

Oxidative Amidation using O₂ and Mechanistic Insight

著者	LI Jing
学位授与機関	Tohoku University
学位授与番号	11301甲第17147号
URL	http://hdl.handle.net/10097/00096934

博士論文

**Oxidative Amidation using O₂ and Mechanistic
Insight**

(酸素を用いる酸化アミノ化反応とその反応機
構解析)

李 静

平成 28 年

Oxidative Amidation using O₂ and Mechanistic Insight

Supervisor:

Yujiro Hayashi

Jing LI

Department of Chemistry, Graduate School of Science

Tohoku University

2016

Acknowledgements

First and foremost, I would like to thank my supervisor, Prof. Yujiro Hayashi (Tohoku University). Looking back, when I came here three years ago, we discuss a lot about the chemistry. At this time, I learn a lot of how to think logically, how to make a logical and reasonable summary, and how to convince other people of my results. In addition, Prof. Hayashi's rich knowledge, logical and deeply thinking, and efficient way to solve problems, affects me a lot for my future life. Without his zealous and continual help, I cannot finish this thesis. The experiences in his group are one of the most important recollections in my life. Although I am sad to be leaving, I am looking forward to the future and will enjoy watching the lab develop during the upcoming years.

Secondly, I want to thank Prof. Martin Lear (University of Lincoln, UK). From the first day I joined this group, he keep teaching me how to make research summary, how to perform experiment and so on. Every time when I meet some difficulties in my life and research, he always use an efficient way to make me cool down and motivate me. Especially when I come out some idea, I got a lot of confidence when shared with him.

I would like to thank Dr. Chiba (Tohoku University) and Dr. Kotaro Iwasaki (Tohoku University) for existing discussion, and they share with me a lot of insightful suggestions and kind encouragements. In addition, they also help me a lot in life. Those kinds of things always motivate me to solve difficult issues in chemistry and in my life.

I would like to thank Prof. Kwon for help in crystal, NMR analysis and calculation study of halogen bonded complex of NIS/NBS and amine, as well as Prof. Itaru Sato (Ibaraki University) and Dr. Shuji Yamashita (Harverd University) for valuable suggestions.

I would like to give my special thanks to Ms. Michiko Fukushima for great help and support.

Finally, I would like to thank Dr. Takasuke Mukaiyama, Dr. Shengen Umemiya, Mr. Daisuke Sakamoto, Mr. Yasuharu Shimasaki, Mr. Shin Ogasawara, Mr. Qianqian Xu, Mr. Yogesh Gupta, Mr. Ryo Fukumoto, Mr. Yuya Kawamoto and all past and current members in Hayashi laboratory.

I would like to take this moment to express my gratitude to all my friends in Tohoku University (Mr. Feng Li, Ms. Bin Wu, Mr. Shuai Mu and so on) who took time to help and motivate me.

This thesis certainly would not have been possible without the love and encouragement of my family: My parents, my parents-in-law, my sister, my brother-in-law and my sister-in-law. Especially, I express my thanks to my wife Ms. Wen-Juan Wang, her understanding and support are one of the most important driving forces to make me finish this thesis. Without all their efforts, kind supports, and encouragements, I would never have completed this Ph.D. program.

Contents

Chapter 1. Introduction	5
1.1 Background of amide synthesis	5
1.2 Umpolung amide synthesis	5
1.3 Previous work and our initial design	6
1.4 Present work	7
Chapter 2. Oxidative Amidation of Nitroalkane with Amine Nucleophiles using Molecular O ₂ and Iodine	10
2.1 Background	10
2.2 Initial design for this work	10
2.3 Optimization of reaction conditions	11
2.4 Substrate scope	12
2.5 Conclusion	14
Chapter 3. Mechanism of Oxidative Amidation of Nitroalkanes with Oxygen and Amine Nucleophiles by Using Electrophilic Iodine	16
3.1 Background	16
3.2 Detail mechanism study for amide formation from primary nitroalkanes	17
3.3 Summary of reaction mechanism	23
Chapter 4. Autocatalytic Conversion of α,α -Diiodonitroalkanes into Amides and Esters by Iodide Byproducts under O ₂	25
4.1 Introduction of autocatalytic reaction	25
4.2 Unexpected sigmoidal kinetic profile in the reaction of α,α -diiodonitroalkane and MeOH /amine	25
4.3 To prove α,α -diiodonitroalkane 4-2a reacting with amine and alcohol is an autocatalytic reaction	26
4.4 Optimization reaction condition for ester formation	30
4.5 Conclusion	32
Chapter 5. Sterically Demanding Oxidative Amidation of α -Substituted Malononitriles with Amines using O ₂	34
5.1 Introduction	34
5.2 Initial design for this work	34
5.3 Screening leaving groups	35
5.4 Substrate scope for amide synthesis	35
5.5 Optimization for sterically hindered amide synthesis	36
5.6 Sterically hindered amide and peptide synthesis	37
5.7 Mechanistic study	38
5.8 Conclusion	40
Chapter 6. Halogen Bonded Complexes between Amines and NBS/NIS: Structure and Reactivity Study	43
6.1 Background of NBS/NIS reacting with amine	43
6.2 NMR study of NIS/NBS with different amines in solution	44
6.3 X-ray crystal structures of halogen bonded complexes of NBS/NIS and amine	46
6.4 Reactivity study of NBS/NIS-quinuclidine complex in halocyclization of olefins	46
6.5 Conclusion	53
Chapter 7. Conclusion	56
Experiment Part	58

List of Publications

Chapter 2

- 1) “Oxidative Amidation of Nitroalkanes with Amine Nucleophiles using Molecular Oxygen and Iodine”.

J. Li, M. J. Lear, Y. Kawamoto, S. Umemiya, A. R. Wong, E. Kwon, I. Sato, Y. Hayashi*.

Angew. Chem. Int. Ed., **2015**, *54*, 12986–12990.

Chapter 3

- 2) “Mechanism of Oxidative Amidation of Nitroalkanes with Oxygen and Amine Nucleophiles by Using Electrophilic Iodine”.

J. Li, M. J. Lear, E. Kwon, Y. Hayashi*. *Chem. Eur. J.* **2016**, *22*, 5538–5542.

Chapter 5

- 3) “Sterically Demanding Oxidative Amidation of α -Substituted Malononitriles with Amines using O₂”.

J. Li, M. J. Lear*, Y. Hayashi*. *Angew. Chem. Int. Ed.*, **2016**, *55*, 9060–9064.

Abbreviations

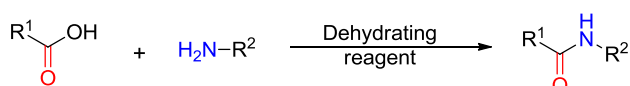
Ac	acetyl
aq.	Aqueous
Boc	tert-butyloxycarbonyl
Cbz	benzyloxycarbonyl
Tr	triphenylmethyl
THF	tetrahydrofuran
TBS	<i>t</i> -butyldimethylsilyl
Bu	butyl
Ts	<i>p</i> -toluenesulfonyl
DMF	<i>N,N</i> -dimethylformamide
<i>dr</i>	diastereomer ratio
ee	enantiomeric excess
Et	ethyl
<i>i</i>	iso
Me	methyl
min	minute(s)
<i>n</i>	normal
NMR	nuclear magnetic resonance
nd	not determined
NOE	nuclear Overhauser effect
Ph	phenyl
Pr	propyl
quant.	quantitative
rt	room temperature
temp.	temperature
NIS	N-iodosuccinimide
NBS	N-bromosuccinimide
I ₂	Iodine

Chapter 1. Introduction

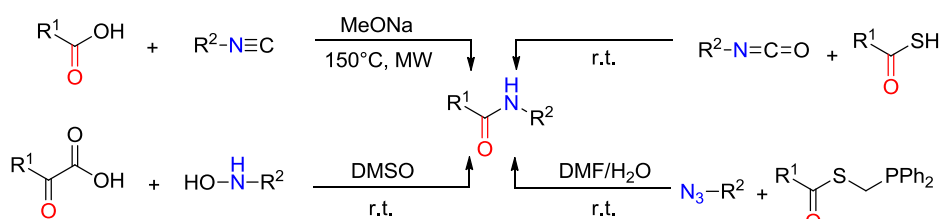
1.1 Background of amide synthesis

Amide bonds are not only the key chemical connections of proteins but they are also the basis for some versatile and widely used synthetic polymers.^[1] Conventional amide bond formation utilizes acids and amines as coupling partners and relies on stoichiometric activating agents for the acid functionality. (Scheme 1a)^[2] Recently, some surrogate reagents and chemical ligands are used in amide and peptide formation. (Scheme 1b)^[2] Isonitriles have been shown to react with carboxylic acids to generate amides under high temperature and microwave conditions, but the harsh reaction conditions and the restricted functional group tolerance to some extent limits the application of this reaction for sensitive peptides or biomolecules.^[3] Isocyanates have also been used to react with thioacids to produce amide linkages.^[4] The Staudinger-type of carboxylic acid derivatives with azides has become a preeminent strategy for amide and peptide formation.^[5] However, the generation of stoichiometric by-products (e.g., $R_3P=O$) often complicates efforts to isolate products, leads to waste disposal issues, and limits the overall synthetic efficiency of this method. Ketoacid-hydroxyl amines are also used to generate an amide group in aqueous conditions without coupling reagents.^[6] But simple and efficient ways to synthesize this α -ketoacid-hydroxylamine ligation are still desirable. In addition, there are some atypical cases of forming reactive *N*-acylating species in a catalytic, manner from alcohols,^[7] aldehydes,^[8,9] and alkyne precursors.^[10](Scheme 1c) The poor substrate scope of this catalytic/oxidative method limits its wide use in complex amide and peptide formation.

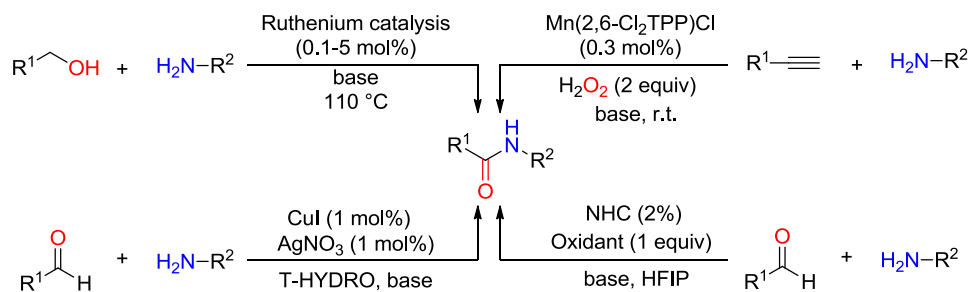
a) Conventional amide synthesis



b) Chemical ligand for amide synthesis



c) Catalysed methods for amide synthesis

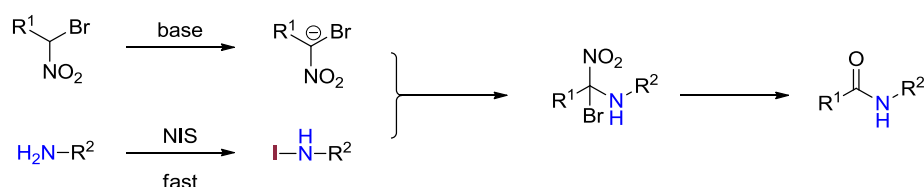


Scheme 1. Previous report about amide synthesis.

1.2 Umpolung amide synthesis

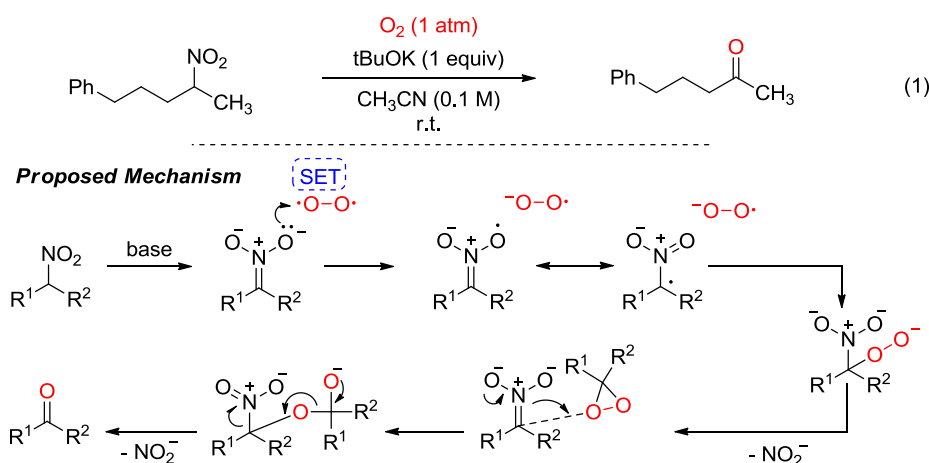
Notably, pre-synthesized α -bromo substituted nitroalkanes have been oxidized with *N*-iodosuccinamide (NIS) and molecular oxygen in the presence of amines.^[11] To account for the apparent umpolung in reactivity of the amine components,

the intermediacy of electrophilic *N*-iodo amines and tetrahedral α -amino, α -bromo nitroalkanes were suggested.^[11,12] From a synthetic point of view, however, methods to achieve direct asymmetric access to α -bromo nitroalkanes are limited in substrate scope^[13] and bromonitroalkanes themselves are potentially explosive.^[8] Comparing with bromonitroalkane, there are a wide variety of catalytic asymmetric methods that adopt nitromethane as a simple, cheap pro-nucleophile to add to both alkyl and aryl aldehydes, imines, enals, enones, and so forth.^[13] In this thesis, my interest was to exploit these readily available primary nitroalkane substrates and develop a direct oxidative method to form amide and peptide bonds in a most economical and practical manner.



Scheme 2. Umpolung amide synthesis using α -bromonitroalkane and amine

1.3 Previous work and our initial design

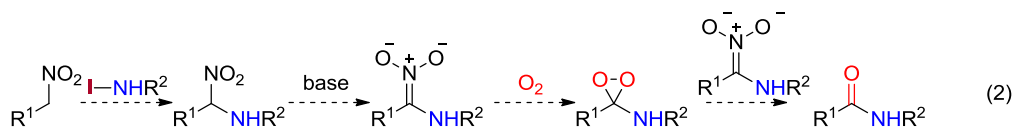


Scheme 3. Metal free Nef reaction and proposed mechanism

In 2013, our group discovered a base-promoted Nef conversion of a key nitroalkene into an enone product under aerobic conditions during the study of the total synthesis of prostaglandin A₁ and E₁ methyl esters^[14]. After that, our group extended this oxidative transformation to a wide range of nitroalkenes and nitroalkanes to produce enones and ketones, respectively (Eq. 1).^[15] Mechanistic insights were gained from [18]O-labeling, nitrite/nitrate ion analysis, intramolecular thioether trapping, and radical clock experiments. In short, the formation of ketones from secondary α -alkylated nitroalkanes was shown to be consistent with a single-electron transfer (SET) mechanism from a charged *aci*-nitronate electron donor to a triplet dioxygen molecule to afford an eventual dioxirane adduct after expelling a nitrite anion. The dioxirane subsequently acts as an electrophilic source of mono-oxygen^[16] that can be captured by another nitronate anion in the surrounding basic medium.

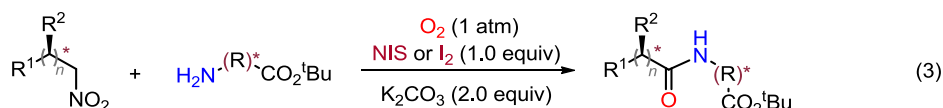
On the basis of these recent mechanistic findings, (Eq. 1)^[14] we reasoned that secondary α -amino nitroalkanes could be formed in situ by reacting primary nitronates with electrophilic *N*-halo amines (Eq. 2). These would be similarly oxidized with oxygen to afford peroxy-adducts bearing amine groups and eventually transform into amides. At this juncture, among other mechanistic concerns, it was not certain whether the formation and reaction of *N*-iodo amines could be achieved in situ and thereby generate the requisite α -amino nitroalkane intermediates (Eq. 2). This was given credence during our

literature search by the suggestion of *N*-iodo amine and α -amino nitroalkane intermediates being reported in a series of oxidative umpolung amide synthesis (UmAS) studies in scheme 2.

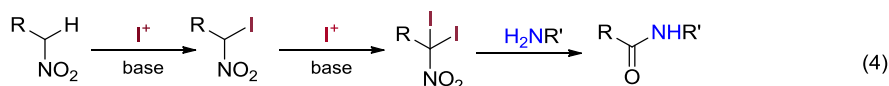


1.4 Present work

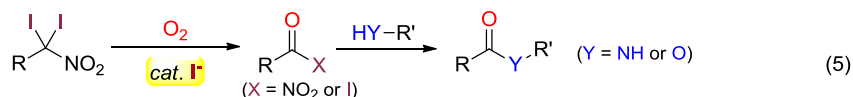
In Chapter 2, a direct oxidative method was developed to make amide and peptide bonds between amines and widely available primary nitroalkanes simply by using I_2 and K_2CO_3 under O_2 . (Eq. 3)



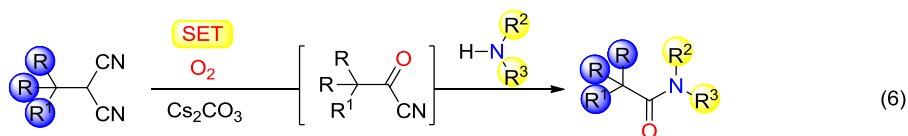
In Chapter 3, during mechanistic study, I observed and isolated α, α -iodonitroalkane intermediates, which further react with an iodine source to form α, α -diiodonitroalkanes; this α, α -diiodo nitroalkane can then directly react with an amine to give the amide or peptide product. (Eq. 4)



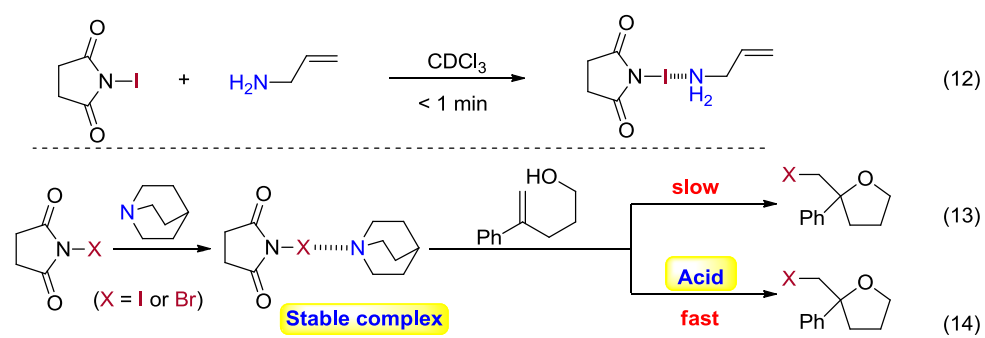
In chapter 4, during mechanistic studies, I identified the α, α -diiodonitroalkane compound as the key intermediate. I identified I^- is an efficient autocatalyst for active ester formation from α, α -diiodonitroalkanes; the active ester can then reacts with amine or MeOH to give amide or ester. (Eq. 5)



In chapter 5, an efficient method for amide and peptide formation between readily available 1,1-dicyanoalkanes and amines was realized simply with molecular oxygen and a carbonate base. This oxidative protocol can be applied to both sterically and electronically challenging substrates in a highly chemoselective, practical, and rapid manner. (Eq. 6)



In chapter 6, I observed and isolated a halogen bonded complex between NIS and allylamine during mechanistic studies of amide formation from primary nitroalkanes using NIS and amine. I further found stable halogen bonded complexes between quinuclidine and NBS/NIS; these complexes are very stable, which show lower reactivity for halocycloetherification, but once acid was added, the reactivity improved dramatically. (Scheme 4)



Scheme 4. Halogen bonded complex between NIS/NBS and amine.

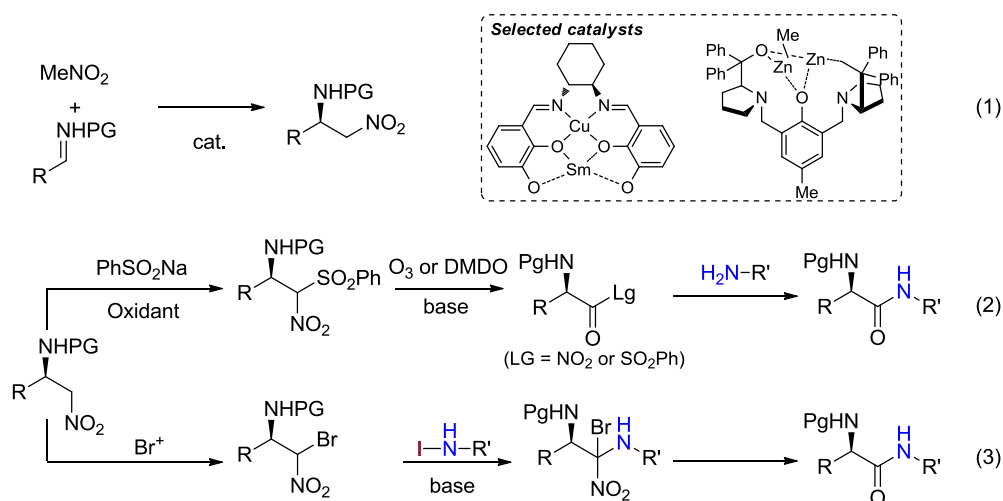
References and Notes

- [1] a) N. Sewald, H. D. Jakubke, in: *Peptides: Chemistry and Biology*, Wiley-VCH, Weinheim, **2002**; b) A. Greenberg, C. M. Breneman, J. F. Liebman, (eds) *The Amide Linkage: Structural Significance in Chemistry, Biochemistry, and Materials Science*, Wiley, **2003**; c) *Peptide Drug Discovery and Development*; Castanho, M., Santos, N., Eds.; Wiley-VCH Verlag GmbH & Co. KGaA: Weinheim, **2011**.
- [2] a) E. Valeur, M. Bradley, *Chem. Soc. Rev.* **2009**, 38, 606–631; b) A. El-Faham, F. Albericio, *Chem. Rev.* **2011**, 111, 6557–6602; c) V. R.; Pattabiraman, J. W. Bode, *Nature* **2011**, 480, 471–479.
- [3] X. Li, S. J. Danishefsky, *J. Am. Chem. Soc.* **2008**, 130, 5446–5448.
- [4] Y. Rao, X. C. Li, S. J. Danishefsky, *J. Am. Chem. Soc.* **2009**, 131, 12924–12926.
- [5] a) H. Staudinger, J. Meyer, *Helv. Chim. Acta* **1919**, 2, 635–646; b) B. L. Nilsson, L. L. Kiessling, R. T. Raines, *Org. Lett.* **2000**, 2, 1939–1941.
- [6] J. W. Bode, R. M. Fox, K. D. Baucom, *Angew. Chem. Int. Ed.* **2006**, 45, 1248–1252.
- [7] C. Gunanathan, Y. Ben-David, D. Milstein, *Science* **2007**, 317, 790–792.
- [8] W.-J. Yoo, C.-J. Li, *J. Am. Chem. Soc.* **2006**, 128, 13064–13065.
- [9] W.-K. Chan, C.-M. Ho, M.-K. Wong, C.-M. Che, *J. Am. Chem. Soc.* **2006**, 128, 14796–14797.
- [10] S. De Sarkar, A. Studer, *Org. Lett.* **2010**, 12, 1992–1999.
- [11] Initial discovery and mechanistic rationale of oxidative umpolung amide synthesis (UmAS): B. Shen, D. M. Makley, J. N. Johnston, *Nature* **2010**, 465, 1027–1032; b) J. P. Shackleford, B. Shen, J. N. Johnston, *Proc. Natl. Acad. Sci. USA* **2012**, 109, 44–46; Application of UmAS in synthesis: c) M. W. Leighty, B. Shen, J. N. Johnston, *J. Am. Chem. Soc.* **2012**, 134, 15233–15236; d) K. E. Schwietzer, J. N. Johnston, *Chem. Sci.* **2015**, 6, 2590–2595; e) K. E. Schwietzer, J. N. Johnston, *Chem. Commun.* **2016**, 52, 152–155.
- [12] Presently accepted mechanism of oxidative umpolung amide synthesis (UmAS): K. E. Schwietzer, B. Shen, J. P. Shackleford, M. W. Leighty, J. N. Johnston, *Org. Lett.* **2014**, 16, 4714–4717.
- [13] a) A. Noble, J. C. Anderson, *Chem. Rev.* **2013**, 113, 2887–2939; b) T. Okino, S. Nakamura, T. Furukawa, Y. Takemoto, *Org. Lett.* **2004**, 6, 625–627; c) B. M. Nugent, R. A. Yoder, J. N. Johnston, *J. Am. Chem. Soc.* **2004**, 126, 3418–3419; d) T. P. Yoon, E. N. Jacobsen, *Angew. Chem. Int. Ed.* **2005**, 44, 466–468; e) H. Gotoh, H. Ishikawa, Y. Hayashi, *Org. Lett.* **2007**, 9, 5307–5309.
- [14] Y. Hayashi, S. Umemiya, *Angew. Chem. Int. Ed.* **2013**, 52, 3450–3452.
- [15] S. Umemiya, K. Nishino, I. Sato, Y. Hayashi, *Chem. Eur. J.* **2014**, 20, 15753–15759.

Chapter 2. Oxidative Amidation of Nitroalkane with Amine Nucleophiles using Molecular O₂ and Iodine

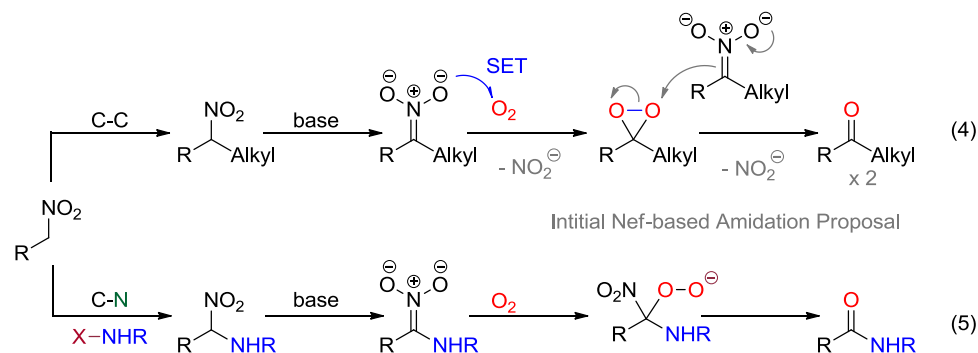
2.1 Background

Nitro compounds are widely available in synthetic chemistry. Especially there are a wide variety of catalytic asymmetric methods that adopt nitromethane as a simple, cheap nucleophile to add imines via Aza-Henry reaction. (Eq. 1)^[1] The conversion of primary nitroalkanes into carbonyl compounds is one of the most important process in organic synthesis. Especially the transformation of primary nitroalkane to aldehyde and carboxylic acid has been widely developed.^[2] The synthesis of an amide from a primary nitroalkane and amine is still rare. The most common approach firstly prepares α -sulfonylnitroalkanes or α -bromonitroalkanes from primary nitroalkane using an oxidative method. α -Sulfonylnitroalkanes further reacts with amine using base and a strong oxidative reagent to afford amide (eg. DMDO or O₃). (Eq. 2)^[2] Pre-formed α -bromonitroalkanes further reacts with an electrophilic amine to afford the amide. (Eq. 3)^[3] In this chapter, our interest was to exploit these readily available primary nitroalkane substrates and develop a direct oxidative method to form amide and peptide bonds in a most economical and practical manner.



Scheme 1. Previous methods for amide formation from primary nitroalkane

2.2 Initial design for this work



Scheme 2. Initial proposal for oxidative amidation from primary nitroalkane.

Recently, our group discovered an oxidative transformation of a wide range of nitroalkenes and nitroalkanes to produce enones and ketones, respectively (Eq. 4).^[4] Mechanistic insights indicated the formation of ketones from secondary α -

alkylated nitroalkanes was consistent with a single-electron transfer (SET) mechanism from a charged aci-nitronate electron donor to a triplet dioxygen molecule to afford an eventual dioxirane adduct after expelling a nitrite anion. The dioxirane subsequently acts as an electrophilic source of mono-oxygen that can be captured by another nitronate anion in the surrounding basic medium. On the basis of these recent mechanistic findings (Eq. 4), we reasoned that secondary α -amino nitroalkanes could be formed in situ by reacting primary nitronates with electrophilic N-halo amines (Eq. 5). These would be similarly oxidized with oxygen to afford peroxy-adducts bearing amine groups and eventually transformed into amides. There was credence for this idea by the suggestion of N-iodo amine and α -amino nitroalkane intermediates being reported in a series of oxidative umpolung amide synthesis (UmAS) studies.^[3]

2.3 Optimization of reaction conditions

In order to check the initial design, we first elected to pursue the base-promoted oxidative coupling of the racemic nitroalkane **2-1** with the hydrochloride salt of (*S*)-phenylalanine methyl ester **2-2** and NIS in acetonitrile (Table 1). In the first instance, the base was varied (entries 1-7). This quickly demonstrated K₂CO₃ (entry 4) to be superior to weaker bases like NaOAc, which gave the α -iodo nitroalkane **2-4** (entry 1). Stronger bases like Cs₂CO₃ and K₃PO₄ gave slightly lower yields of the dipeptide product **2-3** (entries 5 and 6). Soluble bases like DBU were also found inferior to K₂CO₃ (cf. entries 4 and 7), but both conditions resulted in significant amounts of the carboxylic acid **2-5** (30-50% yields). The use of less electrophilic *N*-halosuccinamides did not improve the result and α , α -dichloro nitroalkanes **2-6** (X = Cl) was isolated in one case (entries 8 and 9). A change in the solvent system with NIS and adopting two equivalents of the free amine of **2-2** proved more successful (entries 10 to 17). In particular, the use of molecular I₂ or NIS at room temperature afforded optimal yields of dipeptide **2-3** (67%; entry 18). Generation of the carboxylic side-product **2-5** (15-25%) could not be avoided even under strictly anhydrous conditions. In practice, there was no benefit to using especially dried glassware or super-dry solvents.

Table 1. Optimization of Oxidative Peptide Formation.^a

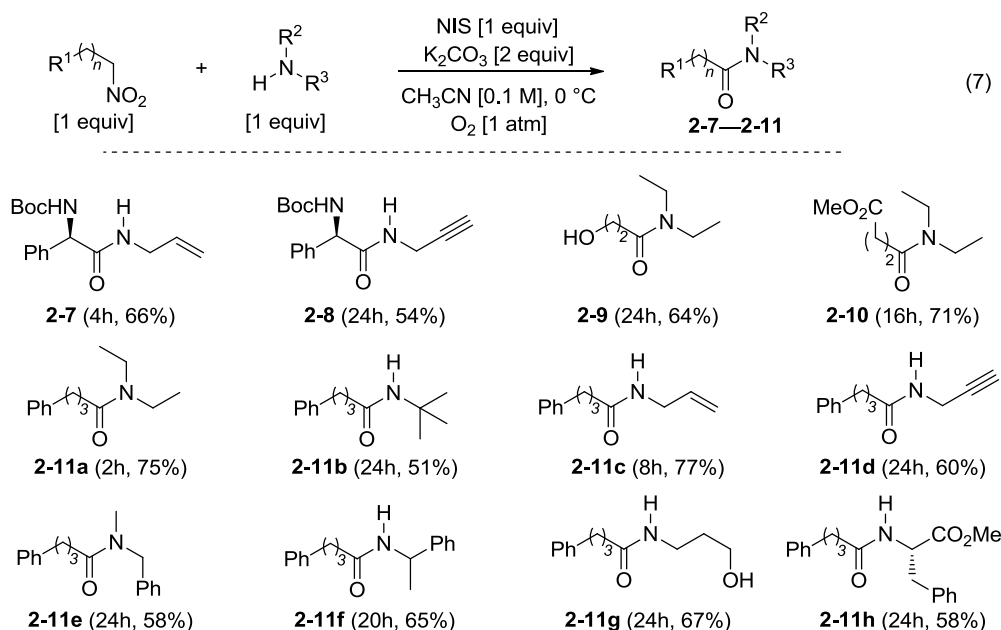
(6)

Entry	Base	X ⁺	Solvent (t, h)	2-3	2-4	2-5
1	NaOAc	NIS	CH ₃ CN (5)	-	5	-
2	KOAc	NIS	CH ₃ CN (5)	20	-	-
3	Na ₂ CO ₃	NIS	CH ₃ CN (15)	5	-	-
4	K ₂ CO ₃	NIS	CH ₃ CN (3)	49	-	30
5	Cs ₂ CO ₃	NIS	CH ₃ CN (2)	30	-	-
6	K ₃ PO ₄	NIS	CH ₃ CN (3)	42	-	-
7	DBU	NIS	CH ₃ CN (12)	30	-	50
8	K ₂ CO ₃	NBS	CH ₃ CN (12)	20	-	-

9	K ₂ CO ₃	NCS	CH ₃ CN (12)	-	- ^[b]	-
10 ^[c]	K ₂ CO ₃	NIS	CH ₃ CN (2.5)	51	-	-
11 ^[c]	K ₂ CO ₃	NIS	THF (7.5)	51	-	-
12 ^[c]	K ₂ CO ₃	NIS	PhCH ₃ (48)	15	-	60
13 ^[c]	K ₂ CO ₃	NIS	DMSO (48)	15	-	30
14 ^[c,d]	K ₂ CO ₃	NIS	1:1 media (12)	59	-	30
15 ^[c,e]	K ₂ CO ₃	I ₂	1:1 media (4)	67	-	25

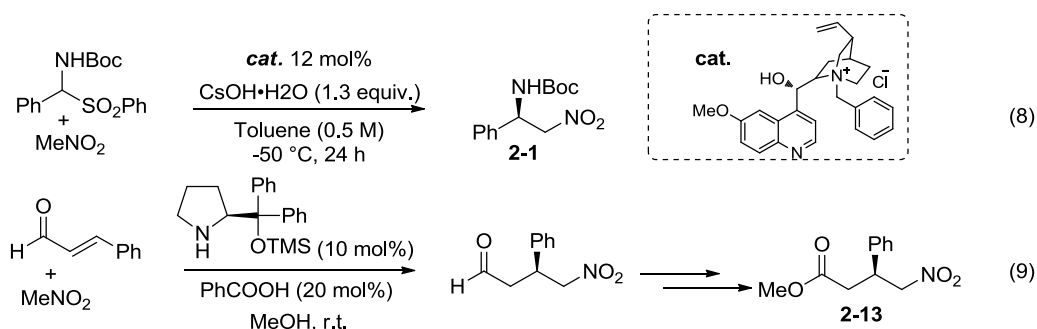
[a] Unless noted otherwise, all reactions were conducted with nitroalkane **1** [0.2 mmol], amine·HCl salt **2-2** [0.2 mmol], base [0.6 mmol], halonium (X⁺) source [0.2 mmol] at 0 °C in solvent [2 mL] under O₂ [1 atmosphere] and isolated yields (%) are given. [b] Dichlorinated nitroalkane **2-6** (X = Cl) was isolated in 10% yield. [c] For entries 10 to 17, two equivalents of the free amine **2-2** [0.4 mmol] and base [0.4 mmol] were used. [d] 1:1 toluene/THF mixture was used. [e] Reaction performed at room temperature with free amine **2-2** [0.4 mmol] and base [0.4 mmol]; a similar result was obtained with NIS [0.2 mmol] over 12 h.

2.4 Substrate scope



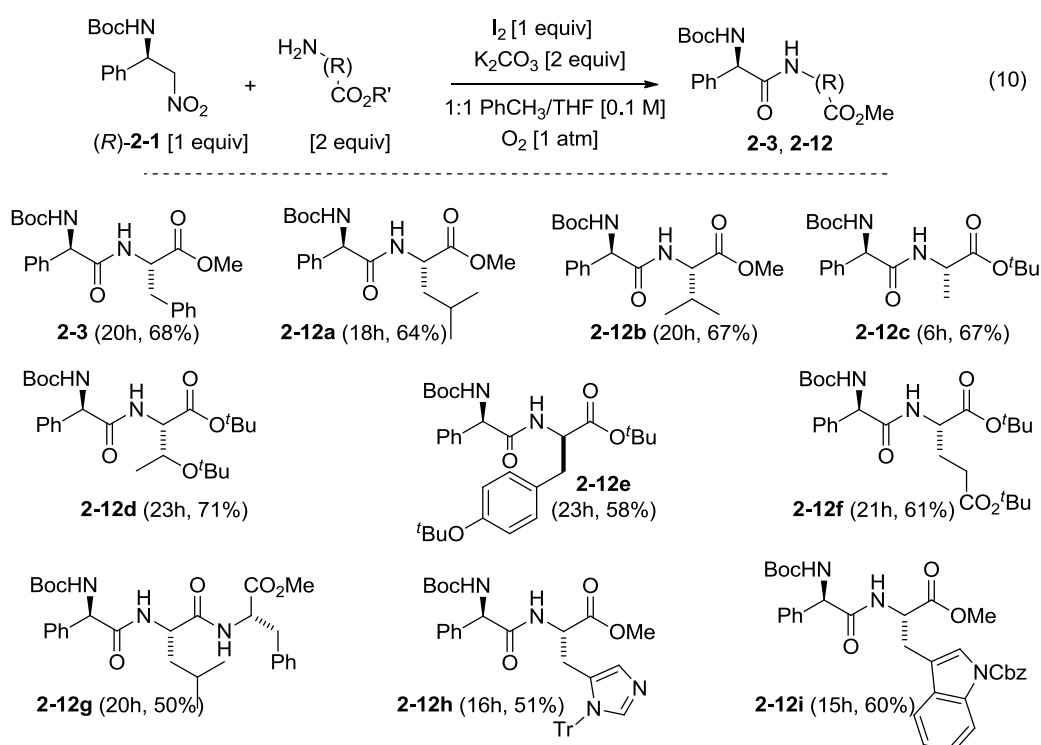
Scheme 3. Oxidative amidation of nonchiral nitroalkanes using NIS/O₂.

First, we used nonchiral nitroalkanes to react with different amines to investigate the scope of the oxidative amidation method (Scheme 3). We found when unsaturated amines were used (eg. allylamine alkynylamine, *N*-Methylbenzylamine), NIS give better result, as I₂ can quickly react with unsaturated amine to give some side product (I₂ addition to double bond or triple bond). For diethylamine, *t*-butylamine and (*S*)-phenylalanine methyl ester, both NIS and I₂ gave good results. Next we decided to use NIS for the substrate scope study. Unsaturated functionality such as benzyl, allyl, and alkynyl groups remained unreacted, and the amidation method also tolerated unprotected hydroxyl groups (**2-9**, **2-11g**). In addition, diethylamine and *t*-butylamine still works very well to give the desired amide. Furthermore, the desired amide was obtained in moderate yield and no epimerization when L-phenylalanine methyl ester was used.

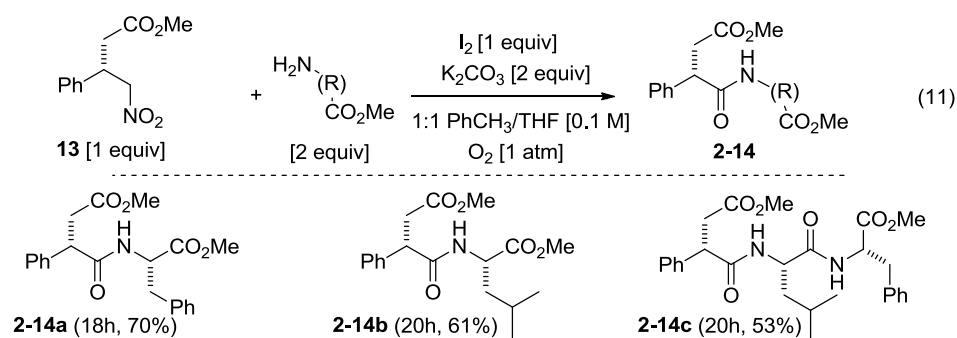


Scheme 4. Synthesis of chiral primary nitroalkanes.

We next focused the reaction of chiral nitroalkane (*R*)-**2-1** with amino acids in order to generate dipeptides. First, the chiral (*R*)-**2-1** was prepared via an aza-Henry reaction from readily available nitromethane and imine using phase transfer catalysis. (Eq. 8). Next, different amino acid esters were used to react with chiral nitroalkane (*R*)-**2-1**. Here, the reaction was performed with I_2 instead of NIS in 1:1 THF/toluene (Eq. 10), because NIS can react with amine to afford a less soluble halogen bonded complex in 1:1 THF/toluene. In addition, I_2 is much cheaper and more [convenient](#) than NIS. In fact, the dipeptide and tripeptide products (**2-3**, **2-12**) were produced with complete stereochemical integrity. No epimerization of potentially labile α -stereocenters was observed. Further extension of this transformation was applied to chiral nitroalkyl Michael adducts **2-13**, which can be easily prepared in high enantioselectivity from chiral nitroalkanes via the asymmetric organocatalyzed Michael reaction between nitromethane and α , β -enals, as developed by our group. (Eq. 9) The same tolerances were found for readily prepared, chiral nitroalkyl Michael adducts (**2-13** \rightarrow **2-14**, Eq. 11) and standard protecting groups (e.g., *O*-*t*-Bu, *N*-Tr, *N*-Cbz, *N*-Boc) were also found compatible.



Scheme 5. Peptide formation using I_2/O_2 .



Scheme 6. Oxidative amidation using I₂/O₂.

2.5 Conclusion

In this chapter, a direct oxidative method was developed to make amide and peptide bonds between amines and widely available primary nitroalkanes simply by using I₂ and K₂CO₃ under O₂. The method is straightforward in operation, chemoselective in functional group tolerance, and stereochemically robust to potentially epimerizable substrates. Importantly, a whole range of primary nitroalkane starting materials for our reaction method can be readily prepared in chiral form via a plethora of asymmetric methods.

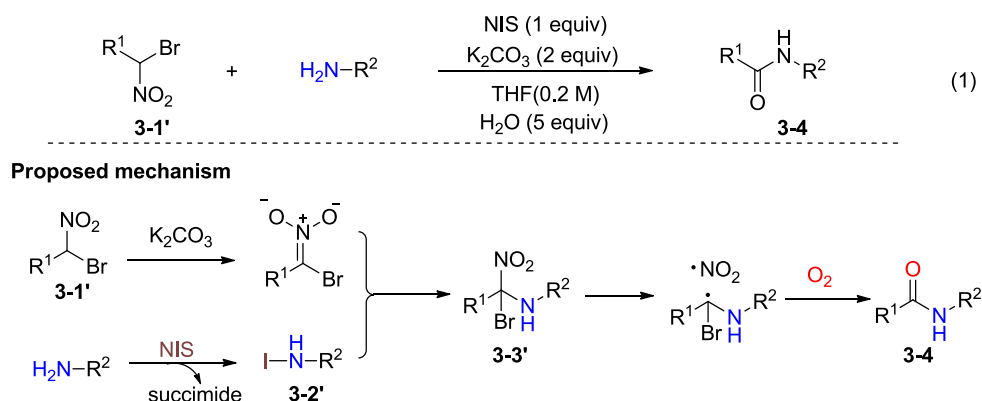
References and Notes

- [1] a) A. Noble, J. C. Anderson, *Chem. Rev.* **2013**, *113*, 2887–2939; b) T. Okino, S. Nakamura, T. Furukawa, Y. Takemoto, *Org. Lett.* **2004**, *6*, 625–627; c) B. M. Nugent, R. A. Yoder, J. N. Johnston, *J. Am. Chem. Soc.* **2004**, *126*, 3418–3419; d) T. P. Yoon, E. N. Jacobsen, *Angew. Chem. Int. Ed.* **2005**, *44*, 466–468; e) H. Gotoh, H. Ishikawa, Y. Hayashi, *Org. Lett.* **2007**, *9*, 5307–5309.
- [2] a) R. Ballini, M. Petrini, *Tetrahedron*, **2004**, *60*, 1017–1047; b) R. Ballini, M. Petrini, *Adv. Synth. Catal.* **2015**, *357*, 2371 – 2402.
- [3] B. Shen, D. M. Makley, J. N. Johnston, *Nature* **2010**, *465*, 1027–1032.
- [4] S. Umemiya, K. Nishino, I. Sato, Y. Hayashi, *Chem. Eur. J.* **2014**, *20*, 15753–15759.

Chapter 3. Mechanism of Oxidative Amidation of Nitroalkanes with Oxygen and Amine Nucleophiles by Using Electrophilic Iodine

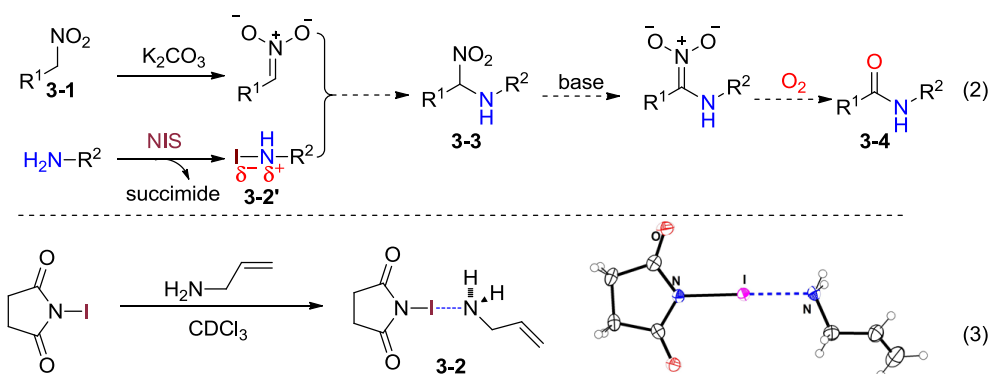
3.1 Background

In 2010, the Johnston group developed the oxidative amidation between α -bromonitroalkanes and an amine using NIS and this reaction is termed *umpolung amide synthesis* (UmAS).^[1] The method centers on α -bromo substituted nitroalkanes **3-1'** reacting with electrophilic *N*-iodo amines **3-2'** (*in situ* generated with NIS) to form reactive tetrahedral α -amino, α -bromo nitroalkanes **3-3'** (Scheme 1). This proposed tetrahedral intermediate **3-3'** couples with molecular oxygen in a homogenic manner to eventually form the amide product **3-4** (Eq. 1).^[1,2]



Scheme 1. Umpolung amide synthesis (UmAS)

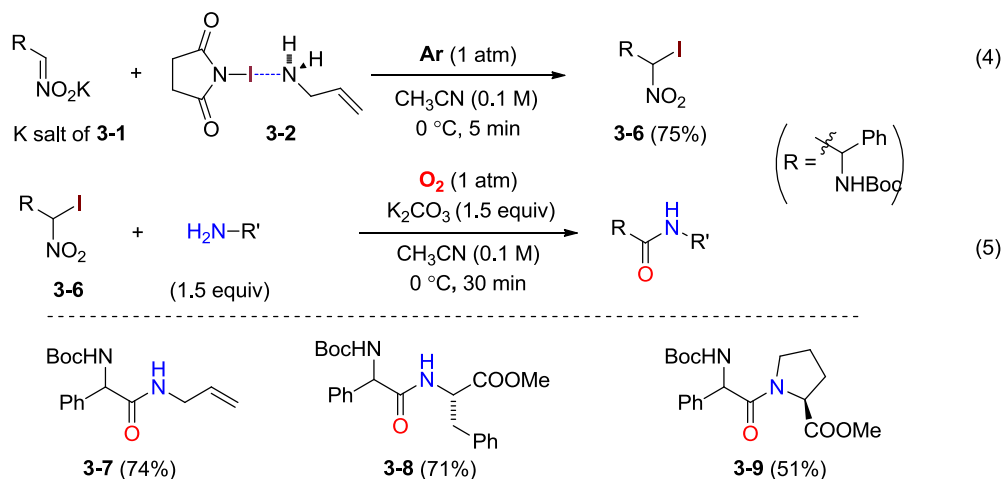
Our initial reaction design was based on our mechanistic finding of the Nef reaction.^[3] We thought an α -aminonitroalkane **3-3** can be easily generated via electrophilic iodo-amine **3-2'** reacting with *aci*-nitronate anion of **3-1**, the α -aminonitroalkane intermediate **3-3** can be further oxidized by O_2 to give amide **4**.^[3] (Scheme 2) However, all attempts to prepare, infer, or observe the anticipated *N*-iodo amines **3-2'**,^[1] were not confirmed in our hands. Instead, we discovered through NMR experiments that allylamine readily react with NIS to form precipitates, which behave chemically as sources of electrophilic iodine and nucleophilic amine. Eventually, we were able to obtain a single crystal and the structure of allylamine/NIS complex **3-2** by X-ray crystallography. (Eq. 3) The isolation of NIS-amine complex **3-2** instead of iodo-amine **3-2'** put our initial proposal into question. We thus decided to do a systematic investigation of the reaction mechanism.



Scheme 2. Our initial design for amide synthesis

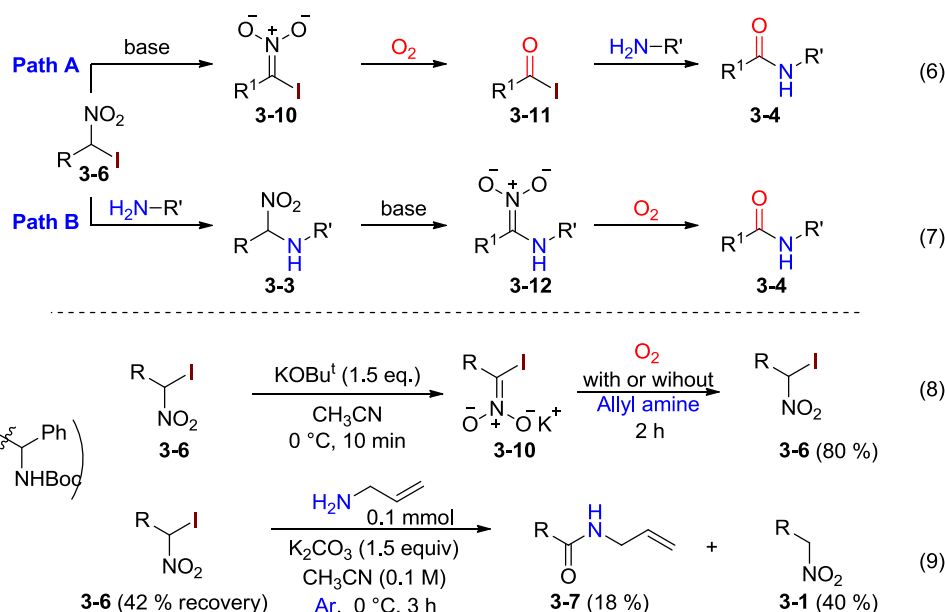
3.2 Detail mechanism study for amide formation from primary nitroalkanes

Firstly, the reaction of the *aci*-nitronate anion of **3-1** with **3-2** was tested; in this case, only α -iodo nitroalkane **3-6** was obtained and isolated in 75% yield within 5 minutes. (Eq. 4) Next, the pre-prepared **3-7** was tested for its ability to form amides directly and electrophilic halogen sources were omitted in the presence of K_2CO_3 , O_2 , and a slight excess of allylamine, phenylalanine methyl ester or L-proline methyl ester. The anticipated amides were isolated in good yields at 0 °C within 30 min. (Eq. 5) The iodo nitroalkane **3-6** was even reactive enough to couple with the methyl ester of L-proline, a secondary amino ester often displaying unique reactivity, giving its respective dipeptide **3-9** in 51% yield. These reactions indicated α -iodo nitroalkane **3-6** to be the key intermediate.



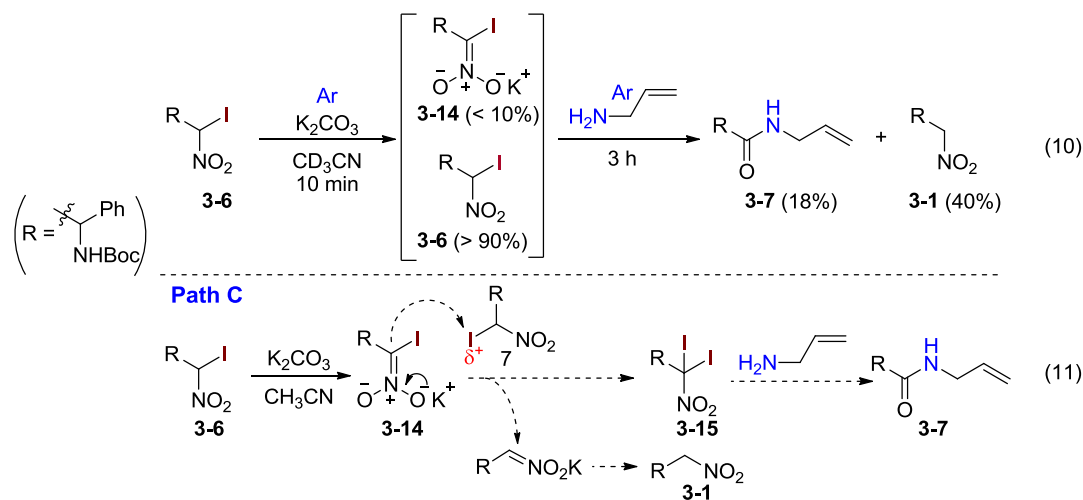
Scheme 3. Mono- α -iodonitroalkane **3-6** is a key intermediate.

Thus, we confirmed the formation of α -iodonitroalkane **3-6** from *aci*-nitronate anion of **3-1** and complex **3-2**. We next considered two interconnected pathways (cf. Eq. 6 and 7) for the formation of amide **3-4** from the α -iodonitroalkane **3-6** based on our previous mechanistic study of Nef reaction using O_2 .^[3] In one case, (Eq. 6, Path A) the α -iodonitroalkane **3-6** first reacts with base to form an *aci*-nitronate anion **3-11**, which further reacts with O_2 via SET and radical coupling to give active ester **3-11**, which further traps amine to give the amide **3-4**. In another case (Eq. 6, Path B), the α -amino nitroalkane intermediate **3-3** can form by attack of an amine onto the α -iodine of **3-6** via S_N2 -type reaction, the anion **3-12** can be generated in-situ in the presence of base; the anion **3-12** further reacts with O_2 via SET and radical coupling to give amide **3-4**. At this time, we were unclear which pathway was more favorable. We thus checked each pathway one by one. First, path A was taken into consideration. We thus prepared the potassium salt of **3-6** and determined if it would react with oxygen directly. We carried these reactions with and without amine being present. (Eq. 8) However, no amide formed at all and α -iodonitroalkane **3-6** was recovered. These two experiments clearly demonstrated that, molecular oxygen does not react with the *aci*-nitronate intermediate of **3-6** at all and the path A (Eq. 6) does not operate.^[3] Next, Path B was taken into consideration (Eq. 7). We performed the reaction of monoiodide nitroalkane **6** with allylamine under Ar in order to observe or isolate the α -amino nitroalkane intermediate **3-3**. In fact, the anaerobic reaction of the monoiodide nitroalkane **3-6** with allylamine and K_2CO_3 not only produced the amide **3-7** (18%), but also a significant amount (40%) of the de-iodinated nitroalkane **3-1** (Scheme 2, Eq. 9); we never observed the formation of the α -amino nitroalkane intermediate **3-3**. This result indicated the path B does not operate. Thus, further control reactions were carried out to understand how the amide **3-7** is generated under Ar.



Scheme 4. Proposed reaction mechanism for amide formation from mono α -iodonitroalkane **3-10**.

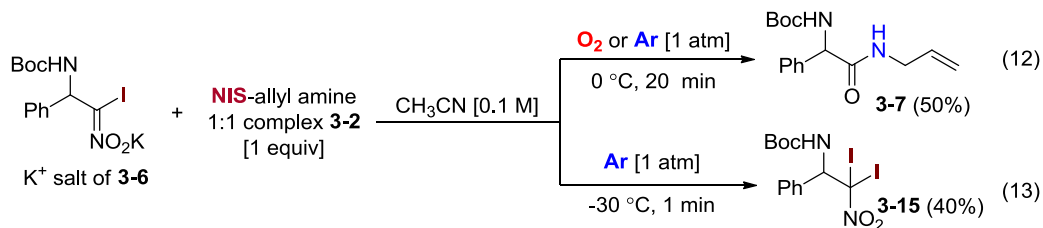
Further ^1H NMR studies were carried out to understand the reaction of mono-iodide **3-6** with K_2CO_3 in CD_3CN . In fact, ^1H NMR shows formation of the *aci*-nitronate intermediate **3-14** is very slow and most mono-iodo nitroalkane **3-6** remained unreacted in CD_3CN after 10 min. When the amine was added to the reaction mixture, the desired amide **3-7** and de-iodo nitroalkane **3-1** formed after 3h. These results led to the idea that the mono-iodide **3-7** can act a source of electrophilic iodine for α -carbanions **3-14**. This would logically produce a unobserved α,α -diodidonitroalkane intermediate **3-15** and the isolated de-iodinated compound **3-1**.



Scheme 5. Further proposed reaction mechanism for amide formation from mono-iodonitroalkane **3-6**.

Suspecting the need for iodine-transfer by **3-6**, we thus decided to study the reactivity of the pure anion of **3-6** with one equivalent of the NIS-amine complex **3-2** under O_2 and under Ar (Scheme 2). The amide **3-8** formed in moderate yields in 20 min when conducted at 0°C both under Ar or O_2 (Eq. 6). Markedly, the potassium salt of **3-6** rapidly produced the diiodide **3-15** at -30°C with the NIS-amine complex **3-2** when the reaction was stopped within 1 min (Eq. 7). Longer

reaction times or higher temperatures produced the expected amide **3-7** and the diiodide **3-15** was not observed. These results further suggested the diiodide **3-15** was a key intermediate to amide **3-7** from mono-iodonitroalkane **3-6**.



Scheme 6. Further proposed reaction mechanism for amide formation from mono-iodonitroalkane **3-6**.

Suspecting these type of dihalogenated species **3-15** as reactive tetrahedral intermediates to the amide **3-7**, we prepared and compared the reactivity of the di-halo nitroalkanes **3-6** (X^1 , X^2 = Cl, Br, and/or I) under both Ar and O_2 . These experiments clearly showed the amide **3-7** formed directly from the dihalide intermediate **3-15**, whereby higher reactivity and yields resulted with the introduction of at least one iodine substituent. Exceptional reactivity, within 20-60 min, was observed with the unstable diiodide **3-15** (X^1 , X^2 = I), which likely accounts for our difficulty in observing **3-15** during our initial amidation studies, unlike the unreactive dichloride (Chapter 2, Table 1).

Table 1. Direct Amidation of Dihalogenated Nitroalkanes **3-15**.^[a]

$ \begin{array}{c} \text{BocHN} \\ \\ \text{Ph}-\text{C}-\text{C}(\text{NO}_2)(\text{X}^1)(\text{X}^2) \\ \text{3-15 [1 equiv]} \end{array} + \text{H}_2\text{N}-\text{CH}_2\text{CH}=\text{CH}_2 \text{ [1.5 equiv]} \xrightarrow[\text{CH}_3\text{CN [0.1 M], 0 }^\circ\text{C}]{\text{Ar or O}_2 \text{ [1 atm], K}_2\text{CO}_3 \text{ [1.5 equiv]}} \begin{array}{c} \text{BocHN} \\ \\ \text{Ph}-\text{C}-\text{C}(\text{NH}-\text{CH}_2\text{CH}=\text{CH}_2) \\ \text{3-7} \end{array} \quad (14) $				
Entry	X^1	X^2	Ar: yield (%) ^b	O_2 : yield (%) ^c
1	Cl	Cl	trace	<5
2	Cl	Br	35	20
3	Cl	I	48	72
4 ^e	Br	Br	10	31
5	Br	I	55	70
6 ^d	I	I	50	60

[a] Unless noted otherwise, all reactions were conducted with dihalogenated nitroalkanes **3-6** [0.1 mmol], allyl amine [0.15 mmol], and K_2CO_3 [0.15 mmol] at 0 °C in CH_3CN [1 mL] under O_2 or Ar [1 atmosphere] and isolated yields (%) are given. [b] Reactions under Ar were conducted over 48 h, except entry 6 was over 1 h. [c] Reactions under O_2 were conducted over 24 h, except entry 6 was over 20 min. [d] Di-iodide of **3-6** was unstable and used immediately after preparation. [e] Reaction conducted at room temperature.

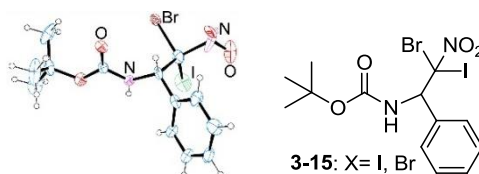


Figure 1. ORTEP X-Ray Structure of dihalo-nitroalkane **3-15** (X = Br, I) with thermal ellipsoids drawn at the 30 % probability level.

After we confirmed the dihalogenated species **3-15** can form amides under Ar and O_2 , we found that our reaction was

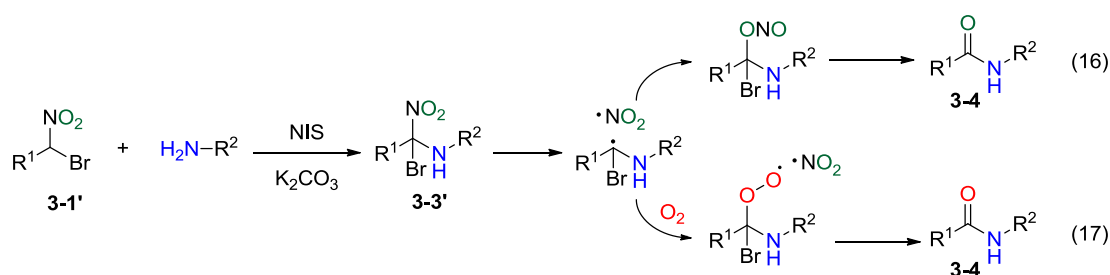
very similar to a recent UmAS study. (Eq. 15)^[1] The difference was that the Johnston group proposed an α -amino, α -halonitroalkane **3-3'** as the key intermediate that further converts to the amide with O₂ or without O₂. (Scheme 7) Further evidence presented in this UmAS labeling study^[1b] also shows that residual H₂¹⁸O and N[¹⁸O]₂-labeled α -halonitroalkanes **3-1'** do not result in significantly [18]O enriched amides **3-4** under [16]-O₂. (Table 2) However, we identified a tetrahedral α -iodo, α -halonitroalkane **3-15** instead of an α -amino, α -halonitroalkane **3-3'** as the key intermediate to the amide product.

Table 2. ¹⁸O label reaction by Johnston group^[a]

(15)

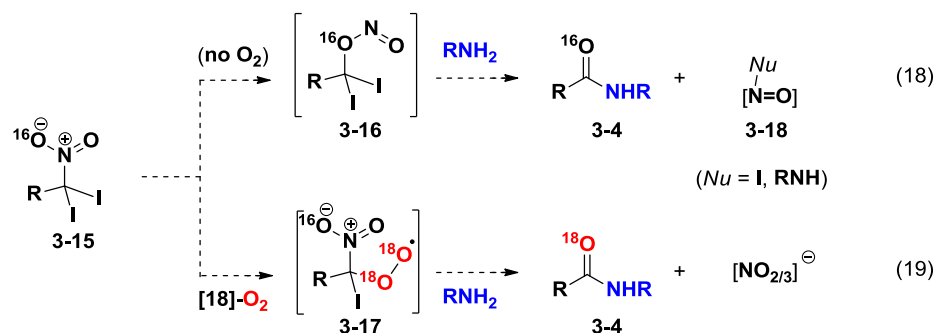
Entry	NO ₂ label (% ¹⁸ O)	H ₂ O (% ¹⁸ O)	Atmosphere	Amide (% ¹⁸ O)	Yield (%)
1	0	>99	open	<1	75
2	82	0	Ar	66	70
3	0	0	¹⁸ O ₂	83	68

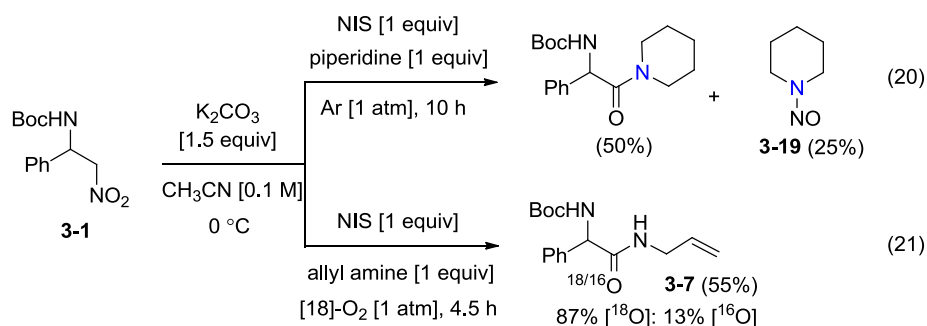
[a] Reactions employed one equivalent of α -bromo nitroalkane (0.2M in THF), with N-iodosuccinimide (one equivalent) added as the final reagent at 0 °C. “Open” atmosphere refers to use of a static atmosphere provided by a cap or septum. Other variations used a balloon of the indicated gas. Isotopic distribution determined by high resolution mass spectrometry.



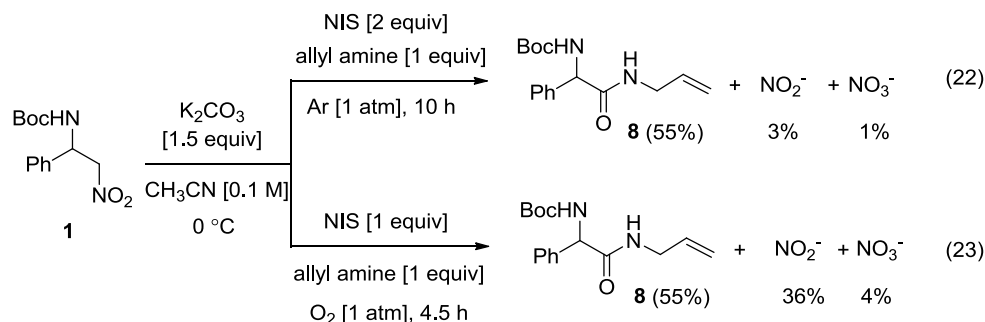
Scheme 7. Proposed mechanism for amide formation by Johnston group.^[1b]

Thus, having discounted dioxygen reacting directly with the anion of **3-1**, two proposed pathways to form the amide **3-4** were reasoned to occur via the tetrahedral α,α -diiodonitroalkane **3-15** (Scheme 8, Eq. 18 and 19). Both radical and ionic modes were considered feasible, and the generation of *N*-nitroso amines **3-18** (Nu = amine) were also deemed possible as byproducts from diiodo nitrites **3-16**, the rearranged adducts of **3-15** (Eq. 18). The fate of the nitro group was thus uncertain under anaerobic and aerobic conditions, for example, to form either nitrate or nitrite salts from the congested peroxy nitroalkane **3-17** (Eq. 19), and a further set of control experiments were performed to discern such fates (Eq. 20 and 21). Specifically, we measured the resultant concentration of nitrate/nitrite salts and the level of [18]O incorporation by converting **3-1** into **3-4** under both Ar and [18]-O₂.^[5]



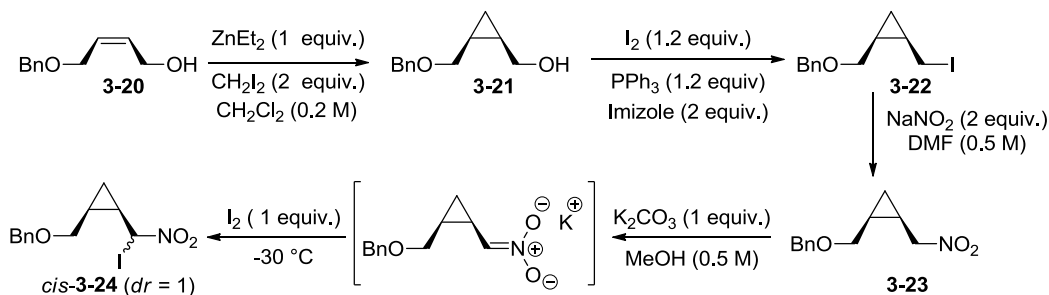


Scheme 8. Nitroso-Trapping and [18]-O₂ labelling Studies of **3-1**.



Scheme 9. The amount of NO₂⁻/NO₃⁻.

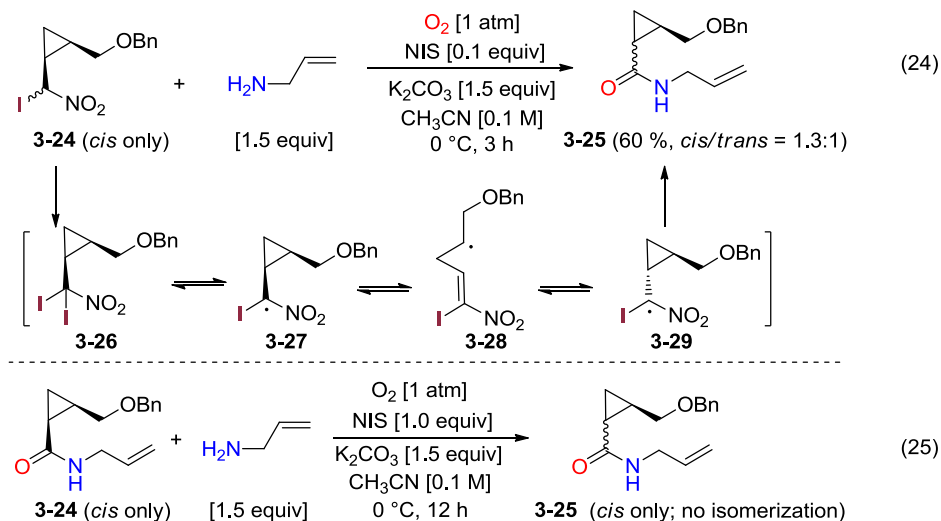
In the event, piperidine was chosen as a less volatile amine reactant, compared to allylamine, which allowed for the anticipated and known *N*-nitroso amine **3-19**^[11] to be isolated reliably (Eq. 20). Under Ar, **3-19** was isolated in 25% yield. Under O₂, **3-19** was isolated in 11% yield. If the nitrosyl iodide **3-19** (Nu = I) forms, it would be expected to also convert to I₂ and NO gas.^[7] The fact that *N*-nitroso amines were isolated supports the existence of nitrite intermediates **3-16**. Next, isotope labelling experiments with allylamine as the nucleophile revealed an 87% of [18]O incorporation in the amide product **3-7** in a chemical yield of 55% under [18]-O₂ (Eq. 21). The resultant nitro-derived salt ratios were calculated to be 36% nitrite (NO₂⁻) and 4-6% nitrate (NO₃⁻) under O₂ (Eq. 23), whereas 3% NO₂⁻ and 1-2% NO₃⁻ were detected under anaerobic conditions (Eq. 22). While these data support the nitro-nitrite rearrangement **15** → **16** (Eq. 18) as the predominant fate under anaerobic conditions, the data suggest that both pathways can occur concomitantly under aerobic conditions. Presumably, the proximity and local concentration of solvated O₂ gas to the diiodide **3-15** will be a factor in pathway selection, and NO_{2/3} salt counts were found to be low due to *N*-nitroso amine formation and loss of NO gas (and I₂) via species like I-N=O.^[7]



Scheme 10. Synthesis of *cis*-cyclopropanes **3-24**.

In order to provide evidence that the reaction proceeds via a radical mechanistic pathway (Eq. 19), we decided to synthesize the *cis*-cyclopropanes **3-20** (Scheme 10) for radical clock experiments. Cyclopropanation of alcohol **3-21** was

easily obtained by employing diethyl zinc and diiodomethane in dichloromethane.^[8] Treatment of the cyclopropane **3-21** with iodine, triphenylphosphine and imidazole gave the iodide compound **3-22**. The iodide compound **3-22** was converted into the corresponding nitroalkane **3-23** via displacement of iodide with nitrite. Next, *cis*-cyclopropanes **3-24** were synthesized from nitroalkane **3-23** using K₂CO₃ and I₂ in MeOH at -30°C.



Scheme 11. Radical clock control experiments of pure *cis*-**3-24** and *cis*-**3-25**.

Next, we performed radical clock experiments (Scheme 11).^[8] Thus, the pure *cis*-cyclopropanes **3-24** and **3-21** were prepared and reacted with allylamine under our oxidative conditions. Starting from *cis*-**3-24**, a 1.3:1 *cis/trans* ratio of **3-25** was generated in 60 % yield (Eq. 24). In order to exclude epimerization occurring after amide formation, the purified *cis*-cyclopropyl amide **3-25** was similarly treated with NIS, K₂CO₃ and O₂. This gave complete recovery of the *cis*-cyclopropyl amide, even after 12 h (Eq. 25). These results support the existence of a cyclopropylcarbinyl radical being generated and undergoing ring opening (**3-27**→**3-28**) and ring closure (**3-28**→**3-29**).

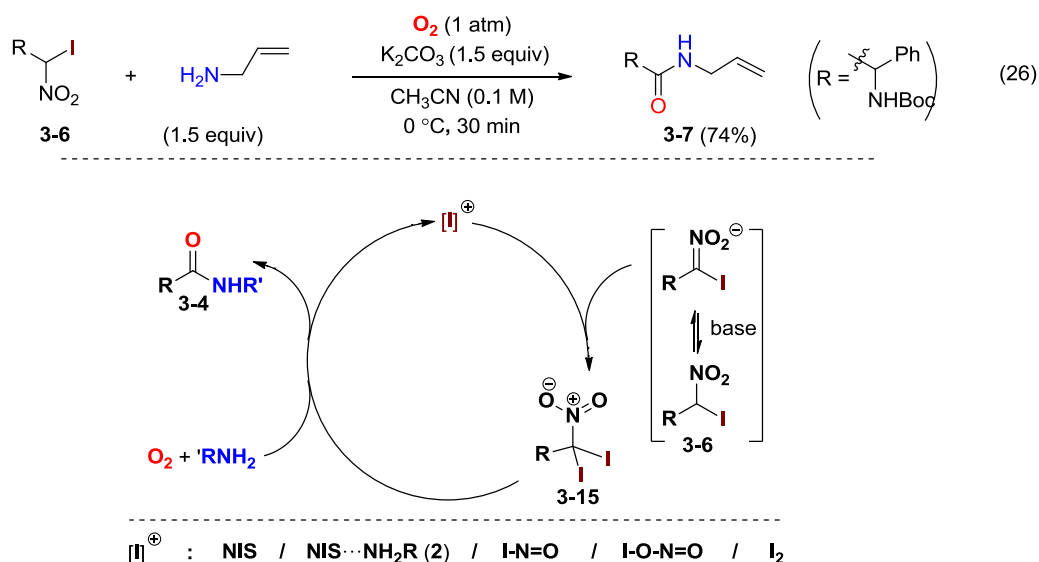


Figure 2. Generic Process to Regenerate an Iodonium Source.

Lastly, the regeneration and intermediacy of putative iodonium sources needs to be considered under our reaction conditions (Figure 2). In other words, presuming the diiodide **3-15** is the key intermediate, the oxidative amidation of the

mono-iodo nitroalkane **3-6** (in the absence of additional NIS or I₂) is expected to occur via an initial iodine transfer to its anion to afford the diiodide **3-15** and eventually regenerate an equivalent amount of an iodinating agent. Furthermore, despite observing the mono-iodonitroalkane **3-6** being oxidized to the amide **3-4** with amine and oxygen under basic conditions (Eq. 26), oxygen does not first react with the anion of **6** (Eq. 6), but more likely O₂ and amine reacts with the di-iodide **3-15** after it forms via iodine-transfer of **3-6** to its nitronate anion. Here, we suggest an extra equivalent of I₂, I⁻N=O^[7] and/or I-O-NO species is generated under our reaction conditions (Figure 2). These iodonium species can thus react under either radical or ionic reaction modes and allow the amide oxidation state of **3-4** to be achieved from mono-iodide **3-6**.

3.3 Summary of reaction mechanism

Collectively, my findings are consistent with the mechanism illustrated in Figure 3. I thus propose the primary nitroalkane **3-1** first becomes α-iodinated with NIS from the halogen bonded amine complex **3-2** to afford the mono-iodide **3-6** (Eq. 27). After further deprotonation, the α-iodo *aci*-nitronate becomes α-iodinated with another iodonium species (I⁺) to afford the di-iodide **3-15**. I propose it is this congested, tetrahedral di-iodinated nitroalkane **3-15** that can either rearrange in a homogenic, anaerobic manner to form the nitrite ester **3-16** (Eq. 28) or react with molecular oxygen to afford a peroxy radical adduct **3-17** (Eq. 29). From these intermediates onwards, several additive-eliminative pathways, under either radical or ionic reaction modes, can be proposed to afford the amide product **3-4**.

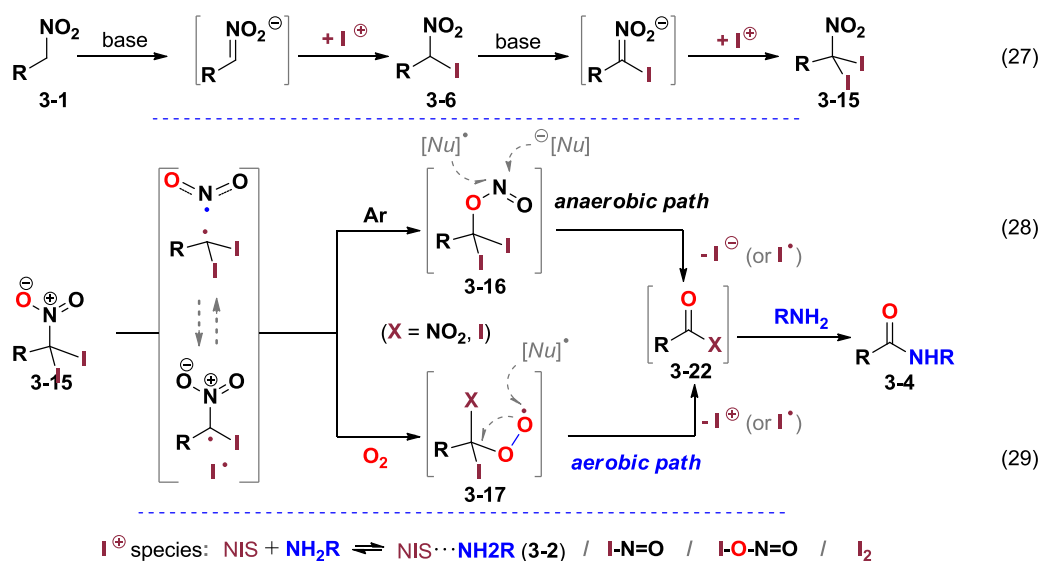


Figure 3. Proposed oxidative amidation of **3-1** via α-iodide **3-6** and diiodide **3-15**.

References and Notes

- [1] Initial discovery and mechanistic rationale of oxidative umpolung amide synthesis (UmAS): B. Shen, D. M. Makley, J. N. Johnston, *Nature* **2010**, *465*, 1027–1032; b) J. P. Shackleford, B. Shen, J. N. Johnston, *Proc. Natl. Acad. Sci. USA* **2012**, *109*, 44–46; Application of UmAS in synthesis: c) M. W. Leighty, B. Shen, J. N. Johnston, *J. Am. Chem. Soc.* **2012**, *134*, 15233–15236; d) K. E. Schwieten, J. N. Johnston, *Chem. Sci.* **2015**, *6*, 2590–2595; e) K. E. Schwieten, J. N. Johnston, *Chem. Commun.* **2016**, 52 152–155.
- [2] Presently accepted mechanism of oxidative umpolung amide synthesis (UmAS): K. E. Schwieten, B. Shen, J. P. Shackleford, M. W. Leighty, J. N. Johnston, *Org. Lett.* **2014**, *16*, 4714–4717.
- [3] J. Li, M. J. Lear, Y. Kawamoto, S. Umemiya A. Wong, E. Kwon, I. Sato, Y. Hayashi, *Angew. Chem. Int. Ed.* **2015** *44*, 12986–12990; *Angew. Chem.* **2015**, *44*, 13178–13182.
- [4] Y. Hayashi, S. Umemiya, *Angew. Chem. Int. Ed.* **2013**, *52*, 3450–3452; *Angew. Chem.* **2013**, *125*, 3534–3536.
- [5] S. Umemiya, K. Nishino, I. Sato, Y. Hayashi, *Chem. Eur. J.* **2014**, *20*, 15753–15759.
- [6] For peroxy-adduct generation from dihaloalkanes, see: a) X. Ge, K. L. M. Hoang, M. L. Leow, X.-W. Liu, *RSC Adv.* **2014**, *4*, 45191–45197; b) J. M. Beames, F. Liu, L. Lu, M. I. Lester, *J. Am. Chem. Soc.* **2012**, *134*, 20045–20048.
- [7] N. Tokitoh, R. J. Okazaki, *Bull. Chem. Soc. Jpn.*, **1987**, *60*, 3291–3297.
- [8] P. W. Atkins, T. L. Overton, J. P. Rourke, M. T. Weller, F. A. Armstrong The Group 15 Elements. In *Inorganic Chemistry*, 6th Edition, Oxford University Press, Oxford, **2014**, pp. 424.
- [9] Radical clock studies: a) E. L. Spence, G. J. Langley, T. D. H. Bugg, *J. Am. Chem. Soc.* **1996**, *118*, 8336–8343; b) T. Benkovics, J. Du, I. A. Guzei, T. P. Yoon, *J. Org. Chem.* **2009**, *74*, 5545–5552; c) J. F. Van Humbeck, S. P. Simonovich, R. R. Knowles, D. W. C. MacMillan, *J. Am. Chem. Soc.* **2010**, *132*, 10012–10014; d) E. Arceo, I. D. Jurberg, A. Alvarez-Fernandez, P. Melchiorre, *Nature Chem.* **2013**, *5*, 750–756.
- [10] H. Shimakoshi, Y. Hisaeda. *Angew. Chem. Int. Ed.* **2015**, *54*, 15439–15443.

Chapter 4. Autocatalytic Conversion of α,α -Diiodonitroalkanes into Amides and Esters by Iodide Byproducts under O_2

4.1 Introduction of autocatalytic reaction

An autocatalytic reaction is defined as a system in which a reaction product serves as a catalyst for its own production. (Figure 1a) This is a relatively rare phenomenon in synthesis and is often considered key to the chemical origins of life. The generally accepted experimental signatures of an autocatalytic process include: a) observation of an enhancement in reaction rate with one or more reaction products added to the reaction vessel, and b) observation of a temporal product concentration profile that exhibits a sigmoidal shape (Figure 1b).^[1]

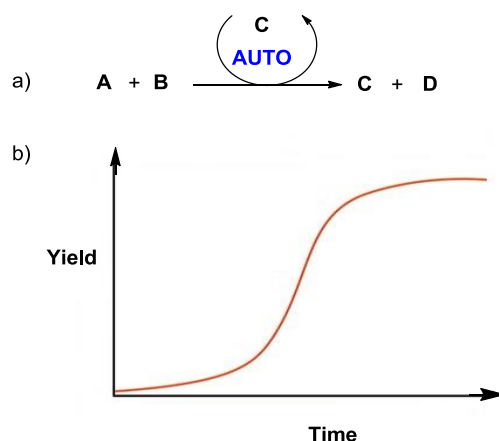
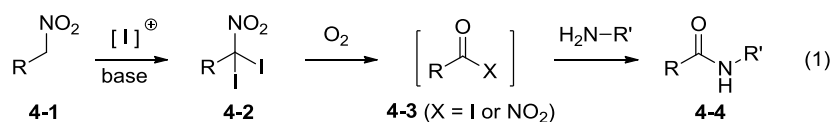


Figure 1. Autocatalytic reaction: a) Catalytic model; b) Kinetic profile.

4.2 Unexpected sigmoidal kinetic profile in the reaction of α,α -diiodonitroalkane and MeOH /amine

In chapter 3, we studied the mechanism of the direct conversion of primary nitroalkanes into amides in the presence of O_2 , I_2 or NIS, and nucleophilic amines (Figure 2). The key intermediate was identified to be the labile, doubly α -iodinated derivative **4-2** of the nitroalkane **4-1** [Eq. 1]. We proposed the amide product **4-4** is generated by nucleophilic amine attack on an activated acyl intermediate **4-3**, as derived by addition of O_2 onto **4-2** through homolytic cleavage of a C–I or C– NO_2 bond.^[2b] Clearly the activated ester **4-3** can also react with other nucleophiles, such as alcohols to form esters. If made synthetically useful under mild conditions, for example, with less nucleophilic amines or alcohols, such a development would help advance the transformation of nitroalkanes into other useful functionalities.^[2]



Scheme 1. Mechanism of amide **4-4** formation from primary nitroalkane **4-1**.

At first we compared the reactivity of differing amines and alcohols with **4-2** under established conditions (Chapter 3) in a qualitative manner (Eq. 2). Here, we anticipated that methanol in excess would display a similar reaction rate to one equivalent of a primary amine due to the high reactivity of **4-3** (Eq. 1) and relative nucleophilicities. The isolated α,α -diiodonitroalkane **4-2a** (X-ray structure of **4-2a** in Figure 3), however, showed a significantly higher reactivity with amines than with methanol. Eventually, we settled on studying the weaker nucleophiles 2,2,2-trifluoroethylamine and methanol at room temperature by quantitative ^1H NMR analysis, and also examined the reaction of **4-2a** with benzylamine at room temperature and at -10°C (Figure 2).

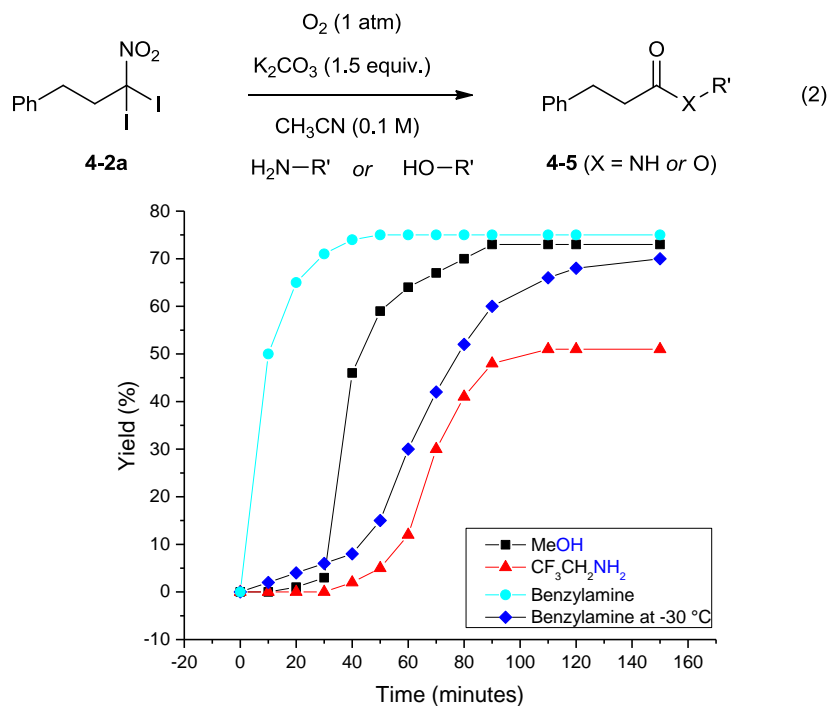


Figure 2. ^1H NMR reaction profiles of α,α -diiodonitroalkane **4-2a** with MeOH (5 equiv.) or amine (1.5 equiv.)

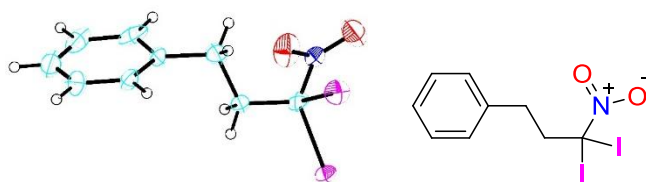


Figure 3. ORTEP X-Ray Structure of α,α -diiodonitroalkane **4-2a** with thermal ellipsoids drawn at the 50 % probability level.

Most strikingly, the reactions from **4-2a** to **5** (Eq. 2) with relatively weak nucleophiles (CH_3OH , $\text{CF}_3\text{CH}_2\text{NH}_2$) displayed clear sigmoidal kinetic profiles at room temperature on the NMR timescale (Figure 2, red and black curves). In contrast, the initial reaction between **4-2a** and benzylamine proceeded exponentially with no slow induction period at room temperature, whereas an uncommon sigmoidal profile was observed at $-10\text{ }^\circ\text{C}$ (Figure 2, cyan and blue curves). Several mechanistic reasons can be attributed to cause these sigmoidal kinetic profiles; for example, a product, intermediate or byproduct of the reaction accelerating a rate-determine step in an autoinductive or autocatalytic fashion.^[7] We thus decided to study the oxidative conversion of the α,α -diiodonitroalkane **4-2a** to the carboxylic derivatives **4-6/4-7** and quantify the kinetic effects of adding each identifiable reaction product at 20 mol% by ^1H NMR (Eq. 3, Figure 4a).

4.3 To prove α,α -diiodonitroalkane **4-2a** reacting with amine and alcohol is an autocatalytic reaction

In the first instance without any additives, the methyl ester **4-6** and carboxylic acid **4-7** were isolated in 75% and 25% yields, respectively, and characterized by ^1H NMR (Eq. 3). This reaction under standard conditions also produced nitrite salts (KNO_2) and I_2 crystals as byproducts, as detected by ion chromatography and observed after solvent removal. Next, we monitored the effect of adding each reaction product at the start of the reaction, including the ester **4-6**, carboxylate **4-7**, nitrite, and hydrogen carbonate salts (Figure 4a). All these cases displayed sigmoidal kinetic profiles similar to the reaction with no additives, although small variations in initial induction times were observed.

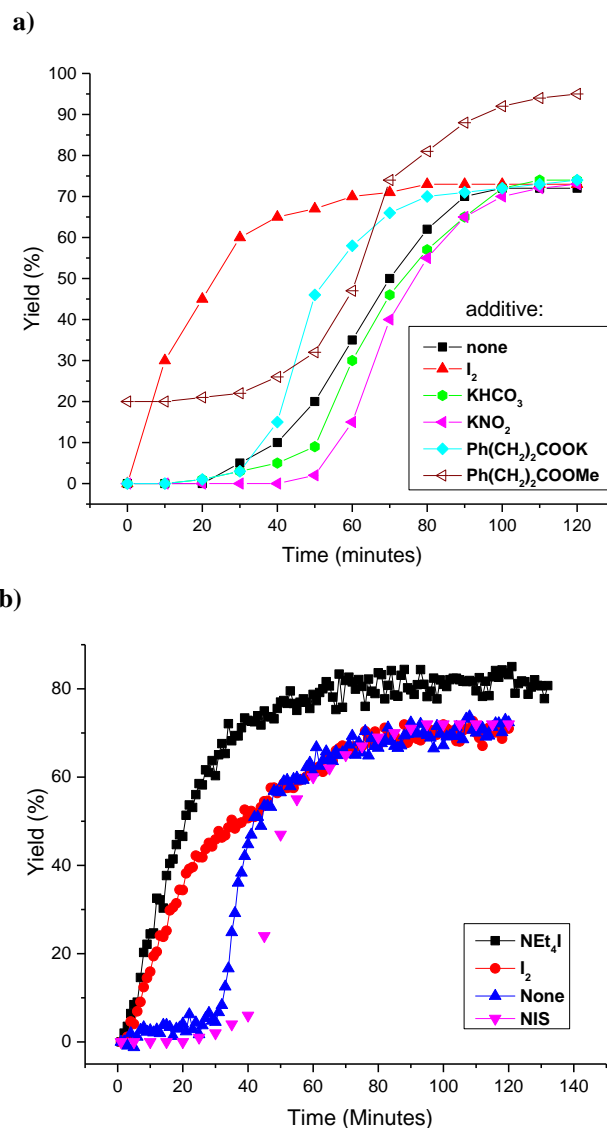
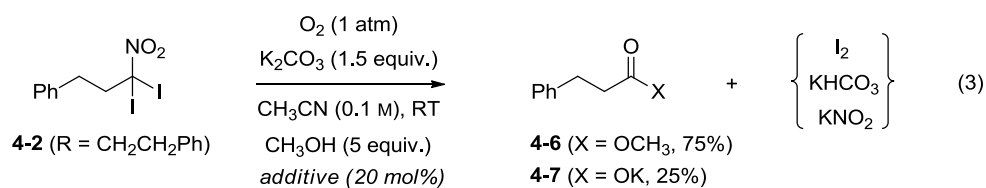


Figure 4. ¹H NMR reaction profiles of α,α-diiodonitroalkane **4-2a** with MeOH (5 equiv.) **a)** ¹H NMR analysis with various reaction product additives (20 mol%); **b)** React-FT-IR analysis with various iodine sources (20 mol%).

Eventually, I₂ was selected as an additive to the reaction [Eq. 3]. This gave a dramatic improvement in the initial reaction rate, similar to conventional pseudo-first-order kinetic profiles (Figure 4b, red curve). Here, the addition of I₂ gave a sustained purple-red color throughout the course of the reaction. In comparison, without pre-adding I₂, the reaction turned from yellow to a similar purple-red colour after 30 minutes, at which time the rapid formation of the ester product was clearly observed. (cf. Figure 4b, red and black curves). The effect of I₂ was therefore studied in more detail by monitoring the in-situ consumption of the α,α-diiodonitroalkane **4-2a** and the in-situ formation of ester **4-6** by React-IR (Figure 4b). Again, we followed the standard reaction without any additive [Eq. 3] and, although the IR-data were consistent with our initial ¹H NMR analysis, the 0–30 min induction periods were much better resolved (cf. Figure 4a, black curve; Figure 4b,

blue curve). Addition of I_2 also gave a similar conventional kinetic profile to our 1H NMR analysis, which produced the desired ester **4-4-4-6** within 80 min (cf. Figure 4a and 4b, red curves).

Since I_2 can act as a dual source of cationic iodonium (I^+) and anionic iodide (I_3^- or I^-) species in solution,^[3] we performed separate reactions by adding 20 mol% of NIS as an I^+ source and 20 mol% of NEt_4I as an I^- source. While NIS demonstrated a slight retardation on the initial reaction rate (cf. Figure 4b, purple and blue curves), NEt_4I dramatically accelerated the induction period and the overall reaction rate (Figure 4b, blue curve). Furthermore, a similar iodide-mediated acceleration effect was observed in the case of $CF_3CH_2NH_2$ reacting with **4-2a** to form the amide **4-5a**. (Figure 5) Collectively, these data support iodide byproducts (I^-) to be the principal species which catalyse the oxidative conversion of the diiodide **4-2** to the ester **4-6**.

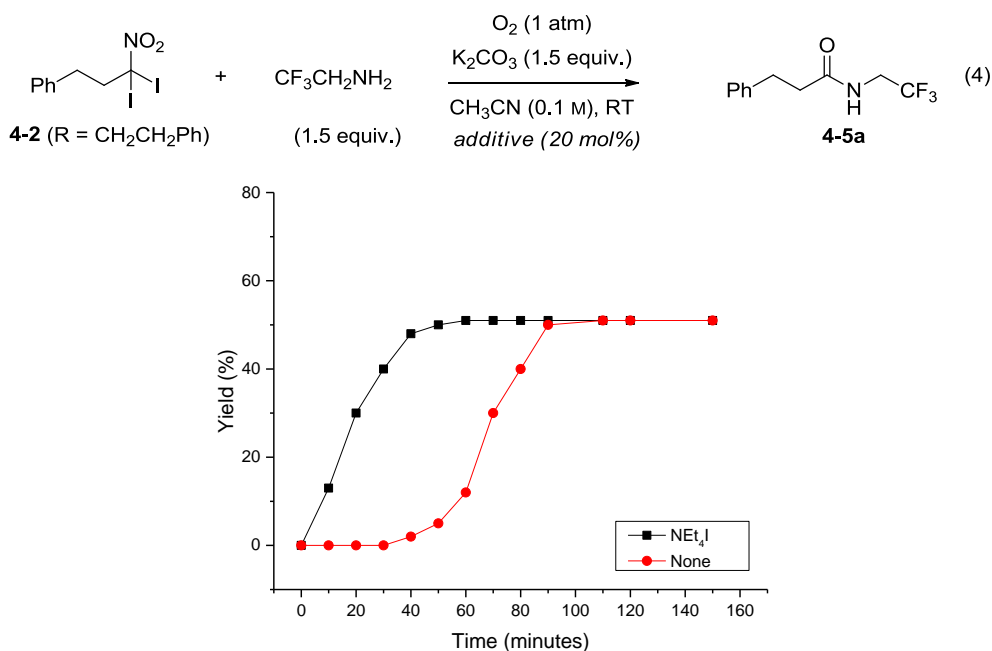
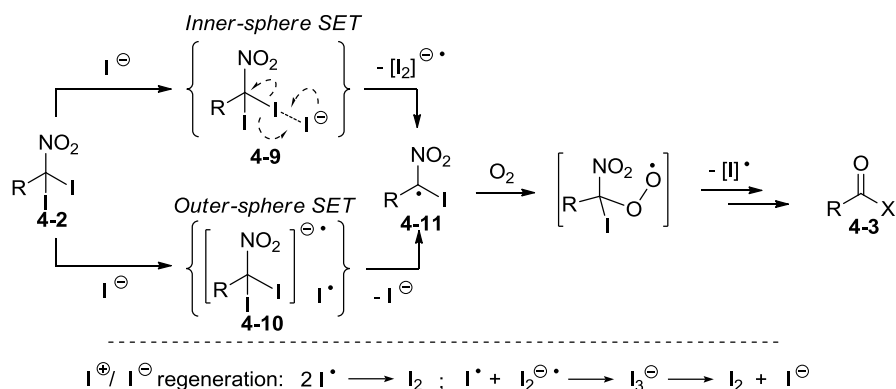


Figure 5. 1H NMR reaction profiles of α,α -diiodonitroalkane **4-2a** with $CF_3CH_2NH_2$ (1.5 equiv.) with or without NEt_4I .

The mechanistic implications of these findings are thought provoking, especially when we take related studies (chapter 3) into account. Our current interpretation for the α,α -diiodo-nitroalkane **4-2** is presented in Scheme 1. From our previous mechanistic studies, we consider the direct addition of O_2 to an α -iodo *aci*-nitronate derived from the α,α -diiodonitroalkane **4-2** to be unlikely. Such anionic intermediates of **4-2** can conceivably be formed by attack of an iodide anion or another nucleophile onto the α -iodine of **4-2**. Here, we propose two alternative single-electron transfer (SET) pathways to proceed from **4-2** by the action of iodide anions to generate the carbon radical **4-11**, either in an inner-sphere or outer-sphere sense (Scheme 2). We thus consider the highly electron deficient α,α -diiodonitroalkane **4-2** to be a good electron acceptor^[4] and I^- to be a good electron donor.^[5,6] For the inner-sphere pathway, an iodine-bridged halogen bonded^[7] complex **4-9** is proposed to form, after which **4-9** undergoes SET-induced homolytic fragmentation to give a diiodide radical anion ($I_2^{\cdot-}$) and the carbon radical **4-11**.^[4] The $I_2^{\cdot-}$ byproduct can then couple with a liberated mono-iodine radical (I^{\cdot}) to generate I_3^- as a known source of I_2 and I^- .^[8] For the outer-sphere pathway, we propose I^- to react directly with the α,α -diiodonitroalkane electron-acceptor **4-2** via SET to give a mono-iodine radical (I^{\cdot}) and the radical anion **4-10**. This activated form of **4-2** can then fragment to a mono-iodide anion (I^-) and the carbon radical **4-11**, which can then be trapped with O_2 .^[9] In this case, the homogenic coupling of I^{\cdot} gives I_2 . Although the contributions of the two SET pathways to form the carbon radical **4-11** are not certain, we have previously evidenced the formation of **4-11** through radical clock experiments in chapter 3. In either case, cationic iodine species (I_2) and anionic iodide species (I^-) are proposed to be regenerated.



Scheme 2. Proposed autocatalytic role of iodide byproduct (I^-) with α, α -diiodonitroalkanes **4-2**, by either inner or outer single-electron transfer (SET) events, and proposed regeneration of diiodine (I_2) and mono-iodide (I^-).

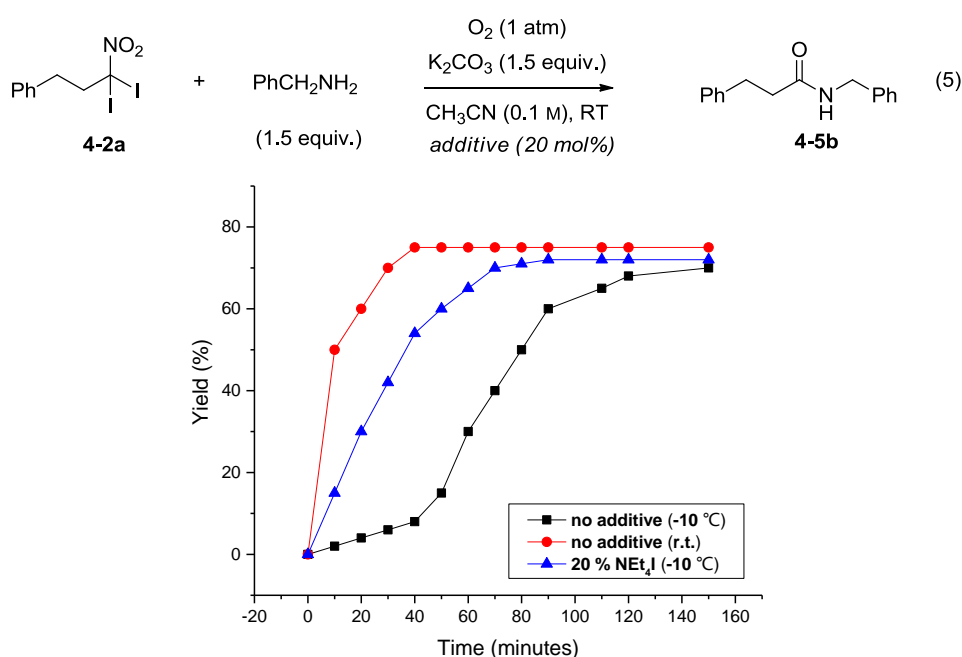


Figure 6. ^1H NMR reaction profiles of α, α -diiodonitroalkane **4-2a** with benzylamine (1.5 equiv.)

On the basis of the mechanism proposed in Scheme 1, the differing kinetic profiles of benzylamine at room temperature and $-10\text{ }^\circ\text{C}$ needed some further clarification. (cf. Figure 6, red and black curves) Indeed, the addition of 20 mol% of NEt_4I for the reaction at $-10\text{ }^\circ\text{C}$ exhibited a conventional kinetic profile with no induction period. (Figure 6, blue curve) Without iodide additives at room temperature, further ^1H NMR experiments showed that benzylamine quickly reacts with **4-2a** to generate a mono α -iodinated derivative of **4-2a** (cf. Figure 7, blue and purple curves) and plausibly iodobenzylamine. This iodobenzylamine can further transform to imine, which is evidenced by benzaldehyde being isolated after work up. At $-10\text{ }^\circ\text{C}$, in spite of a halogen bonded amine complex being observed, deiodinated **4-2a** and benzaldehyde were not detected. These results suggest that **4-2a** can transfer an iodine to the amino group of benzylamine at room temperature, which presumably results in imine formation and the release of iodide catalyst. However, under unfavorable conditions with a weak nucleophile, the α, α -diiodonitroalkane **4-2a** would slowly dissociate into the carbon radical **4-11**. Once intermediate **4-11** reacts with O_2 to form acyl products **4-3**, iodide anions can be generated and the reaction can proceed autocatalytically as proposed in Scheme 2. Reactions with methanol at room temperature or benzylamine at $-10\text{ }^\circ\text{C}$ thus necessitate the

gradual generation of iodide anions in sufficient concentrations to autocatalyse the generation of **4-11** from the key intermediate **4-2a**, which is reflected in their kinetic profiles (cf. Figures 2 and 4).

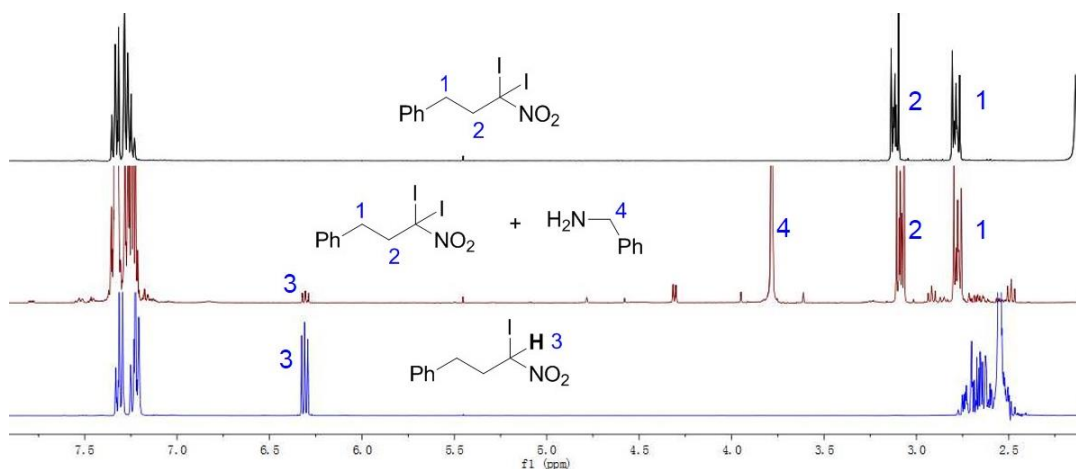


Figure 7. ^1H NMR study of α,α -diiodonitroalkane **4-2a** with benzylamine (1.5 equiv.) at r.t.

4.4 Optimization reaction condition for ester formation

On the mechanistic basis of iodide-mediated autocatalysis, we thus decided to explore the oxidative esterification between primary nitroalkanes and primary alcohols with a slight excess of I_2 (1.2 equiv.) under a variety of basic conditions (Table 1). Here, the premise was that the iodide anions, generated during the formation of the known mono α -iodinated nitroalkane and α,α -diiodonitroalkane **4-2** intermediates, would persist in at least 20 mol% through all stages of the reaction and thereby ensure the esterification process proceeds rapidly. Thus I_2 was chosen to act as a dual source of iodonium cations to not only form **4-2**, but also to form iodide anions that facilitate the homolytic cleavage of **4-2** into O_2 -reactive radical species **4-11** (Scheme 2). Compared to conventional methods, which first convert primary nitroalkanes to carboxylic acids before ester formation,^[10] our aim was to develop a one-pot procedure to make more challenging, sterically hindered esters in a direct way via in-situ formed α,α -diiodonitroalkane intermediates **4-2**.

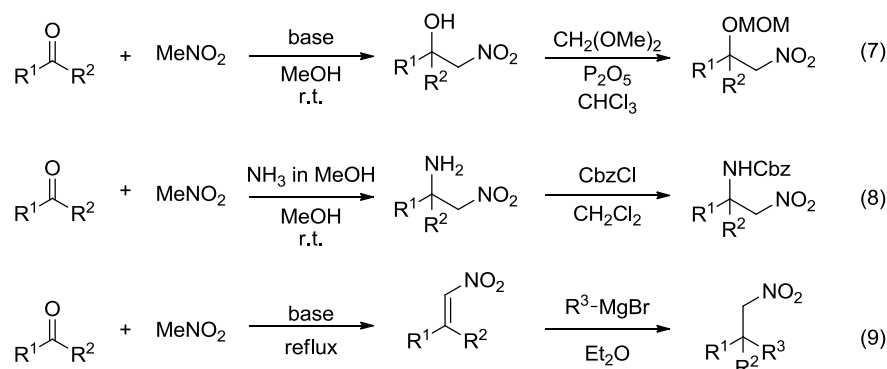
Table 1. Optimization of Oxidative Esterification Process.^[a]

$ \begin{array}{c} \text{Me} \quad \text{NH} \text{Boc} \\ \diagdown \quad \diagup \\ \text{C} \\ \diagup \quad \diagdown \\ \text{Me} \quad \text{CH}_2 \quad \text{NO}_2 \end{array} + \text{MeOH} \xrightarrow[\text{base (2 or 3 equiv)}]{\text{O}_2 (1 \text{ atm}), \text{I}_2 (1.2 \text{ equiv})} \begin{array}{c} \text{Me} \quad \text{NH} \text{Boc} \\ \diagdown \quad \diagup \\ \text{C} \\ \diagup \quad \diagdown \\ \text{Me} \quad \text{C} = \text{O} \\ \quad \quad \quad \text{OMe} \end{array} $ <p style="text-align: center;">(6)</p> <p style="text-align: center;">4-12a 4-13a</p> <p style="text-align: center;">(5 equiv) solvent, RT</p>				
Entry	Base	Solvent	Time [h]	Yield [%]
1	K_2CO_3	CH_3CN	24h	trace
2	K_2CO_3	THF	24 h	trace
3	K_2CO_3	CH_2Cl_2	24 h	trace
4 ^b	K_2CO_3	MeOH	6 h	70
5 ^b	Li_2CO_3	MeOH	6 h	60
6 ^b	Na_2CO_3	MeOH	12h	50
7 ^b	Cs_2CO_3	MeOH	1h	20
8 ^b	NaOMe	MeOH	1h	40

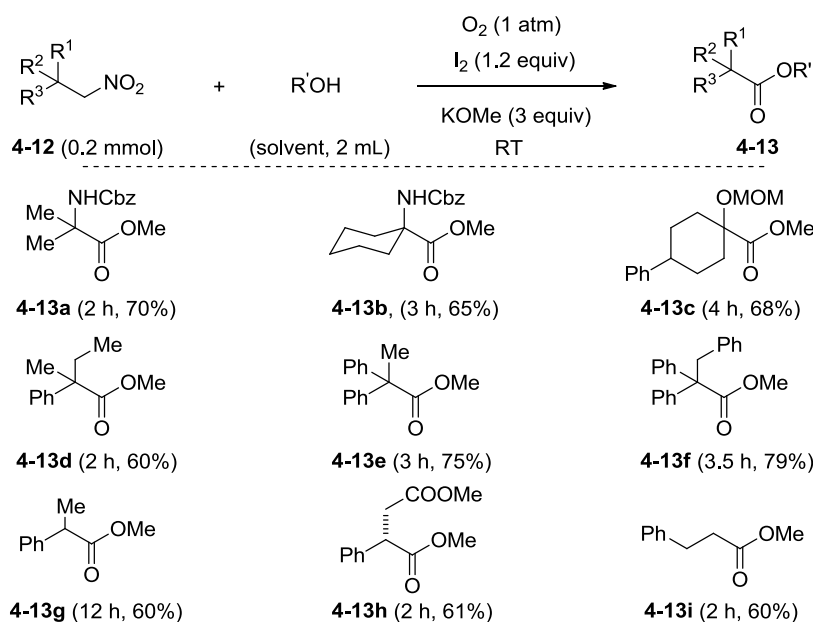
9 ^b	KOMe	MeOH	1h	60
10 ^{b,c}	KOMe	MeOH	1h	70

[a] Reactions were conducted with nitroalkane **4-12a** (0.2 mmol), MeOH (1.0 mmol), base (0.4 mmol) under O₂ atmosphere in CH₃CN (2 mL); [b] MeOH (2 mL) was used as the solvent; [c] KOMe (3 equiv) was used.

As a model system, we selected the readily prepared *N*-protected 1,1-dimethyl-2-nitroethanamine **4-12a** and methanol for optimization to form the sterically hindered methyl ester **4-13a** (Table 1, Eq. 6). From our previous procedures in Chapter 2, K₂CO₃ was first selected as a suitable base in solvents of CH₃CN, THF or CH₂Cl₂. These reactions were found to be very slow due to the low solubility of K₂CO₃ limiting the formation of α-iodo nitroalkane intermediates (entries 1–3). Carbonate bases in MeOH as the solvent improved the overall reaction rate and yields (entries 4–7). Eventually, KOMe was demonstrated to be a superior choice to NaOMe (cf. entries 8 and 9), especially when used in 3 equivalents (entry 10).



Scheme 3. Synthesis of hindered primary nitroalkanes.



Scheme 4. Oxidative esterification of readily prepared primary nitroalkanes into sterically congested methyl or ethyl esters.

The hindered primary nitroalkanes were readily prepared by the addition of nitromethane to ketones (Eq. 7) or to imines (Eq. 8), or by the conjugate addition of a Grignard reagent to β,β-disubstituted nitroalkenes (Eq. 9). With optimized conditions in hand (Table 1, entry 10), the substrate scope was screened with hindered primary nitroalkanes **4-12**. (Scheme 4) Notably, the α-hydroxy, α-alkyl, α-benzyl or α-phenyl functionalized α,α,α-trisubstituted methyl esters **4-13a–13f** all formed in good yields in a direct and rapid manner. (Scheme 4) Although an increase in the bulkiness of the β-position of

the starting nitroalkane gave slightly longer reaction times, the chemical yields remained good (cf. **4-13d-f**). In addition, α -chiral substituted chiral esters such as **4-13h** also can be prepared in good yield.

4.5 Conclusion

During the mechanistic investigation of the I_2/O_2 -based conversion of primary nitroalkanes to amides and esters via recently identified α,α -diiodonitroalkanes **4-2**, I observed unusual sigmoidal reaction profiles with relatively weak amine and alcohol nucleophiles through quantitative 1H NMR and React-IR studies (Figure 1). Systematic addition of sub-stoichiometric amounts of potential products derived from **4-2** (Eq. 3) clearly identified mono-iodide byproducts to accelerate the reaction. Due to the regeneration of iodide anions, we thus propose a rare case of autocatalysis, whereby the iodide-mediated formation of O_2 -reactive carbon radicals **4-11** from **4-2** can occur through inner or outer sphere single-electron transfer (SET) events (Scheme 1). Under this mechanistic framework, I developed a convenient one-pot oxidative transformation of readily prepared β,β,β -trisubstituted nitroalkanes into sterically encumbered α,α,α -trisubstituted esters, which are difficult to access by conventional methods.

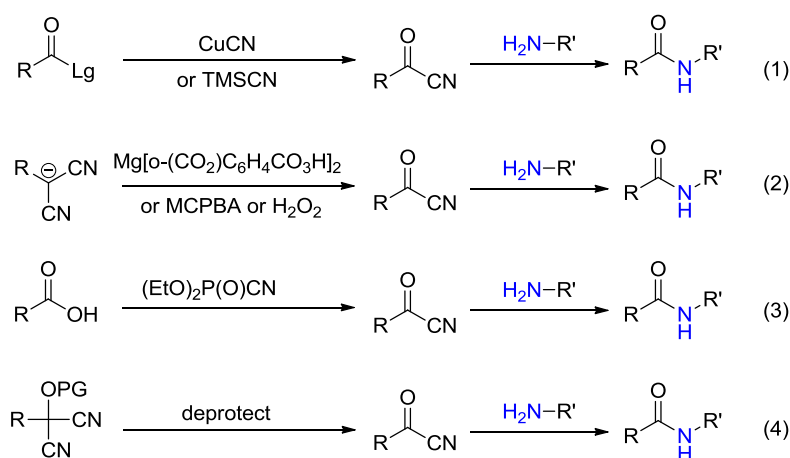
References and Notes

- [1] a) D. G. Blackmond, *Angew. Chem. Int. Ed.* **2005**, *44*, 4302; b) D. G. Blackmond, *J. Am. Chem. Soc.* **2015**, *137*, 10852–10866; c) G.-J. Cheng, X. Zhang, L. W. Chung, L. Xu, Y.-D. Wu *J. Am. Chem. Soc.*, **2015**, *137*, 1706–1725.
- [2] Classical and emerging uses of readily available nitroalkanes in synthesis: a) D. Seebach, E. W. Colvin, F. Lehr, T. Weller, *Chimia* **1979**, *33*, 1; b) A. G. M. Barrett, D. Dhanak, G. G. Graboski, S. J. Taylor, *Organic Synthesis* **1990**, 68, 8; c) *Nitro Compounds—Recent Advances in Synthesis and Chemistry: Organic Nitro Chemistry Series* (Eds.: H. Feuer, A. T. Nielsen), VCH, Weinheim, **1990**; d) N. Ono, *The Nitro Group in Organic Synthesis*, Wiley-VCH, New York, **2001**; e) R. Ballini, M. Petrini, *Tetrahedron*, **2004**, *60*, 1017–1047; f) M. W. Leighty, B. Shen, J. N. Johnston, *J. Am. Chem. Soc.* **2012**, *134*, 15233–15236; g) K. E. Schwietzer, J. N. Johnston, *Chem. Sci.* **2015**, *6*, 2590–2595; h) R. Ballini, M. Petrini, *Adv. Synth. Catal.* **2015**, *357*, 2371–2402; i) K. E. Schwietzer, J. N. Johnston, *Chem. Commun.* **2016**, 52 152–155.
- [3] D. M. Stanbury, *Adv. Inorg. Chem.* **1989**, *33*, 69–138.
- [4] L. Li, W. B. Liu, H. Y. Zeng, X. Y. Mu, G. Cosa, Z. T. Mi, C.-J. Li, *J. Am. Chem. Soc.* **2015**, *137*, 8328–8331.
- [5] For iodide salt catalysed C–I bond cleavage in polymer synthesis, see: A. Goto, A. Ohtsuki, H. Ohfuji, M. Tanishima, H. Kaji, *J. Am. Chem. Soc.* **2013**, *135*, 11131–11139.
- [6] Due to single-electron transfer (SET) events principally occurring over short distances, a two-electron donor-acceptor pre-complexation event is proposed to precede an SET event: N. Zhang, S. R. Samanta, B. M. Rosen, V. Percec, *Chem. Rev.* **2014**, *114*, 5848–5958.
- [7] Halogen bonding of C–I bonds by Lewis bases, although being well characterized non-bonding interactions in solid-state and supramolecular chemistry, are attracting increasing attention and importance in solution-based chemical synthesis: a) A. V. Jentzsch, *Pure Appl. Chem.* **2015**, *87*, 15–41; b) H. Takezawa, T. Murase, G. Resnati, P. Metrangolo, M. Fujita, *Angew. Chem. Int. Ed.* **2015**, *54*, 8411–8414; *Angew. Chem.* **2015**, *127*, 8531–8534; c) M. S. Taylor, *Nat. Chem.* **2014**, *6*, 1029–1031; d) T. M. Beale, M. G. Chudzinski, M. G. Sarwar, M. S. Taylor, *Chem. Soc. Rev.* **2013**, *42*, 1667–1680; e) M. Erdélyi, *Chem. Soc. Rev.* **2012**, *41*, 3547–3557; f) S. E. Denmark, W. E. Kuester, M. T. Burk, *Angew. Chem. Int. Ed.* **2012**, *51*, 10938–10953.
- [8] Gardner, J. M.; Abrahamsson, M.; Farnum, B. H.; Meyer, G. J. *J. Am. Chem. Soc.* **2009**, *131*, 16206–16214.
- [9] a) X. Ge, K. L. M. Hoang, M. L. Leow, X.-W. Liu, *RSC Adv.* **2014**, *4*, 45191–45197; b) J. M. Beames, F. Liu, L. Lu, M. I. Lester, *J. Am. Chem. Soc.* **2012**, *134*, 20045–20048.
- [10] a) N. Kornblum, P. A. Wade, *J. Org. Chem.* **1973**, *38*, 1418–1420; b) C. Matt, A. Wagner, C. Mioskowski, *J. Org. Chem.* **1997**, *62*, 234–235.
- [11] Y. Hayashi, Y. Kawamoto, M. Honada, D. Okamura, S. Umemiya, Y. Noguchi, T. Mukaiyama, I. Sato. *Chem. Eur. J.*, **2014**, *38*, 12072–12082.

Chapter 5. Sterically Demanding Oxidative Amidation of α -Substituted Malononitriles with Amines using O_2

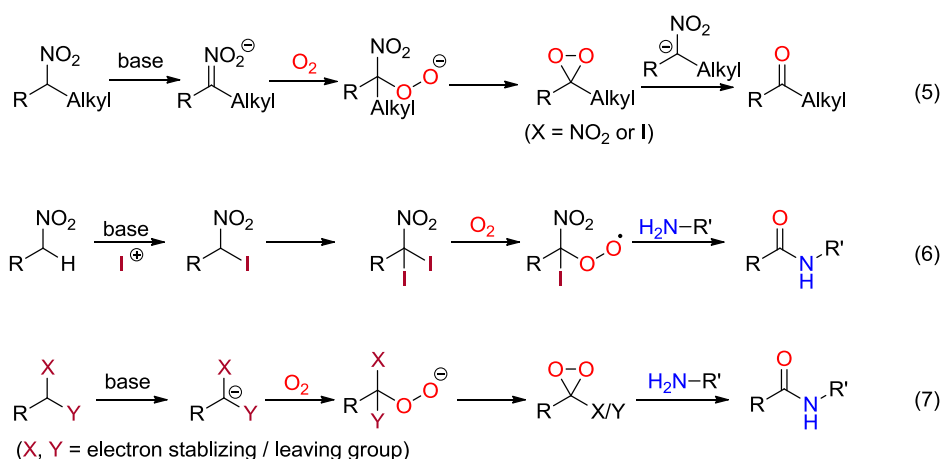
5.1 Introduction

Acyl cyanides are useful synthetic intermediates in organic synthesis as they can be utilized in a variety of transformations. Especially, acyl cyanides serve as highly reactive activated esters during amide and peptide syntheses.^[1] In previous reports, acyl cyanides can be synthesized by cyanation of acyl chlorides using CuCN/TMSCN (Eq.1)^[2] or by the oxidation of malononitriles using strong oxidative reagents by various reported methods (Eq. 2)^[3] and further reacted with amines to form amides. In addition, activating carboxylic acids with traditional reagents (e.g. with phosphorocyanidates) generates acyl cyanides (Eq. 3)^[4] and pre-oxidized hydroxyl malononitriles as masked acyl cyanides (MAC) (Eq.4)^[5] are also used in amide and peptide methods.



Scheme 1. Acyl cyanide serves as an active ester precursor in amide synthesis.

5.2 Initial design for this work



Scheme 2. Mechanistic rationales for oxidative amidation.

The stimulus for this new work to make amides began during the discovery and development of the base-promoted Nef oxidation of nitroalkenes or nitroalkanes to form their ketones with oxygen by our group (Eq. 5). During the further development of a direct halogenative method to form amides under aerobic conditions in Chapter 3, we isolated α,α -diiodinated nitroalkanes (Eq. 6) and recognized the mechanistic need to make intermediates that bear two electron-

stabilizing groups X and Y (Eq. 7). These substituents can thus not only stabilize transient radicals and anions, but also act as one-electron or two-electron leaving groups. We thus proposed to explore an oxidative amidation sequence via putative dioxirane intermediates, which can act as sources of electrophilic mono-oxygen and transform into reactive acyl derivatives to form amide bonds in a new powerful way.

5.3 Screening leaving groups

First, we explored $-\text{NO}_2$ ^[6], $-\text{CN}$ ^[7], $-\text{SO}_2\text{R}$ ^[8] and $-\text{PO}(\text{OR})_2$ ^[9] as suitable X/Y groups for the proposed oxidative amidation sequence (Eq. 7). These studies are summarized in Table 1 (Eq. 8). Under our established oxidative conditions from Chapter 2,^[10c] reactions of α -sulfonyl or α -chloro substituted nitroalkanes **5-1** with allylamine **5-2** produced no amide product **5-3** at all (entries 1–2). Suspecting the need for alternative electron withdrawing groups to facilitate single electron transfer (SET) mechanisms with O_2 ,^[5b] we prepared and explored various α -substituted nitrile derivatives (**1**, X = CN). To our delight, when the 1,1-dicyanide **5-1** (X, Y = CN) was exposed to the amine **5-2** in the presence of K_2CO_3 under O_2 , the desired amide was generated in 96% chemical yield within 3.5 h at room temperature (entry 3). Further studies revealed the cooperative nature of $-\text{CN}$ and $-\text{SO}_2\text{Ph}$ groups in **5-1**, which gave a 70% yield of **5-3**, albeit over three days (entry 4). Otherwise, only trace amounts of the amide **5-3** were observed (entries 5–7).

Table 1. Screening of functionality for oxidative amide formation.^[a]

(8)

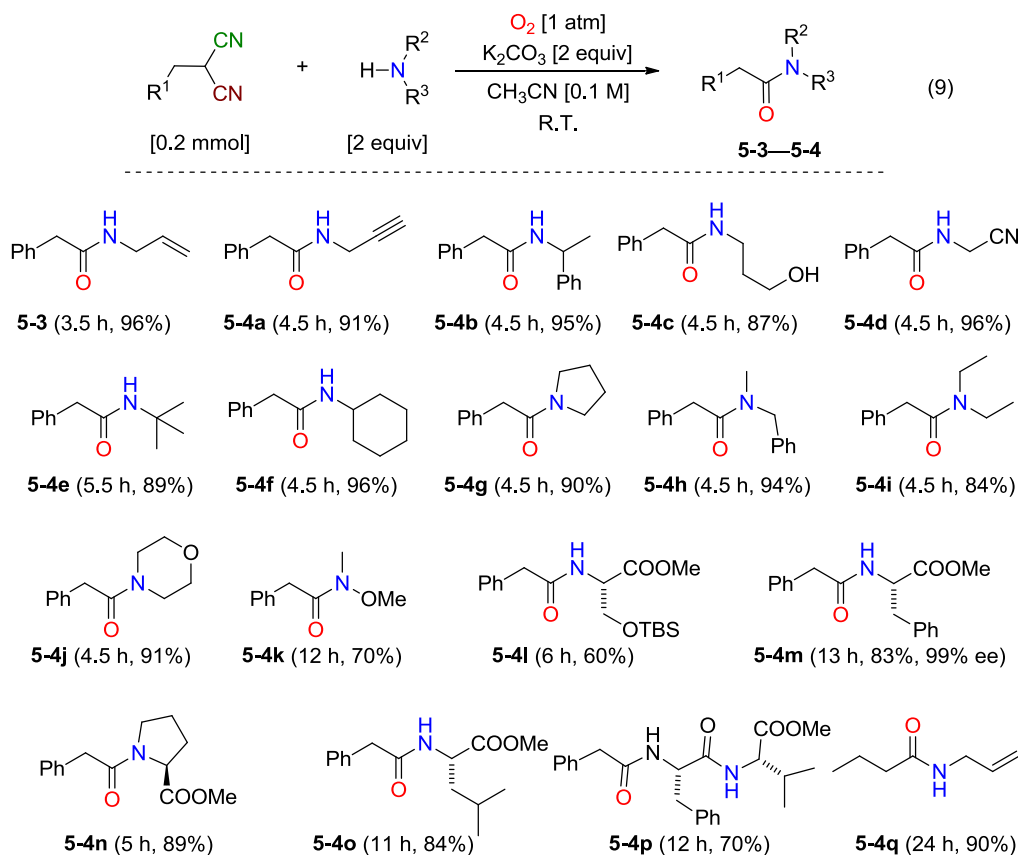
Entry	X	Y	Time [h]	Yield [%]
1	NO ₂	SO ₂ Ph	12	< 5
2	NO ₂	Cl	12	< 5
3	CN	CN	3.5	96
4	CN	SO ₂ Ph	90	70
5	CN	PO(OEt) ₂	60	< 5
6	CN	COOMe	60	< 5
7	CN	OTs	24	< 5

[a] Reactions were conducted with **5-1** (0.2 mmol), allyl amine **5-2** (0.4 mmol) and K_2CO_3 (0.4 mmol) at room temperature under O_2 (1 atm).

5.4 Substrate scope for amide synthesis

With appropriate functionality and initial conditions in place for the 1,1-dicyanide **5-1** (X, Y = CN), the scope of the oxidative amidation method was investigated by changing the amine component (Scheme 3). Common functional groups, such as allyl, propargyl and benzyl amines, displayed high reactivity to amide formation (**5-3**, **5-4a/b**). The unprotected hydroxyl amine generated the corresponding amide **5-4c** chemoselectively in 87% yield and the electron deficient 2-aminoacetonitrile gave the desired amide in 96% yield (**5-4d**). Amines with increasing steric hindrance, including *t*-butylamine, cyclohexylamine, pyrrolidine, *N*-methyl-benzylamine and diethylamine, all gave the desired amides in greater than 80% yield (**5-4e–5-4j**). The conditions were also found suitable for Weinreb amide formation (**5-4k**). Notably, coupling of **5-1** with amino acid methyl esters or an amine-free dipeptide generated the corresponding amides and peptides

in 70–84% isolated yields (**5-4–5-4p**) without epimerization. Moreover, 2-propylmalononitrile reacts with allyl amine to give the desired amide **5-4q** in 90% yield.

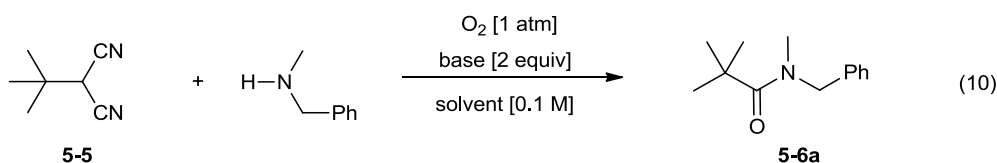


Scheme 3. Oxidative amidation of unhindered α -alkylated malononitriles.

5.5 Optimization for sterically hindered amide synthesis

Next, our aim was to apply this oxidative method to make more challenging amides. As a model system, we selected the α -*tert*-butyl malononitrile **5-5** and *N*-methylbenzylamine for optimization to the sterically hindered amide **5-6a** (Table 2, Eq. 10). The reaction was very slow when K_2CO_3 was used as base, even at 50 °C (entry 1). Changing the solvent from acetonitrile to THF or DMF, for example, gave no product at all (entry 2). Eventually, Cs_2CO_3 was demonstrated to be superior to bases like K_2CO_3 , KOAc, and K_3PO_4 , as well as to stronger bases like $KOtBu$ and $CsOH$ (entries 3–7). Increasing the temperature to 50 °C slightly improved the reaction speed and gave a higher yield of 20% (cf. entries 7 and 8). During these optimization studies (entries 1–8), the major side product was identified as the corresponding carboxylic acid, presumably derived from **5** reacting with residual water. Therefore, strictly anhydrous conditions were adopted and pre-dried 4Å molecular sieves and Cs_2CO_3 dramatically improved the yield. (60%; entry 9) Finally, for sterically demanding systems, it was optimal to adopt two equivalents of the *N*-methylbenzylamine. This gave the amide **5-6a** in 70% yield (entry 10).

Table 2. Oxidative amidation study to form a sterically hindered amide.^[a]

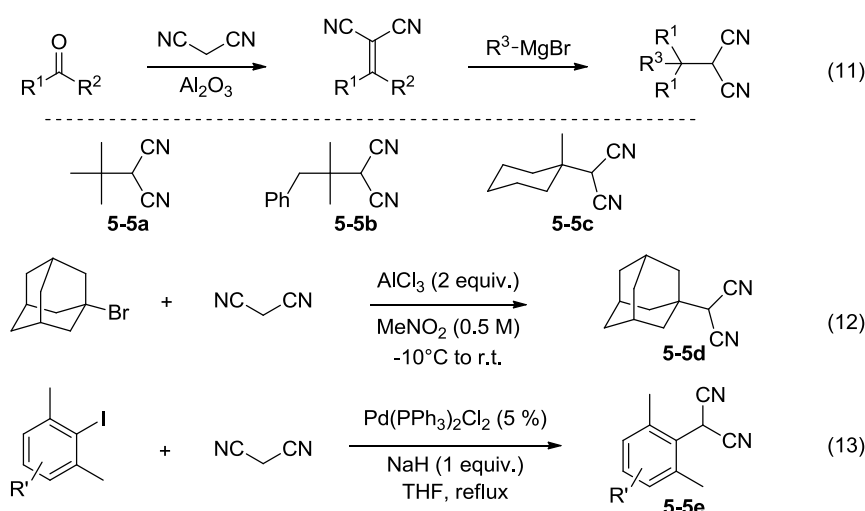


Entry	Base	Solvent	Conditions	4Å MS	Yield [%]
1	K ₂ CO ₃	CH ₃ CN	rt, 24 h; or	-	15
			50 °C, 12 h	-	15
2	K ₂ CO ₃	THF or DMF	rt, 24 h	-	< 5%
3	KOAc	CH ₃ CN	rt, 24 h	-	< 5%
4	K ₃ PO ₄	CH ₃ CN	rt, 24 h	-	< 5%
5	KO ^t Bu	CH ₃ CN	rt, 24 h	-	< 5%
6	CsOH	CH ₃ CN	rt, 24 h	-	< 5%
7	Cs ₂ CO ₃	CH ₃ CN	rt, 24 h	-	15
8	Cs ₂ CO ₃	CH ₃ CN	50 °C, 12 h	-	20
9 ^[b]	Cs ₂ CO ₃	CH ₃ CN	50 °C, 12 h	100 mg	60
10 ^[b,c]	Cs ₂ CO ₃	CH ₃ CN	50 °C, 12 h	100 mg	70

[a] Reactions were conducted with malononitrile **5-5** (0.2 mmol), *N*-methylbenzylamine (0.2 mmol), base (0.4 mmol) under O₂ atmosphere; [b] Cs₂CO₃ and 4Å MS were flame dried under vacuum and saturated with O₂ before use; [c] *N*-methylbenzylamine (0.4 mmol) was used.

5.6 Sterically hindered amide and peptide synthesis

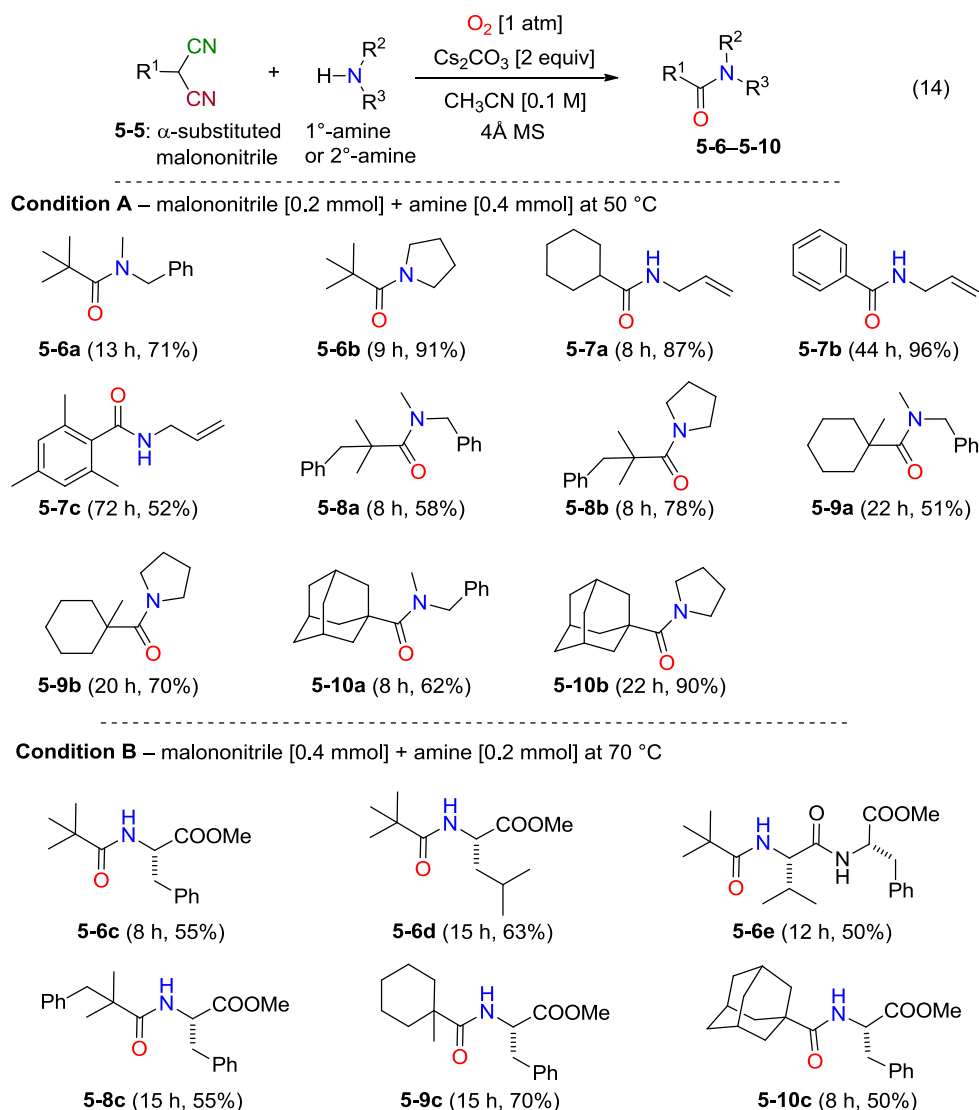
Sterically hindered α -substituted malononitriles **5-5** can be easily synthesized from widely available starting material using simple procedures. The conjugate addition of a Grignard reagent to isopropylidenemalononitrile gave **5-5a** and **5-5b** and the addition of Grignard reagent to 2-cyclohexylidenemalononitrile gave **5-5c**. (Eq. 11).^[11] Malononitrile **5-5d** can be easily synthesized from malononitrile and alkyl halide via a Friedel-Crafts type reaction. (Eq. 12).^[12] Malononitrile **5-5e** also can be prepared from malononitrile and aryl iodide via Pd-catalyzed coupling. (Eq. 12)^[13]



Scheme 4. Sterically hindered α -substituted malononitrile synthesis.

Next, the substrate scope was screened with hindered malononitriles **5-5** (Scheme 5). Besides the notable formation of the congested aromatic amide **5-7c** with allylamine, the formation of amides **5-6-5-10** proceeded in good yield at 50 °C,

despite both sides of the amide bond being fully substituted (Conditions A). Furthermore, chiral amino acid methyl esters and amides could be coupled with sterically hindered malononitriles in acceptable yields and reaction times at 70 °C (Conditions B) with complete stereochemical integrity in the amine component.



Scheme 5. Oxidative amidation of sterically hindered α -alkylated malononitriles and steric *N*-capping of amino acid esters / peptides.

5.7 Mechanistic study

On the basis of our previous mechanistic studies into making ketones^[10a,10b] and amides from nitroalkanes as described in chapter 2 and chapter 3, one plausible pathway for the oxidative amidation of malononitriles with amines is proposed in Figure 1. Thus, the α -substituted malononitrile first deprotonates to generate an anion **5-11**, which is then capable of single-electron transfer (SET) and addition with molecular oxygen, either directly or indirectly. If a radical pair is produced, they would couple to form the peroxide adduct **5-13**. From **5-13** to **5-16**, we proposed two possible pathways. In one case, the dioxygenated adduct **5-13** can cyclize to form a four membered ring anion **5-17**, which further expel cyanate anion and form an acylating species **5-16**. In the other case, the dioxygenated adduct **5-13** can cyclize and expel cyanide anion to form the reactive dioxirane intermediate **5-14**. In turn, electrophilic mono-oxygen transfer from the dioxirane **5-14** to another 1,1-dicyano carbanion **5-11** produces a *bis*-tetrahedral adduct **5-15** that can fragment into two acylating species **5-**

16 capable of being intercepted by the amine nucleophile.

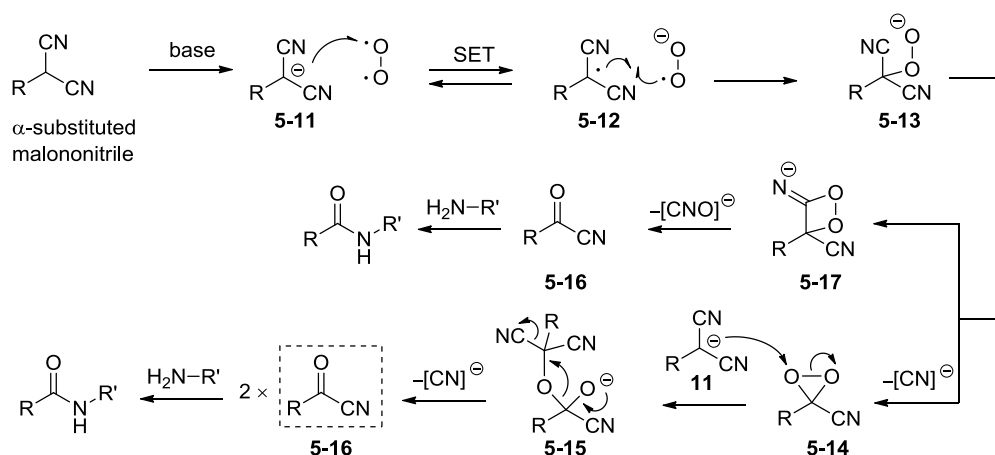
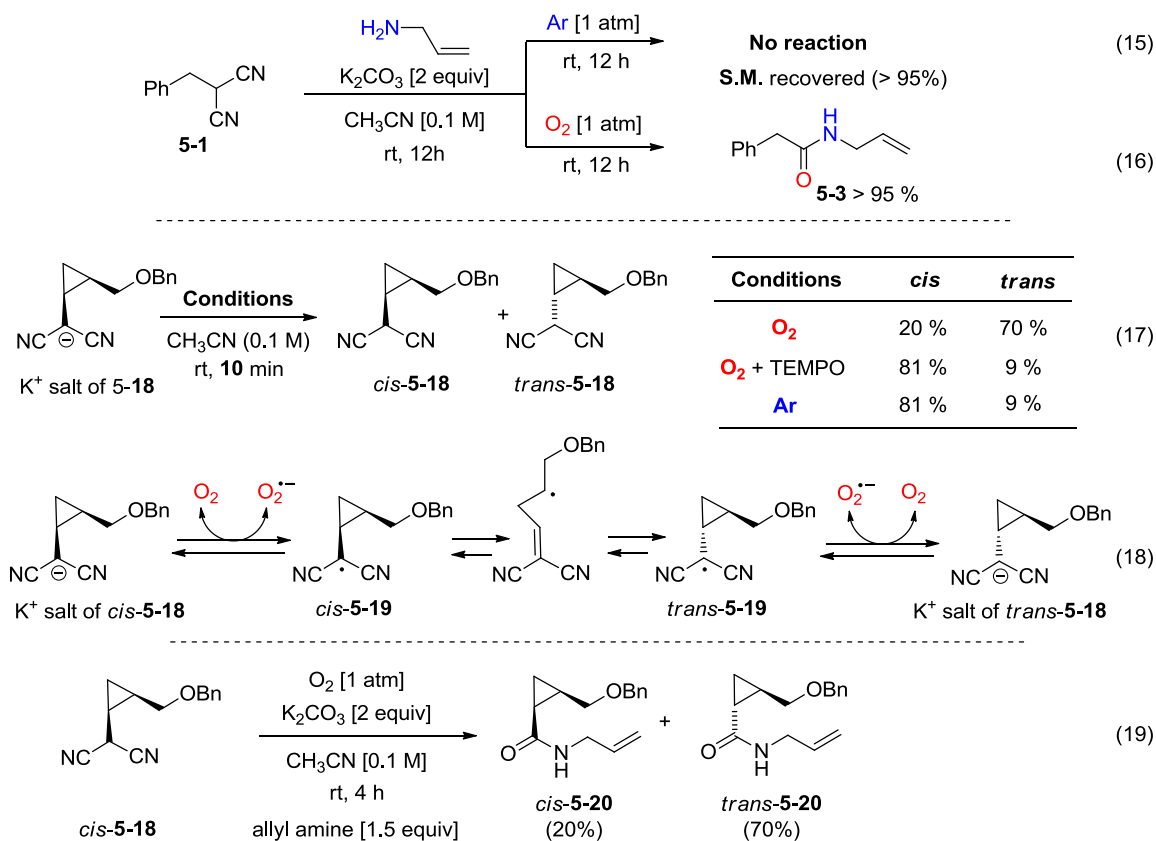


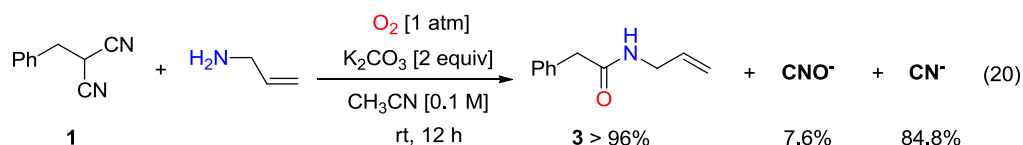
Figure 1. Proposed reaction mechanism.



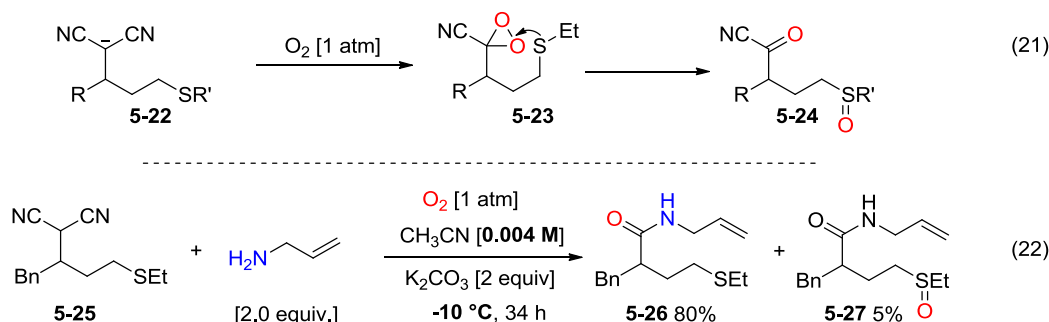
Scheme 6. The reaction of O₂ with malononitrile.

The role of O₂ was considered first, when the malononitrile **5-1** (X, Y = CN) was mixed with allylamine in the presence of K₂CO₃ under Ar, no amide **5-3** formed and **5-1** was recovered completely. (Eq. 15) This is in stark contrast to when the reaction was conducted under O₂ (Eq. 16, 96% yield of **5-3**). Next, in order to determine the existence of radical species like **5-12**, we prepared the α -cyclopropyl malononitrile **cis-5-18** as its pure *cis* isomer for suitable radical clock experiments.^[15] Exposure of the pre-formed potassium salt of **cis-5-18** to O₂ for 10 minutes gave a 1:3 **cis-5-18**/**trans-5-18**

mixture in 90% yield. Control experiments with added TEMPO (1.0 equiv.) and under strictly O₂-free atmospheres gave near complete recovery of the *cis* starting material (around 90%). (Eq. 17) These results indicated the anion **5-18** reacted reversibly with O₂ via SET to form a radical **5-19**. Moreover, when *cis*-**5-18** was exposed to the allylamine in the presence of K₂CO₃ under O₂, the cyclopropyl amide was isolated as a 1:3.5 *cis*-**5-20**/*trans*-**5-21** mixture in 90% yield after 4 h (Eq. 19). Further experiments demonstrated a mixture of the *cis* starting material **5-18** and *cis* amide product **5-20** to be isomerically stable to the reaction conditions under Ar. These control reaction indicated the anion **5-11** reacting reversibly with O₂ via SET to form a radical **5-12**, which can conceivably couple with superoxide to form a peroxide adduct **5-13** and further convert to amide in the presence of amines as shown in Figure 1.



The fate of the cyano groups was also considered. Thus, the quantities of cyanide and cyanate anions were determined by ion chromatography as produced from the reaction given in the generation of **5-3**. (Eq. 20) With respect to a total theoretical yield of 2 equivalents, cyanate ions were detected in low yield (7.6%), whereas cyanide ions were formed in high yield (84.8%). On the basis of these results, we further suggest the peroxide adduct **5-13** cyclizes to form a dioxirane intermediate **5-14**, releasing the first equivalent of cyanide, after which the second equivalent of cyanide would be generated after amine addition to the proposed acyl cyanide **5-16** to give the amide product **5-17** (see Figure 1).

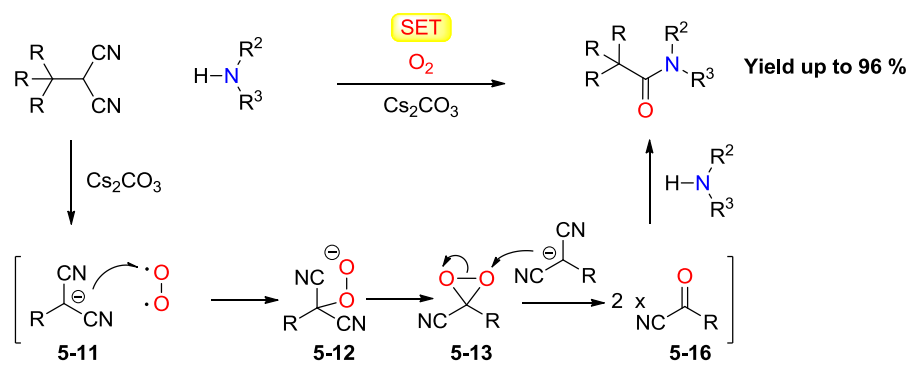


Scheme 7. Dioxirane intermediate trapping reaction.

Next, in order to prove the formation of the electrophilic dioxirane intermediate **5-14**, (Figure 1) intramolecular thioether-trapping experiments were performed in O₂-saturated CH₃CN. The anion **5-22** reacts with molecular O₂ would generate electrophilic dioxirane intermediate **5-23**, which can further react form compound **5-24** via intramolecular reaction. (Eq. 21).^[10b] In the event, the δ-ethylsulfenyl β-benzyl malononitrile **5-25** was prepared and reacted under dilute conditions at −20 °C. (Eq. 22) This gave the oxidized sulfinyl amide **5-27** reliably in 5% yield. The direct oxidation of the sulfide starting material **5-25** or sulfide product **5-26** by O₂ was excluded by additional control experiments at room temperature over 48 h.

5.8 Conclusion

In this chapter, an efficient method for amide and peptide formation between readily available 1,1-dicyanoalkanes and amines was realized simply with molecular oxygen and a carbonate base. This oxidative protocol can be applied to both sterically and electronically challenging substrates in a highly chemoselective, practical, and rapid manner. Mechanistic studies support an initial SET pathway between the anion **5-11** of the α-substituted malononitrile and O₂ to form an α-peroxide adduct **5-12** as a precursor to the dioxirane intermediate **5-13**, which generates the acyl cyanide intermediate **5-16** that further reacts with the amine to give the final amide product.



References and Notes

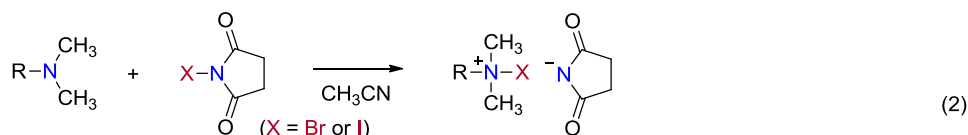
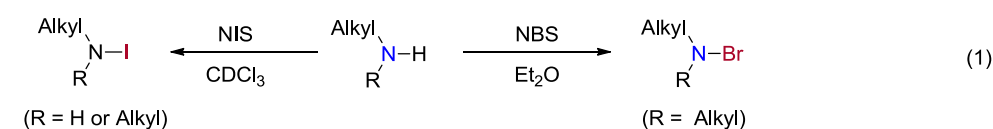
- [1] a) E. Valeur, M. Bradley, *Chem. Soc. Rev.* **2009**, 38, 606–631; b) A. El-Faham, F. Albericio, *Chem. Rev.* **2011**, 111, 6557–6602.
- [2] a) S. Hünig, R. Schaller, *Angew. Chem. Int. Ed.* **1982**, 21, 36–49; b) S. Takuma, Y. Hamada, T. Shioiri, *Chem. Pharm. Bull.* **1982**, 30, 3147–3135;
- [3] a) Y. Sugiura, Y. Tachikawa, Y. Nagasawa, N. Tada, A. Itoh, *RSC Adv.* **2015**, 5, 70883–70886; b) M. Brünjes, M. J. Ford, H. Dietrich, K. Wilson, *Synlett* **2015**, 26, 1365–1370; c) X. Chen, T. Chen, Q. Li, Y. Zhou, L.-B. Han, S.-F. Yin, *Chem. Eur. J.* **2014**, 20, 12234–12238. For amide and ester formations, see: d) S.-I. Murahashi, T. Naota, N. Nakajima, *Tetrahedron Lett.* **1985**, 26, 925–928; e) S. Förster, O. Tverskoy, G. Helmchen, *Synlett* **2008**, 2803–2806; f) T. Arai, T. Moribatake, H. Masum, *Chem. Eur. J.* **2015**, 21, 10671–10675.
- [4] S. Lundgren, E. Wingstrand, C. Moberg, *Adv. Synth. Catal.* **2007**, 349, 364–372; d) H. H. Choi, Y. H. Son, M. S. Jung, E. J. Kung, *Tetrahedron Lett.* **2011**, 52, 2312–2315.
- [5] a) H. Nemoto, Y. Kubota, Y. Yamamoto, *J. Org. Chem.* **1990**, 55, 4515–4516. b) Yang, K. S.; Nibbs, A. E.; Turkmen, Y. E.; Rawal, V. H. *J. Am. Chem. Soc.* **2013**, 135, 16050–16053; c) K. S. Yang, V. H. Rawal, *J. Am. Chem. Soc.* **2014**, 136, 16148–16151;
- [6] R. Ballini, M. Petrini, *Tetrahedron* **2004**, 60, 1017–1047.
- [7] A. McNally, C. K. Prier, D. W. C. MacMillan, *Science* **2011**, 334, 1114–1117. a) S. S. Kulp, M. J. McGee, *J. Org. Chem.*, **1983**, 48, 4097–4098; b) N. Rabjohn, C. A. Harbert, *J. Org. Chem.*, **1970**, 35, 3240–3243; c) S. H. Kim, K. H. Kim, J. N. Kim, *Adv. Synth. Catal.* **2011**, 353, 3335–3339.
- [8] M. Y. Chang, C. Y. Tsai, *Tetrahedron Lett.* **2014**, 55, 5548–5550.
- [9] J. Motoyoshiya, T. Ikeda, S. Tsuboi, T. Kusaura, Y. Takeuchi, S. Hayashi, S. Yoshioka, Y. Takaguchi, H. Aoyama, *J. Org. Chem.* **2003**, 68, 5950–5955.
- [10] a) Y. Hayashi, S. Umemiya, *Angew. Chem. Int. Ed.* **2013**, 52, 3450–3452; b) S. Umemiya, K. Nishino, I. Sato, Y. Hayashi, *Chem. Eur. J.* **2014**, 20, 15753–15759; c) J. Li, M. J. Lear, Y. Kawamoto, S. Umemiya A. Wong, E. Kwon, I. Sato, Y. Hayashi, *Angew. Chem. Int. Ed.* **2015**, 54, 12986–12990; *Angew. Chem.* **2015**, 127, 13178–13182; d) J. Li, M. J. Lear, E. Kwon, Y. Hayashi, *Chem. Eur. J.* **2016**, 5538–5542.
- [11] a) Texier-Boullet, F.; Foucand, A. *Tetrahedron Lett.* **1982**, 23, 4927. B) R. C. Wheland, E. L. Martin, *J. Org. Chem.*, **1975**, 40, 3101–3109.
- [12] S. Rayat, M. Qian, R. Glaser, *Chem. Res. Toxicol.* **2005**, 18, 1211–1218.
- [13] M. Uno, K. Setp, M. Masuda, W. Ueda, S. Takahashi. *Tetrahedron Lett.* **1985**, 26, 1553–1556.
- [15] a) E. L. Spence, G. J. Langley, T. D. H. Bugg, *J. Am. Chem. Soc.* **1996**, 118, 8336–8343; b) T. Benkovics, J. Du, I. A. Guzei, T. P. Yoon, *J. Org. Chem.* **2009**, 74, 5545–5552; c) J. F. Van Humbeck, S. P. Simonovich, R. R. Knowles, D. W. C. MacMillan, *J. Am. Chem. Soc.* **2010**, 132, 10012–10014; d) E. Arceo, I. D. Jurberg, A. Alvarez-Fernandez, P. Melchiorre, *Nature Chem.* **2013**, 5, 750–756.

Chapter 6. Halogen Bonded Complexes between Amines and NBS/NIS: Structure and Reactivity Study

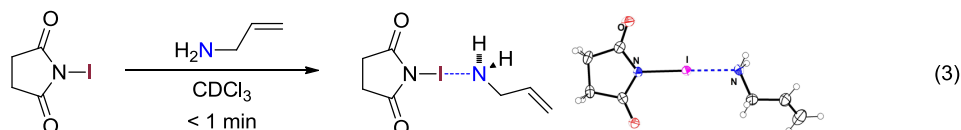
6.1 Background of NBS/NIS reacting with amine

NIS and NBS are commercially available, convenient sources of iodine/bromine for electrophilic addition reactions. Based on previous reports, NBS and NIS are one of the most common reagents used to oxidize the N–H bond to N–X.^[1a] Primary and secondary amines can be readily oxidized by NIS to give *N*-iodo amines.^[1b] Secondary amines can be readily oxidized by NBS to generated bromo-amines.^[1c,1d] Also, tertiary amines can readily react with NIS or NBS to form ammonium salts.^[2] Recently, we developed an efficient oxidative amidation of primary nitroalkanes with amines using NIS under O₂ (Chapter 2, 3). During my mechanistic study in Chapter 3, I observed and isolated a novel stable 1:1 adduct between allylamine and NIS instead of the iodo-amine. (Eq. 3) Based on literature study, I identified this complex belongs to a halogen bonded complex between the amine base and NIS Lewis acid.^[3]

a) Previous report



b) Our result



Scheme 1. Unexpected halogen bonded complex between allylamine and NIS.

Halogen bonding (XB) is the non-covalent interaction that occurs between a halogen atom (Lewis acid) and a Lewis base.^[3] The interaction angle is typically close to 180°, and the R–X...LB distance is shorter than the sum of the van-der-Waals radii of the interacting atoms and the R–X bond is slightly elongated. So far, most applications of halogen bonding are concerned with the solid state, e.g. in crystal engineering,^[4] self-assembly^[5] and organic semiconductors^[6]. The investigation of halogen bonding has considerably lagged behind, but today, it is used in various solution-phase applications.^[7] This includes fundamental studies^[8] and receptor anion transport.^[9] The study of halogen bonding in organic synthesis is currently in its infancy, such as the use of halogen bonded complexes as reagents^[10] and using halogen bonding as Lewis acidic activators or to initiate catalytic events.^[11]

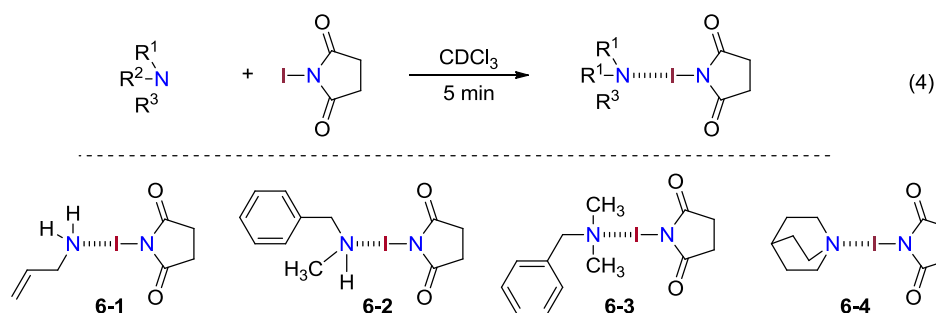


Figure 1. Schematic model of a halogen bond.

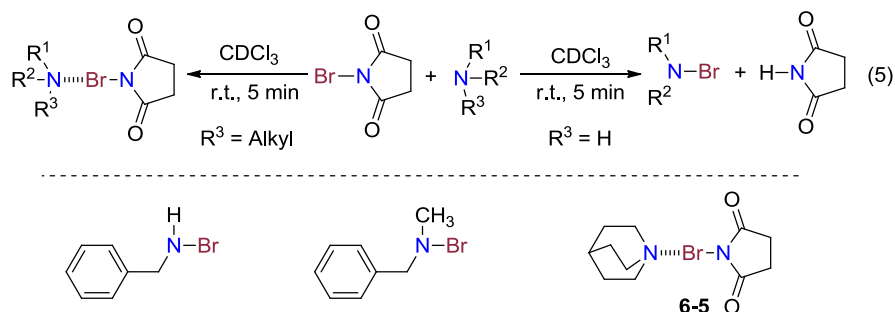
Indeed, the study of halogen bonding in catalysis or as reagents in halofunctionalizations is still rare. To date, there has been no systematic study about the character and reactivity of halogen bonded complexes between amines and NBS/NIS, and their application in catalytic halo-functionalizations.^[12] Herein, we present our fundamental findings about halogen

bonded complexes between amine and NBS/NIS serve as key intermediates in halocyclizations.

6.2 NMR study of NIS/NBS with different amines in solution



NIS reaction with different amines (Eq. 4): Different amines (1 equiv.) were mixed with NIS (1 equiv.) in CDCl_3 and monitored by ^1H NMR. We quickly observed that some signals of NIS were shifted upfield compared with free NIS, and some signals of the amine component were shifted downfield compared with the free amine. (Figure 2a) The pure halogen bonded complex can be readily obtained as a solid by evaporating the solvent and washing with dry Et_2O . Interestingly, I found the thermal stability of complex **6-1–6-4** both in solid and solution forms to highly depend on the type of amine. For example, the allylamine-NIS complex **1** and *N*-methylbenzylamine-NIS complex **2** slowly darken and decompose to a complex mixture at r.t. within 1 day. *N,N*-dimethylbenzylamine:NIS complex **3** quickly darkens and decomposes at r.t. within 10 minutes. However, all complexes can be stored at $-30\text{ }^\circ\text{C}$ for more than three months. The quinuclidine:NIS complex **6-4** is very stable and can be stored at r.t. for more than 3 month without any decomposition.



NBS react with amine (Eq. 5): Next, different amines were used to react with NBS. Primary benzylamine and secondary *N*-methylbenzylamine can be easily oxidized to bromoamine and release succinimide even at low temperature as evidenced by NMR. (Figure 2b)^[1c,1d] However, when NBS was mixed with quinuclidine (1:1), I observed an NBS signal (figure 2b) being shifted upfield, compared with free NBS, and an amine signal (Figure 2b) being shifted downfield, as compared with free quinuclidine as quinuclidine serve as Lewis base donated electron to NBS. Here, I only obtain pure complex solid **6-5** after evaporated the solvent and washed by Et_2O , this complex was stable at r.t. for more than 3 month without any decomposition.

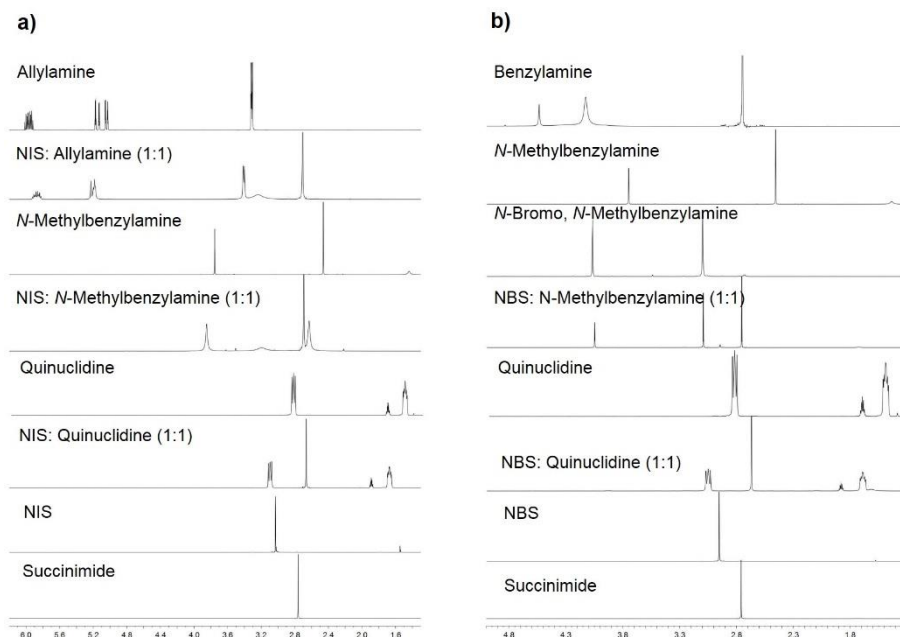


Figure 2. Comparison of the ^1H NMR spectra of NIS with different amines: a) NIS; b) NBS.

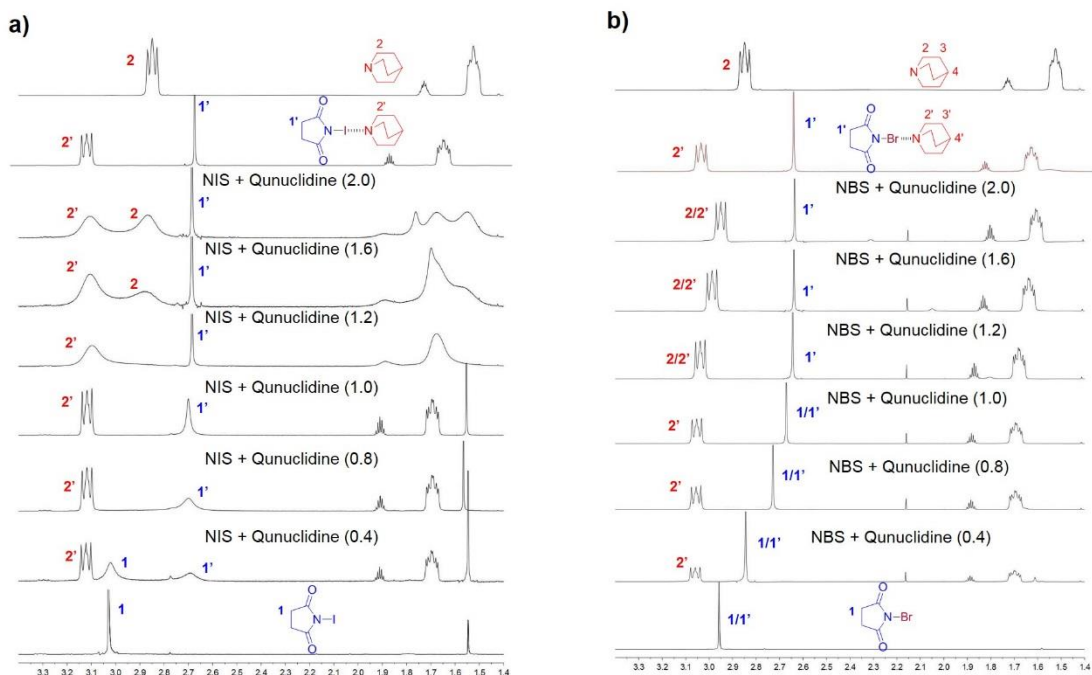


Figure 3. Stack plot of the ^1H NMR spectra of NIS/NBS at 298 K with increasing equivalents of quinuclidine: a) NIS; b) NBS.

Next, the titration of NIS and NBS with quinuclidine at room temperature (Figure 2) allowed the nature of the halogen bonding complex to be assessed in solution. First, the addition of quinuclidine to NIS in CDCl_3 was investigated and monitored by ^1NMR spectroscopy. (We shall discuss proton $1/1'$ of NIS and $2/2'$ of quinuclidine; see Figure 3a) In fact, when quinuclidine (0.4 equiv.) was added to NIS in CDCl_3 , the proton signals of **1** and **1'** appeared independently, and both signals of **1** and **1'** broadened at the same time. When the amount of quinuclidine was increased to 0.8 equiv., the signal of proton **1** disappeared and proton **1'** became sharp. Further increasing the amount of quinuclidine to 1.6 equiv., the peaks of **2** and **2'** broadened independently. This kind of observation due to the reversible ligand exchange of NIS in

and out of the complex **4** is slow on the NMR time scale. Next, the addition of quinuclidine to NBS in a solution of CDCl_3 was also investigated. Gradually increasing the amount of quinuclidine to the NBS solution, the signals of **2/2'** shifted upfield relative to **2**, and only one signal was observed between free NBS and the quinuclidine-NBS complex **5** due to the fast exchange of NBS in the complex **5** on the NMR time scale.

6.3 X-ray crystal structures of halogen bonded complexes of NBS/NIS and amine

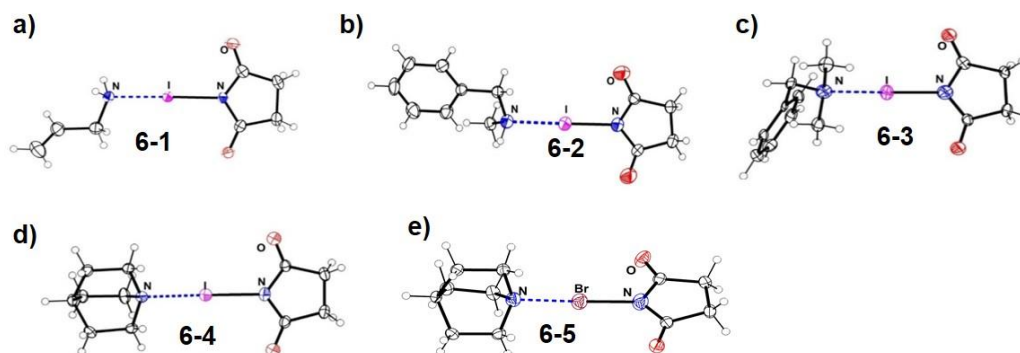


Figure 4. X-ray structure of halogen bonded complexes between NXS and amine: **a)** Allylamine:NIS (**6-1**); **b)** *N*-Methylbenzylamine:NIS (**6-2**); **c)** *N,N'*-Dimethylbenzylamine:NIS (**6-3**); **d)** Quinuclidine:NIS (**6-4**); **e)** Quinuclidine: NBS (**6-5**).

Table 1. Bond length and bond angle of halogen bonded complex **6-1–6-5**.

	6-1	6-2	6-3	6-4	6-5
Bond length of N---X (Å)	2.369	2.399	2.433	2.370	2.211
Bond length of X–N (Å)	2.190	2.165	2.170	2.185	2.030
Angle [deg]: N---X–N (°)	178.54	178.81	175.20	178.80	178.54

All the single crystals of **6-1–6-5** were obtained by slowly decreasing the temperature of a 1:1 mixture of NIS/NBS and amine in a solvent mixture of CH_2Cl_2 and hexane. The structures of complexes **6-1–6-5** were determined by single-crystal X-ray diffraction analysis as shown in Figure 4. The bond length and angle are summarized in Table 1. All the angles of N---I–N of complexes **6-1–6-4** are near to 180° , having essentially linear geometry, ranging from 175.2° to 178.8° , which are in agreement with the fundamental characters of halogen bonding.^[3] The corresponding N---I distances of NIS-amine complexes between Lewis basic amine and NIS vary from 2.369 to 2.433 Å, which are markedly shorter than the sum of the van der Waals radii of the involved atoms (3.53 Å).^[13] In addition, the N–I bond of NIS vary from 2.165–2.196 Å, which are longer than the N–I bond (1.96 Å) of NIS.^[ref] In the case of NBS-quinuclidine complex **6-5**, the angle of N---Br–N is essentially linear at 178.5° and the N---Br bond is 2.21 Å, which is much shorter than the van der Waals radii of the involved atoms (3.40 Å).^[14]

6.4 Reactivity study of NBS/NIS-quinuclidine complex in halocyclization of olefins

Modified chinchona alkaloid derivatives are widely used as catalysts in highly enantioselective chloro-, bromo- and iodocyclizations.^[15] The most commonly used modified chinchona alkaloid derivatives are shown in Figure 5. All the chinchona alkaloid derivatives feature a quinuclidine moiety. Investigation of the reactivity of the quinuclidine complexes **6-4** and **6-5** (stable at room temperature) might provide mechanistic insights into chinchona alkaloid-catalyzed halocyclizations.

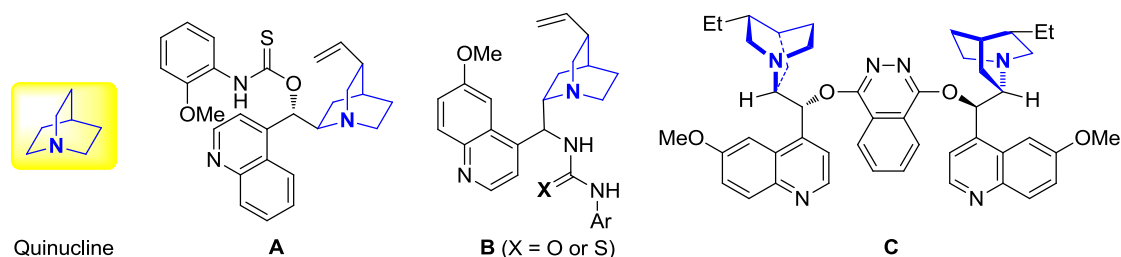


Figure 5. Selected modified chinchona alkaloid derivatives for halocyclization.

As model substrates, we decided to use the widely available δ -unsaturated alcohol **6-6** and acid **6-7** to test the reactivity of the halogen bonded complexes **6-4/6-5**. The δ -unsaturated alcohol **6-6** was first used to demonstrate the reactivity of the NBS-quinuclidine complex **6-5** to using NBS alone. The reaction mixture was homogenous after the δ -unsaturated alcohol **6-6** and complex **6-5** or NBS were mixed in CDCl_3 . Reaction progress and yield of cyclization of the products **6-8** and **6-9** were assayed by ^1H NMR integration based on an internal standard (1,2,4,5-tetrachlorobenzene). In this case of cycloetherification, the reaction speed of the NBS-quinuclidine complex **6-5** is a little slower to afford **6-8** as compared with NBS. (cf. Figure 6a, black and red curves)

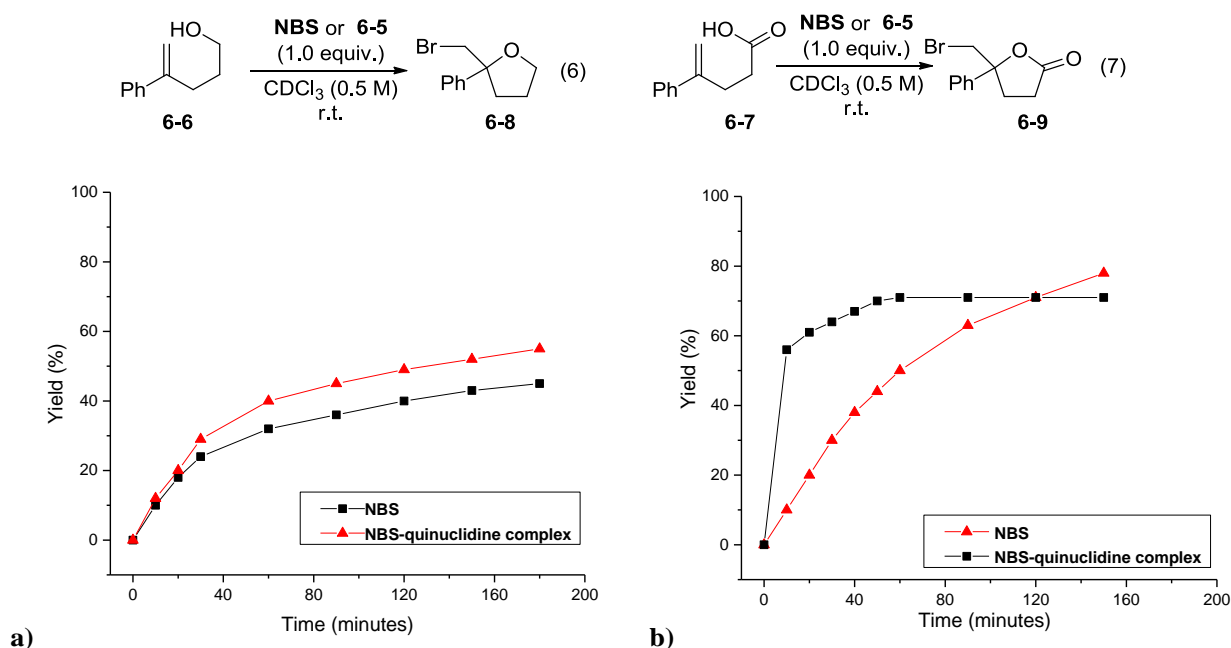
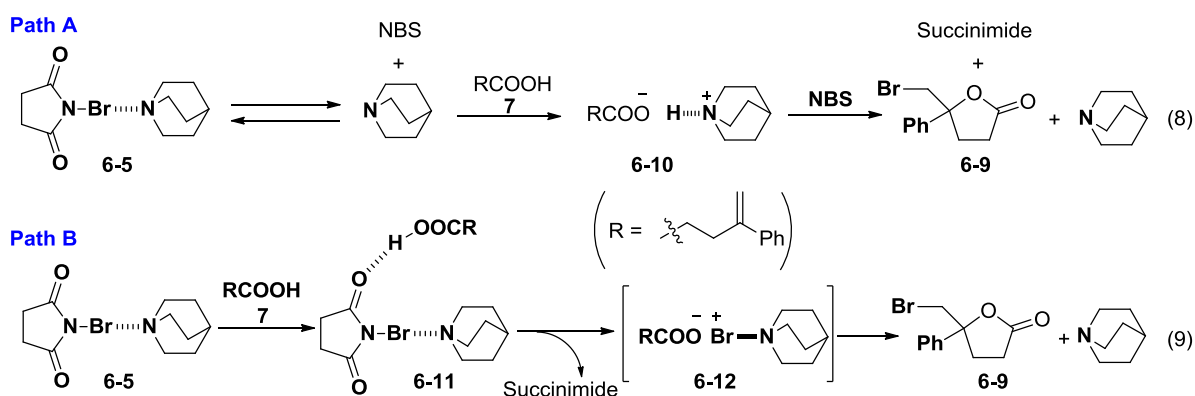


Figure 6. Reactivity of NBS and NBS-quinuclidine complex **6-5**: **a)** unsaturated alcohol **6-6**; **b)** unsaturated alcohol acid **6-7**.

Next, the reactivity of the γ -unsaturated acid **6-7** was assessed with the NBS-quinuclidine complex **6-5** and NBS. When NBS was used, the reaction proceeded slowly to give the lactone **6-9**, whereas the reaction was dramatically faster when the NBS-quinuclidine complex **6-5** was used, but the reaction suddenly slowed down and finally leveled out at 70% yield, leaving the uncyclized acid **6-7** and the unreacted NBS-quinuclidine complex **6-5**. (cf. Figure 6b, black and red curves) Based on these results, several aspects required further investigation: 1) Why does the NBS-quinuclidine complex **6-5** react with the acid substrate **6-7** much faster than the alcohol substrate **6-6**? (cf. Figure 6a and Figure 6b); 2) Why does the reaction of the acid substrate **6-7** with complex **6-5** stop at 70%, even when NBS-quinuclidine **6-5** and unsaturated acid **6-7** still remain? (Figure 6b).

First, we considered why the NBS-quinuclidine complex **6-5** reacts with the unsaturated acid **6-7** much faster

than unsaturated alcohol **6-6**. After a literature study,^[15] two possible explanations are proposed in Scheme 2. In one case (Scheme 2, Path A), the complex **6-5** can release free NBS and the free quinuclidine in solution.^[16] The quinuclidine serves as a base to react with the acid substrate **6-7** and forms a more nucleophilic ammonium salt **6-10**, which reacts with NBS and quickly affords **6-9** thereby releasing quinuclidine and succinimide. In order to clarify path A as a possibility, a soluble potassium salt of **6-7** was prepared in CDCl₃ (unsaturated acid **6-7** with potassium carbonate and 18-crown-6) as a mimic of the ammonium salt **6-10**, before adding NBS in CDCl₃. In this case, the product **6-9** formed slowly and the soluble potassium salt of **6-7** remained unreacted over 12 hours. This indicates path A to be unlikely. According to Path B (Scheme 2), the unsaturated acid **6-7** first reacts with the NBS-quinuclidine complex **6-5** to form a hydrogen-bonded-activated intermediate **6-11**, which fragments into a reactive *N*-bromonium carboxylate salt **6-12**, releasing succinimide, and cyclizes to the lactone **6-9** via intramolecular or intermolecular mechanisms, releasing quinuclidine as a byproduct. This pathway model is similar to the Lewis base / Lewis acid co-catalyzed halocyclization mechanisms reported by Denmark.^[17] Here, however, we suggest the Brønsted acid activates the halogen-bonded NBS-quinuclidine complex **6-5** to form a reactive “Br⁺” species via hydrogen bonding and, eventually, proton transfer to form succinimide.



Scheme 2. Possible mechanism for unsaturated acid **6-7** reacting with complex **6-5**.

If path B is correct, other Brønsted acids instead of the unsaturated acid **6-7** can also activate the NBS-quinuclidine complex **6-5** to form a reactive “Br⁺” species like **6-12**. To test this hypothesis, the δ -unsaturated alcohol **6-6** (1.0 equiv.) was used to check the existence of the “Br⁺” species like **6-12**. In fact, when the δ -unsaturated alcohol **6-6** was added to the reaction mixture of the NBS-quinuclidine **6-5** and CH₃COOH in CDCl₃, compound **6-8** formed quantitatively and the starting materials **6** were completely consumed within 10 minutes (Figure 6b). The reaction speed dramatically improved compared with only using the NBS-quinuclidine complex **6-5**. (cf. Figure 6b, red and black curves) Further ¹H NMR studies were carried out to check the reaction of the NBS-quinuclidine complex **6-5** and CH₃COOH; for example, when CH₃COOH (1.0 equiv.) was added to the NBS-quinuclidine complex **5** in CDCl₃, we observed the proton signals in complex **5** to quickly shift downfield relative to complex **6-5**. Especially, we found *proton-1* to overlap with the proton of succinimide. (Figure 7a) *Proton-2* shifted downfield. In addition, a small amount of new species were generated at the same time.

Based on the reactivity and ¹H NMR spectra, the reactive species **6-12** proposed by previous reports cannot be confirmed unambiguously. At this stage, our conclusion is that the NBS-quinuclidine complex **6-5** can react with Brønsted acids to form in situ reactive “Br⁺” species. This reasonably explains why complex **6-5** reacts with the unsaturated acid substrate **6-7** much faster than the unsaturated alcohol substrate, because the acid substrate **6-7** can promote the NBS-quinuclidine complex **6-5** to form a reactive “Br⁺” species. (cf. Figure 6a and Figure 6b) The reaction of the unsaturated acid substrate **6-7** with the NBS-quinuclidine complex **6-5** stopped at 70% (Figure 8) can also be explained by Path B (Scheme 2). Free quinuclidine is thus generated as a byproduct when NBS-

quinuclidine complex **6-5** is consumed. (Scheme 2, Eq. 9) Quinuclidine can further react with the acid substrate **6-7** to form an ammonium salt **6-10**. The reaction will thus slow down and finally stop due to the lack of enough free acid **6-7** to promote the NBS-quinuclidine complex **6-5** to form a reactive “Br⁺” species. In fact, when extra CH₃COOH was added to the reaction mixture, the reaction proceeded until the acid substrate **6-7** was completely consumed. (cf. Figure 8, black and red curves)

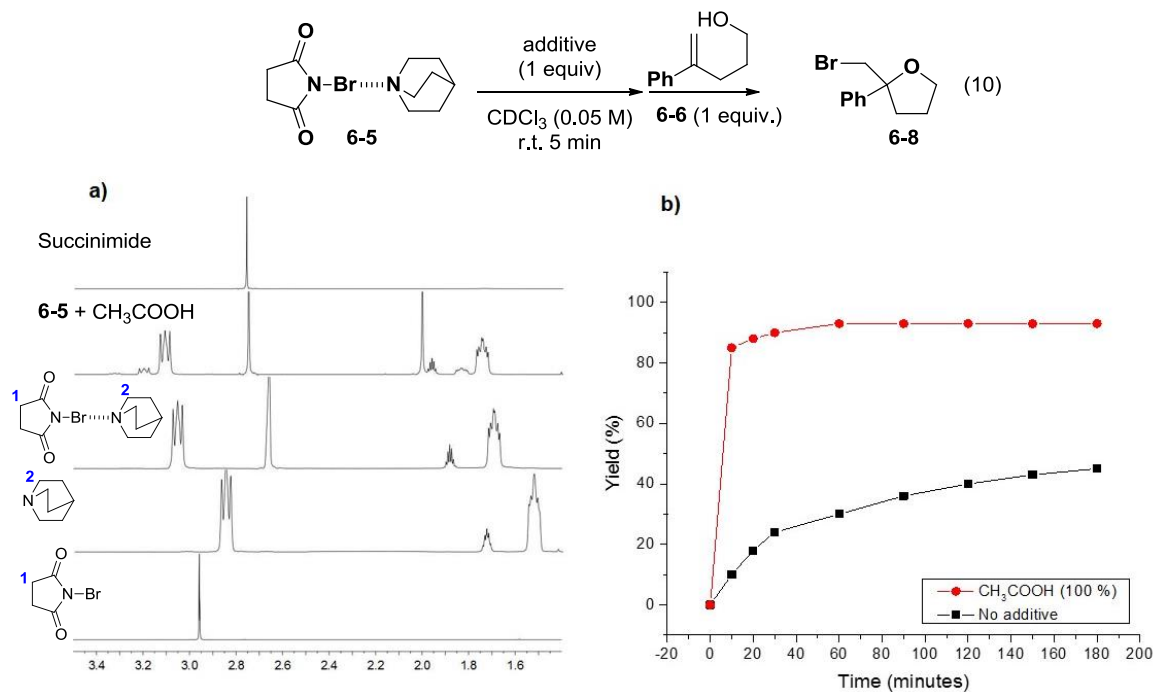


Figure 7. Acid affect on the activation of Quinuclidine-NIS complex **6-5**.

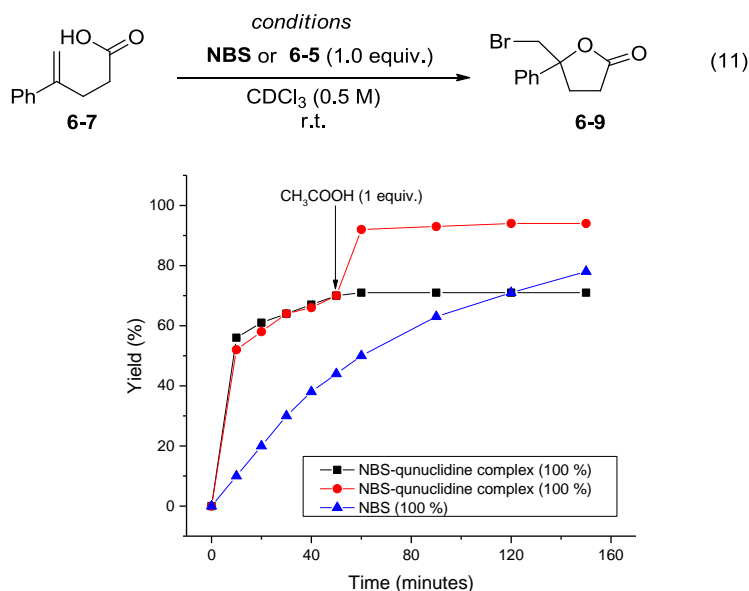


Figure 8. Acid affect on the activation of Quinuclidine-NBS complex **6-5**.

I further extended this study to the NIS-quinuclidine complex **6-4**. When complex **6-4** reacts with the alcohol substrate **6-6** in CDCl₃, almost no reaction occurred even after 3h. (Figure 9b, black curve). Based on acid improving the reactivity

of the NBS-quinuclidine complex **6-5**, CH_3COOH (1 equiv.) was added to the NIS-quinuclidine complex **6-5** in CDCl_3 in order to produce some reactive “ I^+ ” species. However, the reaction only accelerated a little compared with the NIS-quinuclidine **6-5**. (cf. Figure 9b, black and red curve) On the reasoning that the NIS-quinuclidine complex **6-4** is more stable to the NBS-Quinuclidine complex **6-5**, I added a stronger acid to help the complex **6-5** form a reactive “ I^+ ” species. To our delight, the reaction dramatically accelerated to give the desired iodocycloether in more than 90% yield within 10 minutes with the addition of ClCH_2COOH ($\text{pK}_a = 2.9$ in water) instead of CH_3COOH ($\text{pK}_a = 4.8$). (cf. Figure 9b, red and blue curves).

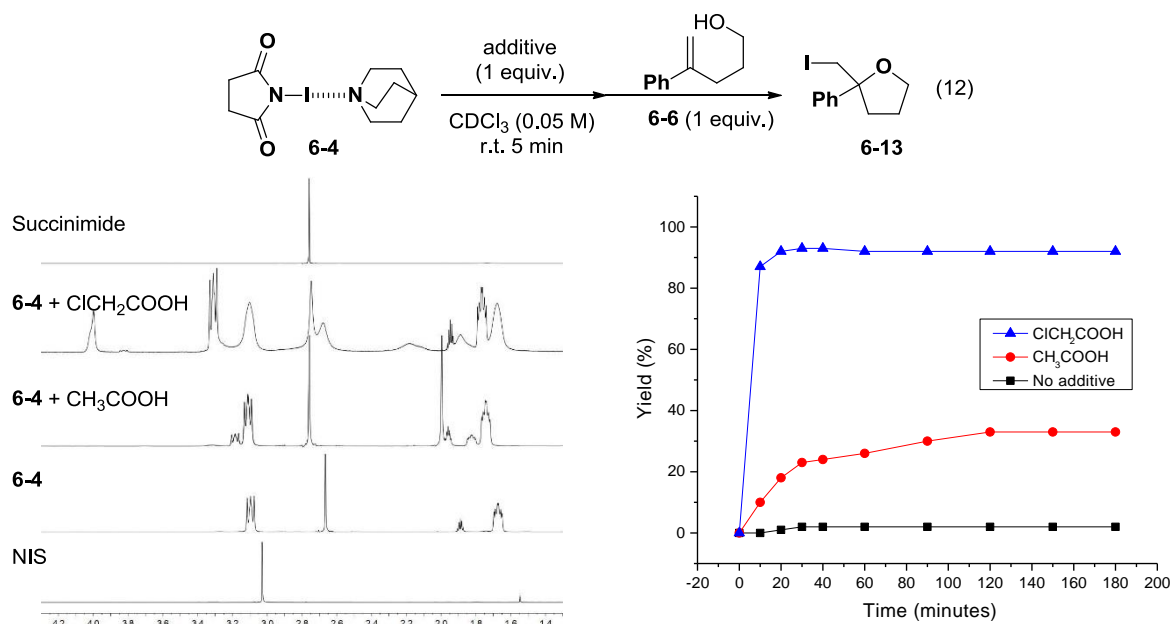


Figure 9. Acid affect on the activation of quinuclidine-NIS complex **6-4**.

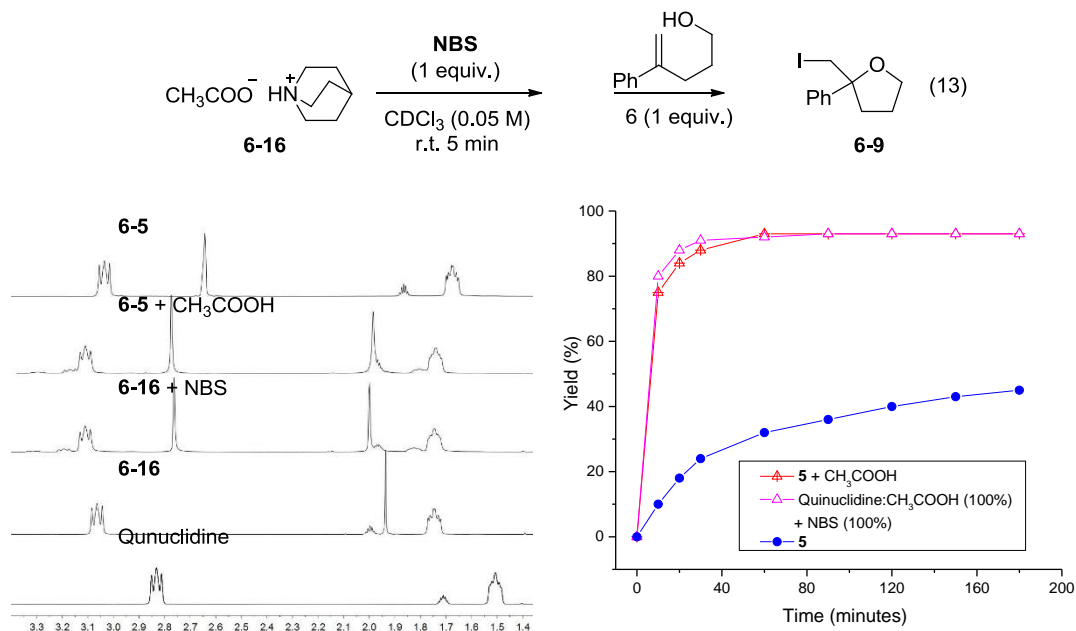
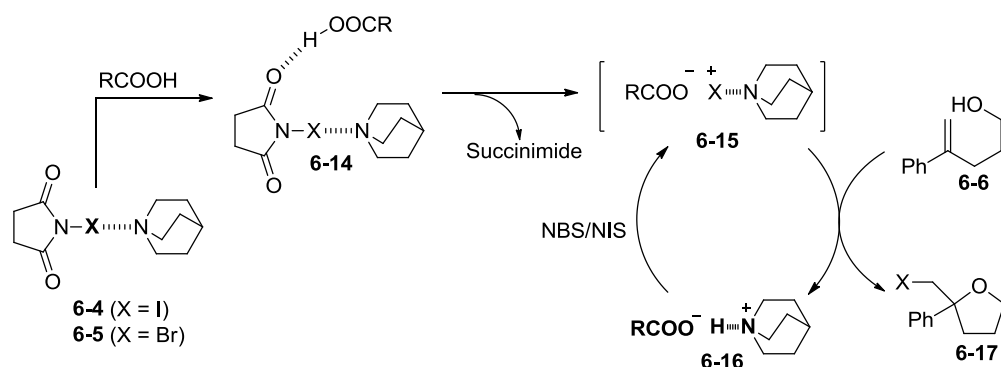


Figure 10. The reaction of ammonium salt **6-16** react with NBS.

During the study of the reactions of Eq. 10 and Eq. 12, I observed and isolated stoichiometric amounts of ammonium salts after the reactions finished. This suggested the possibility that ammonium salts can react with NBS or NIS

to form some reactive “X⁺” species or not. To investigate this possibility, NBS was directly added to the likely pre-formed ammonium salt (quinuclidine + CH₃COOH) in CDCl₃, before adding the unsaturated alcohol **6-9** to the reaction mixture. This reaction showed similar speeds in the formation of **6-9** when compared to using the NBS-quinuclidine (1 equiv.) / CH₃COOH (1 equiv.) reagent system. (cf. Figure 10b, red and purple curves) In addition, we observed the same ¹H NMR profiles when using the reagent systems of ammonium salt **6-16** / NBS as opposed to the NBS-quinuclidine complex **6-5** / CH₃COOH. (Figure 10a)

Having provided evidence that NBS can react with the ammonium salt **6-16** of quinuclidine and CH₃COOH to generate some sort of reactive “Br⁺” species, we propose substoichiometric amounts of a sufficiently strong Brønsted acid and NXS-quinuclidine complex **6-4** or **6-5** can serve as a catalytic system for the halocyclization of **6-6** with NBS or NIS. (Scheme 7)



Scheme 7. Proposed catalytic cycle for acid activated complex **6-4** or **6-5**.

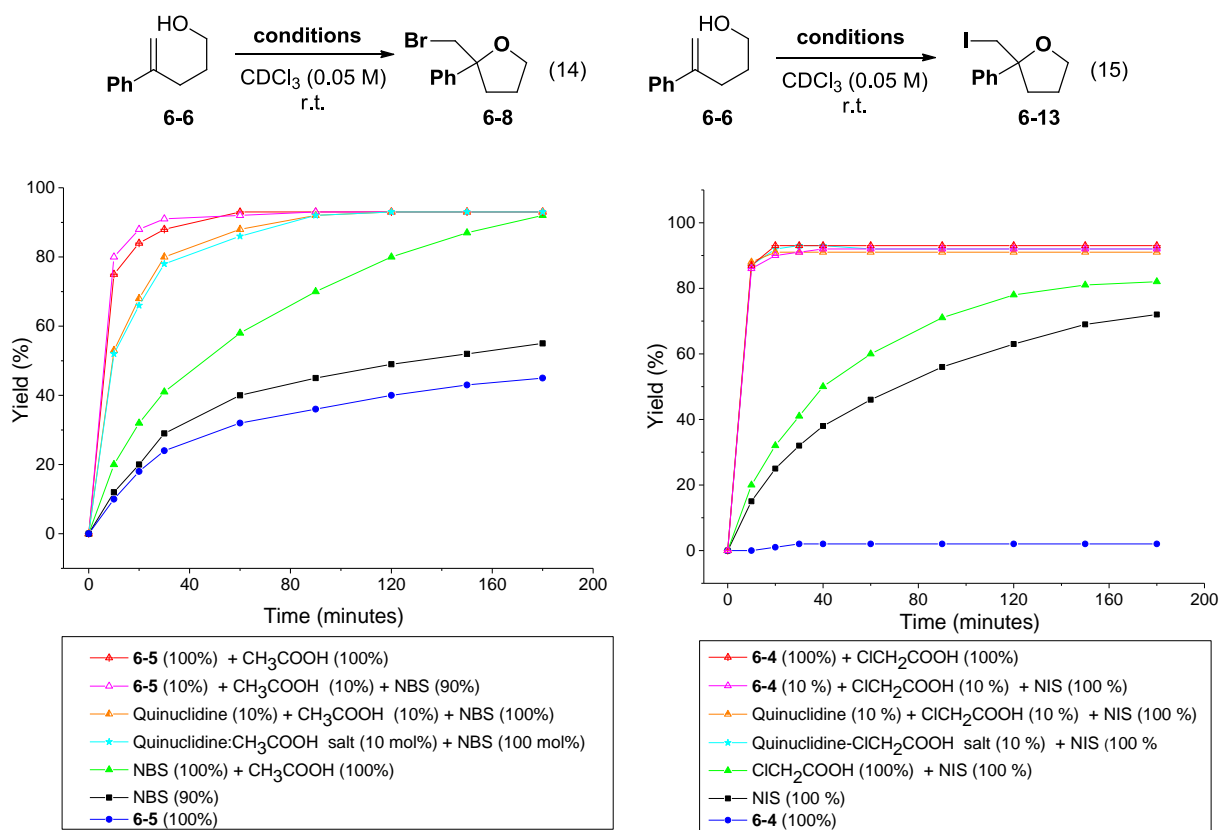


Figure 11. Catalytic amounts of NBS/NIS-Quinuclidine **6-5/6-4** promote halocycloetherification: **a)** NBS; **b)** NIS.

Compared with complex **6-5** (100%) / CH₃COOH (100%), reactions with NBS (100%) / CH₃COOH (100%), NBS-quinuclidine complex **6-5** or just NBS all proceeded slowly (cf. Figure 8a, green, blue, and black curves with the red curve). Next, several separate reactions were carried out using catalytic amounts of NBS-quinuclidine complex **6-5** and an acid (Figure 11a): **1**) δ -unsaturated alcohol **6-6** (1 equiv.) was dissolved in CDCl₃, NBS (0.9 equiv.) + 10 % quinuclidine complex **5** + CH₃COOH (10%) were added collectively in one-portion. We found this reaction to show a similar reaction speed as the complex **6-5** (1.0 equiv.) + CH₃COOH (1.0 equiv.). (cf. Figure 8a, purple and red curves); **2**) When quinuclidine (0.1 equiv.) + CH₃COOH (0.1 equiv.) + NBS (1 equiv.) were used, we obtained a similar speed compared to using stoichiometric complex **6-5** / CH₃COOH; (cf. Figure 11a, yellow and red curves); **3**) When the pre-formed ammonium salt (10%) + NBS (100%) were used, a similar reaction speed was obtained to using stoichiometric complex **6-5** / CH₃COOH. (cf. Figure 11a, cyan and red curves). In the case of the NIS-quinuclidine complex **6-4**, the only difference to the NBS-quinuclidine complex **6-5** was that a stronger acid (ClCH₂COOH) was needed, instead of CH₃COOH. (Figure 11b) Based on all the reactions in Figure 9, a substoichiometric amount of complex **6-4** or **6-5** in combination with a substoichiometric amount of acid can serve as an efficient catalytic system for halocyclization of the δ -unsaturated alcohol **6-6** with NBS or NIS, whether the complex **6-4** and **6-5** is pre-formed or formed in-situ.

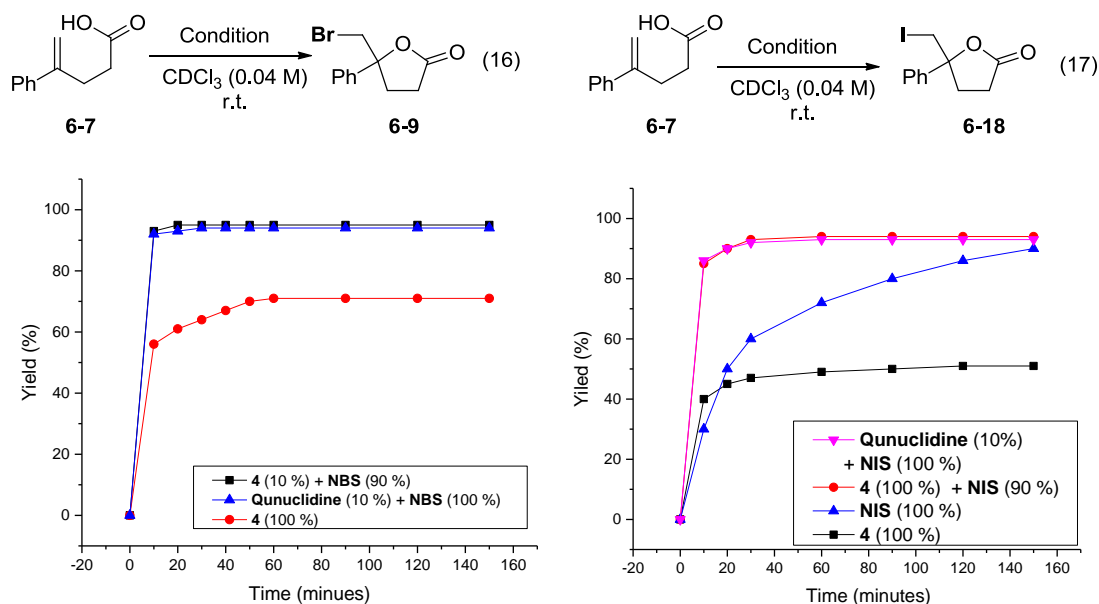


Figure 12. Catalytic amounts of NBS/NIS-Quinuclidine **6-5/6-4** promotes halolactonization: **a**) NBS; **b**) NIS.

Finally, the unsaturated acid **6-7** was studied with NBS and NIS complexes **6-5** and **6-4**, respectively. Here, there was no need to add extra acid, because compound **6-7** serves as a Brønsted acid itself. First, the NBS-quinuclidine complex **6-4** and NBS were investigated (Figure 12a): **1**) The reaction stopped at 70% with only the addition of the NBS-quinuclidine complex **6-4** (100%); **2**) When NBS-quinuclidine complex **6-4** (10%) + NBS (90%) were added in one-portion to a solution of compound **6-7**, the lactone **6-9** was produced in more than 90% within 10 min; **3**) When quinuclidine (10%) + NBS (100%) were used, similar results were obtained compared to using complex **6-5** (10 %) / NBS (100%). (cf. Figure 12a, blue and black curves) Similar results were observed in the case of the NIS-quinuclidine complex **6-4** and NIS. (Figure 12b). **1**) Only NIS used, the reaction slowly proceed; **2**) The reaction stopped at 50% with only the addition of the NBS-quinuclidine complex **6-4** (100%); **3**) When catalytic amount of NIS-quinuclidine complex **6-5** or quinuclidine used, the reaction quickly proceeded and finished within 10 minutes.

6.5 Conclusion

In this chapter, I characterized several novel halogen bonded complexes between various amines and NBS or NIS. The bonding character of this complex was achieved through NMR and X-ray structural studies. A systematic examination of the Brønsted acid affect of NBS/NIS-quinuclidine complexes **6-5/6-4** on the rate of halofunctionalization reactions was conducted. We found the cyclization reaction of unsaturated acids and alcohols with NBS and NIS were dramatically accelerated by adding Brønsted acids, especially ClCH_2COOH was needed in the case of the NIS-quinuclidine complex **6-4** (which is more stable than the NIS-quinuclidine complex **6-5**, which can be activated using a weaker acid CH_3COOH).

References and Notes

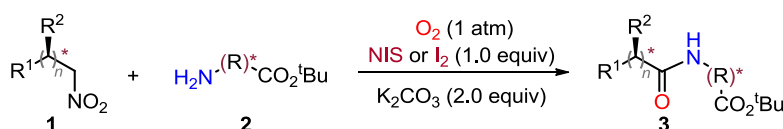
- [1] a) P. Kovacic, M. K. Lowery, K. W. Field, *Chem. Rev.* **1970**, *70*, 639–665; b) B. Shen, D. M. Makley, J. N. Johnston, *Nature* **2010**, *465*, 1027–1032; c) J. E. M. N. Klein, H. Müller-Bunz, P. Evans, *Org. Biomol. Chem.*, **2009**, *7*, 986–995; d) E. J. Corey, C.-P. Chen, G. A. Reichard, *Tetrahedron Lett.* **1989**, *30*, 5547–5550.
- [2] H. G. Stenmark, A. Brazzale, Z. K. Ma, *J. Org. Chem.* **2000**, *65*, 3875–3876.
- [3] a) Metrangolo, P.; Meyer, F.; Pilati, T.; Resnati, G.; Terraneo, G. *Angew. Chem., Int. Ed.* **2008**, *47*, 6114–6127; b) Risannen, K. *Cryst. Eng. Comm.* **2008**, *10*, 1107–1113. c) Politzer, P.; Lane, P.; Concha, M. C.; Ma, Y.; Murray, J. S. *J. Mol. Model.* **2007**, *13*, 305–311. d) Metrangolo, P.; Neukirch, H.; Pilati, T.; Resnati, G. *Acc. Chem. Res.* **2005**, *38*, 386–395.
- [4] P. Metrangolo, G. Resnati, T. Pilati, S. Biella, *Struct. Bond.* **2008**, *126*, 105–136.
- [5] L. C. Gilday, S. W. Robinson, T. A. Barendt, M. J. Langton, B. R. Mullaney, P. D. Beer, *Chem. Rev.* **2015**, *115*, 7118–7195.
- [6] a) H. M. Yamamoto, J.I. Yamaura, R. Kato, *J. Am. Chem. Soc.* **1998**, *120*, 5905–5913; b) M. Fourmigue, P. Batail, *Chem. Rev.* **2004**, *104*, 5379–5418.
- [7] Halogen bonding in solution: a) T. M. Beale, M. G. Chudzinski, M. G. Sarwar, M. S. Taylor. *Chem. Soc. Rev.*, **2013**, *42*, 1667–1680; b) M. Erdelyi, *Chem. Soc. Rev.* **2012**, *41*, 3547–3557.
- [8] Fundamental study of halogen bonding: Halogen Bonding: Fundamentals and Applications; Metrangolo, P., Resnati, G., Eds.; Springer: Berlin, Germany, **2008**.
- [9] A.V. Jentzsch, S. Matile, *Halogen Bonding I: Impact on Materials Chemistry and Life Sciences* **2015**, 358, 205–239.
- [10] Halogen bonded complex used as –CF₃ reagent: F. Sladojevich, E. McNeill, J. Boergel, S.-L. Zheng, T. Ritter, *Angew. Chem. Int. Ed.* **2015**, *54*, 3712.
- [11] Selected example of Halogen bonding in organic synthesis: a) Bruckmann, A.; Pena, M. A.; Bolm, C. *Synlett* **2008**, *6*, 900. b) Jungbauer, S. H.; Schindler, S.; Kniep, F.; Walter, S. M.; Rout, L.; Huber, S. M. *Synlett* **2013**, *24*, 2624. c) Jungbauer, S. H.; Walter, S. M.; Schindler, S.; Rout, L.; Kniep, F.; Huber, S. M. *Chem. Commun.* **2014**, *50*, 6281; d) He, W.; Ge, Y.-C.; Tan, C.-H. *Org. Lett.* **2014**, *16*, 3244.
- [12] Selected reviews about halocyclization: a) A. Castellanos, S. P. Fletcher, *Chem. Eur. J.* **2011**, *17*, 5766–5776; b) Chen, G.; Ma, S. *Angew. Chem., Int. Ed.* **2010**, *49*, 8306–8308; c) Tan, C. K.; Zhou, L.; Yeung, Y.-Y. *Synlett* **2011**, 1335–1339; d) Castellanos, A.; Fletcher, S. P. *Chem. Eur. J.* **2011**, *17*, 5766–5776; e) Hennecke, U. *Chem. Asian J.* **2012**, *7*, 456–465; f) Denmark, S. E.; Kuester, W. E.; Burk, M. T. *Angew. Chem., Int. Ed.* **2012**, *51*, 10938–10953. f) Tan, C. K.; Yeung, Y.-Y. *Chem. Commun.* **2013**, *49*, 7985–7996; g) Murai, H.; Fujioka, H. *Heterocycles* **2013**, *87*, 763–805. h) Nolsøe, J. M. J.; Hansen, T. V. *Eur. J. Org. Chem.* **2014**, 3051–3065; i) Tripathi, C. B.; Mukherjee, S. *Synlett* **2014**, *25*, 163–169.
- [13] The van der Waals radii between N and I atom: Bondi, A. *J. Phys. Chem.* **1964**, *64*, 441.
- [14] The van der Waals radii between N and Br atom: <http://www.sdsc.edu/CCMS/Packages/cambridge/volume1/z1c07076.html>
- [15] Selected examples of chinchona alkaloid derivatives catalyzing halocyclizations: a) Zhang, W.; Xu, H. D.; Xu, H.; Tang, W. P. *J. Am. Chem. Soc.* **2009**, *131*, 3832; b) W. Zhang, S. Zheng, N. Liu, J. B. Werness, I. A. Guzei, W. P. Tang, *J. Am. Chem. Soc.*, **2010**, *132*, 3664–3665; c) Michael Wilking, Christian Mück-Lichtenfeld, Constantin G. Daniliuc, and Ulrich Hennecke. *J. Am. Chem. Soc.*, **2013**, *135*, 8133–8136; d) D. C. Whitehead, R. Yousefi, A. Jaganathan, B. Borhan, *J. Am. Chem. Soc.*, **2010**, *132*, 3298–3300; e) R. Miyaji, K. Asano, S. Matsubara, *J. Am. Chem. Soc.*, **2015**, *137*, 6766–6769.
- [16] Halogen bonding complex as for release base: S. Dordonne, B. Crouses, D. Bonnet-Delpon, J. Legros, *Chem. Comm.* **2011**, *47*, 5855–5857.

- [17] Development and Mechanism of an Enantioselective Bromocyclo etherification Reaction via Lewis Base/Chiral Brønsted Acid Cooperative Catalysis: a) S. E. Denmark, M. T. Burk, *Org. Lett.*, **2012**, *14*, 256–259; b) S. E. Denmark, M. T. Burk, *Chirality*, **2014**, *26*, 344–355.

Chapter 7. Conclusion

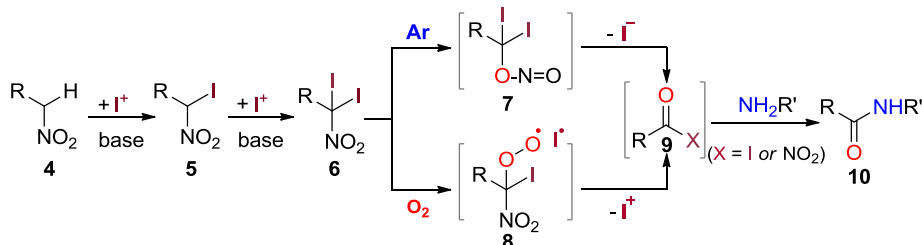
In this thesis, I studied and developed efficient ways to construct different types of amide and peptide bonds using O₂ under mild reaction conditions. In addition, the structure and reactivity of halogen bonded complexes between amines and NIS/NBS were investigated in a systematic and detailed fashion.

In Chapter 2, a direct oxidative method was developed to make amide and peptide bonds between widely available primary nitroalkanes **1** and amines **2** simply by using I₂ and K₂CO₃ under O₂. (Scheme 1) The method is straightforward in operation, chemoselective in functional group tolerance, and stereochemically robust to potentially epimerizable substrates. Importantly, a whole range of primary nitroalkane starting materials for this reaction method can be readily prepared in chiral form via a plethora of asymmetric methods.



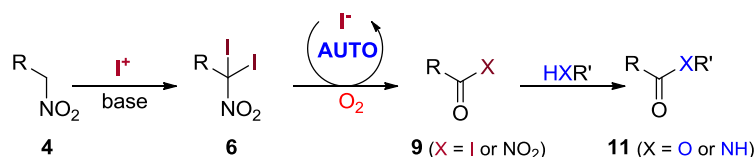
Scheme 1. Halogen bonded complex between NIS/NBS and amine.

In Chapter 3, I systematically investigated the oxidative mechanism and possible intermediates. I observed and isolated the α-iodonitroalkane intermediate **5**, which further reacts with an iodonium source to form α,α-diiodonitroalkane **6**. In particular, my evidence supports α,α-diiodonitroalkane **6** reacting with molecular oxygen to form a peroxy adduct **8**; alternatively, this α,α-diiodonitroalkane **6** can rearrange anaerobically into a cleavable nitrite ester **7**. In either case, the activated ester **9** are proposed form, which eventually react with nucleophilic amines to form the amide **10**. In addition, the generation of an extra equimolar amount of “I⁺” under O₂ during the conversion of the α,α-diiodonitroalkane **6** to the activated ester intermediate **9** is proposed.



Scheme 2. Halogen bonded complex between NIS/NBS and amine.

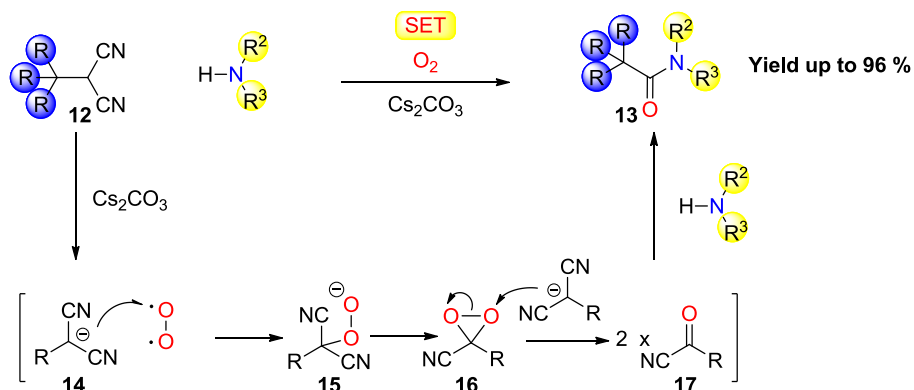
In chapter 4, during mechanistic studies, I identified I⁻ as an efficient autocatalyst to forming the acyl ester **9** from the α,α-diiodonitroalkane **6**; this acylating ester **9** can further react with an amine or MeOH to give an amide or ester. I thus developed a new and rapid I₂/O₂-based method to synthesize sterically hindered esters from primary nitroalkanes by in-situ iodide-mediated catalysis. (Scheme. 3)



Scheme 3. Halogen bonded complex between NIS/NBS and amine.

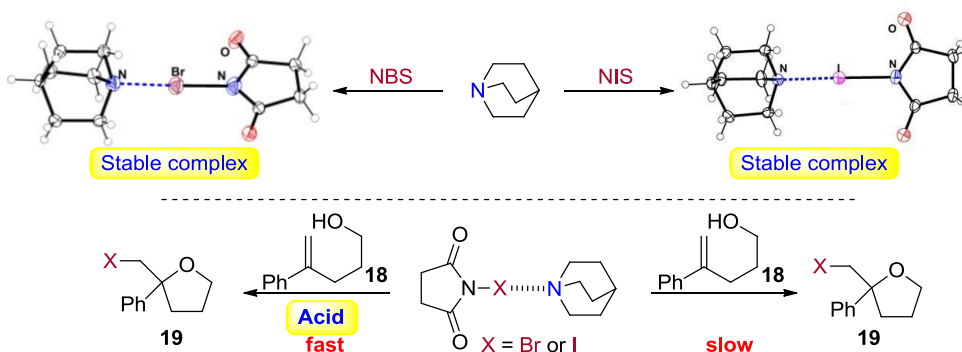
In chapter 5, an efficient method for amide and peptide **13** formation between readily available 1,1-dicyanoalkanes **12**

and amines was realized simply with molecular oxygen and a carbonate base. This oxidative protocol can be applied to both sterically and electronically challenging substrates in a highly chemoselective, practical, and rapid manner. Mechanistic studies support an initial SET pathway between the anion **14** of the α -substituted malononitrile **12** and O_2 to form an α -peroxide adduct **15** as a precursor to the dioxirane intermediate **16**, which generates acyl cyanide intermediates **17** (Scheme 4).



Scheme 4. Halogen bonded complex between NIS/NBS and amine.

In chapter 6, I observed, prepared and isolated a stable halogen bonded complex between NIS/NBS and quinuclidine. I further found the halogen bonded complex to be very stable at r.t., which showed low reactivity for halo-cycloetherification from **18** to **19**, but once acid was added, the reactivity improved dramatically. (Scheme 5)



Scheme 5. Halogen bonded complex between NIS/NBS and amine.

Experiment Part

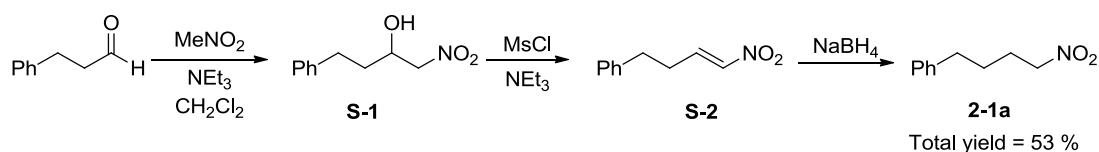
Chapter 2

2.1 General Information

Glassware was oven-dried at 120 °C for all non-aqueous reactions. All reagents and solvents were commercial grade and purified prior to use when necessary. Acetonitrile (CH₃CN), toluene, and tetrahydrofuran (THF) were dried by passage through a column of activated alumina.

Analytical thin-layer chromatography (TLC) was performed using E. Merck Silica gel 60 F254 pre-coated plates. Column chromatography was performed using 40-50 µm Silica Gel 60N (Kanto Chemical Co., Inc.). ¹H-NMR (400 MHz) and ¹³C-NMR (100 MHz) spectra were recorded on an Agilent 400MR spectrometer. Chemical shifts are reported in (ppm) down field from tetramethylsilane with reference to solvent signals [¹H NMR: CHCl₃ (7.26), ⁶d-DMSO (2.50); ¹³C NMR: CDCl₃ (77.16), ⁶d-DMSO (40.00)]. Signal patterns are indicated as s, singlet; d, doublet; t, triplet; q, quartet; m, multiplet; br, broad peak, coupling constant (Hz), integration and assignment. Infrared (IR) spectra were recorded on a PERKIN ELMER Spectrum BX FT-IR System spectrometer. Optical rotations ([α]_D) were measured on a JASCO P-2200 polarimeter. High resolution mass spectra were measured on Thermo Fisher Scientific Orbitrap Discovery (ESI LTQ Orbitrap). HPLC analysis was performed on a HITACHI Elite LaChrom Series HPLC, and UV detection was monitored at appropriate wavelength, respectively, using CHIRALPAK IC (0.46 cm × 25 cm), CHIRAL-CELOD-H (0.46 cm × 25 cm), CHIRALPAK IE (0.46 cm × 25 cm). CHIRALPAK AD (0.46 cm × 25 cm).

2.2 Preparing starting materials



Scheme S-1. Synthesis of nitroalkane **2-1a**

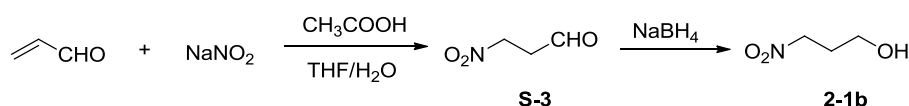
S-1: To a stirred mixture of 3-phenylpropanal (9.85 mL, 75 mmol) and nitromethane (16.05 mL, 300 mmol) in CH₂Cl₂ (15 mL) under Ar at 0 °C was added NEt₃ (52 mL, 375 mmol) through a dropping funnel over 30 min. The reaction was allowed to warm to R.T. and monitored by TLC until the aldehyde disappeared; 100 mL 1N HCl was then added slowly and stirring continued for 5 min. The reaction was extracted with CH₂Cl₂ (100 mL×2) and the combined organic phase was washed with brine and dried over anhydrous MgSO₄. After filtering off solids, the solvent was evaporated to give a dark yellow solid, which was further purified through silica gel chromatography (hexane/EA = 3/1) to afford **S-1** as white solid (12.2 g, 84%).

S-2: To a stirred solution of **S-1** (12.0 g, 62.8 mmol) in CH₂Cl₂ (330 mL), cooled to -35 °C under Ar, MeSO₂Cl (5.8 mL, 75.4 mL) was added over 3 min. Then NEt₃ (21.1 mL, 150.8 mmol) was added dropwise over 10 min and quenched with 1N HCl, then allowed to warm to R.T and extracted with CH₂Cl₂ (50 × 2 mL). The combined organic layers were washed with brine (10 mL), dried (MgSO₄), filtered and concentrated under reduced pressure to give crude **S2**, which was further purified by silica gel chromatography to obtain **S-2** (10.0 g, 90%) as a clear oil.

2-1a: To a stirred solution of **S-2** (56.5 mmol) in THF/Methanol (10/1, 560 mL) at 0 °C under Ar was added NaBH₄ (2.12 g, 56.5 mmol) in 3 portions, quenched with sat. aq NaHCO₃ (10 mL) and extracted with EtOAc (3×10 mL) after 40 min. The combined organic layers were washed with brine (10 mL), dried (MgSO₄), filtered and concentrated under reduced pressure to give crude **2-1a**, which was further purified by silica gel chromatography (hexane/EA=7/1) to obtain a clear oil (7.1 g, 71%).

¹H NMR (CDCl₃, 400 MHz): δ 1.69-1.77 (m, 2H), 2.00-2.08 (m, 2H), 2.68 (t, J = 7.2 Hz, 2H), 4.38 (t, J = 6.8 Hz, 2H), 7.16-7.32 (m, 5 H).

¹³C NMR (CDCl₃, 100 MHz): δ 26.96, 28.00, 35.12, 75.62, 126.28, 128.48, 128.63, 141.15.



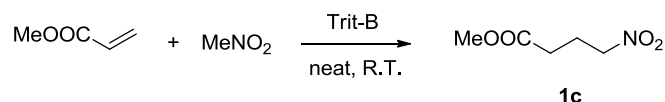
Scheme S-2. Synthesis of compound **1b**

S-3:^[1] To a well-stirred solution of NaNO₂ (4.15 g, 60.0 mmol) and acrolein (2.8 g, 50.0 mmol) in a mixture of H₂O (10 mL) and THF (20 mL) was slowly added glacial acetic acid (3.3 g, 55.0 mmol) at 0 °C under Ar. The resulting mixture was stirred at 0 °C for 4 h, quenched with *sat.* NaHCO₃ solution (10 mL) and extracted with EtOAc (3×10 mL). The combined organic layers were washed with brine (10 mL), dried (MgSO₄), filtered and concentrated under reduced pressure to give crude **S-3** (4.58) as a clear oil.

2-1b: The crude **S-3** was dissolved in 50 mL of methanol, cooled to 0 °C, then NaBH₄ was added slowly, stirred for 10 min and evaporated before water was added and extracted with EtOAc. The combined organic layers were dried (MgSO₄), filtered and concentrated under reduced pressure to give crude **1b**, which was further purified by silica gel chromatography to give **2-1b** (4.0 g, 70%) as an oil. The spectroscopic data are consistent with those reported in the literature.^[1]

¹H NMR (CDCl₃, 400 MHz): δ 2.21-2.27 (m, 2H), 3.77 (t, *J* = 6.0 Hz, 2H), 4.54 (t, *J* = 6.8 Hz, 2H).

¹³C NMR (CDCl₃, 100 MHz): δ 29.93, 59.11, 72.62.

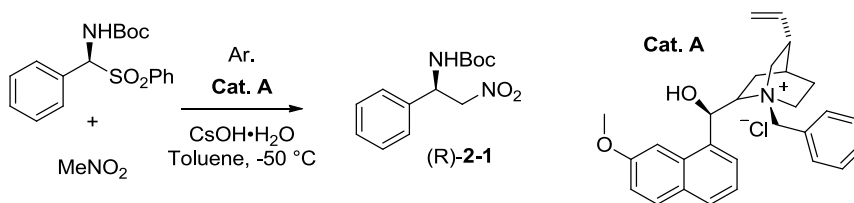


Scheme S-3. Synthesis of nitroalkane **1c**.

Methyl 5-nitropentanoate 1c:^[2] To a stirred solution of methyl acrylate (1.72 g, 20 mmol) in MeNO₂ (60 mL) was added Triton-B (0.2 mL, 40 wt % solution in MeOH) at 25 °C, stirred for 12 h, and then concentrated under reduced pressure to ca. 5 mL. Et₂O (10 mL) was added, and the mixture was washed with water (10 mL×2), saturated aqueous NaCl solution (20 mL) and then dried over MgSO₄. The mixture was concentrated in vacuum to give crude Methyl 4-nitrobutanoate as a light yellowish liquid, then purified by silica gel chromatography to give **1c** (2.25 g, 70 %). The spectroscopic data are consistent with those reported in the literature.^[2]

¹H NMR (CDCl₃, 400 MHz): δ 2.26-2.33 (m, 2H), 2.46 (t, *J* = 6.8 Hz, 2H), 3.67 (s, 3H), 4.46 (t, *J* = 6.4 Hz, 2H).

¹³C NMR (CDCl₃, 100 MHz): δ 22.45, 30.32, 52.00, 74.42, 172.41.



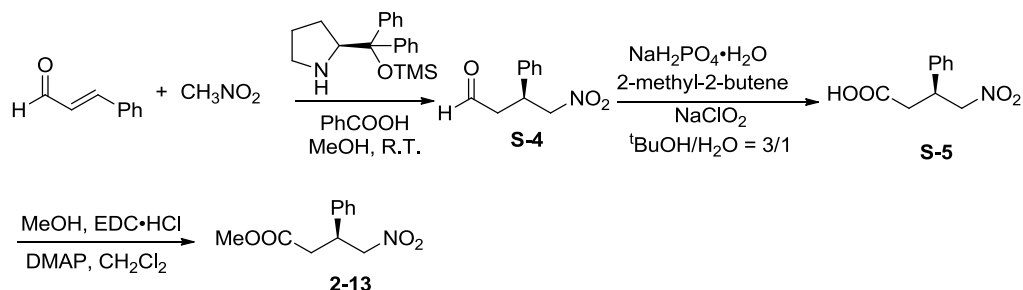
Scheme S-4. Synthesis of compound **R-1**^[3]

To a mixture of the corresponding α-amidosulfone (20.0mmol) and N-benzylquininium chloride (**Cat. A**, 1.08g, 2.6mmol) in toluene (60mL) was added CH₃NO₂ (5.3 mL, 100mmol) and, after cooling to -50 °C, CsOH·H₂O (4.3 g, 22mmol) was then added. The reaction mixture was stirred under an Argon atmosphere at the same temperature for 40 hours. The mixture was quenched with HCl (50 mL, 0.1 N) and extracted with CH₂Cl₂ (50×2mL). The organic layer was washed with HCl (10 ×2 mL, 0.1 N), dried over MgSO₄, and concentrated under reduced pressure. The crude product was purified by flash

column chromatography (ethyl acetate/hexane = 5/1) to give (*R*)-**2-1** (3.67 g, 70 %; after recrystallization, ee > 98%). The enantiomeric ratio was determined by HPLC analysis using a Daicel Chiralpak IC column (Hex/i-Pr = 19/1, 1 mL/min, 20 °C, 210 nm, $t_{\text{minor}} = 25.8$ min, $t_{\text{major}} = 15.0$ min). The spectroscopic data are consistent with those reported in the literature.

¹H NMR (CDCl₃, 400 MHz): δ 1.44 (s, 9H), 4.67-4.71 (m, 1H), 4.83 (br s, 1H), 5.36 (br s, 1H), 7.29-7.40 (m, 5H).

¹³C NMR (CDCl₃, 100 MHz): δ 28.37, 52.99, 79.04, 80.80, 126.46, 128.81, 129.31, 137.04, 154.89.



Scheme S-5. Synthesis of compound **2-13**

S-4:^[4] To a MeOH solution of cinnamaldehyde (4.0 g, 30 mmol) under Ar was added benzoic acid (244 mg, 2 mmol, 10 %) and nitromethane (3.2 mL, 60 mmol), then catalyst (640 mg, 6mmol, 10 %), stirred at R.T. for 24 h, then quenched by sat. NaHCO₃ solution, extracted with EtOAc, and the collected organic phases were dried over anhydrous MgSO₄. Filtration and solvent evaporation afforded a crude product, which was further purified by silica gel chromatography (Hex/EA = 5/1) to afford **S-4**.

S-5: Under Ar, **S-4** (4.96 g, 26 mmol) was dissolved in ^tBuOH:H₂O (3:1, 52 mL) and then cooled to 0°C, NaH₂PO₄·2H₂O (8.01 g, 2.0 eq.) was added, followed by 2-methyl-2-butene (10.08 mL, 4.0 eq.) and NaClO₂ (6.96g, 3.0 eq.). The ice bath was removed, and the reaction was stirred for 2 hr, then quenched by sat. NH₄Cl solution and extracted with EtOAc. The combined organic phases were dried over anhydrous MgSO₄, filtered, the solvent evaporated, and the crude product purified via silica gel chromatography to give the carboxylic acid **S-5**.

(S)-methyl 4-nitro-3-phenylbutanoate 2-13: Under Ar, **S-5** (3.78 g, 18 mmol) was dissolved in CH₂Cl₂ (180 mL) and MeOH (7.3 mL) was added. The reaction mixture was cooled to 0°C and EDC·HCl (3.8 g, 19.6 mmol) was added, followed by DMAP (0.22 g, 1.8 mmol). After 1.5 hr, the reaction was quenched with sat. NH₄Cl solution, extracted with Et₂O and the combined organic phases were dried over anhydrous MgSO₄, filtered and evaporate to afford the crude product, which was purified by silica gel chromatography (Hex/EA = 5/1) and recrystallized (yield = 80 %, ee % > 98 %). Enantiomeric ratio was determined by using a Daicel Chiralpak IC HPLC column (Hex/i-Pr = 19/1, 1 mL/min, 20 °C, 210 nm, $t_{\text{minor}} = 20.13$ min, $t_{\text{major}} = 21.30$ min).

¹H NMR (CDCl₃, 400 MHz): 2.75-2.77 (m, 2H), 3.62 (s, 3H), 3.97 (quint, $J = 7.6$ Hz, 1H), 4.63 (dd, $J = 12.8, 8$ Hz, 1H), 4.72 (dd, $J = 12.8, 7.2$ Hz, 1H), 7.19-7.35 (m, 5H).

¹³C NMR (CDCl₃, 100 MHz): 37.67, 40.30, 52.10, 79.53, 127.43, 128.21, 129.24, 138.43, 171.21.

IR (neat): 2954, 1737, 1555, 1496, 1436, 1378, 1171, 1004, 766, 700 cm⁻¹.

HRMS (ESI) m/z calcd. for C₁₁H₁₃NNaO₄ (M+Na)⁺ 246.0737; found: 246.0740.

$[\alpha]_D^{20}$ -15.6 (c 1.30, CHCl₃).

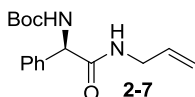
2.3 Characterization of amide and peptide products

General procedure:

Procedure A: To a reaction tube, the nitro-alkane (0.2 mmol), amine (0.2 mmol), dry CH₃CN (2 mL) were mixed and put under an O₂-balloon atmosphere. After cooling to 0 °C, NIS (0.2 mmol) and K₂CO₃ (0.4 mmol) were added under fast, but smooth stirring. After the nitroalkane disappeared by TLC monitoring, CHCl₃ or ethyl acetate was added to the reaction

and the precipitate filtered through a short silica gel column with additional solvent then washed by *sat.* Na₂S₂O₃. The combined organic solution was dried over anhydrous magnesium sulfate, the solvent removed *in vacuo* and the crude product purified by silica gel chromatography to give the pure amide product.

Procedure B: To a reaction tube, nitro-alkane (0.2 mmol), amine (0.4mmol), dry THF/Toluene = 1:1(v/v) (2 mL) were mixed and put under an O₂-balloon atmosphere. Keep the reaction stirring at R.T., K₂CO₃ (0.4 mmol) and I₂ (0.2 mmol) were added sequentially. Upon complete consumption of starting nitroalkane by TLC monitoring, CHCl₃ or ethyl acetate was added to the reaction and the precipitate filtered through a short silica gel column with additional solvent then washed by *sat.* Na₂S₂O₃. The combined organic solution was dried over anhydrous magnesium sulfate, the solvent removed *in vacuo* and the crude product purified by silica gel chromatography to give the pure amide product.



(R)-tert-butyl 4-(allylamino)-4-oxo-3-phenylbutanoate(2-7)

Following the Procedure A, white solid, yield = 66 %.

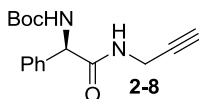
¹H NMR (400 MHz, CDCl₃): δ 1.40 (s, 9H), 3.83-3.86 (m, 2H), 4.98-5.06 (m, 2H), 5.16 (br s, 1H), 5.69-5.79 (m, 1H), 5.84 (br s, 1H), 5.92 (br s, 1H), 7.30-7.35 (m, 5H).

¹³C NMR (CDCl₃, 100 MHz): δ 28.43, 42.06, 58.62, 80.19, 116.44, 127.31, 128.45, 129.11, 133.72, 138.60, 155.34, 170.18.

IR (neat): 3312, 2976, 1700, 1654, 1522, 1497, 1364, 1249, 1169, 697.

HRMS (ESI): *m/z* calcd. for C₂₇H₃₄N₂NaO₆ (M+Na)⁺ 313.1523; found:313.1555.

[α]_D²⁰-97.1 (c 1.5, CHCl₃).



(R)-tert-butyl (2-oxo-1-phenyl-2-(prop-2-yn-1-ylamino)ethyl)carbamate(2-8)

Following the Procedure A, white solid, yield = 54 %.

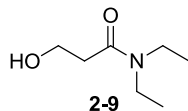
¹H NMR (400 MHz, CDCl₃): δ 1.41 (s, 9H), 2.19 (t, *J* = 2.4 Hz, 1 H), 3.94(ddd, *J* = 2.4, 5.2, 8.0 Hz, 1H), 4.07 (ddd, *J* = 2.8, 6.0, 8.4 Hz, 1H), 5.21 (br s, 1H), 5.80 (br s, 1H), 6.31(br s, 1H), 7.29-7.36 (m, 5H).

¹³C NMR (CDCl₃, 100 MHz): δ 28.30, 29.42, 58.36, 71.87, 78.90, 80.26, 127.23, 128.43, 129.01, 137.86, 155.19, 169.96.

IR (neat): 3311, 2976, 1700, 1658, 1528, 1497, 1367, 1251, 1169, 698 cm⁻¹.

HRMS (ESI): *m/z* calcd. for C₂₇H₃₄N₂NaO₆ (M+Na)⁺ 311.1366; found: 311.1392.

[α]_D²⁰-103.0 (c 1.00, CHCl₃).



N,N-diethyl-3-hydroxypropanamide(2-9)

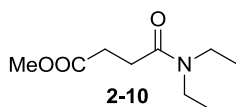
Following the Procedure A, colorless oil, yield = 65 %.

¹H NMR (400 MHz, CDCl₃): δ 1.10-1.19 (m, 6H), 2.52 (t, *J* = 5.2 Hz, 2H), 3.26-3.41 (m, 4H), 3.69 (br s, 1H), 3.86 (t, *J* = 5.2 Hz, 2H).

¹³C NMR (CDCl₃, 100 MHz): δ 13.16, 14.16, 34.65, 40.14, 41.96, 58.90, 171.94.

IR (neat): 3417, 2973, 1621, 1454, 1144, 1064 cm⁻¹.

HRMS (ESI) *m/z* calcd. for C₇H₁₅NNaO₂ (M+Na)⁺ 168.0995; found: 168.1002.



Methyl 4-(diethylamino)-4-oxobutanoate(2-10)

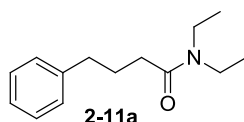
Following the Procedure A, colorless oil, yield = 71 %.

¹H NMR (400 MHz, CDCl₃): δ 1.09 (t, *J* = 7.2 Hz, 3H), 1.18 (t, *J* = 7.2 Hz, 3H), 2.58-2.62 (m, 2H), 2.64-2.68 (m, 2H), 3.31-3.38 (m, 4H), 3.67 (s, 3H).

¹³C NMR (CDCl₃, 100 MHz): δ 13.17, 14.24, 28.02, 29.36, 40.41, 41.91, 51.81, 170.33, 173.91.

IR (neat): 2975, 1738, 1643, 1436, 1365, 1223, 1172, 1142 cm⁻¹.

HRMS (ESI) *m/z* calcd. for C₉H₁₇NNaO₃ (M+Na)⁺ 210.1101; found: 210.1131.



N-diethyl-4-phenylbutanamide(2-11a)

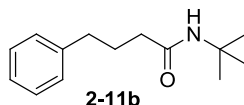
Following the Procedure A; colorless oil, yield = 75 %.

¹H NMR (400 MHz, CDCl₃): δ 1.09-1.13 (m, 6H), 1.99 (quint, *J* = 7.6 Hz, 2H), 2.30 (t, *J* = 7.6 Hz, 2H), 2.68 (t, *J* = 7.6 Hz, 2H), 3.23 (q, *J* = 7.2 Hz, 2H), 3.37 (q, *J* = 7.2 Hz, 2H), 7.16-7.30 (m, 5H).

¹³C NMR (CDCl₃, 100 MHz): δ 13.09, 14.28, 26.82, 32.17, 35.31, 40.05, 41.88, 125.81, 128.29, 128.48, 141.85, 171.83.

IR (neat): 2934, 1713, 1555, 1495, 1453, 1349, 749, 700 cm⁻¹.

HRMS (ESI) *m/z* calcd. for C₁₄H₂₂NO (M+H)⁺ 220.1696; found: 220.1699.



N-(tert-butyl)-4-phenylbutanamide(2-11b)

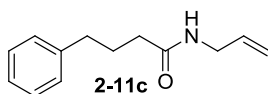
Following the Procedure A, colorless oil, yield = 51 %.

¹H NMR (400 MHz, CDCl₃): δ 1.33 (s, 9H), 1.90-1.98 (m, 2H), 2.08 (t, *J* = 7.6 Hz, 2H), 2.64 (t, *J* = 7.6 Hz, 2H), 5.23 (br s, 1H), 7.16-7.20 (m, 3H), 7.25-7.29 (m, 2H).

¹³C NMR (CDCl₃, 100 MHz): δ 27.24, 28.95, 35.22, 36.87, 51.20, 126.02, 128.47, 128.62, 141.77, 172.13.

IR (neat): 3310, 2965, 1645, 1549, 1453, 1363, 1225, 744, 698.

HRMS (ESI) *m/z* calcd. C₁₄H₂₁NNaO (M+Na)⁺ 242.1515; found: 242.1523.



N-allyl-4-phenylbutanamide(2-11c)

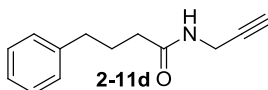
Following the Procedure A, colorless oil, yield = 77 %.

¹H NMR (400 MHz, CDCl₃): δ 1.93-2.08 (m, 2H), 2.18 (t, *J* = 7.6 Hz), 2.65 (t, *J* = 7.6 Hz), 3.84-3.87 (m, 2H), 5.09-5.18 (m, 2H), 5.52 (br s, 1H), 5.76-5.86 (m, 1H), 7.15-7.28 (m, 5H).

¹³C NMR (CDCl₃, 100 MHz): δ 27.22, 35.31, 35.97, 42.01, 116.51, 126.09, 128.51, 128.61, 134.42, 141.59, 172.60.

IR (neat): 3287, 3083, 2925, 1643, 1547, 1496, 1454, 1257, 989, 920, 745, 699.

HRMS (ESI): *m/z* calcd. for C₁₃H₁₇NNaO (M+Na)⁺ 226.1202; found: 226.1211.



4-phenyl-N-(prop-2-yn-1-yl)butanamide(2-11d)

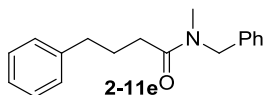
Following the Procedure A, colorless oil, yield = 60 %.

¹H NMR (400 MHz, CDCl₃): δ 1.95-2.03 (m, 2H), 2.19 (t, *J* = 7.6 Hz, 2H), 2.30 (t, *J* = 2.4 Hz, 1H), 2.66 (t, *J* = 7.6 Hz, 2H), 4.06 (q, *J* = 2.4 Hz, 2H), 5.54 (br s, 1H), 7.17-7.31 (m, 5H).

¹³C NMR (CDCl₃, 100 MHz): δ 26.82, 29.06, 35.02, 35.41, 71.48, 79.55, 125.95, 128.36, 128.44, 141.29, 172.38.

IR (neat): 3288, 2928, 1648, 1541, 1496, 1453, 1420, 1253, 1147, 1029, 746, 700 cm⁻¹.

HRMS (ESI): *m/z* calcd. for C₂₇H₃₄N₂NaO (M+Na)⁺ 224.1046; found:224.1045.



N-benzyl-N-methyl-4-phenylbutanamide(2-11e)

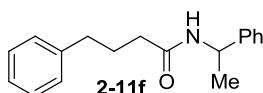
Following the Procedure A, colorless oil, yield = 58 % (A mixture of two rotamers A and B).

¹H NMR (400 MHz, CDCl₃): δ 1.97-2.07 (m, 2H, A+B), 2.38 (t, *J* = 7.6 Hz, 2H), 2.64-2.73 (m, 2H, A+B), 2.85 (s, 3aH, A), 2.95 (s, 3bH, B), 4.67 (s, 2bH, B), 4.59 (s, 2aH, A), 7.10-7.37 (m, 10H, A+B).

¹³C NMR (CDCl₃, 100 MHz): δ 26.51(A), 26.69(B), 32.17(B), 32.55(A), 33.93(B), 34.68 (A), 35.20(B), 35.24(A), 50.69(A), 53.25 (B), 125.79, 125.83, 126.23, 127.24, 127.50, 127.95, 128.27, 128.30, 128.40, 128.46, 128.51, 128.84, 136.60, 137.40, 141.64, 141.68, 172.82(A), 173.19(B).

IR (neat): 3025, 2927, 1646, 1495, 1452, 1403, 1116, 1028, 745, 699 cm⁻¹.

HRMS (ESI): *m/z* calcd. for C₁₈H₂₁NNaO (M+Na)⁺ 290.1515; found: 290.1525.



4-phenyl-N-(1-phenylethyl)butanamide(11f)

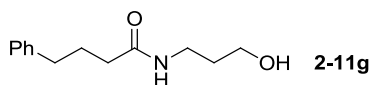
Following the Procedure A, colorless oil, yield = 65%.

¹H NMR (400 MHz, CDCl₃): δ 1.48 (d, *J* = 6.8 Hz, 3H), 1.94-2.01 (m, 2H), 2.15- 2.19 (m, 2H), 2.64 (t, *J* = 7.2 Hz, 2H), 5.15 (m, 1H), 5.56 (br s, 1H), 7.14-7.36 (m, 10H).

¹³C NMR (CDCl₃, 100 MHz): δ 21.64, 27.03, 35.06, 35.85, 48.55, 125.89, 126.12, 127.30, 128.32, 128.44, 128.60, 141.41, 143.16, 171.67.

IR (neat):3292, 3027, 2929, 1643, 1538, 1495, 1453, 1377, 745, 698 cm⁻¹.

HRMS (ESI): *m/z* calcd. for C₁₈H₂₁NNaO (M+Na)⁺ 290.1515; found: 290.1525.



N-(3-hydroxypropyl)-4-phenylbutanamide(2-11g)

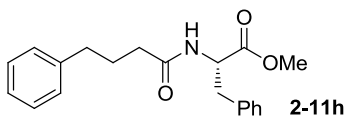
Following the Procedure A, white solid, yield = 67 %.

¹H NMR (400 MHz, CDCl₃): δ 1.61-1.67 (m, 2H), 1.92-1.99 (m, 2H), 2.18 (t, *J* = 7.2 Hz, 2H), 2.64 (t, *J* = 7.6 Hz, 2H), 3.38 (q, *J* = 6.0 Hz, 2H), 3.60 (t, *J* = 5.6, 2H), 5.86 (br s, 1H), 7.14-7.19 (m, 3H), 7.24-7.28 (m, 2H).

¹³C NMR (CDCl₃, 100 MHz): δ 27.29, 32.46, 35.31, 35.94, 36.33, 59.38, 126.15, 128.55, 128.61, 141.49, 174.24.

IR (neat): 3299, 2938, 1644, 1556, 1454, 1070, 700 cm⁻¹.

HRMS (ESI)*m/z* calcd. for C₁₃H₁₉NNaO₂ (M+Na)⁺ 244.1308; found: 244.1311.



(S)-methyl 3-phenyl-2-(4-phenylbutanamido)propanoate(2-11h)

Following the Procedure A, white solid, yield = 58 %. The enantiomeric ratio was determined by HPLC analysis using Daicel Chiralpak IE column (Hex/i-Pr = 10/1, 2 mL /min, 20 °C, 210 nm, t_{major} = 11.09 min, t_{minor} = 13.89 min).

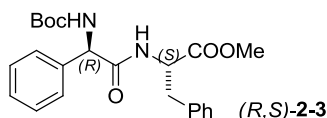
^1H NMR (400 MHz, CDCl_3): δ 1.90-1.97 (m, 2H), 2.17 (t, J = 7.2 Hz, 2 H), 2.61 (t, J = 7.2 Hz, 2H), 3.08(dd, J = 5.6, 13.6 Hz, 1H), 3.16 (dd, J = 6.0, 14 Hz, 1H), 3.73 (s, 3H), 4.91 (dd, J = 6.0, 14.0 Hz, 1 H), 5.82 (br d, J = 8.0 Hz, 1H), 7.07-7.29 (m, 10 H).

^{13}C NMR (CDCl_3 , 100 MHz): δ 26.87, 34.98, 35.55, 37.87, 52.30, 52.89, 125.92, 127.11, 128.35, 128.45, 128.56, 129.19, 135.81, 141.36, 172.14, 172.24.

IR (neat): 3297, 3027, 2950, 1745, 1648, 1540, 1496, 1454, 1436, 1215, 746, 700 cm^{-1} .

HRMS (ESI): m/z calcd. for $\text{C}_{20}\text{H}_{23}\text{NNaO}_3$ ($\text{M}+\text{Na}$) $^+$ 348.1570; found: 348.1586.

$[\alpha]_D^{20}$ 66.8 (c 0.90, CHCl_3).



N-Boc-Phenylglycine-(L)Phe-OMe(R,S-2-3)

Following the Procedure B, white solid, yield = 68 %. The enantiomeric ratio was determined by HPLC analysis using Daicel Chiralpak OD/H column (Hex/i-Pr = 19/1, 0.5 mL /min, 20 °C, 210 nm, t_{minor} = 18.30 min, t_{major} = 21.28 min).

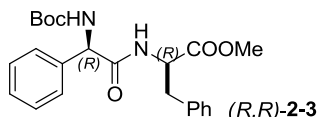
^1H NMR (400 MHz, CDCl_3): δ 1.39 (s, 9H), 2.94-2.97 (m, 2H), 3.69 (s, 3H), 4.87-4.91 (m, 1H), 5.11 (br s, 1H), 5.79 (br s, 1H), 6.13 (br s, 1H), 6.62 (d, J = 6.8 Hz, 2H), 7.03-7.37 (m, 8H).

^{13}C NMR (CDCl_3 , 100 MHz): δ 28.27, 37.59, 52.40, 52.99, 58.58, 80.00, 126.96, 127.16, 127.26, 128.38, 128.47, 128.60, 129.07, 129.13, 135.05, 138.36, 154.93, 169.36, 171.32.

IR (neat): 3318, 2977, 1743, 1662, 1497, 1456, 1366, 1050, 731, 699.

HRMS (ESI): m/z calcd. for $\text{C}_{27}\text{H}_{34}\text{N}_2\text{NaO}_6$ ($\text{M}+\text{Na}$) $^+$ 435.1890; found: 435.1900.

$[\alpha]_D^{20}$ -1.9 (c 1.00, CHCl_3).



N-Boc-Phenylglycine-(D)Phe-OMe (R,R-2-3)

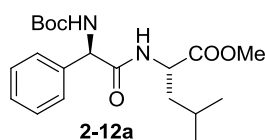
Following the Procedure B, white solid, yield = 67 %.

The enantiomeric ratio was determined by HPLC analysis using Daicel Chiralpak OD/H column (Hex/i-Pr = 19/1, 1 mL /min, 20 °C, 210 nm, t_{minor} = 21.23 min, t_{major} = 18.33 min).

^1H NMR (400 MHz, CDCl_3): δ 1.42 (s, 9H), 3.06 (dd, J = 14.0, 6.0 Hz, 1H), 3.16 (dd, J = 14.0, 5.6 Hz, 1H), 3.64 (s, 3H), 4.80 (ddd, J = 7.6, 6.0, 6.0 Hz, 1H), 5.10 (br s, 1H), 5.65 (br s, 1H), 6.21 (br s, 1H), 7.04-7.06 (m, 2H), 7.26-7.35 (m, 8H).

^{13}C NMR (CDCl_3 , 100 MHz): δ 28.40, 37.81, 52.42, 53.58, 58.88, 80.28, 127.30, 127.32, 128.53, 128.74, 128.93, 129.10, 129.37, 135.70, 137.84, 155.15, 169.86, 171.45.

$[\alpha]_D^{20}$ -93.0 (c 1.15, CHCl_3).



N-Boc-Phenylglycine-Leu-OMe(2-12a)

Following the Procedure B, white solid, yield = 64 %.

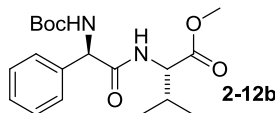
^1H NMR (400 MHz, CDCl_3): δ 0.77 (d, J = 6.54 Hz, 6H), 1.40 (s, 9H), 1.25-1.46 (m, 2H), 1.56 (ddd, J = 14.0, 8.4, 5.2 Hz, 1H), 3.72 (s, 3H), 4.59 (ddd, J = 9.2, 9.2, 4.8 Hz, 1H), 5.17 (br s, 1H), 5.75 (br s, 1H), 6.25 (d, J = 8.8 Hz, 1H), 7.27-7.37 (m, 5H).

¹³C NMR (CDCl₃, 100 MHz): δ 21.72, 22.83, 24.72, 28.38, 41.34, 50.93, 52.53, 58.81, 80.23, 127.34, 128.52, 129.12, 138.43, 169.96, 173.31.

IR (neat): 3316, 2957, 1744, 1717, 1682, 1522, 1496, 1367, 1246, 1169 cm⁻¹.

HRMS (ESI): *m/z* calcd. for C₂₇H₃₄N₂NaO₆ (M+Na)⁺ 401.2047; found: 401.2051.

[α]_D²⁰ -79.9 (c 1.00, CHCl₃).



N-Boc-Phenylglycine-Val-OMe(2-12b)

Following the Procedure B, white solid, yield = 67%.

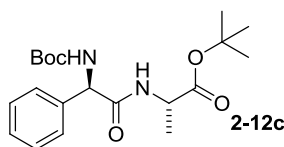
¹H NMR (400 MHz, CDCl₃): δ 0.66 (d, *J* = 7.2 Hz, 3H), 0.72 (d, *J* = 7.2 Hz, 3H), 1.39 (s, 9H), 2.03-2.08 (m, 1H), 3.72 (s, 3H), 4.53 (dd, *J* = 8.8, 4.8 Hz, 1H), 5.13 (br s, 1H), 5.69 (br s, 1H), 6.19 (br d, *J* = 8.0 Hz, 1H), 7.28-7.40 (m, 5H).

¹³C NMR (100 MHz, CDCl₃): δ 17.40, 18.87, 28.42, 31.49, 52.40, 57.16, 59.16, 80.29, 127.35, 128.60, 129.22, 138.60, 155.12, 169.99, 172.23.

IR (neat): 3322, 2977, 2934, 1723, 1673, 1497, 1392, 1367, 1240, 1167, 1083 cm⁻¹.

HRMS (ESI): *m/z* calcd. for C₁₉H₂₈N₂NaO₅ (M+Na)⁺ 387.1890; found: 387.1892.

[α]_D²⁰ -48.0 (c 0.96, CHCl₃).



N-Boc-Phenylglycine-Ala-OBu^t(2-12c)

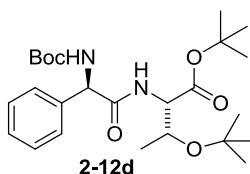
Following the Procedure B, white solid, yield = 67 %.

¹H NMR (400 MHz, CDCl₃): δ 1.23 (d, *J* = 7.2 Hz, 3H), 1.39 (s, 9H), 1.43 (s, 9H), 4.38-4.45 (m, 1H), 5.13 (br s, 1H), 5.71 (br d, *J* = 2.4 Hz, 1H), 6.29 (br d, *J* = 7.2 Hz, 1H), 7.27-7.38 (m, 5H).

¹³C NMR (100 MHz, CDCl₃): δ 18.41, 28.06, 28.41, 49.02, 58.74, 80.16, 82.40, 127.38, 128.46, 129.15, 138.52, 155.17, 169.47, 171.96.

IR (neat): 3418, 2976, 1747, 1713, 1650, 1486, 1434, 1366, 1170, 1056, 1024.

[α]_D²⁰ -63.1 (c 0.95, CHCl₃).



N-Boc-Phenylglycine-Thr(Obu^t)-Obu^t(2-12d)

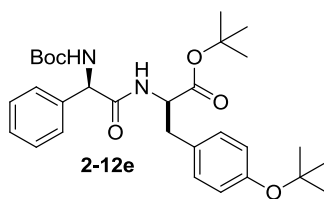
Following the Procedure B, sticky oil, yield = 71 %.

¹H NMR (400 MHz, CDCl₃): δ 0.86 (d, *J* = 6.0 Hz, 3H), 1.05 (s, 9H), 1.40 (s, 9H), 1.44 (s, 9H), 4.07-4.12 (m, 1H), 4.27 (dd, *J* = 8.8, 2.0 Hz, 1H), 5.17 (br s, 1H), 5.73 (br s, 1H), 6.47 (br d, *J* = 8.0 Hz, 1H), 7.24-7.41 (m, 5H).

¹³C NMR (100 MHz, CDCl₃): δ 20.60, 28.22, 28.44, 28.75, 58.59, 59.11, 67.33, 73.80, 80.06, 82.13, 127.37, 128.37, 129.08, 138.73, 155.04, 169.67, 170.23.

HRMS (ESI): *m/z* calcd. for C₂₅H₄₀N₂NaO₆ (M+Na)⁺ 487.2779; found: 487.2788.

[α]_D²⁰ -34.7 (c 1.40, CHCl₃).



N-Boc-Phenylglycine-Tyr(OBu^t)-OBu^t(2-12e)

Following the Procedure B, white solid, yield = 58 %.

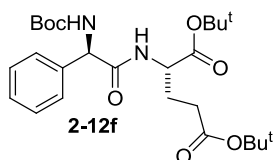
¹H NMR (400 MHz, CDCl₃): δ 1.26 (s, 9H), 1.31 (s, 9H), 1.39 (s, 9H), 3.01 (d, *J* = 6.4 Hz, 2H), 4.61 (dd, *J* = 12.8, 5.6 Hz, 1H), 5.08 (br s, 1H), 5.70 (br d, *J* = 2.8 Hz, 1H), 6.20 (br d, *J* = 3.6 Hz, 1H), 6.86-6.89 (m, 2H), 6.98 (d, *J* = 8.4 Hz, 2H), 7.25-7.33 (m, 5 H).

¹³C NMR (100 MHz, CDCl₃): δ 27.94, 28.40, 28.97, 37.45, 54.13, 58.99, 78.51, 80.22, 82.51, 124.21, 127.29, 128.50, 129.13, 130.09, 130.88, 138.11, 154.48, 155.21, 169.50, 169.91.

IR (neat): 3316, 2977, 1720, 1663, 1507, 1366, 1237, 1163, 898 cm⁻¹.

HRMS (ESI): *m/z* calcd. for C₃₀H₄₂N₂NaO₆ (M+Na)⁺ 549.2935; found: 549.2936;

[α]_D²⁰ -55.3 (c 1.30, CHCl₃).



N-Boc-Phenylglycine-Glu(OBu^t)-OBu^t(2-12f)

Following the Procedure B, sticky oil, yield = 61 %.

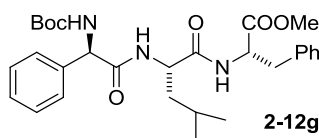
¹H NMR (400 MHz, CDCl₃): δ 1.33 (s, 9H), 1.39 (s, 9H), 1.42 (s, 9H), 1.85-1.93 (m, 1H), 2.04-2.12 (m, 1H), 2.18-2.32 (m, 2H), 4.39 (ddd, *J* = 8.0, 8.0, 4.8 Hz, 1H), 5.11 (br s, 1H), 5.74 (br s, 1H), 6.46 (br d, *J* = 7.6 Hz, 1H), 7.26-7.36 (m, 5H).

¹³C NMR (100 MHz, CDCl₃): δ 27.61, 27.99, 28.21, 28.43, 31.51, 52.86, 58.82, 80.18, 80.95, 82.50, 127.40, 128.50, 129.12, 138.19, 155.18, 169.95, 170.35, 172.42.

IR (neat): 3322, 2977, 2934, 1722, 1673, 1496, 1456, 1391, 1367, 1249, 1167, 1083 cm⁻¹.

HRMS (ESI): *m/z* calcd. for C₂₆H₄₀N₂NaO₇ (M+Na)⁺ 515.2728; found: 515.2729;

[α]_D²⁰ -46.3 (c 1.05, CHCl₃).



N-Boc-Phenylglycine-Leu-Phe-OMe(2-12g)

Following the Procedure B, white solid, yield = 50%.

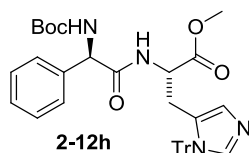
¹H NMR (400 MHz, ⁶d-DMSO): δ 0.55-0.66 (m, 6H), 0.81-0.86 (m, 1H), 1.12-1.26 (m, 1H), 1.38 (s, 9H), 1.62-1.64 (m, 1H), 2.94 (dd, *J* = 6.0, 14.0 Hz, 1H), 3.02 (dd, *J* = 6.0, 14.0 Hz), 3.55 (s, 3H), 4.16 (t, *J* = 8.0 Hz, 1H), 4.46 (dd, *J* = 14.0, 6.4 Hz, 1H), 5.30 (brd, *J* = 8.4 Hz, 1H), 5.17-7.30 (m, 10 H), 7.44 (d, *J* = 6.8 Hz, 2H), 8.15 (d, *J* = 8.8 Hz, 1H), 8.53 (d, *J* = 7.2 Hz, 1H).

¹³C NMR (100 MHz, ⁶d-DMSO): δ 10.60, 14.99, 23.72, 28.16, 36.53, 36.91, 51.74, 53.55, 56.18, 57.38, 78.40, 126.51, 127.06, 127.40, 128.06, 128.24, 129.04, 137.09, 139.18, 154.77, 169.83, 171.00, 171.71.

IR (neat): 3286, 2966, 1746, 1643, 1545, 1366, 1169, 697.

HRMS (ESI): *m/z* calcd. for C₂₇H₃₄N₂NaO₆ (M+Na)⁺ 548.2731; found: 548.2777.

[α]_D²⁰ -35.6 (c 0.2, CHCl₃).



N-Boc-Phenylglycine-His(Tr)-OMe(2-12h)

Following the Procedure B, white solid, yield =51 %.

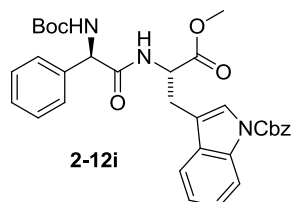
¹H NMR (400 MHz, CDCl₃): δ 1.36 (s, 9H), 2.80 (dd, *J* = 14.4, 4.0 Hz, 1H), 2.95 (dd, *J* = 14.8, 4.2 Hz, 1H), 3.59 (s, 3H), 4.61 (ddd, *J* = 7.2, 4.8, 4.8 Hz, 1H), 5.18 (br s, 1H), 5.90 (br s, 1H), 6.40 (s, 1H), 6.99-7.39 (m, 20 H), 7.80 (d, *J* = 6.4 Hz, 1H).

¹³C NMR (100 MHz, CDCl₃): δ 28.46, 29.40, 52.33, 53.13, 58.76, 75.43, 79.86, 119.52, 127.26, 128.11, 128.22, 128.26, 128.89, 129.89, 136.33, 138.84, 138.95, 142.35, 155.08, 170.15, 171.53.

IR (neat): 3318, 3061, 2977, 1747, 1715, 1678, 1493, 1445, 1366, 1240, 1170, 1131, 910 cm⁻¹.

HRMS (ESI): *m/z* calcd. for C₃₉H₄₁N₄O₅ (M+H)⁺ 645.3071; found: 645.3074.

[α]_D²⁰ -12.6 (c 0.80, CHCl₃).



N-Boc-Phenylglycine-Trp(Cbz)-OMe(2-12i)

Following the Procedure B, white solid, yield =60 %.

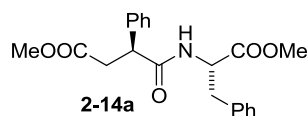
¹H NMR (400 MHz, CDCl₃): δ 1.35 (s, 9H), 3.03-3.12 (m, 2H), 3.64 (s, 3H), 4.90-4.95 (m, 1H), 5.08 (br s, 1H), 5.42 (dd, *J* = 16, 4.0 Hz, 2H), 6.57 (br s, 1H), 6.14 (br s, 1H), 7.06-7.50 (m, 14 H), 8.09 (d, *J* = 7.2 Hz, 1H).

¹³C NMR (100 MHz, CDCl₃): δ 27.65, 28.38, 52.26, 52.69, 58.74, 68.82, 80.18, 115.45, 115.48, 118.83, 123.20, 123.75, 125.03, 127.20, 128.49, 128.64, 128.95, 129.08, 129.43, 130.12, 135.20, 135.50, 138.10, 150.63, 169.99, 155.08, 169.97, 171.75.

IR (neat): 3316, 2977, 1720, 1663, 1507, 1366, 1237, 1163 898 cm⁻¹.

HRMS (ESI): *m/z* calcd. for C₃₃H₃₅N₃NaO₇ (M+Na)⁺ 608.2367; found: 608.2379;

[α]_D²⁰ -9.1 (c 0.85, CHCl₃).



(S)-methyl4-(((S)-1-methoxy-1-oxo-3-phenylpropan-2-yl)amino)-4-oxo-3-phenyl butanoate(2-14a)

Following the Procedure B, white solid, yield = 70 %.

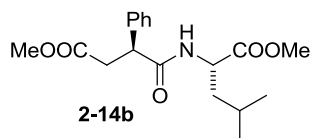
¹H NMR (400 MHz, CDCl₃): δ 2.63 (dd, *J* = 16.8, 6.0 Hz, 1H), 3.03 (dd, *J* = 5.6, 13.6 Hz, 1H), 3.10 (dd, *J* = 5.6, 13.6 Hz, 1H), 3.24 (dd, *J* = 9.2, 16.8 Hz, 1H), 3.61(s, 3H), 3.64 (s, 3H), 3.91 (dd, *J* = 8.8, 6.0 Hz, 1H), 4.76 (ddd, *J* = 8.0, 6.0, 6.0 Hz, 1H), 5.91 (d, *J* = 4.4 Hz, 1H), 7.03-7.05 (m, 2H), 7.19-7.32 (m, 8H);

¹³C NMR (CDCl₃, 100 MHz): δ 37.60, 37.83, 48.63, 51.97, 52.33, 53.54, 127.19, 127.91, 128.02, 128.67, 129.16, 129.39, 135.83, 138.26, 171.67, 171.82, 172.43;

IR (neat): 3330, 1739, 1675, 1522, 1436, 1171, 700 cm⁻¹.

HRMS (ESI): *m/z* calcd. for C₂₇H₃₄N₂NaO₆ (M+Na)⁺ 392.1468; found:392.1474;

[α]_D²⁰ 86.84 (c 1.00, CHCl₃).



(S)-methyl 2-((S)-4-methoxy-4-oxo-2-phenylbutanamido)-4-methylpentanoate(2-14b)

Following the Procedure B, white solid, yield = 61 %.

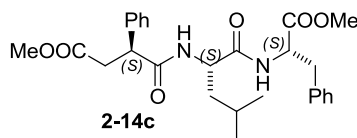
¹H NMR (400 MHz, CDCl₃): δ 0.88 (d, *J* = 1.2 Hz, 3H), 0.90 (d, *J* = 1.2 Hz, 3H), 1.42-1.49 (m, 1H), 1.54-1.64 (m, 2H), 2.61 (dd, *J* = 5.6, 16.4 Hz, 1H), 3.25 (dd, *J* = 9.2, 16.8 Hz, 1H), 3.61 (s, 3H), 3.62 (s, 3H), 3.95 (dd, *J* = 6.0, 9.2 Hz, 1H), 4.55 (ddd, *J* = 8.4, 8.4, 5.2 Hz, 1H), 5.80 (d, *J* = 8.4 Hz, 1H), 7.24-7.35 (m, 5H).

¹³C NMR (CDCl₃, 100 MHz): δ 21.90, 22.73, 24.76, 37.70, 41.39, 48.43, 50.97, 51.80, 52.16, 127.77, 127.99, 129.00, 138.26, 171.94, 172.37, 173.07.

IR (neat): 3292, 2957, 1740, 1644, 1560, 1437, 1252, 1020, 699.

HRMS (ESI): *m/z* calcd. for C₁₈H₂₅KNO₅ (M+K)⁺ 374.1364; found: 374.1362.

[α]_D²⁰ 74.7 (c 1.00, CHCl₃).



(S)-methyl 4-(((S)-1-(((S)-1-methoxy-1-oxo-3-phenylpropan-2-yl)amino)-4-methyl-1-oxopentan-2-yl)amino)-4-oxo-3-phenylbutanoate(2-14c)

Following the Procedure B, white solid, yield = 53 %.

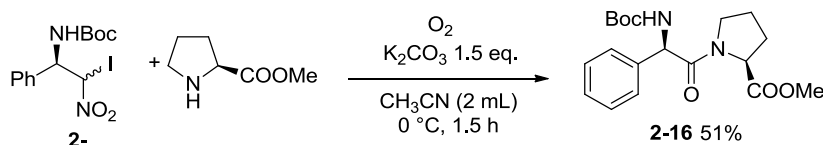
¹H NMR (400 MHz, CDCl₃): δ 0.80-0.83 (m, 6H), 0.90-0.98 (m, 1H), 1.20-1.27 (m, 1H), 1.80-2.03 (m, 1H), 2.66 (dd, *J* = 16.4, 5.6 Hz, 1H), 2.89 (dd, *J* = 14.0, 6.8 Hz, 1H), 2.98 (dd, *J* = 14.0, 5.6 Hz, 1H), 3.26 (dd, *J* = 17.2, 8.8 Hz, 1H), 3.64 (s, 3H), 3.67 (s, 3H), 3.94 (dd, *J* = 8.8, 5.6 Hz, 1H), 4.21 (dd, *J* = 8.8, 6.0 Hz, 1H), 4.72 (ddd, *J* = 7.6, 6.4, 6.4 Hz, 1H), 5.94 (d, *J* = 8.8 Hz, 1H), 6.05 (d, *J* = 8.0 Hz, 1H), 6.91-6.93 (m, 2H), 7.17-7.34 (m, 8H).

¹³C NMR (CDCl₃, 100 MHz): δ 11.50, 15.37, 24.65, 37.07, 37.65, 37.83, 48.75, 52.01, 52.47, 53.17, 57.90, 127.27, 127.93, 128.01, 128.74, 129.25, 129.31, 135.69, 138.50, 170.33, 171.60, 172.17, 172.47.

IR (neat): 3277, 3071, 2960, 1744, 1639, 1552, 1496, 1436, 1370, 1204, 1170, 990, 741, 699 cm⁻¹.

HRMS (ESI): *m/z* calcd. for C₂₇H₃₄N₂NaO₆ (M+Na)⁺ 505.2309; found: 505.2338.

[α]_D²⁰ 80.06 (c 1.00, CHCl₃).



N-Boc-Phenylglycine-Pro-OMe(2-16)

To a reaction tube, nitro-alkane **4** (0.2 mmol), L-proline methyl ester (0.3 mmol), dry CH₃CN (2 mL) were mixed and then put under an O₂-balloon atmosphere before K₂CO₃ (0.3 mmol) was added. The reaction was stirred at R.T. until **4** disappeared; CHCl₃ was then added to the reaction and the solid removed by washing through a short silica-gel column with CHCl₃. The eluent obtained was then washed with *sat.* Na₂S₂O₃, dried over MgSO₄, and purified via silica gel chromatography (Hex/EA = 3/1) to yield **16** as a white solid (yield = 51%).

¹H NMR (400 MHz, CDCl₃) major rotamer: δ 1.36 (s, 9H), 1.74-1.78 (m, 1H), 1.90-2.05 (m, 3H), 3.08-3.12 (m, 1H), 3.66-3.78 (m, 1H), 3.73 (s, 3H), 4.40 (dd, *J* = 8.0, 3.2 Hz, 1H), 5.39 (br d, *J* = 7.2 Hz, 1H), 6.06 (br d, *J* = 7.2 Hz, 1H), 7.24-7.37 (m, 5H).

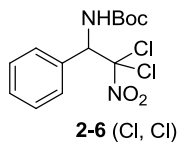
¹³C NMR (100 MHz, CDCl₃) major rotamer: δ 24.64, 28.45, 29.08, 46.83, 52.45, 56.74, 59.39, 79.72, 128.07, 128.33,

129.03, 137.79, 154.91, 168.96, 172.47.

IR (neat): 3418, 2977, 1747, 1713, 1650, 1487, 1434, 1306, 1171, 1056, 1025 cm^{-1} .

HRMS (ESI): m/z calcd. for $\text{C}_{19}\text{H}_{26}\text{N}_2\text{NaO}_5$ ($\text{M}+\text{Na}$)⁺ 385.1734; found: 385.1744.

$[\alpha]_D^{20}$ -165.4 (c 1.10, CHCl_3).

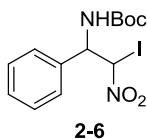


Di-chloro nitroalkane **2-6** (white solid, yield = 10 %)

^1H NMR (400 MHz, CDCl_3): δ 1.43 (s, 9H), 5.60 (br s, 1H), 5.96 (br d, $J = 9.2$ Hz, 1H), 7.37-7.44 (m, 5H).

^{13}C NMR (CDCl_3 , 100 MHz): δ 28.25, 63.88, 81.59, 116.08, 128.78, 128.96, 129.79, 133.25, 154.11.

HRMS (ESI) m/z calcd. for $\text{C}_{13}\text{H}_{16}\text{Cl}_2\text{N}_2\text{NaO}_4$ ($\text{M}+\text{Na}$)⁺ 357.0385, 359.0355; found: 357.0379, 359.0348.



^1H NMR (400 MHz, CDCl_3 , 1:1.67 mixture of diastereomers): δ 1.45, 1.47 (s, 9H), 5.23-5.33, 5.97(m, 2.0H), 6.59-6.61 (m, 1H), 7.27-7.41 (m, 5H).

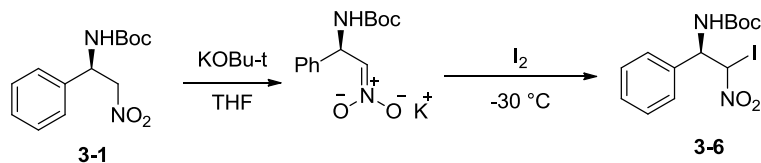
^{13}C NMR (CDCl_3 , 100 MHz, 1:1.67 mixture of diastereomers): δ 28.15, 28.20, 58.07, 81.01, 81.61, 85.20, 126.78, 126.97, 128.50, 129.01, 129.09, 129.13, 129.24, 129.54, 134.69, 135.25, 154.47, 154.74.

IR (neat): 3375, 1682, 1552, 1519, 1171 cm^{-1} .

HRMS (ESI) m/z calcd. for $\text{C}_{13}\text{H}_{17}\text{IN}_2\text{NaO}_4$ ($\text{M}+\text{Na}$)⁺ 415.0125; found: 415.0133.

Chapter 3

3.1. Preparing starting materials or key intermediates



Scheme S-1. Synthesis of α -iodonitroalkane **3-6**

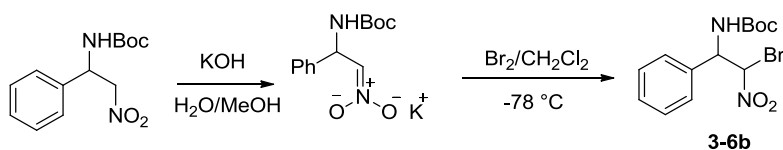
Synthesis of 3-6: Under Ar, nitroalkane (*R*)-**1** (532 mg, 2.0 mmol) was dissolved in THF (10 mL). The reaction mixture was cooled to 0°C and KOBu^t (224 mg, 2 mmol) was added. After 30 min, a white precipitation formed and cooling to -30 °C, I₂ (538 mg, 2.0 mmol) was added in one-portion. After a further 30 min, the reaction was quenched with *sat.* NH₄Cl solution (20 mmol) and extracted with CH₂Cl₂. The combined organic layers were washed with brine (10 mL), dried (MgSO₄), filtered and concentrated under reduced pressure to give crude **3-6**, which was columned via silica gel chromatography (Hex/EA = 5/1) to give pure **3-6** (470mg, 60%) as a white solid (stored at low temperature without light).

¹H NMR (400 MHz, CDCl₃, 1:1.67 mixture of diastereomers): δ 1.45, 1.47 (s, 9H), 5.23-5.33, 5.97(m, 2.0H), 6.59-6.61 (m, 1H), 7.27-7.41 (m, 5H).

¹³C NMR (CDCl₃, 100 MHz, 1:1.67 mixture of diastereomers): δ 28.15, 28.20, 58.07, 81.01, 81.61, 85.20, 126.78, 126.97, 128.50, 129.01, 129.09, 129.13, 129.24, 129.54, 134.69, 135.25, 154.47, 154.74.

IR (neat): 3375, 1682, 1552, 1519, 1171 cm⁻¹.

HRMS (ESI) m/z calcd. for C₁₃H₁₇IN₂NaO₄ (M+Na)⁺ 415.0125; found: 415.0133.



Scheme S-2. Synthesis of α -Bromo nitroalkane **3-6b**

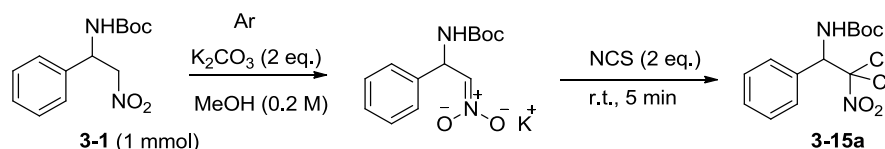
3-6b:^[7] Under Ar, the nitroalkane **1** (532 mg, 2 mmol) was dissolved in KOH solution [116 mg KOH in H₂O (6 mL) + MeOH(2 mL)] until the white solid disappeared. The resulting solution was cooled until it started to freeze and then bromine (324 mg, 1 mmol) in 10 mL of CH₂Cl₂ (pre-cooled to -78°C) was added, all at once, with vigorous stirring. After about 1 min, the layers are separated and the aqueous phase was extracted with 10 mL of CH₂Cl₂. The combined methylene chloride solutions were washed with 10 mL of H₂O and dried over anhydrous magnesium sulfate, and then the solvent was removed to give crude **3-6b**; further purification by silica gel chromatography (Hex/EA = 5/1) gave pure **3-6b** (552 mg, 80 %) as a white solid.

¹H NMR (400 MHz, CDCl₃, 1:1.4 mixture of diastereomers): δ 1.43, 1.44(s, 9H), 5.41-5.43 (m, 1H), 5.64-5.74 (m, 1H), 6.30 (s, 1H), 7.24-7.41 (m, 5H).

¹³C NMR (CDCl₃, 100 MHz, 1:1.4mixture of diastereomers): δ 28.15, 28.20, 58.07, 81.03, 81.62, 85.23, 126.76, 126.95, 129.09, 129.13, 129.25, 134.68, 135.22, 154.72.

IR (neat): 3356, 1691, 1566, 1517, 1367, 1166, 699.

HRMS (ESI) m/z calcd. for C₁₃H₁₇BrN₂NaO₄ (M+Na)⁺ 367.0264; found: 367.0273.



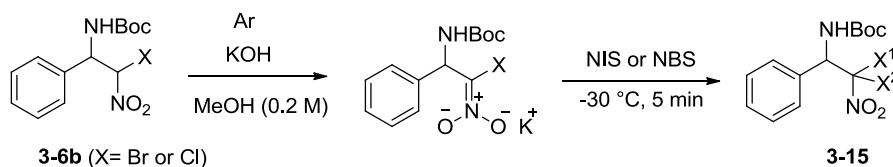
Scheme S-3. Synthesis of di-chloronitroalkane **3-15a**

3-15a: Nitroalkane **3-1** (1 mmol) was dissolved in methanol (5 mL) in a two necked flask. The flask was degassed using freeze-pump-thaw techniques and backfilled with nitrogen (3 cycles). Next, KOH (1.5 eq.) was added in one portion at R.T. and the reaction stirred for 10 min. NCS (2.2 eq.) was added in one portion and stirring continued for 10 min. The mixture was then quenched with *sat.* NH₄Cl (30 mL) and extracted with CH₂Cl₂ (25×2mL). The organic phase was dried over MgSO₄, and concentrated under reduced pressure. Crude product was purified by flash column chromatography (ethyl acetate / hexane = 1 / 5) to give **3-15a** (white solid, yield = 81 %)

¹H NMR (400 MHz, CDCl₃): δ 1.43 (s, 9H), 5.60 (br s, 1H), 5.96 (br d, *J* = 9.2 Hz, 1H), 7.37-7.44 (m, 5H).

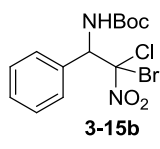
¹³C NMR (CDCl₃, 100 MHz): δ 28.25, 63.88, 81.59, 116.08, 128.78, 128.96, 129.79, 133.25, 154.11.

HRMS (ESI) *m/z* calcd. for C₁₃H₁₆Cl₂N₂NaO₄ (M+Na)⁺ 357.0385, 359.0355; found: 357.0379, 359.0348.



Scheme S-4A. Synthesis of di-halo nitroalkane **3-15**

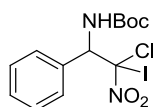
Procedure: Bromo nitroalkane **3-6b** (1 mmol) *or* chloro nitroalkane **3-6c** (1 mmol) was dissolved in methanol (5 mL) in a two necked flask; the flask was degassed using freeze-pump-thaw techniques and backfilled with nitrogen (3 cycles). Next, KOH (1.5 eq.) was added in one portion at 0 °C and the reaction stirred for 5 min. After cooling to -30 °C bath for 5-10 min, NIS or NBS (1.1 eq.) was added in one portion. Warming to 0 °C (over 5 min) produced some precipitate. The mixture was then quenched with *sat.* NH₄Cl (30 mL) and stirred rapidly until a lot of white solid was generated before extraction with CH₂Cl₂ (25×2mL, pre-cooled to -30 °C). The organic phase was dried over MgSO₄ at -30 °C (over a MeOH cooling bath), quickly filtered and the solution concentrated under reduced pressure. The crude product was purified by flash column chromatography (ethyl acetate/hexane = 1/5, pre-cooled to -30 °C for bromo / chloro iodo nitroalkane) to obtain relatively pure compound **3-15**. Further purification via recrystallization (CH₂Cl₂ + Hexane) in refrigerator (-30 °C) gave pure compounds **3-15**.



¹H NMR (400 MHz, CDCl₃, 1:1.9 *syn/anti* mixture of diastereomers): δ 1.41, 1.45 (s, 9H), 5.64-5.71 (m, 1 H), 5.98-6.00 (m, 1H), 7.33-7.47 (m, 5H).

¹³C NMR (CDCl₃, 100 MHz): δ 28.23, 28.28, 64.38, 81.46, 104.46, 105.46, 128.65, 128.76, 128.96, 129.17, 129.69, 129.72, 133.11, 133.66, 153.93, 154.22.

HRMS (ESI) *m/z* calcd. for C₁₃H₁₆BrClN₂NaO₄ (M+Na)⁺ 400.9880, 402.9859; found: 400.9887, 402.9863.

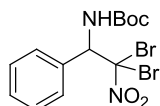


3-15c Yellow solid, yield= 60 %.

¹H NMR (400 MHz, CDCl₃, 1:2.25 *syn/anti* mixture of diastereomers): δ 1.42, 1.49 (s, 9H), 5.58, (d, J = 10.8 Hz, 0.78H), 5.80 (d, J = 10.0 Hz, 0.34H), 5.91 (d, J = 10.0 Hz, 0.31H), 6.06 (d, J = 10.4 Hz, 0.56H), 7.27-7.46 (m, 5H).

¹³C NMR (CDCl₃, 100 MHz): δ 28.33, 28.42, 65.69, 75.95, 81.47, 128.68, 128.84, 128.97, 129.38, 129.61, 129.65, 132.36, 154.31.

HRMS (ESI) *m/z* calcd. for C₁₃H₁₆ClIN₂NaO₄ (M+Na)⁺ 448.9741; found: 448.9737.

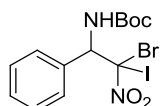


3-15d White solid, yield= 70 %.

¹H NMR (400 MHz, CDCl₃): δ 1.44 (s, 9H), 5.6 (br s, 1H), 5.97 (br d, J = 9.2 Hz, 1H), 7.35-7.45 (m, 5H).

¹³C NMR (CDCl₃, 100 MHz): δ 28.31, 64.71, 81.48, 94.54, 128.65, 129.16, 129.69, 133.77, 154.03.

HRMS (ESI) *m/z* calcd. for C₁₃H₁₆Br₂N₂NaO₄ (M+Na)⁺ 446.9354, 444.9375, 448.9334; found: 446.9349, 444.9370, 448.9326.

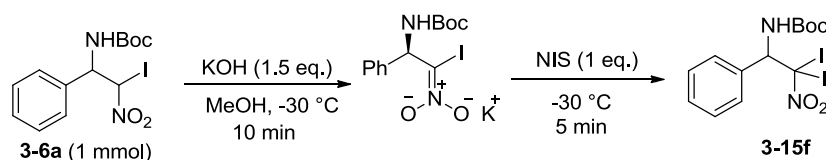


3-15e Yellow solid, yield= 60 %

¹H NMR (400 MHz, CDCl₃, 1:1.45 *syn/anti* mixture of diastereomers): δ 1.43, 1.48 (s, 9H), 7.31-7.48 (m, 5H).

¹³C NMR (CDCl₃, 100 MHz): δ 28.19, 28.26, 64.90, 65.61, 65.91, 77.21, 81.27, 128.45, 128.56, 128.87, 129.25, 129.42, 129.55, 133.07, 153.68, 154.04.

HRMS (ESI) *m/z* calcd. for C₁₃H₁₆BrIN₂O₄ (M+Na)⁺ 492.9236, 494.9215; found: 492.9232, 494.9211.

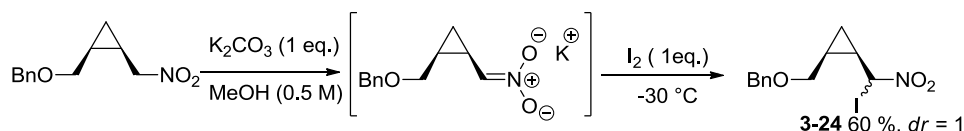


Scheme S-4B. Synthesis of di-iodo nitroalkane **3-15f**

3-15f: Iodo nitroalkane (1 mmol) was dissolved in methanol (5 mL) in a two-necked flask. The solution was degassed using freeze-pump-thaw techniques and backfilled with nitrogen (3 cycles). Next, KOH (1.5 eq.) was added in one portion at -30 °C and the reaction stirred for 10 min, at the same temperature, before NIS (1.5 eq.) was added and stirred continued for 3 min. The mixture was then quenched with *sat.* NH₄Cl (30 mL, pre-cooled to 0 °C) and quickly stirred until copious amounts of white (sticky) solid was generated. The aqueous was then extracted with CH₂Cl₂ (25×2mL, pre-cooled to -30 °C). The organic phase was dried over MgSO₄ (over a -30 °C MeOH bath), quickly filtrated and then concentrated under reduced pressure. The crude product was purified via recrystallization (CH₂Cl₂ + Hexane) in refrigerator (-30 °C) to obtain relatively pure compound **3-6f** (yellow sticky solid, yield = 50 %)

¹H NMR (400 MHz, CDCl₃): δ 1.45 (s,9H), 5.589 (d, J = 9.2 Hz, 1H), 5.733 (d, J = 8.4 Hz, 1H), 7.30-7.44 (m, 5H).

¹³C NMR (CDCl₃, 100 MHz): δ 28.38, 61.19, 66.54, 81.40, 128.64, 129.13, 129.51, 131.10, 153.97.



Scheme S-5. Synthesis of α -iodonitroalkane **3-24**

General procedure: Nitroalkane^[13] (1.105g, 5 mmol) was dissolved in 10 mL MeOH, then K_2CO_3 (1.035 g, 7.5 mmol) was added to stirred at R.T. for 10 min, then filter solid to collect solution. Cooling the solution to -30 , and added I_2 (1.27g, 5 mmol), slowly warm to 0, until the solution become darken, then pour the reaction mixture to 100 mL water, and extract by CH_2Cl_2 (100 mL). The combined organic solution was dried over anhydrous magnesium sulfate, the solvent removed *in vacuo* and the crude product purified by silica gel chromatography to give the pure **3-24** (a *ca.* 1:1 mixture of diastereomers)

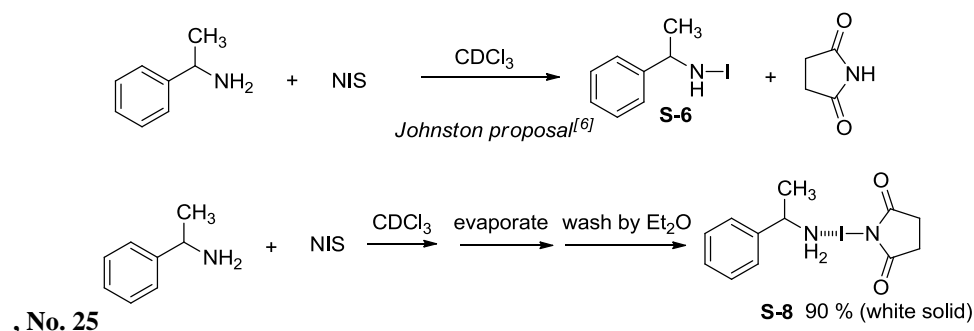
1H NMR (400 MHz, $CDCl_3$): δ 0.53-0.58 (m, 0.5 H), 0.81-0.85 (m, 0.5 H), 1.04-1.09 (m, 0.5 H), 1.14-1.19 (m, 0.5 H), 2.11-2.22 (m, 1H), 3.39 (dd, J = 3.6, 10.8 Hz, 0.5 H), 3.55 (dd, J = 5.6, 11.2 Hz, 0.5 H), 3.66 (dd, J = 4.0, 10.4 Hz, 0.5 H), 4.17-4.57 (m, 2H), 6.08 (d, J = 3.6 Hz, 0.5 H), 6.08-6.12 (m, 1H), 6.98-7.38 (m, 5H).

^{13}C NMR (400 MHz, $CDCl_3$): δ 11.09, 12.52, 18.44, 24.31, 24.51, 24.76, 52.23, 52.30, 66.07, 67.60, 73.15, 73.24, 127.83, 127.85, 127.88, 127.92, 128.46, 128.54, 137.50.

HRMS (ESI) m/z calcd. for $C_{12}H_{14}INNaO_3$ ($M+Na$)⁺ 369.9911; found: 369.9901.

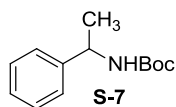
3.2. Mechanistic study

3.2.1 Nature of how NIS reacts with amine



Scheme S-6 NMR Study of amine with NIS in $CDCl_3$

In order to discern the reaction and chemical nature between NIS and α -methyl benzyl amine, we repeated the same reaction as described by Johnston.^[6] Mixing NIS and the amine in $CDCl_3$, we obtained the same 1H NMR spectrum, but were not convinced of the formation of **S-6**. For one experiment, we decided to trap the putative N-iodo amine **S-6** (as proposed by Jonhston) by adding $(Boc)_2O$. This would form a more stable N-iodo N-Boc-amide. From our NMR studies, only compound **S-7** lacking an N-iodo substituent formed. During a separate experiment, a white powder formed rapidly from CH_2Cl_2 , which after NMR and X-ray analysis of the related complex **15**, vide infra, was characterized to be an NIS:amine (1:1) complex **S-8**.



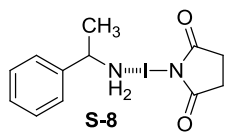
S-7: NIS (112 mg, 0.5 mmol) was added to 5 mL $CDCl_3$ in 0 °C, then 1-phenyl- ethanamine (0.5 mmol) was added. After stirring for 10 min, $(Boc)_2O$ (109 mg, 0.5 mmol) was added and the reaction monitored by 1H NMR. The solvent was eventually removed after stirring overnight and the product purified by column (Hex/EA = 3/1) to afford pure

S-7 (192 mg, 87 %) as a white solid. The spectroscopic data are consistent with those reported in the literature.^[5]

¹H NMR (CDCl₃, 400 MHz): δ 1.41 (s, 12 H), 4.77 (br s, 2H), 7.21-7.33 (m, 5H).

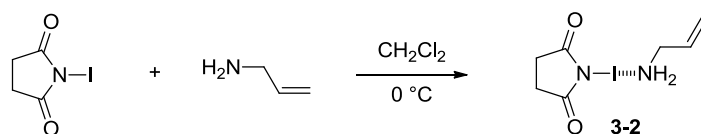
¹³C NMR (CDCl₃, 100 MHz): 22.83, 28.53, 37.47, 50.31, 79.56, 94.79, 126.02, 127.26, 128.70, 144.22, 155.25.

HRMS (ESI) *m/z* calcd. for C₁₄H₂₀NaO₂ (M+Na)⁺ 244.1356; found: 244.1318.



S-8: NIS (112 mg, 0.5 mmol) was added to dry CH₂Cl₂ (5 mL), cooled to 0 °C, then 1-phenylethanamine (0.5 mmol) was added. NIS quickly dissolved and a white solid formed after 5-10 min, which was filtered off, washed with Et₂O, and dried under vacuum to afford a white solid, yield = 90 %; at R.T. this product gradually darkened and decomposed, but was stable under Ar below -10 °C.

¹H NMR (400 MHz): δ 1.36 (d, *J* = 6.4 Hz, 1.5 H), 1.44 (d, *J* = 6.8 Hz, 1.5 H), 3.68 (q, *J* = 2.8 Hz, 0.5 H), 4.00 (q, *J* = 2.8 Hz, 0.5 H), 2.71 (s, 4H), 7.18-7.31 (m, 5H).



Scheme S-7. Synthesis of complex **3-2** of allylamine with NIS.

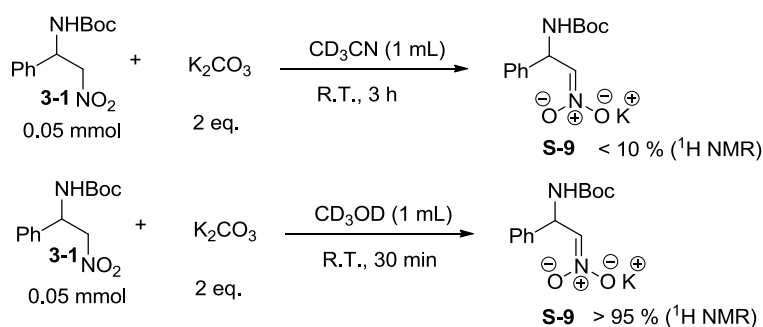
3-2: NIS (112 mg, 0.5 mmol) was dissolved in dry CH₂Cl₂ (5 mL), cooled to 0 °C, then allylamine (0.5 mmol) was added. After stirring for 10 min, the solvent was removed in vacuo and the yellow solid formed was washed with Et₂O and dried under vacuum to afford a white solid, yield = 90 %. At R.T., this product **3-2** darkened and decomposed, but was stable under Ar below -10 °C; latterly, **3-2** was crystallized for X-ray analysis (vide infra).

¹H NMR (CDCl₃, 400 MHz): δ 2.73 (s, 4H), 3.40 (d, *J* = 6.0 Hz, 2H), 5.19-5.24 (m, 2H), 5.83-5.93 (m, 1H).

¹³C NMR (CDCl₃, 100 MHz): δ 30.03, 47.36, 117.92, 135.81, 182.81.

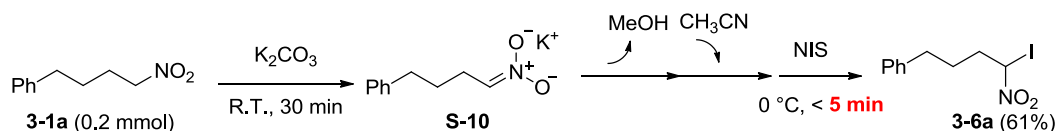
IR (neat): 3160, 1773, 1702, 1617, 1424, 1364, 1292, 1242, 1183, 817, 639 cm⁻¹.

3.2.2 Products formed when *aci*-nitronate salts react with NIS or amine-complex **3-2**



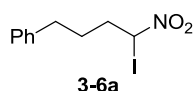
Scheme S-8. ¹H NMR deprotonation study of nitroalkane with base.

In order to understand the formation α-iodo nitroalkane from nitroalkane, the degree of formation of anion **S-9** from nitroalkane was studied by ¹H NMR. When mixed in CD₃CN with K₂CO₃, the nitroalkane **1** generated the anion **S-9** in less than 5 % yield after 3 h, indicating the nitroalkane deprotonates slowly. Suspecting solubility issues of K₂CO₃ in CH₃CN, the NMR solvent was changed to CD₃OD. In this case, we found the anion **S-9** formed in more than 95 % yield, relatively quickly within 30 min.



Scheme S-9A. Formation of α -iodonitroalkane **3-6a** using NIS

In order to determine the reaction of NIS with nitroalkane **3-1a**, the nitroalkane was first deprotonated by K_2CO_3 to form the anion **S-10** in methanol (**Scheme S-11A**). Subsequent removal of methanol, changing the solvent to CH_3CN , cooling to 0 °C, adding NIS (0.2 mmol) in one-portion, stirring for <5 min, quenching with *sat.* NH_4Cl solution, and purifying the crude by silica gel chromatography afforded the α -iodo nitroalkane **3-6a** in 61% yield.

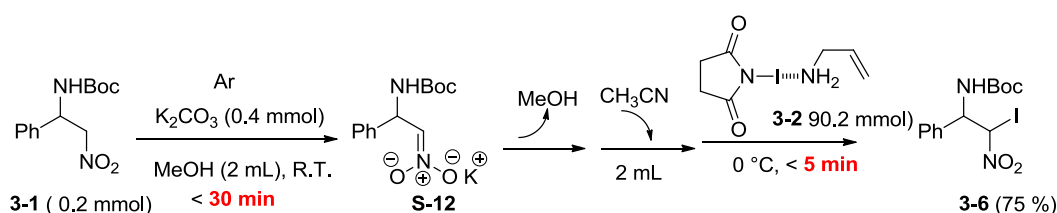


1H NMR ($CDCl_3$, 400 MHz): δ 1.63-1.79 (m, 2H), 2.20-2.28 (m, 1H), 2.29-2.45 (m, 1H), 2.66 (t, J = 7.2 Hz, 2H), 6.13 (t, J = 7.2 Hz, 1H), 7.13-7.30 (m, 5H).

^{13}C NMR ($CDCl_3$, 100 MHz): δ 29.37, 34.53, 38.63, 53.18, 126.46, 128.41, 129.71, 140.54.

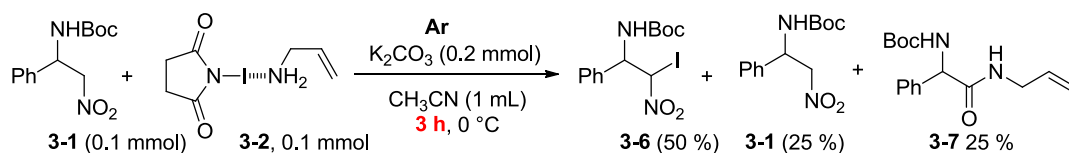
IR (neat): 2934, 1713, 1555, 1495, 1453, 1349, 749, 700 cm^{-1} .

HRMS (ESI) m/z calcd. for $C_{10}H_{12}INNaO_2$ ($M+Na$) $^+$ 327.9810; found 327.9811.



Scheme S-9B. Formation of α -iodo nitroalkane **3-6** using pre-generated anion.

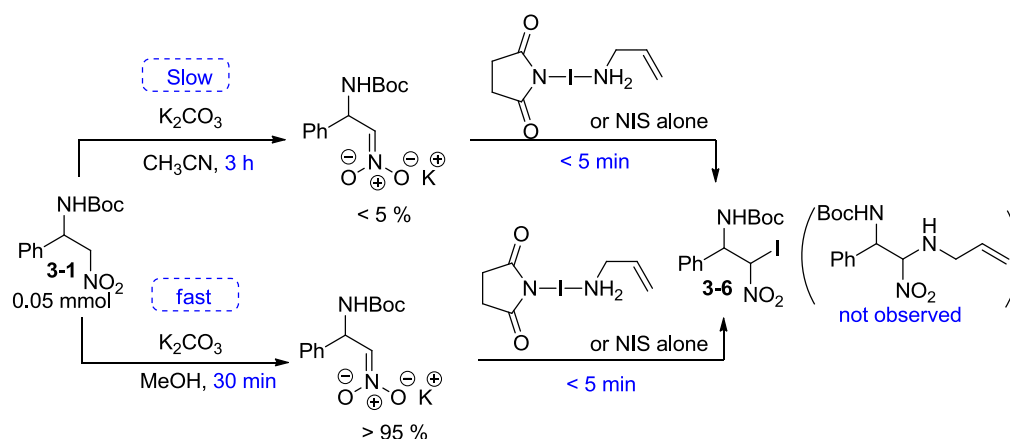
In order to show the NIS-amine complex **3-2** to be a source of electrophilic iodine, the nitroalkane **3-1** was deprotonated by K_2CO_3 to form anion **S-12** in methanol (**Scheme S-11B**). After 30 min, >95 % yield of anion **S-12** was generated. Subsequent removal of methanol, changing the solvent to CH_3CN , cooling to 0 °C, adding the pre-prepared complex **3-6** in one-portion, stirring for <5 min, quenching with *sat.* NH_4Cl solution, and purifying the crude by silica gel chromatography afforded the α -iodo nitroalkane **3-6** in 75 % yield.



Scheme S-9C. Formation of α -iodonitroalkane **3-6** using in situ-generated anion.

Under O_2 , the α -iodo nitroalkane reacts with the amine within 30 minutes. To check the intermediacy of α -iodonitroalkane **3-6**, we conducted reactions of **3-1** with NIS-amine complex **3-2** under Ar in presence of K_2CO_3 (**Scheme S-11C**). After 3 h, about 50 % of α -iodo nitroalkane **3-7**, 25 % amide and 25 % of starting nitroalkane **3-1** were observed. These yields and reaction times are consistent with reactions under O_2 .

Conclusion



Based on the above results, the nitroalkane **3-1** is first deprotonated by K_2CO_3 , which in CH_3CN is relatively slow when compared to MeOH. Once formed, the anion quickly reacts with NIS or the NIS-amine complex **3-2** (< 5 mins). All control reactions demonstrated the α -iodonitroalkane as the primary intermediate. In all cases, we did not observe the intermediacy or isolate any α -amino nitroalkane products.

3.3 Reaction of α -iodo nitroalkanes with amine or NIS-complex

(**Scheme S-10, A**): The α -iodonitroalkane **3-6** was mixed with amine in presence of K_2CO_3 (2 eq.) in CH_3CN at 0 °C under O_2 . After 30 min, the reaction was diluted with $CHCl_3$ and the precipitate removed through a short silica gel plug. Further purification by gel silica gel chromatography gave the pure amide product **3-7** (yield = 74 %).

(**Scheme S-10, B**): The α -iodo nitroalkane **3-6** was mixed with amine in presence of K_2CO_3 (2 eq.) in CH_3CN at 0 °C under Ar. After 3 h, the reaction was diluted with $CHCl_3$ and the precipitate removed through a short silica gel plug. The de-iodinated nitroalkane **3-1** and iodo nitroalkane **3-6** and trace amounts of amide **3-7** were calculated to be in a ratio of **3-6**:**3-1**:**3-7** = 42:40:18 by 1H NMR analysis.

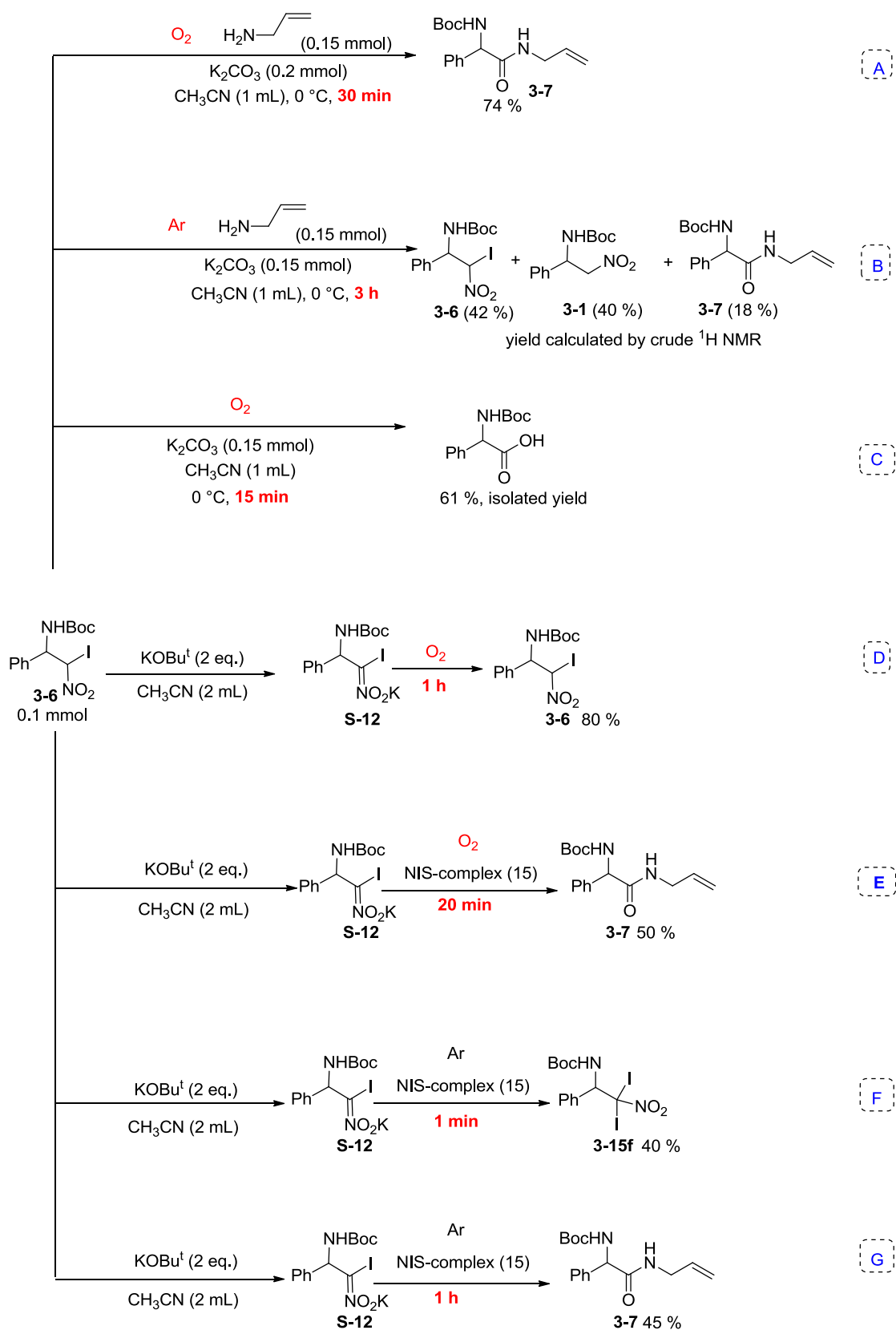
(**Scheme S-10, C**): The α -iodonitroalkane **3-6** was mixed with K_3CO_3 under an O_2 atmosphere. After 15 mins, the α -iodonitroalkane **3-6** reacted completely, as checked by TLC; after aqueous acid work-up, only the carboxylic acid was isolated in 61 % yield.

(**Scheme S-10, D**): The pre-formed pure anion **S-12** was prepared by reacting iodo nitroalkane with $KOBu^t$ (2 eq.) under Ar at -30 °C and the reaction system was saturated with O_2 atmosphere by freeze-thaw techniques. After 1h, the reaction was quenched with *sat.* NH_4Cl . Only the iodo nitroalkane **3-6** was recovered.

(**Scheme S-10, E**): The pre-formed pure anion **S-12** was prepared by reacting iodo nitroalkane with $KOBu^t$ (2 eq.) under Ar at -30 °C and the reaction system was saturated with O_2 atmosphere by freeze-thaw techniques. The NIS-complex **3-2** (1 eq.) was then added in one-portion at 0 °C, at the same temperature for 20 min, then reaction was diluted by $CHCl_3$ and further purify by silicane gel column chromatography (Hex/EA = 3/1), the amide **3-7** (50 %) was isolated.

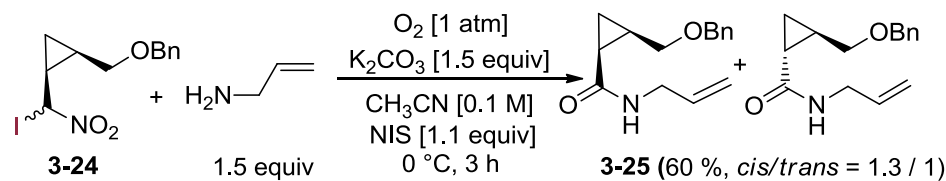
(**Scheme S-10, F**): The pre-formed pure anion **S-12** was prepared by reacting iodo nitroalkane with $KOBu^t$ (2 eq.) under Ar at -30 °C, then NIS-complex **3-2** (1.0 eq.) was added in one-portion. After 1 min, the reaction was quenched with cold *sat.* NH_4Cl (at -30 °C over a MeOH cooling bath). This gave 40 % di-iodo nitroalkane **3-15f** and recovered starting materials.

(**Scheme S-10, G**): The pre-formed pure anion **S-12** was prepared by reacting iodo nitroalkane with $KOBu^t$ (2 eq.) under Ar at -30 °C and the reaction system was saturated with Ar atmosphere by freeze-thaw techniques. The NIS-complex **3-2** (1 eq.) was then added in one-portion at 0 °C, at the same temperature for 1 h, then reaction was diluted by $CHCl_3$ and further purify by silicane gel column chromatography (Hex/EA = 3/1), the amide **3-7** (45 %) was isolated.



Scheme S-10. Reaction of α -iodonitroalkane **3-6**.

3.4 Radical clock reaction



Scheme S-II. Reaction of α -iodonitroalkane **3-24** with allyl amine.

Procedure: The iodo-nitroalkane **3-24** (0.1 mmol), K_2CO_3 (1.5 equiv), CH_3CN (1mL, pre-saturated with O_2) and allyl amine (0.15 mmol) were added to a 10 mL flask. The reaction mixture was then cooling to 0 °C before NIS (0.01 mol) was added, then the reaction put under an O_2 -balloon atmosphere. After the iodonitroalkane **3-24** disappeared by TLC monitoring, $CHCl_3$ was added to the reaction and the precipitate filtered through a short silica gel column. The solvent removed *in vacuo* and the crude product purified via flash silica gel column chromatography (Hexane/Ethyl acetate = 3/2, *cis/trans* = 1.3/1), *cis* and *trans* was determined by NOE.

HRMS (ESI): m/z calcd. for $C_{15}H_{19}NNaO_2$ ($M+Na$)⁺ 268.1308; found: 268.1307.

cis product: R_f = 0.45

1H NMR ($CDCl_3$, 400 MHz): δ 0.93-0.99 (m, 1H), 1.08-1.12 (m, 1H), 1.47-1.60 (m, 2H), 3.52 (dd, J = 9.6, 10.0 Hz, 1H), 3.80 (dd, J = 5.2, 10.0 Hz, 1H), 3.84-3.88 (m, 2H), 4.44 (dd, J = 11.6, 14.4 Hz, 2H), 5.06-5.20 (m, 2H), 5.75-5.85(m, 1H), 5.89 (br s, 1H), 7.23-7.33 (m, 5H).

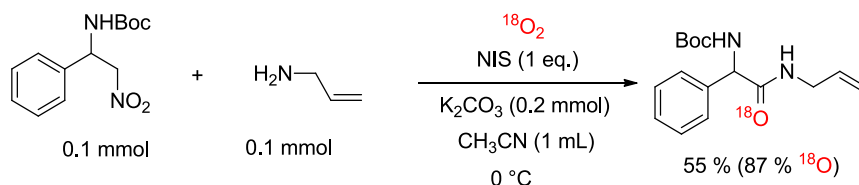
^{13}C NMR ($CDCl_3$, 100 MHz): δ 9.81, 19.57, 19.97, 42.15, 68.65, 72.94, 116.20, 127.50, 127.76, 128.28, 134.36, 138.41, 170.63.

trans product: R_f = 0.44

1H NMR ($CDCl_3$, 400 MHz): δ 0.73-0.77 (m, 1H), 1.18-1.23 (m, 1H), 1.28-1.32 (m, 1H), 1.62-1.76 (m, 1H), 3.31 (dd, J = 6.8, 10.4 Hz, 1H), 3.51 (dd, J = 5.6, 10.4 Hz, 1H), 3.81-3.94 (m, 2H), 4.50 (dd, J = 12.0, 15.2 Hz, 2H), 5.10-5.20 (m, 1H), 5.63 (br s, 1H), 5.78-5.88 (m, 1H), 7.24-7.35 (m, 5H).

^{13}C NMR ($CDCl_3$, 100 MHz): δ 11.83, 20.38, 42.18, 71.64, 72.55, 116.43, 127.63, 128.39, 134.33, 138.20, 172.19.

3.5 ^{18}O labeled reaction.



S-12. Nitroalkane reaction with amine under $^{18}O_2$

Procedure: The nitroalkane (0.1 mmol), K_2CO_3 (2.0 equiv), CH_3CN (1mL) and amine (0.1 mmol) were added to a 10 mL flask. The reaction mixture was then frozen under liquid nitrogen before NIS (0.1 mmol) was added and the reaction sealed with a glass septum screw cap and parafilm. The flask was degassed using three 10 minute freeze-pump-thaw cycles, after which the frozen solution was placed under high vacuum and the $^{18}O_2$ regulator needle was inserted through the septum. The vacuum line was closed and then the $^{18}O_2$ gas regulator was opened to fill the static vacuum. The flask was warmed to 0 °C and allowed to stir for 4.5 h before the reaction mixture was diluted with chloroform, filtered, and concentrated. The residue was purified via flash silica gel column chromatography.

^{18}O Percentage Mass Spectrometry Calculation

The amount of ^{18}O incorporation was determined as follows:

$(^{16}O \text{ ion intensity}) \times (\text{predicted } ^{18}O \text{ ion natural abundance in the unlabeled compound}) / 100 = ^{18}O \text{ ion intensity expected in}$

the unlabeled compound

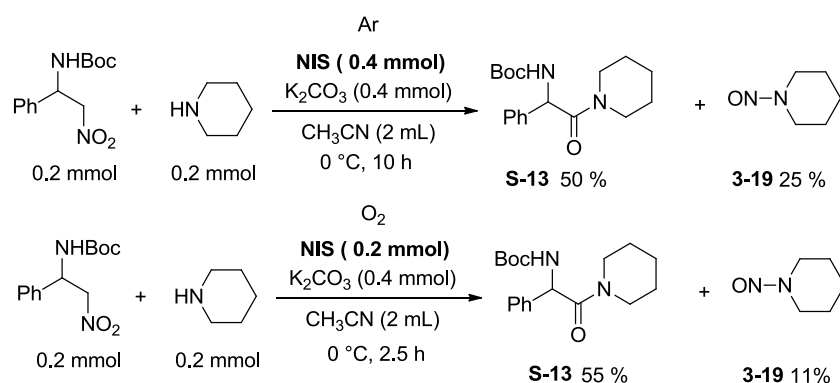
$(^{18}\text{O} \text{ ion intensity}) - (^{18}\text{O} \text{ ion intensity expected in the unlabeled compound}) = \text{corrected } ^{18}\text{O} \text{ ion intensity}$
 $(\text{Corrected } ^{18}\text{O} \text{ ion intensity}) / (\text{Corrected } ^{18}\text{O} \text{ ion intensity} + ^{16}\text{O} \text{ ion intensity}) \times 100 = \text{XX}\% (^{18}\text{O} \text{ incorporation})$

$^{18}\text{O} \text{ ion intensity expected in the unlabeled compound} = 14.96 \times 1.4 / 100 = 0.21$

corrected $^{18}\text{O} \text{ ion intensity} = 100 - 0.21 = 99.79$

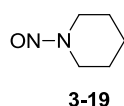
$^{18}\text{O} \text{ incorporation} = 99.79 / (99.79 + 14.96) \times 100 = 87 \%$

3.6 Isolate N-nitroso amines



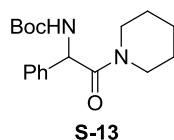
Scheme S-13. N-nitroso amines synthesis

Procedure: To a reaction tube, the nitro-alkane (0.2 mmol), K_2CO_3 (0.4 mmol), amine (0.2 mmol), and dry CH_3CN (2 mL) were added. After freezing in liquid nitrogen, NIS (0.4 mmol) was added and the reaction was sealed with a glass septum screw cap and parafilm. After degassing using three 10 minute freeze-pump-thaw cycles, i.e., saturating the solution with either Ar or O_2 , the solution was warmed over an ice-water bath for 5-10 min. After the nitroalkane disappeared as indicated by TLC, Et_2O was added to the reaction and the precipitate filtered through a short silica gel column. The combined organic solution was dried over anhydrous magnesium sulfate, the solvent removed *in vacuo*, and the crude product purified by silica gel chromatography (Et_2O /pentane = 1/2) to give the pure amide product **S-13** (yield =50 % under Ar; 55 % under O_2) and the N-nitroso amine **3-19** (yield =25 % under Ar; 11 % under O_2). NMR data were consistent with literature ^[12].



^1H NMR (400 MHz, CDCl_3): δ 1.48-1.58 (m, 2 H), 1.72-1.84 (m, 4H), 3.77 (t, J = 6.0 Hz, 2H), 4.18 (t, J = 6.0 Hz, 2H).

^{13}C NMR (CDCl_3 , 100 MHz): δ 24.33, 24.91, 26.57, 39.94, 51.00.

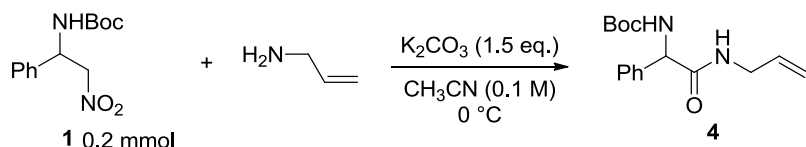


^1H NMR (400 MHz, CDCl_3): δ 0.84-0.94 (m, 1H), 1.25-1.43 (m, 3H), 1.40 (s, 9H), 1.47-1.54 (m, 2H), 3.21-3.29 (m, 2H), 3.37-3.46 (m, 1H), 3.67-3.73 (m, 1H), 5.53 (d, J = 8.0 Hz, 1H), 6.10 (d, J = 7.6 Hz, 1H), 7.23-7.36 (m, 5H).

^{13}C NMR (CDCl_3 , 100 MHz): δ 24.40, 25.49, 25.64, 28.50, 43.54, 46.53, 55.19, 79.65, 127.79, 128.11, 129.06, 138.75, 155.19, 168.12.

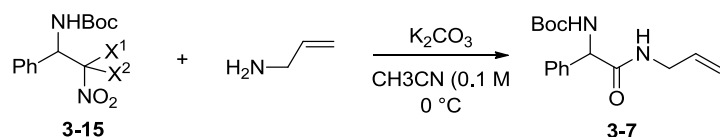
HRMS (ESI) m/z calcd. for $\text{C}_{18}\text{H}_{26}\text{N}_2\text{NaO}_3$ ($\text{M}+\text{Na}$)⁺ 341.1836; found: 341.1835

3.7 The effect of halogen sources^a



entry	NIS (mol %)	NIX-complex ^c (mol %)	other halogen source (mol %)	O ₂ ^b (1 atm)	time (h)	yield (%)
1	100			yes	4	66
2		100		yes	4	50
3		100		no	10	25
4		200		no	10	33
5	200			no	10	35
6			NCS (100)	yes	12	0
7			NBS (100)	yes	48	38
8	10		NBS (100)	yes	18	55
9			I ₂ (100)	yes	4	38
10	100		I ₂ (100)	no	10	26

^a Reactions were performed at 0.1 M of nitroalkane in 2.0 mL of CH₃CN with 1.0 equiv of allylamine; ^b All solutions were first degassed (freeze-pump-thaw cycles), and entries not using oxygen were performed under an argon atmosphere (balloon), whereas entries using oxygen were performed under an oxygen atmosphere (balloon). ^c Reaction performed without adding extra amine separately.



Scheme S-14. Di-halo nitroalkane **3-15** react with allylamine

General procedure: To a two necked flask, nitroalkane (0.1 mmol) in 1.0 mL of CH₃CN, the solutions were first degassed (freeze-pump-thaw cycles), not using oxygen were performed under an argon atmosphere (balloon), whereas using oxygen were performed under an oxygen atmosphere (balloon). Then cooled to 0 °C, allylamine (0.15 mmol) and base (0.15 mmol) were added by one-portion. After reaction finished, CHCl₃ was added to the reaction and the precipitate filtered through a short silica gel column. The crude product purified by silica gel chromatography (Hexane/Ethyl acetate = 3/1) to give the pure amide product.

(±)-tert-butyl 4-(allylamino)-4-oxo-3-phenylbutanoate(3-7)

¹H NMR (400 MHz, CDCl₃): δ 1.40 (s, 9H), 3.83-3.86 (m, 2H), 4.98-5.06 (m, 2H), 5.16 (br s, 1H), 5.69-5.79 (m, 1H), 5.84 (br s, 1H), 5.92 (br s, 1H), 7.30-7.35 (m, 5H).

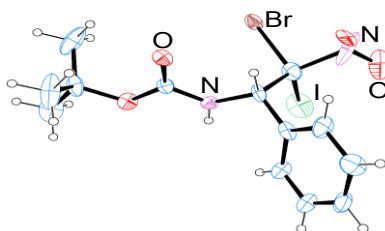
¹³C NMR (CDCl₃, 100 MHz): δ 28.43, 42.06, 58.62, 80.19, 116.44, 127.31, 128.45, 129.11, 133.72, 138.60, 155.34, 170.18.

IR (neat): 3312, 2976, 1700, 1654, 1522, 1497, 1364, 1249, 1169, 697.

HRMS (ESI): m/z calcd. for $C_{27}H_{34}N_2NaO_6$ ($M+Na$)⁺ 313.1523; found:313.1555.

3.8 X-Ray crystal structure and data of Bromo iodo-nitroalkane 3-15 (X = I, Br)

The single crystal of **15** (X = I, Br) suitable for X-ray analysis was grown in a solution of dichloromethane/Hexane at -30 °C under Ar; A colorless prism crystal of $C_{28}H_{32}Br_2I_2N_4O_8$ having approximate dimensions of $0.300 \times 0.100 \times 0.100$ mm was mounted on a glass fiber. All measurements were made on a Rigaku XtaLAB mini diffractometer using graphite monochromated Mo-K radiation. The crystal-to-detector distance was 50.00 mm. The data were collected at a temperature of -123 ± 1 °C to a maximum 2θ value of 55.0° . A total of 540 oscillation images were collected. The structure was solved by direct methods and expanded using Fourier techniques. Some non-hydrogen atoms were refined anisotropically, while the rest were refined isotropically. Crystallographic data has been deposited with the Cambridge Crystallographic Data Center, **CCDC reference number: 1054441**



EXPERIMENTAL DETAILS

A. Crystal Data

Empirical Formula	$C_{28}H_{32}Br_2I_2N_4O_8$
Formula Weight	966.20
Crystal Color, Habit	colorless, prism
Crystal Dimensions	0.300 X 0.100 X 0.100 mm
Crystal System	hexagonal
Lattice Type	Primitive
Lattice Parameters	$a = 21.554(3) \text{ \AA}$ $c = 15.8983(11) \text{ \AA}$ $V = 6396.4(13) \text{ \AA}^3$
Space Group	$P6_5$ (#170)
Z value	6
D_{calc}	1.505 g/cm^3
$F(000)$	2808.00
$m(\text{MoK}\alpha)$	33.962 cm^{-1}

B. Intensity Measurements

Diffractometer	XtaLAB mini
Radiation	MoK α ($\lambda = 0.71075 \text{ \AA}$) graphite monochromated
Voltage, Current	50kV, 12mA
Temperature	-123.0°C
Detector Aperture	75.0 mm (diameter)
Data Images	540 exposures
ω oscillation Range ($c=54.0$, $f=0.0$)	$-60.0 - 120.0^\circ$
Exposure Rate	32.0 sec./°
Detector Swing Angle	30.00°
ω oscillation Range ($c=54.0$, $f=120.0$)	$-60.0 - 120.0^\circ$

Exposure Rate	32.0 sec./°
Detector Swing Angle	30.00°
ω oscillation Range (c=54.0, f=240.0)	-60.0 - 120.0°
Exposure Rate	32.0 sec./°
Detector Swing Angle	30.00°
ω oscillation Range (c=54.0, f=0.0)	-60.0 - 120.0°
Exposure Rate	32.0 sec./°
Detector Swing Angle	30.00°
ω oscillation Range (c=54.0, f=120.0)	-60.0 - 120.0°
Exposure Rate	32.0 sec./°
Detector Swing Angle	30.00°
ω oscillation Range (c=54.0, f=240.0)	-60.0 - 120.0°
Exposure Rate	32.0 sec./°
Detector Swing Angle	30.00°
Detector Position	50.00 mm
Pixel Size	0.073 mm
2θ _{max}	55.0°
No. of Reflections Measured	Total: 67491 Unique: 9748 (R _{int} = 0.0522) Parsons quotients (Flack x parameter): 3780
Corrections	Lorentz-polarization Absorption (trans. factors: 0.358 - 0.712) Secondary Extinction (coefficient: 7.07000e-003)

C. Structure Solution and Refinement

Structure Solution	Direct Methods (SIR2008)
Refinement	Full-matrix least-squares on F ²
Function Minimized	$\sum w (F_o^2 - F_c^2)^2$
Least Squares Weights	$w = 1 / [s^2(F_o^2) + (0.2000 \cdot P)^2 + 0.0000 \cdot P]$ where $P = (\text{Max}(F_o^2, 0) + 2F_c^2) / 3$
2θ _{max} cutoff	55.0°
Anomalous Dispersion	All non-hydrogen atoms
No. Observations (All reflections)	9748
No. Variables	388
Reflection/Parameter Ratio	25.12
Residuals: R1 (I>2.00σ(I))	0.1084
Residuals: R (All reflections)	0.1166
Residuals: wR2 (All reflections)	0.3200
Goodness of Fit Indicator	1.425
Flack parameter (Parsons' quotients = 3780)	0.472(8)
Max Shift/Error in Final Cycle	0.000
Maximum peak in Final Diff. Map	5.69 e ⁻ /Å ³
Minimum peak in Final Diff. Map	-2.49 e ⁻ /Å ³

Table 1. Atomic coordinates and B_{iso}/B_{eq}

atom	x	y	z	B _{eq}
------	---	---	---	-----------------

I2	0.64105(8)	0.23086(9)	0.25027(11)	4.80(4)
I33	0.46693(12)	-0.04374(12)	0.0057(2)	7.78(7)
Br1	0.47984(11)	0.00640(12)	0.20389(14)	3.92(4)
Br30	0.76104(7)	0.35020(7)	0.12158(8)	1.80(3)
O1	0.9019(6)	0.3068(6)	0.1663(8)	3.0(2)
O2	0.8255(6)	0.1963(7)	0.1149(9)	3.4(2)
O3	0.6797(7)	0.0921(6)	0.2179(9)	3.2(2)
O4	0.6770(7)	-0.0123(6)	0.1806(9)	3.5(2)
O26	0.8099(8)	0.4247(7)	0.3038(11)	4.1(3)
O29	0.6942(7)	0.3754(8)	0.3217(10)	3.8(2)
O35	0.4428(14)	0.0792(13)	0.008(2)	8.3(7)
O36	0.5144(12)	0.1452(9)	0.0875(11)	4.9(4)
N23	0.7922(7)	0.2356(7)	0.2246(9)	2.5(2)
N24	0.6214(8)	0.0276(7)	0.1013(9)	2.8(2)
N25	0.7467(8)	0.3734(7)	0.2973(9)	3.1(2)
N34	0.4842(13)	0.1023(17)	0.0669(17)	8.2(10)
C2	0.8464(9)	0.2516(10)	0.1675(9)	2.7(3)
C3	0.6267(9)	0.1055(8)	-0.0147(13)	3.1(3)
C4	0.7990(14)	0.2982(14)	0.5187(14)	4.5(4)
C5	0.5984(8)	0.0754(8)	0.0730(12)	2.9(3)
C6	0.8136(11)	0.3171(12)	0.4351(11)	3.4(3)
C7	0.7154(10)	-0.0150(11)	0.2558(17)	4.3(4)
C8	0.6766(15)	0.1606(14)	-0.1721(14)	4.7(4)
C9	0.7545(13)	0.2211(15)	0.5374(13)	4.4(4)
C10	0.6355(11)	0.0647(10)	-0.0786(12)	3.5(3)
C11	0.7290(13)	0.1760(16)	0.4813(15)	4.8(5)
C12	0.8711(12)	0.2006(15)	0.0457(15)	5.3(6)
C13	0.5124(11)	0.0392(13)	0.0787(16)	4.4(4)
C14	0.7885(15)	0.0492(10)	0.261(3)	7.5(10)
C15	0.8223(17)	0.1277(14)	0.0037(19)	6.1(7)
C16	0.7400(8)	0.3119(8)	0.2465(11)	2.5(2)
C17	0.6453(14)	0.1763(11)	-0.0341(16)	4.6(4)
C18	0.6709(15)	0.2044(12)	-0.1155(19)	5.3(5)
C19	0.7163(17)	-0.0814(13)	0.242(2)	6.5(7)
C20	0.8799(16)	0.2533(15)	-0.0187(18)	5.4(5)
C21	0.952(5)	0.233(8)	0.083(4)	32(7)
C22	0.6746(19)	-0.0197(14)	0.3379(18)	7.0(9)
C27	0.6599(8)	0.0370(9)	0.1709(11)	2.7(3)
C28	0.7381(11)	0.1930(12)	0.3939(11)	3.5(3)
C31	0.7826(9)	0.2667(10)	0.3706(11)	2.8(3)
C32	0.6602(15)	0.0927(15)	-0.1530(14)	4.9(4)
C37	0.965(4)	0.693(4)	0.304(4)	10.9(14)
C39	0.7954(8)	0.2894(8)	0.2788(11)	2.5(2)
C40	0.905(4)	0.634(4)	0.236(5)	12.8(19)

$$B_{eq} = 8/3 p^2(U_{11}(aa^*)^2 + U_{22}(bb^*)^2 + U_{33}(cc^*)^2 + 2U_{12}(aa^*bb^*)\cos g + 2U_{13}(aa^*cc^*)\cos b + 2U_{23}(bb^*cc^*)\cos a)$$

Table 2. Atomic coordinates and B_{iso} involving hydrogen atoms

atom	x	y	z	B _{iso}
H4	0.81679	0.33315	0.56208	5.394

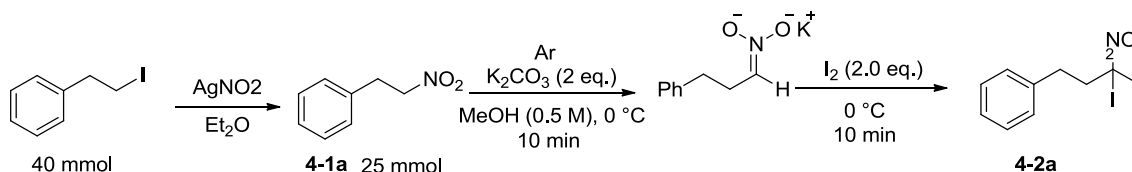
H5	0.61920	0.11705	0.11255	3.491
H6	0.84555	0.36576	0.42100	4.110
H8	0.69273	0.17802	-0.22734	5.616
H9	0.74538	0.20594	0.59436	5.323
H10	0.62337	0.01664	-0.06748	4.163
H11	0.70157	0.12705	0.49700	5.755
H14A	0.81418	0.05489	0.20840	8.962
H14B	0.81492	0.04301	0.30767	8.962
H14C	0.78455	0.09193	0.27149	8.962
H15A	0.77679	0.12444	-0.01215	7.332
H15B	0.81310	0.08909	0.04312	7.332
H15C	0.84586	0.12316	-0.04676	7.332
H17	0.64074	0.20545	0.00744	5.465
H18	0.68353	0.25208	-0.12977	6.381
H19A	0.74182	-0.07765	0.18910	7.831
H19B	0.66704	-0.12143	0.23756	7.831
H19C	0.74073	-0.08970	0.28854	7.831
H20A	0.90272	0.30120	0.00646	6.469
H20B	0.83287	0.24133	-0.04111	6.469
H20C	0.91003	0.25246	-0.06434	6.469
H21A	0.95284	0.19946	0.12476	38.821
H21B	0.96792	0.27924	0.10973	38.821
H21C	0.98527	0.23881	0.03702	38.821
H22A	0.69854	-0.02751	0.38570	8.408
H22B	0.62524	-0.05956	0.33388	8.408
H22C	0.67418	0.02521	0.34606	8.408
H23	0.75532	0.19180	0.22734	3.036
H24	0.60943	-0.01094	0.07092	3.362
H28	0.71545	0.15671	0.35251	4.242
H32	0.66678	0.06473	-0.19437	5.876
H39	0.84450	0.33216	0.27412	3.013

References

- [1] L. M. Hu, F. J. Xiong, X. F. Chen, W. X. Chen, Q. Q. He, F. E. Chen, *Tetrahedron: Asymmetry* **2013**, 24, 207-211.
- [2] G. R. Newkome, H. J. Kim, C. N. Moorefield, H. Maddi, K. S. Yoo, *Macromolecules* **2003**, 36, 4345-4354.
- [3] C. Palomo, M. Oiarbide, A. Laso, R. Lopez, *J. Am. Chem. Soc.* **2005**, 127, 17622-17623.
- [4] H. Gotoh, H. Ishikawa, Y. Hayashi, *Org. Lett.* **2007**, 9, 5307-5309. **Vol. 9, No**
- [5] L. Keller, S. Beaumont, J. M. Liu, S. Thoret, J. S. Bignon, J. Wdzieczak-Bakala, P. Dauban, R. H. Dodd, *J. Med. Chem.* **2008**, 51, 3414-3421.
- [6] (a) B. Shen, D. M. Makley, J. N. Johnston, *Nature* **2010**, 465, 1027-1032. (b) J. P. Shackleford, B. Shen, J. N. Johnston, *Proc. Natl. Acad. Sci. USA* **2012**, 109, 44-46; (c) K. E. Schwieter, B. Shen, J. P. Shackleford, M. W. Leighty, J. N. Johnston, *Org. Lett.* **2014**, 16, 4714-4717; (d) K. E. Schwieter, J. N. Johnston, *Chem. Sci.* **2015**, 6, 2590-2595.
- [7] A. S. Erickson, N. Kornblum, *J. Org. Chem.* **1977**, 42, 3764-3767.
- [8] B. R. Cho, S. J. Lee, Y. K. Kim, *J. Org. Chem.* **1995**, 60, 2072-2076.
- [9] Y. Takeuchi, M. Asahina, A. Murayama, K. Hori, T. Koizumi, *J. Org. Chem.* **1986**, 51, 956-958.
- [10] J. E. M. N. Klein, H. Müller-Bunz, P. Evans, *Org. Biomol. Chem.*, **2009**, 7, 986-995.
- [11] E. J. Corey, C.-P. Chen, G. A. Reichard, *Tetrahedron Lett.* **1989**, 30, 5547-5550.
- [12] N. Tokitoh, R. J. Okazaki, *Bull. Chem. Soc. Jpn.*, **1987**, 60, 3291-3297.
- [13] S. Umemiya, K. Nishino, I. Sato, Y. Hayashi, *Chem. Eur. J.* **2014**, 20, 15753-15759.

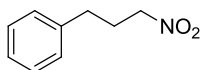
Chapter 4

4.1 Synthesis of α,α -diiodonitroalkane 4-2a.



Scheme S-1. Synthesis of nitroalkane 4-2a

Synthesis nitroalkane 4-1a: Iodide compound was dissolved in dry Et₂O (50 mL), then AgNO₂ was added by one-portion. The reaction mixture was stirred at r.t. until all the iodide compound was completely consumed. Then filter and concentrated under reduced pressure to afford crude compound **4-1a**, which was columned via silica gel chromatography (Hex/EA = 10/1) to give pure **4-1a** (62.5%) as a colorless sticky oil.



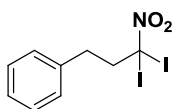
¹H NMR (400 MHz, CDCl₃): δ 2.28-2.35 (m, 2H), 2.71 (t, J = 7.2 Hz, 2H), 4.35 (t, J = 7.2 Hz, 2H), 7.16-7.32 (m, 5H).

¹³C NMR (100 MHz, CDCl₃): δ 28.82, 32.21, 74.64, 126.58, 128.42, 128.70, 139.44.

IR (neat): 2929, 1552, 1383, 701 cm⁻¹.

HRMS (ESI): m/z calcd. for C₉H₁₁NNaO₂ (M + Na)⁺ 188.0682; found: 188.0885.

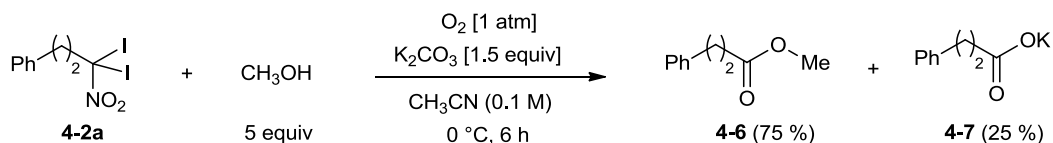
Synthesis α,α -diiodonitroalkane 4-2a: Nitroalkane **4-1a** (25 mmol) was dissolved in methanol (50 mL) in a two necked flask. The flask was degassed using freeze-pump-thaw techniques and backfilled with nitrogen (3 cycles). Next, K₂CO₃ (2.0 equiv.) was added by one portion at 0 °C and the reaction stirred for 10 min. Then cooled the reaction mixture to -30 °C and I₂ (2.0 eq.) was added at same reaction temperature, further stirring for 10 min. The mixture was then quenched with NH₄Cl (400 mL) and extracted with pre-cooled CH₂Cl₂ (-30 °C, 150×2mL). The organic phase was dried over Mg₂SO₄ and keep the flask at -30 °C bath. Then filtered and concentrated under reduced pressure at ice bath to afford yellow solid crude compound. The crude product was purified via recrystallization (CH₂Cl₂ + Hexane) in refrigerator for 3 times (-30 °C) to obtain yellow crystal **4-2a** (yield = 40 %) as show in bellow. (Caution: The key to observe sigmoidal kinetic profile is the purity of α,α -diiodonitroalkane **4-2a**. This compound can be stored at -30 °C more than half one year without any decomposition).



¹H NMR (400 MHz, CD₃CN): δ 2.76-2.80 (m, 2H), 3.01-3.14 (m, 2H), 7.23-7.36 (5H).

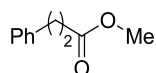
¹³C NMR (100 MHz, CD₃CN): δ 23.29, 42.10, 59.39, 131.91, 133.97, 143.68.

4.2 Kinetic study of α,α -diiodonitroalkane **4-2a** reacting with MeOH and amine using ^1H NMR.



Procedure: To a 10 mL reaction tube, α,α -diiodonitroalkane **4-2a** (0.4 mmol) and dry CH_3CN (4 mL, pre-saturated with O_2) were mixed and put under an O_2 -balloon atmosphere. CH_2Br_2 (0.4 mmol) was added as internal standard. After that, MeOH (2.0 mmol) and K_2CO_3 (0.6 mmol) were added under fast, but smooth stirring at r.t. Every 10 minutes, take out 100 μL reaction mixture and diluted by CDCl_3 (600 μL), checking ^1H NMR to estimate the yield of ester.

Organic phase:

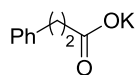


^1H NMR (400 MHz, CDCl_3): δ 2.62 (t, $J = 8.0$ Hz, 2H), 2.94 (t, $J = 8.0$ Hz, 2H), 7.18-7.30 (m, 5H).

^{13}C NMR (100 MHz, CDCl_3): δ 30.92, 35.68, 51.60, 126.25, 128.25, 128.49, 140.49, 173.33.

HRMS (ESI): m/z calcd. for $\text{C}_{10}\text{H}_{12}\text{NaO}_2$ $[\text{M}+\text{Na}]^+$ 187.0730; found: 187.0716.

Water phase:



(The data is consistent with auto-sample)

^1H NMR (400 MHz, D_2O): δ 2.66-2.70 (m, 2H), 2.93-2.97 (m, 2H), 7.18-7.30 (m, 5H).

^{13}C NMR (100 MHz, CDCl_3): δ 27.98, 32.86, 123.79, 125.66, 125.97, 137.54, 175.80.

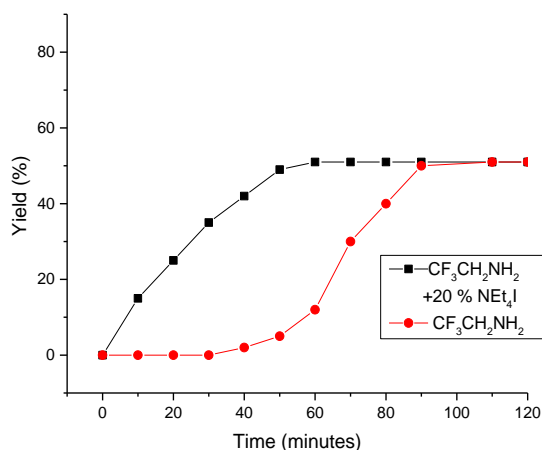
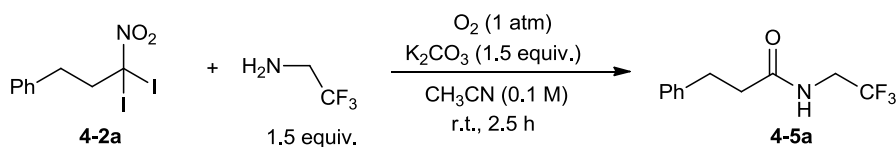
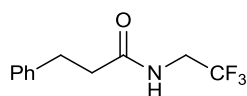


Figure S-1. ^1H NMR study of trifluoroethylamine reacting with α,α -diiodonitroalkane **4-2a**.

Procedure: To a 10 mL reaction tube, α,α -diiodonitroalkane **2a** (0.4 mmol) and dry CH_3CN (4 mL, pre-saturated with O_2) were mixed and put under an O_2 -balloon atmosphere. CH_2Br_2 (0.4 mmol) was added as internal standard. After that, $\text{CF}_3\text{CH}_2\text{NH}_2$ (0.6 mmol) and K_2CO_3 (0.6 mmol) were added under fast, but smooth stirring at r.t. Every 10 minutes, take

out 100 μL reaction mixture and diluted by CDCl_3 (600 μL), checking ^1H NMR to estimate the yield of amide.



White solid, yield = 50%.

^1H NMR (400 MHz, CDCl_3): δ 2.53 (t, $J = 7.6$ Hz, 2H), 2.97 (t, $J = 7.6$ Hz, 2H), 3.82-3.90 (m, 2H), 5.63 (br s, 1H), 7.16-7.30 (m, 5H).

^{13}C NMR (100 MHz, CDCl_3): δ 31.33, 38.11, 40.55 (q, $J = 35$ Hz, 1C), 123.95 (q, $J = 276.8$ Hz, 1C), 126.42, 128.25, 128.61, 140.27.

IR (neat): 3308, 2360, 1662, 1558, 1158, 701 cm^{-1} .

HRMS (ESI): m/z calcd. for $\text{C}_{11}\text{H}_{12}\text{F}_3\text{NNaO}$ ($\text{M} + \text{Na}$) $^+$ 254.0763; found 254.0765.

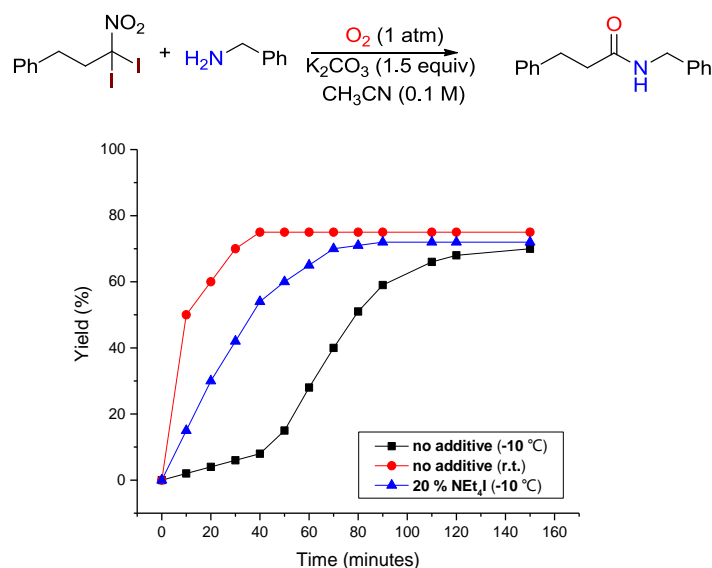
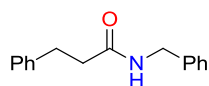


Figure S-2. ^1H NMR study of benzylamine with α,α -diiodonitroalkane **4-2a**

Procedure: To a 10 mL reaction tube, α,α -diiodonitroalkane **2a** (0.4 mmol), dry CH_3CN (4 mL, pre-saturated with O_2) were mixed and put under an O_2 -balloon atmosphere. CH_2Br_2 (0.4 mmol) was added as internal standard. After that, PhCH_2NH_2 (2.0 mmol) and K_2CO_3 (0.6 mmol) were added under fast, but smooth stirring at -10°C . Every 10 minutes, take out 100 μL reaction mixture and diluted by CDCl_3 (600 μL), checking ^1H NMR.

White solid, yield = 75%.



^1H NMR (400 MHz, CDCl_3): δ 2.48 (t, $J = 7.6$ Hz, 2H), 2.96 (t, $J = 7.6$ Hz, 2H), 3.45 (d, $J = 5.6$ Hz, 2H), 5.95 (br s, 1H), 7.11-7.30 (m, 5H).

^{13}C NMR (100 MHz, CDCl_3): δ 31.71, 38.38, 43.49, 126.23, 127.38, 127.68, 128.39, 128.53, 128.61, 138.19, 140.78, 172.02.

IR (neat): 3287, 1637, 1541, 1454, 697 cm^{-1} .

HRMS (ESI): m/z calcd. for $\text{C}_{16}\text{H}_{17}\text{NNaO}$ ($\text{M} + \text{Na}$) $^+$ 262.1202; found: 262.1203.

4.3 React IR analysis

Instrument Information: React IR 15, Probe A: ReactIR 15 (SN:Unspecified) with MCT Detector using HappGenzel

apodization; DiComp (Diamond) probe (SN:Unspecified) connected via AgX 6mm x 1.5m Fiber (Silver Halide); Sampling 2500 to 650 at 8 wavenumber resolution; Scan option: AutoSelect; Gain: 1x.

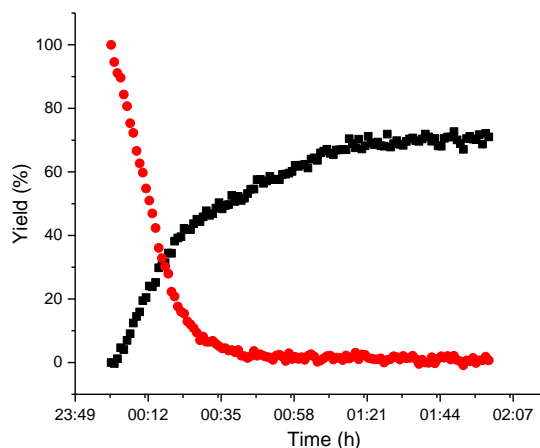
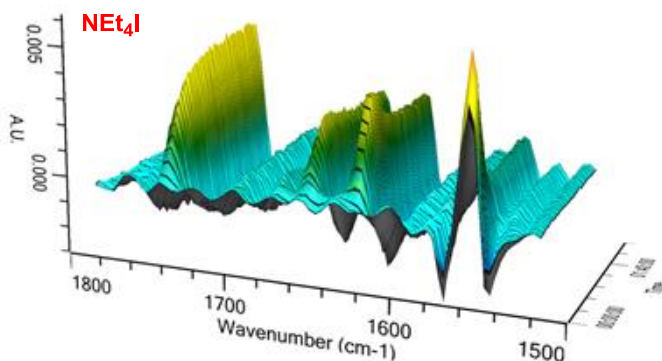
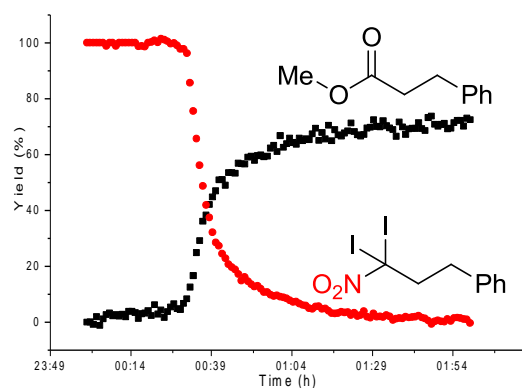
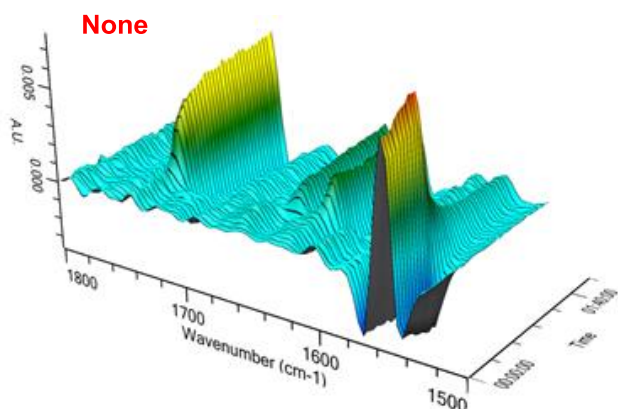
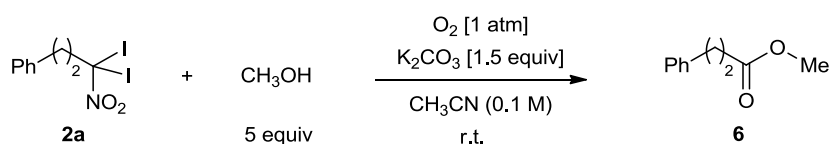


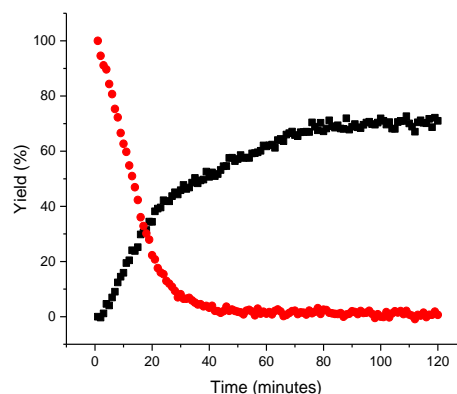
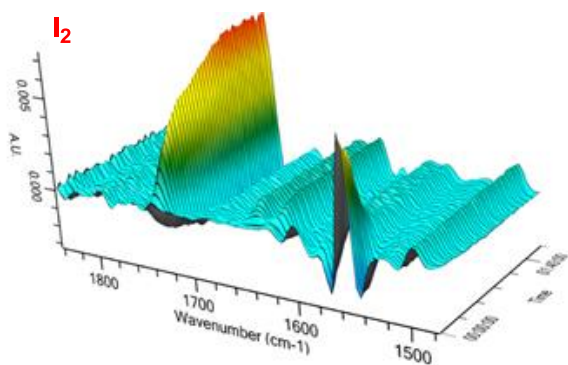
(No reaction proceed)



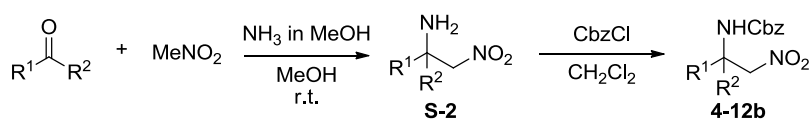
(After reaction proceed)

To a reaction flask (10 mL), α,α -diiodonitroalkane **4-2a** (0.3 mmol), MeOH (1.5 mmol), dry CH₃CN (6 mL, pre-saturated with O₂) were mixed and put under an O₂-balloon atmosphere. Until all the yellow solid dissolved in CH₃CN. The react IR probe was inserted into the solution, then K₂CO₃ (0.15 mmol) were added under fast, but smooth stirring at r.t. Finally, I₂ or NEt₄I was added one portion and the react-IR start record the reaction every 1 minutes. After the reaction was finished, CHCl₃ was added to the reaction and the precipitate filtered through a short silica gel column with additional solvent then washed by *sat.* Na₂S₂O₃. The combined organic solution was dried over anhydrous magnesium sulfate, the solvent removed *in vacuo* and the crude product purified without further purification to give the pure ester without further purification.

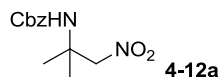




4.4 Preparing starting materials



Procedure: To a 100 mL flask, ketone (1 equiv.) and MeNO₂ (5 equiv.) was dissolved in MeOH (50 mL, pre-saturated with NH₃ gas). The reaction mixture stirred overnight at r.t. After that, all the *volatile* compounds were removed *in vacuo* to give crude product. Further dissolve all the crude product in CH₂Cl₂ and cooled to 0 °C, CbzCl (20 mmol) and NEt₃ (20 mmol) was added and stirred at r.t. for 3 h. The reaction mixture was quenched by sat. NH₄Cl solution and extracted with CHCl₃. The combined organic solution was dried over anhydrous magnesium sulfate, the solvent removed *in vacuo* to give crude product, which was columned via silica gel chromatography (Hexane/ Ethyl Acetate = 3/1) to give pure **4-12**.

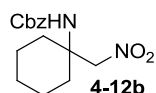


¹H NMR (400 MHz, CDCl₃): δ 1.42 (s, 6H), 4.73 (s, 2H), 4.89 (br s, 1H), 5.09 (s, 2H), 7.30-7.35 (s, 5H).

¹³C NMR (100 MHz, CDCl₃): δ 25.56, 52.25, 66.63, 80.78, 127.97, 128.20, 128.56, 136.12, 154.64.

IR (neat): 2982, 1716, 1550, 1250, 1090 cm⁻¹.

HRMS (ESI): *m/z* calcd. for C₁₂H₁₆N₂NaO₄ (M + Na)⁺ 275.1002; found: 275.1400.

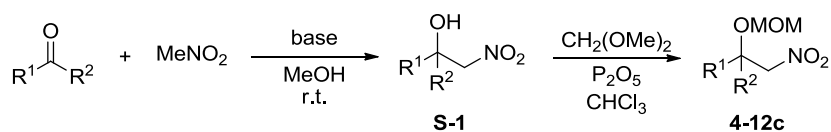


¹H NMR (400 MHz, CDCl₃): δ 1.28-1.31 (m, 1H), 1.46-1.63 (m, 8H), 2.02-2.05 (m, 2H), 4.67 (br s, 1H), 4.77 (s, 2H), 5.10 (s, 2H), 7.29-7.37 (m, 5H).

¹³C NMR (100 MHz, CDCl₃): δ 20.95, 25.07, 32.90, 54.62, 66.60, 80.21, 127.91, 128.17, 128.56, 136.20, 154.64.0, 154.64.

IR (neat): 3342, 2937, 1717, 1547, 1253, 1221 cm⁻¹.

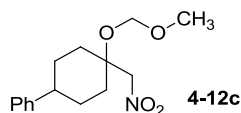
HRMS (ESI): *m/z* calcd. for C₁₅H₂₀N₂NaO₄ (M + Na)⁺ 315.1315; found: 315.1318.



Step1: To a 200 mL flask, MeNO₂ (50 mmol) and ketone (10 mmol) was dissolved in MeOH (50 mL). The reaction mixture

was cooled to 0 °C. After that, NaOH solution (50 mmol in 20 mL water) was slowly added and keep the reaction stirred at the same temperature until the ketone was disappeared by TLC monitoring. The reaction mixture was diluted with water, which was neutralized by 1M HCl solution and extracted with CHCl₃. The combined organic solution was dried over anhydrous magnesium sulfate, the solvent removed *in vacuo* to give crude product, which was columned via silica gel chromatography to give pure **S-1**.

Step 2:

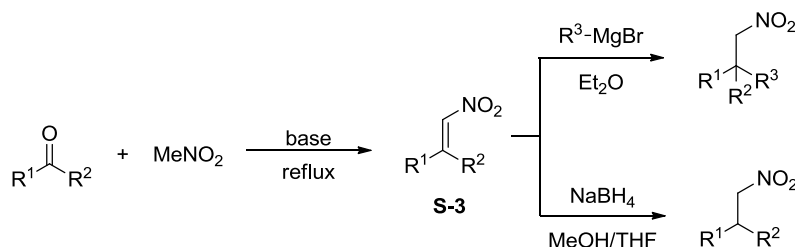


¹H NMR (400 MHz, CDCl₃): δ 1.56-1.66 (m, 2H), 1.76-1.99 (m, 3H), 2.12-2.20 (m, 2H), 2.47-2.54 (m, 2H), 3.47 (s, 3H), 4.55 (s, 2H), 4.83 (s, 2H), 7.17-7.31 (m, 5H).

¹³C NMR (400 MHz, CDCl₃): δ 28.51, 32.93, 33.95, 41.35, 43.06, 56.42, 75.09, 83.15, 91.34, 126.23, 126.71, 128.43, 146.26.

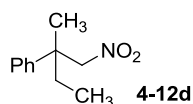
IR (neat): 2360, 1550, 1024, 1141 cm⁻¹.

HRMS (ESI): *m/z* calcd. for C₁₅H₂₁NNaO₄ (M + Na)⁺ 302.1363; found: 302.1366.



Step 1: To a 10 mL flask, MeNO₂ (50 mmol) and ketone (10 mmol) was dissolved in distilled MeOH (50 mL). Then NaOH solution (50 mmol in 20 mL water) was slowly added and reflux overnight. The reaction mixture was diluted with water, which was neutralized by 1M HCl solution and extracted with CHCl₃. The combined organic solution was dried over anhydrous magnesium sulfate, the solvent removed *in vacuo* to give crude product, which was columned via silica gel chromatography to give pure **S-3**.

Step 2: To the solution of **S-3** (5.0 mmol) in 20 ml of anhydrous Et₂O at -20 °C under Ar, Grignard Reagents (1 equiv.) in diethylether was added dropwise to the reaction. The mixture was stirred at -20 °C for 20 min, then warmed to R.T. over 2 hr, then poured onto excess ice. The mixture was made slightly acidic with 1M HCl solution. The aqueous layer was extracted once with ether. The combined organic layers were washed twice with water, made slightly acidic with dilute hydrochloric acid, and washed twice with saturated sodium chloride solution. After drying with anhydrous magnesium sulfate, solvent removal and column purification (Hexane/EA= 1/5).



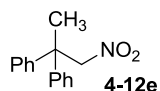
Sticky oil, 70%.

¹H NMR (400 MHz, CDCl₃): δ 0.73 (t, *J* = 7.2 Hz, 3H), 1.71-1.78 (m, 1H), 1.92-1.98 (m, 1H), 4.54 (d, *J* = 10.8 Hz, 1H), 4.59 (d, *J* = 10.8 Hz, 1H), 7.23-7.37 (m, 5H).

¹³C NMR (100 MHz, CDCl₃): δ 8.24, 21.86, 32.31, 42.66, 86.19, 126.17, 126.94, 128.60, 142.02.

IR (neat): 2973, 1549, 1375, 700 cm⁻¹.

HRMS (ESI): *m/z* calcd. for C₁₁H₁₅NNaO₂ (M + Na)⁺ 216.0995; found: 216.0993.



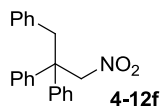
Sticky oil, 70%

¹H NMR (400 MHz, CDCl₃): δ 1.96 (s, 3H), 5.10 (s, 2H), 7.16-7.34 (m, 10H).

¹³C NMR (100 MHz, CDCl₃): δ 25.56, 52.25, 66.63, 80.78, 127.97, 128.20, 128.56, 136.12, 154.64.

IR (neat): 2616, 1552, 699 cm⁻¹.

HRMS (ESI): *m/z* calcd. for C₁₅H₁₅NNaO₂ (M + Na)⁺ 264.0995; found: 264.0992.



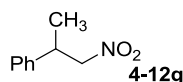
White solid, 80%

¹H NMR (400 MHz, CDCl₃): δ 3.77 (s, 2H), 5.05 (s, 2H), 6.74 (d, *J* = 7.2 Hz, 2H), 7.03-7.32 (m, 13H).

¹³C NMR (400 MHz, CDCl₃): δ 42.60, 51.48, 80.95, 126.80, 127.23, 127.83, 127.96, 128.31, 131.07, 136.04, 143.73.

IR (neat): 3024, 1550, 1493, 1447, 1376, 755, 698 cm⁻¹.

HRMS (ESI): *m/z* calcd. for C₂₁H₁₉NNaO₂ (M+Na)⁺ 340.1308; found 340.1304.



To the solution of **S-3** (5 mmol) in THF/MeOH = 10/1 (20 mL) at 0 °C under argon, NaBH₄ (0.38 g, 10 mmol) was added slowly. After stirring for 20 min, the reaction was treated with 1N HCl and extracted with Et₂O three times, the combined organic layers were washed with brine (30 mL), dried (MgSO₄), filtered and evaporated to leave the crude product, which was purified by column chromatography over silica gel (hexane:ethyl acetate = 9:1) to provide **4-1a** (1.42 g, 91%) as sticky oil.

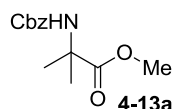
¹H NMR (400 MHz, CDCl₃): δ 1.37 (d, *J* = 6.8 Hz, 3H), 3.59-3.65 (m, 1H), 4.47 (dd, *J* = 8.4, 12 Hz, 1H), 4.54 (dd, *J* = 7.6, 12 Hz, 1H), 7.20-7.35 (m, 5H).

¹³C NMR (100 MHz, CDCl₃): δ 18.71, 38.63, 81.85, 126.89, 127.56, 128.96, 140.86.

IR (neat): 2973, 1552, 1383, 1022, 766, 701 cm⁻¹.

4.5 Characterization of esters.

Typical procedure: To a 10 mL flask, nitroalkanes **4-12** (0.2 mmol) were dissolved in distilled dry MeOH (2 mL, pre-saturated with O₂). Then MeOK (3 equiv.) was added and stirred for 5 min until all the solid completely disappeared. I₂ (1.2 equiv.) was added under fast, but smooth stirring. After the nitroalkane **4-12** disappeared by TLC monitoring, the reaction was quenched with *sat.* Na₂S₂O₃ solution and extracted with CHCl₃. The combined organic solution was dried over anhydrous magnesium sulfate, the solvent removed *in vacuo* to give crude product, which was columned via silica gel chromatography to give pure **4-13**.



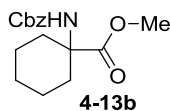
Sticky oil, yield = 70%.

¹H NMR (400 MHz, CDCl₃): δ 1.53 (s, 6H), 3.70 s, (3H), 5.07 (s, 2H), 5.38 (br s, 1H), 7.28-7.35 (m, 5H).

¹³C NMR (100 MHz, CDCl₃): δ 25.14, 52.61, 56.47, 66.52, 128.04, 128.07, 128.48, 128.52, 136.39, 154.88, 175.04.

IR (neat): 3355, 1717, 1552, 1456, 1292, 1252, 1153, 1075, 699 cm⁻¹.

HRMS *m/z* calcd. for C₁₃H₁₇NNaO₄ (M + Na)⁺ 274.1050; found: 274.1054.



Sticky oil, yield = 65%.

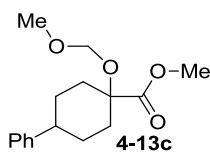
¹H NMR (400 MHz, CDCl₃): δ 1.24-1.33 (m, 1 H), 1.39-1.49 (m, 2H), 1.59-1.63 (m, 3H), 1.80-1.87 (m, 2H), 1.98-2.02 (m, 2H).

¹³C NMR (100 MHz, CDCl₃): δ 3.66 (br s, 3H), 4.95 (br s, 1H), 5.07 (s, 2H), 7.28-7.36 (5H).

¹³C NMR (100 MHz, CDCl₃): δ 21.20, 25.11, 32.60, 52.28, 59.11, 66.67, 128.05, 136.37, 155.19, 174.82.

IR (neat): 3353, 2945, 128.10, 128.48, 128.52, 1734, 1523, 1455, 1281, 1258, 1236, 1069, 740, 699 cm⁻¹.

HRMS *m/z* calcd. for C₁₆H₂₁NNaO₄ (M + Na)⁺ 314.1363; found: 314.1365.



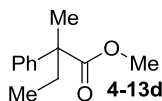
Sticky oil, yield = 68%.

¹H NMR (400 MHz, CDCl₃): δ 1.74-1.87 (m, 6H), 2.18-2.21 (m, 2H), 2.48-2.57 (m, 1H), 3.47 (s, 3H), 3.73 (s, 3H), 4.76 (s, 2H), 7.16-7.31 (m, 5H).

¹³C NMR (100 MHz, CDCl₃): δ 28.42, 32.46, 33.95, 41.35, 43.13, 52.14, 56.46, 77.85, 92.88, 126.112, 126.74, 128.38, 146.72, 175.17.

IR (neat): 2949, 1738, 1450, 1243, 1144, 1028, 701 cm⁻¹.

HRMS *m/z* calcd. for C₁₆H₂₂NaO₄ (M + Na)⁺ 301.1410; found: 301.1410.



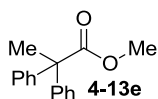
Sticky oil, yield = 60%.

¹H NMR (400 MHz, CDCl₃): δ 0.81 (t, *J* = 7.2 Hz, 3H), 1.52 (s, 3H), 1.92-1.99 (m, 1H), 2.05-2.12 (m, 1H), 3.64 (s, 3H), 7.20-7.35 (m, 5H).

¹³C NMR (100 MHz, CDCl₃): δ 9.11, 22.20, 31.80, 50.65, 52.01, 125.99, 126.58, 128.31, 143.84, 176.80.

IR (neat): 2974, 1731, 1240, 1147, 699 cm⁻¹.

HRMS (ESI): *m/z* calcd. for C₁₂H₁₆NaO₂ (M + Na)⁺ 215.1043; 215.1044.



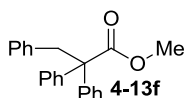
White solid, yield = 75%.

¹H NMR (400 MHz, CDCl₃): δ 1.93 (s, 3H), 3.73 (s, 3H), 7.20-7.32 (m, 5H).

¹³C NMR (100 MHz, CDCl₃): δ 27.09, 52.48, 56.55, 126.81, 127.99, 128.07, 144.38, 175.63.

IR (neat): 2992, 1732, 1496, 1447, 1240, 699 cm⁻¹.

HRMS *m/z* calcd. for C₁₆H₁₆NaO₂ (M + Na)⁺ 263.1043; found: 263.1042.



White solid, yield = 79%.

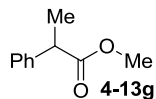
¹H NMR (400 MHz, CDCl₃): δ 3.68 (s, 3H), 3.71 (s, 2H), 6.65-6.67 (s, 2H), 5.38 (br s, 1H), 7.28-7.35 (m, 5H).

¹³C NMR (100 MHz, CDCl₃): δ 44.42, 52.18, 62.04, 126.23, 126.81, 127.44, 127.63, 129.25, 130.83, 137.28, 142.73,

173.99.

IR (neat): 3029, 1732, 1497, 1446, 1219, 700 cm⁻¹.

HRMS *m/z* calcd. for C₂₂H₂₀NaO₂ (M + Na)⁺ 339.1356; found: 339.1355.



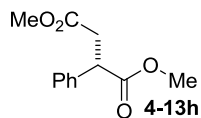
Sticky oil, yield = 60%

¹H NMR (400 MHz, CDCl₃): δ 1.49 (d, *J* = 7.2 Hz, 3H), 3.65 (s, 3H), 3.71 (q, *J* = 7.2 Hz, 1H), 7.22-7.33 (m, 5H).

¹³C NMR (100 MHz, CDCl₃): δ 18.57, 45.39, 51.99, 127.11, 127.44, 128.61, 140.53, 174.99.

IR (neat): 2982, 1736, 1580, 1454, 1209, 1166, 699 cm⁻¹.

HRMS (ESI): *m/z* calcd. for C₁₀H₁₂NaO₂ (M+Na)⁺ 187.0730; Found 187.0727.



Sticky oil, yield = 61%.

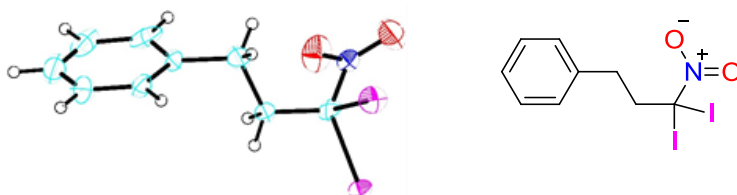
The NMR data is consistent with previous report: Y. X. Gao, L. Chang, H. Shi, B. Liang, K. Wongkhan, D. D. Chaiyaveij, A.S. Batsanov, T. B. Marder, C.-C. Li, Z. Yang, and Y. Huang, *Adv. Synth. Catal.* **2010**, 352, 1955–1966.

¹H NMR (400 MHz, CDCl₃): δ 2.65 (dd, *J* = 5.2, 18.8 Hz, 1H), 3.19 (dd, *J* = 10, 16.8 Hz, 1H), 3.65 (s, 3H), 3.66 (s, 3H), 4.07 (dd, *J* = 5.2, 10Hz, 1H), 7.23-7.33 (m, 5H).

¹³C NMR (100 MHz, CDCl₃): δ 37.60, 47.06, 51.85, 52.35, 127.66, 127.70, 128.87, 137.63, 171.96, 173.41.

6.2 X-Ray structure of α,α-diiodonitroalkane 4-2a

The single crystal of **4-2a** suitable for X-ray analysis was grown in a solution of dichloromethane/Hexane at -30 °C under Ar. A yellow block crystal of C₉H₉I₂NO₂ having approximate dimensions of 0.400×0.400×0.300 mm was mounted on a glass fiber. All measurements were made on a Rigaku XtaLAB mini diffractometer using graphite monochromated Mo-Kα radiation. The crystal-to-detector distance was 50.11 mm. The data were collected at a temperature of -123±1 °C to a maximum 2θ value of 55.0°. A total of 540 oscillation images were collected. A sweep of data was done using ω scans from -60.0 to 120.0° in 1.00° step, at φ=54.0° and θ = 0.0°. The exposure rate was 12.0 [sec./°]. The detector swing angle was 30.00°. A second sweep was performed using ω scans from -60.0 to 120.0° in 1.00° step, at φ=54.0° and θ = 120.0°. The exposure rate was 12.0 [sec./°]. The detector swing angle was 30.00°. Another sweep was performed using ω scans from -60.0 to 120.0° in 1.00° step, at φ=54.0° and θ = 0.0°. The exposure rate was 12.0 [sec./°]. The detector swing angle was 30.20°. Another sweep was performed using ω scans from -60.0 to 120.0° in 1.00° step, at φ=54.0° and θ = 120.0°. The exposure rate was 12.0 [sec./°]. The detector swing angle was 30.20°. The crystal-to-detector distance was 50.11 mm. Readout was performed in the 0.073 mm pixel mode. Crystallographic data has been deposited with the Cambridge Crystallographic Data Center, **CCDC reference number: 1437079**.



EXPERIMENTAL DETAILS

A. Crystal Data

Empirical Formula	C ₉ H ₉ I ₂ NO ₂
Formula Weight	416.98
Crystal Color, Habit	yellow, block
Crystal Dimensions	0.400 × 0.400 × 0.300 mm
Crystal System	orthorhombic
Lattice Type	Primitive
Lattice Parameters	a = 12.08000 Å b = 11.70400 Å c = 16.18200 Å V = 2287.88107 Å ³
Space Group	Pbca (#61)
Z value	8
D _{calc}	2.421 g/cm ³
F ₀₀₀	1536.00
m(MoKα)	54.758 cm ⁻¹

B. Intensity Measurements

Diffractometer	XtaLAB mini
Radiation	MoKα (λ = 0.71075 Å) graphite monochromated
Voltage, Current	50kV, 12mA
Temperature	-123.0 °C
Detector Aperture	75.0 mm (diameter)
Data Images	540 exposures
ω oscillation Range (χ=54.0, φ=0.0)	-60.0 - 120.0°
Exposure Rate	12.0 sec./°
Detector Swing Angle	30.00°
ω oscillation Range (χ=54.0, φ=120.0)	-60.0 - 120.0°
Exposure Rate	12.0 sec./°
Detector Swing Angle	30.00°
ω oscillation Range (χ=54.0, φ=240.0)	-60.0 - 120.0°
Exposure Rate	12.0 sec./°
Detector Swing Angle	30.00°
ω oscillation Range (χ=54.0, φ=0.0)	-60.0 - 120.0°
Exposure Rate	12.0 sec./°
Detector Swing Angle	30.20°
ω oscillation Range (χ=54.0, φ=120.0)	-60.0 - 120.0°
Exposure Rate	12.0 sec./°
Detector Swing Angle	30.20°
ω oscillation Range (χ=54.0, φ=240.0)	-60.0 - 120.0°
Exposure Rate	12.0 sec./°
Detector Swing Angle	30.20°
Detector Position	50.11 mm
Pixel Size	0.073 mm
2θ _{max}	55.0°
No. of Reflections Measured	Total: 20398

Corrections	Unique: 2620 ($R_{\text{int}} = 0.0807$) Lorentz-polarization Absorption (trans. factors: 0.103 - 0.193)
C. Structure Solution and Refinement	
Structure Solution	Charge Flipping (Superflip)
Refinement	Full-matrix least-squares on F^2
Function Minimized	$S \sum w (F_o^2 - F_c^2)^2$
Least Squares Weights	$w = 1 / [s^2(F_o^2) + (0.0820 \cdot P)^2 + 55.3747 \cdot P]$ where $P = (\text{Max}(F_o^2, 0) + 2F_c^2)/3$
$2\theta_{\text{max}}$ cutoff	55.0°
Anomalous Dispersion	All non-hydrogen atoms
No. Observations (All reflections)	2620
No. Variables	127
Reflection/Parameter Ratio	20.63
Residuals: R_1 ($I > 2.00\sigma(I)$)	0.0716
Residuals: R (All reflections)	0.0743
Residuals: wR_2 (All reflections)	0.2096
Goodness of Fit Indicator	1.193
Max Shift/Error in Final Cycle	0.001
Maximum peak in Final Diff. Map	3.43 e ⁻ /Å ³
Minimum peak in Final Diff. Map	-2.81 e ⁻ /Å ³

Table 1. Atomic coordinates and $B_{\text{iso}}/B_{\text{eq}}$

atom	x	y	z	B_{eq}
I1	-0.05195(7)	1.16338(7)	0.13541(5)	2.46(2)
I2	0.17729(8)	1.09930(8)	0.26361(6)	3.22(2)
O7	-0.0352(10)	0.9763(10)	0.3179(6)	4.1(2)
O8	-0.0882(10)	0.8909(10)	0.2095(8)	4.4(2)
N3	-0.0307(9)	0.9582(9)	0.2457(7)	2.62(18)
C6	0.0486(10)	1.0264(10)	0.1891(8)	2.32(19)
C12	0.1920(9)	0.7723(10)	0.0811(7)	2.20(19)
C13	0.0936(10)	0.9522(10)	0.1211(7)	2.19(18)
C14	0.1208(11)	0.6827(11)	0.0630(11)	3.4(3)
C15	0.1427(14)	0.6131(12)	-0.0079(11)	3.7(3)
C16	0.2356(15)	0.6333(13)	-0.0530(9)	4.0(3)
C17	0.3065(12)	0.7200(13)	-0.0327(9)	3.3(2)
C18	0.2842(11)	0.7897(10)	0.0347(8)	2.6(2)
C19	0.1619(14)	0.8498(13)	0.1520(8)	3.5(3)

$$B_{\text{eq}} = 8/3 \pi^2 (U_{11}(aa^*)^2 + U_{22}(bb^*)^2 + U_{33}(cc^*)^2 + 2U_{12}(aa^*bb^*)\cos \gamma + 2U_{13}(aa^*cc^*)\cos \beta + 2U_{23}(bb^*cc^*)\cos \alpha)$$

Table 2. Atomic coordinates and B_{iso} involving hydrogen atoms

atom	x	y	z	B_{iso}
H13A	0.14067	0.99951	0.08454	2.628
H13B	0.03095	0.92332	0.08760	2.628
H14	0.05848	0.66772	0.09711	4.065
H15	0.09318	0.55365	-0.02311	4.485
H16	0.25146	0.58650	-0.09947	4.791

H17	0.37121	0.73246	-0.06483	3.979
H18	0.33369	0.84989	0.04843	3.095
H19A	0.23022	0.87762	0.17909	4.186
H19B	0.11848	0.80646	0.19336	4.186

Table 3. Anisotropic displacement parameters

atom	U ₁₁	U ₂₂	U ₃₃	U ₁₂	U ₁₃	U ₂₃
I1	0.0337(5)	0.0280(4)	0.0316(4)	0.0096(3)	-0.0029(3)	0.0017(3)
I2	0.0401(6)	0.0399(5)	0.0425(6)	-0.0048(4)	-0.0068(4)	0.0006(4)
O7	0.062(7)	0.057(7)	0.036(5)	-0.013(6)	0.008(5)	-0.004(5)
O8	0.044(6)	0.053(7)	0.070(7)	-0.019(5)	0.007(6)	-0.017(6)
N3	0.040(6)	0.027(5)	0.032(5)	0.008(5)	0.001(4)	0.000(4)
C6	0.029(6)	0.027(6)	0.032(6)	0.012(5)	-0.007(5)	0.001(5)
C12	0.027(5)	0.032(6)	0.025(5)	0.018(4)	0.002(4)	0.001(4)
C13	0.031(6)	0.028(6)	0.024(5)	0.007(5)	0.000(4)	0.001(4)
C14	0.031(6)	0.026(6)	0.072(10)	0.009(5)	0.003(6)	0.015(6)
C15	0.054(9)	0.025(6)	0.063(9)	0.005(6)	-0.012(8)	-0.007(6)
C16	0.071(11)	0.039(7)	0.042(8)	0.019(8)	-0.014(7)	-0.013(6)
C17	0.040(7)	0.042(8)	0.044(7)	0.013(6)	0.012(6)	0.000(6)
C18	0.035(6)	0.020(5)	0.042(7)	-0.001(5)	0.005(5)	-0.002(5)
C19	0.056(9)	0.047(8)	0.029(6)	0.026(7)	0.003(6)	0.005(6)

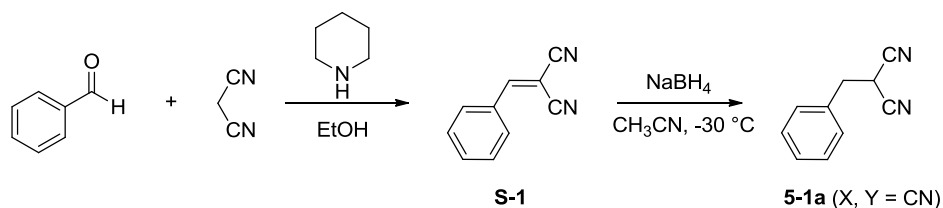
The general temperature factor expression: $\exp(-2p^2(a^2U_{11}h^2 + b^2U_{22}k^2 + c^2U_{33}l^2 + 2a*b*U_{12}hk + 2a*c*U_{13}hl + 2b*c*U_{23}kl))$

Table 4. Bond lengths (Å)

atom	atom	distance	atom	atom	distance
I1	C6	2.191(12)	I2	C6	2.145(12)
O7	N3	1.188(15)	O8	N3	1.202(16)
N3	C6	1.547(16)	C6	C13	1.503(17)
C12	C14	1.387(18)	C12	C18	1.359(17)
C12	C19	1.507(18)	C13	C19	1.54(2)
C14	C15	1.43(2)	C15	C16	1.36(2)
C16	C17	1.37(2)	C17	C18	1.389(19)

Chapter 5

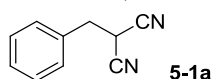
5.1. Preparation of starting materials



Scheme S-1. Synthesis malononitrile **5-1a**.

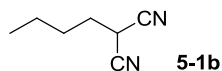
Procedure of preparing 5-1a: Piperidine (2-3 drops) was added to a solution of benzaldehyde (2.12 g, 20 mmol) and malononitrile (1.32 g, 20 mmol) in 20 mL EtOH under argon. The reaction was refluxed for 2–3 h. A precipitate formed upon cooling the reaction mixture to room temperature. The crude product was filtered and recrystallized from ethanol to yield 2-benzylidenemalononitrile **S-1** in 75% yield.^[1]

To the solution of **S-1** (1.54 g, 10 mmol) in CH₃CN (20 mL) at -30 °C under argon, NaBH₄ (0.38 g, 10 mmol) was added slowly. After stirring for 20 min, the reaction was treated with 1N HCl and extracted with Et₂O three times, the combined organic layers were washed with brine (10 mL), dried (MgSO₄), filtered and evaporated to leave the crude product, which was purified by column chromatography over silica gel (hexane:ethyl acetate = 5:1) to provide **5-1a** (1.42 g, 91%) as a white solid; the data was consistent with previous report.^[2]



¹H NMR (400 MHz, CDCl₃): δ 3.27 (d, *J* = 6.8 Hz, 2H), 3.89 (t, *J* = 7.2 Hz, 1H), 7.30-7.42 (m, 5H).

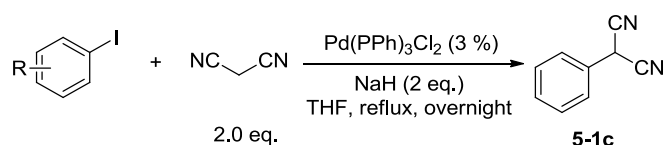
¹³C NMR (100 MHz, CDCl₃): δ 24.98, 36.72, 112.14, 128.81, 129.12, 129.29, 132.91.



The procedure to prepare **1a** was followed.

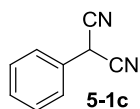
¹H NMR (400 MHz, CDCl₃): δ 1.02 (t, *J* = 7.6 Hz, 3H), 1.61-1.70 (m, 2H), 1.98- 2.02 (m, 2H), 3.07 (t, *J* = 6.8 Hz, 1H).

¹³C NMR (100 MHz, CDCl₃): δ 12.83, 19.93, 22.25, 32.60.



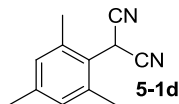
Scheme S-2. Synthesis malononitrile **5-1c**.

Procedure of preparing 5-1c:^[3] To a cooled (0 °C) slurry of NaH (15 mmol, 60 % in oil, pre-washed before use) in THF was added malononitrile (660 mg, 10 mmol) dropwise (caution: gas evolution). Upon complete addition, the mixture was allowed to warm to ambient temperature and, after the evolution of gas ceased, (PPh₃)₃ PdCl₂ (101 mg, 0.15 mmol, 3 mol %) and iodobenzene (1.02 g, 5 mmol) were added. The resulting mixture was stirred at reflux overnight. Afterwards, the mixture was cooled to room temperature, quenched carefully by the addition of water, and concentrated in vacuo. Following extractive workup, the organic layer was dried (anhyd. Na₂SO₄), filtered, and concentrated. The phenylmalononitrile **1c** was purified by chromatography on silica, giving a white solid (646 mg, 91.0 %).



¹H NMR (400 MHz, CDCl₃): δ 5.07 (m, 1H), 7.47 (s, 5H);

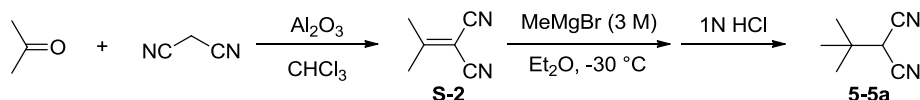
¹³C NMR (100 MHz, CDCl₃): δ 28.07, 111.86, 126.22, 127.21, 130.03, 130.36.1



The procedure to prepare **5-1c** was followed.

¹H NMR (400 MHz, CDCl₃): δ 2.28 (s, 3H), 2.48 (s, 6H), 5.26 (s, 1H), 6.94 (s, 2H);

¹³C NMR (100 MHz, CDCl₃): δ 20.13, 20.89, 21.99, 111.48, 120.79, 130.65, 136.61, 140.47.



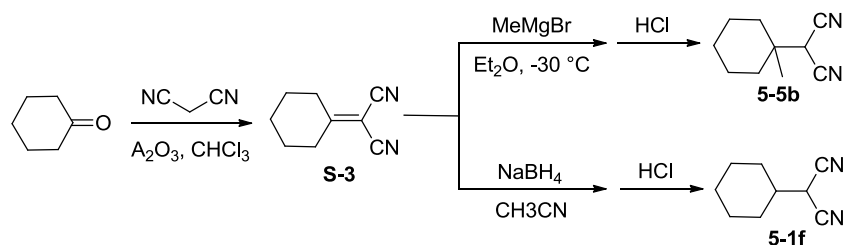
Scheme S-3. Synthesis malononitrile **5-5a**.

Procedure to prepare *t*-Butylmalononitrile **5-5a:**^[4,5] To a stirred solution of acetone (22 mmol) and malononitrile (20 mmol) in 40 mL CHCl₃, A₂O₃ (basic, 10.0 g, 3 times) was added to the reaction mixture until the malononitrile disappeared (as monitored by TLC). The solid was then filtered off and evaporated to leave the crude product, which was purified by column chromatography over silica gel (hexane: ethyl acetate = 5:1) to provide the corresponding isopropylidene malononitrile **S-2** (2.00 g, 95%) as a colourless oil.

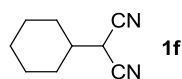
To the solution of isopropylidene malononitrile **S-2** (1.59 g, 15.0 mmol) in 30 ml of anhydrous Et₂O at -20 °C under Ar, methylmagnesium bromide (5 mL, 3 M) in diethylether was added dropwise to the reaction. The mixture was stirred at -20 °C for 20 min, then warmed to R.T. over 2 hr, then poured onto excess ice. The mixture was made slightly acidic with 1M HCl solution. The aqueous layer was extracted once with ether. The combined organic layers were washed twice with water, made slightly acidic with dilute hydrochloric acid, and washed twice with saturated sodium chloride solution. After drying with anhydrous magnesium sulfate, solvent removal and column purification (Hexane/EA= 1/5), a waxy solid was obtained (1.1 g, 60 %).

¹H NMR (400 MHz, CDCl₃): δ 1.24 (s, 9H), 3.44 (s, 1H);

¹³C NMR (100 MHz, CDCl₃): δ 26.91, 35.84, 35.88, 111.97.



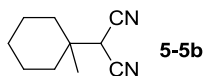
Scheme S-4. Synthesis of malononitriles **5-1e** and **5-1f**.



Following the procedure for the synthesis of **5-1a**, the oily product **5-1f** was obtained in 60 % total yield from cyclohexanone.

¹H NMR (400 MHz, CDCl₃): δ 1.16-1.36 (m, 5 H), 1.70-1.74 (m, 1H), 1.84-1.87(m, 2H), 1.95-2.01 (m, 3H), 3.55 (d, J = 5.2 Hz, 1H);

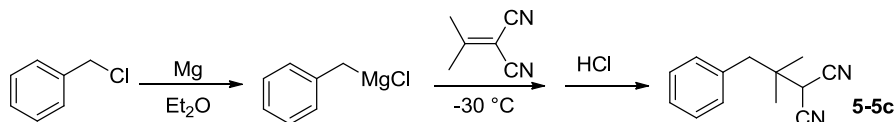
¹³C NMR (100 MHz, CDCl₃): δ 25.09, 25.29, 29.42, 29.99, 39.45, 111.94.



Following the procedure for the synthesis of *t*-butylmalononitrile **5-5a**, the oily product **5-5b** was obtained in a 58 % total yield from cyclohexanone.

¹H NMR (400 MHz, CDCl₃): 1.24 (s, 3H), 1.26-1.30 (m, 1 H), 1.51-1.61 (m, 9H), 3.57 (s, 1H);

¹³C NMR (100 MHz, CDCl₃): δ 21.49, 21.71, 25.14, 34.86, 35.11, 38.28, 111.85.



Scheme S-5. Synthesis malononitrile **5-5c**.

Procedure: Benzylmagnesium bromide (12 mmol) was prepared from benzyl chloride (12 mmol) and Mg (15 mmol) in ether under Ar. The next procedure followed the procedure to prepare **5-5a**; an oil product **5-5c** was obtained, total yield = 50 %.

¹H NMR (400 MHz, CDCl₃): δ 1.25 (s, 6H), 2.82 (s, 2H), 3.39 (s, 1H), 7.17-7.19 (m, 2H), 7.29-7.36 (m, 3H).

¹³C NMR (100 MHz, CDCl₃): δ 24.69, 33.69, 39.39, 45.30, 112.05, 127.53, 128.72, 130.23, 135.09.

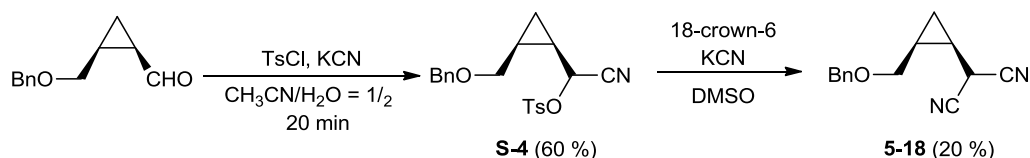


Scheme S-6. Synthesis malononitrile **5-5d**.

Procedure:^[6] The reaction was carried out under Argon. To the solution of aluminum chloride (655 mg, 5 mmol) and malononitrile (330 mg, 5 mmol) in 3 mL of nitromethane in 0 °C under Ar, 1-bromoadamantane (1.07 g, 5 mmol) was added. After that, the reaction mixture was allowed to warm to R.T. The reaction was worked up after 3 h by adding a saturated solution of sodium bicarbonate and extracting with methylene chloride, the combined organic layers were washed with brine (10 mL), dried (MgSO₄), filtered and evaporated to give the crude product, which was purified by column chromatography over silica gel (hexane:ethyl acetate = 5:1) to provide the corresponding **5d** (0.71 g, 71%) as a white solid.

¹H NMR (400 MHz, CDCl₃): δ 3.42(s, H), 1.24 (s, 9H).

¹³C NMR (100 MHz, CDCl₃): δ 28.22, 35.93, 36.45, 37.16, 39.59.

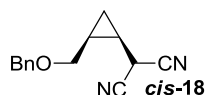


Scheme S-7. Synthesis *cis*-malononitrile **5-18**.

S-4: Aldehyde^[7] (1.4 g, 6 mmol) and TsCl (1.33g, 7 mmol) were dissolved in CH₃CN (7 mL) and cooled to -10 °C, then a KCN solution (10 mmol KCN pre-dissolved in 3.5 mL H₂O) was slowly added to the reaction mixture; after 20 min, the reaction was quenched with *sat.* Na₂S₂O₃ solution and extracted with AcOEt with care; the combined organic layers were washed with brine (10 mL), dried (MgSO₄), filtered and evaporated to leave the crude product, which was purified by

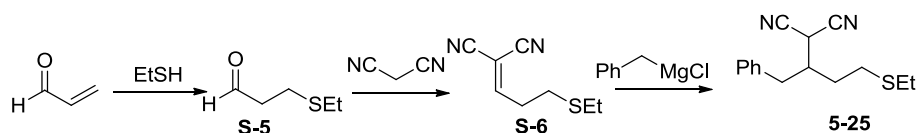
column chromatography over silica gel (hexane:ethyl acetate = 3:1) to provide the corresponding **S-4** (60%) as a sticky oil.

5-18: To DMSO (5 mL), a solution of 18-crown-6 (2.1 g, 8 mmol), KCN (520 mg, 8 mmol) were added; the reaction was stirred for 30 min until all solids disappeared, then **S-4** was added in one-portion, the reaction kept at R.T. for 1.5 h, then quenched by *sat.* Na₂S₂O₃ solution and extracted with CH₂Cl₂. The combined organic phases washed with brine (10 mL), dried (MgSO₄), filtered and evaporated to leave the crude product, which was purified by column chromatography over silica gel (hexane:ethyl acetate = 3:1) to provide the *cis*-**5-18** (20%) as a white solid.



¹H NMR (CDCl₃, 400 MHz): δ 0.73-0.79 (m, 1H), 0.99-1.05 (m, 1H), 1.36-1.44 (m, 1H), 1.52-1.60 (m, 1H), 3.61 (dd, *J* = 5.6, 10.4 Hz, 1H), 3.84 (d, *J* = 10 Hz, 1H), 3.92 (dd, *J* = 3.2, 10.4 Hz, 1H), 4.55 (d, *J* = 12 Hz, 1H), 4.35 (d, *J* = 12 Hz, 1H).

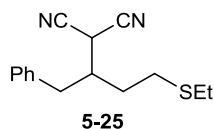
¹³C NMR (CDCl₃, 100 MHz): δ 7.89, 16.22, 16.64, 22.52, 66.26, 73.34, 113.01, 113.07, 127.91, 128.12, 128.62, 137.13.



Scheme S-8. Synthesis δ-sulfenyl malononitrile **5-25**.

S-5: Acrylic aldehyde (30 mmol, 2 mL) and ethanethiol (30 mmol, 2.17 mL) were dissolved in 30 mL CH₂Cl₂, then NEt₃ (10 %, 0.42 mL) was added and the reaction stirred under Ar overnight. The solvent was removed under vacuum to give oil compound **S-5** (Caution: the compound is foul; take care). Next, the crude product was dissolved in CH₂Cl₂ (20 mL) and malononitrile (30 mmol, 1.98g) was added in one-portion, after which A₂O₃ (basic) was added. The reaction mixture was filtered to collect the solution after 20 min. Evaporation of the solvent gave a crude product. Further purification via column chromatography over silica gel (hexane:ethyl acetate = 3:1) provided the corresponding **S-6** (20%) as sticky oil (**Be careful smart smelling**).

5-25: To a solution of **S-6** (1.59 g, 15.0 mmol) in 30 ml of anhydrous Et₂O at -20 °C under Ar, benzylmagnesium chloride (15 mmol, pre-prepared in diethyl ether) was dropwise to the reaction. The mixture was stirred at -20 °C for 20 min, then warmed to R.T. after 2 hr and poured onto excess ice. The mixture was made faintly acidic with 1M HCl solution. The aqueous layer was extracted once with 30 mL ether. The combined organic layers were washed twice with water, made faintly acidic with dilute hydrochloric acid, and washed twice with saturated sodium chloride solution. After drying with anhydrous magnesium sulfate and solvent removal, the crude was purified by column chromatography (Hexane/EA= 1/5) to give a sticky oil **5-25** (1.1 g, 60 %).

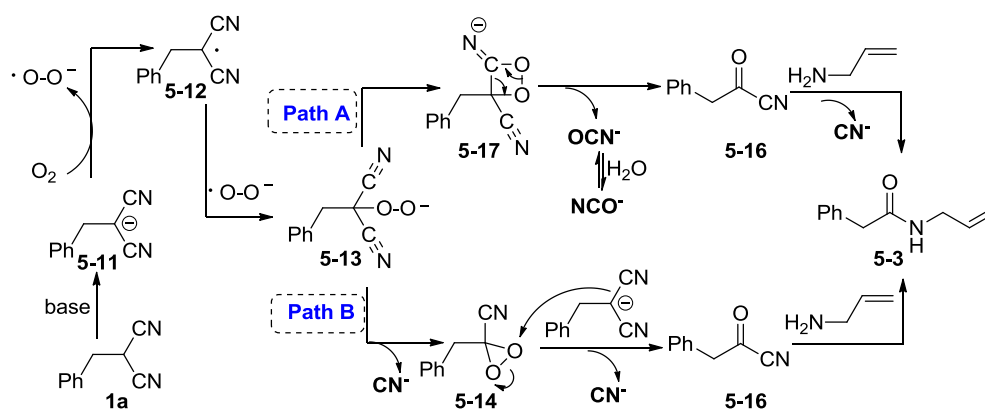


¹H NMR (CDCl₃, 400 MHz): δ 1.25 (t, *J* = 7.2 Hz, 3H), 1.84-1.93 (m, 1H), 1.98-2.07 (m, 1H), 2.49-2.77 (m, 6H), 3.01 (dd, *J* = 5.2, 9.6 Hz, 1H), 3.73 (d, *J* = 4.0 Hz, 1H), 7.18-7.38 (m, 5H).

¹³C NMR (CDCl₃, 100 MHz): δ 14.57, 25.53, 25.51, 26.51, 28.28, 30.11, 37.13, 41.07, 111.46, 112.31, 127.57, 128.90, 129.23, 136.63.

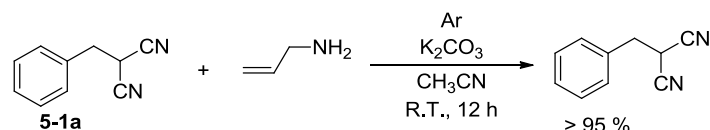
HRMS (ESI) *m/z* calcd. for C₁₅H₁₈N₂NaS (M+Na)⁺ 281.1083; found: 281.1086.

5.3 Mechanistic study



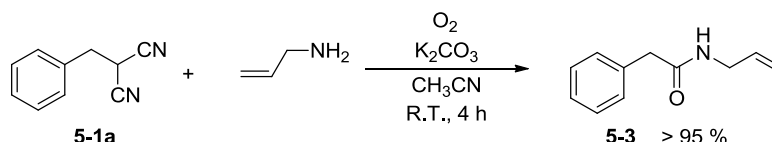
Scheme S-9. Possible mechanistic pathways to form amide **5-3**.

1) To probe the role of O₂



Scheme S-10-A Malononitrile **5-1a** reaction with allyl amine under Ar.

To a two necked flask, malononitrile **1a** (0.2 mmol) in 2.0 mL of CH₃CN was added and the solution was degassed (freeze-pump-thaw cycles) under an argon atmosphere (balloon). Allylamine (0.4 mmol) and K₂CO₃ (0.4 mmol) were added in one-portion. After 12 h, CHCl₃ was added to the reaction and the precipitate filtered through a short silica gel column. After crude NMR, all the starting malononitrile was recovered completely (yield > 96 %); no amide was detected.



Scheme S-10-B. Malononitrile **5-1a** reacts with allyl amine under O₂.

In a two necked flask, malononitrile **5-1a** (0.2 mmol) in 2.0 mL of CH₃CN (pre-saturated with O₂) was degassed (freeze-pump-thaw cycles) and the reaction mixture purged and kept under an oxygen atmosphere (balloon). Allylamine (0.15 mmol) and K₂CO₃ (0.4 mmol) were added in one-portion sequentially. After the reaction finished, CHCl₃ was added to the reaction and the precipitate filtered through a short silica gel column. The crude product **5-3** required no more purification (> 96 % yield).

2) Radical clock reactions.

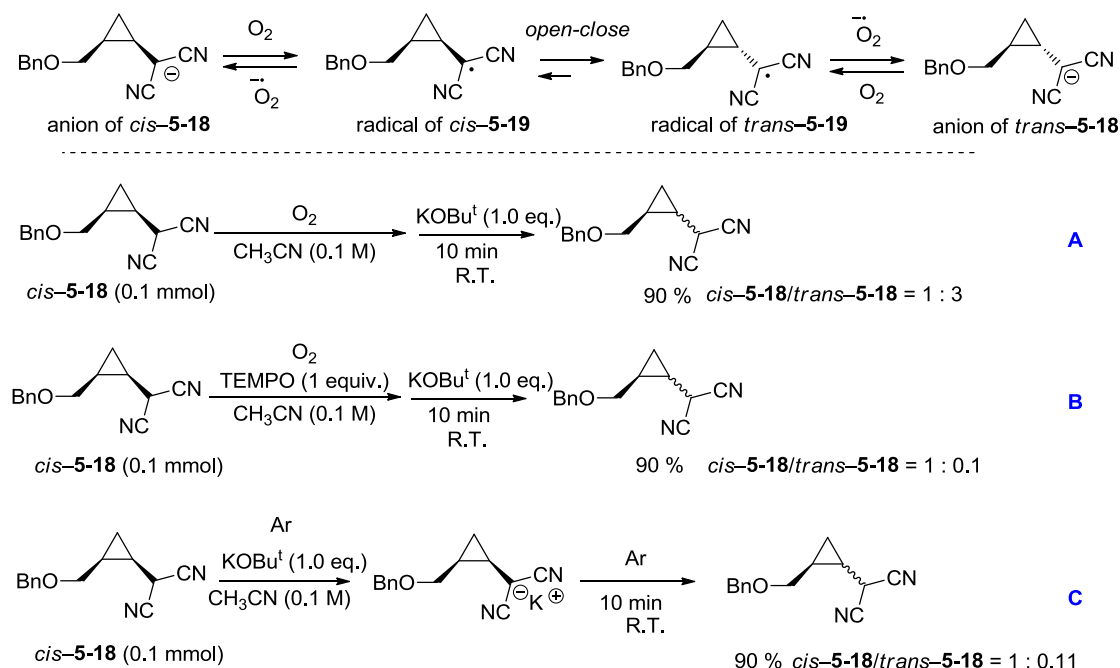
Reaction of anion with O₂.

Cis-**5-18** and *trans*-**5-18** were determined unambiguously by a series of NMR Nuclear Overhauser Effect (NOE) studies.

Scheme S-11 (A): To a two necked flask, malononitrile *cis*-**5-18** (0.1 mmol) in 1.0 mL of CH₃CN was added and the solution was degassed (freeze-pump-thaw cycles) three times before purging under an O₂ atmosphere (balloon), then adding KOBu^t (0.1 mmol) at r.t. After 10 min, the reaction was quenched by adding *sat.* NH₄Cl solution. Extracting with CHCl₃, gave *cis*-**5-18**/*trans*-**5-18** = 1: 3 in 90 % total yield.

Scheme S-11 (B): To a two necked flask, malononitrile *cis*-**5-18** (0.1 mmol) and TEMPO (0.1 mmol, radical quench

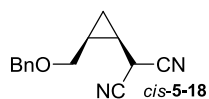
reagent) were added in 1.0 mL of CH₃CN. The solutions were degassed (freeze-pump-thaw cycles) three times, purged with O₂ and the reaction prepared under an O₂ atmosphere (O₂ balloon). After that, KOBu^t (0.1 mmol) was added at RT. The reaction was quenched by adding *sat.* NH₄Cl solution after 10 min, then extracted with CHCl₃ to give *cis*-**5-18**/*trans*-**5-18** = 10:1 in 90 % total yield.



Scheme S-II. K⁺ salt of malononitrile **5-18** reaction with O₂.

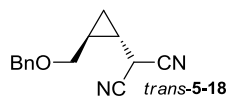
Scheme S-11 (C): To a two necked flask, malononitrile *cis*-**5-18** (0.1 mmol) was dissolved in 1.0 mL of CH₃CN. The solutions were thoroughly degassed (freeze-pump-thaw cycles) 6 times (keep pump time more than 10 minutes) and purged with an argon atmosphere (**Caution:** Ar line was used; if a balloon was used, trace amounts O₂ promoted isomerization of the anion of *cis*-**5-18**). With the solution frozen, KOBu^t was added (0.1 mmol) and the solids subjected to vacuum pump again to make sure the system was not contaminated with O₂. After that, the reaction was warmed to RT to start reaction over 10 min. The reaction was then quenched by adding *sat.* NH₄Cl solution, then extracted with CHCl₃ to give *cis*-**5-18**/*trans*-**5-18** = 10:1.1 in 90 % total yield.

HRMS (ESI): *m/z* calcd. for C₁₄H₁₄N₂NaO (M + Na)⁺ 249.0998. Found 249.0994.



¹H NMR (CDCl₃, 400 MHz): δ 0.73-0.79 (m, 1H), 0.99-1.05 (m, 1H), 1.36-1.44 (m, 1H), 1.52-1.60 (m, 1H), 3.61 (dd, *J* = 5.6, 10.4 Hz, 1H), 3.84 (d, *J* = 10 Hz, 1H), 3.92 (dd, *J* = 3.2, 10.4 Hz, 1H), 4.55 (d, *J* = 12 Hz, 1H), 4.35 (d, *J* = 12 Hz, 1H), 7.24-7.39 (m, 5H).

¹³C NMR (CDCl₃, 100 MHz): δ 5.74, 12.92, 14.96, 22.13, 67.50, 69.83, 109.29, 109.44, 125.05, 125.79, 135.84.

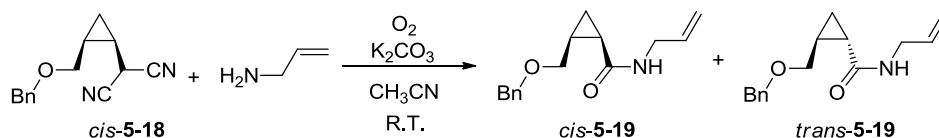


In CDCl₃, the protons of cyclopropane part are overlap, so d⁶-Benzene was used.

¹H NMR (Benzene-D₆, 400 MHz): δ 0.04-0.08 (m, 2H), 0.39-0.45 (m, 1H), 0.61-0.69 (m, 1H), 1.87 (d, *J* = 7.2 Hz, 1H), (m, 1H), 2.68 (dd, *J* = 6.4, 10.0 Hz, 1H), 2.84 (dd, *J* = 6.0, 9.6 Hz, 1H), 4.10 (s, 2H), 7.01-7.18 (m, 5H).

^{13}C NMR (Benzene- D_6 , 100 MHz): δ 8.22, 15.40, 17.43, 24.60, 69.97, 72.31, 111.75, 111.90, 128.26, 138.31.

3) To show radical pathway of **18** when reacting with allylamine under O_2 .



Scheme S-12. Reaction of malononitrile **5-18** reacts with allyl amine under O_2

Procedure: The amine (2.0 equiv) was added to a solution of malononitrile (1.0 equiv, 0.2 mmol) and K_2CO_3 (2.0 equiv) in CH_3CN (2.0 mL, pre-saturated with O_2) at RT under an O_2 atmosphere. The reaction was monitored by TLC. After the malononitrile **5-18** disappeared (about 4 h), the reaction was diluted with CHCl_3 , filtered through a short column, then concentrated and subjected to flash column chromatography on silica gel: Hexane / EA = 3/1; *cis*-**5-20**:*trans*-**5-20** = 23/77 as determined by NOE; *cis* and *trans* products were also separated by flash column).

HRMS (ESI): m/z calcd. for $\text{C}_{15}\text{H}_{19}\text{NNaO}_2$ ($\text{M}+\text{Na}$) $^+$ 268.1308; found: 268.1307.

Cis product: R_f = 0.45

^1H NMR (CDCl_3 , 400 MHz): δ 0.93-0.99 (m, 1H), 1.08-1.12 (m, 1H), 1.47-1.60 (m, 2H), 3.52 (dd, J = 9.6, 10.0 Hz, 1H), 3.80 (dd, J = 5.2, 10.0 Hz, 1H), 3.84-3.88 (m, 2H), 4.44 (dd, J = 11.6, 14.4 Hz, 2H), 5.06-5.20 (m, 2H), 5.75-5.85 (m, 1H), 5.89 (br s, 1H), 7.23-7.33 (m, 5H).

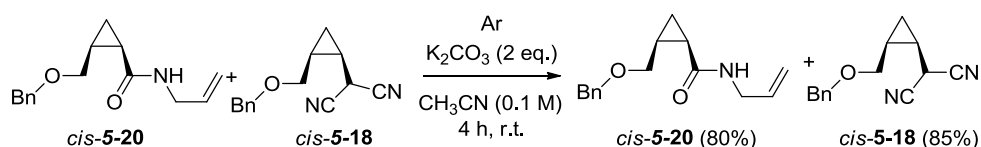
^{13}C NMR (CDCl_3 , 100 MHz): δ 9.81, 19.57, 19.97, 42.15, 68.65, 72.94, 116.20, 127.50, 127.76, 128.28, 134.36, 138.41, 170.63.

Trans product: R_f = 0.44

^1H NMR (CDCl_3 , 400 MHz): δ 0.73-0.77 (m, 1H), 1.18-1.23 (m, 1H), 1.28-1.32 (m, 1H), 1.62-1.76 (m, 1H), 3.31 (dd, J = 6.8, 10.4 Hz, 1H), 3.51 (dd, J = 5.6, 10.4 Hz, 1H), 3.81-3.94 (m, 2H), 4.50 (dd, J = 12.0, 15.2 Hz, 2H), 5.10-5.20 (m, 1H), 5.63 (br s, 1H), 5.78-5.88 (m, 1H), 7.24-7.35 (m, 5H).

^{13}C NMR (CDCl_3 , 100 MHz): δ 11.83, 20.38, 42.18, 71.64, 72.55, 116.43, 127.63, 128.39, 134.33, 138.20, 172.19.

IR (neat): 3295, 2860, 1641, 1547, 1364, 1235 cm^{-1} .

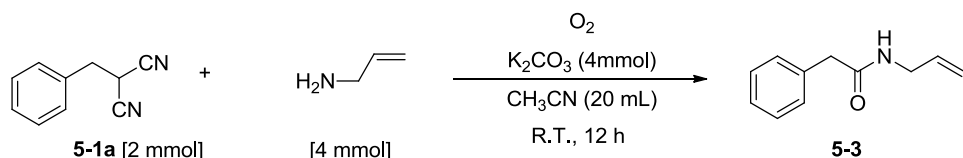


Scheme S-13. Malononitrile *cis*-**18** and amide *cis*-**19** co-reaction with base under Ar.

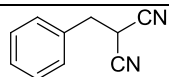
Procedure: The amide *cis*-**5-20** (2.0 equiv.) was added to a solution of the malononitrile *cis*-**5-18** (1.0 equiv., 0.2 mmol) and K_2CO_3 (2.0 equiv.) in CH_3CN (2.0 mL, the solutions were thoroughly degassed (freeze-pump-thaw cycles) 3 times) and purged with an argon atmosphere. After stirring at RT for 4h, the reaction remained unchanged and so was diluted with CHCl_3 , filtered through a short column, then check ^1H NMR

5.4 CN^-/CNO^- analysis

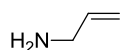
- 1) Required concentration of anion HPLC: [10 – 100 mmol/L]
- 2) Reaction and reagents



Reagent information:



synthesized, purified via flash silica gel column chromatography (purity > 98 %)



Commercial available from **TCI** (purity > 99 %)



Commercial available from **wako** (purity > 99.5 %)



Commercial available from **wako** (purity > 99.5 %)

3) Procedure to make sample

After the reaction completed, all the CH₃CN was removed, pre-cooled NaOH solution (pH = 12) was added in 3 portions (20 mL + 20 mL + 20 mL) and the solution stirred for 20 min to dissolve all inorganic salts. The collected water phase was filtered and transferred to a 100 mL volumetric flask, and NaOH solution (pH = 12) was added to reach 100 mL exactly. (The solution should be stored in dark at low temperature)



volumetric flask

分析結果報告書 (溶液試料)

2016/2/1 依頼整理番号 107275

【分析結果】 (単位 : mmol/L)

	[NCO]	[NCO + CN]	[CN]
平均値	1.52	35.4	33.9
SD	0.03	0.4	
RSD	2.3%	1.2%	

(n=3)

【分析方法】

イオンクロマトグラフを用いて検液中の NCO を測定 (電気伝導度検出)

[NCO] : 試料を適宜希釈、pH12 に調整後測定

[NCO + CN] : 試料を適宜希釈、pH12 に調整後、
クロラミン T によって CN を NCO に酸化して測定 (ref.)

[CN] = [NCO + CN] - [NCO] として算出

ref.) M. Nonomura, *Journal of Chromatography*, 465(1989) pp.395-401

Theoretical concentration (cf. Scheme S-9)

Path A: CN⁻ = 20 mmol/ L,

NCO⁻ = 20 mmol/ L;

Path B: CN⁻ = 40 mmol/ L

4) Results and discussion:

Real results: CN⁻ = 33.9 mmol/ L,

NCO⁻ = 1.52 mmol/ L

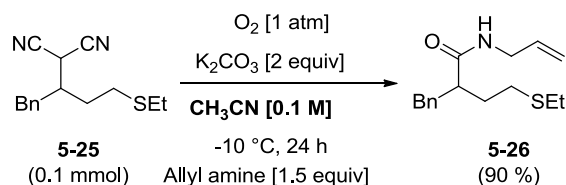
Discussion: Since CN⁻ was obtained in good yield 84.8 %, and NCO⁻ in low yield, **Path B** is the most plausible and preferred (cf. Scheme S-9).

*イオンクロマトグラフ装置条件 (Metrohm 850 Professional IC)

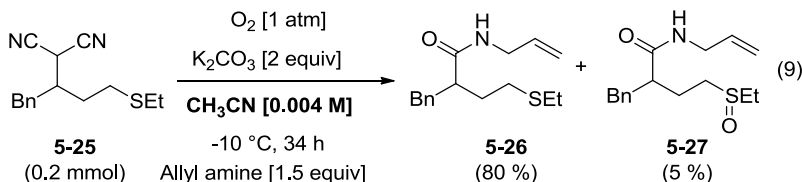
分離カラム :	Metrosep A Supp 4 (Metrohm製、250mmH×4mmID)
ガードカラム :	Metrosep A Supp 4/5 S-Guard /4.0 (Metrohm製)
カラム温度 :	25℃
溶離液組成 :	1.8mmol/L Na ₂ CO ₃ + 1.7mmol/L NaHCO ₃
溶離液流量 :	1mL/min.
試料導入量 :	20μL
サプレッサー :	MSM-HC (Metrohm製、再生液 : 50mmol/L H ₂ SO ₄)
炭酸サプレッサー :	MCS (Metrohm製)
検出器 :	Conductivity detector (Metrohm製)
データ処理ソフト :	MagIC Net™

(金研 材料分析研究コア 権沢)

5.5 Control reaction to trap dioxirane intermediate

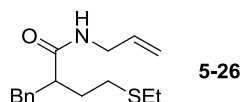


Scheme S-14. A Control reaction to support formation of dioxirane intermediate



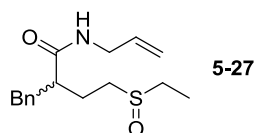
Scheme S-14 B. Control reaction to support formation of dioxirane intermediate

Procedure: The amine (2.0 equiv) was added to a solution of malononitrile **5-20** (1.0 equiv, 0.2 mmol) and K_2CO_3 (2.0 equiv) in CH_3CN (2.0 mL, pre-saturated by O_2) at -20°C under O_2 atmosphere. After the malononitrile **5-20** disappeared by TLC (about 34 h), the reaction was diluted with CHCl_3 , filtered through a short silica column, then concentrated. The ratio of **5-22** was determined by ^1H NMR. Further purification via flash column chromatography on silica gel (hexane / EA = 3/1 gave amide **5-21**; EA/MeOH = 10/1 gave amide **5-22**).



^1H NMR (CDCl_3 , 400 MHz): δ 1.20 (t, $J = 7.2$ Hz, 3H), 1.66-1.74 (m, 1H), 1.99-2.08 (m, 1H), 2.39-2.72 (m, 6H), 2.92 (dd, $J = 9.6$ Hz, 13.2 Hz, 2H), 3.70-3.78 (m, 2H), 4.89-4.99 (m, 2H), 5.41 (br s, 1H), 5.56-5.66 (m, 1H), 7.14-7.26 (m, 5H).
 ^{13}C NMR (CDCl_3 , 100 MHz): δ 14.70, 25.61, 29.40, 31.67, 39.07, 41.61, 48.49, 116.15, 126.33, 128.41, 128.90, 134.02, 139.55, 173.86.

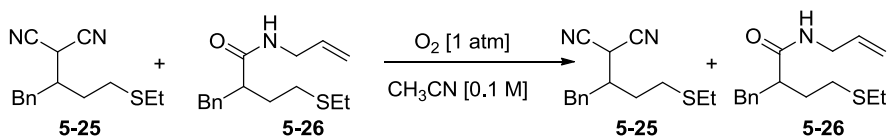
HRMS (ESI): m/z calcd. for $\text{C}_{16}\text{H}_{23}\text{NNaOS}$ ($\text{M}+\text{Na}$) $^+$ 300.1393; found: 300.1398.



(1:1 mixture of diastereomers)

^1H NMR (CDCl_3 , 400 MHz): δ 1.25-1.30 (m, 3H), 1.77-2.19 (m, 2H), 2.54-2.79 (m, 6H), 2.88-2.99 (m, 1H), 3.66-3.80 (m, 2H), 4.87-4.99 (m, 2H), 5.53-5.67 (m, 1H), 5.7 (br, 0.5 H), 6.02 (br, 0.5 H), 7.15-7.26 (m, 5H).
 ^{13}C NMR (CDCl_3 , 100 MHz): δ 6.46, 6.95, 24.87, 27.58, 39.18, 39.32, 41.67, 46.21, 47.96, 48.20, 48.40, 49.00, 116.24, 116.34, 126.43, 126.56, 128.47, 128.54, 128.89, 128.93, 133.82, 133.94, 139.00, 139.11, 173.27, 173.35.

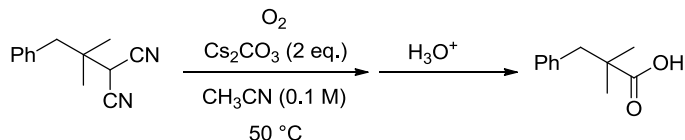
HRMS (ESI): m/z calcd. for $\text{C}_{16}\text{H}_{23}\text{NNaO}_2\text{S}$ ($\text{M}+\text{Na}$) $^+$ 316.1342; found: 316.1332.



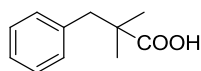
Scheme S-15. Malononitrile **5-25** and amide **5-26** reaction with O_2 .

Procedure: Malononitrile **5-25** (0.1 mmol) and amide **5-26** (0.1 mmol) were added to a 5 mL flask, then CH₃CN (2.0 mL, pre-saturated by O₂) was added, put the reaction under O₂ atmosphere at R.T. for 48 h. Then the reaction mixture was diluted with CHCl₃, then check crude ¹H NMR. Without new compounds generated.

5.6 Control reaction to support acyl cyanide (5-16) formation.



Malononitrile (0.2 mmol) and Cs₂CO₃ (0.4 mmol) were added to a 5 mL flask, then CH₃CN (2.0 mL, pre-saturated by O₂) was added, put the reaction under O₂ atmosphere at 50 °C until malononitrile disappeared. Then collect the solid salt and acidified with 1M HCl, extracted with ethyl acetate, and then the organic phase was collected and dried with anhydride MgSO₄. Concentration in vacuum gave the crude acid in about 60 % yield.



¹H NMR (400 MHz, CDCl₃): δ 1.20 (s, 6H), 2.88 (s, 2 H), 7.15-7.28 (m, 5H), 8.4 (br s, 1H). ¹³C NMR (CDCl₃, 100 MHz): δ 24.83, 43.58, 46.04, 126.69, 128.18, 130.39, 137.72, 184.19.

IR (neat): 2929, 1700, 701 cm⁻¹.

HRMS (ESI): *m/z* calcd. for C₁₁H₁₄NaO₂ (M +Na)+ 201.0886. Found 201.0889.

5.7 General Procedure for Amide Formation

General Procedure A

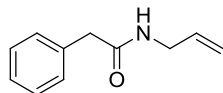
The amine (2.0 equiv.) was added to a solution of malononitrile (1.0 equiv., 0.2 mmol) and K₂CO₃ (2.0 equiv., finer powders will make the reaction faster) in CH₃CN (2.0 mL) at R.T. under O₂ atmosphere. After malononitrile disappears as indicated by TLC, the reaction was diluted with CHCl₃, filtered through a short silica column, then concentrated and subjected to purification by silica gel flash column chromatography.

General Procedure B

In a reaction tube, Cs₂CO₃ (2.0 equiv.) and 4Å MS (100 mg) were dried under flame and saturated with O₂ atmosphere. Then the reaction tube were cooled to R.T. before sequential addition of CH₃CN (2.0 mL), the malononitrile (1.0 equiv., 0.2 mmol), and then the amine (2.0 equiv.). The reaction was heated at 50 °C in O₂ atmosphere until TLC indicated all the malononitrile had disappeared; after which, the reaction was diluted by CHCl₃, filtered through a short silica column, then concentrated and subjected to purification by flash column chromatography on silica gel.

General Procedure C

In a reaction tube, Cs₂CO₃ (2.0 equiv.) and 4Å MS (100 mg) were dried under flame and saturated with O₂ atmosphere. The reaction solids were cooled to R.T. CH₃CN (2.0 mL), the malononitrile (2.0 equiv., 0.4 mmol), and then the amine (1.0 equiv.) were added sequentially. The reaction was heated at 70 °C in O₂ atmosphere until TLC indicated all the malononitrile had disappeared; after which, the reaction was diluted by CHCl₃, filtered through a short silica column, then concentrated and subjected to purification by flash column chromatography on silica gel.



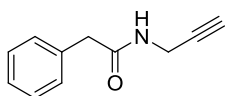
N-allyl-2-phenylacetamide (5-3)

Following the **procedure A**, white solid, yield = 96 %.

¹H NMR (CDCl₃, 400 MHz): 3.56 (s, 2H), 3.81 (t, J = 1.6 Hz, 2H), 5.00-5.05 (m, 2H), 5.64 (br s, 1H), 5.71-5.79 (m, 1H), 7.24-7.35 (m, 5H).

¹³C NMR (CDCl₃, 100 MHz): 41.96, 43.84, 116.11, 127.45, 129.10, 129.52, 134.12, 134.96, 170.93.

IR (neat): 3241, 3061, 1632, 1555, 1454, 1270, 1160, 991, 921, 762, 692, 608, 542 cm⁻¹.



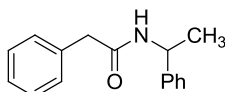
2-phenyl-N-(prop-2-yn-1-yl)acetamide (5-4a)

Following the **procedure A**, white solid, yield = 91 %.

¹H NMR (CDCl₃, 400 MHz): δ 2.16 (t, J = 2.4 Hz, 1H), 3.55 (s, 2H), 3.97 (dd, J = 5.2, 2.4 Hz, 2H), 5.94 (br s, 1H), 7.23-7.35 (m, 5H).

¹³C NMR (CDCl₃, 100 MHz): δ 29.28, 43.37, 71.50, 79.43, 127.40, 129.00, 129.41, 134.45, 170.74.

IR (neat): 3269, 3034, 1664, 1632, 1541, 1449, 1264, 1157, 732, 692, 650, 608, 549 cm⁻¹.



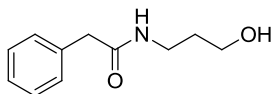
2-phenyl-N-(1-phenylethyl)acetamide (5-4b)

Following the **procedure A**, white solid, yield = 95 %.

¹H NMR (CDCl₃, 400 MHz): δ 1.38 (d, J = 6.8 Hz, 3H), 3.54 (s, 2H), 5.10 (quant, J = 7.2 Hz, 1H), 5.78 (br d, J = 6.0 Hz, 1H), 7.15-7.35 (m, 5H).

¹³C NMR (CDCl₃, 100 MHz): δ 21.89, 43.87, 48.81, 126.02, 127.32, 127.36, 128.67, 129.03, 129.41, 135.04, 132.20, 170.14.

IR (neat): 3316, 3027, 2973, 1648, 1534, 1495, 1452, 1343, 1247, 758, 701 cm⁻¹.



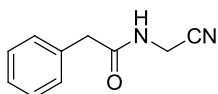
N-(3-hydroxypropyl)-2-phenylacetamide (5-4c)

Prepared according procedure A, white solid, yield = 87 %.

¹H NMR (400 MHz, CDCl₃): δ 1.54-1.60 (m, 2H), 3.29-3.34 (m, 3H), 3.5-3.53 (m, 4H), 6.05 (br s, 1H), 7.20-7.33 (m, 5H);

¹³C NMR (CDCl₃, 100 MHz): δ 32.14, 36.60, 43.70, 59.36, 127.46, 129.09, 129.47, 134.88, 172.52.

IR (neat): 3287, 2927, 1643, 1555, 1495, 1453, 1271, 1071, 695 cm⁻¹.



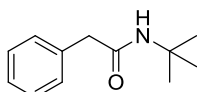
N-(cyanomethyl)-2-phenylacetamide (5-4d)

Prepared according **procedure A**, white solid, yield = 96 %

¹H NMR (400 MHz, CDCl₃): δ 3.55 (s, 2H), 4.00 (d, J = 5.6 Hz, 2H), 6.37 (br s, 1H), 7.20-7.35 (m, 5H);

¹³C NMR (CDCl₃, 100 MHz): 27.66, 43.02, 116.14, 127.78, 129.23, 129.53, 133.85, 171.51;

IR (neat): 3288, 3061, 1660, 1537, 1496, 1454, 1414, 1030, 697 cm⁻¹.



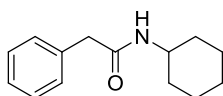
N-(tert-butyl)-2-phenylacetamide (5-4e)

Following the **procedure A**, white solid, yield = 89 %.

¹H NMR (CDCl₃, 400 MHz): δ 1.26 (s, 9H), 3.45 (s, 2H), 5.18 (br s, 1H), 7.20-7.25 (m, 3 H), 7.27-7.34 (m, 2H).

¹³C NMR (CDCl₃, 100 MHz): δ 28.80, 45.02, 51.36, 127.25, 129.03, 129.40, 135.62, 170.40.

IR (neat): 3279, 3076, 2971, 1643, 1556, 1495, 1448, 1428, 1358, 1269, 1230, 947, 700 cm^{-1} .



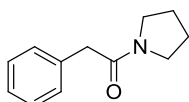
N-cyclohexyl-2-phenylacetamide (5-4f)

Prepared according to **procedure A**, white solid, yield = 96 %

^1H NMR (400 MHz, CDCl_3): δ 0.94-1.11 (m, 3H), 1.24-1.34 (m, 2H), 1.49-1.60 (m, 3H), 1.78-1.89 (m, 2H), 3.50 (s, 2H), 3.67-3.78 (m, 1H), 5.30 (br s, 1H), 7.21-7.33 (m, 5H).

^{13}C NMR (CDCl_3 , 100 MHz): δ 24.79, 25.55, 32.99, 44.09, 48.27, 127.32, 129.04, 129.44, 135.30, 170.13.

IR (neat): 3276, 2931, 2850, 1636, 1559, 1447, 694 cm^{-1} .



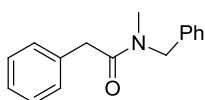
2-phenyl-1-(pyrrolidin-1-yl)ethanone (5-4g)

Following the procedure A, white solid, yield = 90 %.

^1H NMR (CDCl_3 , 400 MHz): 1.79-1.92 (m, 4H), 3.39 (t, J = 6.8 Hz, 2H), 3.46 (t, J = 6.8 Hz, 2H), 3.63 (s, 2H), 7.19-7.31 (m, 5H).

^{13}C NMR (CDCl_3 , 100 MHz): 24.45, 26.25, 42.39, 46.03, 46.98, 126.79, 128.68, 129.07, 135.06, 169.64.

IR (neat): 2972, 2874, 1643, 1495, 1427, 1341, 1191, 742, 720 cm^{-1} .



N-benzyl-N-methyl-2-phenylacetamide (5-4h)

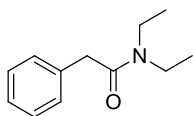
Following the **procedure A**; sticky oil, yield = 94 %.

A mixture of two stereoisomers A and B.

^1H NMR (400 MHz, CDCl_3): δ 2.88 (s, 3aH, A), 2.94 (s, 3bH, B), 3.74 (s, 2bH, B), 3.77 (s, 2aH, A), 4.51 (s, 2bH, B), 4.60 (s, 2aH, A), 7.08 (d, J = 6.8 Hz, 1H), 7.21-7.35 (m, 9H, A+B).

^{13}C NMR (CDCl_3 , 100 MHz): δ 34.09(B), 35.28(A), 40.93(B), 41.27(A), 51.04(A), 53.73(B), 126.46, 126.85, 126.90, 127.42, 127.72, 128.12, 128.63, 128.75, 128.76, 128.86, 128.90, 128.99, 135.03, 135.18, 136.56, 137.37, 171.21(A), 171.55(B).

IR (neat): 3028, 1645, 1494, 1452, 1399, 1110, 730, 697 cm^{-1} .



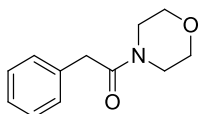
N,N-diethyl-2-phenylacetamide (5-4i)

Following **procedure A**, sticky oil, yield = 84 %.

^1H NMR (400 MHz, CDCl_3): δ 1.05 (t, J = 7.2 Hz, 3H), 1.09 (t, J = 7.2 Hz), 3.26 (q, J = 7.2 Hz, 2H), 3.36 (q, J = 7.2 Hz, 2H), 3.66 (s, 2H), 7.18-7.30 (m, 5H).

^{13}C NMR (CDCl_3 , 100 MHz): δ 13.01, 14.27, 40.22, 40.99, 42.43, 126.72, 128.68, 128.75, 135.61, 170.21.

IR (neat): 2973, 2933, 1642, 1495, 1454, 1133, 726, 696 cm^{-1} .



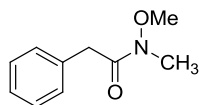
1-morpholino-2-phenylethanone (5-4j)

Prepared according procedure A, white solid, yield = 91 %.

¹H NMR (400 MHz, CDCl₃): δ 3.38-3.45 (m, 4H), 3.60 (s, 4H), 3.69 (s, 2H), 7.19-7.31 (m, 5H).

¹³C NMR (CDCl₃, 100 MHz): δ 40.90, 42.22, 46.59, 66.52, 66.85, 126.97, 128.60, 128.87, 134.88, 169.70.

IR (neat): 2855, 1643, 1454, 1272, 1114, 729, 698 cm⁻¹.

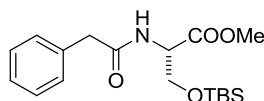


N-methoxy-N-methyl-2-phenylacetamide (5-4k)

Following **procedure A**, HCl•HN(CH₃)OMe was used, K₂CO₃ (3 equiv.), sticky oil, yield = 70 %.

¹H NMR (CDCl₃, 400 MHz): δ 3.17 (s, 3H), 3.58 (s, 3H), 3.76 (s, 2H), 7.20-7.32 (m, 5H).

¹³C NMR (CDCl₃, 100 MHz): δ 32.21, 39.39, 61.25, 126.74, 128.47, 129.27, 134.93.



(S)-methyl-3-((tert-butyldimethylsilyl)oxy)-2-(2-phenylacetamido)propanoate (5-4l)

Prepared according **procedure A**, sticky oil, yield = 60 %.

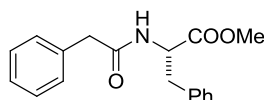
¹H NMR (CDCl₃, 400 MHz): δ -0.10 (s, 3H), -0.82 (s, 3H), 0.74 (s, 9H), 3.61 (d, *J* = 3.2 Hz, 2H), 3.68 (s, 3H), 3.70 (dd, *J* = 2.8, 10.0 Hz, 1H), 3.98 (dd, *J* = 2.4, 10.0 Hz, 1H), 4.62 (ddd, *J* = 2.4, 2.4, 5.6 Hz, 1H), 6.24 (br d, *J* = 8.0 Hz, 1H), 7.25-7.36 (m, 5H).

¹³C NMR (CDCl₃, 100 MHz): δ 18.10, 25.69, 43.79, 52.45, 54.33, 63.35, 127.54, 129.15, 129.60, 134.59, 170.82, 170.90.

IR (neat): 3312, 2952, 2856, 1750, 1654, 1516, 1471, 1254, 1208, 1113, 836, 779, 727 cm⁻¹.

HRMS (ESI) *m/z* calcd. for C₁₈H₂₉NNaO₄Si (*M* + Na)⁺ 374.758. Found: 374.1763.

[α]_D²⁷ 25.30 (c 1.7, CHCl₃).



(S)-methyl 3-phenyl-2-(2-phenylacetamido)propanoate (5-4m)

Prepared according **procedure A**, white solid, yield = 83 %, ee > 99 %.

The enantiomeric ratio was determined by HPLC analysis using Daicel Chiralpak IC column (Hex/i-Pr = 10/1, 2 mL/min, 20 °C, 210 nm, *t*_{minor} = 32.99 min, *t*_{major} = 19.86 min).

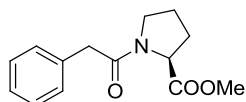
¹H NMR (CDCl₃, 400 MHz): δ 2.99 (dd, *J* = 14.0, 6.0 Hz, 1H), 3.07 (dd, *J* = 13.6, 5.6 Hz, 1H), 3.54 (s, 2H), 3.69 (s, 3H), 4.85 (ddd, *J* = 6.0, 6.0, 8.0 Hz, 1H), 5.90 (br d, *J* = 7.2 Hz, 1H), 6.88-6.92 (m, 2H), 7.17-7.21 (m, 5H), 7.26-7.35 (m, 5H);

¹³C NMR (CDCl₃, 100 MHz): δ 37.58, 43.58, 52.26, 52.96, 127.00, 127.32, 128.49, 128.94, 129.10, 129.36, 134.42, 135.56, 170.41, 171.77;

IR (neat): 3287, 3028, 2949, 1744, 1653, 1541, 1496, 1454, 1217, 727, 699 cm⁻¹.

HRMS (ESI) *m/z* calcd. for C₁₈H₁₉NNaO₃ (*M* + Na)⁺ 320.1257. Found: 320.1262.

[α]_D²⁷ 45.76 (c 1.5, CHCl₃).



(S)-methyl 1-(2-phenylacetyl)pyrrolidine-2-carboxylate (5-4n)

Prepared according **procedure A**, white solid, yield = 89 %.

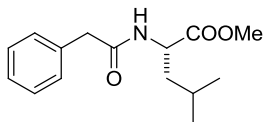
A mixture of two stereo isomers A and B in approximately 5:1 ratio.

¹H NMR (400 MHz, CDCl₃): δ 1.83-2.17 (m, 5H, A+B), 3.43-3.67 (m, 5 H, A+B), 4.39-4.49 (m, 2H), 7.18-7.30 (m, 5H).
¹³C NMR (CDCl₃, 100 MHz): δ 22.52(B), 24.94(A), 29.28(A), 31.56(B), 41.91(B), 41.96(A), 46.67(B), 47.38(A), 52.22(A), 52.58(B), 58.95(A), 59.59(B), 126.84(B), 126.92(A), 128.65(A+B), 129.05(A+B), 134.48(A+B), 169.85(B), 169.94(A), 172.70(B), 172.84(A).

IR (neat): 2953, 1745, 1650, 1496, 1422, 1198, 1029, 722 cm⁻¹.

HRMS (ESI) *m/z* calcd. for C₁₄H₁₇NNaO₃ (M + Na)⁺ 270.1101. Found: 270.1110.

[α]_D²⁷ -69.47 (c 1.9, CHCl₃).



(S)-methyl 4-methyl-2-(2-phenylacetamido)pentanoate (5-4o)

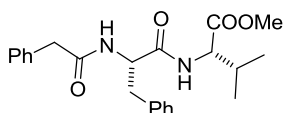
Prepared according **procedure A**, white solid, yield =84 %.

¹H NMR (CDCl₃, 400 MHz): 0.87 (d, *J* = 5.2 Hz, 3H), 0.88 (d, *J* = 5.2 Hz, 3H), 1.40-1.62 (m, 3H), 3.60 (s, 2H), 3.70 (s, 3H), 4.62 (ddd, *J* = 5.2, 8.8, 8.8 Hz, 1H), 5.75 (br d, *J* = 7.6 Hz, 1H), 7.26-7.38 (m, 5H).

¹³C NMR (CDCl₃, 100 MHz): 22.09, 22.87, 25.01, 41.56, 43.77, 50.92, 52.39, 127.54, 129.13, 29.54, 134.70, 170.80, 173.50.

IR (neat): 3286, 2956, 1747, 1648, 1543, 1496, 1437, 1203, 1165, 727, 696 cm⁻¹.

HRMS (ESI) *m/z* calcd. for C₁₅H₂₁NNaO₃ (M + Na)⁺ 286.1414. Found: 286.1419.



(S)-methyl 3-methyl-2-((S)-3-phenyl-2-(2-phenylacetamido)propanamido)butanoate (5-4p)

Prepared according **procedure A**, white solid, yield = 70 %.

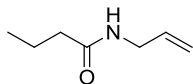
¹H NMR (CDCl₃, 400 MHz): δ 0.82 (d, *J* = 4.4 Hz, 3H), 0.84 (d, *J* = 4.4 Hz, 3H), 1.41-1.56 (m, 3H), 2.92 (dd, *J* = 7.2, 14 Hz, 1H), 2.99 (dd, *J* = 6.8, 14Hz, 1H), 3.47 (s, 2H), 3.66 (s, 3H), 4.43-4.49 (m, 1H), 4.70 (ddd, *J* = 7.2, 7.2, 7.2 Hz, 1H), 6.21 (br d, *J* = 8.0 Hz, 1H), 6.62 (br d, *J* = 8.0 Hz, 1H), 7.01-7.03 (m, 2H), 7.08-7.11 (m, 2H), 7.16-7.19 (m, 3H), 7.23-7.29 (m, 3H).

¹³C NMR (CDCl₃, 100 MHz): δ 21.96, 22.78, 24.84, 37.79, 41.20, 43.59, 50.99, 52.32, 54.16, 126.95, 127.44, 128.61, 129.06, 129.39, 129.41, 134.42, 136.35, 170.79, 171.15, 172.89.

IR (neat): 3268, 3075, 2956, 1749, 1642, 1556, 1495, 1438, 1248, 1196, 1157, 731, 701 cm⁻¹.

HRMS (ESI) *m/z* calcd. for C₂₄H₃₀N₂NaO₄ (M + Na)⁺ 433.2098. Found: 433.2103.

[α]_D²⁷ -19.06 (c 0.8, CHCl₃).

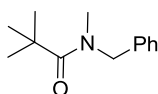


N-allylbutyramide (5-4q)

Prepared according **procedure A**, sticky oil, yield = 90 %.

¹H NMR (CDCl₃, 400 MHz): δ 0.90-1.01 (m, 3H), 1.60-1.69 (m, 2H), 2.07-2.17 (m, 2H), 3.84-3.88 (m, 2H), 5.08-5.18 (m, 2H), 5.60 (br s, 1H), 5.76-5.86 (m, 1H).

¹³C NMR (CDCl₃, 100 MHz): δ 13.75, 19.14, 38.64, 41.81, 116.23, 134.35.

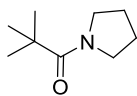


N-benzyl-N-methylpivalamide (5-6a)

Following the **procedure B**, sticky oil, yield = 71 %.

¹H NMR (CDCl₃, 400 MHz): δ 1.31 (s, 9H), 2.96 (s, 3H), 4.62 (s, 2H), 7.16-7.33 (m, 5H).

¹³C NMR (CDCl₃, 100 MHz): δ 28.39, 36.08, 38.89, 53.19, 127.16, 127.26, 128.59, 137.56, 177.80.

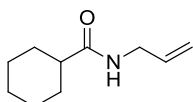


2,2-dimethyl-1-(pyrrolidin-1-yl)propan-1-one (5-6b)

Following the **procedure B**, sticky oil, yield = 91 %.

¹H NMR (CDCl₃, 400 MHz): δ 1.21 (s, 9H), 1.81 (br s, 4H), 3.49 (br s, 4H).

¹³C NMR (CDCl₃, 100 MHz): δ 27.46, 38.89, 47.81, 176.42.



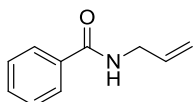
N-allylcyclohexanecarboxamide (5-7a)

Prepared according **procedure B**, white solid, yield = 87 %.

¹H NMR (400 MHz, CDCl₃): δ 1.14-1.28 (m, 3H), 1.36-1.45 (m, 2H), 1.62-1.65 (m, 1H), 1.73-1.85 (m, 4H), 2.03-2.11 (m, 1H), 3.81-3.84 (m, 2H), 5.05-5.15 (m, 2H), 5.68 (br s, 1H), 5.68-5.84 (m, 1H).

¹³C NMR (CDCl₃, 100 MHz): δ 25.86, 29.71, 29.95, 41.75, 45.61, 116.16, 134.60, 176.07.

IR (neat): 3289, 2928, 2851, 1636, 1547, 1447, 984, 018, 704 cm⁻¹.



N-allylbenzamide (5-7b)

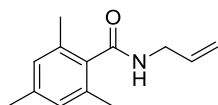
Prepared according **procedure B**, white solid, yield = 96 %.

¹H NMR (400 MHz, CDCl₃): δ 4.04-4.08 (m, 2H), 5.14-5.26 (m, 2H), 5.87-5.96 (m, 1H), 6.49 (br s, 1H), 7.38-7.40 (m, 2H), 7.41-7.42 (m, 1H), 7.46-7.80 (m, 2H).

¹³C NMR (CDCl₃, 100 MHz): δ 42.51, 116.66, 127.05, 128.62, 131.55, 134.26, 134.56, 167.52.

IR (neat): 3315, 3066, 1643, 1578, 1537, 1489, 1422, 1307, 993, 922, 694 cm⁻¹.

HRMS (ESI) *m/z* calcd. for C₁₁H₁₄NaO₂ (M+Na)⁺ 201.0886, found 201.0889.



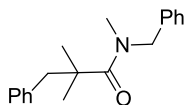
N-allyl-2,4,6-trimethylbenzamide (5-7c)

Following the **procedure B**, white solid, yield = 52 %.

¹H NMR (400 MHz, CDCl₃): δ 2.27 (s, 3H), 2.28 (s, 6H), 4.06-4.09 (m, 2H), 5.16-5.28 (m, 2H), 5.72 (br s, 1H), 5.88-5.97 (m, 1H), 6.83 (s, 2H).

¹³C NMR (CDCl₃, 100 MHz): δ 19.11, 21.04, 41.96, 116.83, 128.17, 134.05, 134.11, 134.79, 138.42, 170.34.

HRMS (ESI) *m/z* calcd. for C₁₃H₁₇NNaO (M+Na)⁺ 226.1202. Found 226.1199.



N-benzyl-N,2,2-trimethyl-3-phenylpropanamide (5-8a)

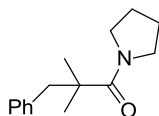
Following the **procedure B**, sticky oil, yield = 58 %.

¹H NMR (CDCl₃, 400 MHz): 1.30 (s, 6H), 2.97 (s, 2H), 2.99 (s, 3H), 4.61 (s, 2H), 7.08-7.11 (m, 2H), 7.20-7.33 (m, 8H);

^{13}C NMR (CDCl_3 , 100 MHz): 26.82, 36.52, 43.96, 46.27, 53.69, 126.53, 127.39, 127.86, 128.15, 128.71, 130.40, 137.60, 138.19, 176.86.

IR (neat): 2924, 1626, 1495, 1453, 1394, 1087, 737, 700 cm^{-1} .

HRMS (ESI) m/z calcd. for $\text{C}_{19}\text{H}_{24}\text{NO}$ ($\text{M}+\text{H}$) $^+$ 282.1852; found: 282.1866.



2,2-dimethyl-3-phenyl-1-(pyrrolidin-1-yl)propan-1-one (5-8b)

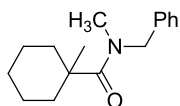
Following the **procedure B**, sticky oil, yield = 78 %.

^1H NMR (CDCl_3 , 400 MHz): 1.24 (s, 6H), 1.72 (br s, 4H), 2.85 (s, 2H), 3.39 (br s, 4H), 7.08-7.10 (m, 2H), 7.15 (m, 3H).

^{13}C NMR (CDCl_3 , 100 MHz): 23.00, 26.05, 44.09, 46.35, 47.67, 48.31, 126.29, 127.68, 129.90, 129.85, 130.11, 138.37, 175.27.

IR (neat): 2968, 2874, 1613, 1402, 1378, 1156, 762, 743, 702 cm^{-1} .

HRMS (ESI) m/z calcd. $\text{C}_{15}\text{H}_{21}\text{NNaO}$ ($\text{M} + \text{Na}$) $^+$ 254.1515; Found: 254.1524.



N-benzyl-N,1-dimethylcyclohexanecarboxamide (5-9a)

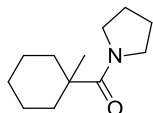
Following the **procedure B**, sticky oil, yield = 51 %.

^1H NMR (CDCl_3 , 400 MHz): δ 1.26 (s, 3H), 1.33-1.55 (m, 8H), 2.09-2.95 (m, 2H), 2.95 (3H), 4.63 (s, 2H), 7.18-7.33 (5H).

^{13}C NMR (CDCl_3 , 100 MHz): δ 23.17, 24.28, 25.98, 36.21, 37.05, 42.93, 53.35, 127.12, 127.38, 128.55, 137.75, 177.25.

IR (neat): 2930, 2856, 1641, 921, 732 cm^{-1} .

HRMS (ESI) m/z calcd. $\text{C}_{16}\text{H}_{23}\text{NNaO}$ ($\text{M} + \text{Na}$) $^+$ 268.1672. Found: 268.1673.



(1-methylcyclohexyl)(pyrrolidin-1-yl)methanone (5-9b)

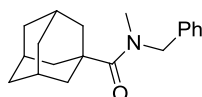
Following the **procedure B**, sticky oil, yield = 70 %.

^1H NMR (400 MHz, CDCl_3): δ 1.14 (s, 3H), 1.22-1.32 (m, 3H), 1.38-1.52 (m, 5H), 1.82 (br s, 4H), 2.08-2.13 (m, 2H), 3.50-3.53 (m, 4H).

^{13}C NMR (CDCl_3 , 100 MHz): δ 23.27, 24.17, 26.12, 36.39, 43.46, 48.01, 175.84.

IR (neat): 2930, 1605, 1391, 1087, 921, 732 cm^{-1} .

HRMS (ESI) m/z calcd. $\text{C}_{12}\text{H}_{21}\text{NNaO}$ ($\text{M} + \text{Na}$) $^+$ 218.1515; Found: 218.1510.



(3r,5r,7r)-N-benzyl-N-methyladamantane-1-carboxamide (5-10a)

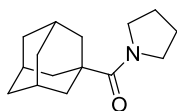
Following the **procedure B**, sticky oil, yield = 62 %.

^1H NMR (CDCl_3 , 400 MHz): 2.96 (s, 3H), 4.67 (s, 2H), 7.15 -7.33 (m, 5H).

^{13}C NMR (CDCl_3 , 100 MHz): 28.63, 36.38, 36.76, 39.21, 42.06, 53.56, 127.29, 128.73, 137.72, 177.32.

IR (neat): 2904, 2849, 1624, 1451, 1384, 1052, 726, 697 cm^{-1} .

HRMS (ESI) m/z calcd. $\text{C}_{19}\text{H}_{25}\text{NNaO}$ ($\text{M} + \text{Na}$) $^+$ 306.1828. Found 306.1858.



(3r,5r,7r)-adamantan-1-yl(pyrrolidin-1-yl)methanone (5-10b)

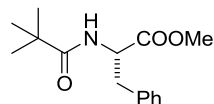
Following the **procedure B**, white solid, yield = 90 %.

¹H NMR (400 MHz, CDCl₃): δ 1.66-1.72 (m, 6H), 1.81 (br s, 4H), 1.93-2.00 (m, 9H), 3.55 (br s, 4H).

¹³C NMR (CDCl₃, 100 MHz): δ 28.34, 28.51, 36.79, 38.31, 41.82, 48.04, 175.98.

IR (neat): 2903, 1602, 1397 cm⁻¹.

HRMS (ESI) *m/z* calcd. C₁₅H₂₃NNaO (M + Na)⁺ 256.1672. Found: 256.1674.



(S)-methyl 3-phenyl-2-pivalamidopropanoate (5-6c)

Prepared according **procedure C**, white solid, yield = 55 %, ee > 97 %.

The enantiomeric ratio was determined by HPLC analysis using Daicel Chiralpak ID column (Hex/i-Pr = 15/1, 1 mL/min, 20 °C, 208 nm, *t*_{minor} = 10.84 min, *t*_{major} = 13.53 min).

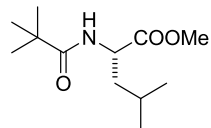
¹H NMR (400 MHz, CDCl₃): δ 1.29 (s, 9H), 3.07 (dd, *J* = 6.0, 14 Hz, 1H), 3.16 (dd, *J* = 6.0, 13.6 Hz, 1H), 3.72 (s, 3H), 4.82-4.87 (m, 1H), 6.01 (br d, *J* = 6.8 Hz, 1H), 7.05-7.07 (m, 2H), 7.20-7.29 (m, 4H).

¹³C NMR (CDCl₃, 100 MHz): δ 27.33, 37.76, 38.64, 52.27, 52.81, 127.09, 128.48, 129.27, 135.90, 172.27, 177.83.

IR (neat): 3361, 2960, 1744, 1647, 1527, 1204 cm⁻¹.

HRMS (ESI) *m/z* calcd. for C₁₅H₂₁NNaO₃ (M+Na)⁺ 286.1414, found 286.1418.

[α]_D²⁷ 60.2 (c 1.35, CHCl₃).



(S)-methyl 4-methyl-2-pivalamidopentanoate (5-6d)

Prepared according **procedure C**, white solid, yield = 63 %.

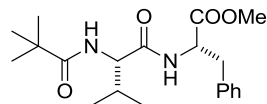
¹H NMR (400 MHz, CDCl₃): δ 0.91 (s, 3H), 0.93 (s, 3H), 1.19 (s, 9H), 1.47-1.66 (m, 3H), 3.70 (s, 3H), 4.57-4.62 (m, 1H), 5.96 (br d, *J* = 7.2 Hz, 1H).

¹³C NMR (CDCl₃, 100 MHz): δ 22.04, 22.77, 24.95, 27.41, 38.63, 41.69, 50.56, 52.20, 173.83, 178.18.

IR (neat): 3008, 2961, 1740, 1654, 1619, 1218 cm⁻¹.

HRMS (ESI) *m/z* calcd. for C₁₂H₂₃NNaO₃ (M+H)⁺ 252.1570, found 252.1575.

[α]_D²⁷ 0.78 (c 0.90, CHCl₃).



(S)-methyl 2-((S)-3-methyl-2-pivalamidobutanamido)-3-phenylpropanoate (5-6e)

Prepared according **procedure C**, HCl•aimne used, Cs₂CO₃ (3 eq.), white solid, yield = 50 %.

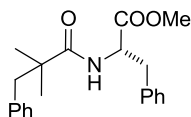
¹H NMR (400 MHz, CDCl₃): δ 0.87 (d, *J* = 6.8 Hz, 3H), 0.89 (d, *J* = 6.8 Hz, 1H), 1.18 (s, 9H), 2.05-2.10 (m, 1H), 3.03-3.14 (m, 2H), 3.69 (s, 3H), 4.22 (dd, *J* = 6.4, 8.4 Hz, 1H), 4.79-4.84 (m, 1H), 6.15 (br d, *J* = 8.4 Hz, 1H), 6.27 (br d, *J* = 7.6 Hz, 1H), 7.06-7.08 (m, 2H), 7.19-7.28 (m, 3H).

¹³C NMR (CDCl₃, 100 MHz): δ 17.81, 18.95, 27.40, 31.00, 37.72, 38.75, 52.23, 53.04, 57.81, 127.11, 128.57, 129.05, 135.43, 170.86, 171.49, 178.19.

IR (neat): 3291, 2961, 1749, 1635, 1539, 1210 cm^{-1} .

HRMS (ESI) m/z calcd. for $\text{C}_{20}\text{H}_{31}\text{N}_2\text{O}_4$ ($\text{M}+\text{H}$)⁺ 363.2278, found 363.2277.

$[\alpha]_D^{27}$ 18.0 (c 0.80, CHCl_3).



(S)-methyl 2-(2,2-dimethyl-3-phenylpropanamido)-3-phenylpropanoate (5-8c)

Prepared according **procedure C**, white solid, yield = 55 %.

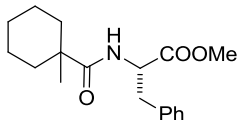
^1H NMR (400 MHz, CDCl_3): δ 1.11 (s, 3H), 1.13 (s, 3H), 2.71 (d, J = 13.2, 1H), 2.92 (d, J = 13.2, 1H), 2.96 (dd, J = 5.6, 13.6 Hz, 1H), 3.05 (dd, J = 5.6, 13.6 Hz, 1H), 3.67 (s, 3H), 4.83-4.88 (m, 1H), 5.88 (br d, J = 7.6 Hz, 1H), 6.79-6.82 (m, 2H), 7.17-7.27 (m, 8H).

^{13}C NMR (CDCl_3 , 100 MHz): δ 24.26, 25.61, 37.88, 43.40, 46.47, 52.18, 52.74, 126.47, 127.03, 127.96, 128.43, 129.21, 130.37, 135.70, 137.90, 171.93, 176.37.

IR (neat): 1744, 1653, 1510, 1454, 1213 cm^{-1} .

HRMS (ESI) m/z calcd. for $\text{C}_{21}\text{H}_{26}\text{NO}_3$ ($\text{M} + \text{H}$)⁺ 340.1907, found 340.1916.

$[\alpha]_D^{27}$ 47.75 (c 1.55, CHCl_3).



(S)-methyl 2-(1-methylcyclohexanecarboxamido)-3-phenylpropanoate (5-9c)

Prepared according **procedure C**, white solid, yield = 70 %.

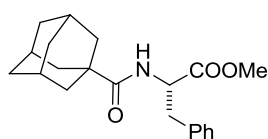
^1H NMR (400 MHz, CDCl_3): δ 1.05 (s, 3H), 1.19-1.51 (m, 8H), 1.78-1.83 (m, 2H), 3.07 (dd, J = 5.6, 13.6 Hz, 1H), 3.16 (dd, J = 5.6, 13.6 Hz, 1H), 8.85-4.90 (m, 1H), 6.02 (br d, J = 7.2 Hz, 1H), 7.07-7.09 (m, 2H), 7.19-7.28 (m, 3H).

^{13}C NMR (CDCl_3 , 100 MHz): δ 22.69, 25.68, 35.44, 35.48, 37.85, 42.66, 52.25, 52.72, 127.06, 128.50, 129.23, 135.97, 172.40, 177.19.

IR (neat): 3356, 2932, 2862, 1747, 1642, 1526, 1211 cm^{-1} .

HRMS (ESI) m/z calcd. for $\text{C}_{18}\text{H}_{26}\text{NO}_3$ ($\text{M}+\text{H}$)⁺ 304.1907, found 304.1916.

$[\alpha]_D^{27}$ 45.00 (c 1.65, CHCl_3).



(S)-methyl 2-((3S,5S,7S)-adamantane-1-carboxamido)-3-phenylpropanoate (5-10c)

Prepared according **procedure C**, white solid, yield = 50 %.

^1H NMR (400 MHz, CDCl_3): δ 1.63-1.78 (m, 12H), 1.99 (br s, 3H), 3.07 (dd, J = 5.6, 14.0 Hz, 1H), 3.14 (dd, J = 5.6, 14 Hz, 1H), 3.71 (s, 3H), 4.82-4.87 (m, 1H), 6.01 (br, d, J = 7.6 Hz, 1H), 7.05-7.06 (m, 2H), 7.22-7.29 (m, 3H).

^{13}C NMR (CDCl_3 , 100 MHz): δ 28.02, 36.42, 37.78, 39.02, 49.56, 52.25, 52.65, 127.05, 128.45, 129.31, 135.94, 172.29, 177.31.

IR (neat): 3351, 2907, 2850, 1744, 1643, 1516, 1453, 1214 cm^{-1} .

HRMS (ESI) m/z calcd. for $\text{C}_{21}\text{H}_{28}\text{NO}_3$ ($\text{M}+\text{H}$)⁺ 342.2064, found 342.2073.

$[\alpha]_D^{27}$ 63.3 (c 0.85, CHCl_3).

References:

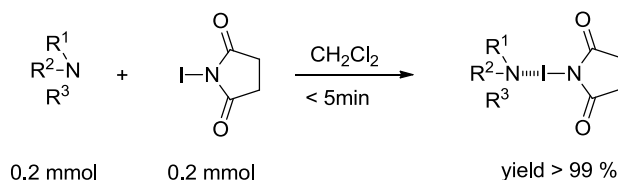
- (1) P. Bobal, J. Bobalova. *Molecules* **2013**, *18*, 2212-2221.
- (2) B. C. Ranu, S. Samanta. *Tetrahedron* **2003**, *59*, 7901–7906.
- (3) M. Uno, K. Setp, M. Masuda, W. Ueda, S. Takahashi. *Tetrahedron Lett.*, **1985**, *26*, 1553-1556.
- (4) Texier-Boullet, F.; Foucand, A. *Tetrahedron Lett.* **1982**, *23*, 4927.
- (5) R. C. Wheland, E. L. Martin, *J. Org. Chem.*, **1975**, *40*, 3101.
- (6) S. Rayat, M. Qian, R. Glaser, *Chem. Res. Toxicol.* **2005**, *18*, 1211-1218.
- (7) A.B. Charette, H. Juteau , H. Lebel, C. Molinaro, *J. Am. Chem. Soc.*, **1998**, *120*, 11943-11952.

Chapter 6

6.1 General information.

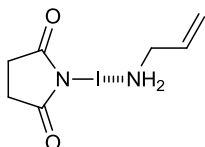
N-Bromosuccinimide (NBS) was recrystallized from hot H₂O, dried under vacuum at room temperature, stored at -20 °C, and protected from light. *N*-Iodosuccinimide was recrystallized from THF/CH₂Cl₂, dried under vacuum at room temperature, ground in a mortar and pestle, stored at -20 °C and protected from light. CDCl₃ was treated with basic Al₂O₃ overnight and distilled, stored without light at r.t. Quinuclidine purchased from TCI (Q0062) without further purification. CH₃COOH was distilled. ClCH₂COOH was without further purification.

6.2 General procedure to make halogen bonded complex 6-1, 6-2, 6-4, 6-5.



Scheme S-1. Synthesis of complex **6-1**, **6-2**, **6-4**, **6-5**.

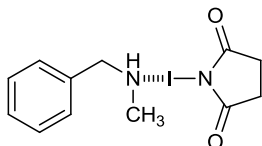
NIS (112 mg, 0.5 mmol) or NBS (89 mg, 0.5 mmol) was dissolved in dry CH₂Cl₂ (5 mL), cooled to 0 °C, then amine (0.5 mmol) was added by one-potion. After stirring for 10 min until all the solid disappeared, the solvent was removed in vacuum and the slightly yellow solid formed was washed with Et₂O and dried under vacuum to afford a yellow to white solid, yield > 95 %. Which can store under Ar below -30 °C for more than 3 months; latterly, **6-1–6-3**, **6-5** were crystallized for X-ray analysis (vide infra).



¹H NMR (CDCl₃, 400 MHz): δ 2.73 (s, 4H), 3.40 (d, *J* = 6.0 Hz, 2H), 5.19-5.24 (m, 2H), 5.83-5.93 (m, 1H).

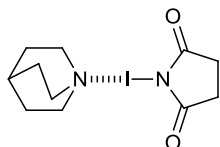
¹³C NMR (CDCl₃, 100 MHz): δ 30.03, 47.36, 117.92, 135.81, 182.81.

IR (neat): 3160, 1773, 1702, 1617, 1424, 1364, 1292, 1242, 1183, 817, 639 cm⁻¹.



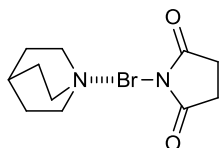
¹H NMR (CDCl₃, 400 MHz): δ 2.630 (br s, 2H) 2.694 (s, 4H), 3.85 (br s, 2H), 7.25-7.34 (m, 5H).

¹³C NMR (CDCl₃, 100 MHz): δ 29.888, 37.742, 57.679, 128.142, 128.736, 128.926, 136.484, 183.193.



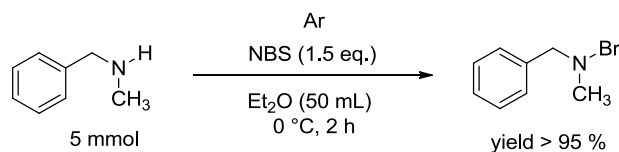
¹H NMR (CDCl₃, 400 MHz): δ 1.65-1.70 (m, 6H), 1.87-1.91 (m, 1H), 2.67 (s, 4H), 3.10 (dd, *J* = 8.0, 8.0 Hz, 6 H);

¹³C NMR (CDCl₃, 100 MHz): δ 18.41, 26.58, 29.90, 51.22, 183.77;



¹H NMR (CDCl₃, 400 MHz): δ 1.64-1.69 (m, 6H), 1.84-1.87 (m, 1H), 2.62 (s, 4H), 3.03 (t, *J* = 8.0 Hz, 6 H);

^{13}C NMR (CDCl_3 , 100 MHz): δ 19.31, 26.45, 29.59, 50.09, 180.55;



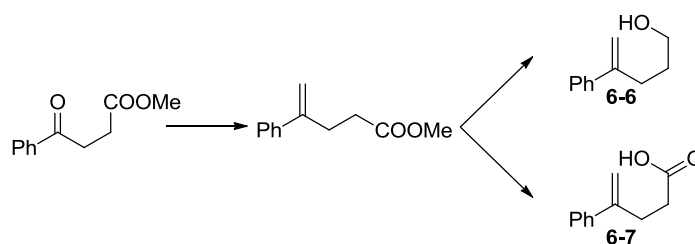
Scheme S-2. Preparing compound *N*-bromo, *N*-methylbenzylamine

Procedure to prepare N-bromo amine: Under Ar, *N*-methylbenzylamine (5 mmol) was dissolved in 50 mL Et₂O, the flask was cooled down over an ice bath for 10 min before NBS was added in one-portion. The reaction was stirred at the same temperature for 2 h and the succinimide filtered off. Collection of the organic solution and evaporating off Et₂O (whilst immersing in an ice-water bath) *in vacuo* gave a thick yellow oil, which was found to be unstable and should be used immediately, or stored at low temperature, in a yield of about 95 %.

^1H NMR (400 MHz, CDCl_3): δ 3.10 (s, 3H), 4.07 (s, 2H), 7.32-7.36 (m, 5H).

^{13}C NMR (CDCl_3 , 100 MHz): δ 54.23, 71.94, 128.12, 128.51, 129.19, 137.81.

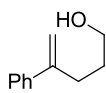
6.3 Preparation of unsaturated acid 6-7 and unsaturated alcohol 6-6.



Scheme S-8. Preparing of unsaturated acid 6-7 and unsaturated alcohol 6-6

Step 1: Methyltriphenylphosphonium bromide (17.8 g, 50 mmol, 1.0 equiv) was dissolved in dry THF (120 mL) and cooled to ca. 0 °C on an ice bath. NaOBu^t (4.8 g, 50 mmol, 1.0 equiv.) was slowly added and the resulting solution was stirred for 30 min. Then methyl 3-benzoylpropionate (7.68 g, 40 mmol, 0.8 equiv) was added dropwise by syringe. The resulting solution was then stirred while warming to room temperature for 12 h. On cooling, the reaction was quenched by the addition of saturated ammonium chloride (200 mL) and the resulting slurry was diluted with water (100 mL) and extracted with ethyl acetate (3×100 mL). The combined organics were washed with brine (100 mL), dried over anhydrous Na₂SO₄, and concentrated by rotary evaporation. The residue was purified by column chromatography on silica gel (10% ethyl acetate in hexanes) to give 5.7 g (75% yield) of the desired methyl 4-phenylpent-4-enoate.

Synthesis of 6-6: This substance was used immediately without characterization in the following saponification reaction. The ester (15 mmol, 1 equiv) was dissolved in THF (40 mL) and cooled to ca. 0 °C on an ice bath. LiAlH₄ (550 mg, 15 mmol, 1.0 equiv) was slowly added. The resulting solution was allowed to warm to room temperature while stirring for 1 h. The reaction was quenched by slowly adding ice until no more bubble, the *con.* HCl solution was added until the two phase was separated, extracted with ethyl acetate (3×50 mL). The combined organics were washed with brine (100 mL), dried over anhydrous Na₂SO₄, and concentrated by rotary evaporation. The residue was purified by column chromatography on silica gel (30% ethyl acetate in hexanes) to give 2.1 g (87% yield) of the desired unsaturated alcohol 6-6.



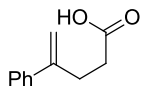
The NMR data is consistent with previous report. (J. F. Hartwig *et al.* *J. Am. Chem. Soc.*, **2006**, 128, 6042–

6043.)

¹H NMR (CDCl₃, 400 MHz): δ 1.70-1.75 (m, 2H), 2.58-2.62 (m, 2H), 3.65 (t, J = 6.4 Hz, 2H), 5.08-5.09 (m, 1H), 5.28-5.29 (m, 1H), 7.23-7.41 (m, 5H).

¹³C NMR (CDCl₃, 100 MHz): δ 31.15, 31.55, 62.43, 112.56, 126.10, 127.42, 128.31, 140.99, 147.95.

Synthesis of 6-7: The methyl 4-phenylpent-4-enoate (15 mmol, 1 equiv) was dissolved in THF (20 mL) and cooled to ca. 0 °C on an ice bath. A solution of lithium hydroxide monohydrate (600 mg, 14.30 mmol, 5.07 equiv) in water (20 mL) was added dropwise. The resulting solution was allowed to warm to room temperature while stirring for 18 h. The solution was acidified to pH = 1, extracted with ethyl acetate (3×50 mL). The combined organics were washed with brine (100 mL), dried over anhydrous Na₂SO₄, and concentrated by rotary evaporation to give pure unsaturated acid **6-7**.

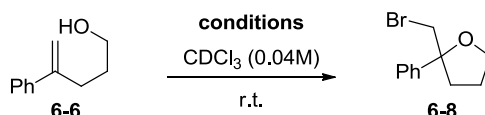


The NMR data is consistent with previous report. (Y. Y. Yeung *et al.* *J. Am. Chem. Soc.* **2011**, 133, 9164–9167.)

¹H NMR (CDCl₃, 400 MHz): δ 2.50-2.54 (m, 2H), 2.84 (m, 2H), 5.09 (d, J = 0.8 Hz, 1H), 5.31 (s, 1H), 7.24-7.40 (m, 5H).

¹³C NMR (CDCl₃, 100 MHz): δ 30.12, 32.85, 112.95, 126.06, 127.66, 128.41, m 140.38, 146.51, 179.07.

6.4 General procedure for kinetic study of unsaturated acid 6-7 and unsaturated alcohol 6-6.

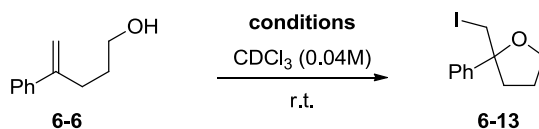


A 10-mL, flame-dried reaction tube, fitted with a septum and a magnetic stir bar, was charged with unsaturated alcohol **6** (0.2 mmol) and an internal standard (1,2,4,5-tetrachlorobenzene, 0.1 mmol). Then CDCl₃ (5 mL) was added via syringe. The flask was wrapped in Al-foil and then was evacuated. After that, NBS or NBS-quinuclidine complex **6-5** were added by one-portion. Then a solution of CH₃COOH in CDCl₃ (0.1 M) was added rapidly via syringe, and the resulting solution was stirred for at room temperature. The reaction progress was monitored by ¹H NMR. After unsaturated alcohol 6-6 was disappeared, saturated aq. Na₂S₂O₃ solution (5 mL) was added, and the resulting biphasic mixture was transferred to separatory funnel where it was diluted with H₂O (10 mL) and was extracted with CH₂Cl₂ (4 x 10 mL). The combined organic extracts were dried over MgSO₄, filtered and concentrated in vacuum. The residue was purified by column chromatography (Hexane/Ethylacetate = 10/1) to provide 207 mg (81%) of **6-8** as an oil.

The NMR data is consistent with previous report: M. Greb, J. Hartung, F. Köhler, K. Špehar, R. Kluge, R. Csuk, *Eur. J. Org. Chem.* **2004**, 3799-3812.

¹H NMR (CDCl₃, 400 MHz): δ 1.78-1.88 (m, 1H), 1.99-2.09 (m, 1H), 2.21-2.28 (m, 1H), 2.37-2.45 (m, 1H), 3.64 (s, 2H), 3.89-3.95 (m, 1H), 4.05-4.10 (m, 1H), 7.25-7.42 (m, 5H).

¹³C NMR (CDCl₃, 100 MHz): δ 26.12, 36.43, 42.17, 68.64, 85.24, 125.53, 127.38, 128.25, 143.93.



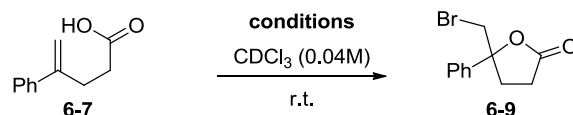
A 10-mL, flame-dried reaction tube, fitted with a septum and a magnetic stir bar, was charged with unsaturated alcohol **6-6** (0.2 mmol) and an internal standard (1,2,4,5-tetrachlorobenzene, 0.1 mmol). Then CDCl₃ (5 mL) was added via syringe. The flask was wrapped in Al-foil and then was evacuated. After that, NIS or NIS-quinuclidine complex **6-4** were added by one-portion. Then a solution of ClCH₂COOH in CDCl₃ (0.1 M) was added rapidly via syringe, and the resulting solution was stirred for at room temperature. The reaction progress was monitored by ¹H NMR. After unsaturated alcohol **6-6** was

disappeared, saturated *aq.* Na₂S₂O₃ solution (5 mL) was added, and the resulting biphasic mixture was transferred to separatory funnel where it was diluted with H₂O (10 mL) and was extracted with CH₂Cl₂ (4× 10 mL). The combined organic extracts were dried over MgSO₄, filtered and concentrated in vacuum. The residue was purified by column chromatography (Hexane/Ethylacetate = 10/1) to provide 207 mg (90%) of **6-13** as an oil.

The NMR data is consistent with previous report (S. H. Kang, C. M. Park, S. B. Lee, M. Kim, *Synlett* **2004**, 7, 1279-1281.)

¹H NMR (CDCl₃, 400 MHz): δ 1.77-1.88 (m, 1H), 2.05-2.10 (m, 1H), 2.26-2.37 (m, 2H), 3.51-3.57 (m, 2H), 3.89-3.94 (m, 1H), 4.04-4.10 (m, 1H), 4.23-4.40 (m, 5H).

¹³C NMR (CDCl₃, 100 MHz): δ 19.15, 26.24, 37.64, 68.45, 84.57, 125.38, 127.29, 128.26, 143.93.

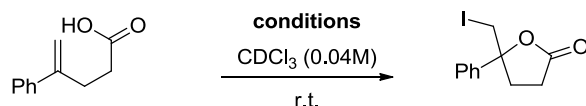


A 10-mL, flame-dried reaction tube, fitted with a septum and a magnetic stir bar, was charged with unsaturated acid **6-7** (0.2 mmol) and an internal standard (1,2,4,5-tetrachlorobenzene, 0.1 mmol). Then CDCl₃ (5 mL) was added via syringe. The flask was wrapped in Al-foil and then was evacuated. After that, NBS or NBS-quinuclidine complex **6-5** were added by one-portion and the resulting solution was stirred for at room temperature. The reaction progress was monitored by ¹H NMR. After unsaturated acid **6-7** was disappeared, saturated *aq.* Na₂S₂O₃ solution (5 mL) was added, and the resulting biphasic mixture was transferred to separatory funnel where it was diluted with H₂O (10 mL) and was extracted with CH₂Cl₂ (4× 10 mL). The combined organic extracts were dried over MgSO₄, filtered and concentrated in vacuum. The residue was purified by column chromatography (Hexane/Ethylacetate = 10/2) to provide 207 mg (90%) of **6-13** as an oil.

The NMR data is consistent with previous report (L.Zhou, C. K.Tan, X. J. Jiang, F. Chen, Y. Y. Yeung, *J. Am. Chem. Soc.* **2010**, 132, 15474–15476.)

¹H NMR (CDCl₃, 400 MHz): δ 2.47-2.59 (m, 2H), 2.74-2.85 (m, 2H), 3.70 (d, *J* = 11.2 Hz, 1H), 3.73 (d, *J* = 11.2 Hz, 1H), 7.31-7.41 (m, 5H).

¹³C NMR (CDCl₃, 100 MHz): δ 29.06, 32.37, 41.02, 86.42, 124.89, 128.67, 128.84, 140.72, 175.53.



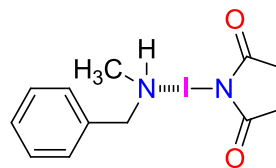
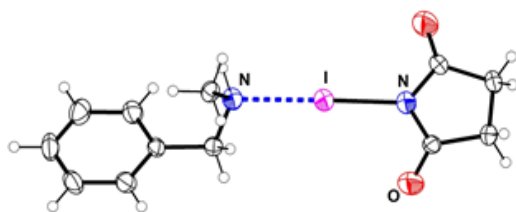
A 10-mL, flame-dried reaction tube, fitted with a septum and a magnetic stir bar, was charged with unsaturated acid **6-7** (0.2 mmol) and an internal standard (1,2,4,5-tetrachlorobenzene, 0.1 mmol). Then CDCl₃ (5 mL) was added via syringe. The flask was wrapped in Al-foil and then was evacuated. After that, NIS or NIS-quinuclidine complex **6-4** were added by one-portion and the resulting solution was stirred for at room temperature. The reaction progress was monitored by ¹H NMR. After unsaturated acid **6-7** was disappeared, saturated *aq.* Na₂S₂O₃ solution (5 mL) was added, and the resulting biphasic mixture was transferred to separatory funnel where it was diluted with H₂O (10 mL) and was extracted with CH₂Cl₂ (4× 10 mL). The combined organic extracts were dried over MgSO₄, filtered and concentrated in vacuum. The residue was purified by column chromatography (Hexane/Ethylacetate = 10/2) to provide 207 mg (95%) of **6-18** as an oil.

The NMR data is consistent with previous report (H. Nakatsuji, Y. Sawamura, A. Sakakura, K. Ishihara, *Angew. Chem. Int. Ed.* **2014**, 53, 6974-6977.)

¹H NMR (CDCl₃, 400 MHz): δ 2.18-2.53 (m, 4H), 3.40 (d, *J* = 11.2 Hz, 1H),, 3.70 (d, *J* = 11.2 Hz, 1H), 7.05-7.14 (m, 5H).

¹³C NMR (CDCl₃, 100 MHz): δ 16.30, 29.20, 33.93, 86.01, 124.84, 128.56, 128.81, 140.58, 175.33.

6.5 X-ray data



The single crystal of **6-2** suitable for X-ray analysis was grown in a solution of dichloromethane/Hexane at -30 °C under Ar, an orange block crystal of $C_{25}H_{30}Cl_2I_2N_4O_4$ having approximate dimensions of $0.400 \times 0.100 \times 0.100$ mm was mounted on a glass fiber. All measurements were made on a Rigaku XtaLAB mini diffractometer using graphite monochromated Mo-K α radiation. The crystal-to-detector distance was 50.00 mm. The structure of **6-2** was solved by use of SHELXTL program. Refinement was performed on F^2 anisotropically for all the non-hydrogen atoms by the full-matrix least-squares method. Crystallographic data has been deposited with the Cambridge Crystallographic Data Center, **CCDC reference number: 1495217**

A. Crystal Data

Empirical Formula	$C_{25}H_{30}Cl_2I_2N_4O_4$
Formula Weight	775.25
Crystal Color, Habit	yellow, prism
Crystal Dimensions	$0.400 \times 0.100 \times 0.100$ mm
Crystal System	monoclinic
Lattice Type	Primitive
Lattice Parameters	$a = 13.0962(10)$ Å $b = 19.8246(16)$ Å $c = 1.8508(9)$ Å $\beta = 103.699(7)^\circ$ $V = 2989.3(4)$ Å ³
Space Group	$P2_1/c$ (#14)
Z value	4
D_{calc}	1.722 g/cm^3
F_{000}	1520.00
μ (MoK)	23.196 cm^{-1}

B. Intensity Measurements

Diffractometer	XtaLAB mini
Radiation	MoK α ($\lambda = 0.71075$ Å)
	graphite monochromated
Voltage, Current	50kV, 12mA
Temperature	-123.0°C
Detector Aperture	75.0 mm (diameter)
Data Images	540 exposures
ω oscillation Range ($\chi=54.0$, $\phi=0.0$)	$-60.0-120.0^\circ$
Exposure Rate	16.0 sec./°
Detector Swing Angle	30.00°

ω oscillation Range ($\chi=54.0$, $\phi=120.0$)	-60.0 - 120.0 $^{\circ}$
Exposure Rate	16.0 sec./ $^{\circ}$
Detector Swing Angle	30.00 $^{\circ}$
ω oscillation Range ($\chi=54.0$, $\phi=240.0$)	-60.0 - 120.0 $^{\circ}$
Exposure Rate	16.0 sec./ $^{\circ}$
Detector Swing Angle	30.00 $^{\circ}$
Detector Position	50.00 mm
Pixel Size	0.146 mm
$2\theta_{\max}$	55.0 $^{\circ}$
No. of Reflections Measured	Total: 31041 Unique: 6845 ($R_{\text{int}} = 0.0361$)
Corrections	Lorentz-polarization Absorption (trans. factors: 0.527 - 0.793)

C. Structure Solution and Refinement

Structure Solution	Direct Methods (SIR2008)
Refinement	Full-matrix least-squares on F^2
Function Minimized	$\omega (F_o^2 - F_c^2)^2$
Least Squares Weights	$\omega = 1 / [\sigma^2(F_o^2) + (0.0185 \cdot P)^2 + 2.2517 \cdot P]$ where $P = (\text{Max}(F_o^2, 0) + 2F_c^2)/3$
$2\theta_{\max}$ cutoff	55.0 $^{\circ}$
Anomalous Dispersion	All non-hydrogen atoms
No. Observations (All reflections)	6845
No. Variables	334
Reflection/Parameter Ratio	20.49
Residuals: R_1 ($I > 2.00\sigma(I)$)	0.0241
Residuals: R (All reflections)	0.0290
Residuals: ωR_2 (All reflections)	0.0538
Goodness of Fit Indicator	1.078
Max Shift/Error in Final Cycle	0.001
Maximum peak in Final Diff. Map	0.87 e $^{-}/\text{\AA}^3$
Minimum peak in Final Diff. Map	-0.55 e $^{-}/\text{\AA}^3$

Table 1. Atomic coordinates and $B_{\text{iso}}/B_{\text{eq}}$

atom	x	y	z	B_{eq}
I1	-0.05365(2)	0.38951(2)	0.40888(2)	1.700(4)
I2	-0.04684(2)	0.14835(2)	0.47285(2)	1.678(4)
Cl1	-0.58109(6)	0.17781(4)	0.95953(7)	3.569(14)
Cl2	-0.57782(6)	0.21359(5)	0.72075(7)	3.988(16)
O1	-0.08901(13)	0.48205(9)	0.16067(15)	2.17(3)

O2	-0.31509(17)	0.37331(14)	0.3345(2)	4.82(6)
O3	-0.03805(14)	0.20145(10)	0.20947(15)	2.57(3)
O4	-0.31049(14)	0.17425(10)	0.38343(16)	2.69(3)
N1	-0.18303(15)	0.42128(10)	0.26624(17)	1.89(3)
N2	0.08821(16)	0.35392(10)	0.56017(17)	1.76(3)
N3	-0.15802(15)	0.18479(10)	0.31976(17)	1.74(3)
N4	0.07898(15)	0.10847(10)	0.64138(17)	1.76(3)
C1	-0.17151(19)	0.45716(12)	0.1699(2)	1.76(4)
C2	-0.2763(2)	0.45986(13)	0.0821(2)	2.30(4)
C3	-0.3510(2)	0.42070(15)	0.1383(3)	2.98(5)
C4	-0.2852(2)	0.40174(14)	0.2572(3)	2.80(5)
C5	0.1629(2)	0.31461(13)	0.5114(2)	2.31(4)
C6	0.1379(2)	0.41321(13)	0.6272(2)	2.36(4)
C7	0.2304(2)	0.39606(12)	0.7252(2)	1.94(4)
C8	0.3327(2)	0.41262(13)	0.7206(2)	2.55(5)
C9	0.4170(2)	0.39625(14)	0.8126(3)	3.00(5)
C10	0.3994(2)	0.36373(14)	0.9089(3)	2.78(5)
C11	0.2984(2)	0.34596(13)	0.9133(2)	2.47(5)
C12	0.2142(2)	0.36200(13)	0.8224(2)	2.13(4)
C13	-0.26564(19)	0.18830(12)	0.3079(2)	1.98(4)
C14	-0.3164(2)	0.21323(14)	0.1865(2)	2.43(5)
C15	-0.2248(2)	0.22325(14)	0.1289(2)	2.40(5)
C16	-0.12881(19)	0.20247(12)	0.2201(2)	1.89(4)
C17	0.1442(2)	0.16500(13)	0.6972(2)	2.23(4)
C18	0.1417(2)	0.05242(13)	0.6096(2)	2.13(4)
C19	0.21976(19)	0.02276(12)	0.7120(2)	1.98(4)
C20	0.1850(2)	-0.01258(13)	0.7973(2)	2.60(5)
C21	0.2560(3)	-0.03833(14)	0.8933(3)	3.17(5)
C22	0.3629(2)	-0.02958(15)	0.9046(3)	3.31(6)
C23	0.3983(2)	0.00505(15)	0.8205(3)	3.09(5)
C24	0.3270(2)	0.03127(14)	0.7247(2)	2.52(5)
C26	-0.5043(2)	0.20654(16)	0.8653(2)	3.00(5)

$$B_{eq} = 8/3 \pi^2 (U_{11}(aa^*)^2 + U_{22}(bb^*)^2 + U_{33}(cc^*)^2 + 2U_{12}(aa^*bb^*)\cos \gamma + 2U_{13}(aa^*cc^*)\cos \beta + 2U_{23}(bb^*cc^*)\cos \alpha)$$

Table 2. Atomic coordinates and B_{iso} involving hydrogen atoms

atom	x	y	z	B_{iso}
H3	0.41169	-0.04742	0.97020	3.976
H7	0.45666	0.35352	0.97242	3.338
H8	0.14500	0.34976	0.82632	2.557
H10A	0.18008	0.06917	0.55254	2.551
H10B	0.09337	0.01636	0.57152	2.551
H11	0.11179	-0.01913	0.78951	3.118
H13A	-0.27133	0.43860	0.00801	2.760

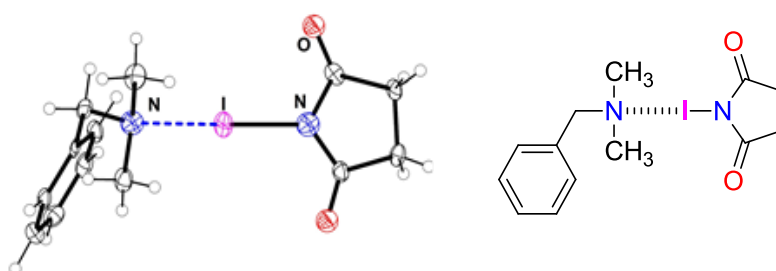
H13B	-0.30016	0.50707	0.06674	2.760
H14	0.28669	0.32257	0.97902	2.964
H15	0.48664	0.40754	0.80894	3.598
H16A	-0.23337	0.19465	0.05874	2.882
H16B	-0.21960	0.27100	0.10641	2.882
H17A	0.08449	0.43677	0.65953	2.829
H17B	0.16127	0.44480	0.57373	2.829
H18A	-0.35402	0.25623	0.18954	2.917
H18B	-0.36663	0.17951	0.14357	2.917
H19A	-0.41147	0.44905	0.14509	3.573
H19B	-0.37753	0.37991	0.09255	3.573
H24	0.34503	0.43517	0.65432	3.065
H25	0.35199	0.05528	0.66724	3.021
H26A	-0.47404	0.25112	0.89232	3.604
H26B	-0.44532	0.17480	0.86840	3.604
H33	0.23141	-0.06197	0.95143	3.807
H34	0.47158	0.01101	0.82812	3.711
H36A	0.09938	0.19935	0.72033	2.675
H36B	0.18139	0.18469	0.64240	2.675
H36C	0.19541	0.14868	0.76599	2.675
H37A	0.12583	0.27716	0.46523	2.769
H37B	0.21848	0.29672	0.57475	2.769
H37C	0.19407	0.34377	0.46180	2.769

Table 3. Anisotropic displacement parameters

atom	U ₁₁	U ₂₂	U ₃₃	U ₁₂	U ₁₃	U ₂₃
I1	0.02061(8)	0.02379(8)	0.01938(8)	-0.00155(6)	0.00315(6)	0.00175(6)
I2	0.01781(8)	0.02548(8)	0.01994(8)	0.00165(6)	0.00341(6)	0.00128(6)
Cl1	0.0397(4)	0.0558(5)	0.0424(4)	0.0036(4)	0.0143(3)	0.0014(4)
Cl2	0.0414(4)	0.0702(6)	0.0382(4)	-0.0108(4)	0.0059(3)	0.0003(4)
O1	0.0241(9)	0.0321(9)	0.0274(9)	0.0019(7)	0.0083(8)	0.0033(8)
O2	0.0364(12)	0.0907(18)	0.0525(14)	-0.0316(13)	0.0039(11)	0.0234(14)
O3	0.0273(10)	0.0431(11)	0.0304(10)	0.0064(8)	0.0131(8)	0.0064(8)
O4	0.0238(9)	0.0469(11)	0.0336(10)	0.0028(8)	0.0107(8)	0.0080(9)
N1	0.0206(10)	0.0281(11)	0.0201(10)	-0.0034(8)	-0.0011(8)	0.0024(8)
N2	0.0220(10)	0.0234(10)	0.0203(10)	0.0015(8)	0.0024(8)	-0.0002(8)
N3	0.0195(10)	0.0262(10)	0.0199(10)	0.0035(8)	0.0036(8)	0.0031(8)
N4	0.0188(10)	0.0267(11)	0.0202(10)	0.0031(8)	0.0019(8)	0.0016(8)
C1	0.0266(13)	0.0197(11)	0.0194(11)	0.0053(10)	0.0027(10)	-0.0036(9)
C2	0.0277(13)	0.0324(14)	0.0227(12)	0.0039(11)	-0.0032(11)	-0.0023(11)
C3	0.0247(13)	0.0394(16)	0.0399(16)	-0.0074(12)	-0.0105(12)	0.0017(13)
C4	0.0283(14)	0.0390(15)	0.0348(15)	-0.0126(12)	-0.0011(12)	0.0037(13)
C5	0.0295(13)	0.0301(13)	0.0279(13)	0.0045(11)	0.0065(11)	-0.0019(11)
C6	0.0312(14)	0.0267(13)	0.0272(13)	0.0024(11)	-0.0021(11)	-0.0028(11)

C7	0.0258(12)	0.0234(12)	0.0228(12)	0.0011(10)	0.0018(10)	-0.0031(10)
C8	0.0318(14)	0.0305(14)	0.0357(15)	-0.0040(11)	0.0098(12)	0.0017(12)
C9	0.0202(13)	0.0406(16)	0.0508(18)	-0.0049(11)	0.0039(13)	-0.0049(14)
C10	0.0277(14)	0.0333(14)	0.0366(15)	0.0035(11)	-0.0085(12)	-0.0046(12)
C11	0.0356(15)	0.0322(14)	0.0235(13)	0.0043(11)	0.0018(11)	0.0023(11)
C12	0.0226(12)	0.0304(13)	0.0271(13)	0.0007(10)	0.0041(10)	-0.0019(11)
C13	0.0203(12)	0.0252(12)	0.0291(13)	0.0015(10)	0.0048(10)	0.0007(10)
C14	0.0242(13)	0.0369(14)	0.0288(13)	0.0053(11)	0.0014(11)	0.0051(12)
C15	0.0294(14)	0.0372(15)	0.0237(13)	0.0085(11)	0.0043(11)	0.0076(11)
C16	0.0260(13)	0.0229(12)	0.0239(12)	0.0043(10)	0.0076(10)	0.0014(10)
C17	0.0273(13)	0.0317(13)	0.0230(12)	-0.0002(11)	0.0006(10)	-0.0039(11)
C18	0.0277(13)	0.0288(13)	0.0232(12)	0.0056(10)	0.0037(10)	-0.0018(10)
C19	0.0250(12)	0.0249(12)	0.0235(12)	0.0061(10)	0.0018(10)	-0.0036(10)
C20	0.0320(14)	0.0315(14)	0.0339(14)	0.0042(11)	0.0051(12)	0.0027(12)
C21	0.0524(19)	0.0337(15)	0.0328(15)	0.0070(13)	0.0066(14)	0.0082(13)
C22	0.0450(17)	0.0400(16)	0.0317(15)	0.0169(14)	-0.0094(13)	-0.0028(13)
C23	0.0241(14)	0.0489(17)	0.0395(16)	0.0087(12)	-0.0025(12)	-0.0090(14)
C24	0.0280(13)	0.0353(14)	0.0320(14)	0.0032(11)	0.0064(11)	-0.0037(12)
C26	0.0236(13)	0.0511(18)	0.0397(16)	0.0055(12)	0.0080(12)	-0.0084(14)

The single crystal of **6-3** suitable for X-ray analysis was grown in a solution of dichloromethane/Hexane at -30 °C under Ar. A colorless block crystal of C₁₃H₁₇IN₂O₂ having approximate dimensions of 0.400 × 0.400 × 0.300 mm was mounted on a glass fiber. All measurements were made on a Rigaku XtaLAB mini diffractometer using graphite monochromated Mo-K α radiation. The crystal-to-detector distance was 49.99 mm. The structure of **6-3** was solved by use of SHELXTL program. Refinement was performed on F² anisotropically for all the non-hydrogen atoms by the full-matrix least-squares method. Crystallographic data has been deposited with the Cambridge Crystallographic Data Center, **CCDC reference number: 1495215**



A. Crystal Data

Empirical Formula	C ₁₃ H ₁₇ IN ₂ O ₂
Formula Weight	360.19
Crystal Color, Habit	colorless, block
Crystal Dimensions	0.400 × 0.400 × 0.300 mm
Crystal System	monoclinic
Lattice Type	Primitive
Lattice Parameters	a = 10.131(13) Å b = 7.209(9) Å

	$c = 10.194(12) \text{ \AA}$
	$= 109.143(16)^\circ$
	$V = 703.3(15) \text{ \AA}^3$
Space Group	$P2_1$ (#4)
Z value	2
D_{calc}	1.701 g/cm^3
F000	356.00
$\mu(\text{MoK}\alpha)$	22.741 cm^{-1}

B. Intensity Measurements

Diffractometer	XtaLAB mini
Radiation	MoK α ($\lambda = 0.71075 \text{ \AA}$) graphite monochromated
Voltage, Current	50kV, 12mA
Temperature	-123.0 °C
Detector Aperture	75.0 mm (diameter)
Data Images	540 exposures
ω oscillation Range ($=54.0$, $=0.0$)	-60.0 - 120.0 $^\circ$
Exposure Rate	20.0 sec./ $^\circ$
Detector Swing Angle	30.00 $^\circ$
ω oscillation Range ($=54.0$, $=120.0$)	-60.0 - 120.0 $^\circ$
Exposure Rate	20.0 sec./ $^\circ$
Detector Swing Angle	30.00 $^\circ$
ω oscillation Range ($=54.0$, $=240.0$)	-60.0 - 120.0 $^\circ$
Exposure Rate	20.0 sec./ $^\circ$
Detector Swing Angle	30.00 $^\circ$
ω oscillation Range ($=54.0$, $=0.0$)	-60.0 - 120.0 $^\circ$
Exposure Rate	20.0 sec./ $^\circ$
Detector Swing Angle	30.40 $^\circ$
ω oscillation Range ($=54.0$, $=120.0$)	-60.0 - 120.0 $^\circ$
Exposure Rate	20.0 sec./ $^\circ$
Detector Swing Angle	30.40 $^\circ$
ω oscillation Range ($=54.0$, $=240.0$)	-60.0 - 120.0 $^\circ$
Exposure Rate	20.0 sec./ $^\circ$
Detector Swing Angle	30.40 $^\circ$
Detector Position	49.99 mm
Pixel Size	0.073 mm
$2\theta_{\text{max}}$	55.0 $^\circ$
No. of Reflections Measured	Total: 6423 Unique: 3154 ($R_{\text{int}} = 0.0557$) Parsons quotients (Flack x parameter): 1164
Corrections	Lorentz-polarization

Absorption
(trans. factors: 0.275 - 0.505)
Secondary Extinction
(coefficient: 8.32000e-003)

C. Structure Solution and Refinement

Structure Solution	Direct Methods (SIR2008)
Refinement	Full-matrix least-squares on F^2
Function Minimized	$\sum w (F_o^2 - F_c^2)^2$
Least Squares Weights	$w = 1 / [\sigma^2(F_o^2) + (0.0257 \cdot P)^2 + 0.0000 \cdot P]$ where $P = (\text{Max}(F_o^2, 0) + 2F_c^2)/3$
$2\theta_{\text{max}}$ cutoff	55.0°
Anomalous Dispersion	All non-hydrogen atoms
No. Observations (All reflections)	3154
No. Variables	164
Reflection/Parameter Ratio	19.23
Residuals: R1 ($I > 2.00\sigma(I)$)	0.0376
Residuals: R (All reflections)	0.0391
Residuals: wR2 (All reflections)	0.0794
Goodness of Fit Indicator	0.915
Flack parameter (Parsons' quotients = 1164)	0.04(4)
Max Shift/Error in Final Cycle	0.000
Maximum peak in Final Diff. Map	1.17 e ⁻ /Å ³
Minimum peak in Final Diff. Map	-1.62 e ⁻ /Å ³

Table 1. Atomic coordinates and $B_{\text{iso}}/B_{\text{eq}}$

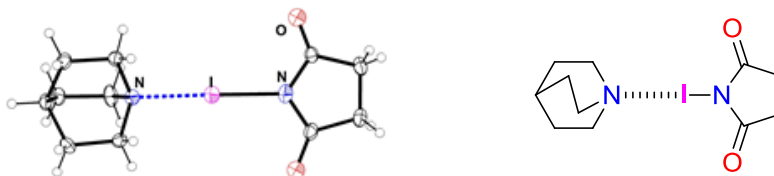
atom	x	y	z	B_{eq}
I1	0.09307(4)	0.87496(13)	0.68843(4)	1.287(13)
O14	0.1018(6)	0.6297(9)	0.9724(7)	2.65(13)
O19	-0.2426(6)	0.9634(7)	0.6609(6)	1.85(10)
N2	0.2446(7)	0.9288(8)	0.5500(7)	1.64(14)
N10	-0.0481(7)	0.8061(8)	0.8017(7)	1.34(12)
C1	0.1631(7)	0.871(2)	0.4081(7)	2.13(12)
C3	0.2869(8)	1.1274(11)	0.5450(8)	1.64(14)
C4	-0.0136(8)	0.6984(11)	0.9155(9)	1.58(14)
C5	0.3632(8)	1.2208(10)	0.6787(8)	1.33(13)
C6	-0.2560(8)	0.7752(11)	0.8542(8)	1.56(14)
C7	0.2909(8)	1.3368(11)	0.7423(9)	1.73(19)
C8	0.5763(9)	1.2982(11)	0.8622(10)	2.00(15)
C9	0.5044(9)	1.4155(11)	0.9224(9)	1.92(19)
C11	0.5070(8)	1.2052(11)	0.7401(9)	1.58(14)
C15	0.3596(9)	1.4347(10)	0.8619(9)	1.98(16)

C16	0.3689(9)	0.8070(11)	0.6046(10)	2.09(16)
C17	-0.1395(9)	0.6775(13)	0.9657(10)	1.97(16)
C18	-0.1872(7)	0.866(2)	0.7599(7)	1.46(12)

$$B_{eq} = 8/3 \pi^2 (U_{11}(aa^*)^2 + U_{22}(bb^*)^2 + U_{33}(cc^*)^2 + 2U_{12}(aa^*bb^*)\cos \gamma + 2U_{13}(aa^*cc^*)\cos \beta + 2U_{23}(bb^*cc^*)\cos \alpha)$$

Table 2. Atomic coordinates and B_{iso} involving hydrogen atoms

atom	x	y	z	B _{iso}
H1A	0.22436	0.86569	0.35105	2.555
H1B	0.08774	0.95993	0.36778	2.555
H1C	0.12302	0.74758	0.41085	2.555
H3A	0.34627	1.13410	0.48490	1.971
H3B	0.20137	1.20015	0.49881	1.971
H6A	-0.32766	0.68499	0.80187	1.869
H6B	-0.30122	0.86926	0.89608	1.869
H7	0.19235	1.34838	0.70226	2.081
H8	0.67402	1.28120	0.90508	2.401
H9	0.55302	1.48265	1.00417	2.298
H11	0.55853	1.12978	0.69783	1.891
H15	0.30898	1.51412	0.90257	2.382
H16A	0.33848	0.67788	0.60432	2.508
H16B	0.42222	0.84416	0.69970	2.508
H16C	0.42794	0.81850	0.54572	2.508
H17A	-0.16229	0.54509	0.97271	2.367
H17B	-0.12184	0.73735	1.05722	2.367



Experimental

The single crystal of **6-4** suitable for X-ray analysis was grown in a solution of dichloromethane/Hexane at 0 °C under Ar. A colorless chunk crystal of C₁₁H₁₇IN₂O₂ having approximate dimensions of 0.400 × 0.300 × 0.200 mm was mounted on a glass fiber. All measurements were made on a Rigaku XtaLAB mini diffractometer using graphite monochromated Mo-Kα radiation. The crystal-to-detector distance was 450.00 mm. The structure of **6-4** was solved by use of SHELXTL program. Refinement was performed on F² anisotropically for all the non-hydrogen atoms by the full-matrix least-squares method. Crystallographic data has been deposited with the Cambridge Crystallographic Data Center, **CCDC reference number: 1495214**

A. Crystal Data

Empirical Formula	C ₁₁ H ₁₇ IN ₂ O ₂
Formula Weight	336.17
Crystal Color, Habit	colorless, chunk
Crystal Dimensions	0.400 × 0.300 × 0.200 mm
Crystal System	monoclinic

Lattice Type	Primitive
Lattice Parameters	$a = 9.9099(10) \text{ \AA}$ $b = 10.4515(10) \text{ \AA}$ $c = 12.5123(13) \text{ \AA}$ $\beta = 106.827(8)^\circ$ $V = 1240.5(2) \text{ \AA}^3$
Space Group	$P2_1/n$ (#14)
Z value	4
D_{calc}	1.800 g/cm^3
F000	664.00
$\mu(\text{MoK}\alpha)$	25.714 cm^{-1}

B. Intensity Measurements

Diffractometer	XtaLAB mini
Radiation	MoK α ($\lambda = 0.71075 \text{ \AA}$) graphite monochromated
Voltage, Current	50kV, 12mA
Temperature	-123.0 °C
Detector Aperture	75.0 mm (diameter)
Data Images	540 exposures
ω oscillation Range ($\chi=54.0$, $\phi=0.0$)	-60.0 - 120.0°
Exposure Rate	64.0 sec./°
Detector Swing Angle	30.00°
ω oscillation Range ($\chi=54.0$, $\phi=120.0$)	-60.0 - 120.0°
Exposure Rate	64.0 sec./°
Detector Swing Angle	30.00°
ω oscillation Range ($\chi=54.0$, $\phi=240.0$)	-60.0 - 120.0°
Exposure Rate	64.0 sec./°
Detector Swing Angle	30.00°
ω oscillation Range ($\chi=54.0$, $\phi=0.0$)	-60.0 - 120.0°
Exposure Rate	64.0 sec./°
Detector Swing Angle	30.00°
oscillation Range ($\chi=54.0$, $\phi=120.0$)	-60.0 - 120.0°
Exposure Rate	64.0 sec./°
Detector Swing Angle	30.00°
ω oscillation Range ($\chi=54.0$, $\phi=240.0$)	-60.0 - 120.0°
Exposure Rate	64.0 sec./°
Detector Swing Angle	30.00°
Detector Position	50.00 mm
Pixel Size	0.073 mm
$2\theta_{\text{max}}$	55.0°
No. of Reflections Measured	Total: 12350

	Unique: 2829 ($R_{\text{int}} = 0.0258$)
Corrections	Lorentz-polarization
	Absorption
	(trans. factors: 0.503 - 0.598)

C. Structure Solution and Refinement

Structure Solution	Direct Methods (SHELXS97)
Refinement	Full-matrix least-squares on F^2
Function Minimized	$\sum w (F_o^2 - F_c^2)^2$
Least Squares Weights	$w = 1 / [\sigma^2(F_o^2) + (0.0156 \cdot P)^2 + 0.7506 \cdot P]$ where $P = (\text{Max}(F_o^2, 0) + 2F_c^2)/3$
$2\theta_{\text{max}}$ cutoff	55.0°
Anomalous Dispersion	All non-hydrogen atoms
No. Observations (All reflections)	2829
No. Variables	145
Reflection/Parameter Ratio	19.51
Residuals: R_1 ($I > 2.00\sigma(I)$)	0.0167
Residuals: R (All reflections)	0.0174
Residuals: wR_2 (All reflections)	0.0430
Goodness of Fit Indicator	1.154
Max Shift/Error in Final Cycle	0.001
Maximum peak in Final Diff. Map	0.35 e ⁻ /Å ³
Minimum peak in Final Diff. Map	-0.73 e ⁻ /Å ³

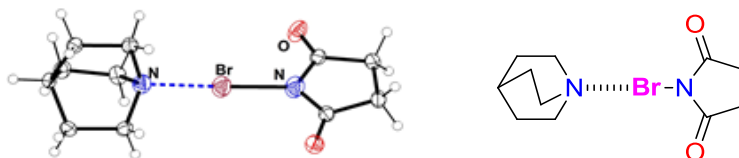
Table 1. Atomic coordinates and $B_{\text{iso}}/B_{\text{eq}}$

atom	x	y	z	B_{eq}
I1	0.22943(2)	-0.00987(2)	0.49820(2)	1.287(4)
O2	0.31957(15)	-0.11838(12)	0.76535(11)	2.18(2)
O6	0.28034(19)	-0.31710(13)	0.43354(11)	2.96(3)
N13	0.15962(14)	0.18353(12)	0.39868(11)	1.15(2)
N17	0.29402(16)	-0.19008(13)	0.58673(12)	1.54(2)
C4	0.08041(19)	0.39010(16)	0.28673(14)	1.63(3)
C5	0.33111(17)	-0.20229(16)	0.70143(14)	1.47(3)
C7	0.0443(2)	0.39588(17)	0.39731(15)	1.83(3)
C8	0.23964(19)	0.37234(17)	0.31160(15)	1.74(3)
C9	0.3681(2)	-0.40452(17)	0.62163(15)	1.88(3)
C10	0.0979(2)	0.27303(17)	0.46415(15)	1.89(3)
C11	0.3874(2)	-0.33652(17)	0.73335(15)	1.96(3)
C12	0.00547(19)	0.27432(18)	0.22030(15)	1.87(3)
C14	0.3098(2)	-0.30278(16)	0.53421(15)	1.75(3)
C15	0.28280(19)	0.24473(18)	0.37414(16)	2.04(3)
C16	0.0515(2)	0.15322(17)	0.29161(14)	1.88(3)

$$B_{eq} = 8/3 \pi^2 (U_{11}(aa^*)^2 + U_{22}(bb^*)^2 + U_{33}(cc^*)^2 + 2U_{12}(aa^*bb^*)\cos \gamma + 2U_{13}(aa^*cc^*)\cos \beta + 2U_{23}(bb^*cc^*)\cos \alpha)$$

Table 2. Atomic coordinates and B_{iso} involving hydrogen atoms

atom	x	y	z	B _{iso}
H4	0.04977	0.47057	0.24324	1.959
H7A	-0.05903	0.40339	0.38298	2.201
H7B	0.08928	0.47170	0.44057	2.201
H8A	0.28971	0.44418	0.35799	2.082
H8B	0.26570	0.37155	0.24096	2.082
H9A	0.45927	-0.43748	0.61564	2.256
H9B	0.30125	-0.47681	0.61318	2.256
H10A	0.17014	0.29548	0.53464	2.271
H10B	0.01870	0.23053	0.48337	2.271
H11A	0.33336	-0.38017	0.77798	2.355
H11B	0.48815	-0.33408	0.77705	2.355
H12A	0.03065	0.26656	0.14956	2.240
H12B	-0.09797	0.28519	0.20201	2.240
H15A	0.32136	0.18633	0.32796	2.447
H15B	0.35753	0.26065	0.44489	2.447
H16A	-0.03161	0.11404	0.30745	2.253
H16B	0.09055	0.09036	0.24931	2.253



The single crystal of **6-5** suitable for X-ray analysis was grown in a solution of dichloromethane/Hexane at 0 °C under Ar. A colorless prism crystal of C₁₁H₁₇BrN₂O₂ having approximate dimensions of 0.400 × 0.200 × 0.200 mm was mounted on a glass fiber. All measurements were made on a Rigaku XtaLAB mini diffractometer using graphite monochromated Mo-K α radiation. The crystal-to-detector distance was 50.00 mm. The structure of **6-5** was solved by use of SHELXTL program. Refinement was performed on F² anisotropically for all the non-hydrogen atoms by the full-matrix least-squares method. Crystallographic data has been deposited with the Cambridge Crystallographic Data Center, **CCDC reference number: 1495216**

A. Crystal Data

Empirical Formula	C ₁₁ H ₁₇ BrN ₂ O ₂
Formula Weight	289.17
Crystal Color, Habit	colorless, prism
Crystal Dimensions	0.400 X 0.200 X 0.200 mm
Crystal System	monoclinic
Lattice Type	Primitive
Lattice Parameters	a = 9.9776(13) Å

	$b = 10.2427(13) \text{ \AA}$
	$c = 12.2501(16) \text{ \AA}$
	$\beta = 106.868(8)^\circ$
	$V = 1198.1(3) \text{ \AA}^3$
Space Group	$P2_1/n$ (#14)
Z value	4
D_{calc}	1.603 g/cm^3
F_{000}	592.00
$\mu(\text{MoK}\alpha)$	34.293 cm^{-1}

B. Intensity Measurements

Diffractometer	XtaLAB mini
Radiation	MoK α ($\lambda = 0.71075 \text{ \AA}$) graphite monochromated
Voltage, Current	50kV, 12mA
Temperature	-123.0°C
Detector Aperture	75.0 mm (diameter)
Data Images	540 exposures
ω oscillation Range ($\chi=54.0, \phi=0.0$)	$-60.0 - 120.0^\circ$
Exposure Rate	24.0 sec./°
Detector Swing Angle	30.00°
ω oscillation Range ($\chi=54.0, \phi=120.0$)	$-60.0 - 120.0^\circ$
Exposure Rate	24.0 sec./°
Detector Swing Angle	30.00°
ω oscillation Range ($\chi=54.0, \phi=240.0$)	$-60.0 - 120.0^\circ$
Exposure Rate	24.0 sec./°
Detector Swing Angle	30.00°
ω oscillation Range ($\chi=54.0, \phi=0.0$)	$-60.0 - 120.0^\circ$
Exposure Rate	24.0 sec./°
Detector Swing Angle	30.00°
ω oscillation Range ($\chi=54.0, \phi=120.0$)	$-60.0 - 120.0^\circ$
Exposure Rate	24.0 sec./°
Detector Swing Angle	30.00°
ω oscillation Range ($\chi=54.0, \phi=240.0$)	$-60.0 - 120.0^\circ$
Exposure Rate	24.0 sec./°
Detector Swing Angle	30.00°
Detector Position	50.00 mm
Pixel Size	0.073 mm
$2\theta_{\text{max}}$	55.0°
No. of Reflections Measured	Total: 12299 Unique: 2742 ($R_{\text{int}} = 0.0408$)
Corrections	Lorentz-polarization

Absorption
(trans. factors: 0.348 - 0.504)
Secondary Extinction
(coefficient: 8.29000e-003)

C. Structure Solution and Refinement

Structure Solution	Direct Methods (SHELXS97)
Refinement	Full-matrix least-squares on F^2
Function Minimized	$\sum w (F_o^2 - F_c^2)^2$
Least Squares Weights	$w = 1 / [\sigma^2(F_o^2) + (0.0182 \cdot P)^2 + 0.8468 \cdot P]$ where $P = (\text{Max}(F_o^2, 0) + 2F_c^2)/3$
$2\theta_{\text{max}}$ cutoff	55.0°
Anomalous Dispersion	All non-hydrogen atoms
No. Observations (All reflections)	2742
No. Variables	146
Reflection/Parameter Ratio	18.78
Residuals: R1 ($I > 2.00\sigma(I)$)	0.0241
Residuals: R (All reflections)	0.0277
Residuals: wR2 (All reflections)	0.0584
Goodness of Fit Indicator	1.064
Max Shift/Error in Final Cycle	0.000
Maximum peak in Final Diff. Map	0.36 e ⁻ /Å ³
Minimum peak in Final Diff. Map	-0.40 e ⁻ /Å ³

Table 1. Atomic coordinates and $B_{\text{iso}}/B_{\text{eq}}$

atom	x	y	z	B_{eq}
Br1	0.28120(2)	0.48943(2)	0.50484(2)	1.541(6)
O3	0.18340(15)	0.39658(13)	0.23707(11)	2.15(2)
O6	0.24229(18)	0.18809(14)	0.57675(12)	2.84(3)
N4	0.21945(17)	0.31952(14)	0.41973(13)	1.66(3)
N17	0.34382(15)	0.67347(14)	0.60041(12)	1.30(2)
C2	0.4560(2)	0.89033(18)	0.60135(16)	1.87(3)
C5	0.1358(2)	0.10433(18)	0.38444(16)	1.83(3)
C7	0.2047(2)	0.20509(18)	0.47367(16)	1.73(3)
C8	0.17455(19)	0.31040(17)	0.30244(16)	1.55(3)
C10	0.3999(2)	0.76628(18)	0.53140(16)	1.81(3)
C11	0.4199(2)	0.88427(18)	0.71425(16)	1.67(3)
C12	0.1143(2)	0.17453(18)	0.27009(16)	1.83(3)
C13	0.4946(2)	0.76715(19)	0.78228(16)	1.97(3)
C15	0.4547(2)	0.64356(18)	0.70832(16)	1.86(3)
C16	0.22127(19)	0.73151(19)	0.62804(17)	1.83(3)
C18	0.2607(2)	0.86504(18)	0.68768(16)	1.73(3)

$$B_{\text{eq}} = 8/3 \pi^2 (U_{11}(\text{aa}^*)^2 + U_{22}(\text{bb}^*)^2 + U_{33}(\text{cc}^*)^2 + 2U_{12}(\text{aa}^*\text{bb}^*)\cos \gamma + 2U_{13}(\text{aa}^*\text{cc}^*)\cos \beta + 2U_{23}(\text{bb}^*\text{cc}^*)\cos \alpha)$$

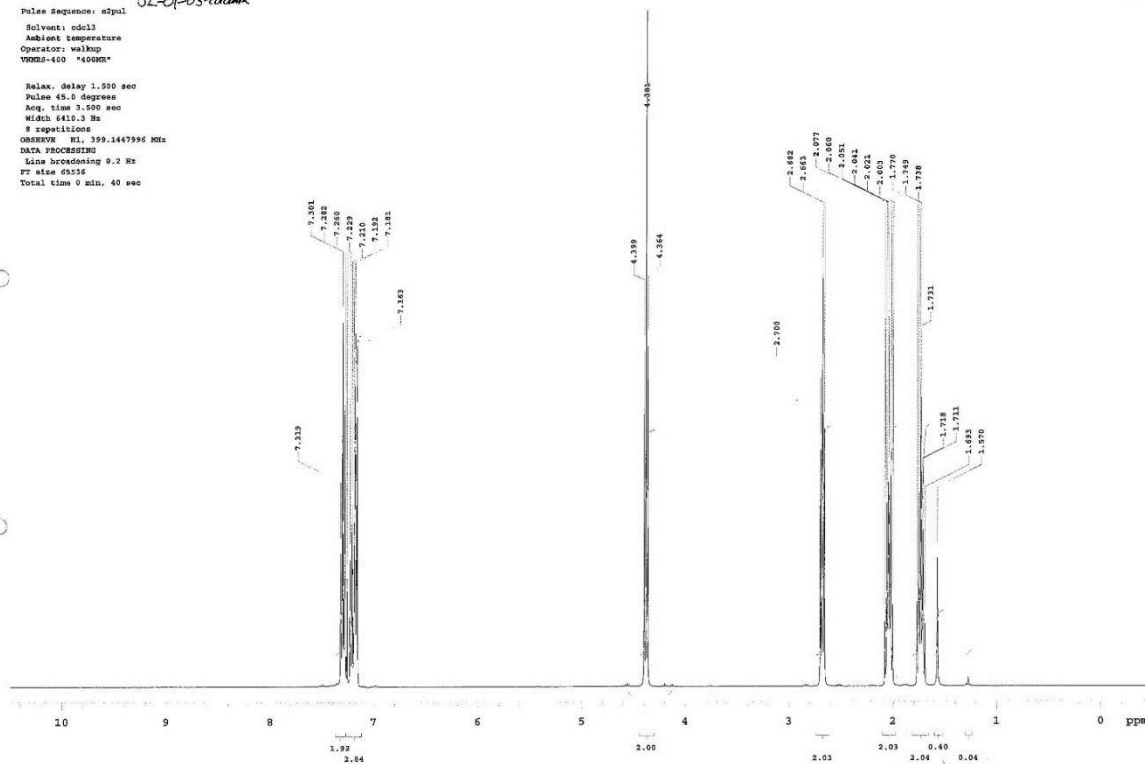
Table 2. Atomic coordinates and B_{iso} involving hydrogen atoms

atom	x	y	z	B _{iso}
H2A	0.55875	0.89606	0.61619	2.247
H2B	0.41306	0.96883	0.55798	2.247
H5A	0.04504	0.07582	0.39392	2.198
H5B	0.19695	0.02703	0.38976	2.198
H10A	0.32489	0.79036	0.46164	2.178
H10B	0.47638	0.72404	0.50788	2.178
H11	0.44941	0.96664	0.75851	2.006
H12A	0.16465	0.12887	0.22253	2.201
H12B	0.01361	0.17929	0.22752	2.201
H13A	0.46662	0.75731	0.85304	2.367
H13B	0.59725	0.78047	0.80375	2.367
H15A	0.53847	0.60891	0.69037	2.234
H15B	0.42043	0.57576	0.75127	2.234
H16A	0.18896	0.67174	0.67871	2.198
H16B	0.14357	0.74318	0.55706	2.198
H18A	0.21054	0.93601	0.63732	2.081
H18B	0.23340	0.86736	0.75918	2.081

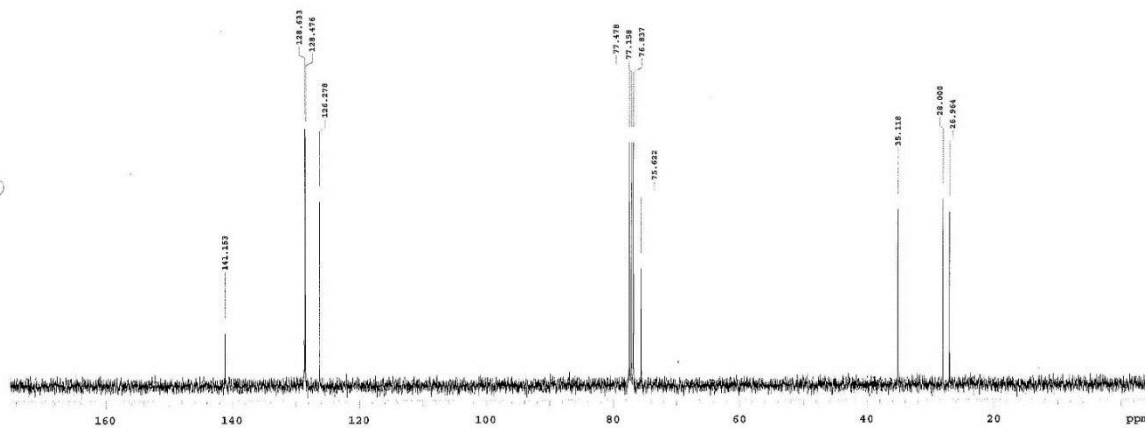
Spectra

Spectra

File: exp
 Pulse Sequence: sfpul
 Solvent: cdcl3
 Ambient temperature
 Operator: walkup
 VMDR-400 "400MHz"
 Relax. delay 1.500 sec
 Pulse 45.0 degrees
 Acq. time 3.500 sec
 Width 6410.3 Hz
 8 repetitions
 OBSERVE H1, 399.1447996 MHz
 DATA PROCESSING
 Line broadening 9.2 Hz
 FT size 65536
 Total time 0 min, 40 sec

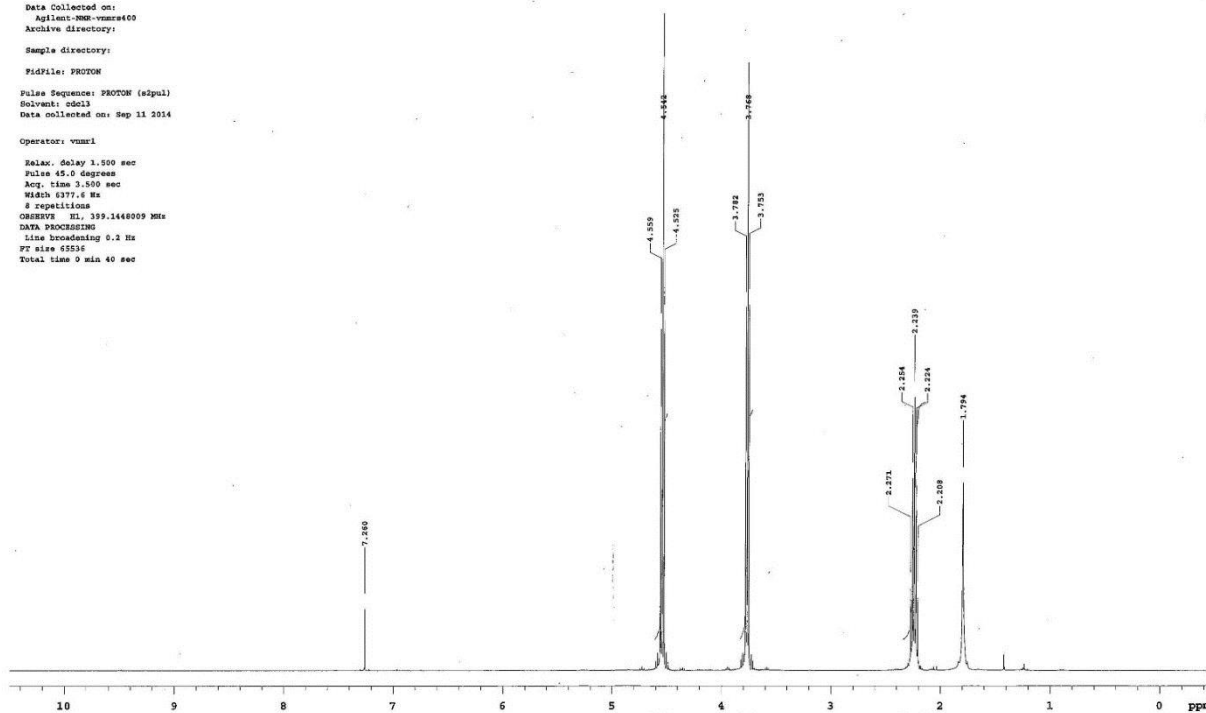


File: exp
 Pulse Sequence: sfpul
 Solvent: cdcl3
 Ambient temperature
 Operator: walkup
 VMDR-400 "400MHz"
 Relax. delay 0.780 sec
 Pulse 45.0 degrees
 Acq. time 1.300 sec
 Width 24860.8 Hz
 64 repetitions
 OBSERVE C13, 100.6260774 MHz
 DECOUPLE H1, 399.1448033 MHz
 Power 41 dB
 continuously on
 WALTZ-16 modulated
 DATA PROCESSING
 Line broadening 1.0 Hz
 FT size 65536
 Total time 2 min, 9 sec

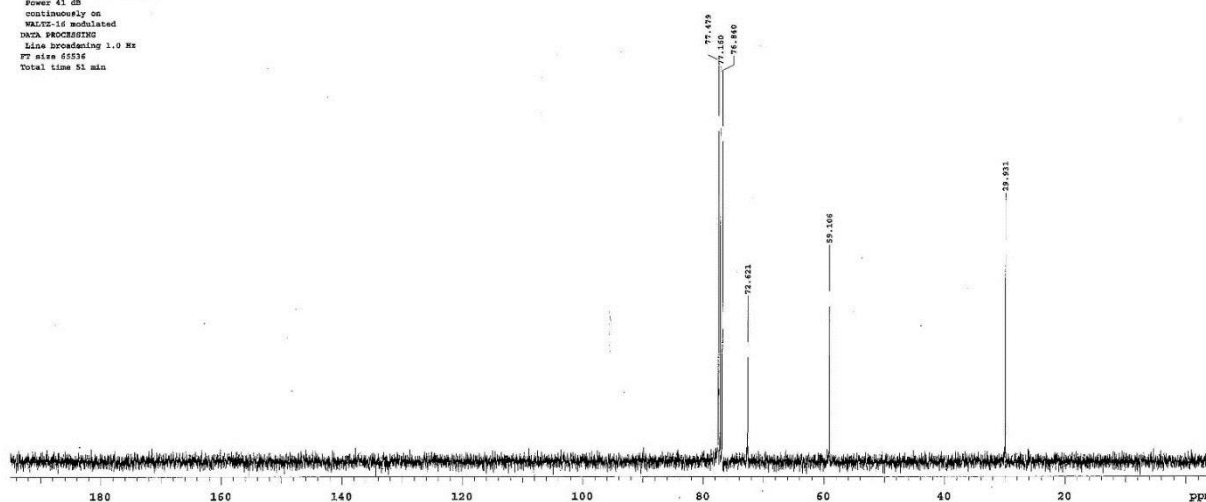




Sample Name:
 Data Collected on:
 Agilent-900-vnmr400
 Archive directory:
 Sample directory:
 FidFile: PROTON
 Pulse Sequence: PROTON (s2pul)
 Solvent: cdcl3
 Data collected on: Sep 11 2014
 Operator: vnmr1
 Relax. Delay 1.500 sec
 Pulse 45.0 degrees
 Acq. time 3.500 sec
 Width 6377.6 Hz
 8 repetitions
 OBSERVE RL 399.1448009 MHz
 DATA PROCESSING
 Line broadening 0.2 Hz
 FT size 65535
 Total time 9 min 40 sec

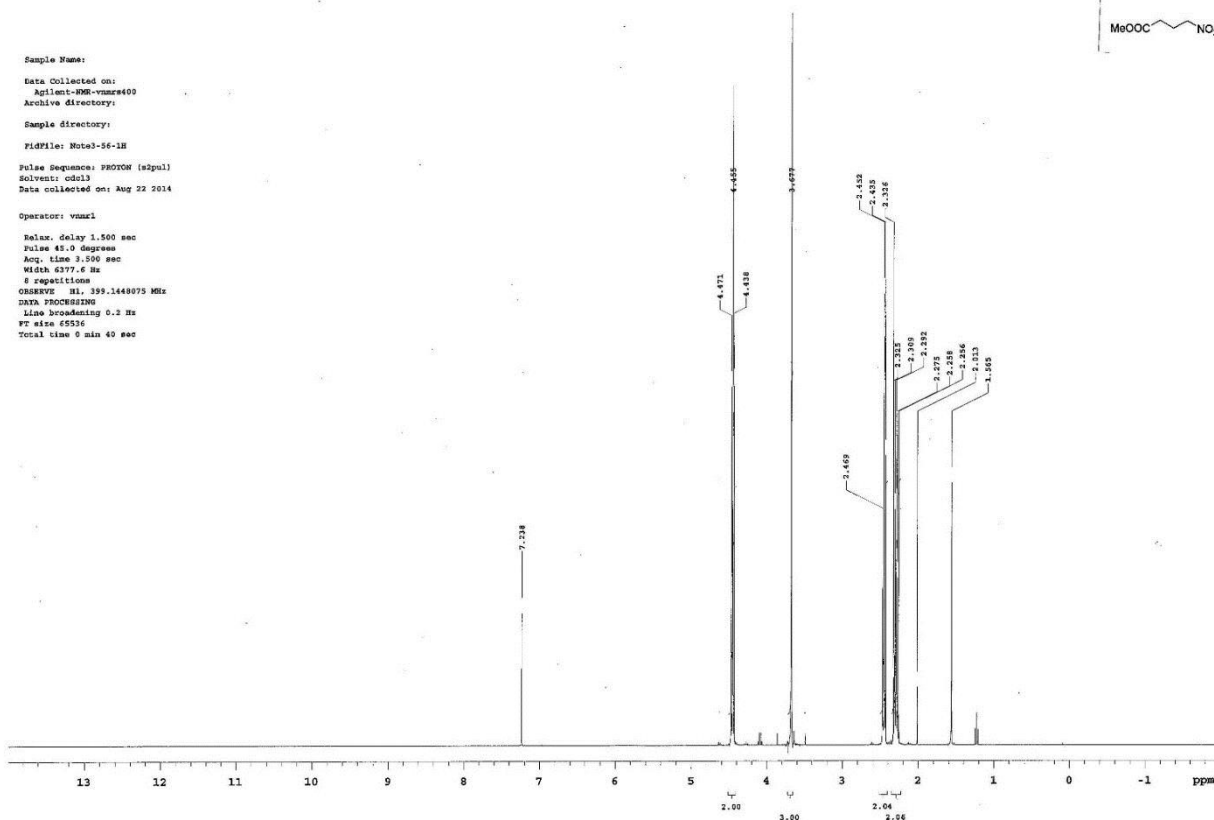


Sample Name:
 Data Collected on:
 Agilent-900-vnmr400
 Archive directory:
 Sample directory:
 FidFile: CARBON
 Pulse Sequence: CARBON (s2pul)
 Solvent: cdcl3
 Data collected on: Sep 11 2014
 Temp. 26.3 C / 299.4 K
 Operator: vnmr1
 Relax. Delay 1.689 sec
 Pulse 45.0 degrees
 Acq. time 1.311 sec
 Width 25000.0 Hz
 64 repetitions
 OBSERVE C13, 100.3650265 MHz
 DECOUPLE RL 399.1448009 MHz
 Power 41 dB
 continuously on
 WALTZ-16 modulated
 DATA PROCESSING
 Line broadening 1.0 Hz
 FT size 65536
 Total time 51 min



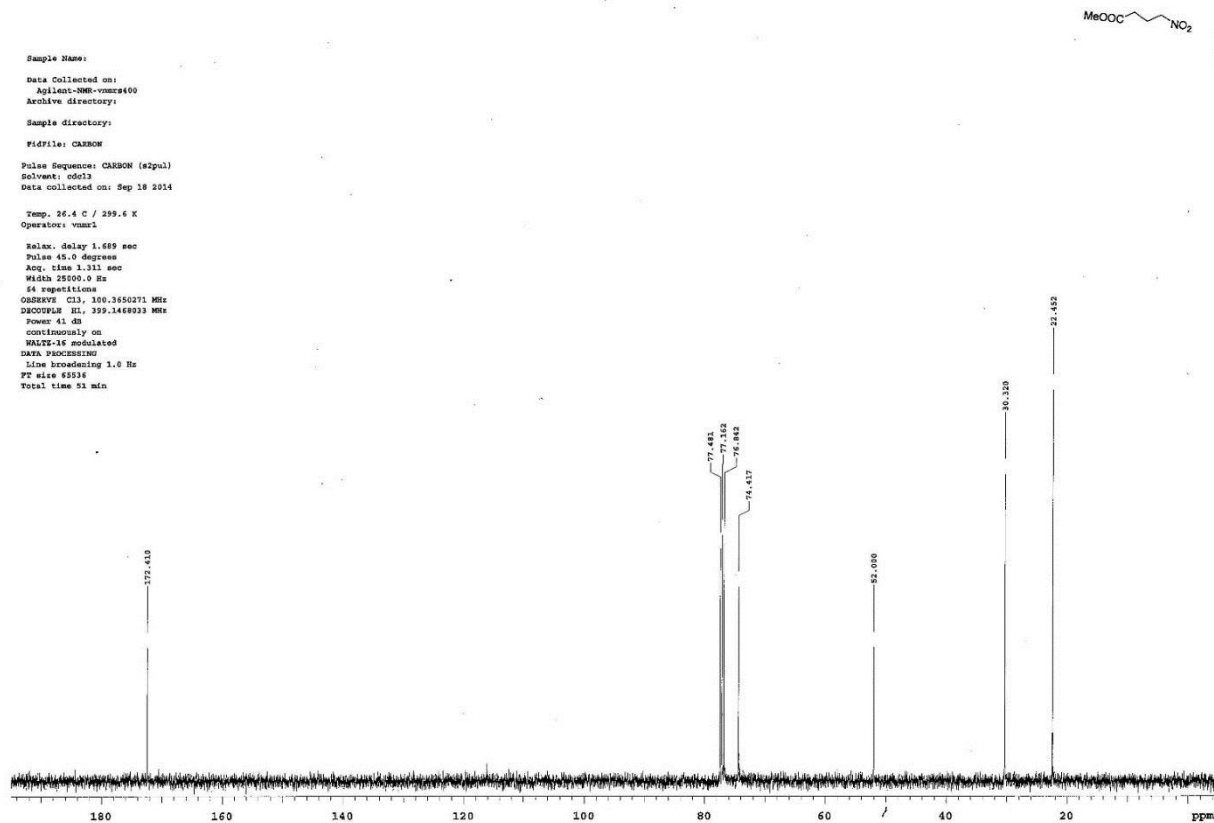
Sample Name:
 Data Collected on:
 Agilent-WNM-vnmr400
 Archive directory:
 Sample directory:
 FIDFile: M03-56-1H
 Pulse Sequence: PROTON (zgpg30)
 Solvent: cdcl3
 Data collected on: Aug 22 2014

Operator: vnmr1
 Relax. delay 1.500 sec
 Pulse 45.0 degrees
 Acq. time 3.500 sec
 Width 6377.6 Hz
 8 repetitions
 OBSERVE HL 399.1449075 MHz
 DATA PROCESSING
 Line broadening 0.2 Hz
 FT size 65536
 Total time 6 min 40 sec

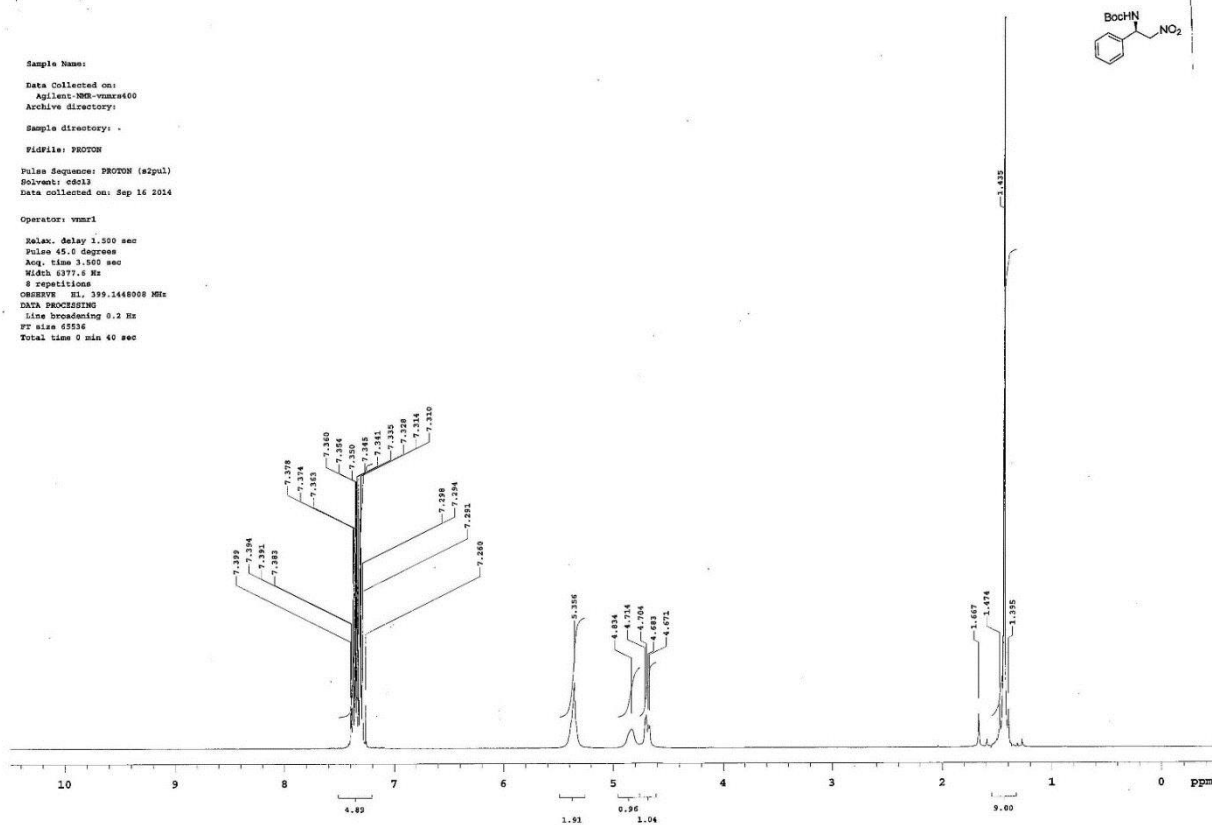


Sample Name:
 Data Collected on:
 Agilent-WNM-vnmr400
 Archive directory:
 Sample directory:
 FIDFile: CARBON

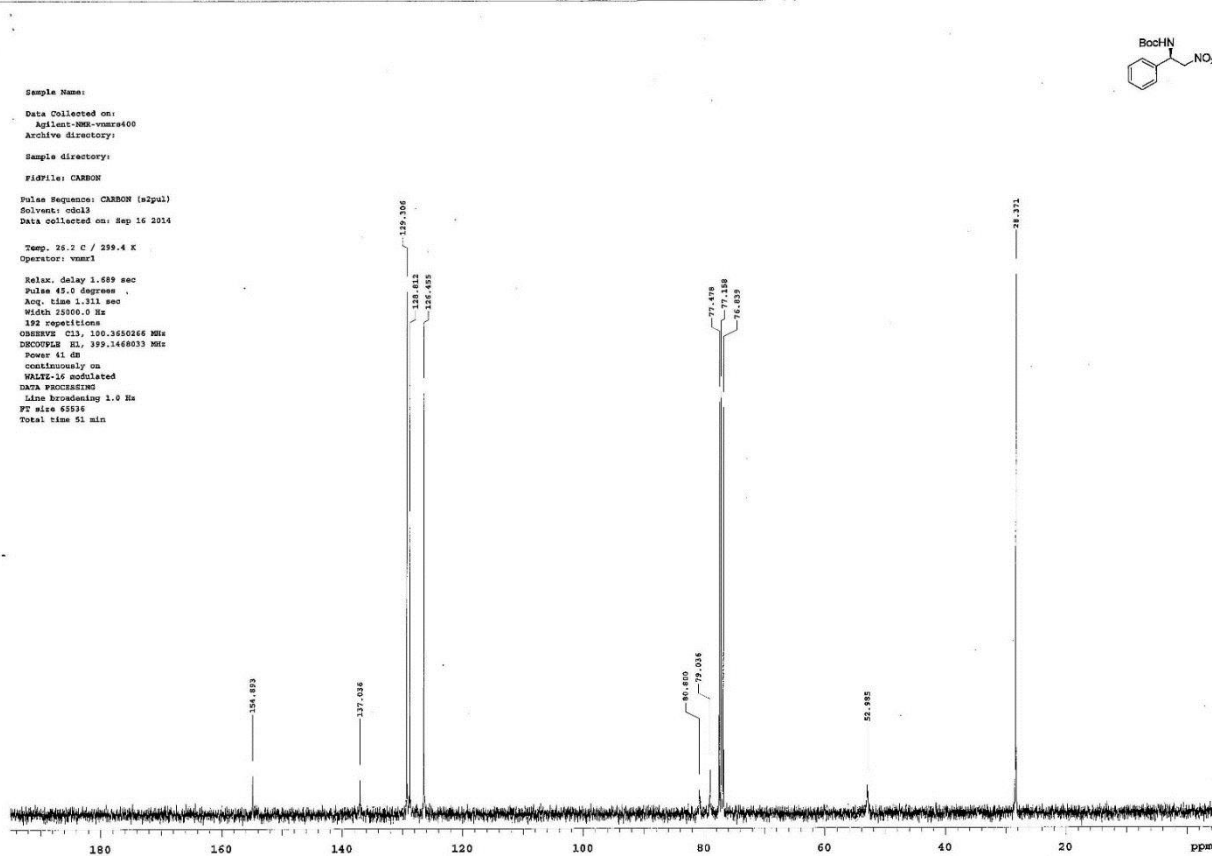
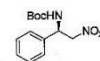
Pulse Sequence: CARBON (zgpg30)
 Solvent: cdcl3
 Data collected on: Sep 18 2014
 Temp. 26.4 C / 299.6 K
 Operator: vnmr1
 Relax. delay 1.689 sec
 Pulse 45.0 degrees
 Acq. time 1.311 sec
 Width 25100.0 Hz
 64 repetitions
 OBSERVE CH 100.6250271 MHz
 DECOUPLE HL 399.1448933 MHz
 Power 41 dB
 Continuously on
 WALTZ-16 modulated
 DATA PROCESSING
 Line broadening 1.0 Hz
 FT size 65536
 Total time 51 min



Sample Name:
 Data Collected on:
 Agilent-NMR-vnmr400
 Archive directory:
 Sample directory:
 FIDFile: PROTON
 Pulse Sequence: PROTON (s2pul)
 Solvent: cdcl3
 Data collected on: Sep 16 2014
 Operator: vnmr1
 Relax. delay 1.550 sec
 Pulse 45.0 degrees
 Acq. time 3.502 sec
 Width 6377.6 Hz
 8 repetitions
 OBSERVE EL 399.1448000 MHz
 DATA PROCESSING
 Line broadening 0.2 Hz
 FT size 65536
 Total time 0 min 40 sec



Sample Name:
 Data Collected on:
 Agilent-NMR-vnmr400
 Archive directory:
 Sample directory:
 FIDFile: CARBON
 Pulse Sequence: CARBON (s2pul)
 Solvent: cdcl3
 Data collected on: Sep 16 2014
 Temp. 25.2 C / 299.4 K
 Operator: vnmr1
 Relax. delay 1.559 sec
 Pulse 45.0 degrees
 Acq. time 1.311 sec
 Width 25100.0 Hz
 192 repetitions
 OBSERVE C13, 100.3550266 MHz
 DECOUPLE EL 399.1448000 MHz
 Power 41.0m
 continuously on
 WALTZ-16 modulated
 DATA PROCESSING
 Line broadening 1.0 Hz
 FT size 65536
 Total time 31 min



3-137aruda

Sample Name:

Data Collected on:

Agilent-VNM-vmr400

Archive directory:

Sample directory:

FidFile: PROTON

Pulse Sequence: PROTON (s2pul)

Solvent: cdcl3

Data collected on: Sep 15 2014

Operator: vmr400

Relax. delay 1.500 sec

Pulse 45.0 degrees

Acq. time 3.500 sec

Width 6377.6 Hz

8 repetitions

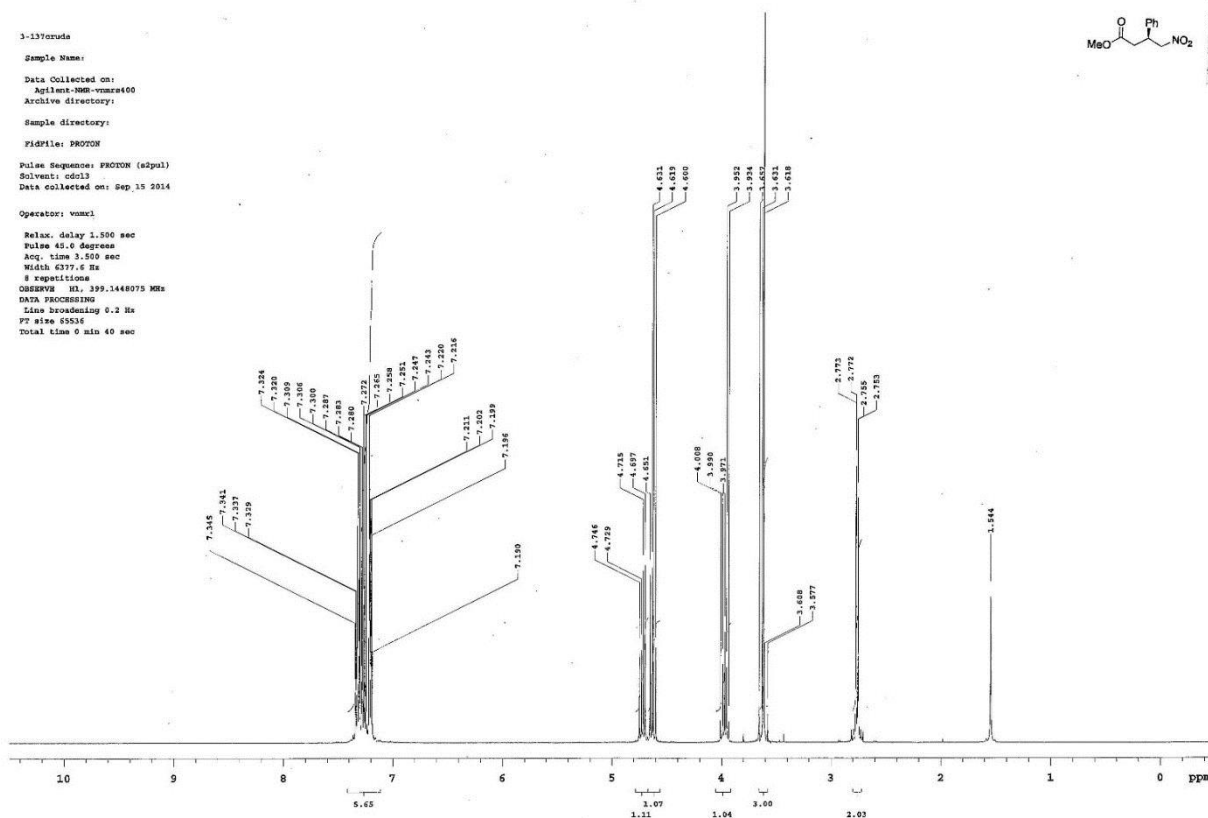
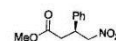
OBSERVE HL 399.1448075 MHz

DATA PROCESSING

Line broadening 5.2 Hz

FT size 65536

Total time 0 min 40 sec



Sample Name:

Data Collected on:

Agilent-VNM-vmr400

Archive directory:

Sample directory:

FidFile: CARBON

Pulse Sequence: CARBON (s2pul)

Solvent: cdcl3

Data collected on: Sep 15 2014

Temp. 25.9 C / 299.1 K

Operator: vmr400

Relax. delay 1.689 sec

Pulse 45.0 degrees

Acq. time 1.311 sec

Width 25000.0 Hz

128 repetitions

OBSERVE C13, 100.3650145 MHz

DCOUPLE HL 399.1448075 MHz

Power 41 dB

continuously on

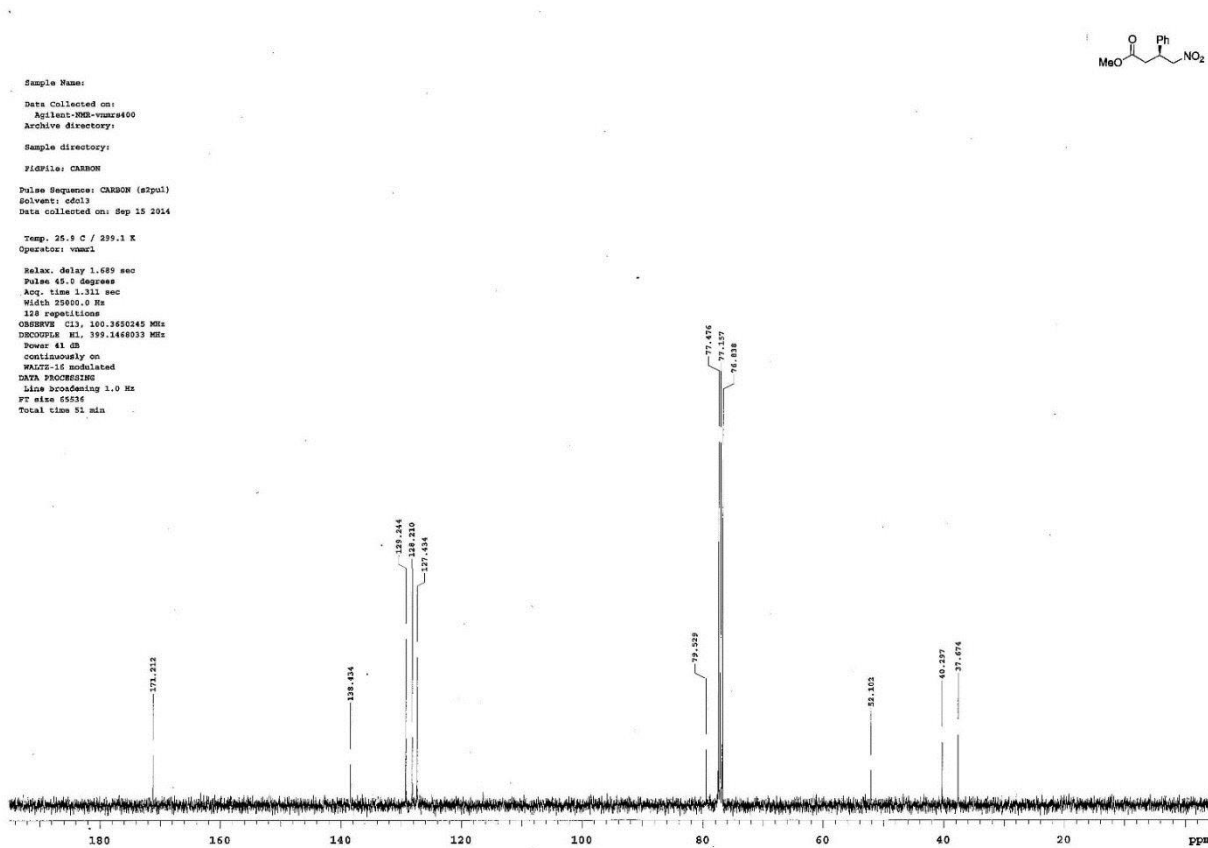
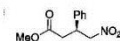
WALTZ-16 modulated

DATA PROCESSING

Line broadening 1.0 Hz

FT size 65536

Total time 31 min

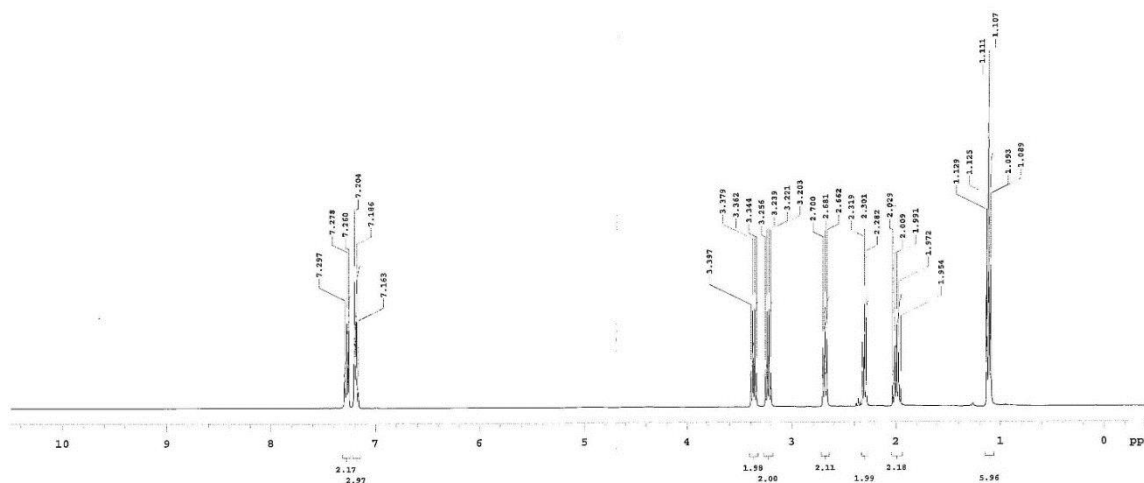
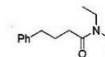


3-136-1

File: exp

Pulse Sequence: zgpg30
Solvent: cdcl3
Ambient temperature
Operator: walup
VME52-400 "400MHz"

Relax. delay 1.500 sec
Pulse 45.0 degrees
Acq. time 3.500 sec
Width 4415.3 Hz
8 repetitions
OBSERVE F1, 399.1447982 MHz
DATA PROCESSING
Line broadening 0.2 Hz
PT size 65536
Total time 0 min, 40 sec

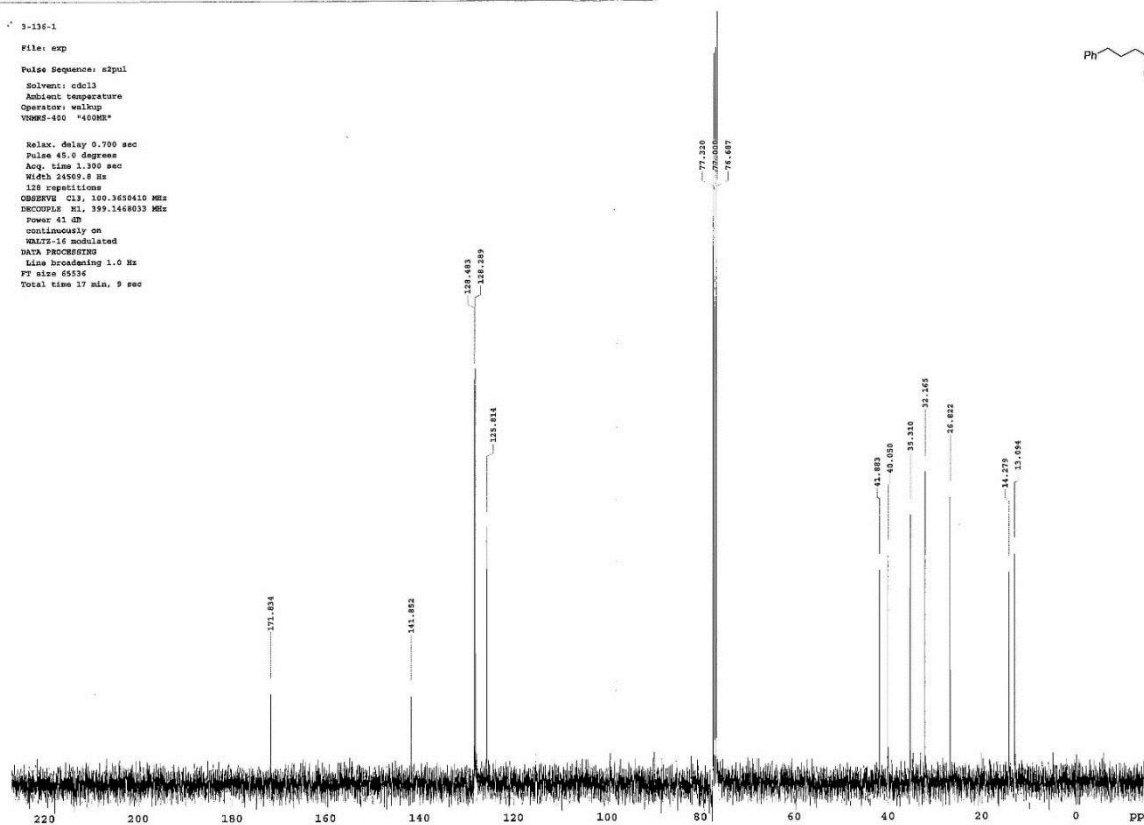
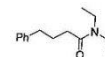


3-136-1

File: exp

Pulse Sequence: zgpg30
Solvent: cdcl3
Ambient temperature
Operator: walup
VME52-400 "400MHz"

Relax. delay 0.700 sec
Pulse 45.0 degrees
Acq. time 1.300 sec
Width 24500.8 Hz
128 repetitions
OBSERVE C13, 100.626010 MHz
DECOUPLE H1, 399.1448033 MHz
Power 41 dB
Continuously on
WALTZ-16 modulated
DATA PROCESSING
Line broadening 1.0 Hz
PT size 65536
Total time 17 min, 9 sec

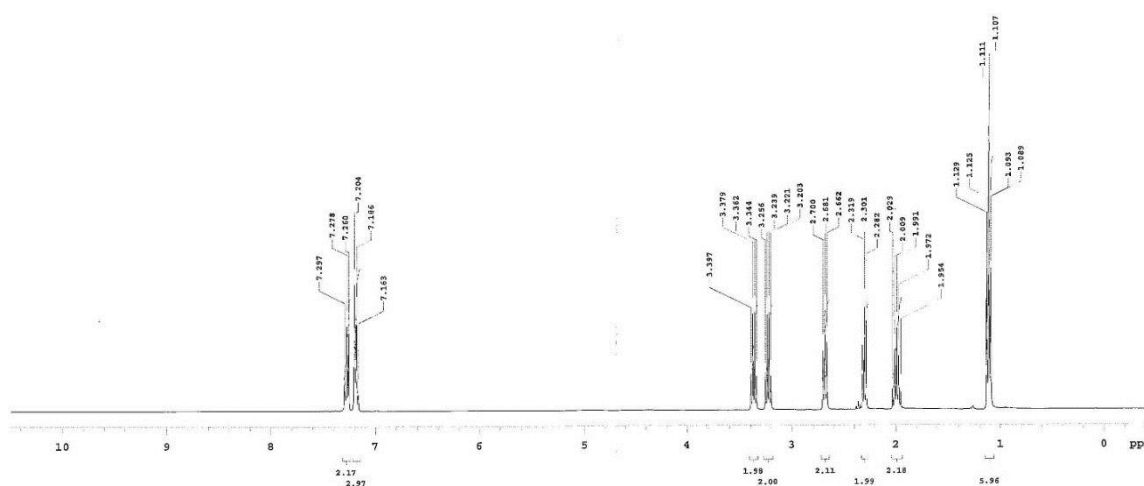
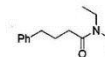


3-136-1

File: exp

Pulse Sequence: zgpg30
Solvent: cdcl3
Ambient temperature
Operator: walup
VME52-400 "400MHz"

Relax. delay 1.500 sec
Pulse 45.0 degrees
Acq. time 3.500 sec
Width 4415.3 Hz
8 repetitions
OBSERVE F1, 399.1447982 MHz
DATA PROCESSING
Line broadening 0.2 Hz
PT size 65536
Total time 0 min, 40 sec

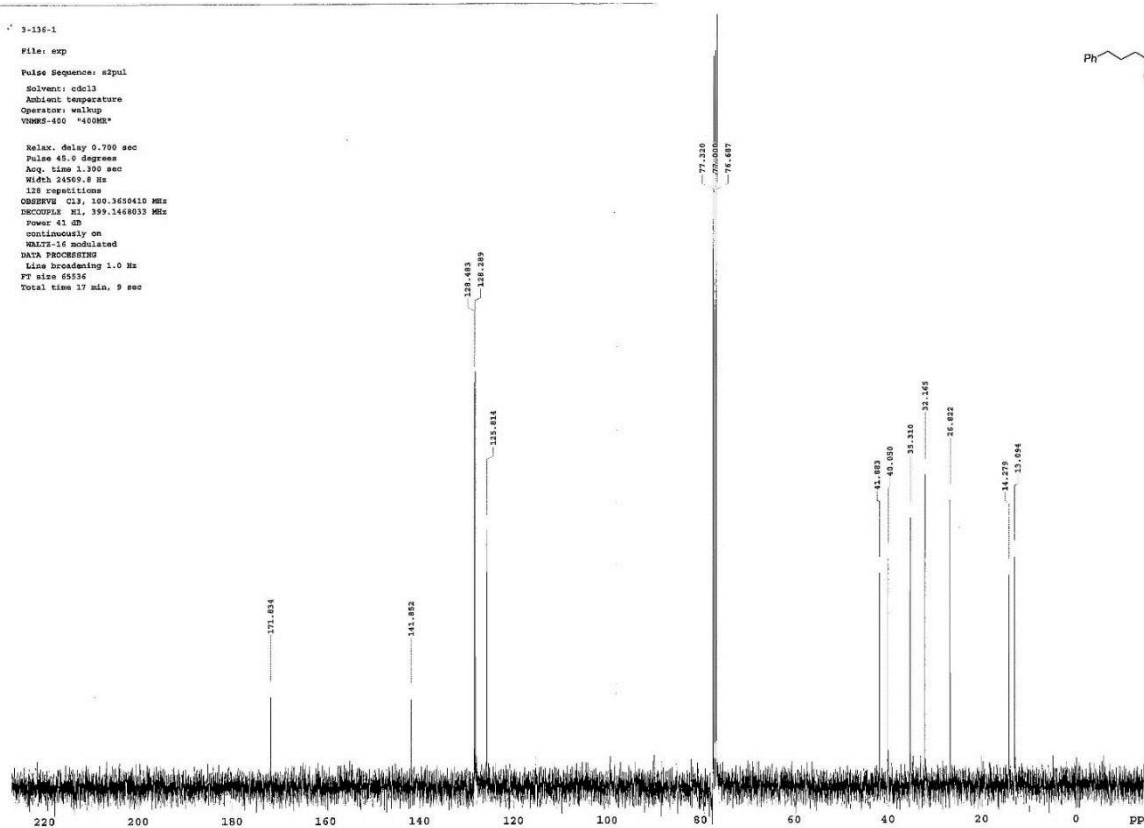
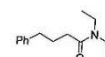


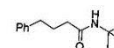
3-136-1

File: exp

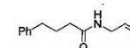
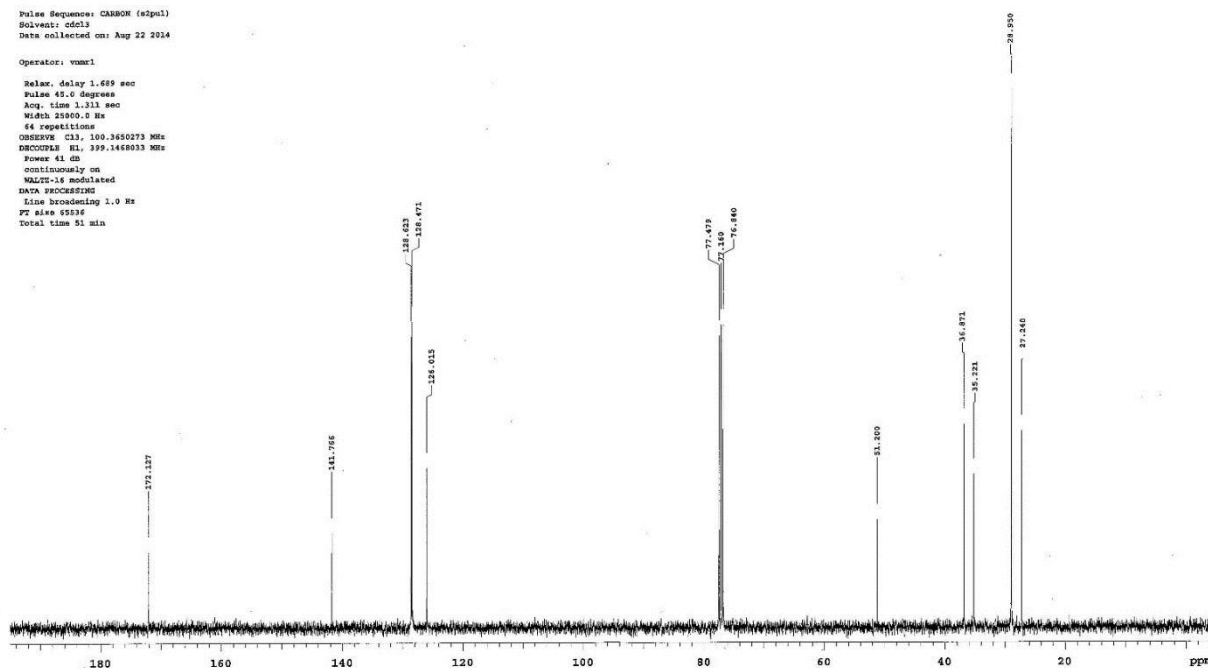
Pulse Sequence: zgpg30
Solvent: cdcl3
Ambient temperature
Operator: walup
VME52-400 "400MHz"

Relax. delay 0.700 sec
Pulse 45.0 degrees
Acq. time 1.300 sec
Width 24500.8 Hz
128 repetitions
OBSERVE C13, 100.626010 MHz
DECOUPLE H1, 399.1448033 MHz
Power 41 dB
Continuously on
WALTZ-16 modulated
DATA PROCESSING
Line broadening 1.0 Hz
PT size 65536
Total time 17 min, 9 sec

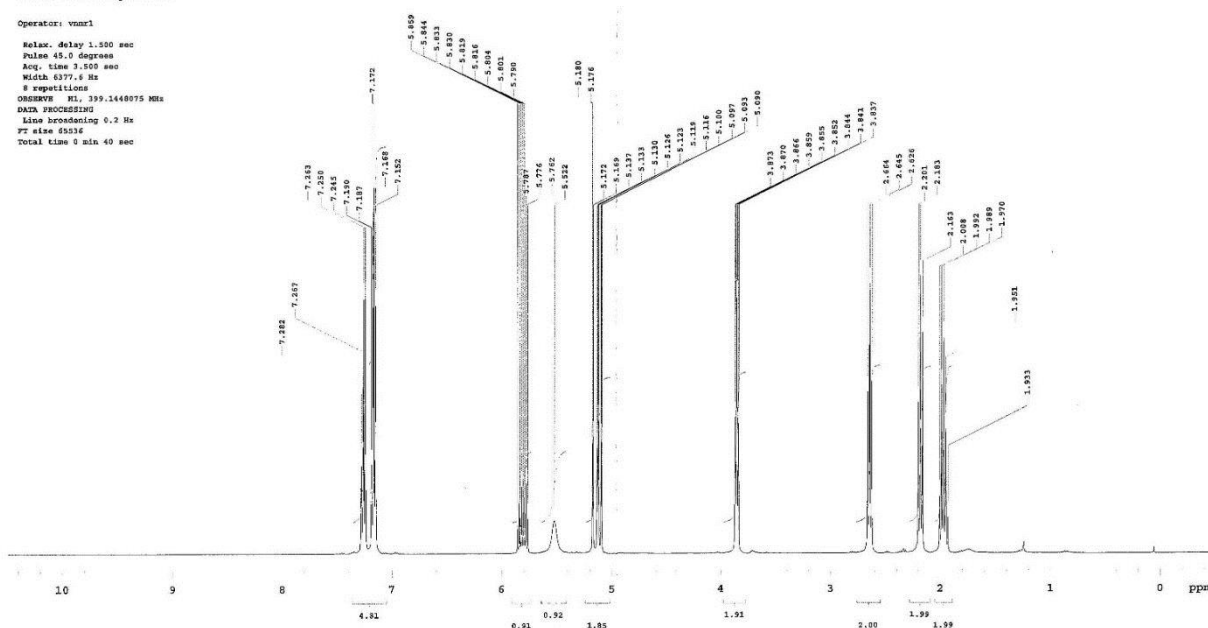




Sample Name:
Data Collected on:
Agilent-NMR-vnmr400
Archive directory:
Sample directory:
FidFile: Nmr3-45-13C
Pulse Sequence: CARBON (zgpg1)
Solvent: cdcl3
Data collected on: Aug 22 2014
Operator: vnmr1
Relax. delay 1.689 sec
Pulse 45.0 degrees
Acq. time 1.313 sec
Width 25900.5 Hz
44 repetitions
OBSERVE CH1: 100.625073 MHz
DECODED CH1: 100.625073 MHz
Power 41 dB
continuously on
WALTZ-16 modulated
DATA PROCESSING
Line broadening 1.0 Hz
PT size 65536
Total time 51 min



3-165-1
Sample Name:
KMYT_allylamine
Data Collected on:
Agilent-NMR-vnmr400
Archive directory:
Sample directory:
FidFile: PROTON
Pulse Sequence: PROTON (zgpg1)
Solvent: cdcl3
Data collected on: Apr 13 2014
Operator: vnmr1
Relax. delay 1.500 sec
Pulse 45.0 degrees
Acq. time 3.500 sec
Width 6377.4 Hz
8 repetitions
OBSERVE CH1: 399.1448075 MHz
DATA PROCESSING
Line broadening 0.2 Hz
PT size 65536
Total time 8 min 40 sec



nakadai-008-008-P23.4
chose...

Sample Name:

Data Collected on:
Agilent-VNMRS-vnmr400
Archive directory:

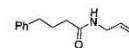
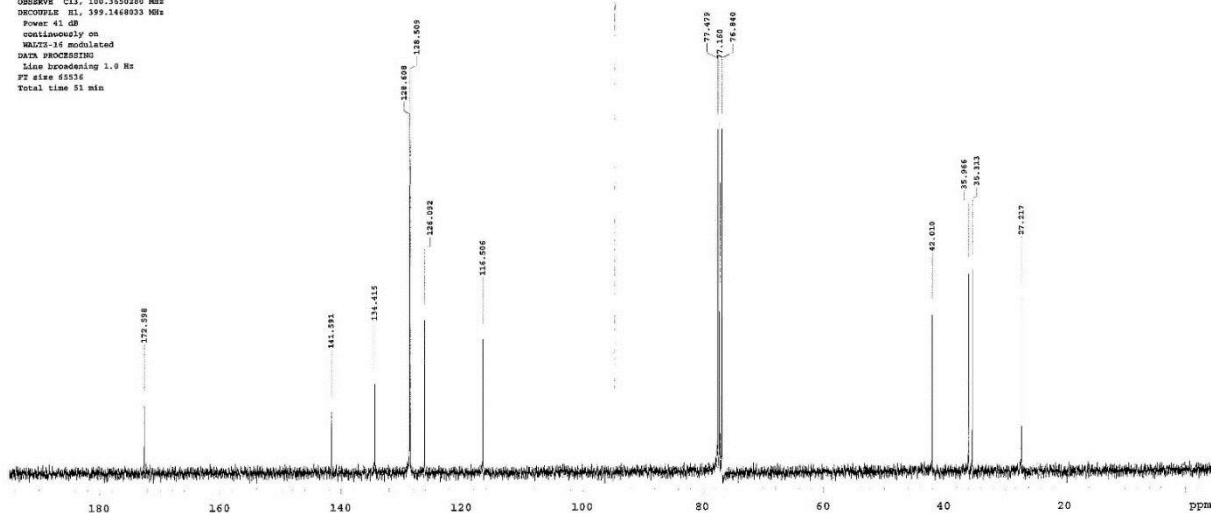
Sample directory:

FidFile: CARBON

Pulse Sequence: CARBON (zgpg3)
Solvent: cdcl3
Data collected on: Apr 13 2014

Temp: 24.9 C / 297.9 K
Operator: vnmr1

Relax. delay 1.500 sec
Pulse 45.0 degrees
Acq. time 1.311 sec
Width 23400.0 Hz
120 repetitions
OBSERVE CH3, 100.3650280 MHz
DECOUPLE H1, 399.1448333 MHz
Power 41 dB
continuously on
WALTZ-16 modulated
DATA PROCESSING
Line broadening 1.0 Hz
FT size 65536
Total time 51 min



3-149-1

Sample Name:

Archive directory:

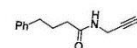
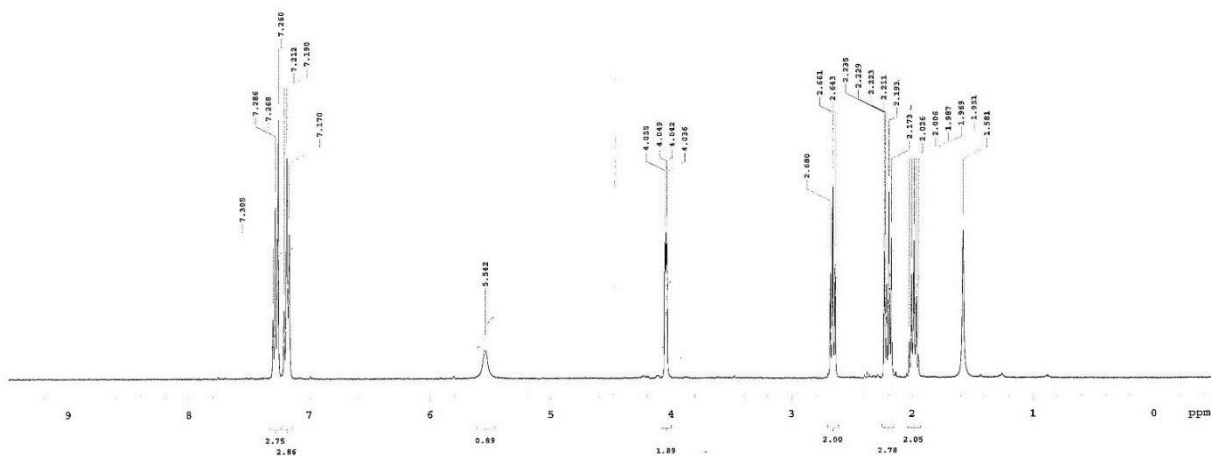
Sample directory:

FidFile: 3-149-1-20131113

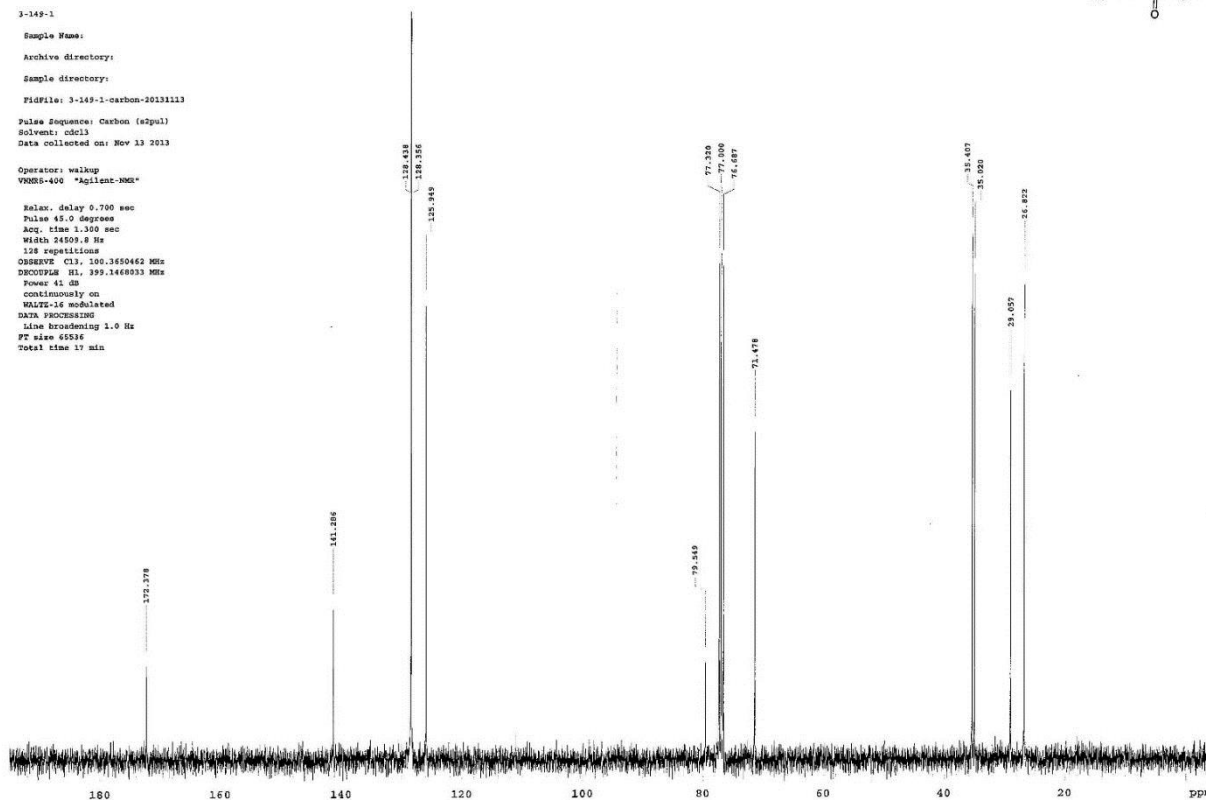
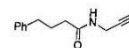
Pulse Sequence: Proton (zgpg3)
Solvent: cdcl3
Data collected on: Nov 13 2013

Operator: walkup
VNMRS-400 "Agilent-VNM"

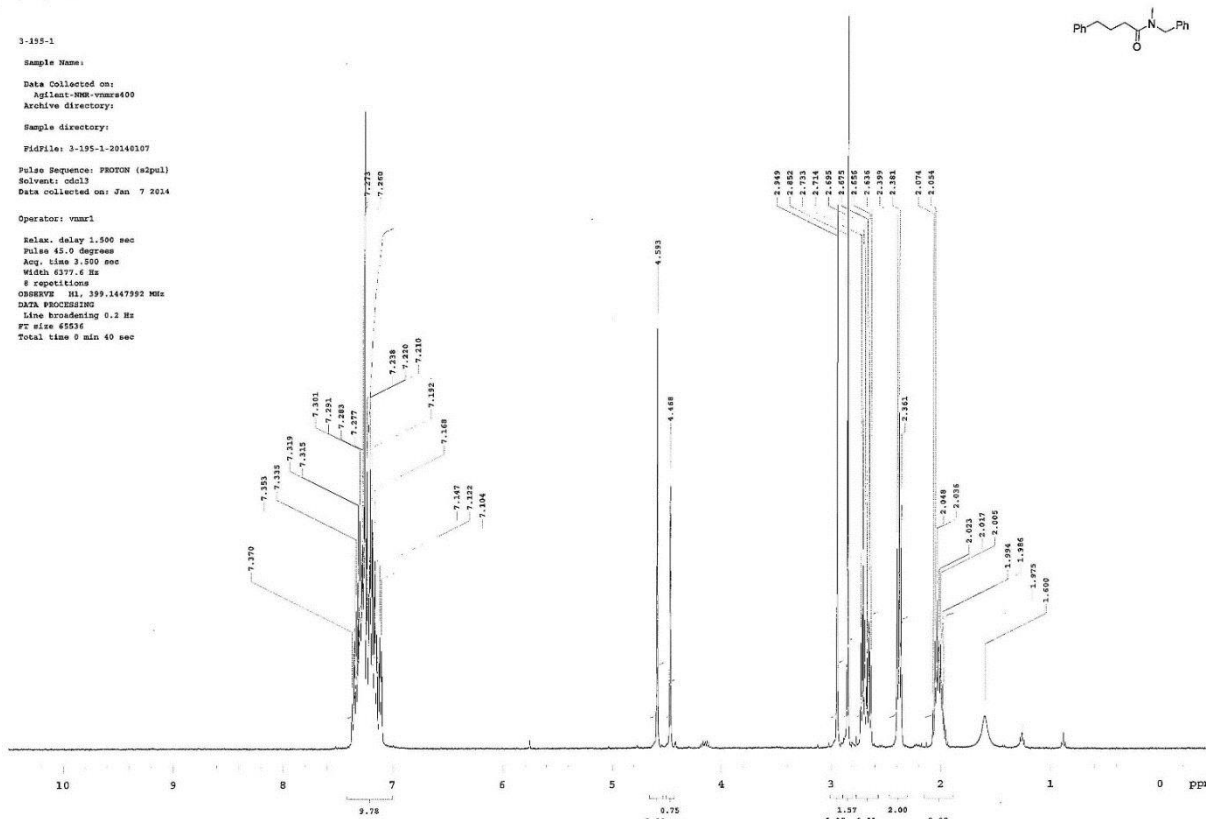
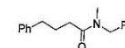
Relax. delay 1.500 sec
Pulse 45.0 degrees
Acq. time 3.500 sec
Width 6410.3 Hz
8 repetitions
OBSERVE H1, 399.1447991 MHz
DATA PROCESSING
Line broadening 0.2 Hz
FT size 65536
Total time 0 min 40 sec



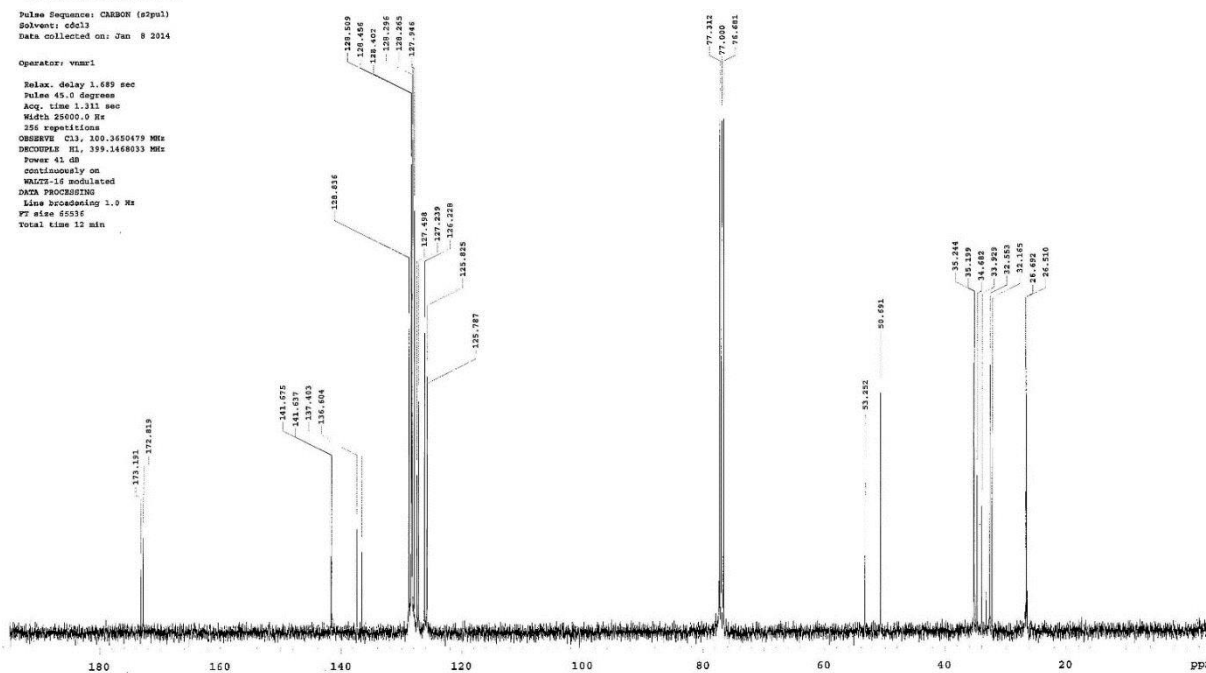
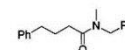
3-149-1
 Sample Name:
 Archive directory:
 Sample directory:
 FidFile: 3-149-1-carbon-20131113
 Pulse Sequence: Carbon (w2pul)
 Solvent: cdcl3
 Data collected on: Nov 13 2013
 Operator: walkup
 VNMRS-400 "Agilent-NMR"
 Relax. delay 0.700 sec
 Pulse 45.0 degrees
 Acq. time 1.350 sec
 Width 24509.8 Hz
 128 repetitions
 OBSERVE C13, 100.350463 MHz
 DECOUPLE H1, 399.1468933 MHz
 Power 41 dB
 continuously on
 WALTZ-16 modulated
 DATA PROCESSING
 Line broadening 1.0 Hz
 FT size 65536
 Total time 17 min



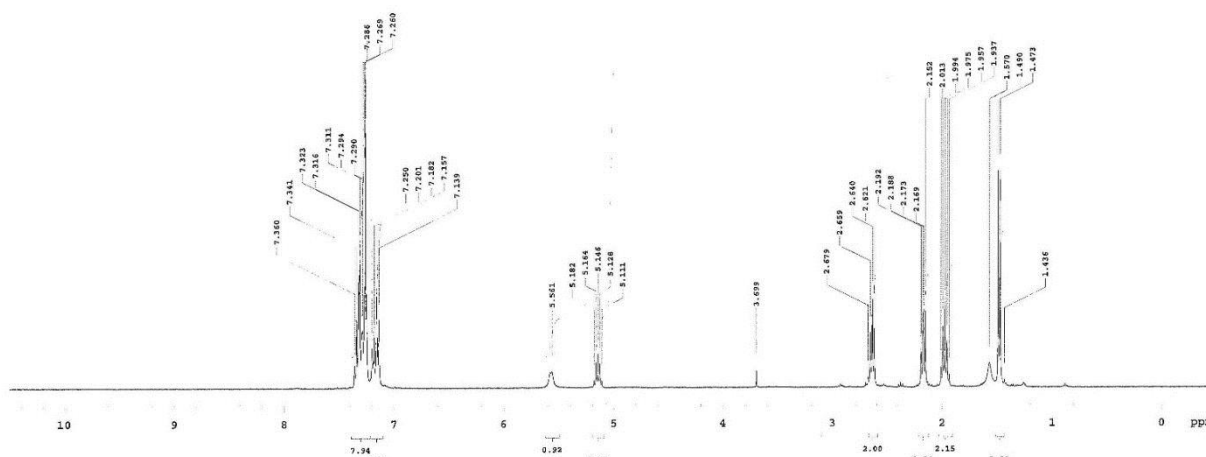
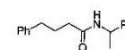
3-155-1
 Sample Name:
 Data Collected on:
 Agilent-NMR-vnmr400
 Archive directory:
 Sample directory:
 FidFile: 3-155-1-20140107
 Pulse Sequence: PROTON (w2pul)
 Solvent: cdcl3
 Data collected on: Jan 7 2014
 Operator: vnmr1
 Relax. delay 1.500 sec
 Pulse 45.0 degrees
 Acq. time 1.500 sec
 Width 6377.6 Hz
 8 repetitions
 OBSERVE H1, 399.1447992 MHz
 DATA PROCESSING
 Line broadening 0.2 Hz
 FT size 65536
 Total time 0 min 40 sec



3-195-1
 Sample Name:
 Data Collected on:
 Agilent-VNM-vmx400
 Archive directory:
 Sample directory:
 FIDFile: 3-195-1-carbon-20140108
 Pulse Sequence: CARRION (s2pul)
 Solvent: cdcl3
 Data collected on: Jan 9 2014
 Operator: vmx1
 Relax. delay 1.450 sec
 Pulse 45.0 degrees
 Acq. time 1.311 sec
 Width 25600.0 Hz
 356 repetitions
 OBSERVE CH, 100.6250479 MHz
 DECOUPLE H1, 399.1468333 MHz
 Power 41.00
 continuously on
 WALTZ-16 modulated
 DATA PROCESSING
 Line broadening 1.0 Hz
 FT size 65536
 Total time 12 min



3-185-1
 Sample Name:
 Data Collected on:
 Agilent-VNM-vmx400
 Archive directory:
 Sample directory:
 FIDFile: 3-185-1-20131217
 Pulse Sequence: PROTON (s2pul)
 Solvent: cdcl3
 Data collected on: Dec 17 2013
 Operator: vmx1
 Relax. delay 1.500 sec
 Pulse 45.0 degrees
 Acq. time 3.500 sec
 Width 6377.6 Hz
 9 repetitions
 OBSERVE H1, 399.1447966 MHz
 DATA PROCESSING
 Line broadening 0.2 Hz
 FT size 65536
 Total time 0 min 40 sec



3-185-1

Sample Name:

Data Collected on:
Agilent-800-vnmr400
Archive directory:

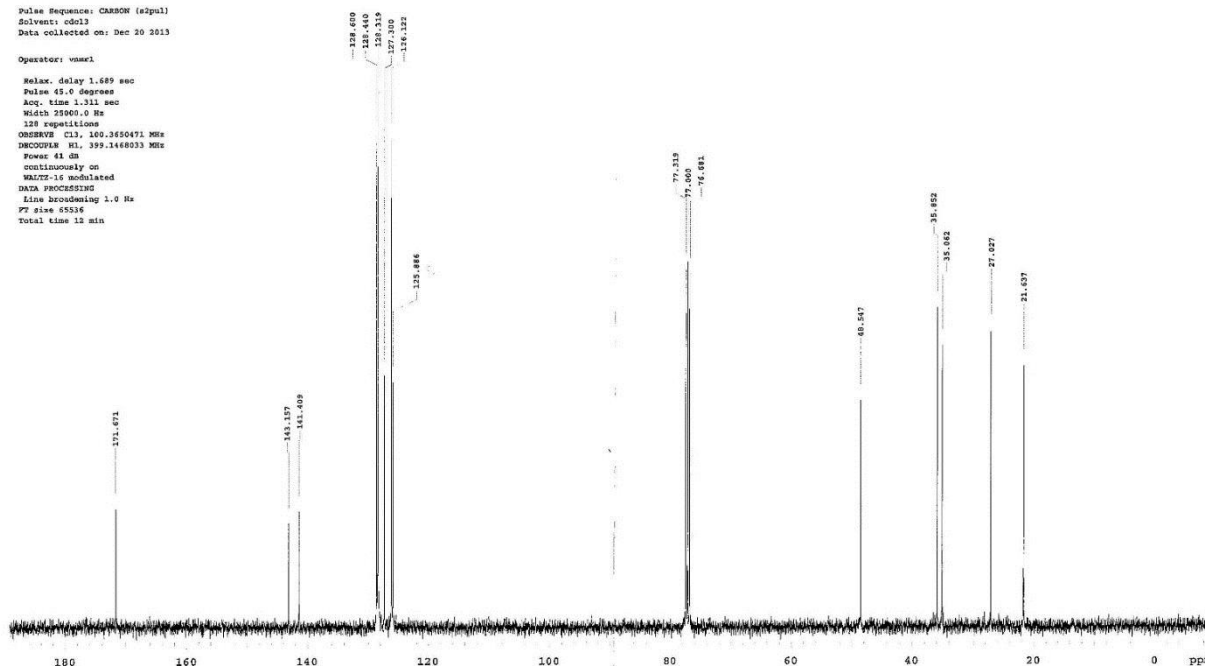
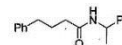
Sample directory:

Fidfile: CARBON

Pulse Sequence: CARBON (zgpg3)
Solvent: cdcl3
Data collected on: Dec 20 2013

Operator: vnmr1

Relax. delay 1.650 sec
Pulse 45.0 degrees
Acq. time 1.311 sec
Width 23900.0 Hz
128 repetitions
OBSERVE CH: 100.6250471 MHz
PROBHD: 5mm 1H/13C QNP 1H/13C
Pulse 45.0 degrees
continuously on
WALTZ-16 modulated
DATA PROCESSING
Line broadening 2.0 Hz
PT size 65536
Total time 13 min



Sample Name:

Data Collected on:
Agilent-800-vnmr400
Archive directory:

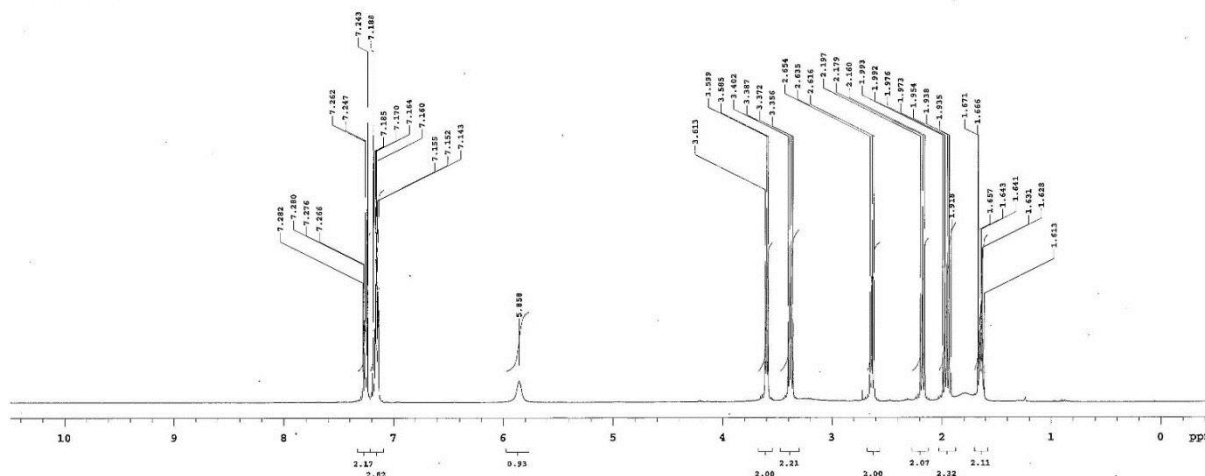
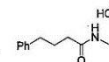
Sample directory:

Fidfile: PROTON

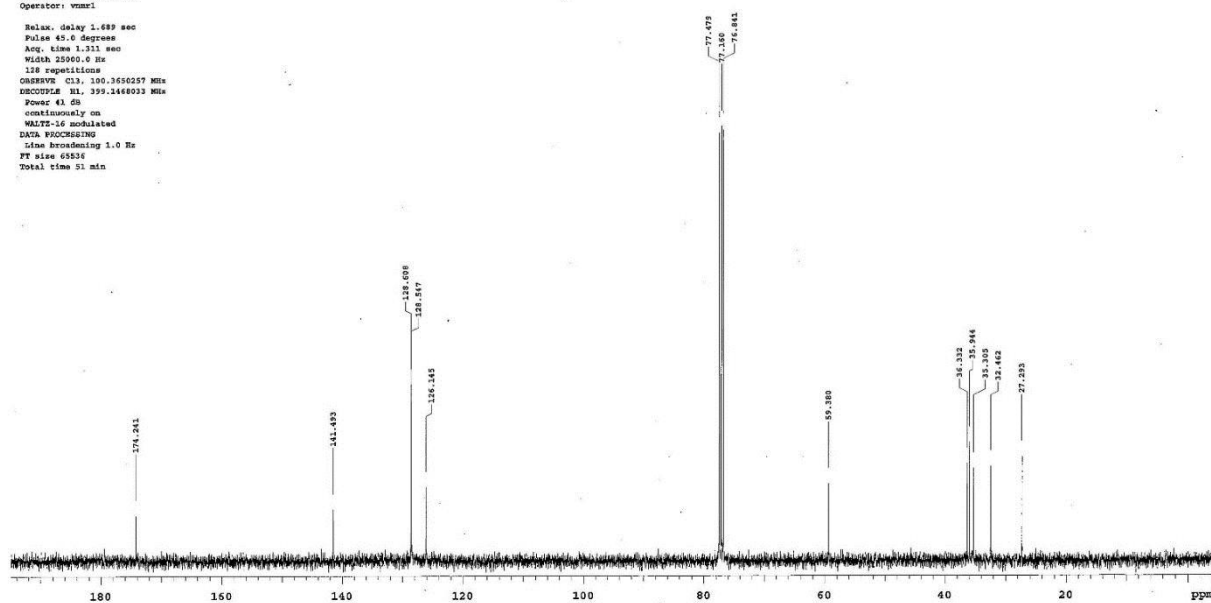
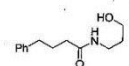
Pulse Sequence: PROTON (zgpg3)
Solvent: cdcl3
Data collected on: Sep 15 2014

Operator: vnmr1

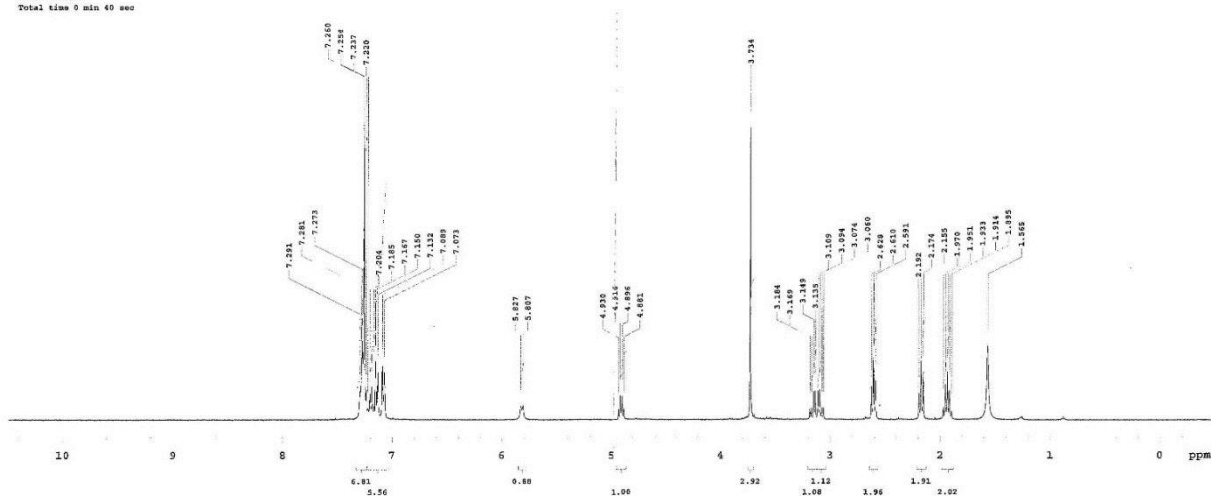
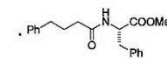
Relax. delay 1.550 sec
Pulse 45.0 degrees
Acq. time 3.590 sec
Width 6377.6 Hz
8 repetitions
OBSERVE CH: 400.146075 MHz
PROBHD: 5mm 1H/13C QNP 1H/13C
Pulse 45.0 degrees
DATA PROCESSING
Line broadening 0.2 Hz
PT size 65536
Total time 5 min 40 sec



Sample Name:
Data Collected on:
Agilent-100-vnmr400
Archive directory:
Sample directory:
FIDFile: CARBON
Pulse Sequence: CARBON (zgpg3)
Solvent: cdcl3
Data collected on: Sep 15 2014
Temp: 26.2 C / 299.4 K
Operator: vnmr1
Relax. delay 1.689 sec
Pulse 45.0 degrees
Acq. time 1.311 sec
Width 25940.0 Hz
128 repetitions
OBSERVE CH1, 100.6260597 MHz
FIDRES 0.11, 399.1446033 MHz
Power 41.00
continuously on
WALTZ-16 modulated
DATA PROCESSING
Line broadening 1.0 Hz
FT size 65536
Total time 51 min



3-186-4
Sample Name:
Data Collected on:
Agilent-100-vnmr400
Archive directory:
Sample directory:
FIDFile: PROTON
Pulse Sequence: PROTON (zgpg3)
Solvent: cdcl3
Data collected on: Dec 20 2013
Operator: vnmr1
Relax. delay 1.500 sec
Pulse 45.0 degrees
Acq. time 3.500 sec
Width 6177.6 Hz
8 repetitions
OBSERVE H1, 399.1447388 MHz
DATA PROCESSING
Line broadening 0.2 Hz
FT size 65536
Total time 9 min 40 sec



3-131-1-2

File: exp

Pulse Sequence: zgpg30

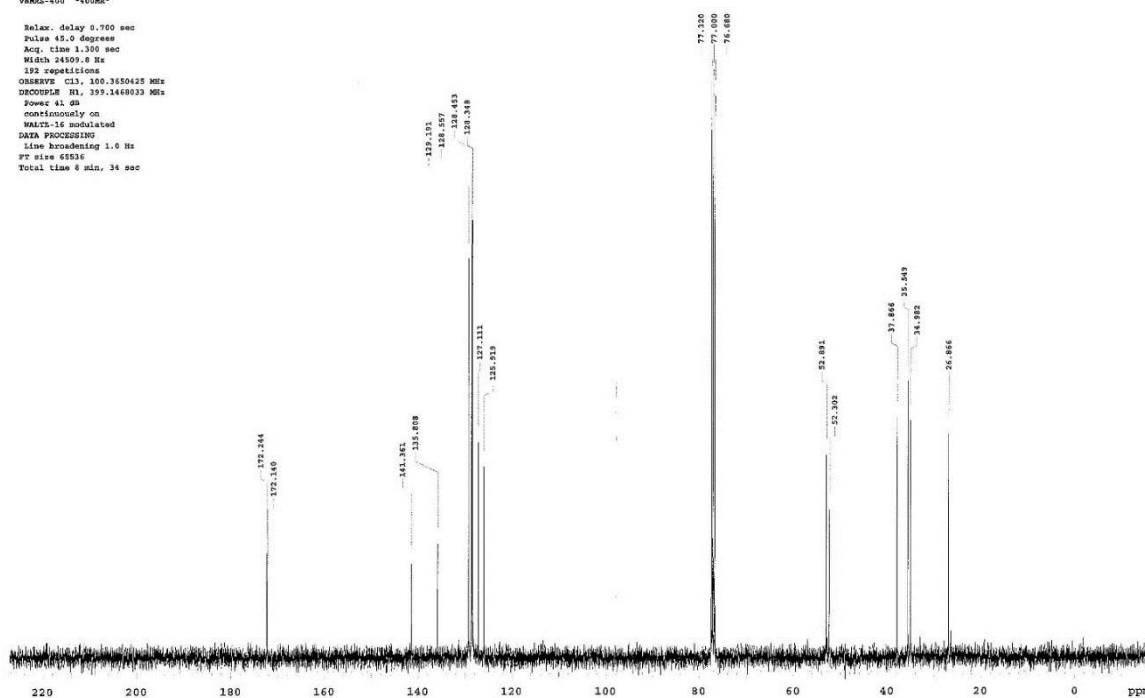
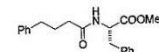
Solvent: cdcl3

Ambient temperature

Operator: walkup

VERBOL-400 "400MHz"

Relax. delay 8.700 sec
Pulse 45.0 degrees
Acq. time 1.350 sec
Width 24509.8 Hz
192 repetitions
OBSERVE C13, 100.6250425 MHz
DECOUPLE H1, 399.1448033 MHz
Power 41.00
continuously on
WALTZ-16 modulated
DATA PROCESSING
Line broadening 1.0 Hz
FT size 65536
Total time 8 min, 34 sec



Sample Name:

Data Collected on:

Agilent-MS-vmars400

Archive directory:

Sample directory:

File: PROTON

Pulse Sequence: PROTON (zgpg30)

Solvent: cdcl3

Data collected on: Sep 12 2014

Operator: vmars1

Relax. delay 1.500 sec

Pulse 45.0 degrees

Acq. time 3.500 sec

Width 6377.6 Hz

8 repetitions

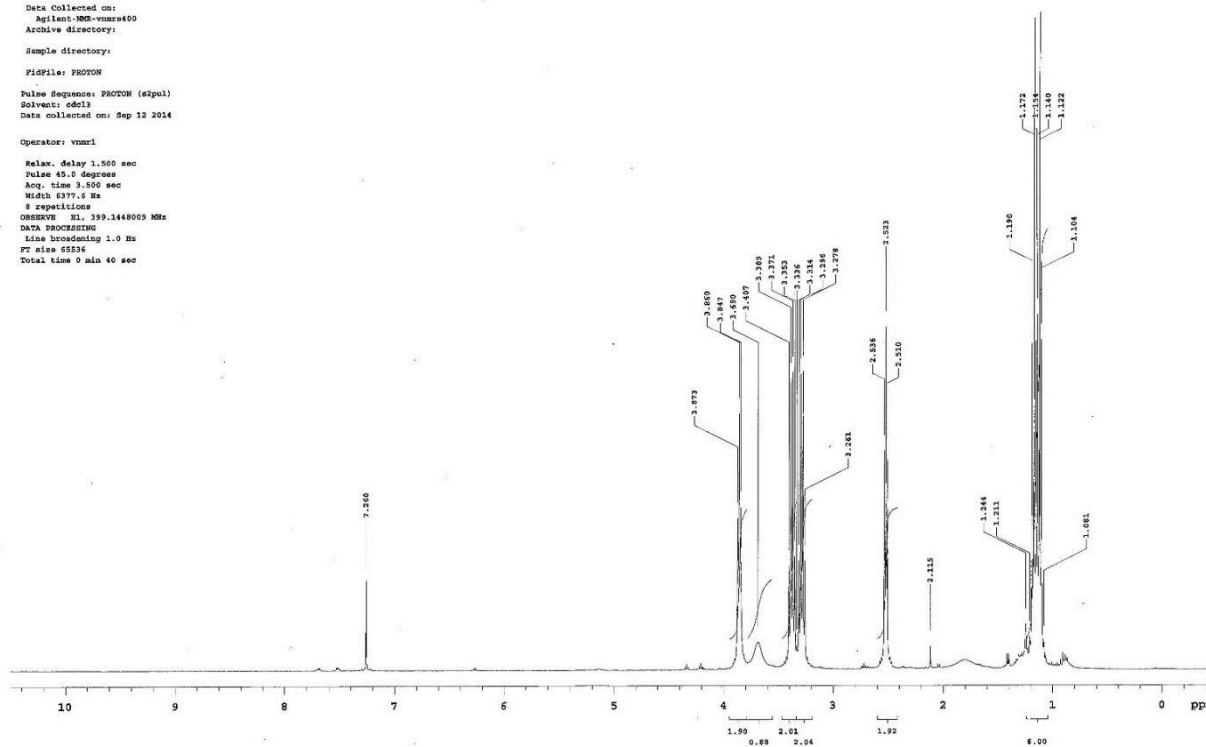
OBSERVE H1, 399.1448009 MHz

DATA PROCESSING

Line broadening 1.0 Hz

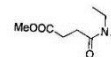
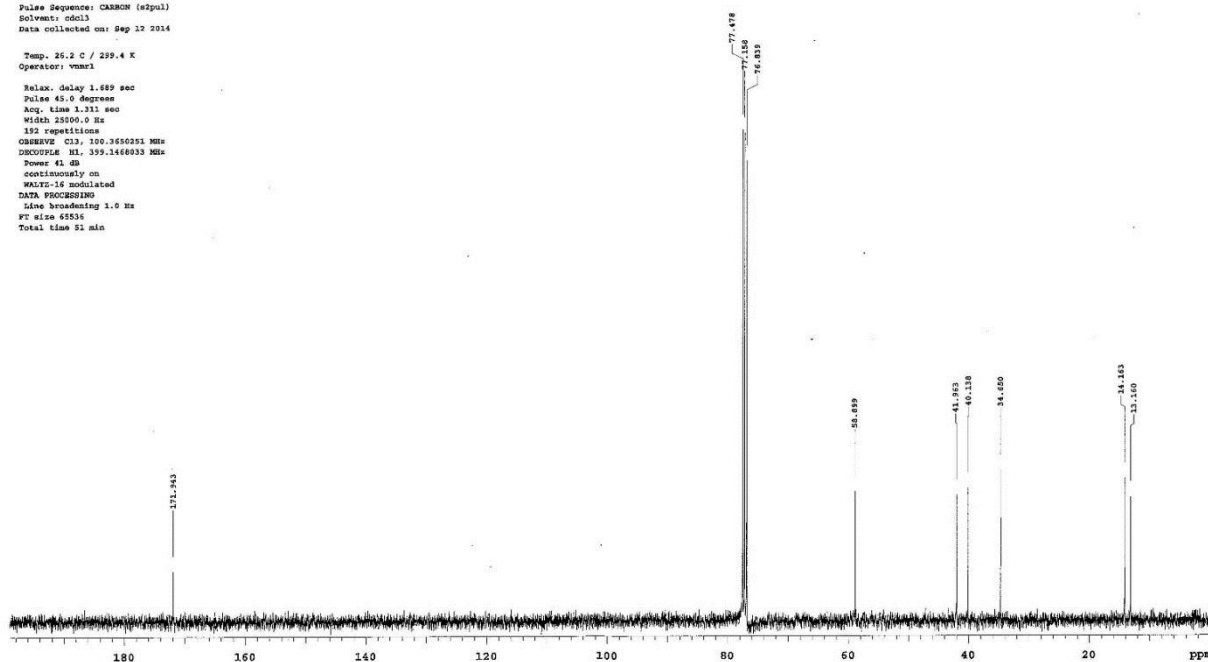
FT size 65536

Total time 9 min 40 sec

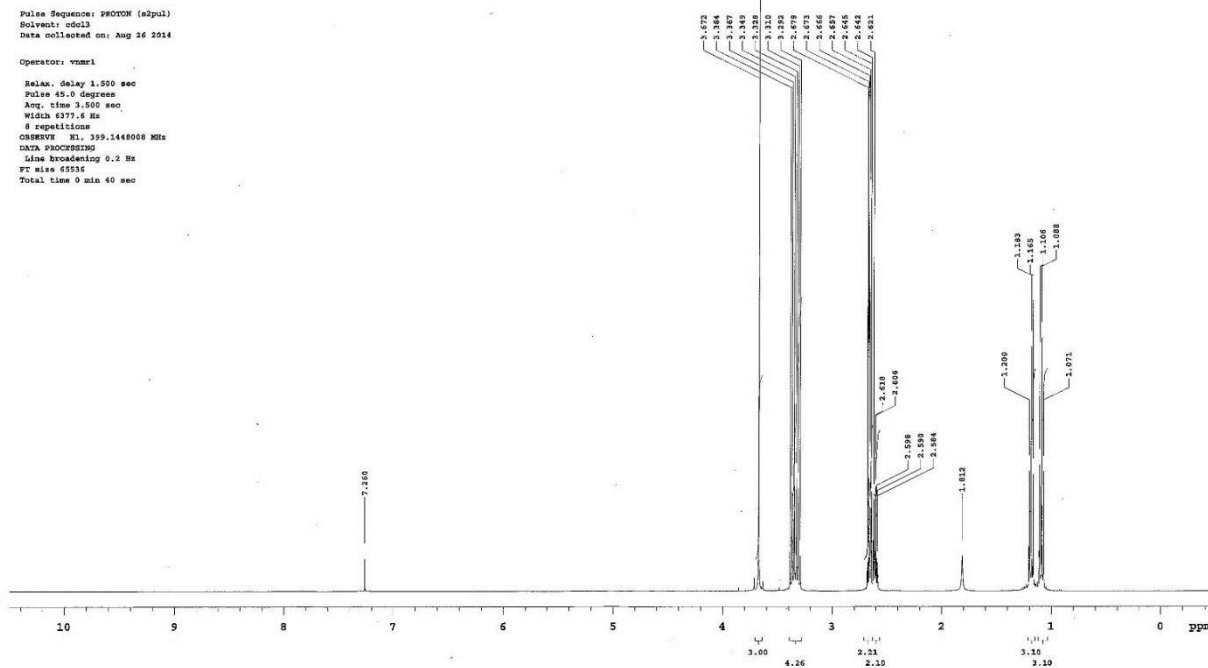


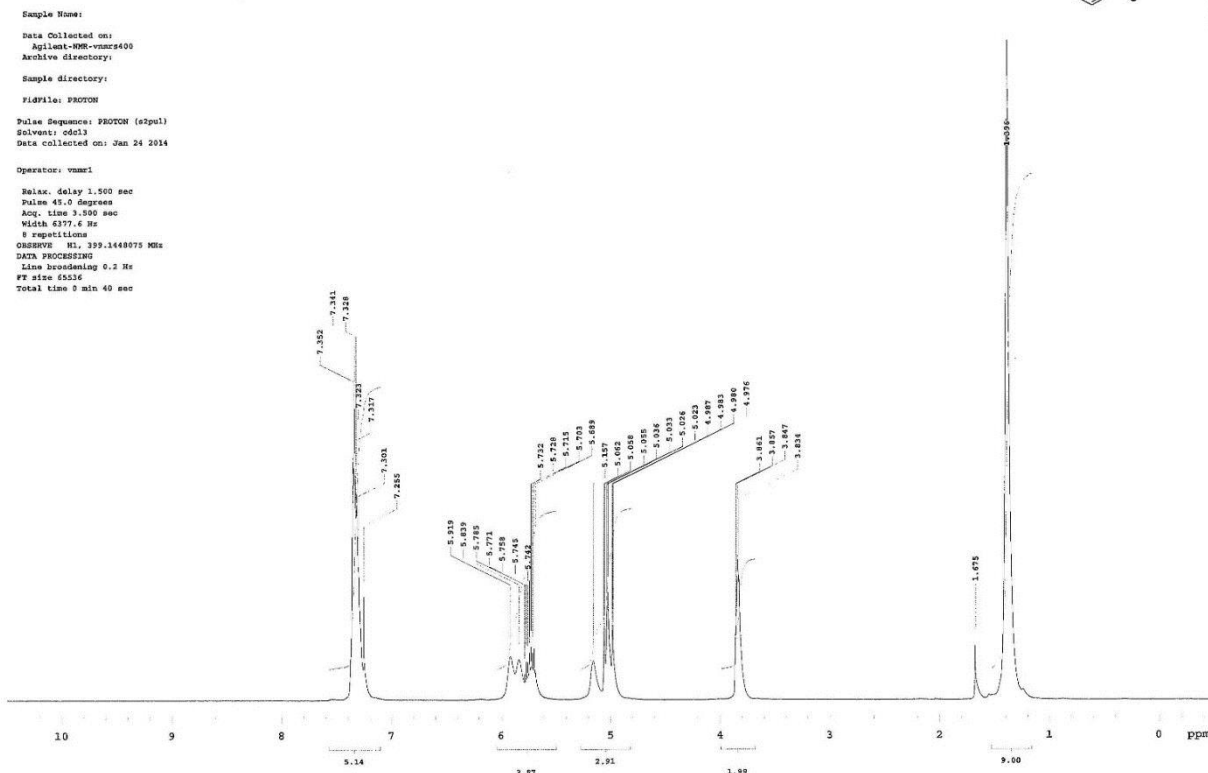
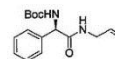
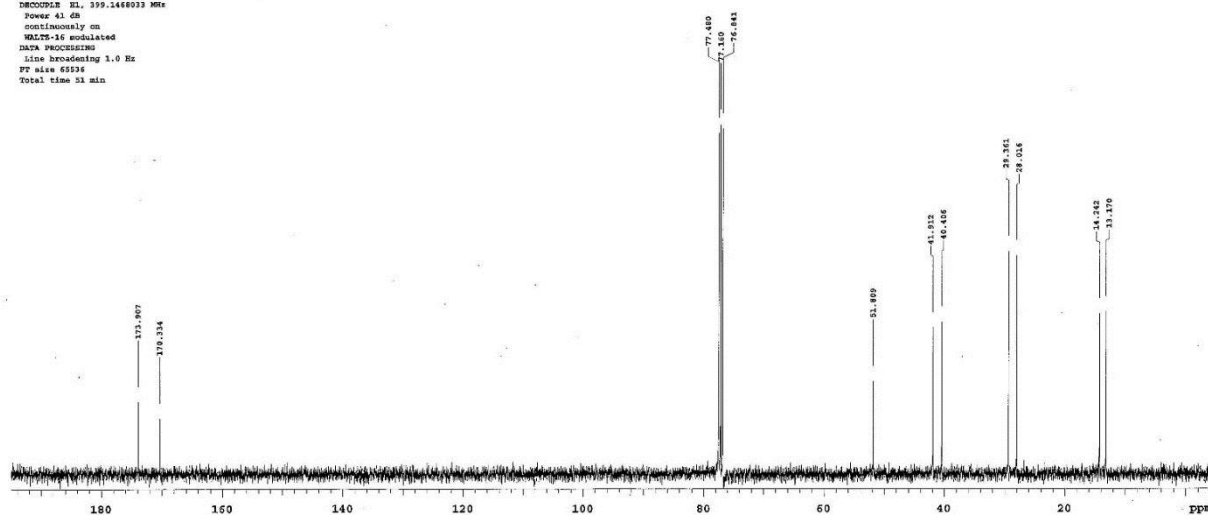
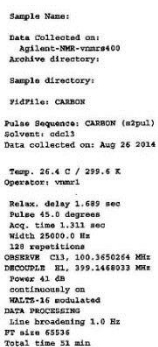


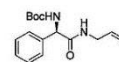
Sample Name:
Data Collected on:
Agilent-DMX-vnmr400
Archive directory:
Sample directory:
FidFile: CARBON
Pulse Sequence: CARBON (s2pul)
Solvent: cdcl3
Data collected on: Sep 17 2014
Temp. 25.2 C / 259.4 K
Operator: vnmr1
Relax. delay 1.559 sec
Pulse 45.0 degrees
Acq. time 3.311 sec
Width 25000.0 Hz
192 repetitions
OBSERVE CH: 100.3550251 MHz
PROBHD: HL 399.1468033 MHz
Power 41 dB
continuously on
WALTZ-16 modulated
DATA PROCESSING
Line broadening 1.0 Hz
FT size 65536
Total time 51 min



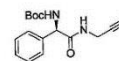
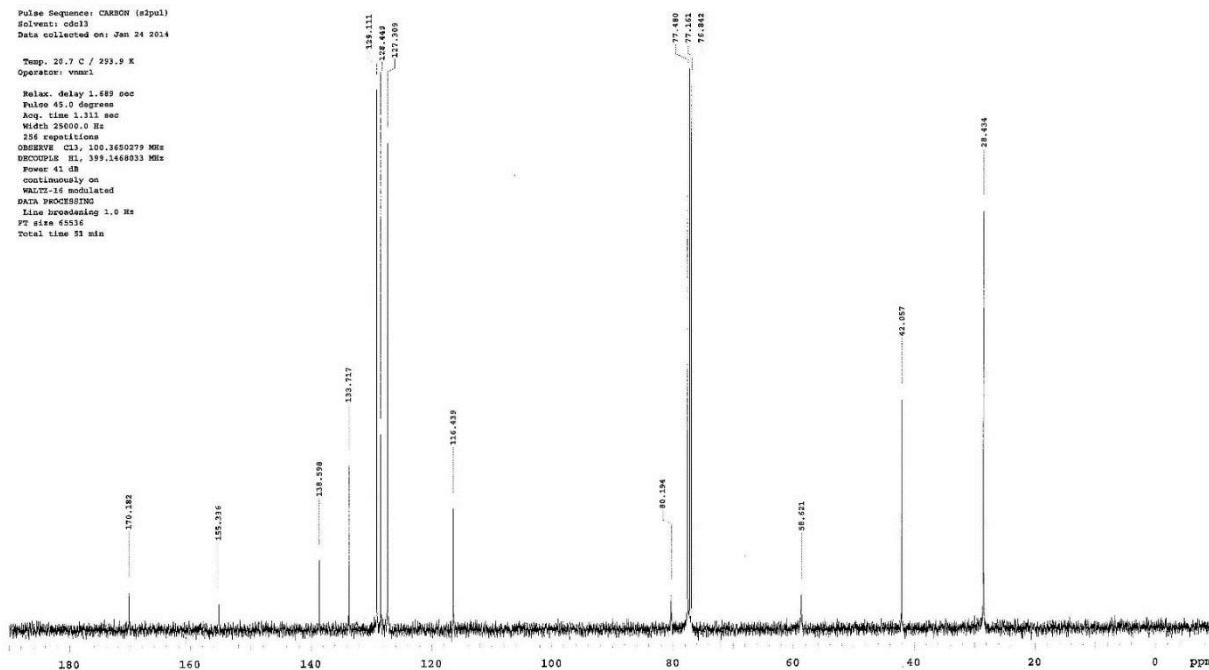
Sample Name:
Data Collected on:
Agilent-DMX-vnmr400
Archive directory:
Sample directory:
FidFile: Metab-59-1H
Pulse Sequence: PROTON (s2pul)
Solvent: cdcl3
Data collected on: Aug 16 2014
Operator: vnmr1
Relax. delay 1.550 sec
Pulse 45.0 degrees
Acq. time 3.500 sec
Width 6377.6 Hz
8 repetitions
OBSERVE CH: 399.1468008 MHz
DATA PROCESSING
Line broadening 0.2 Hz
FT size 65536
Total time 0 min 40 sec



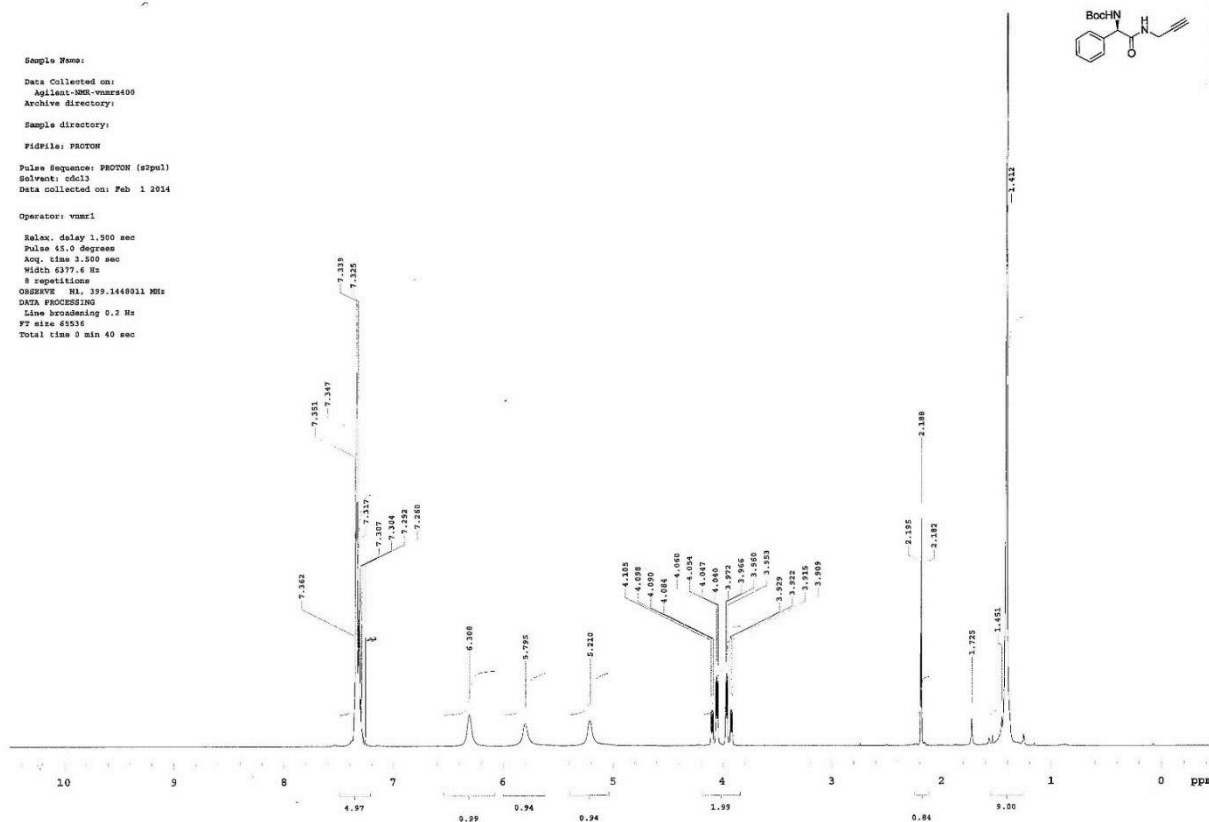


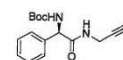


Sample Name:
 Data Collected on:
 Agilent-900-vnmr400
 Archive directory:
 Sample directory:
 FIDFile: CARBON
 Pulse Sequence: CARBON (zgpg3)
 Solvent: cdcl3
 Data collected on: Jan 24 2014
 Temp. 20.7 C / 293.9 K
 Operator: vnmr1
 Relax. delay 1.400 sec
 Pulse 45.0 degrees
 Acq. time 1.311 sec
 Width 25600.0 Hz
 256 repetitions
 OBSERVE CH1 100.6250779 MHz
 DECOUPLE HL 399.1468933 MHz
 Power 41 dB
 continuously on
 WALTZ-16 modulated
 DATA PROCESSING
 Line broadening 1.0 Hz
 FT size 65536
 Total time 51 min

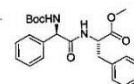
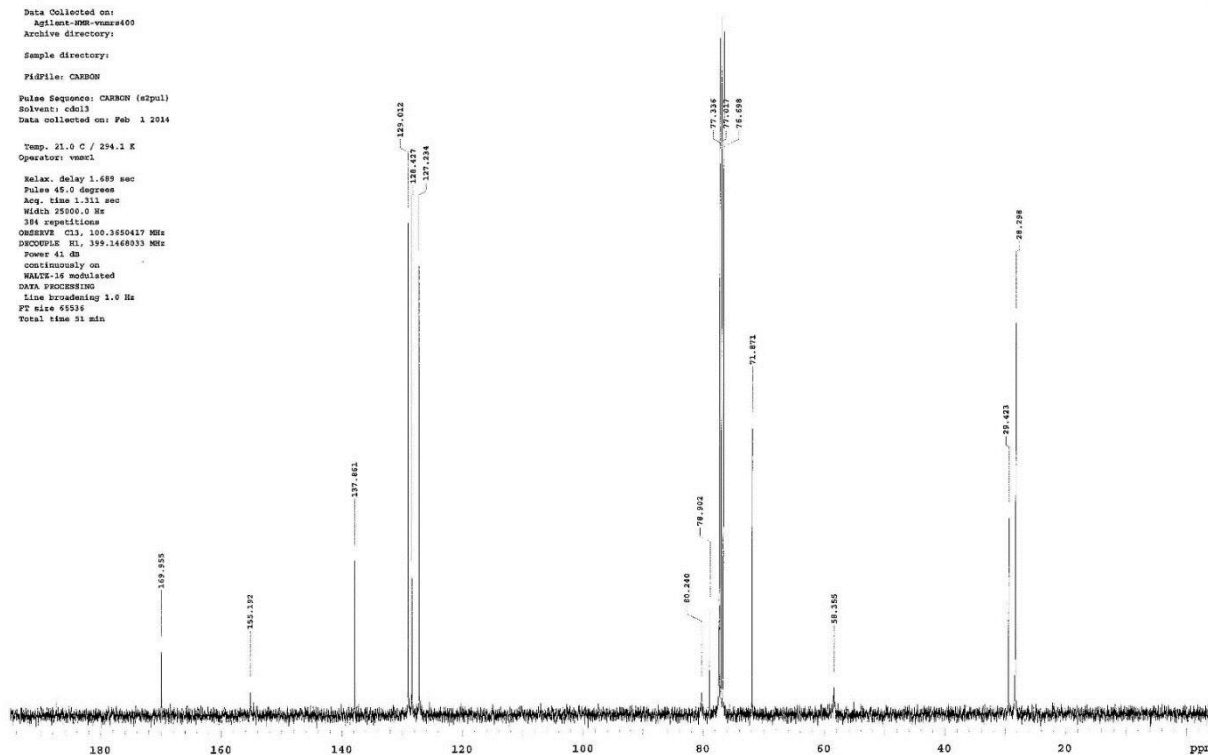


Sample Name:
 Data Collected on:
 Agilent-900-vnmr400
 Archive directory:
 Sample directory:
 FIDFile: PROTON
 Pulse Sequence: PROTON (zgpg3)
 Solvent: cdcl3
 Data collected on: Feb 1 2014
 Operator: vnmr1
 Relax. delay 1.500 sec
 Pulse 45.0 degrees
 Acq. time 3.100 sec
 Width 6377.6 Hz
 8 repetitions
 OBSERVE HL 399.1468911 MHz
 DATA PROCESSING
 Line broadening 0.2 Hz
 FT size 65536
 Total time 0 min 40 sec

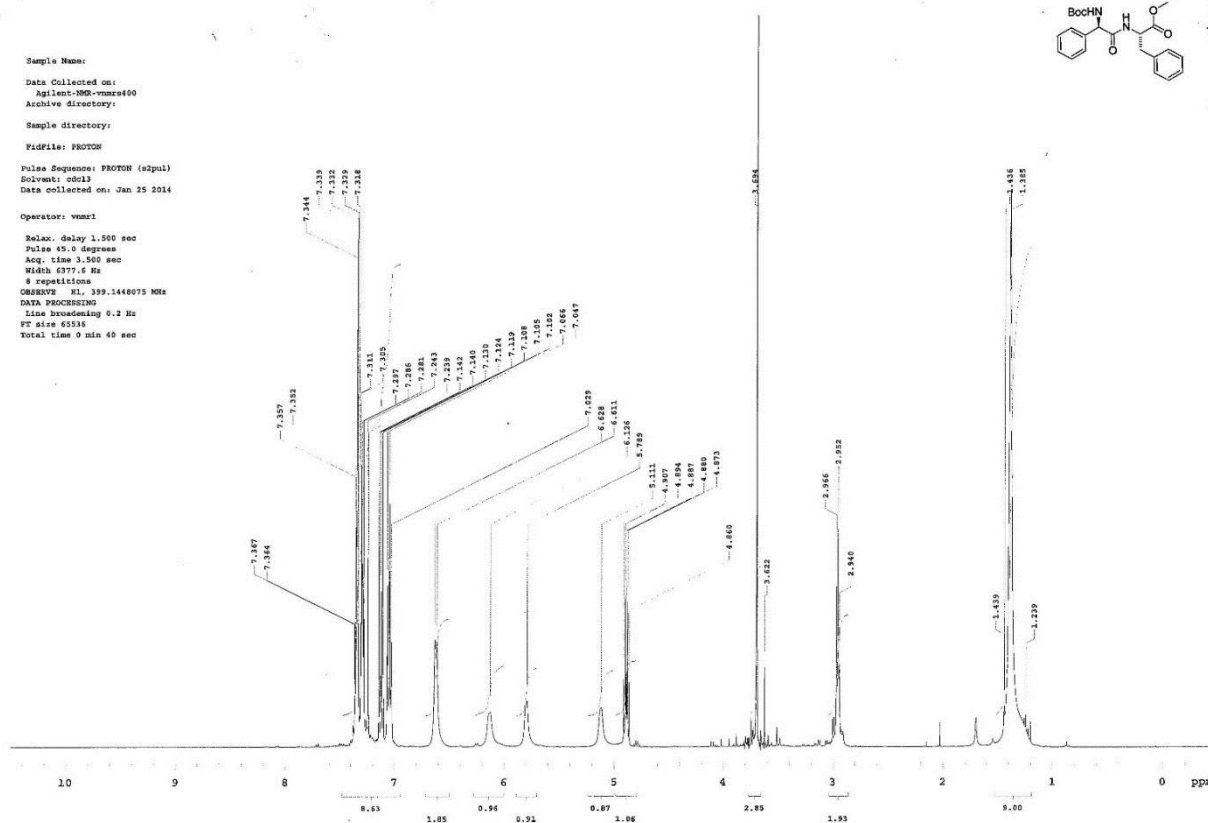




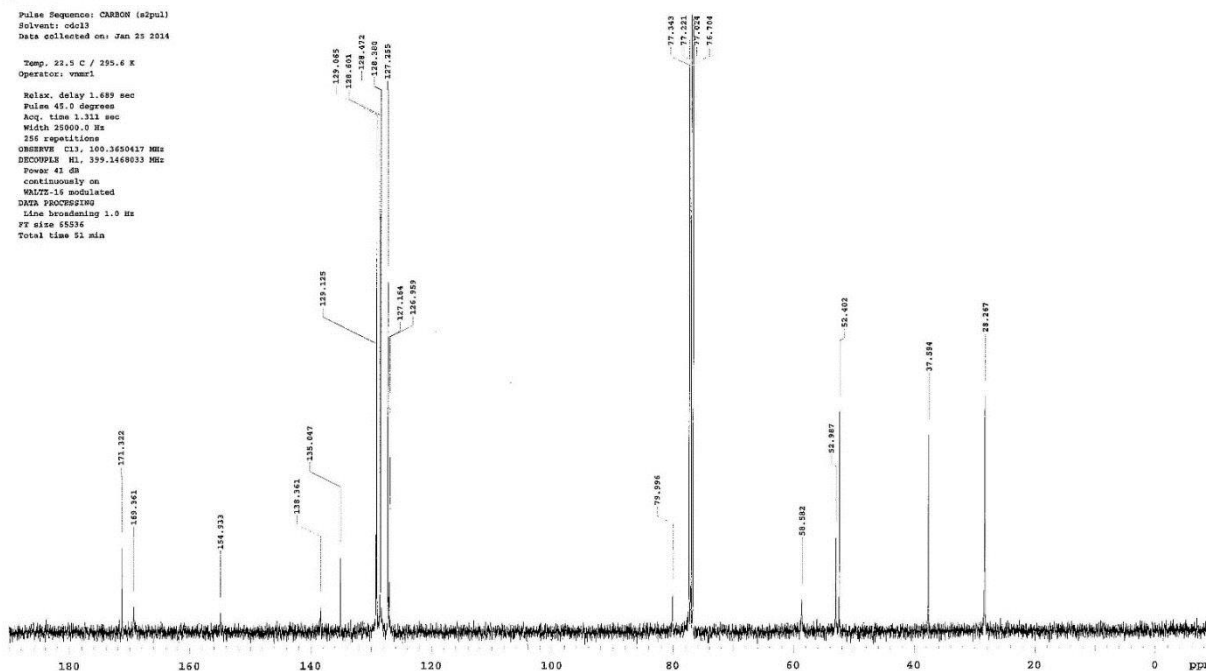
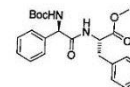
Sample Name:
Data Collected on:
Agilent-800-mm400
Archive directory:
Sample directory:
Fidfile: CARBON
Pulse Sequence: CARBON (s2pul)
Solvent: cdcl3
Data collected on: Feb 1 2014
Temp. 21.0 C / 254.1 K
Operator: vmwrl
Relax. delay 1.689 sec
Pulse 45.0 degrees
Acq. time 1.311 sec
Width 25000.0 Hz
384 repetitions
OBSERVE CH, 100.6250417 MHz
DECOUPLE H1, 399.1468033 MHz
Power 41 dB
continuously on
WALTZ-16 modulated
DATA PROCESSING
Line broadening 1.0 Hz
FT size 65536
Total time 31 min



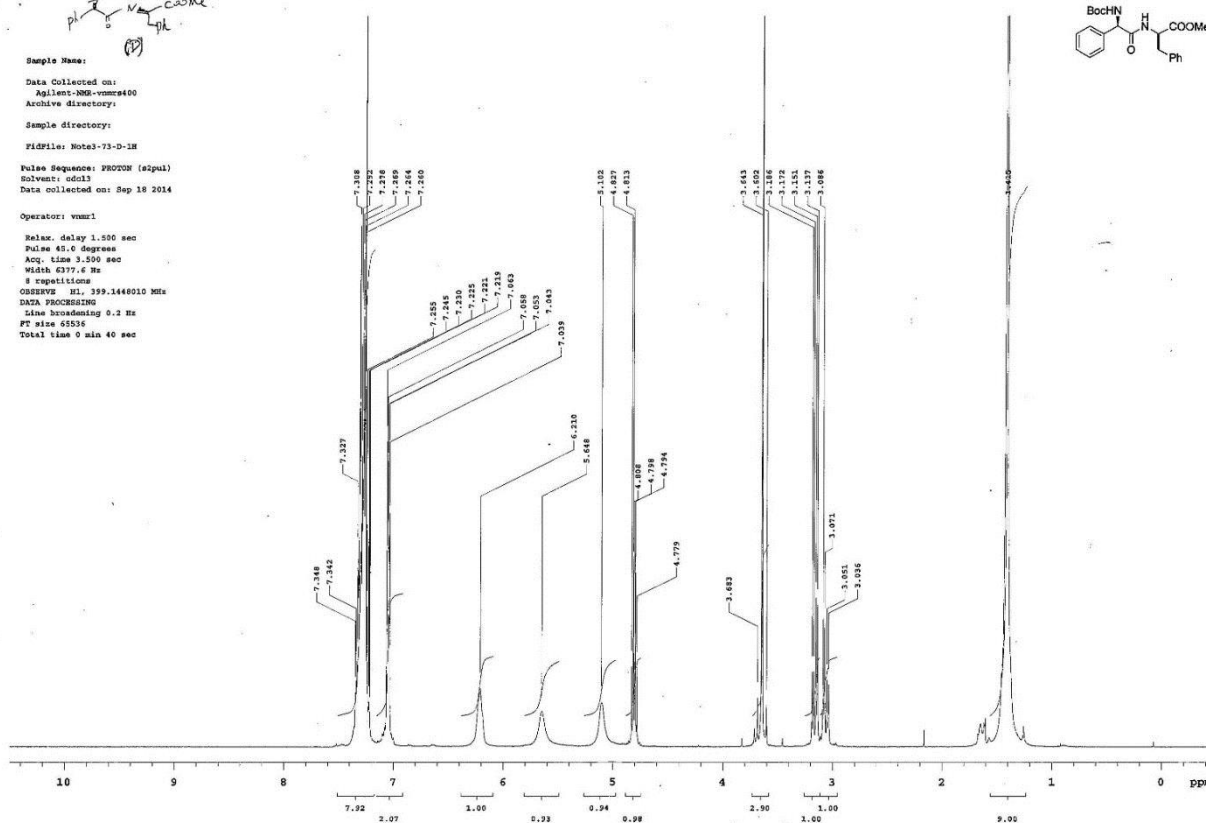
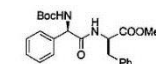
Sample Name:
Data Collected on:
Agilent-800-mm400
Archive directory:
Sample directory:
Fidfile: PROTON
Pulse Sequence: PROTON (s2pul)
Solvent: cdcl3
Data collected on: Jan 25 2014
Operator: vmwrl
Relax. delay 1.560 sec
Pulse 45.0 degrees
Acq. time 3.560 sec
Width 6777.6 Hz
8 repetitions
OBSERVE H1, 399.1468075 MHz
DATA PROCESSING
Line broadening 0.2 Hz
FT size 65536
Total time 9 min 40 sec



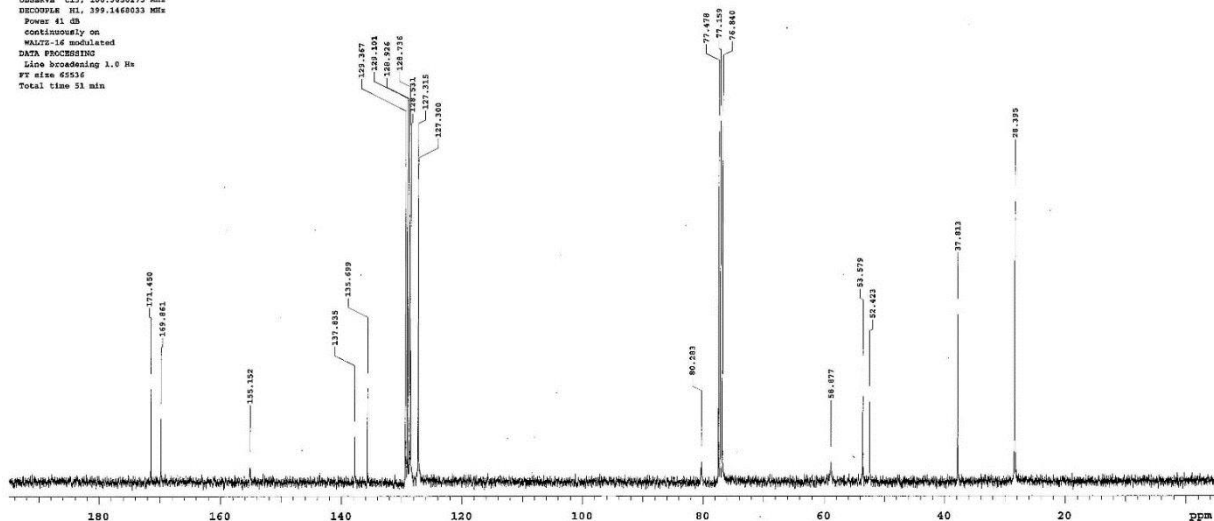
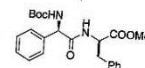
Sample Name:
 Data Collected on:
 Agilent-900-vnmr400
 Archive directory:
 Sample directory:
 FIDFile: CARBON
 Pulse Sequence: CARBON (zgpg3)
 Solvent: cdcl3
 Data collected on: Jan 25 2014
 Temp: 22.5 C / 295.6 K
 Operator: vnmr1
 Relax. delay 1.693 sec
 Pulse 45.0 degrees
 Acq. time 1.311 sec
 Width 25000.0 Hz
 256 repetitions
 OBSERVE CH: 100.6260417 MHz
 DECOUPLE N1: 399.1460033 MHz
 Power 41 dB
 continuously on
 WALTZ-16 modulated
 DATA PROCESSING
 Line broadening 1.0 Hz
 FT size 65536
 Total time 51 min



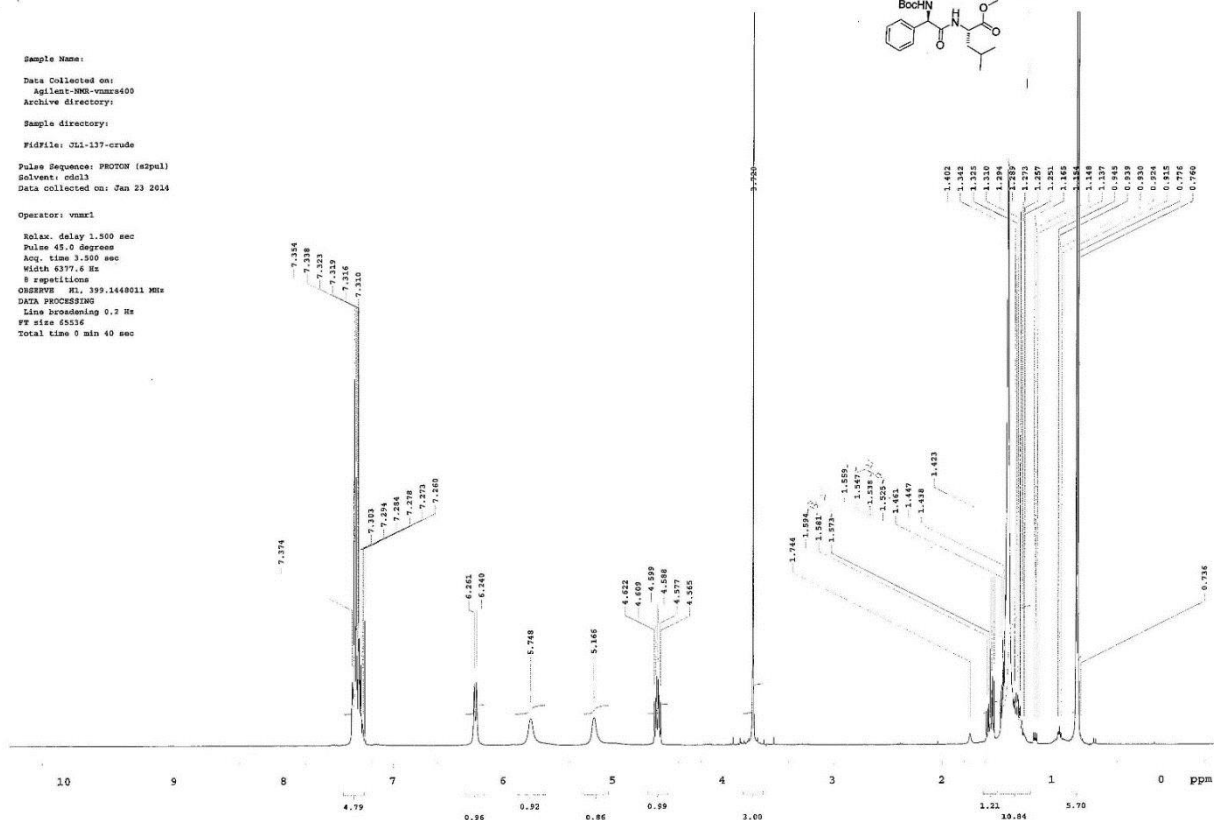
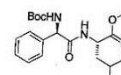
Sample Name:
 Data Collected on:
 Agilent-900-vnmr400
 Archive directory:
 Sample directory:
 FIDFile: M063-73-D-1H
 Pulse Sequence: PROTON (zgpg3)
 Solvent: cdcl3
 Data collected on: Sep 18 2014
 Operator: vnmr1
 Relax. delay 1.550 sec
 Pulse 45.0 degrees
 Acq. time 3.590 sec
 Width 6177.6 Hz
 8 repetitions
 OBSERVE CH: 399.1460010 MHz
 DATA PROCESSING
 Line broadening 0.2 Hz
 FT size 65536
 Total time 0 min 40 sec



Sample Name:
 Data Collected on:
 Agilent-MRM-vnmr400
 Archive directory:
 Sample directory:
 FIDFile: CARBON
 Pulse Sequence: CARBON (zgpg3)
 Solvent: cdcl3
 Data collected on: Sep 19 2014
 Temp: 25.6 C / 298.8 K
 Operator: vnmr1
 Relax. delay 1.689 sec
 Pulse 45.0 degrees
 Acq. time 1.311 sec
 Width 23900.0 Hz
 320 repetitions
 OBSERVE CH1: 120.3450273 MHz
 DECOUPLE H1: 399.1460033 MHz
 Power 41 dB
 continuously on
 WALTZ-16 modulated
 DATA PROCESSING
 Line broadening 1.0 Hz
 FT size 65536
 Total time 31 min

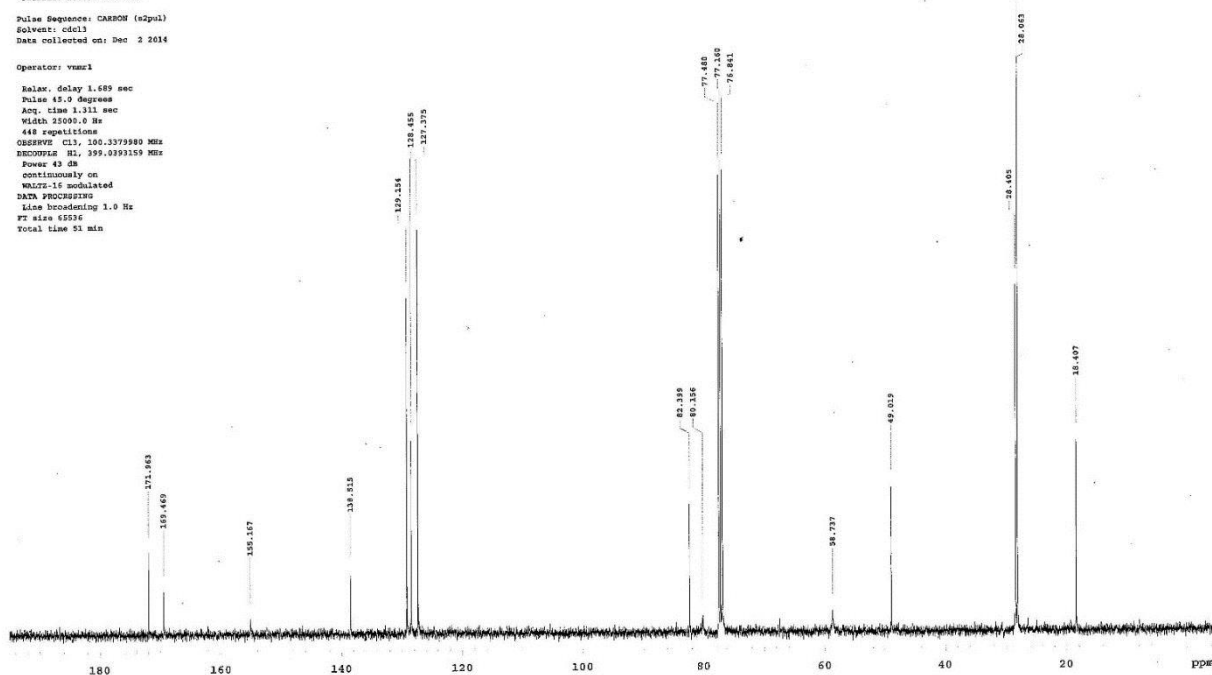
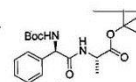


Sample Name:
 Data Collected on:
 Agilent-MRM-vnmr400
 Archive directory:
 Sample directory:
 FIDFile: JLI-137-crude
 Pulse Sequence: PROTON (zgpg3)
 Solvent: cdcl3
 Data collected on: Jan 23 2014
 Operator: vnmr1
 Relax. delay 1.500 sec
 Pulse 45.0 degrees
 Acq. time 3.500 sec
 Width 6377.6 Hz
 8 repetitions
 OBSERVE H1: 399.1448011 MHz
 DATA PROCESSING
 Line broadening 0.2 Hz
 FT size 65536
 Total time 9 min 40 sec



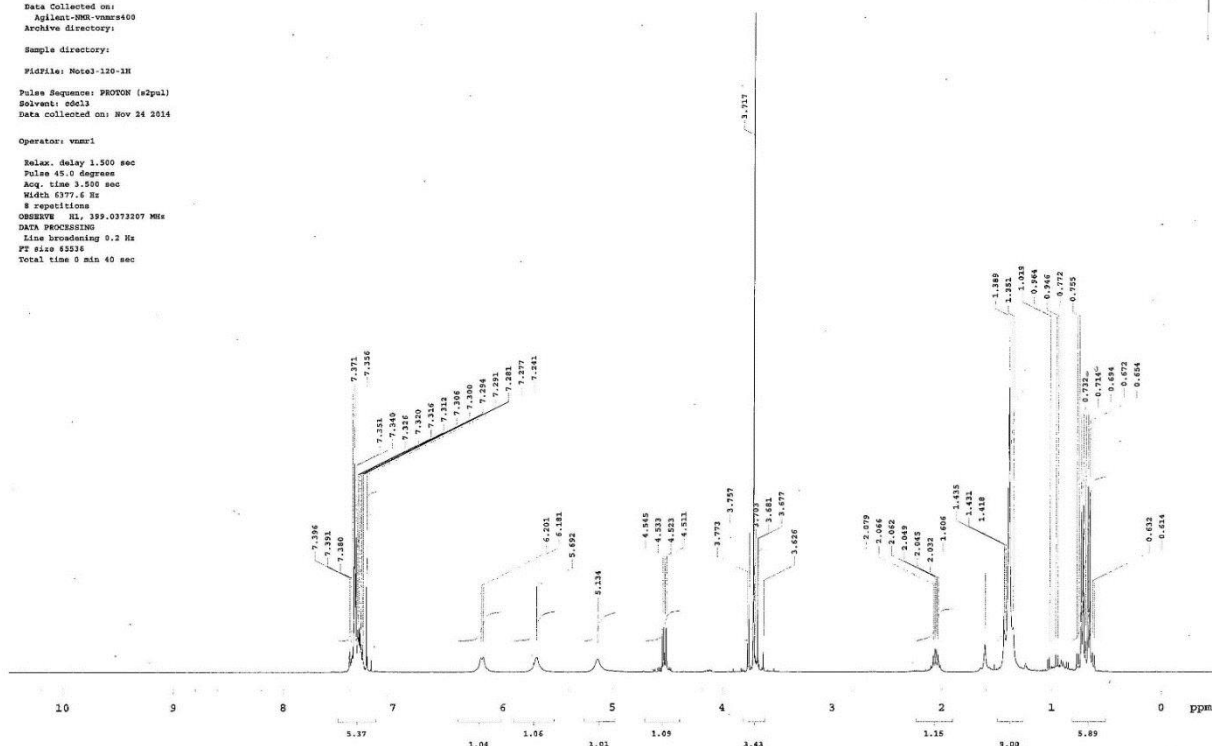
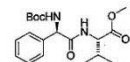
Sample Name:
Data Collected on:
Agilent-MSD-vnmr400
Archive directory:
Sample directory:
FidFile: Note3-130-13C-2
Pulse Sequence: CARBON (zgpg3)
Solvent: cdcl3
Data collected on: Dec 2 2014

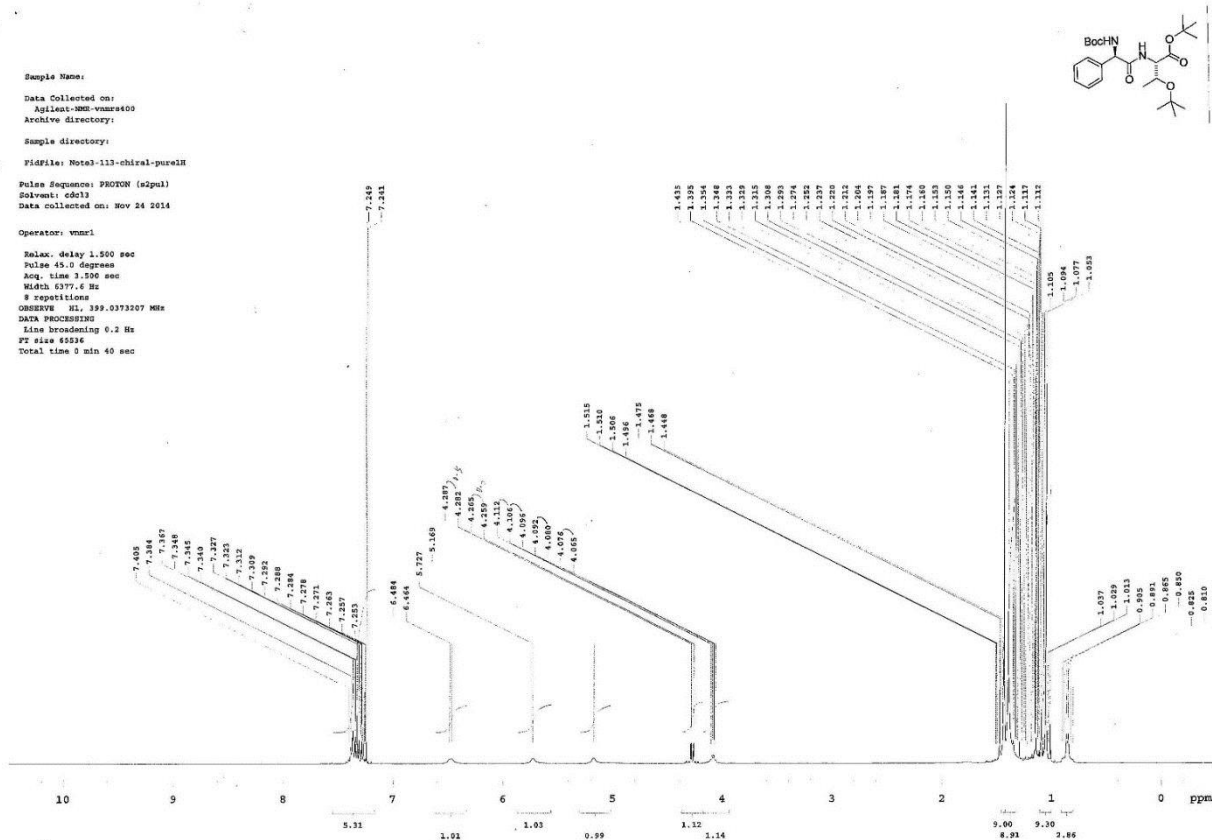
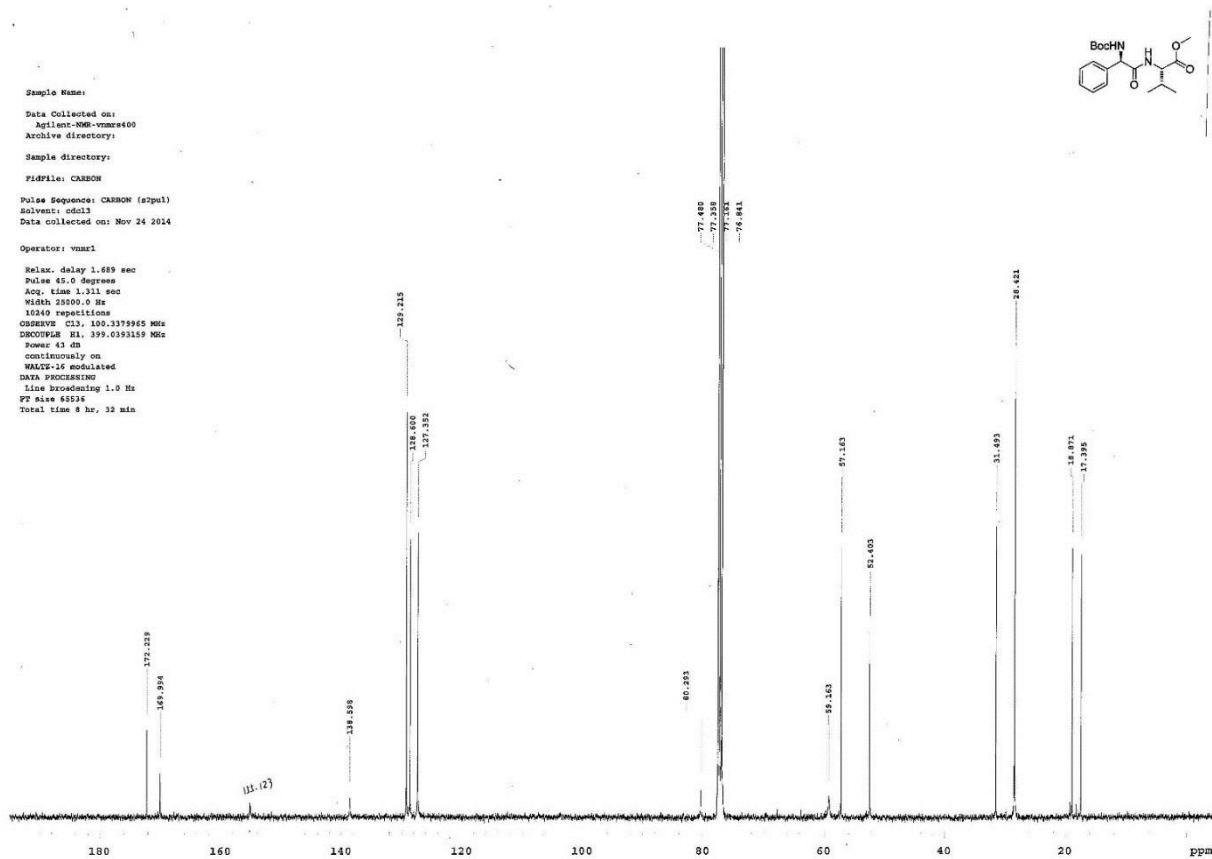
Operator: vnmr1
Pulpr. delay 1.689 sec
Pulse 45.0 degrees
Acq. time 1.311 sec
Width 15000.0 Hz
448 repetitions
OBSERVE CH, 100.6279980 MHz
RECOVER CH, 399.0293159 MHz
Power 41.00
continuously on
WALTZ-16 modulated
DATA PROCESSING
Line broadening 1.0 Hz
FT size 65536
Total time 51 min



Sample Name:
Data Collected on:
Agilent-MSD-vnmr400
Archive directory:
Sample directory:
FidFile: Note3-130-1H
Pulse Sequence: PROTON (zgpg3)
Solvent: cdcl3
Data collected on: Nov 24 2014

Operator: vnmr1
Pulpr. delay 1.500 sec
Pulse 45.0 degrees
Acq. time 3.500 sec
Width 6377.6 Hz
8 repetitions
OBSERVE CH, 399.0373207 MHz
DATA PROCESSING
Line broadening 0.2 Hz
FT size 65536
Total time 0 min 40 sec

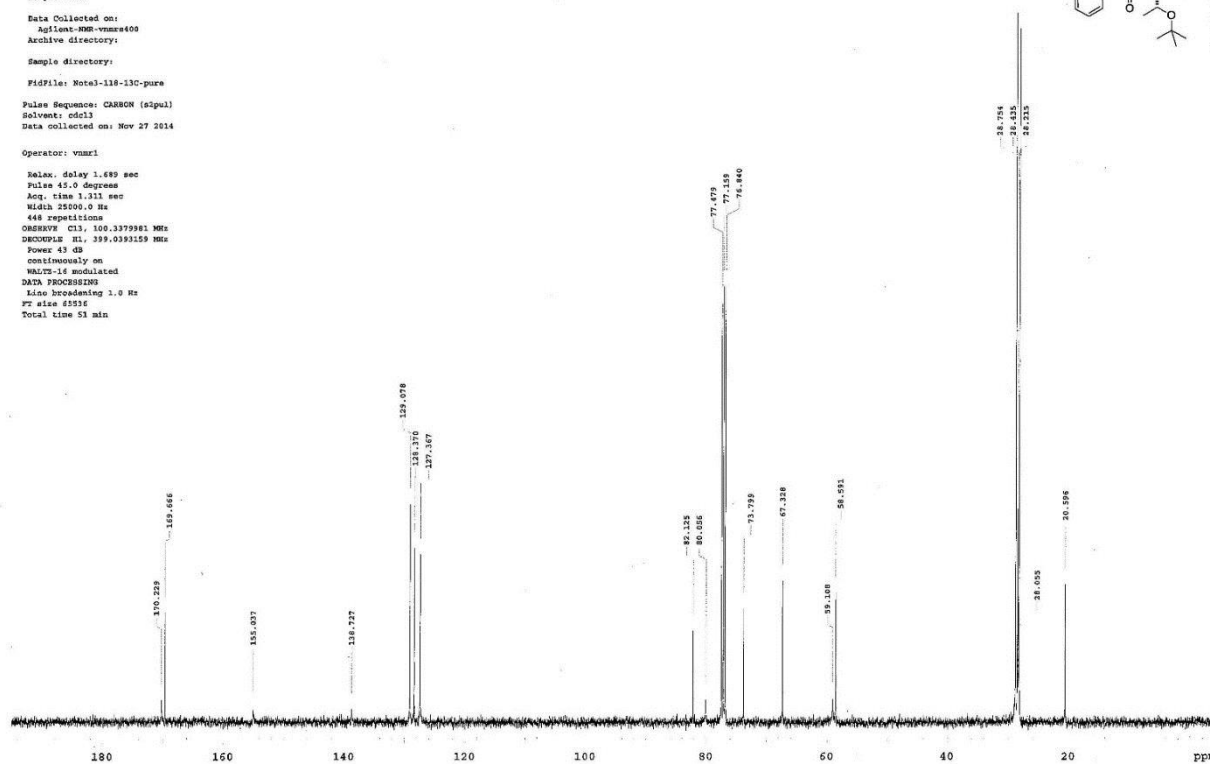
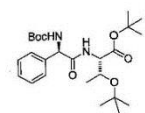




yu01145-1m5
 Sample Name:
 Data Collected on:
 Agilent-MMR-vnmr400
 Archive directory:
 Sample directory:
 FIDFile: Notal-118-13C-pure
 Pulse Sequence: CARBON (zgpg3)
 Solvent: cdcl3
 Data collected on: Nov 27 2014

Operator: vnmr1

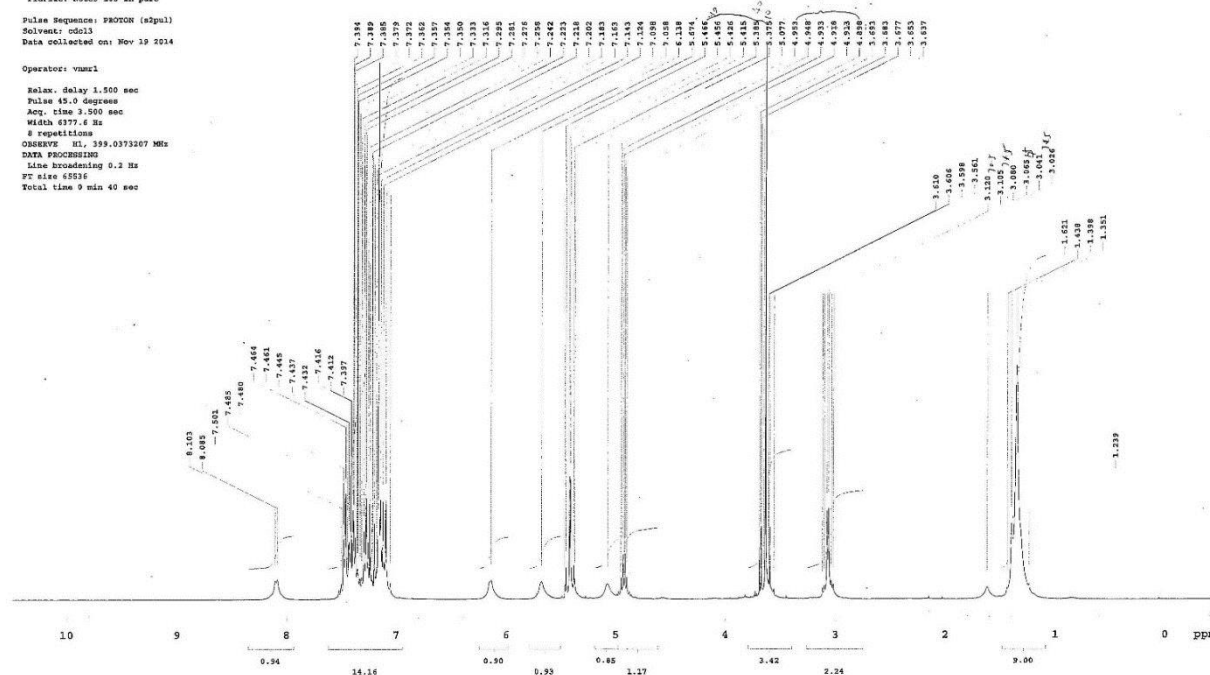
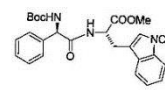
Relax. delay 1.689 sec
 Pulse 45.0 degrees
 Acq. time 1.511 sec
 Width 25500.0 Hz
 448 repetitions
 OBSERVE Ch1, 100.6279981 MHz
 DECOUPLE H1, 399.0393159 MHz
 Power 43 dB
 continuously on
 WALTZ-16 modulated
 DATA PROCESSING
 Line broadening 1.0 Hz
 FT size 65536
 Total time 51 min

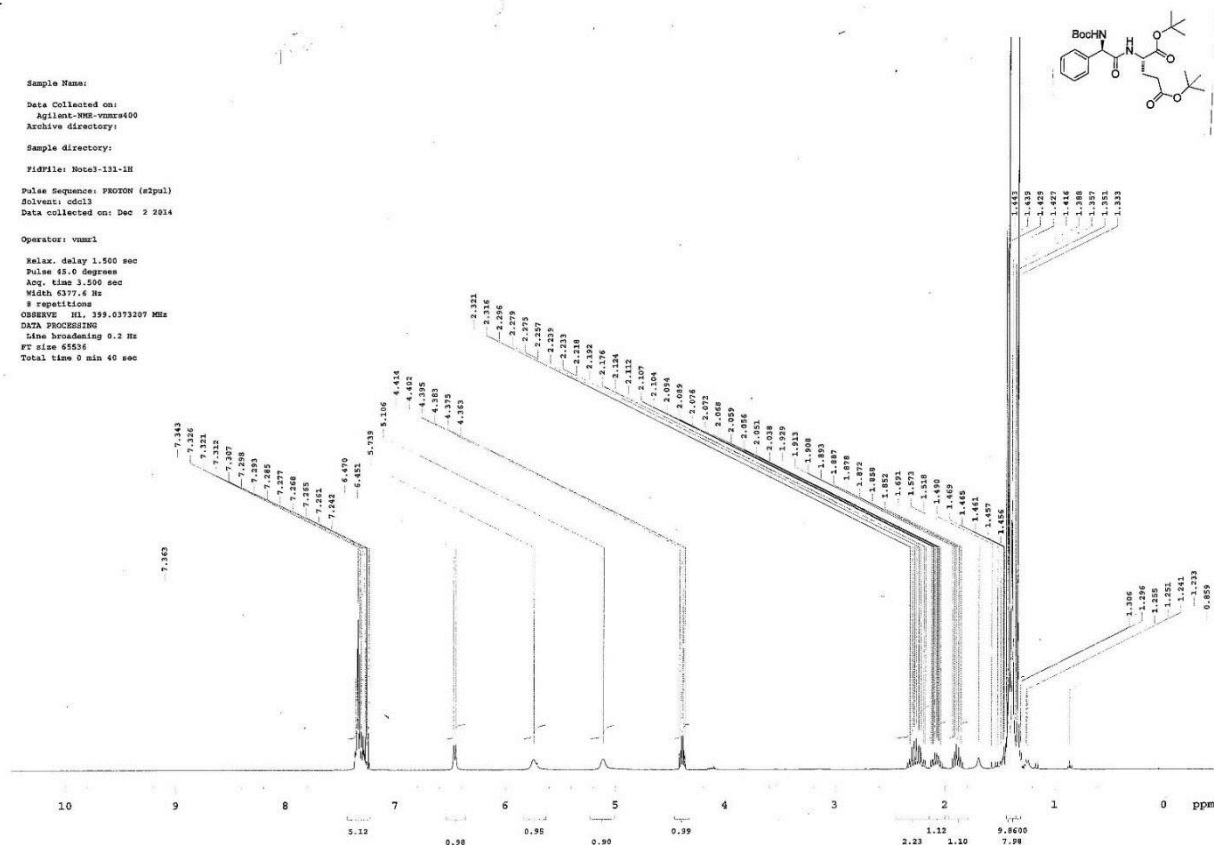
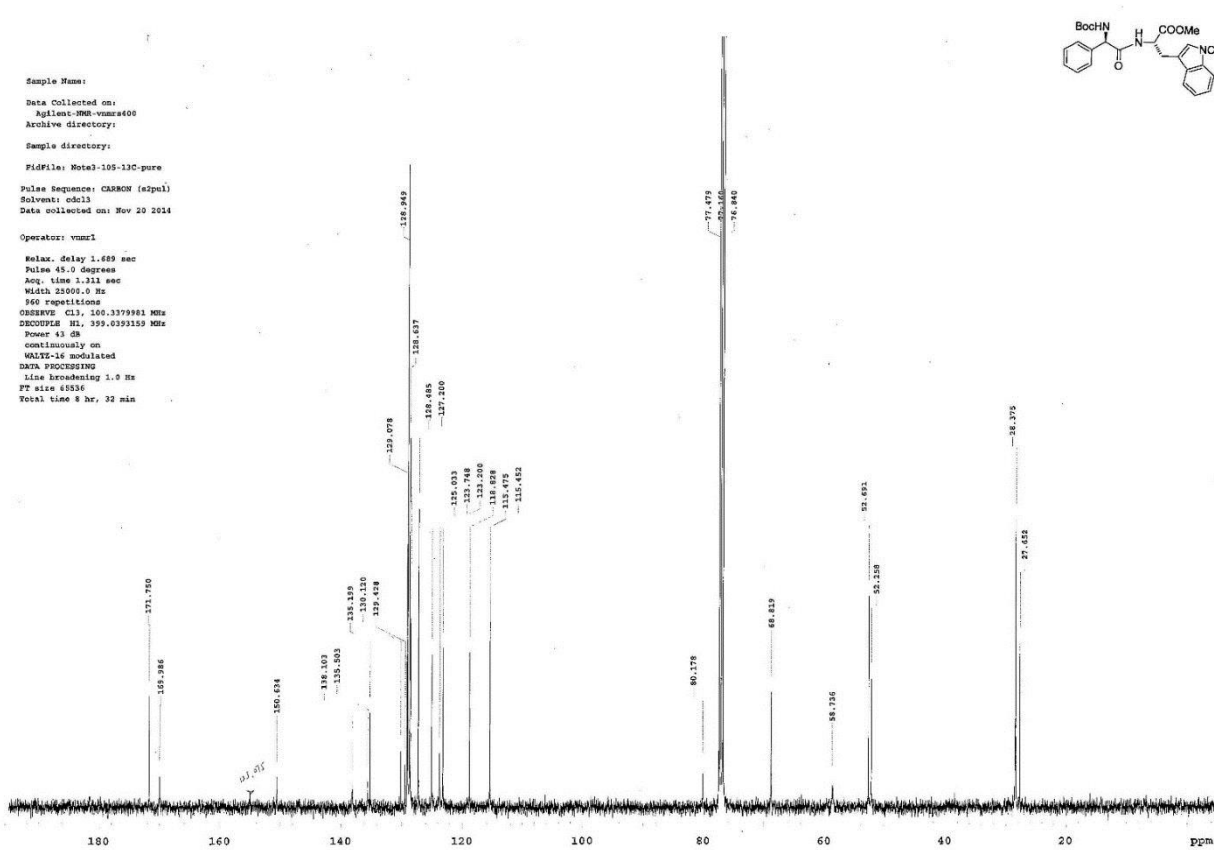


Sample Name:
 Data Collected on:
 Agilent-MMR-vnmr400
 Archive directory:
 Sample directory:
 FIDFile: Notal-105-1H-pure
 Pulse Sequence: PROTON (zgpg3)
 Solvent: cdcl3
 Data collected on: Nov 10 2014

Operator: vnmr1

Relax. delay 1.500 sec
 Pulse 45.0 degrees
 Acq. time 3.500 sec
 Width 6777.6 Hz
 8 repetitions
 OBSERVE H1, 399.0373207 MHz
 DATA PROCESSING
 Line broadening 0.2 Hz
 FT size 65536
 Total time 9 min 40 sec



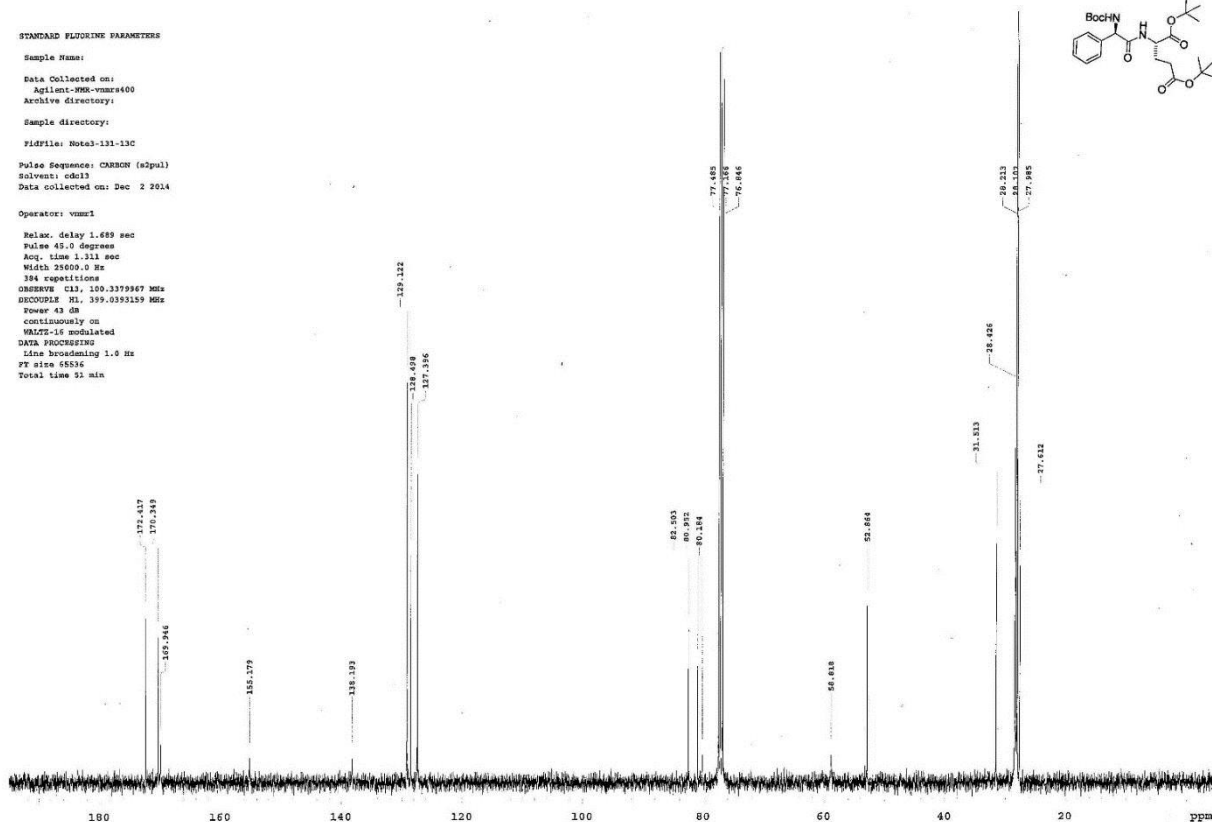


STANDARD FLUORINE PARAMETERS

Sample Name:
Data Collected on:
Agilent-MRM-vnmr400
Archive directory:
Sample directory:
FidFile: Notal-131-13C
Pulse Sequence: CARRON (a2pul)
Solvent: cdcl3
Data collected on: Dec 2 2014

Operator: vnmr1

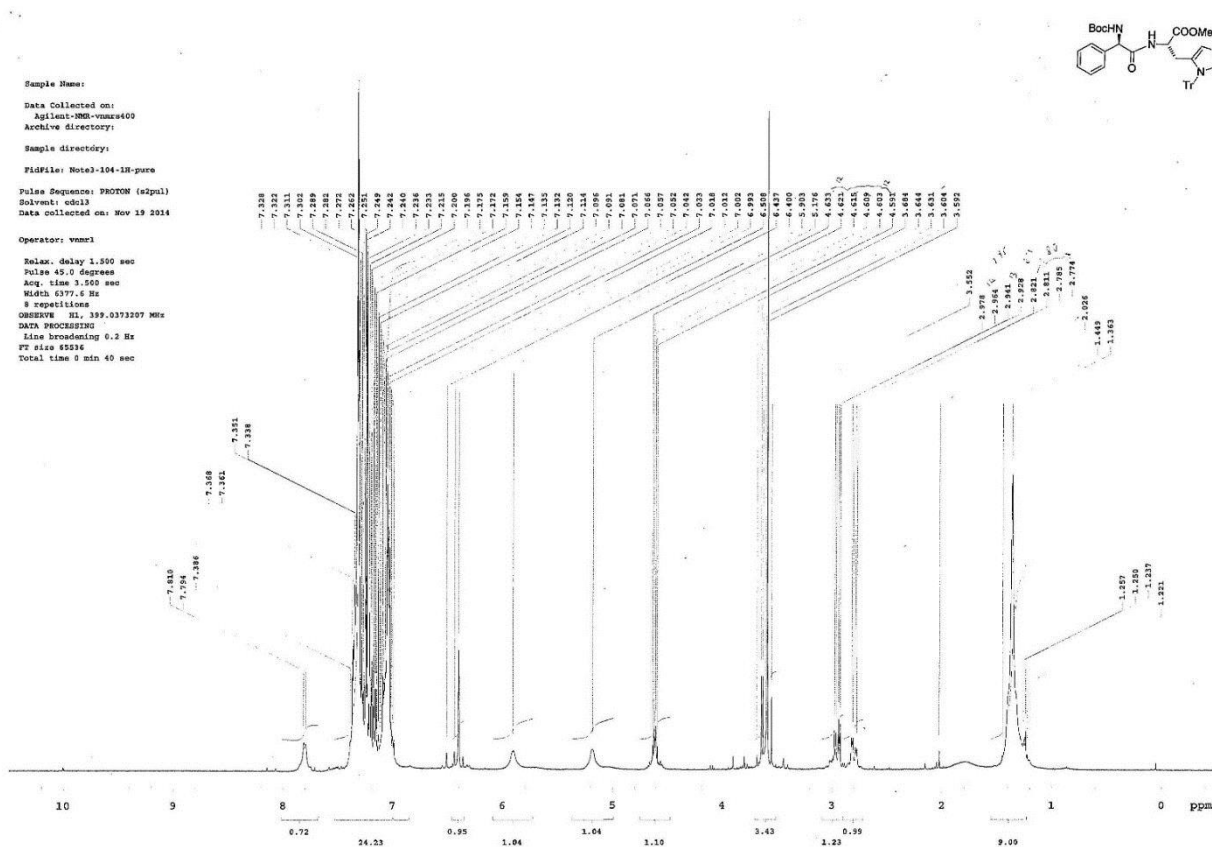
Relax. delay 1.689 sec
Pulse 45.0 degrees
Acq. time 1.311 sec
Width 25600.0 Hz
394 repetitions
OBSERVE H1, 100.3379967 MHz
DECOUPLE H1, 399.0393159 MHz
Power 43 dB
continuously ON
WALTZ-16 modulated
DATA PROCESSING
Line broadening 1.0 Hz
FT size 65536
Total time 51 min

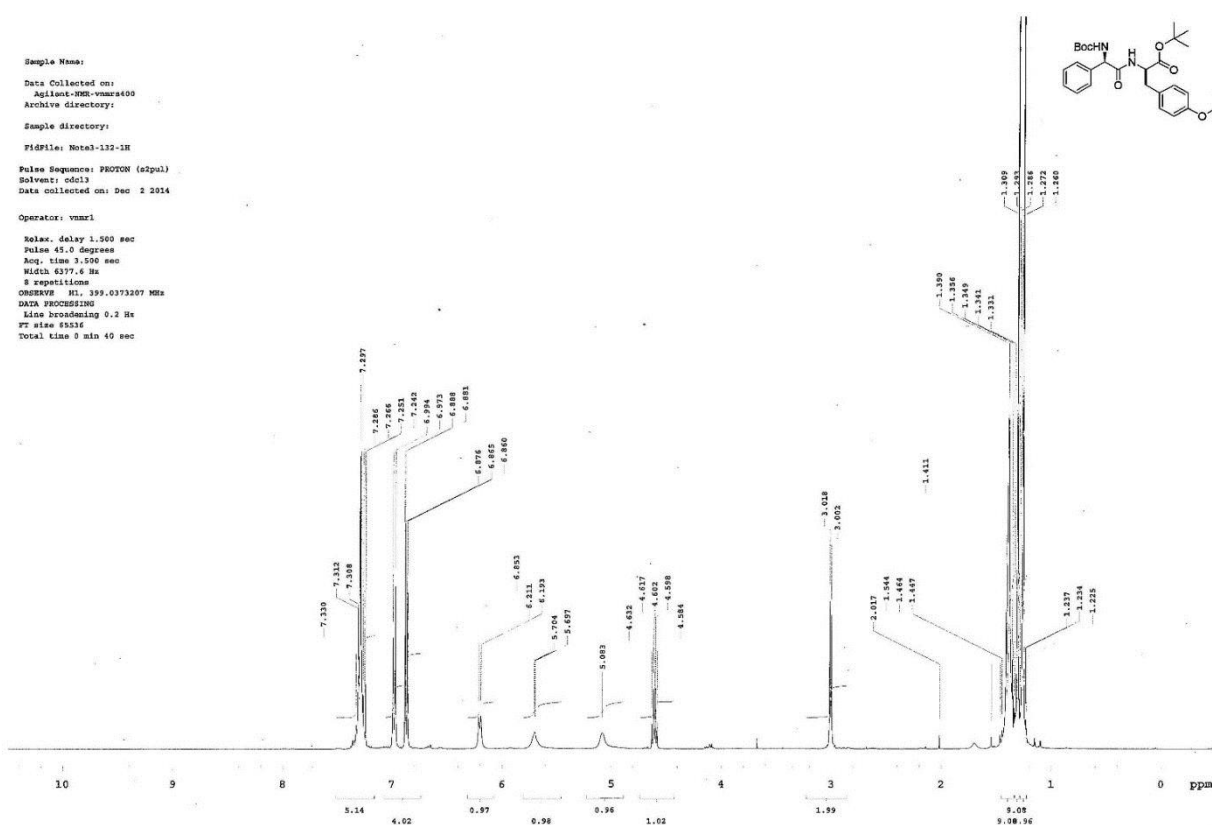
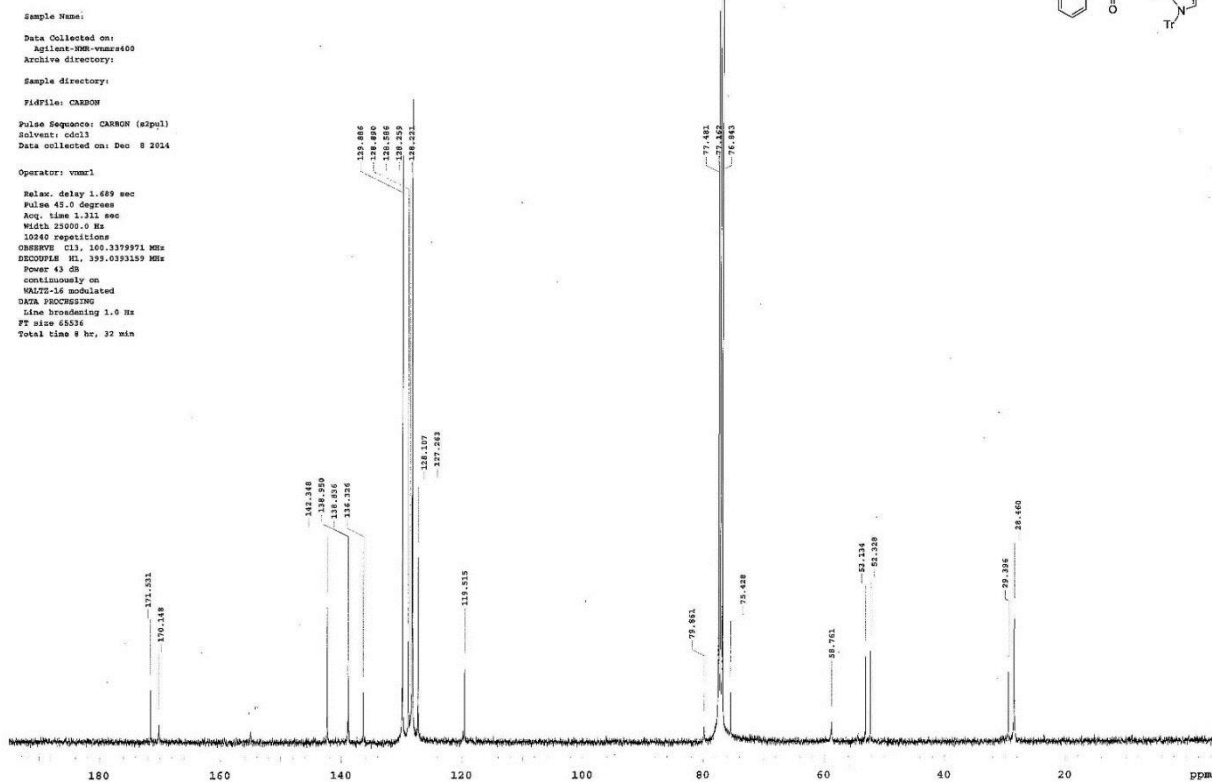


Sample Name:
Data Collected on:
Agilent-MRM-vnmr400
Archive directory:
Sample directory:
FidFile: Notal-104-1H-pure
Pulse Sequence: PROTON (a2pul)
Solvent: cdcl3
Data collected on: Nov 19 2014

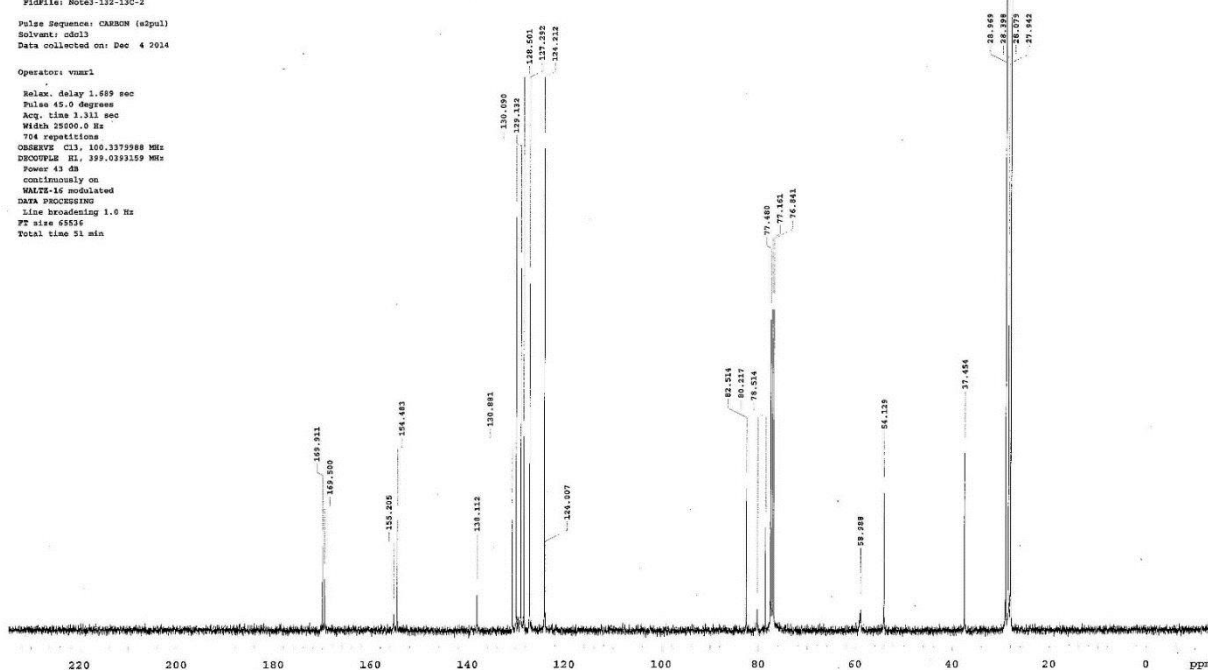
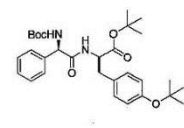
Operator: vnmr1

Relax. delay 1.500 sec
Pulse 45.0 degrees
Acq. time 3.560 sec
Width 6377.6 Hz
8 repetitions
OBSERVE H1, 399.0371207 MHz
DATA PROCESSING
Line broadening 0.2 Hz
FT size 65536
Total time 5 min 40 sec

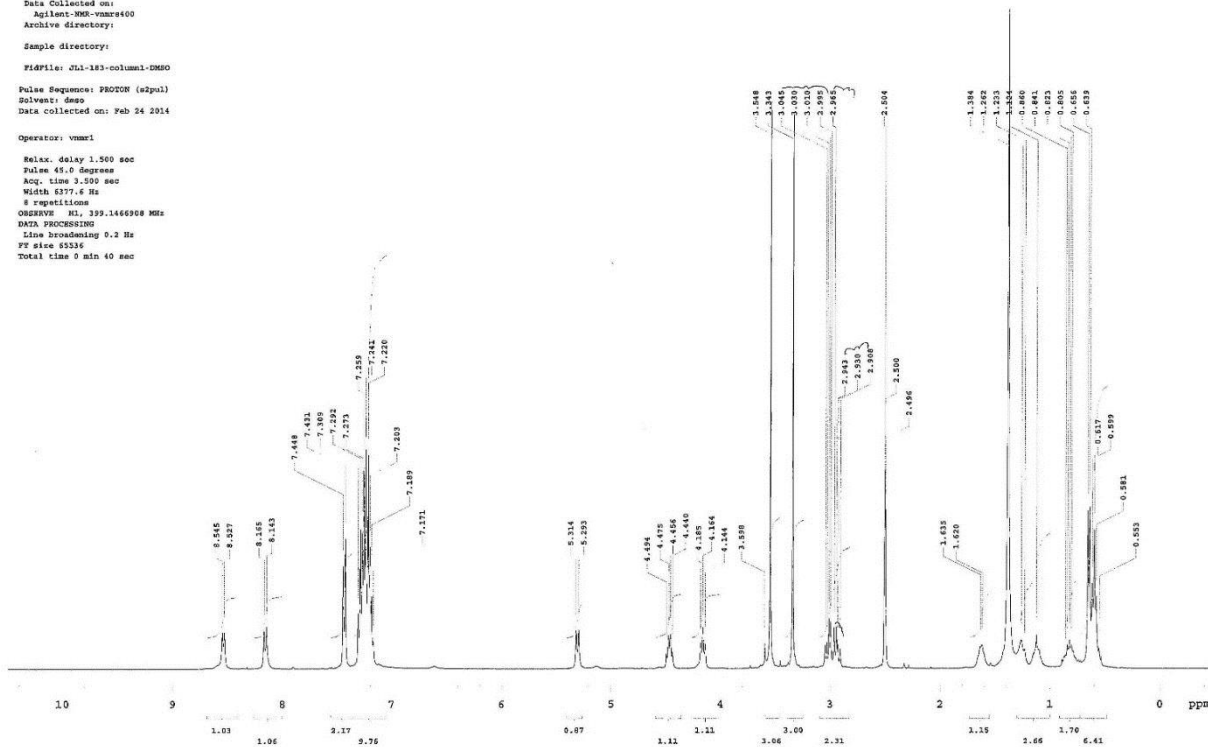
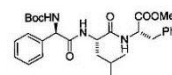




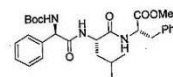
nakadai-2-062
 JCI-Pr-THS90-Ma-B01-75%
 Sample Name:
 Data Collected on:
 Agilent-800-mmrs400
 Archive directory:
 Sample directory:
 Fidfile: Notel-132-130-2
 Pulse Sequence: CARBON (s2pul)
 Solvent: cdcl3
 Data collected on: Dec 4 2014
 Operator: vmur
 Relax. delay 1.689 sec
 Pulse 45.0 degree
 Acq. time 1.311 sec
 Width 25000.0 Hz
 T04 repetitions
 OBSERVE CH1, 100.375968 MHz
 DECOUPLE H1, 399.0393159 MHz
 Power 43 dB
 continuously on
 WALTZ-16 modulated
 DATA PROCESSING
 Line broadening 1.0 Hz
 FT size 65526
 Total time 31 min



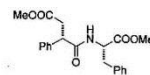
Sample Name:
 Data Collected on:
 Agilent-800-mmrs400
 Archive directory:
 Sample directory:
 Fidfile: JCI-183-column1-DMSO
 Pulse Sequence: PROTON (s2pul)
 Solvent: dms
 Data collected on: Feb 24 2014
 Operator: vmur
 Relax. delay 1.500 sec
 Pulse 45.0 degree
 Acq. time 3.500 sec
 Width 6377.6 Hz
 8 repetitions
 OBSERVE H1, 399.1466908 MHz
 DATA PROCESSING
 Line broadening 5.2 Hz
 FT size 65536
 Total time 0 min 40 sec



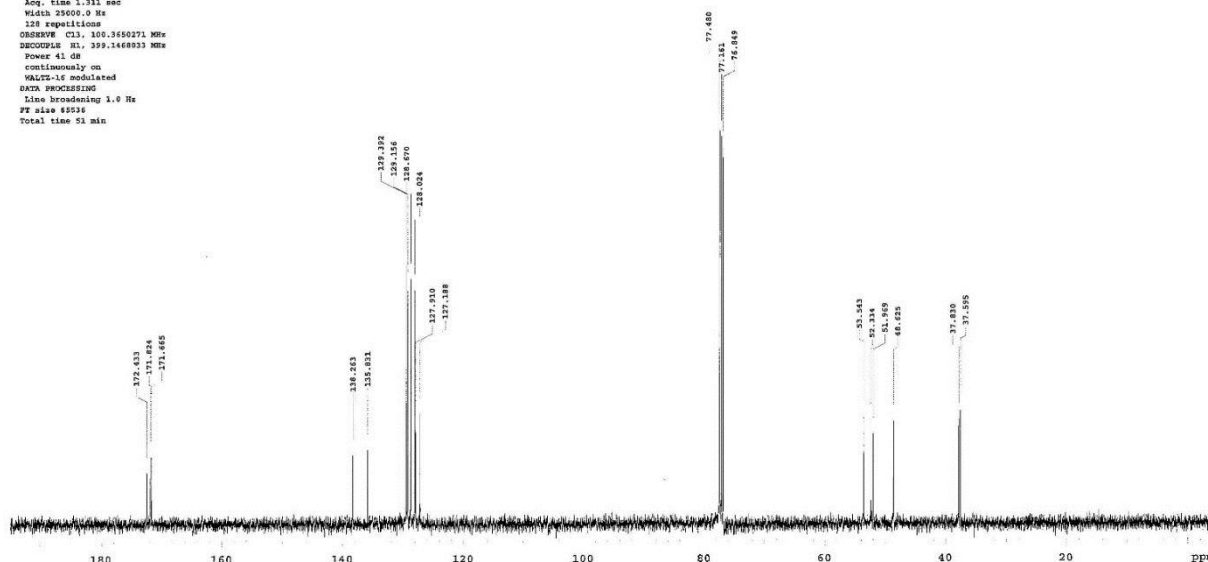
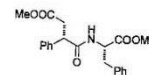
Relax. delay 1.689 sec
Pulse 45.0 degrees
Acq. time 1.311 sec
Width 25900.0 Hz
768 repetitions
OBSERVE CH1, 100.3655594 MHz
DECOUPLE M1, 399.1486992 MHz
Power 41 dB
continuously on
WALTZ-16 modulated
DATA PROCESSING
Line broadening 1.0 Hz
PF case 85536
Total time 51 min



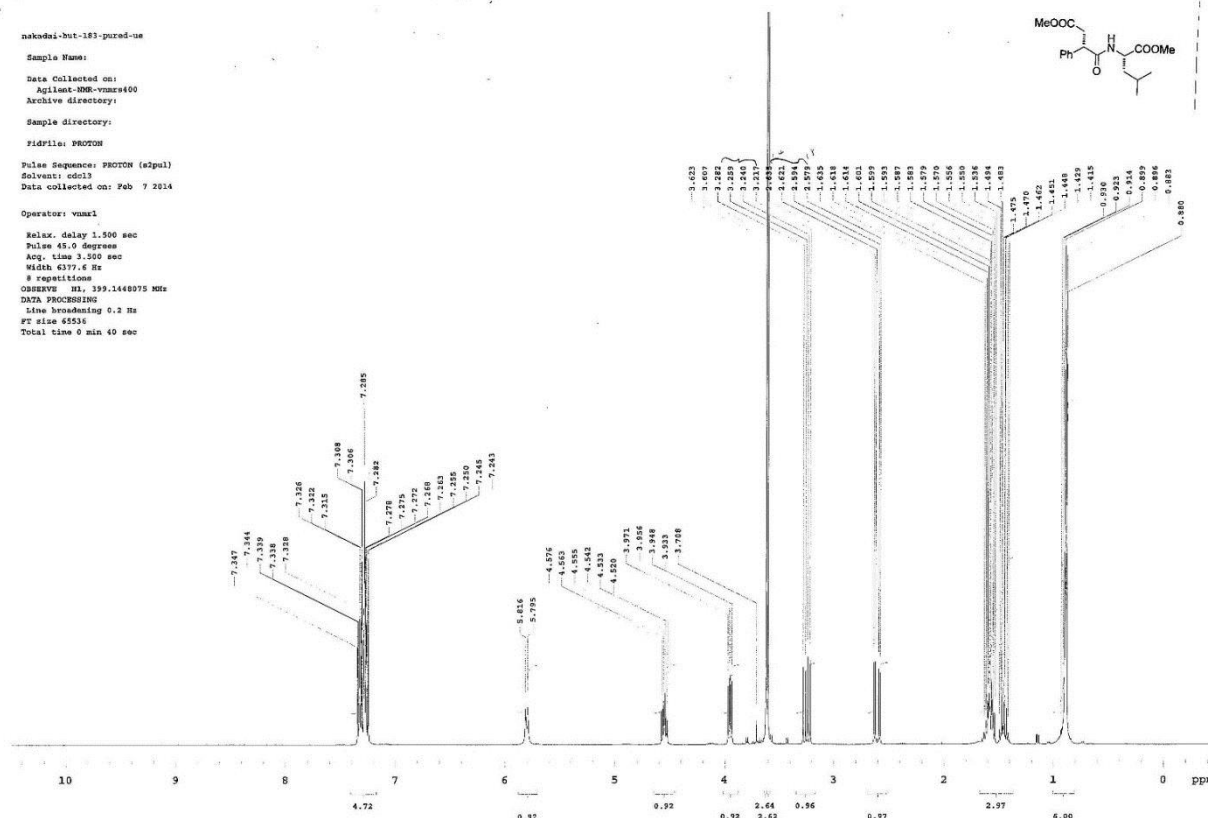
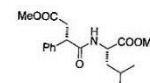
```
Relax. delay 1.500 sec
Pulse 45.0 degrees
Acq. time 3.500 sec
Width 6377.6 Hz
8 repetitions
OBSERVE H1, 399.1448075 MHz
DATA PROCESSING
Line broadening 0.2 Hz
FT size 65536
Total time 0 min 40 sec
```



Sample Name:
 Data Collected on:
 Agilent-MMR-vnmr400
 Archive directory:
 Sample directory:
 FIDFile: JLI-137-column-p2-13C
 Pulse sequence: CARBON (zgpg3)
 Solvent: cdcl3
 Data collected on: Jan 21 2014
 Operator: vnmr1
 Relax. delay 1.689 sec
 Pulse 42.0 degree
 Acq. time 1.314 sec
 Width 25000.0 Hz
 128 repetitions
 OBSERVE Ch1: 100.6260271 MHz
 DECOUPLE H1: 399.1468033 MHz
 Power 41 dB
 continuously on
 WALTZ-16 modulated
 DATA PROCESSING
 Line broadening 1.0 Hz
 FT size 65536
 Total time 51 min

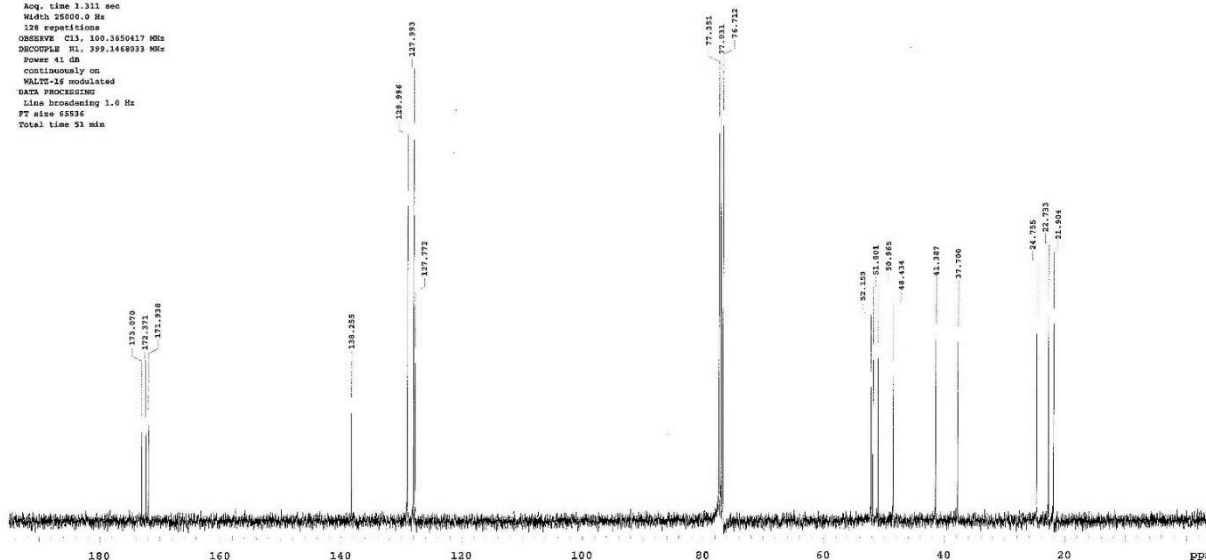
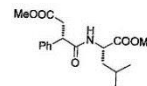


Sample Name:
 Data Collected on:
 Agilent-MMR-vnmr400
 Archive directory:
 Sample directory:
 FIDFile: PHOTON
 Pulse Sequence: PHOTON (zgpg3)
 Solvent: cdcl3
 Data collected on: Feb 7 2014
 Operator: vnmr1
 Relax. delay 1.500 sec
 Pulse 45.0 degree
 Acq. time 3.500 sec
 Width 6377.6 Hz
 8 repetitions
 OBSERVE H1: 399.1468075 MHz
 DATA PROCESSING
 Line broadening 0.2 Hz
 FT size 65536
 Total time 0 min 40 sec



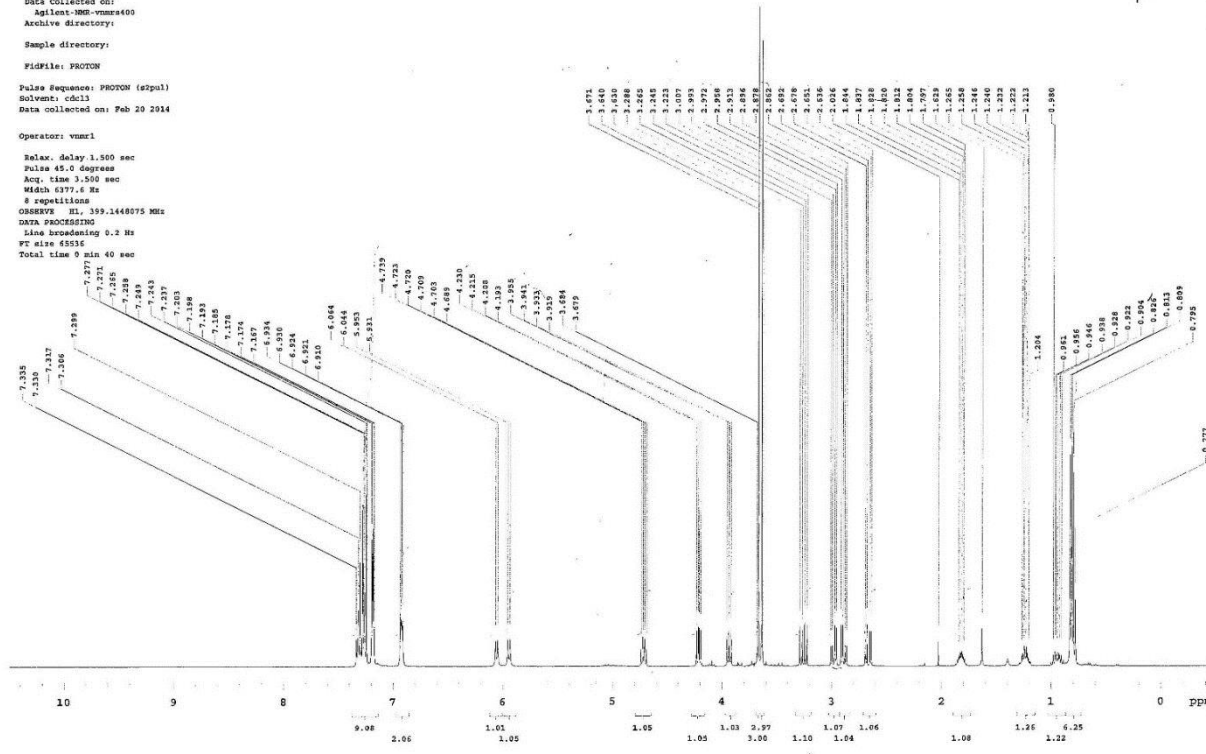
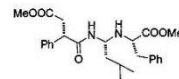
nakadai-but-189-pured-up
 Sample Name:
 Data Collected on:
 Agilent-MMR-vnmr400
 Archive directory:
 Sample directory:
 FIDfile: CARBON
 Pulse Sequence: CARBON (zgpg3)
 Solvent: cdcl3
 Data collected on: Feb 7 2014

Temp: 17.9 C / 291.1 K
 Operator: vnmr1
 Relax. delay 1.500 sec
 Pulse 45.0 degrees
 Acq. time 3.311 sec
 Width 25000.0 Hz
 128 repetitions
 OBSERVE CH: 100.6250417 MHz
 DECOUPLE H1: 299.1448933 MHz
 Power 41.00
 continuously on
 VOLTAGE modulated
 DATA PROCESSING
 Line broadening 1.0 Hz
 FT size 65836
 Total time 23 min

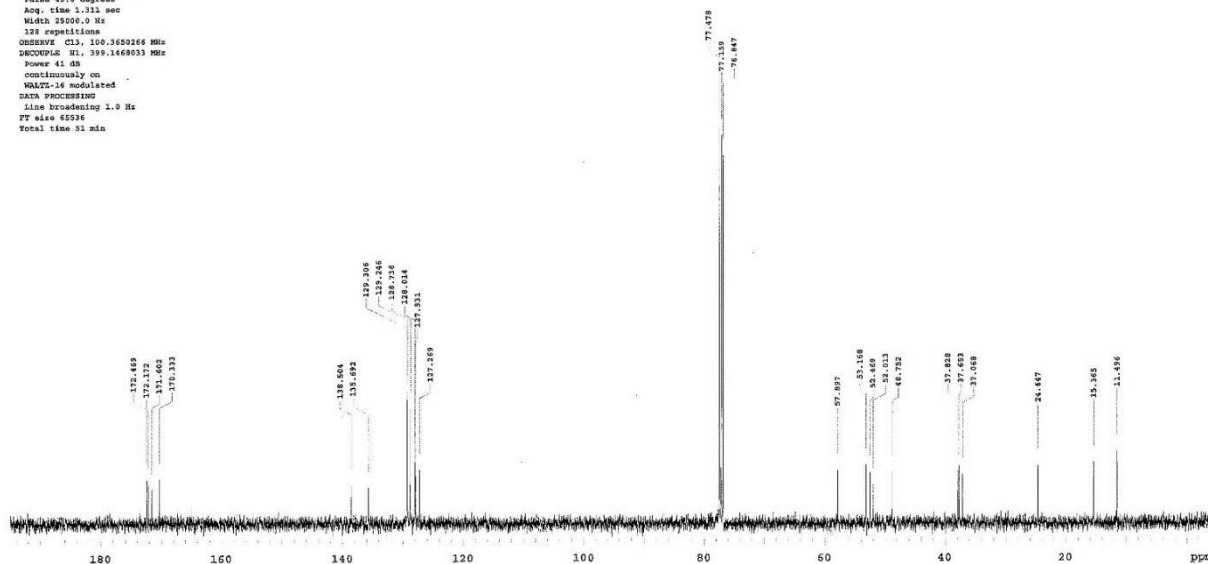
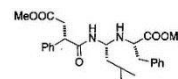


Sample Name:
 Data Collected on:
 Agilent-MMR-vnmr400
 Archive directory:
 Sample directory:
 FIDfile: PROTON
 Pulse Sequence: PROTON (zgpg3)
 Solvent: cdcl3
 Data collected on: Feb 20 2014

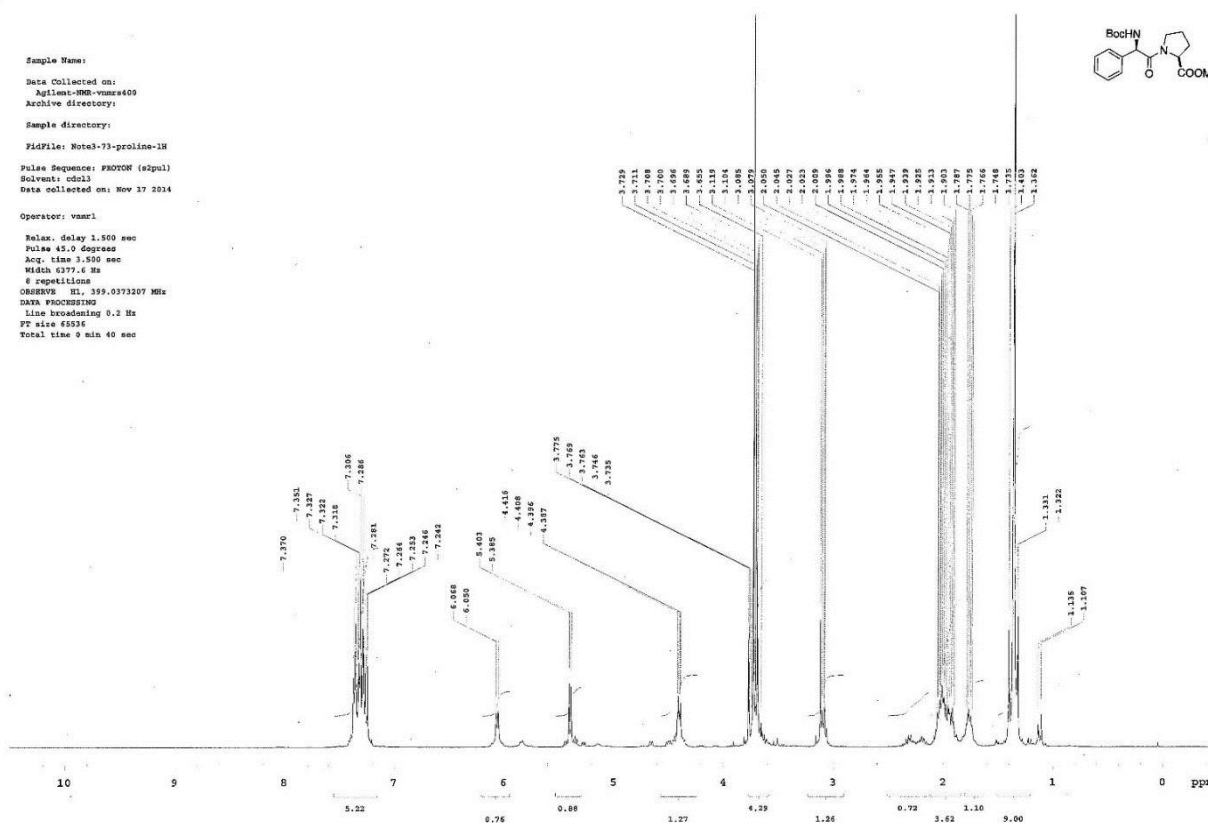
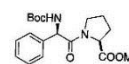
Operator: vnmr1
 Relax. delay 1.500 sec
 Pulse 45.0 degrees
 Acq. time 3.500 sec
 Width 6377.6 Hz
 8 repetitions
 OBSERVE H1: 399.1448075 MHz
 DATA PROCESSING
 Line broadening 0.2 Hz
 FT size 65536
 Total time 9 min 40 sec



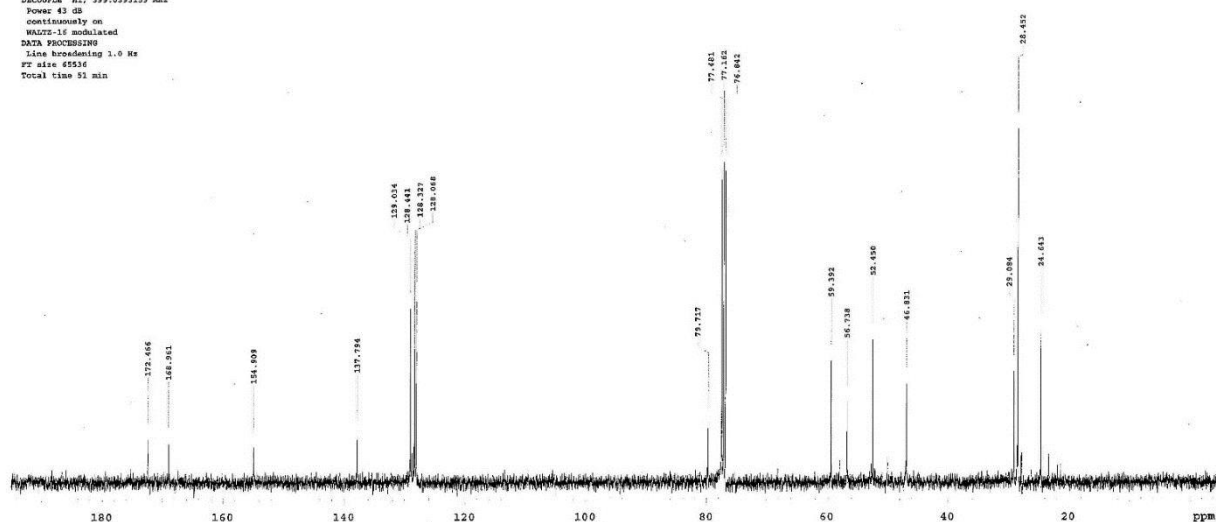
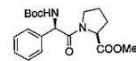
Sample Name:
 Data Collected on:
 Apolima-900-vnmr400
 Archive directory:
 Sample directory:
 Fidfile: CARBON
 Pulse Sequence: CARBON (a2pul)
 Solvent: cdcl3
 Data collected on: Feb 20 2014
 Temp: 19.3 C / 292.4 K
 Operator: vnmr1
 Relax delay 1.689 sec
 Pulse 45.0 degrees
 Acq time 1.311 sec
 Width 25000.0 Hz
 128 repetitions
 OBSERVE CH1: 100.6250264 MHz
 DECOUPLE H1: 399.1468933 MHz
 Power 41 dB
 continuously on
 WALTZ-16 modulated
 DATA PROCESSING
 Line broadening 1.0 Hz
 FT size 65536
 Total time 51 min



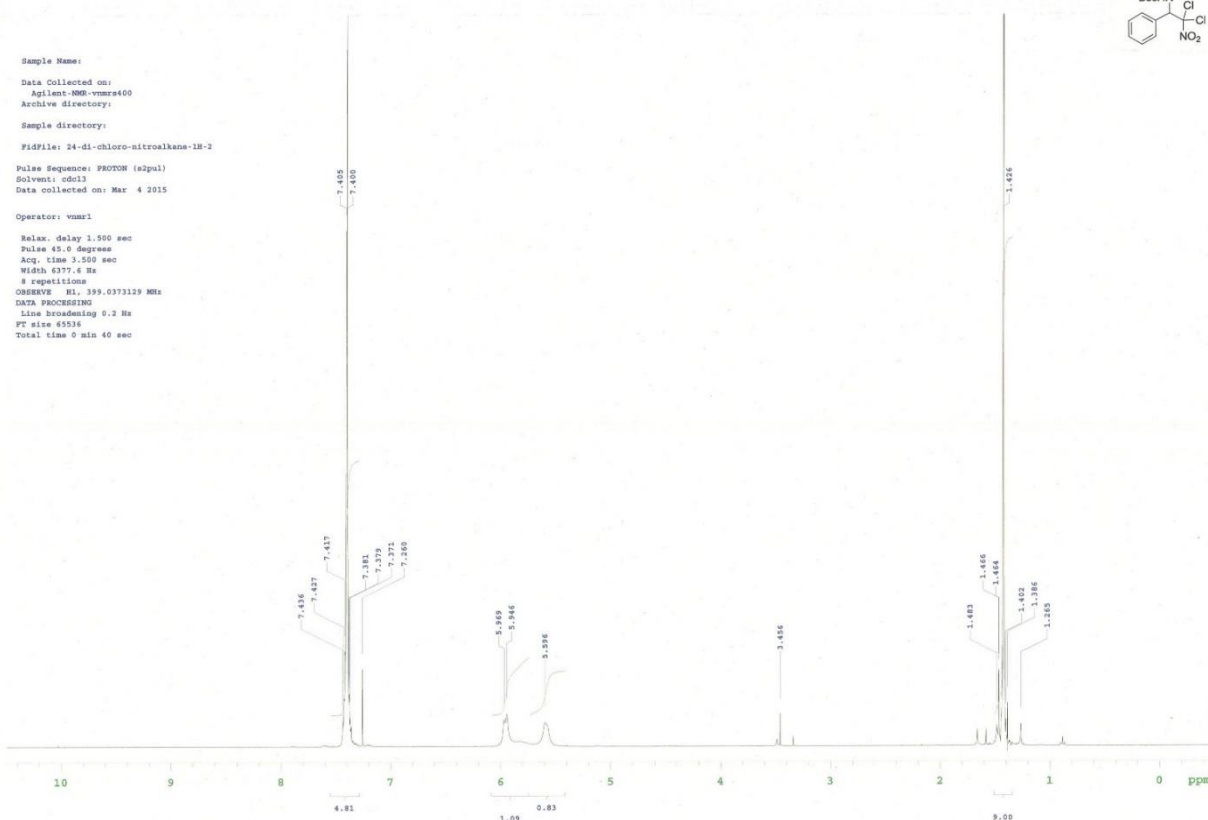
Sample Name:
 Data Collected on:
 Apolima-900-vnmr400
 Archive directory:
 Sample directory:
 Fidfile: N0241-73-proline-1H
 Pulse Sequence: PROTON (a2pul)
 Solvent: cdcl3
 Data collected on: Nov 17 2014
 Operator: vnmr1
 Relax delay 1.500 sec
 Pulse 45.0 degrees
 Acq time 1.500 sec
 Width 6177.6 Hz
 8 repetitions
 OBSERVE H1: 399.0373207 MHz
 DATA PROCESSING
 Line broadening 0.2 Hz
 FT size 65536
 Total time 9 min 40 sec



Sample Name:
 Data Collected on:
 Agilent-NMR-vnmr400
 Archive directory:
 Sample directory:
 FIDFile: Notal-73-proline-13C
 Pulse Sequence: CARBON (s2pul)
 Solvent: cdcl3
 Data collected on: Nov 17 2014
 Operator: vnmr1
 Relax: delay 1.489 sec
 Pulse 45.0 degrees
 Acq. time 1.313 sec
 Width 25000.0 Hz
 128 repetitions
 OBSERVE C13, 100.3379994 MHz
 DECOUPLE H1, 399.0393159 MHz
 Power 42 dB
 continuously on
 WALTZ-16 modulated
 DATA PROCESSING
 Line broadening 1.0 Hz
 FT size 65536
 Total time 31 min

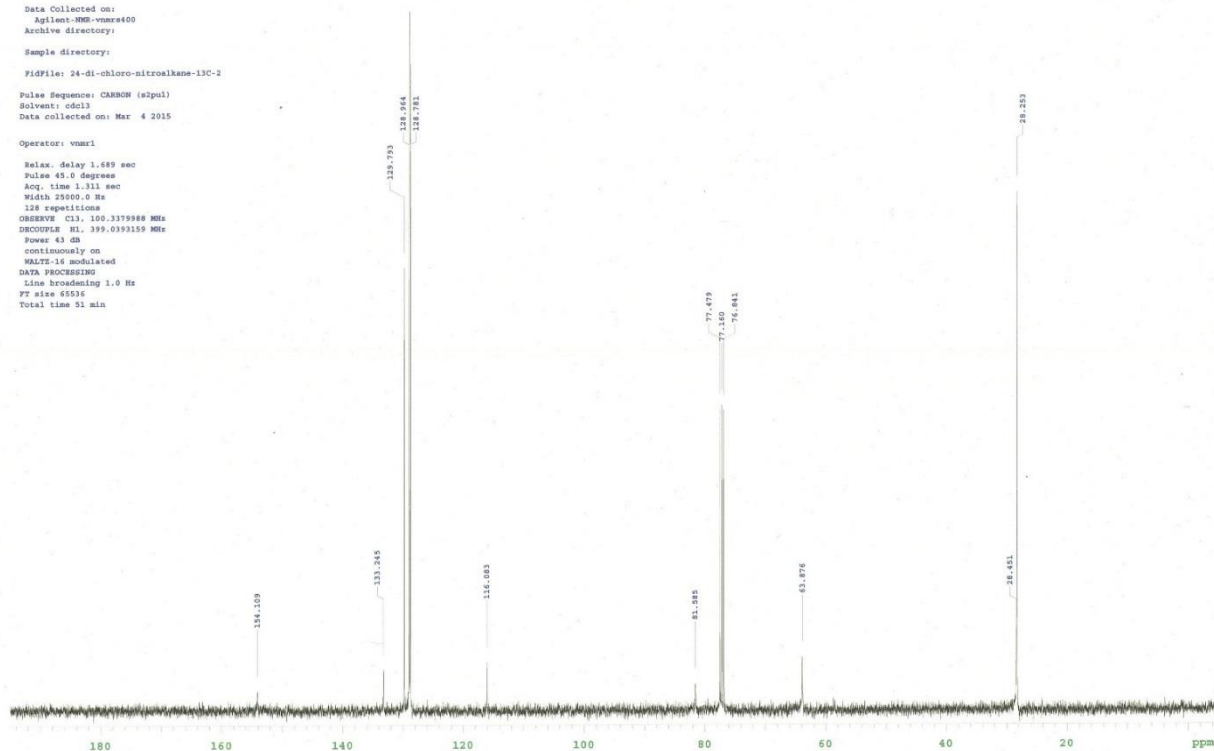


Sample Name:
 Data Collected on:
 Agilent-NMR-vnmr400
 Archive directory:
 Sample directory:
 FIDFile: 24-di-chloro-nitroalkane-18-2
 Pulse Sequence: PROTON (s2pul)
 Solvent: cdcl3
 Data collected on: Mar 4 2015
 Operator: vnmr1
 Relax: delay 1.500 sec
 Pulse 45.0 degrees
 Acq. time 3.550 sec
 Width 6377.6 Hz
 8 repetitions
 OBSERVE H1, 399.0373129 MHz
 DATA PROCESSING
 Line broadening 0.2 Hz
 FT size 65536
 Total time 0 min 40 sec

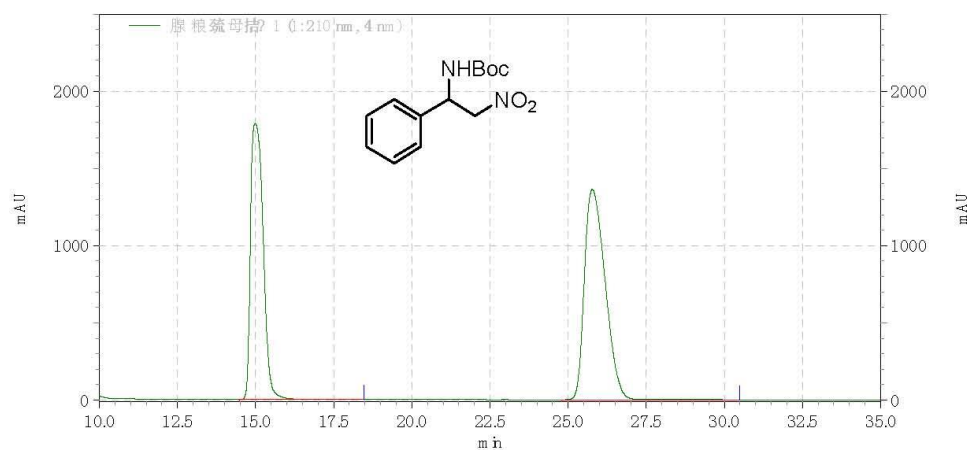




Sample Name:
 Data Collected on:
 Agilent-WW-vnmr400
 Archive directory:
 Sample directory:
 FIDFile: 24-di-chloro-nitroalkane-13C-2
 Pulse Sequence: CARBON (s2pul)
 Solvent: cdcl3
 Data collected on: Mar 4 2015
 Operator: vnmr1
 Relax delay 1.489 sec
 Pulse 45.0 degrees
 Acq. time 1.311 sec
 Width 25000.0 Hz
 128 repetitions
 OBSERVE C13, 100.3379988 MHz
 DECOUPLE H1, 399.6393159 MHz
 Power 43 dB
 continuously on
 WALTZ-16 modulated
 DATA PROCESSING
 Line broadening 1.0 Hz
 FT size 65536
 Total time 51 min

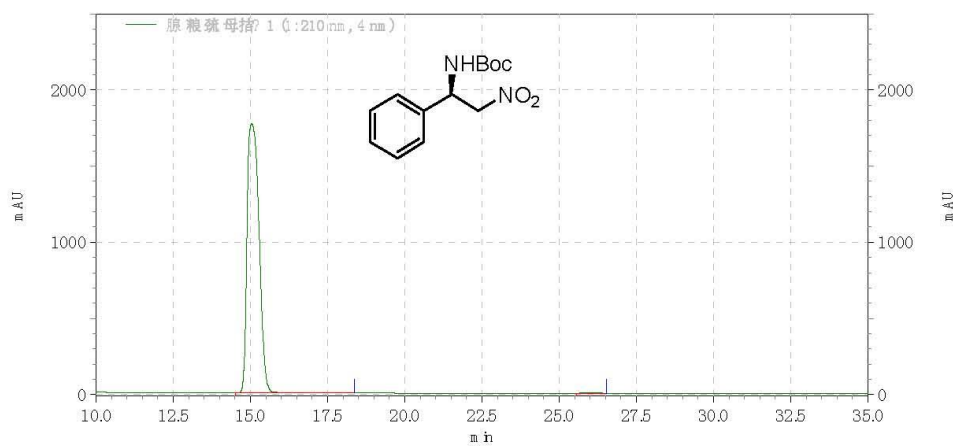


Daicel Chiralpak IC column (Hex/i-Pr = 19/1, 1 mL /min, 20 °C, 210 nm).



1: 210 nm, 4 nm結果

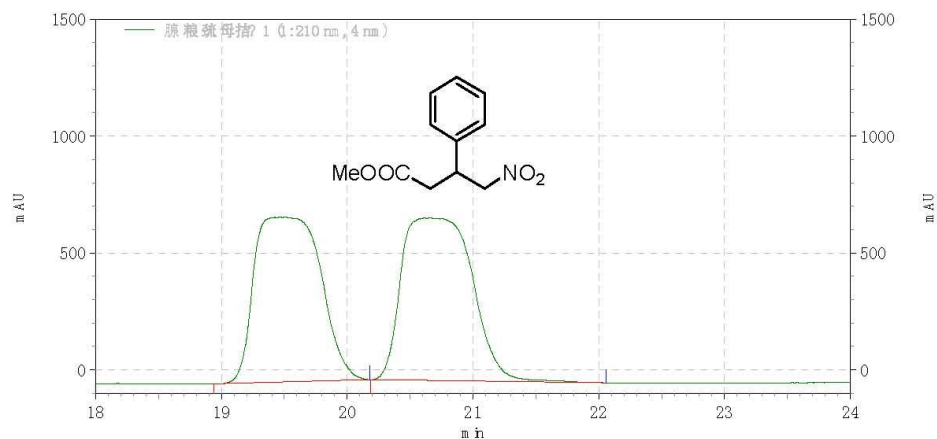
Pk #	名前	保持時間	面積	面積%	ベースラインコード
1		14.99	200931890	44.452	MM
2		25.77	251089907	55.548	MM



1: 210 nm, 4 nm結果

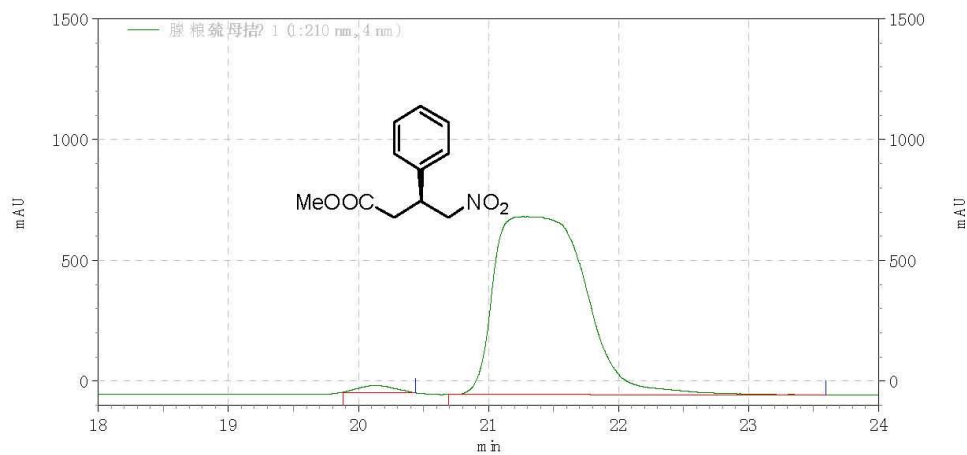
Pk #	名前	保持時間	面積	面積%	ベースラインコード
1		15.04	191047311	99.639	MM
2		26.04	691295	0.361	MM

Daicel Chiralpak IC column (Hex/i-Pr = 19/1, 1 mL/min, 20 °C, 210 nm).



1: 210 nm, 4 nm結果

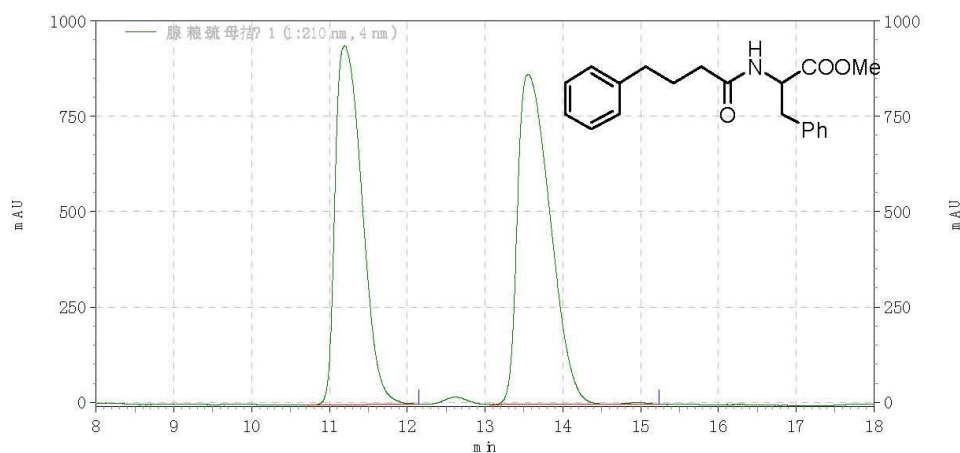
Pk #	名前	保持時間	面積	面積%	ベースラインコード
1		19.47	103090397	48.742	MM
2		20.65	108411154	51.258	MM



1: 210 nm, 4 nm結果

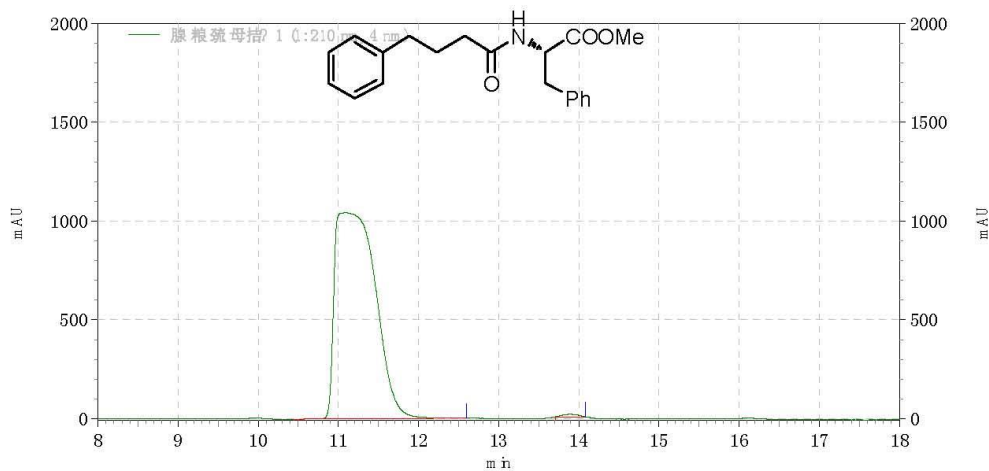
Pk #	名前	保持時間	面積	面積%	ベースラインコード
1		20.13	2197149	1.515	MM
2		21.30	142825299	98.485	MM

Daicel Chiralpak IE column (Hex/i-Pr = 10/1, 2 mL /min, 20 °C, 210 nm)



1: 210 nm, 4 nm結果

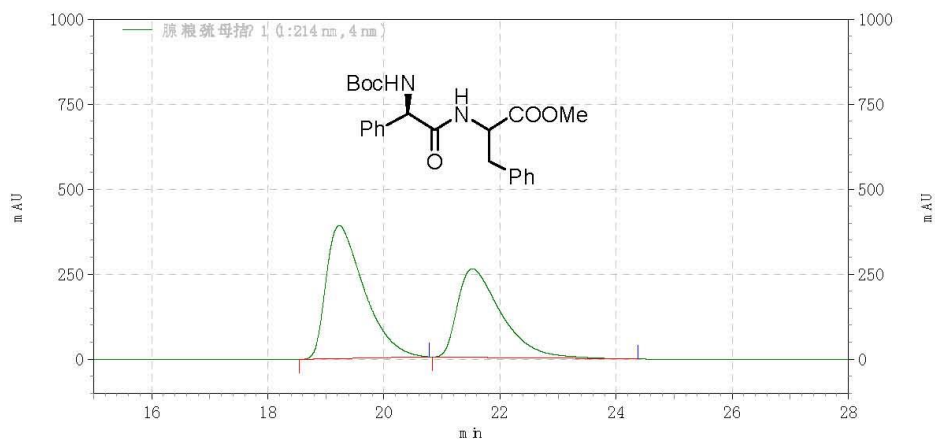
Pk #	名前	保持時間	面積	面積%	ベースラインコード
1		11.20	90179536	47.179	MM
2		13.55	100965014	52.821	MM



1: 210 nm, 4 nm結果

Pk #	名前	保持時間	面積	面積%	ベースラインコード
1		11.09	147572882	99.529	MM
2		13.89	698477	0.471	MM

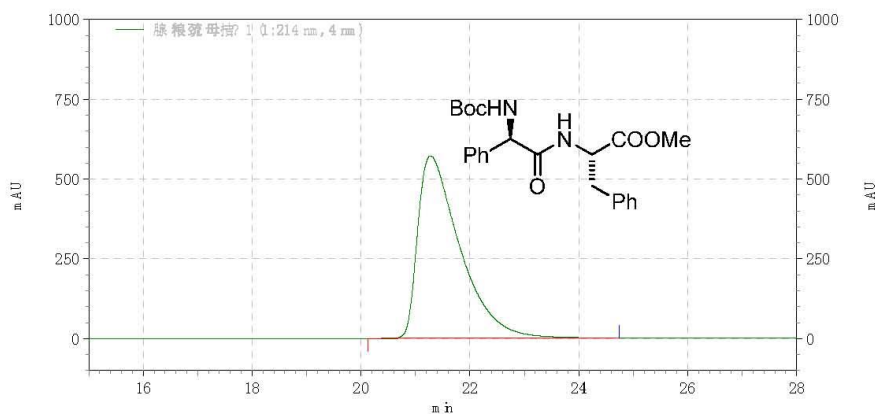
Daicel Chiralpak OD/H HPLC column (Hex/i-Pr = 19/1, 0.5 mL/min, 20 °C, 210 nm, $t_{\text{minor}} = 20.13$ min, $t_{\text{major}} = 21.30$ min).



1: 214 nm, 4 nm

結果

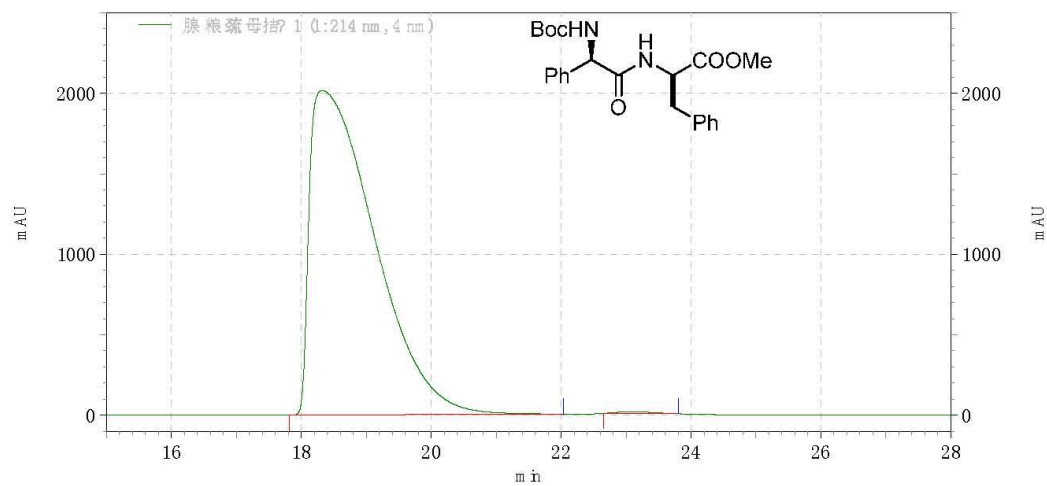
名前	保持時間	面積	面積%	ピークコード*
	19.23	71173771	56.679	MM
	21.53	54399286	43.321	MM



1: 214 nm, 4 nm

結果

名前	保持時間	面積	面積%	ピークコード*
	21.28	122965799	100.000	MM

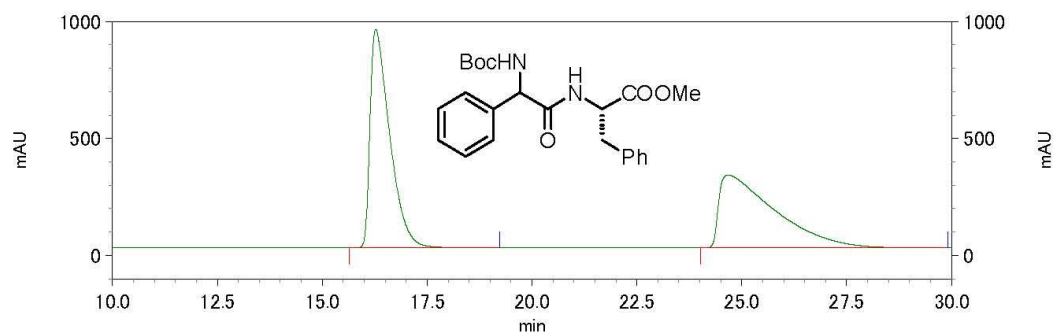


1: 214 nm, 4 nm

結果

名前	保持時間	面積	面積%	ピークコード
	18.33	560290168	99.687	MM
	23.09	1760001	0.313	MM

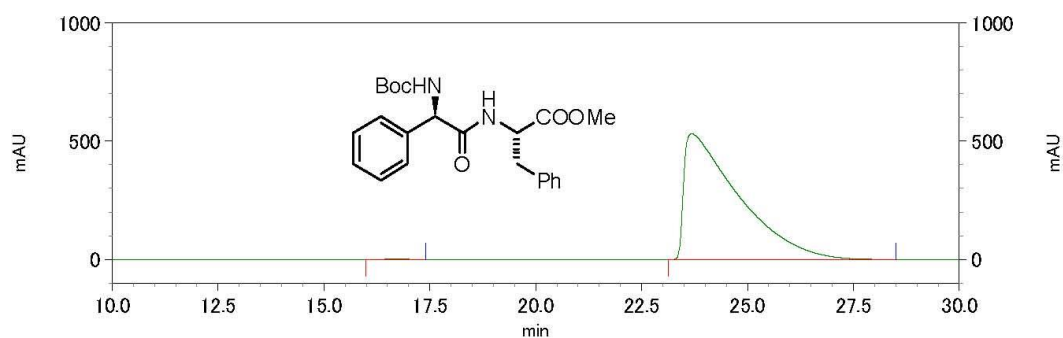
Daicel Chiralpak ID HPLC column (Hex/i-Pr = 4/1, 1 mL/min, 20 °C, 210 nm).



1: 212 nm, 4 nm結

果

Pk #	名前	保持時間	面積	面積%	ベースラインコード
1		16.28	122014974	51.311	MM
2		24.68	115781045	48.689	MM

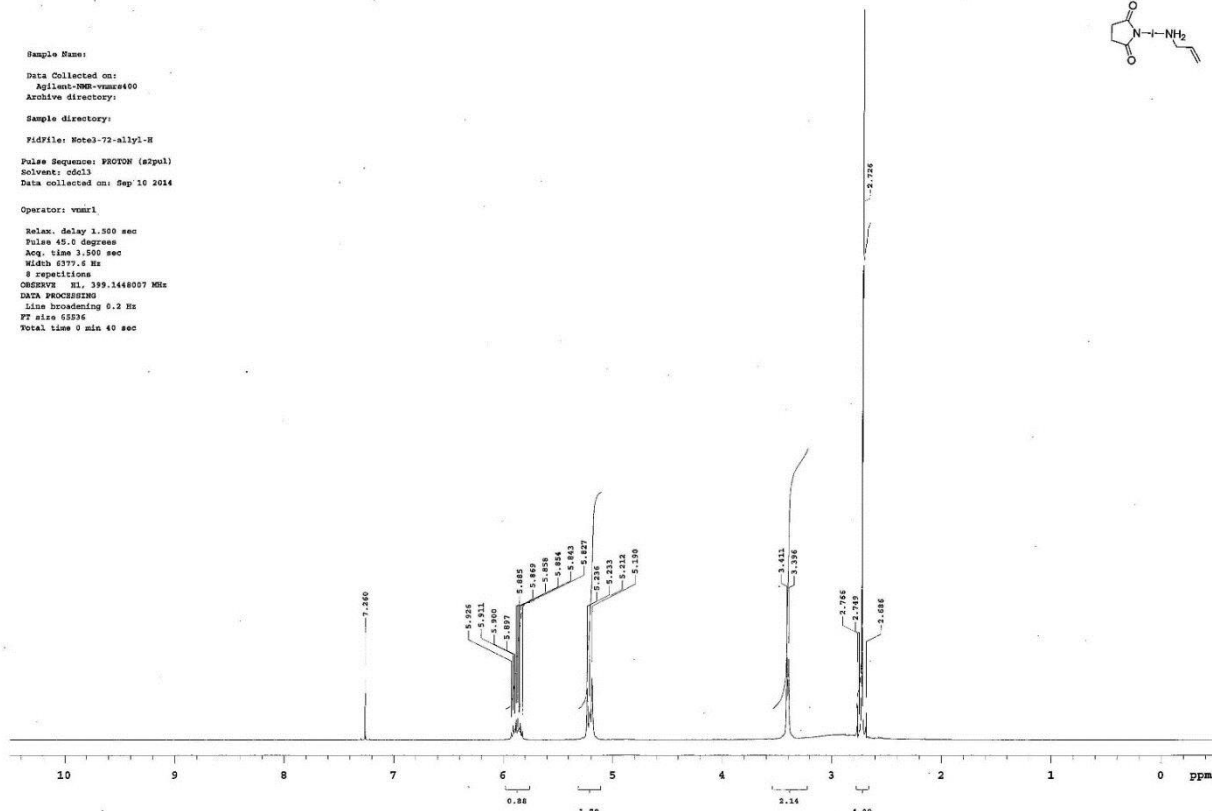


1: 212 nm, 4 nm結

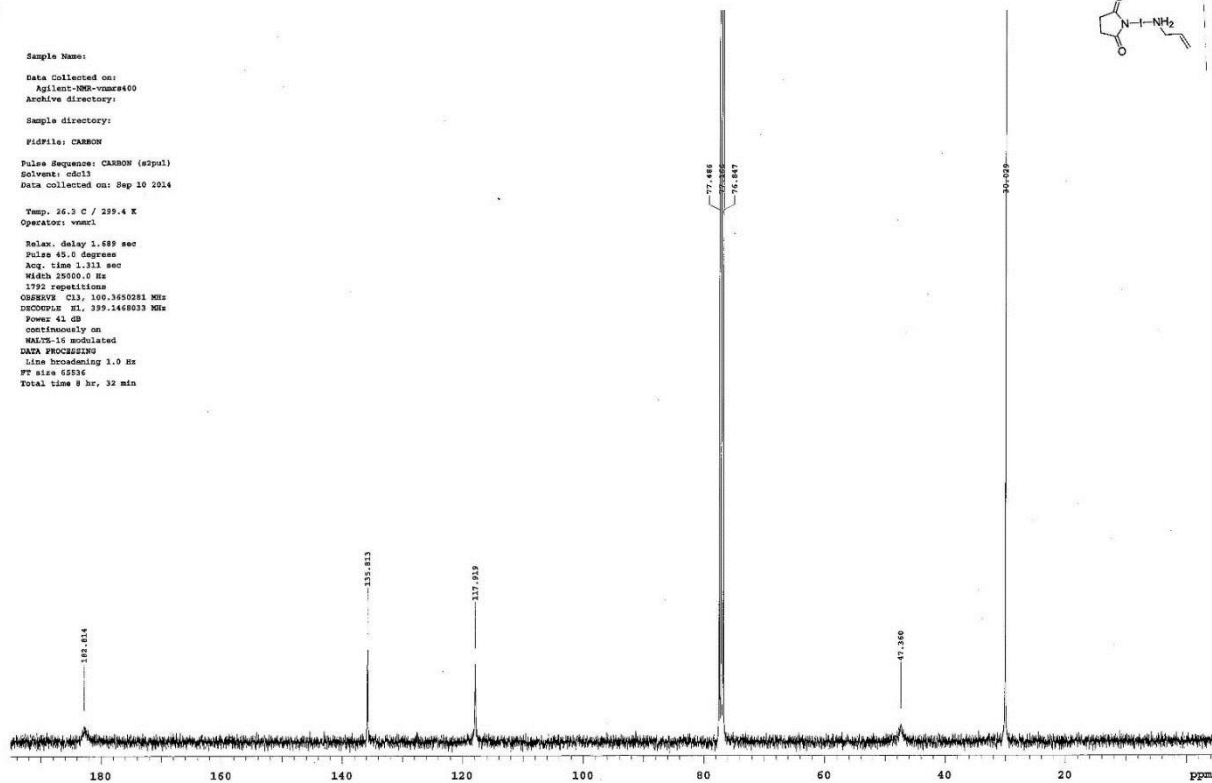
果

Pk #	名前	保持時間	面積	面積%	ベースラインコード
1		16.71	449358	0.235	MM
2		23.69	190797561	99.765	MM

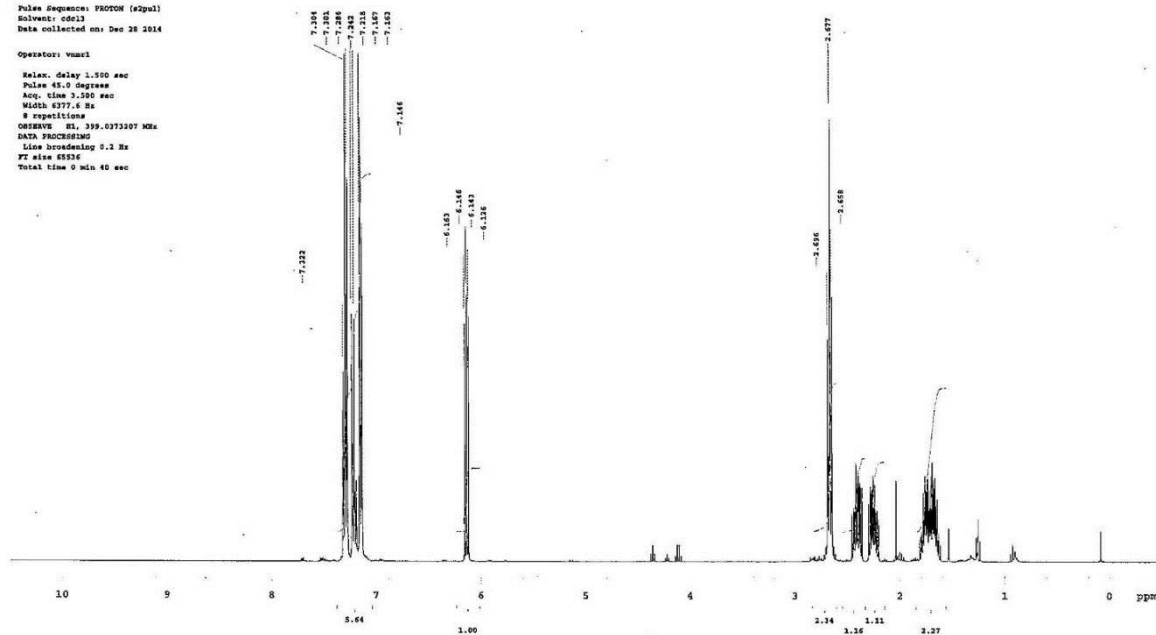
Sample Name:
 Data Collected on:
 Agilent-VNM-vmx400
 Archive directory:
 Sample directory:
 FidFile: M063-72-allyl-H
 Pulse Sequence: F2DOTN (s2pul)
 Solvent: cdcl3
 Data collected on: Sep 10 2014
 Operator: vmxrl
 Relax. delay 1.500 sec
 Pulse 45.0 degrees
 Acq. time 3.500 sec
 Width 6377.6 Hz
 8 repetitions
 OBSERVE HL 399.1448007 MHz
 DATA PROCESSING
 Line broadening 0.2 Hz
 FT size 65836
 Total time 0 min 40 sec



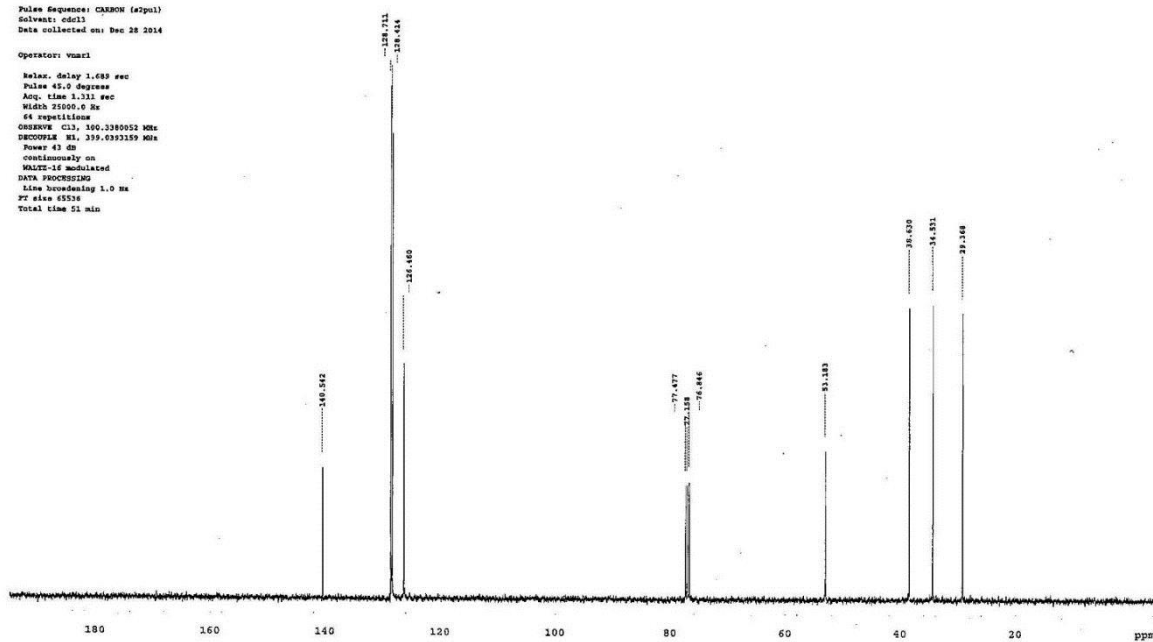
Sample Name:
 Data Collected on:
 Agilent-VNM-vmx400
 Archive directory:
 Sample directory:
 FidFile: CARBON
 Pulse Sequence: CARBON (s2pul)
 Solvent: cdcl3
 Data collected on: Sep 10 2014
 Temp. 24.3 C / 299.4 K
 Operator: vmxrl
 Relax. delay 1.689 sec
 Pulse 45.0 degrees
 Acq. time 1.311 sec
 Width 20000.0 Hz
 1792 repetitions
 OBSERVE CL3 100.6260281 MHz
 DECOUPLE HL 399.1448003 MHz
 Power 41 dB
 continuously on
 WALTZ-16 modulated
 DATA PROCESSING
 Line broadening 1.0 Hz
 FT size 62036
 Total time 8 hr, 32 min



Sample Name:
 Data Collected on:
 Agilent-VNMR-vnmr400
 Archive directory:
 Sample directory:
 FIDFile: M043-160-pure-2H
 Pulse Sequence: PROTON (zgpg3)
 Solvent: cdcl3
 Data collected on: Dec 28 2014
 Operator: vnmr1
 Relax. delay 1.500 sec
 Pulse 45.0 degrees
 Acq. time 1.250 sec
 Width 6377.6 Hz
 8 repetitions
 OBSERVE M1 399.6373207 MHz
 DATA PROCESSING
 Line broadening 0.2 Hz
 FT size 65536
 Total time 0 min 40 sec



Sample Name:
 Data Collected on:
 Agilent-VNMR-vnmr400
 Archive directory:
 Sample directory:
 FIDFile: M043-160-pure-13C
 Pulse Sequence: CARBON (zgpg3)
 Solvent: cdcl3
 Data collected on: Dec 28 2014
 Operator: vnmr1
 Relax. delay 1.689 sec
 Pulse 45.0 degrees
 Acq. time 1.311 sec
 Width 25500.0 Hz
 64 repetitions
 OBSERVE C13 100.6280052 MHz
 DECOUPLE M1 399.6393159 MHz
 Power 47 dB
 continuously on
 WALTZ-16 modulated
 DATA PROCESSING
 Line broadening 1.0 Hz
 FT size 65536
 Total time 51 min

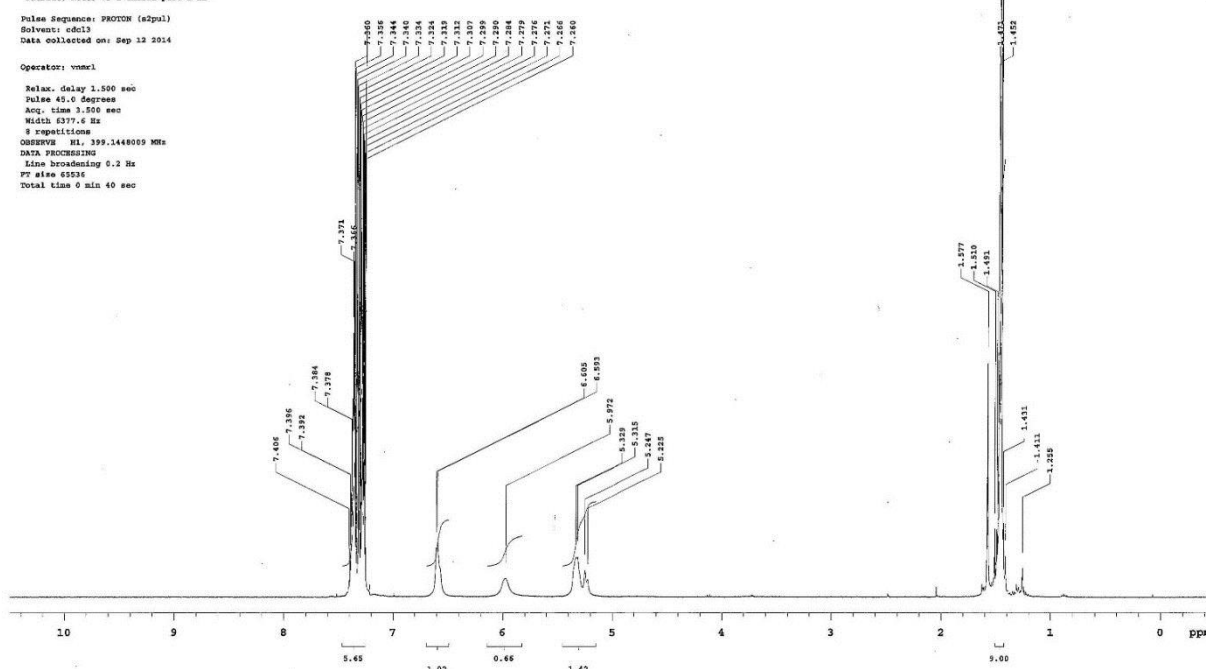


Sample Name:
 Data Collected on:
 Agilent-VNM-vmr400
 Archive directory:
 Sample directory:
 FIDFile: M063-73-1-chiral-pure-1-1R

Pulse Sequence: PROTON (s2pul)
 Solvent: cdcl3
 Data collected on: Sep 12 2014

Operator: vmr41

Relax. delay 1.500 sec
 Pulse 45.0 degrees
 Acq. time 3.500 sec
 Width 6377.6 Hz
 8 repetitions
 OBSERVED HL 399.1448009 MHz
 DATA PROCESSING
 Line broadening 5.2 Hz
 FT size 65536
 Total time 0 min 40 sec

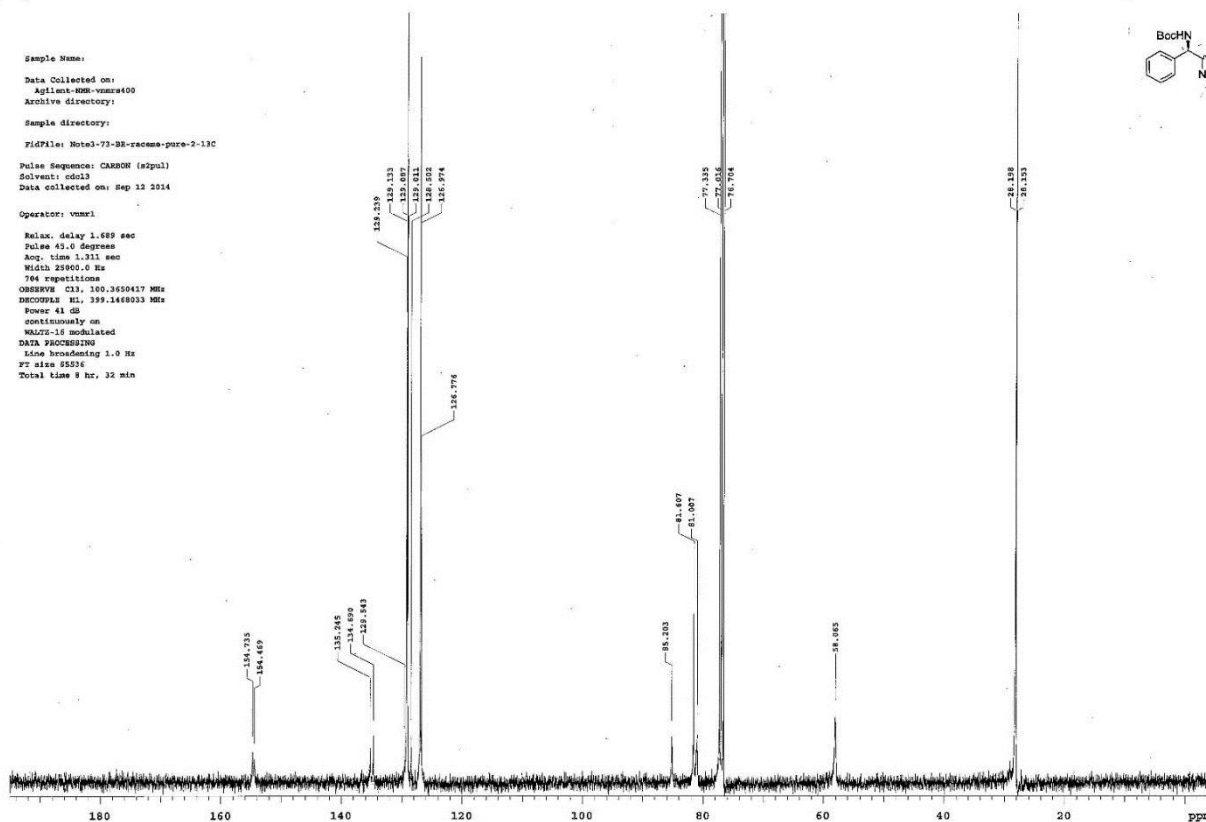


Sample Name:
 Data Collected on:
 Agilent-VNM-vmr400
 Archive directory:
 Sample directory:
 FIDFile: M063-73-1R-2-13C

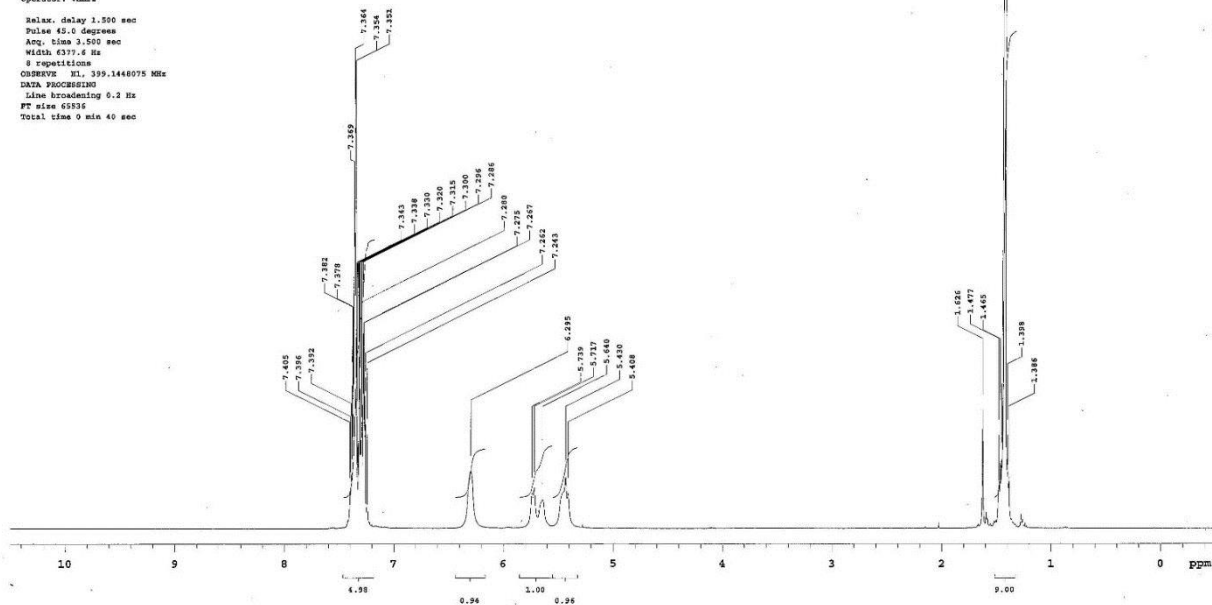
Pulse Sequence: CARBON (s2pul)
 Solvent: cdcl3
 Data collected on: Sep 12 2014

Operator: vmr41

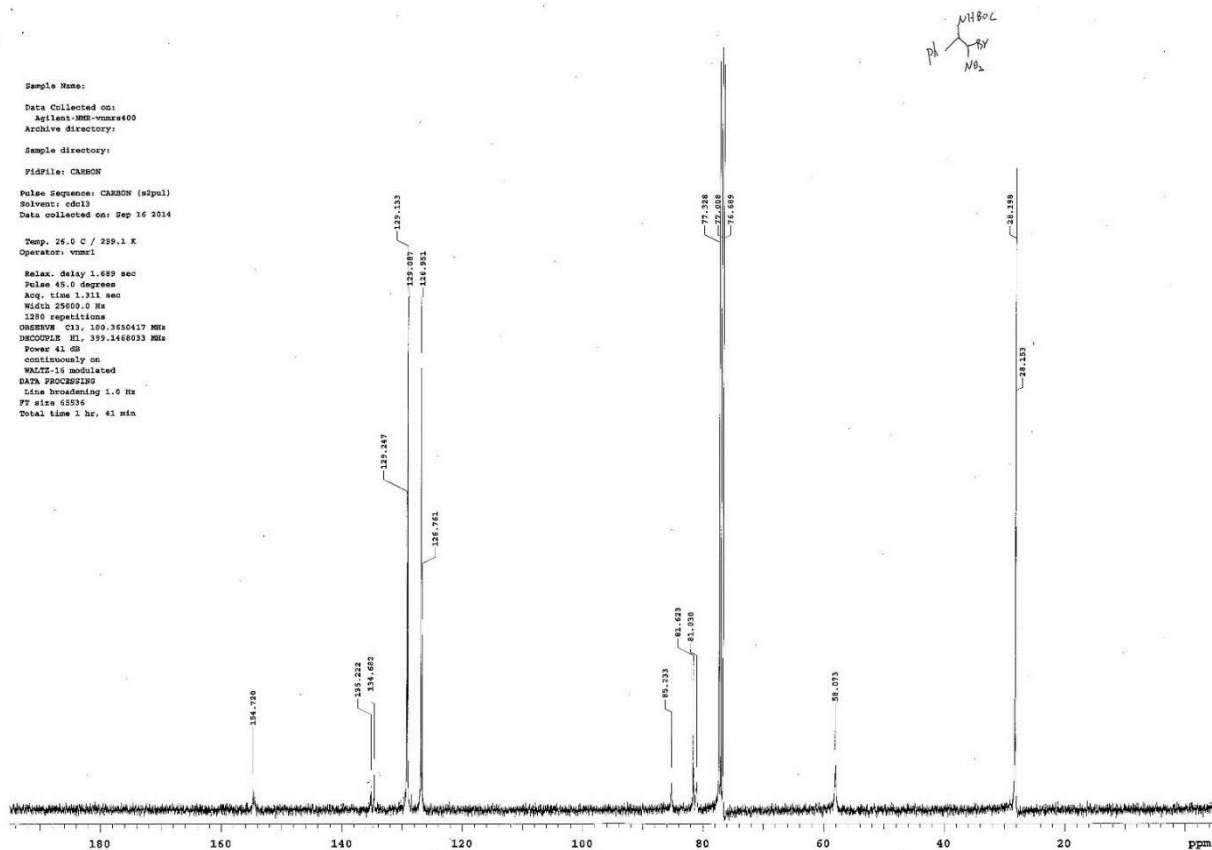
Relax. delay 1.689 sec
 Pulse 45.0 degrees
 Acq. time 1.311 sec
 Width 25900.0 Hz
 794 repetitions
 OBSERVED CH 100.6250417 MHz
 DECOUPLE HL 399.1448009 MHz
 Power 41 dB
 continuously on
 WALTZ-16 modulated
 DATA PROCESSING
 Line broadening 1.0 Hz
 FT size 65536
 Total time 8 hr, 32 min

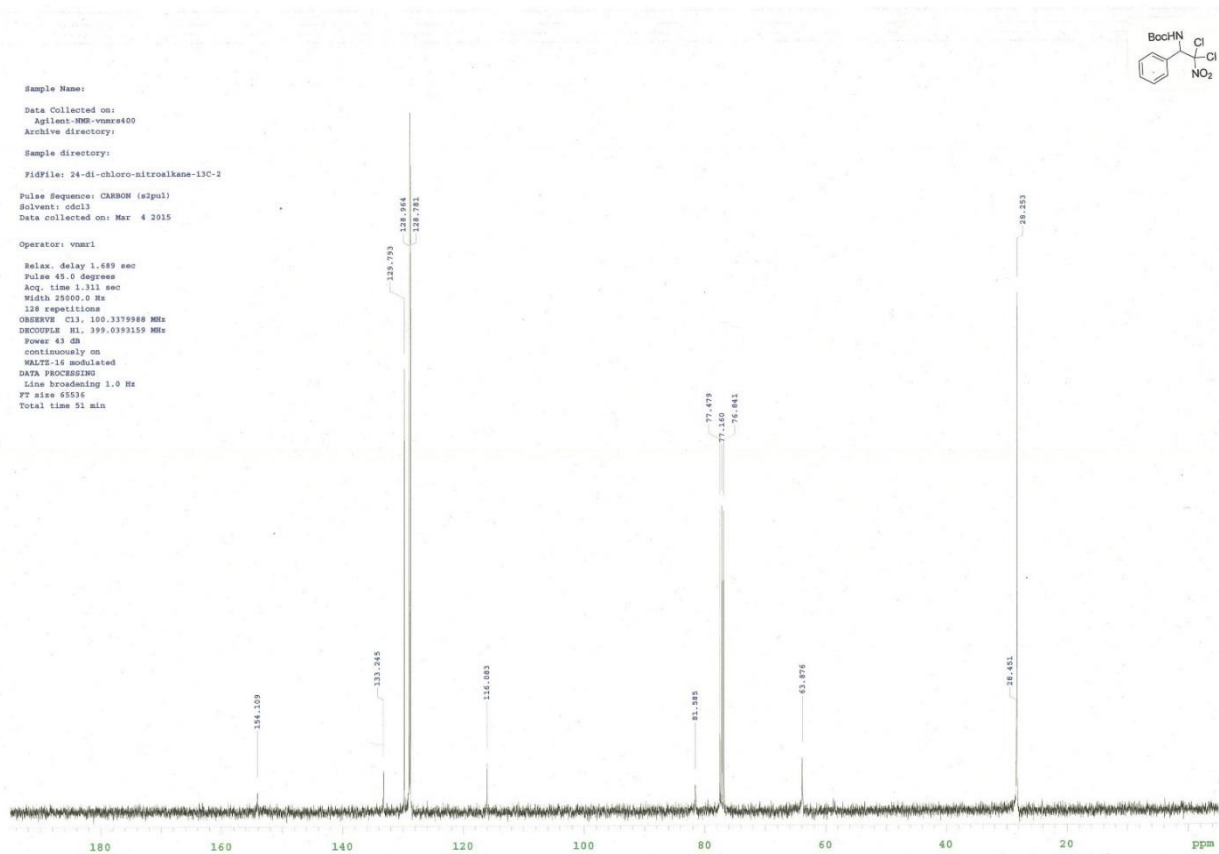
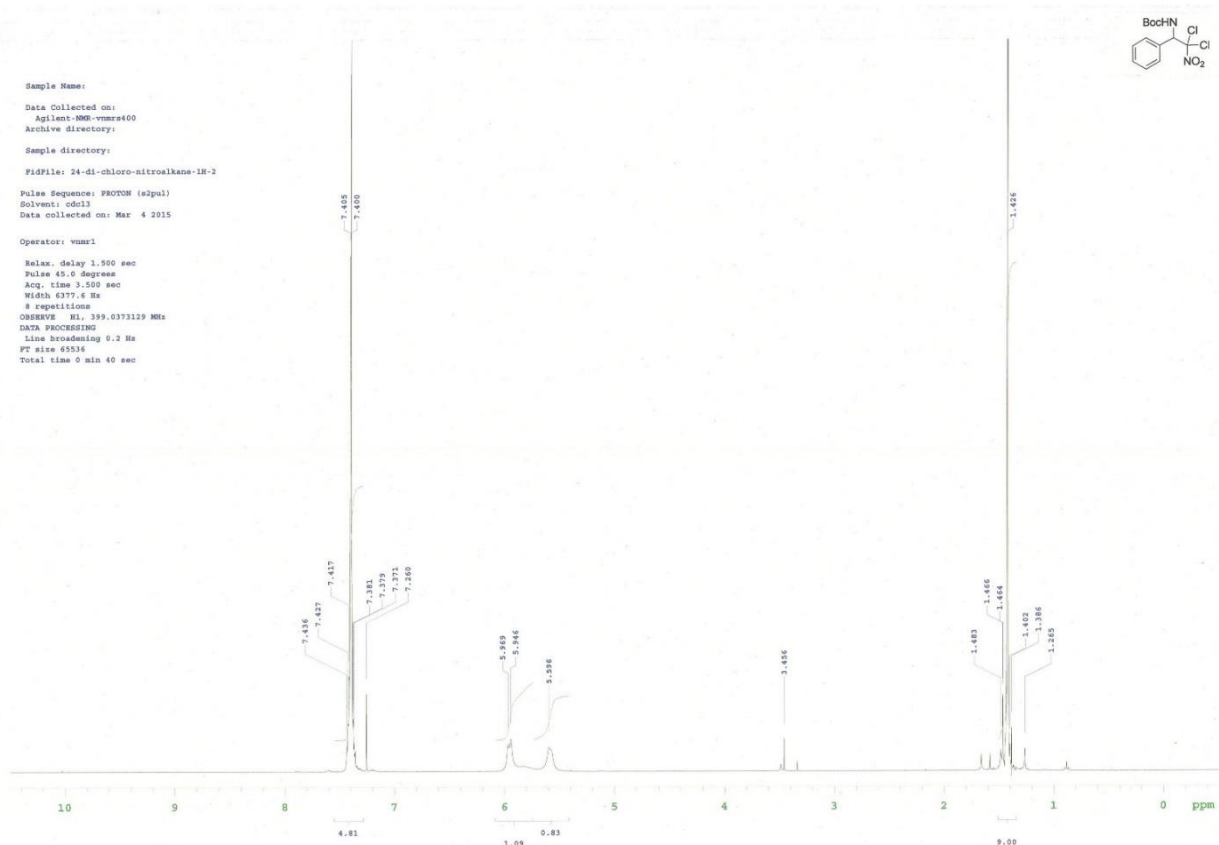


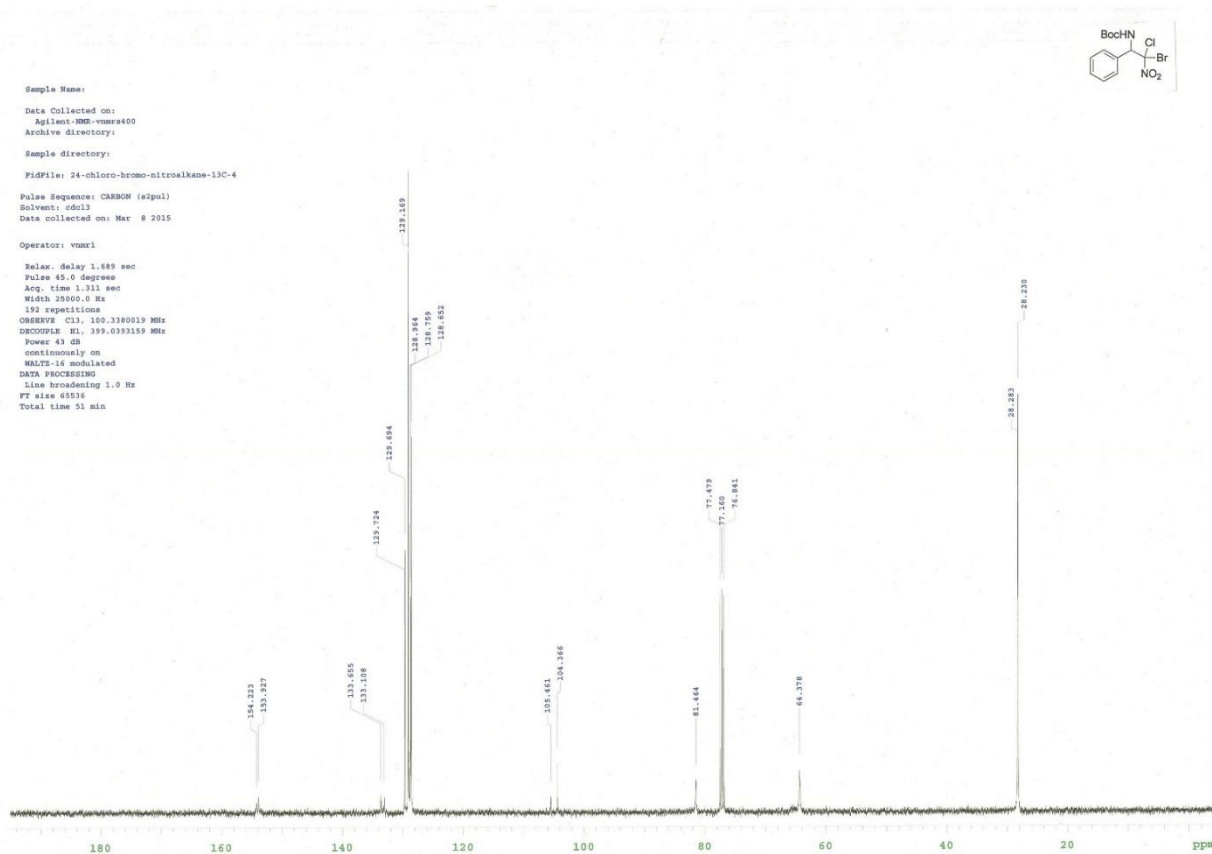
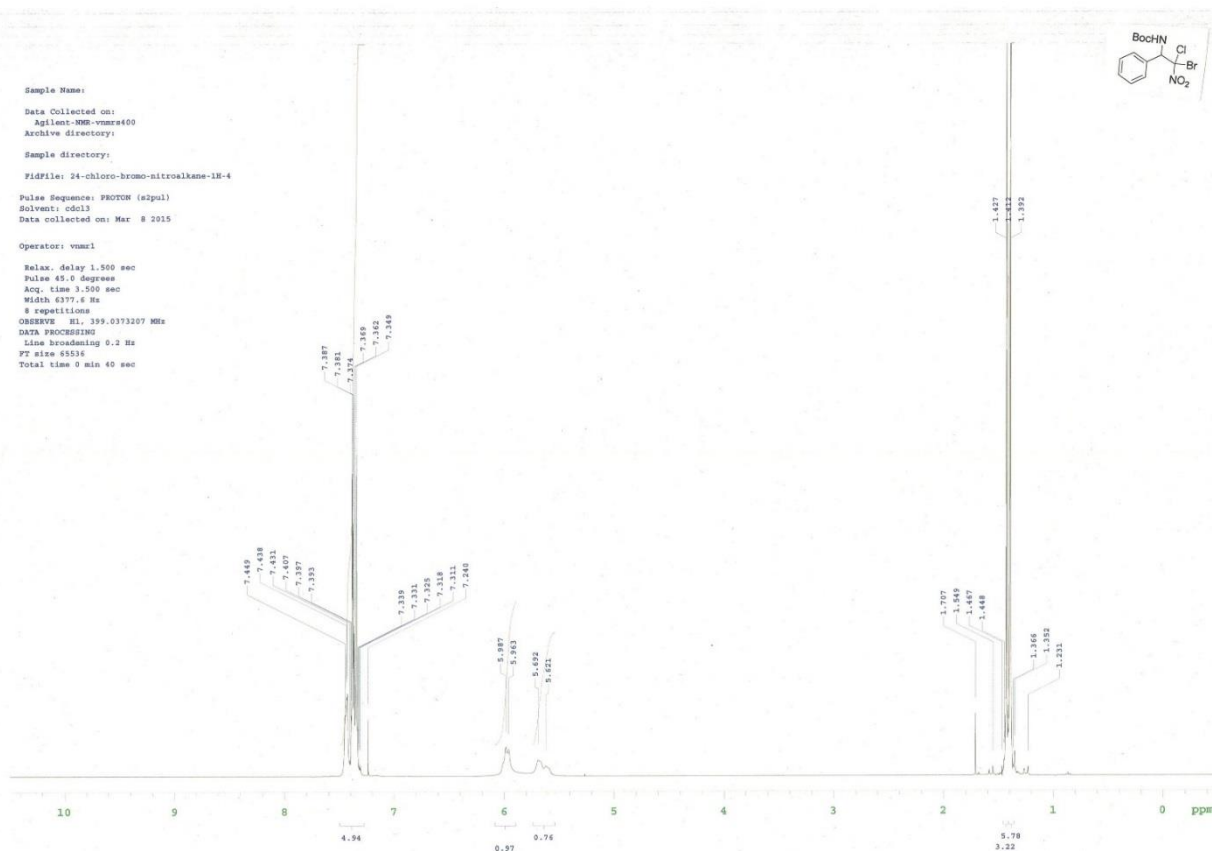
Sample Name:
 Data Collected on:
 Agilent-DMG-vnmr400
 Archive directory:
 Sample directory:
 FIDFile: PROTON
 Pulse Sequence: PROTON (s2pul)
 Solvent: cdcl3
 Data collected on: Sep 16 2014
 Operator: vnmr1
 Relax. delay 1.550 sec
 Pulse 45.0 degrees
 Acq. time 3.500 sec
 Width 6377.6 Hz
 8 repetitions
 OBSERVE HL 399.1446075 MHz
 DATA PROCESSING
 Line broadening 0.2 Hz
 FT size 65536
 Total time 0 min 40 sec

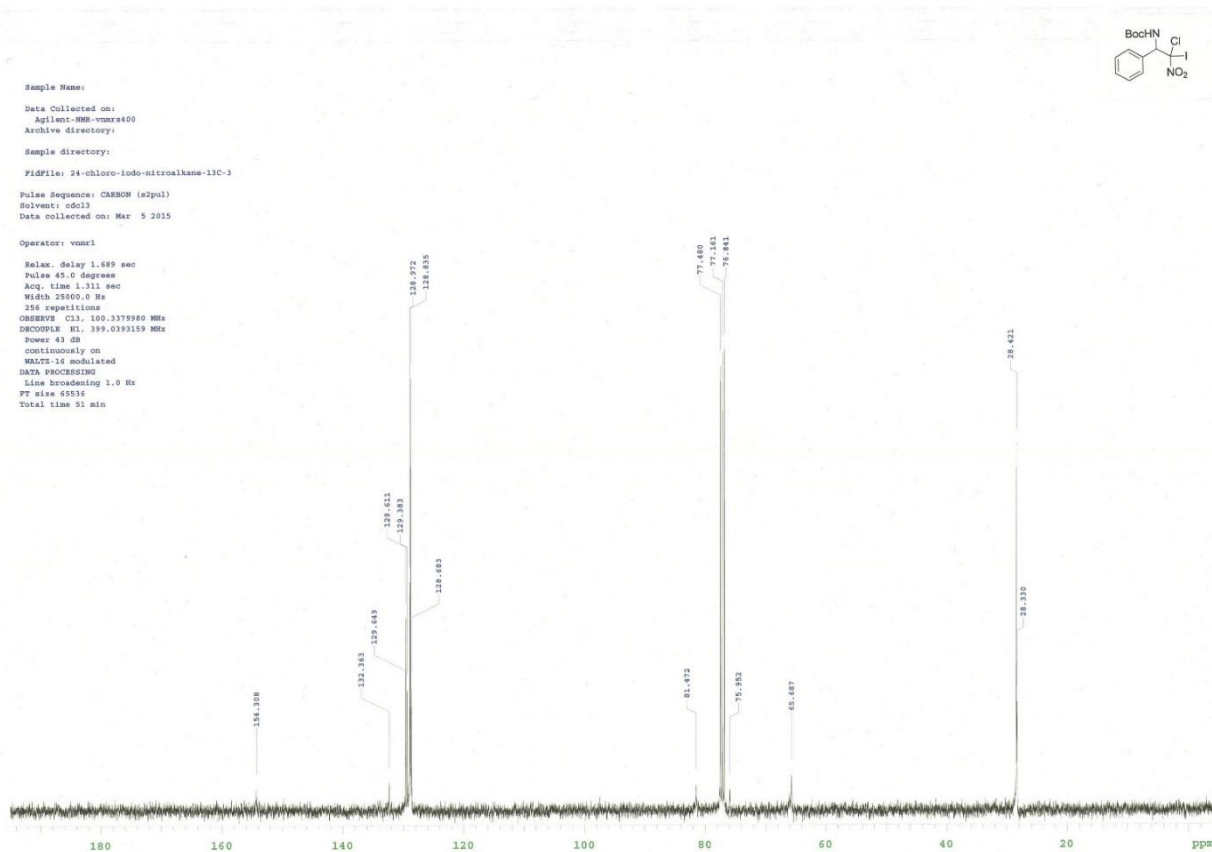
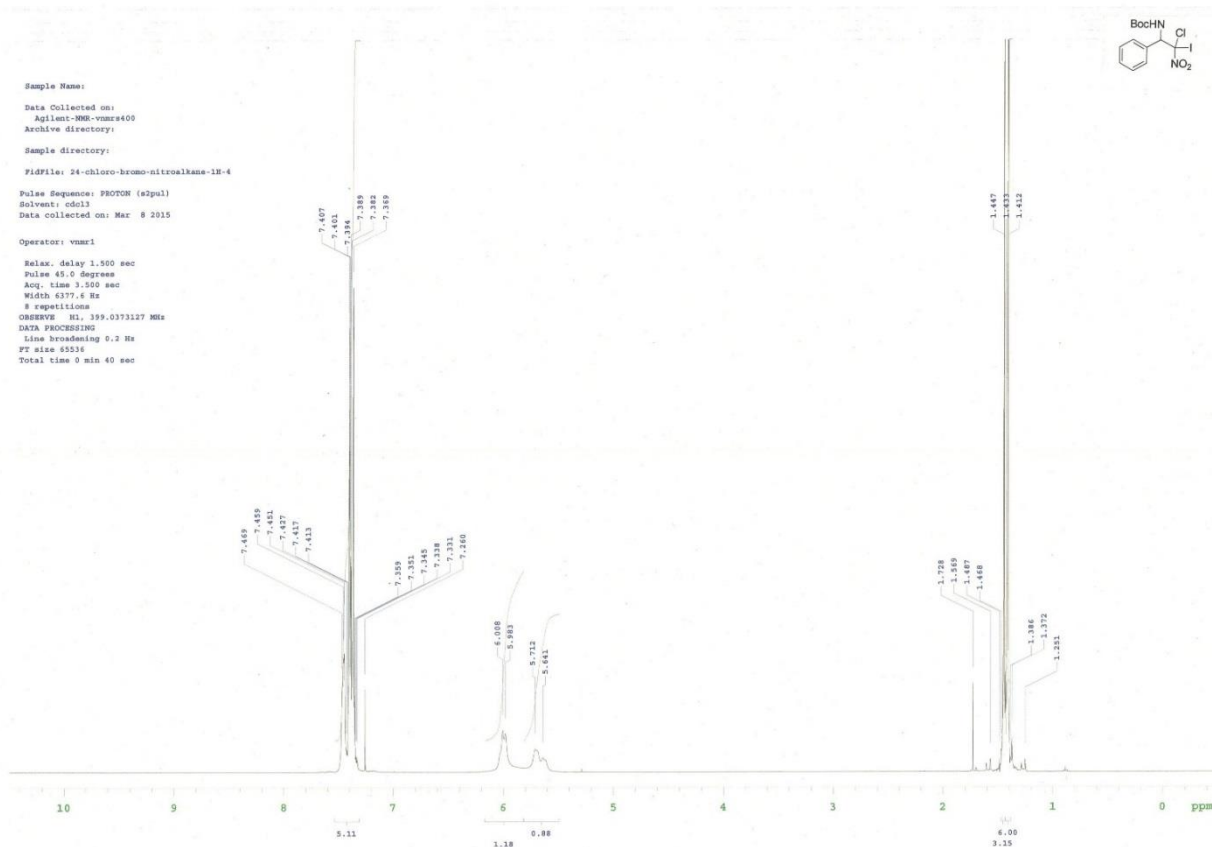


Sample Name:
 Data Collected on:
 Agilent-DMG-vnmr400
 Archive directory:
 Sample directory:
 FIDFile: CARBON
 Pulse Sequence: CARBON (s2pul)
 Solvent: cdcl3
 Data collected on: Sep 16 2014
 Temp. 26.0 C / 299.1 K
 Operator: vnmr1
 Relax. delay 1.669 sec
 Pulse 45.0 degrees
 Acq. time 1.311 sec
 Width 25000.0 Hz
 1280 repetitions
 OBSERVE C13 100.6250417 MHz
 DECOUPLE HL 399.1446075 MHz
 Power 41.0W
 continuously on
 WALTZ-16 modulated
 DATA PROCESSING
 Line broadening 1.0 Hz
 FT size 65536
 Total time 1 hr, 41 min

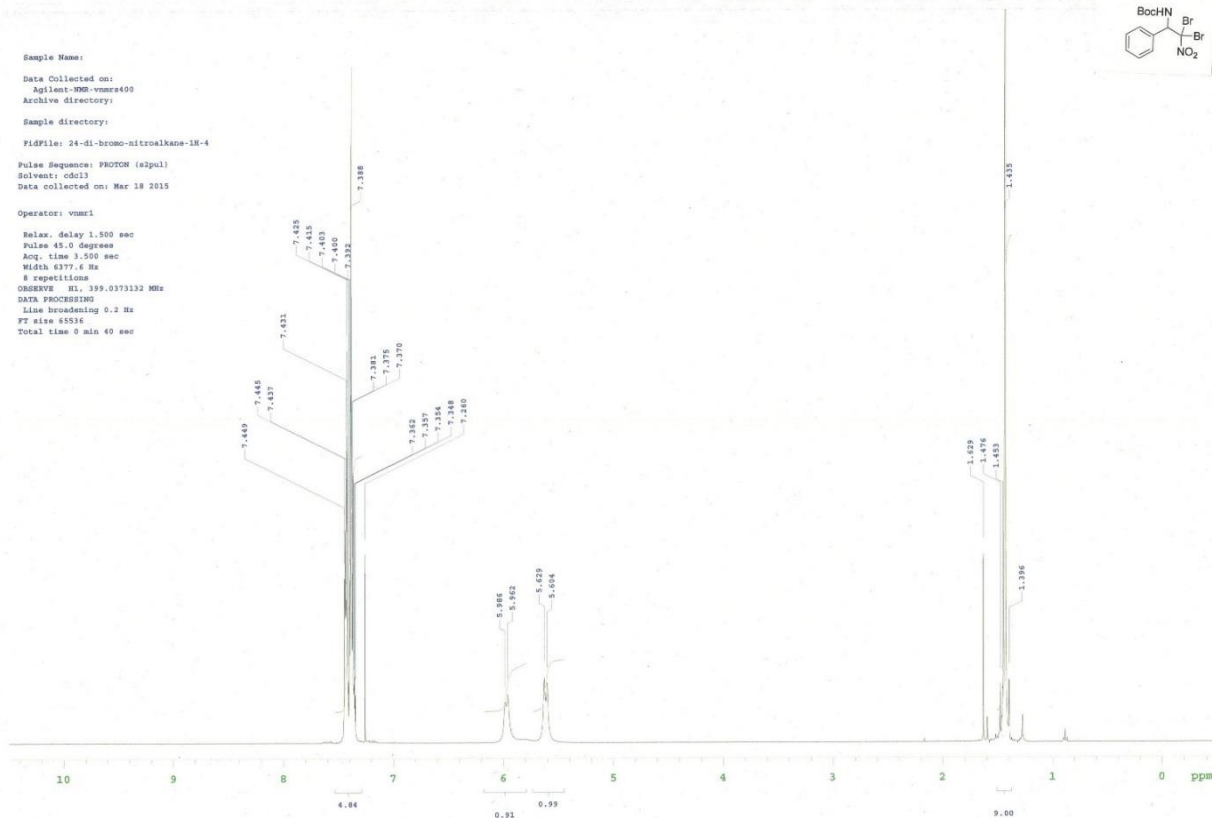




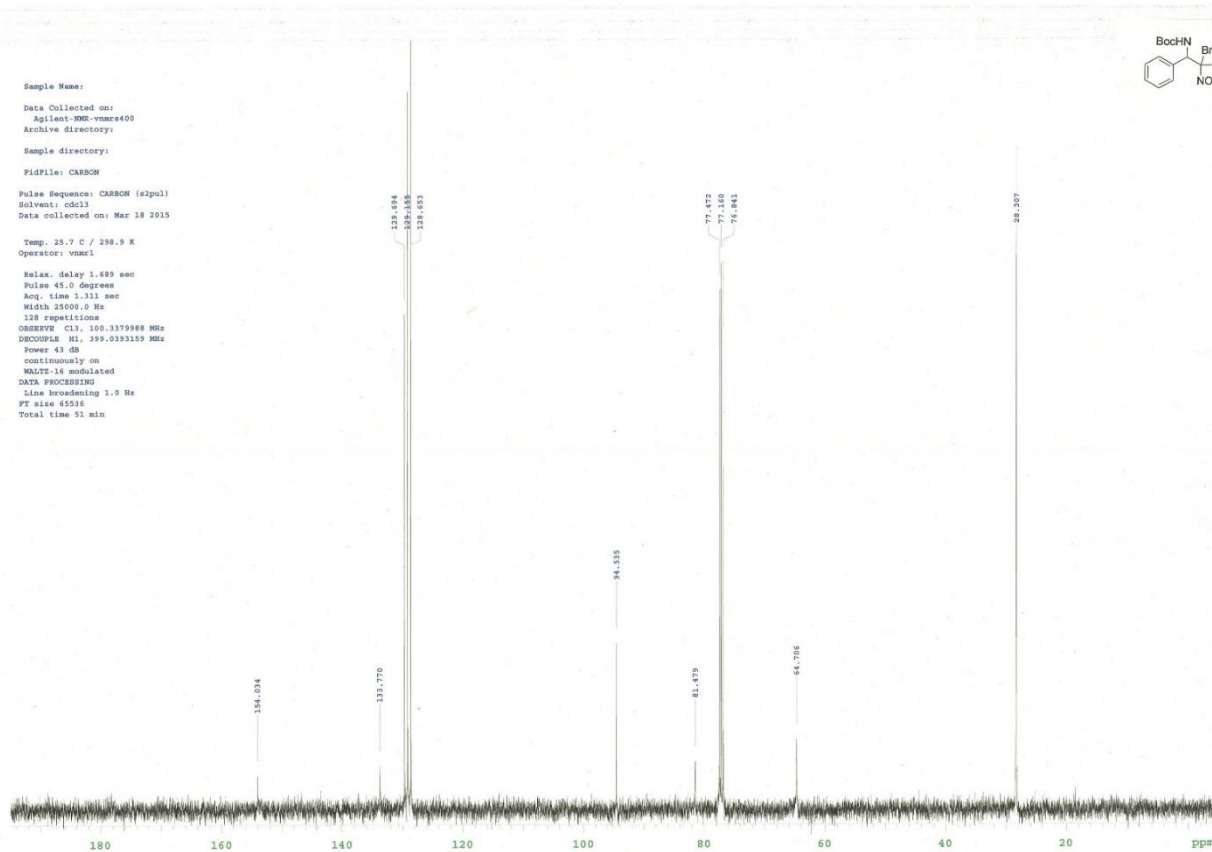


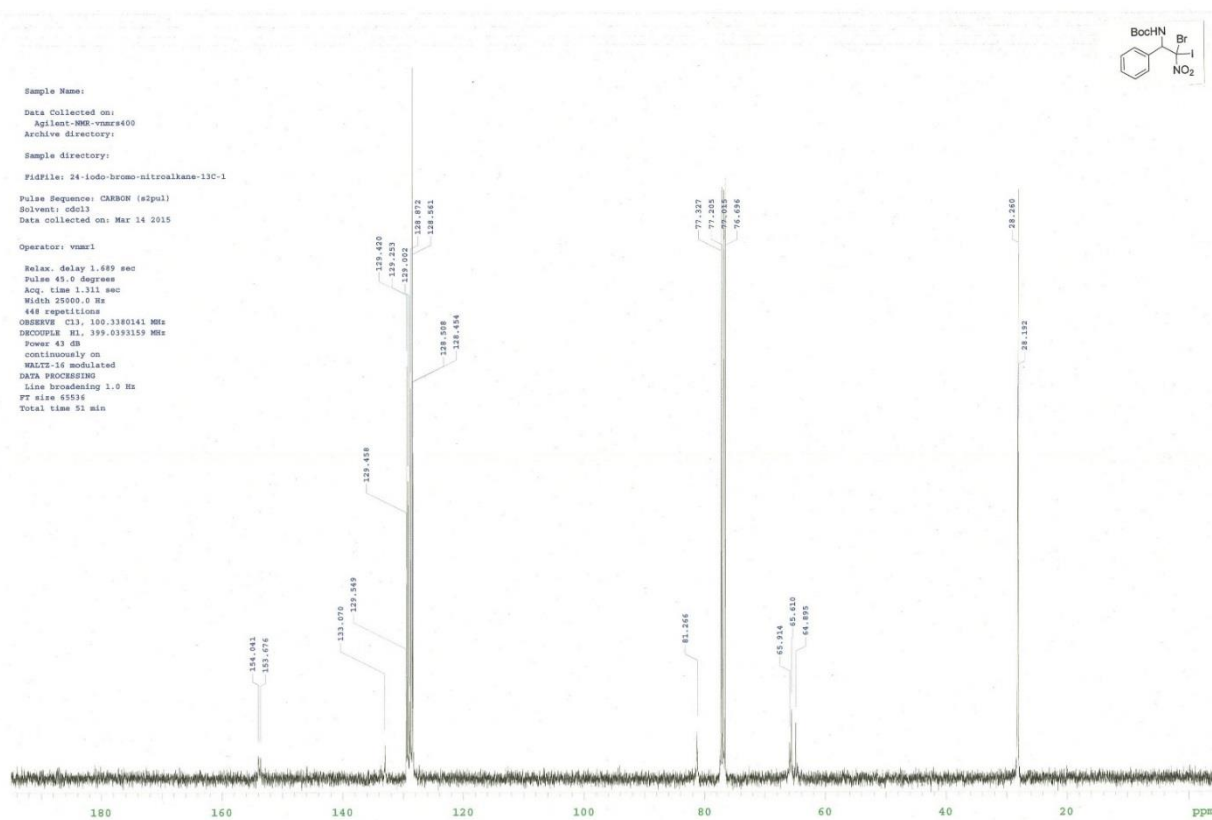
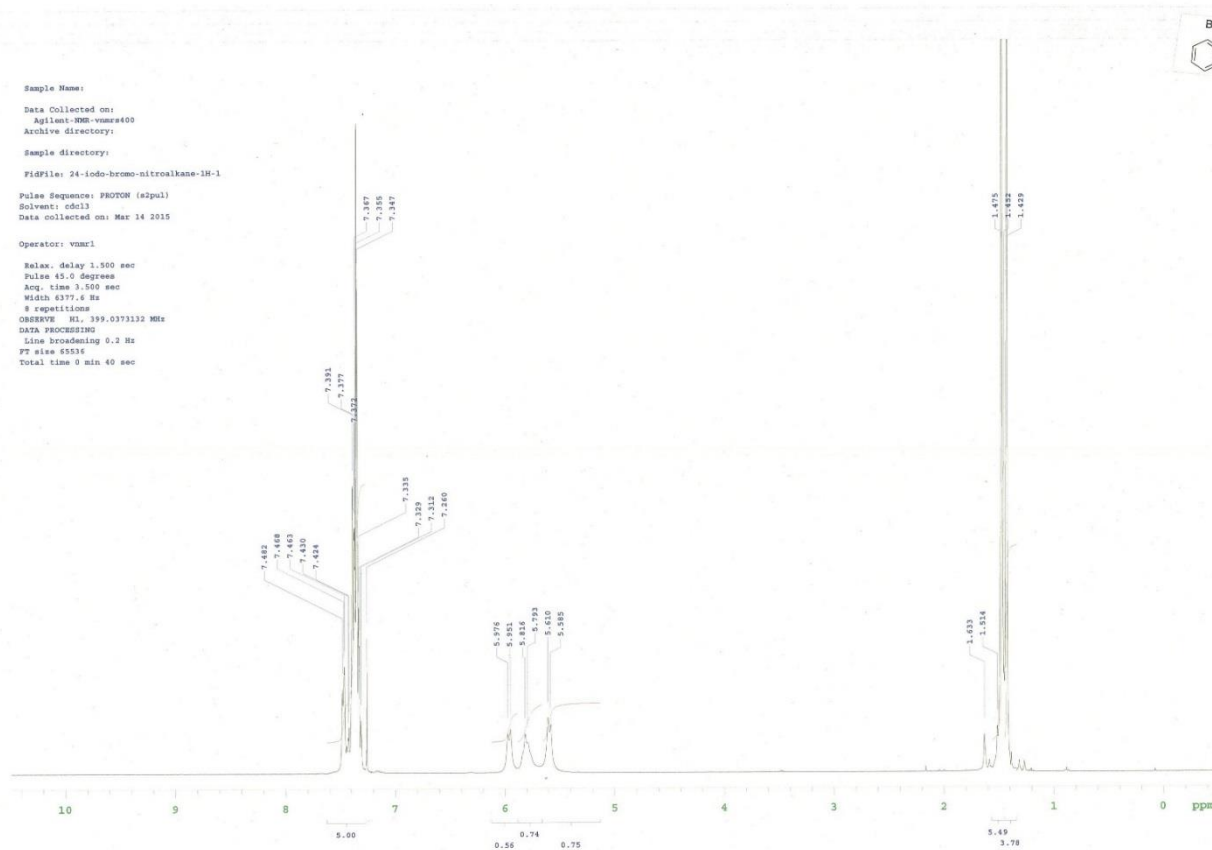


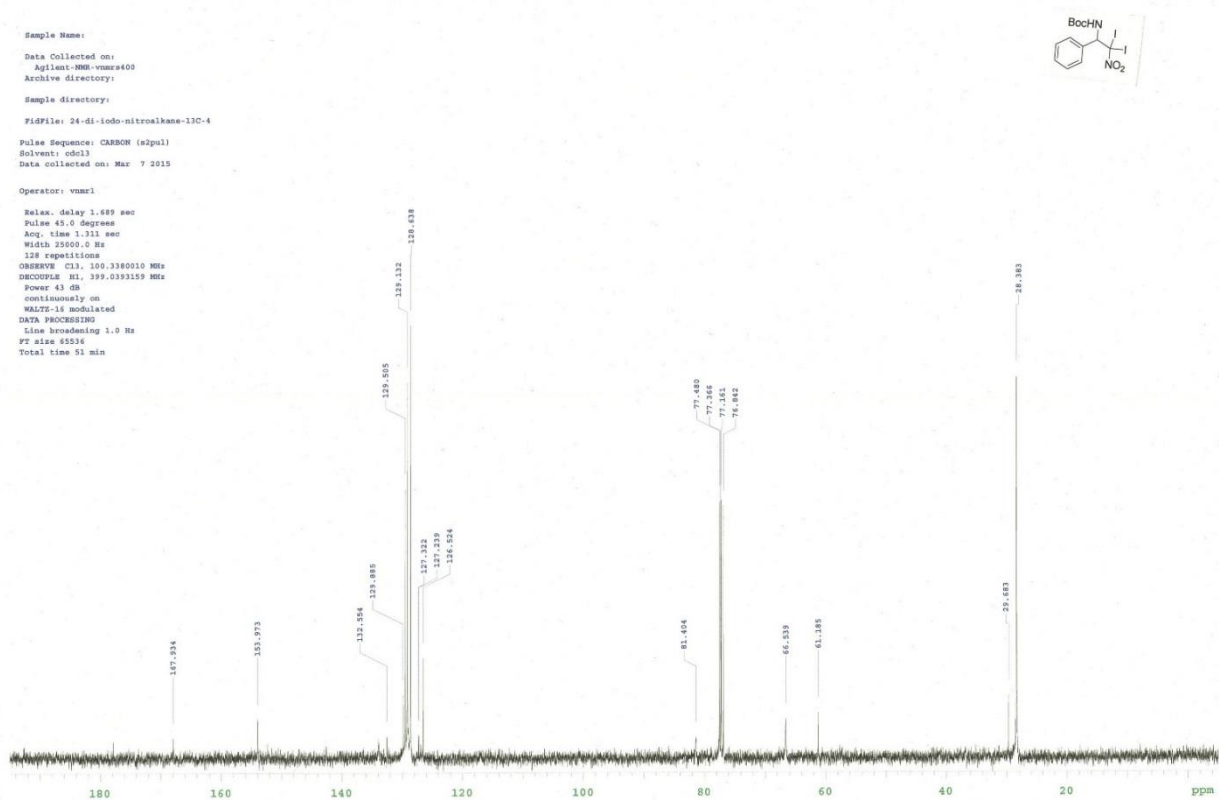
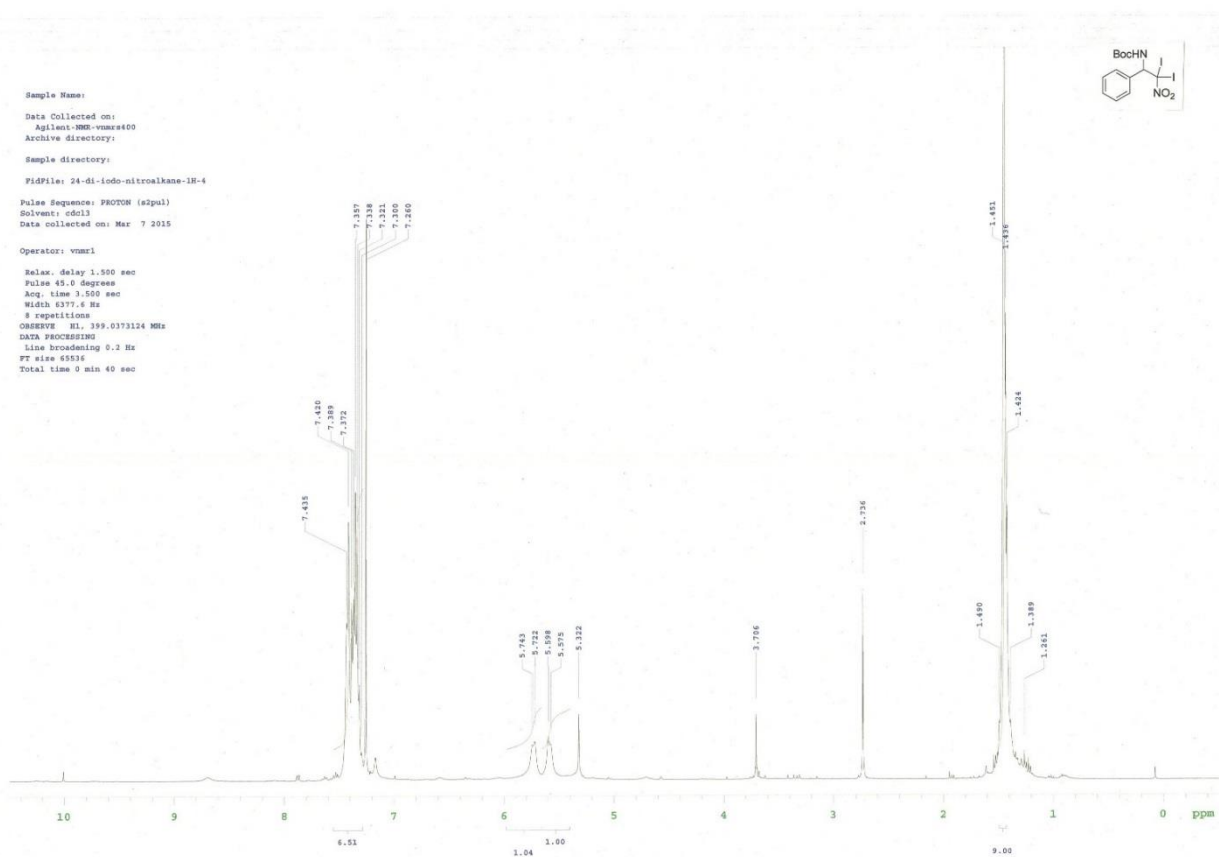
Sample Name:
 Data Collected on:
 Agilent-MMR-vnmr400
 Archive directory:
 Sample directory:
 FIDFile: 24-di-bromo-nitroalkane-1H-4
 Pulse Sequence: PROTON (a2pul)
 Solvent: cdcl3
 Data collected on: Mar 18 2015
 Operator: vnmr1
 Relax. delay 1.500 sec
 Pulse 45.0 degree
 Acq. time 3.500 sec
 Width 6377.6 Hz
 8 repetitions
 OBSERVE H1, 399.0375132 MHz
 DATA PROCESSING
 Line broadening 0.2 Hz
 FT size 65536
 Total time 0 min 40 sec

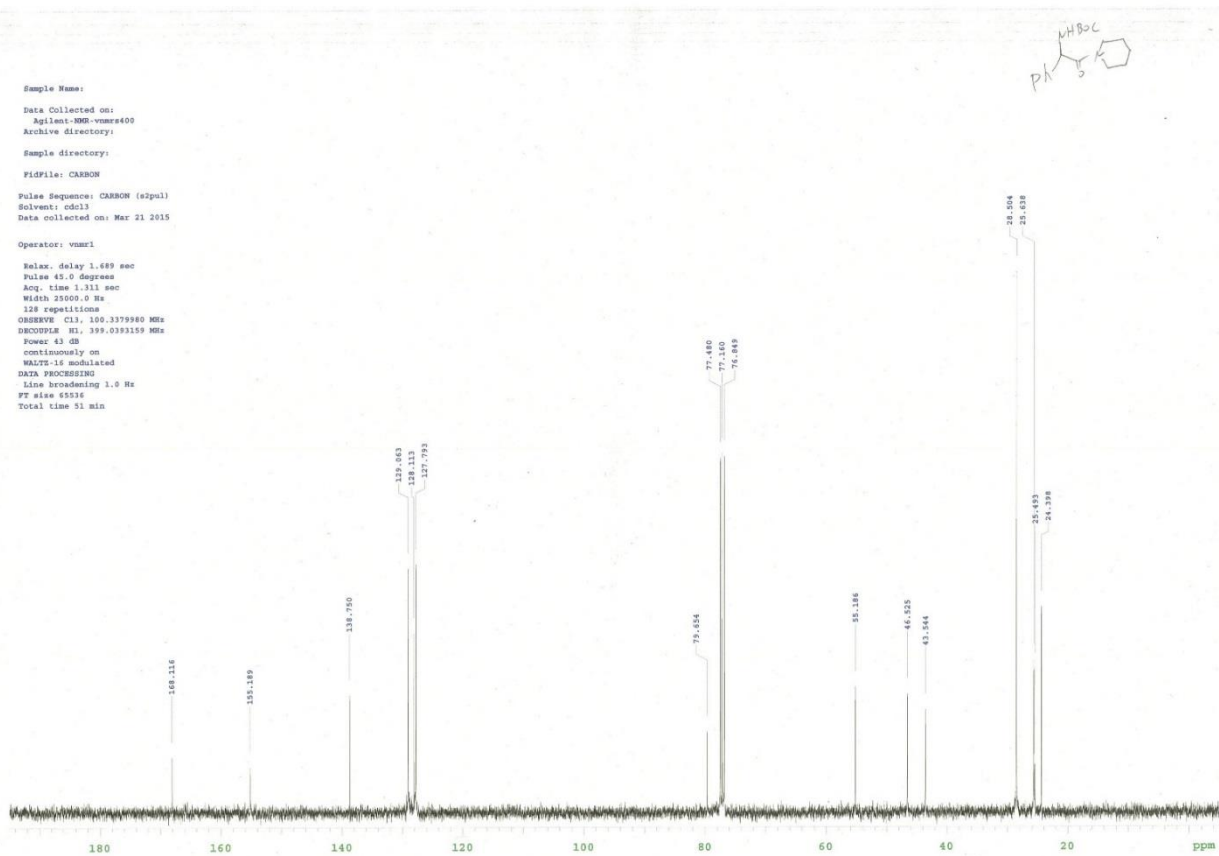
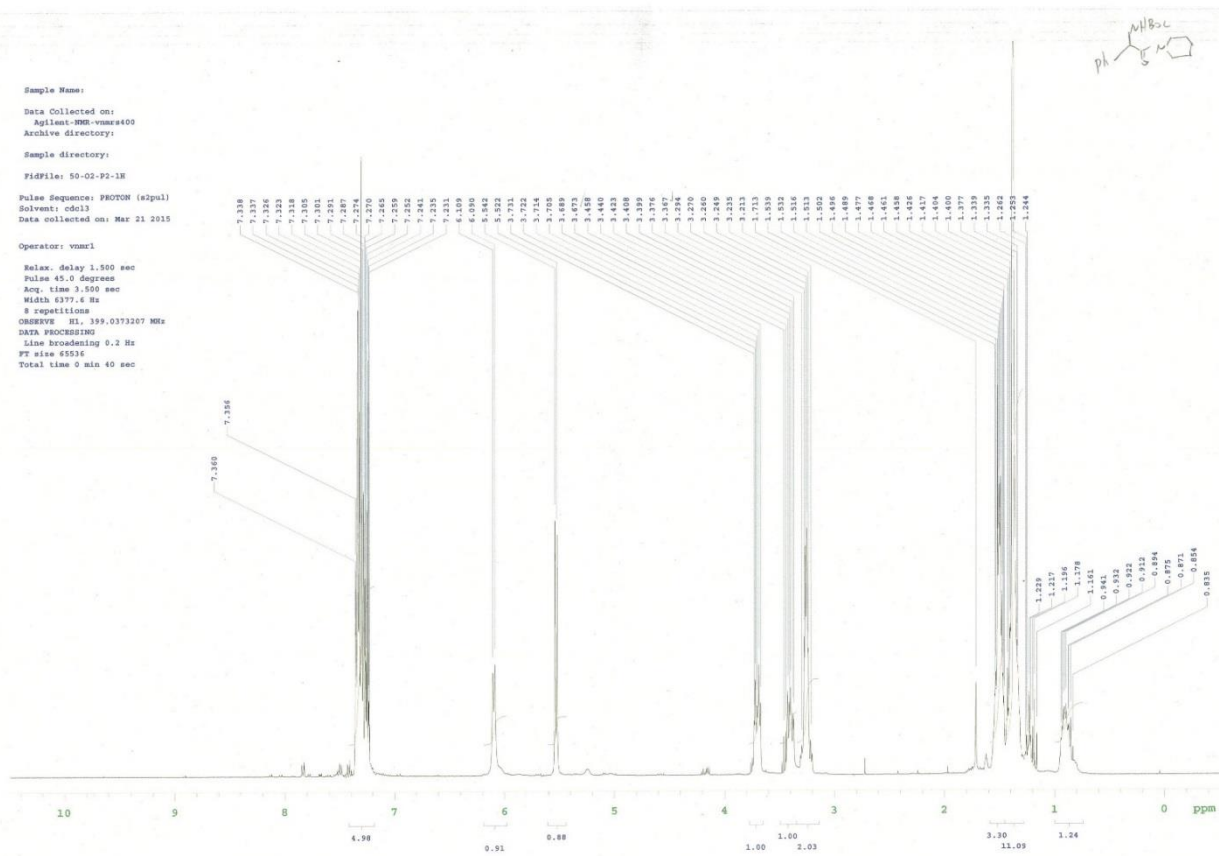


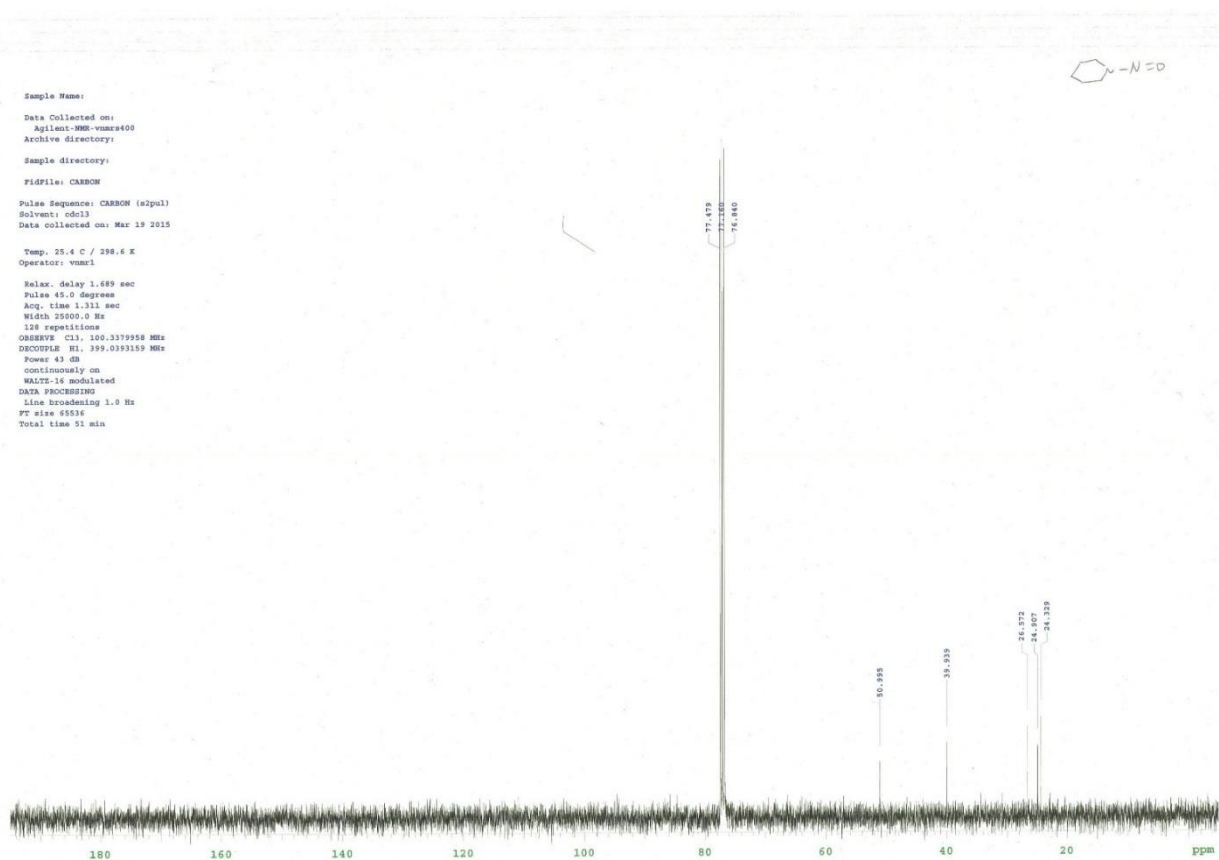
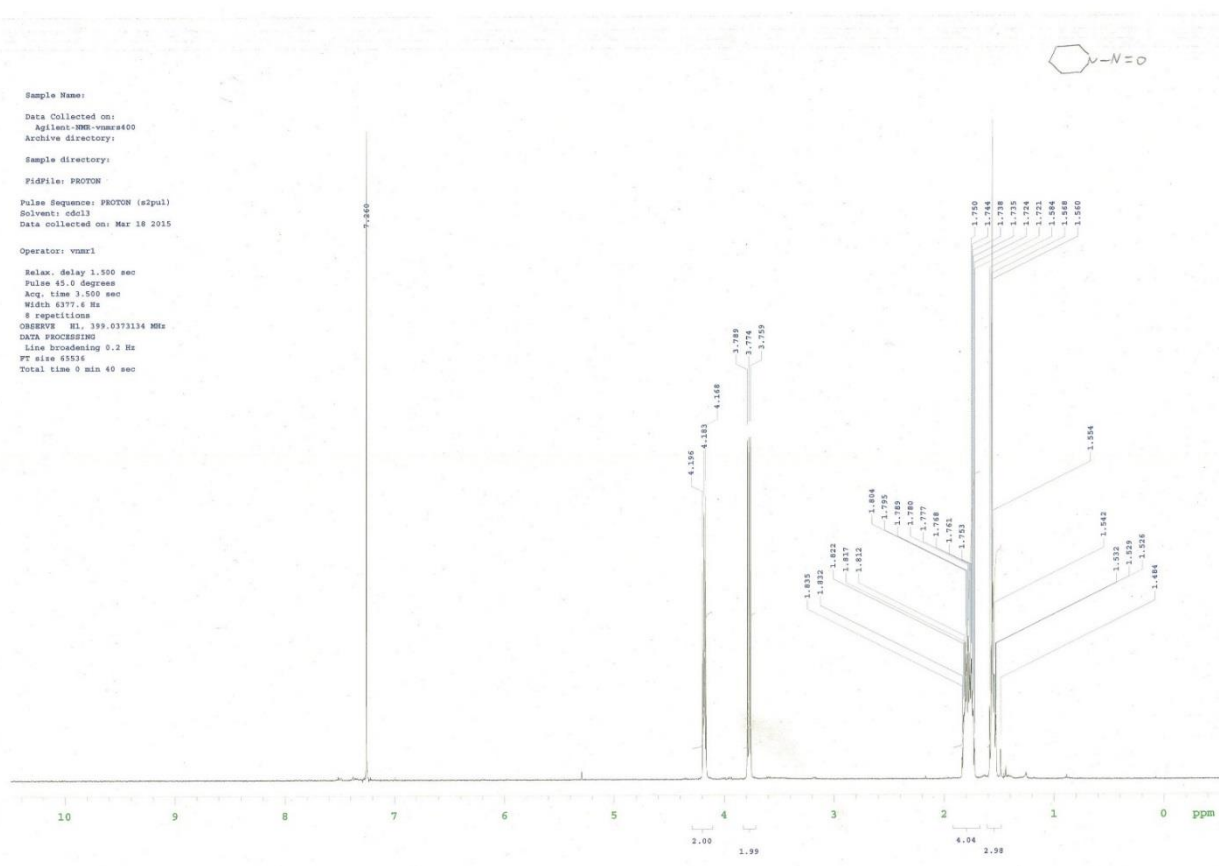
Sample Name:
 Data Collected on:
 Agilent-MMR-vnmr400
 Archive directory:
 Sample directory:
 FIDFile: CARBON
 Pulse Sequence: CARBON (a2pul)
 Solvent: cdcl3
 Data collected on: Mar 18 2015
 Temp. 25.7 C / 259.9 K
 Operator: vnmr1
 Relax. delay 1.689 sec
 Pulse 45.0 degree
 Acq. time 1.311 sec
 Width 25000.0 Hz
 128 repetitions
 OBSERVE C13, 100.3779868 MHz
 DECOUPLE H1, 399.0393159 MHz
 Power 43 dB
 continuously on
 WALTZ-16 modulated
 DATA PROCESSING
 Line broadening 1.0 Hz
 FT size 65536
 Total time 51 min

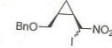
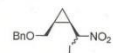


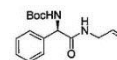




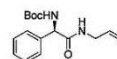
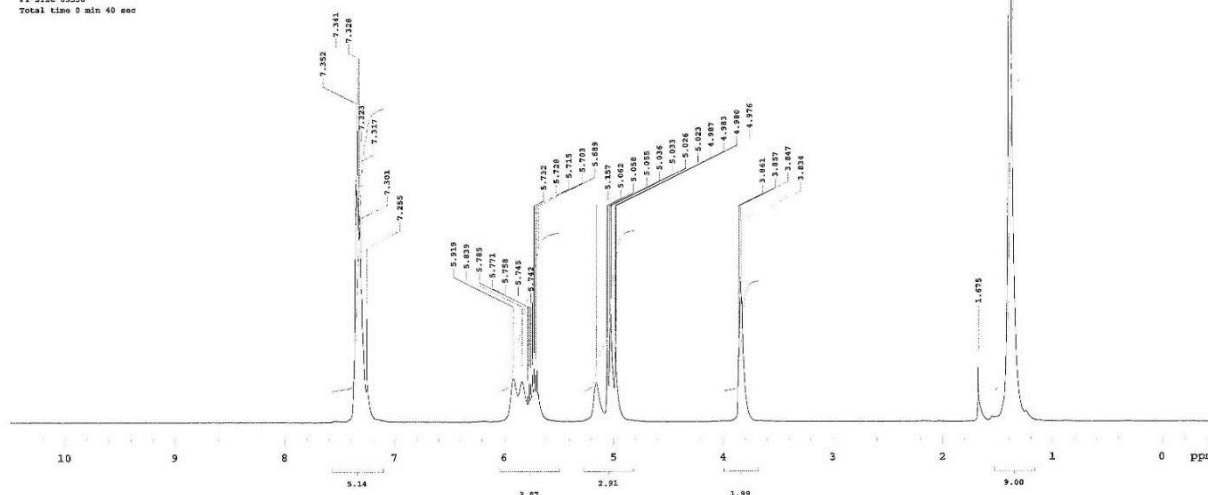




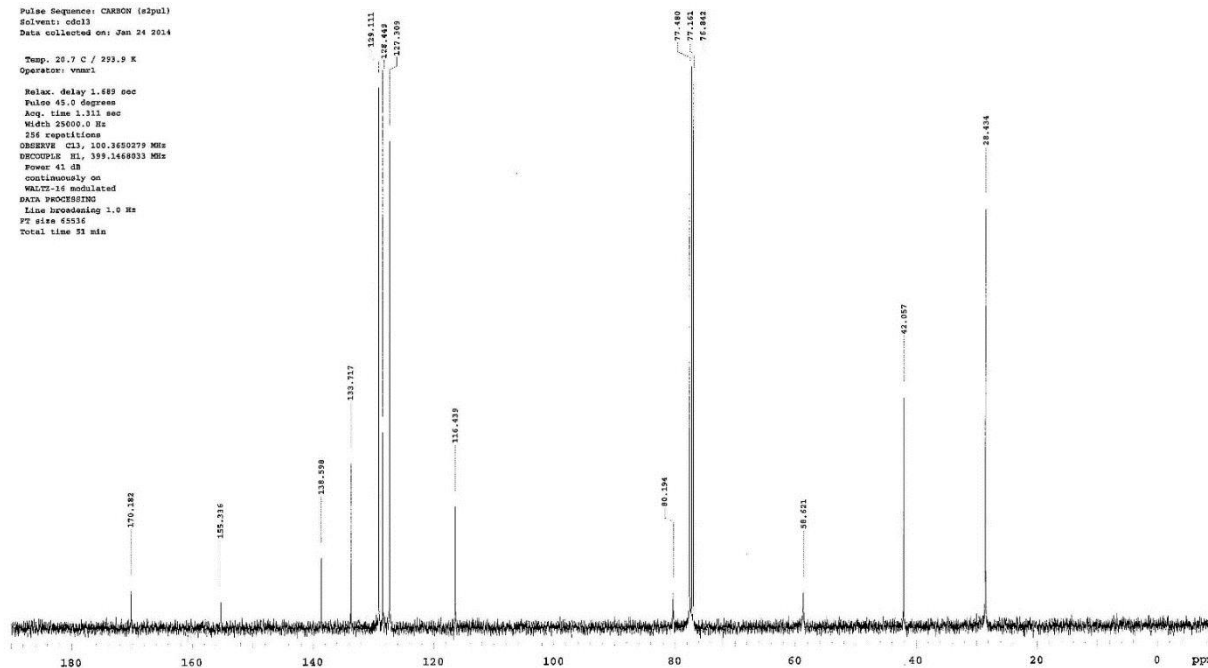


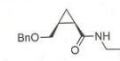
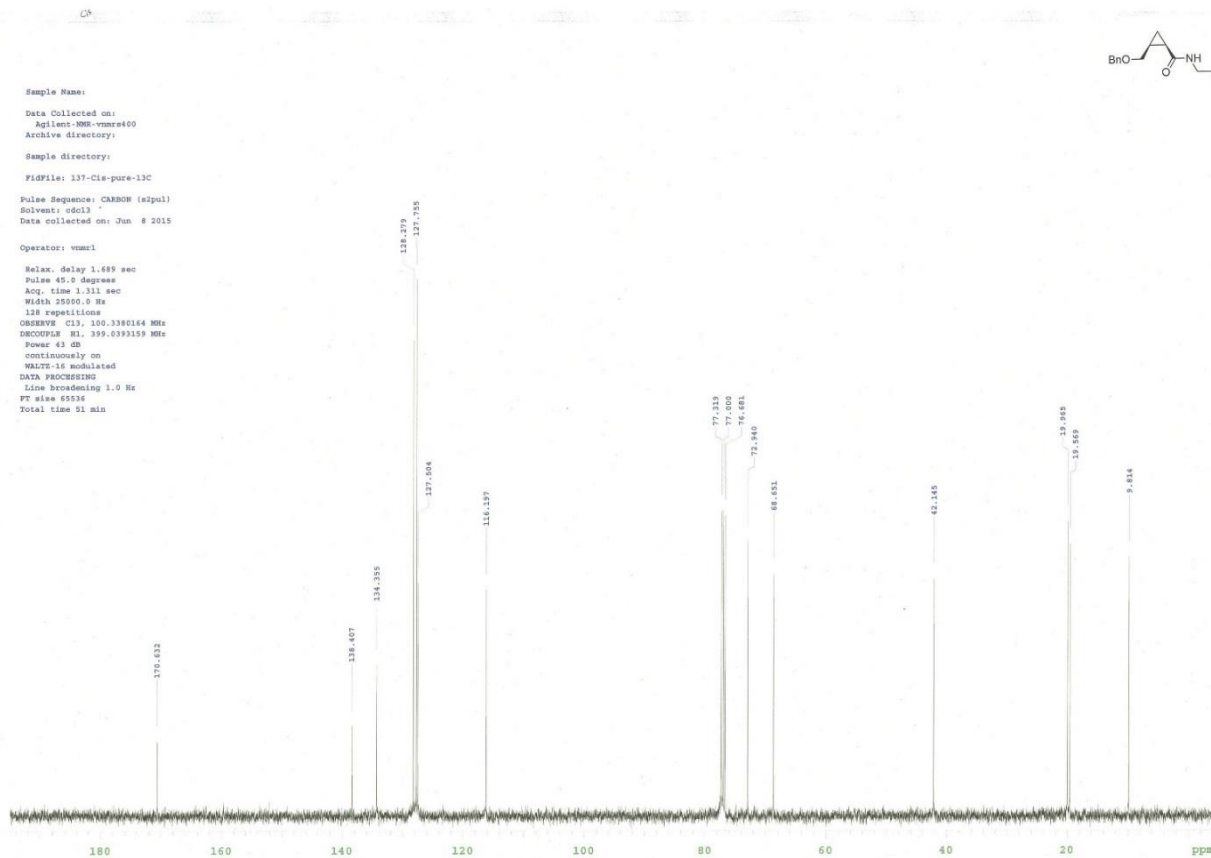
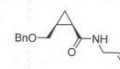
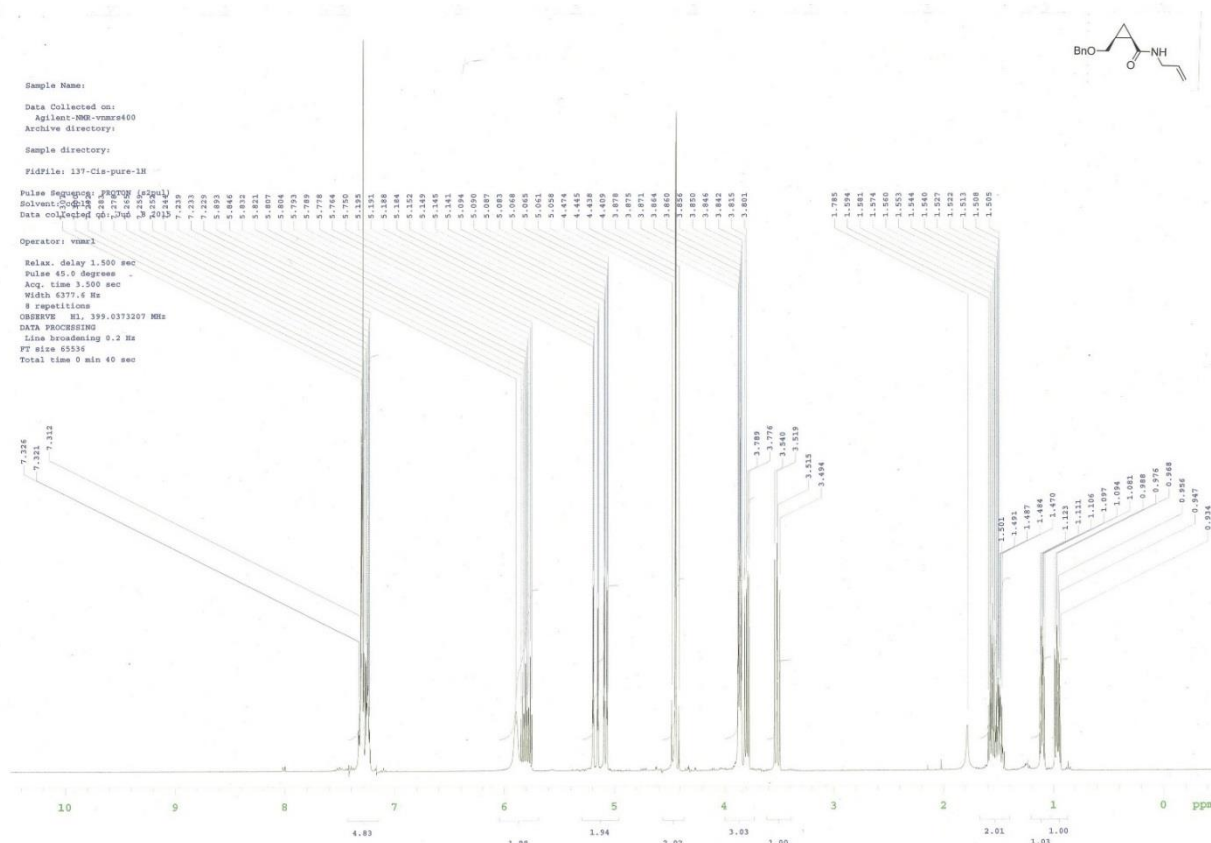


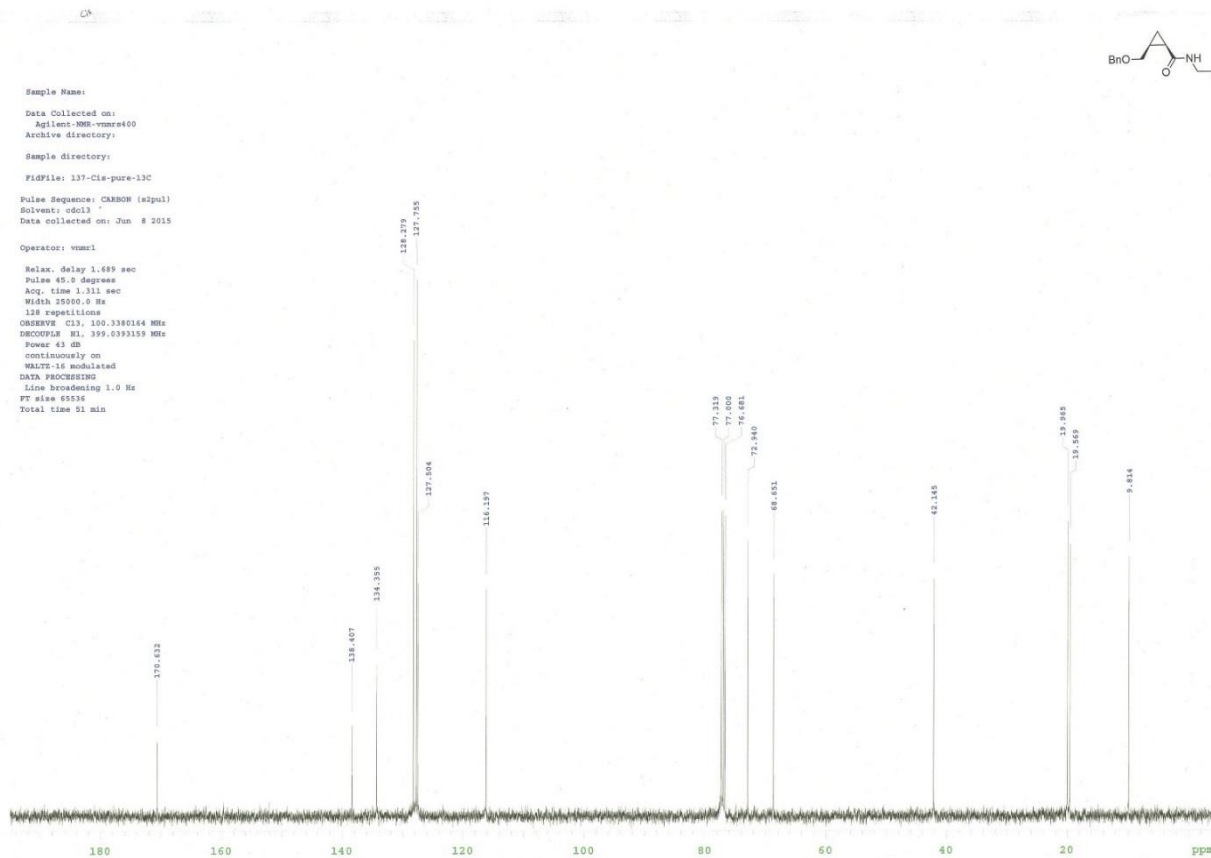
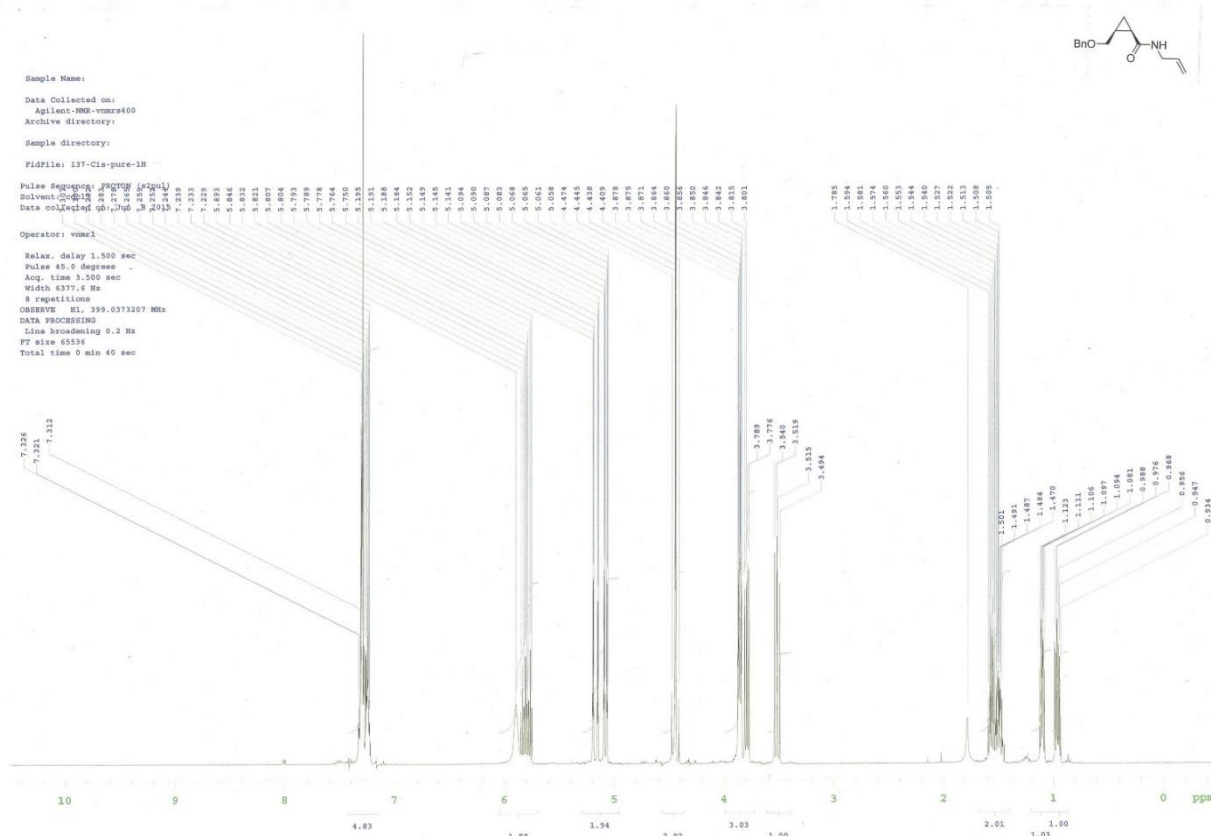
Sample Name:
 Data Collected on:
 Agilent-900-vnmr400
 Archive directory:
 Sample directory:
 FIDFile: PROTON
 Pulse Sequence: PROTON (zgpg3)
 Solvent: cdcl3
 Data collected on: Jan 24 2014
 Operator: vnmr1
 Relax. delay 1.500 sec
 Pulse 45.0 degrees
 Acq. time 3.500 sec
 Width 6377.6 Hz
 8 repetitions
 OBSERVE H1, 399.1448073 MHz
 DATA PROCESSING
 Line broadening 0.2 Hz
 FT size 65536
 Total time 8 min 40 sec



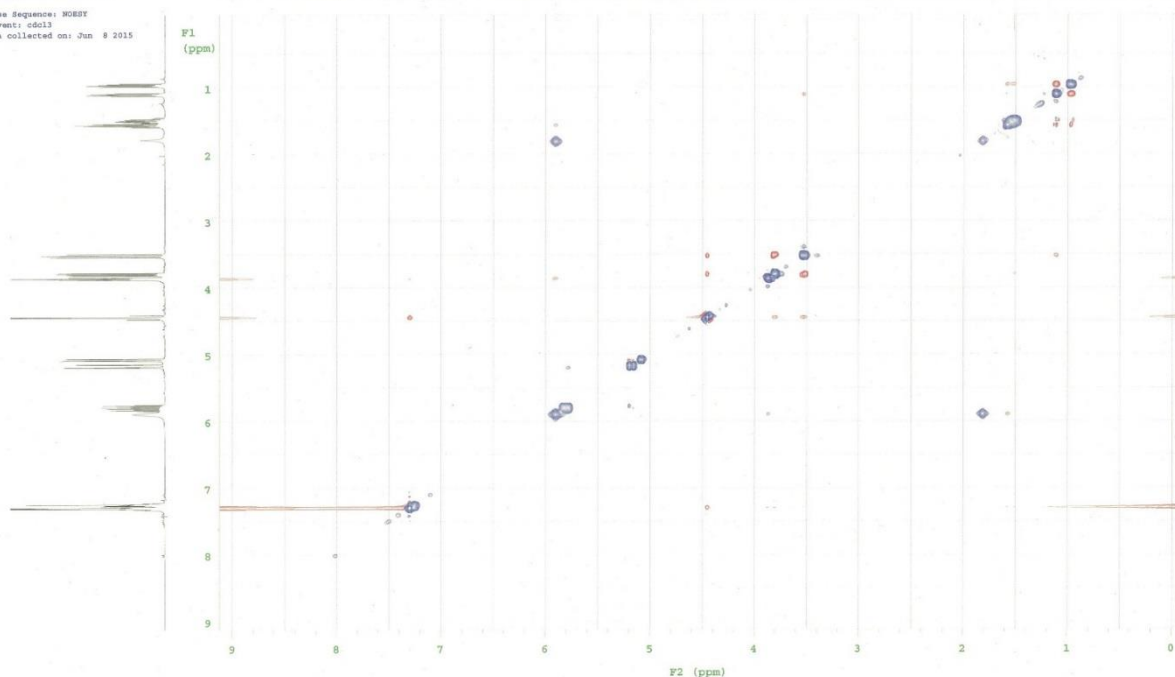
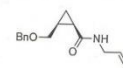
Sample Name:
 Data Collected on:
 Agilent-900-vnmr400
 Archive directory:
 Sample directory:
 FIDFile: CARBON
 Pulse Sequence: CARBON (zgpg3)
 Solvent: cdcl3
 Data collected on: Jan 24 2014
 Temp: 25.7 C / 299.9 K
 Operator: vnmr1
 Relax. delay 1.400 sec
 Pulse 45.0 degrees
 Acq. time 1.311 sec
 Width 25600.0 Hz
 256 repetitions
 OBSERVE C13, 100.625073 MHz
 DECOUPLE H1, 399.1448073 MHz
 Power 41 dB
 continuously on
 WALTZ-16 modulated
 DATA PROCESSING
 Line broadening 1.0 Hz
 FT size 65536
 Total time 23 min



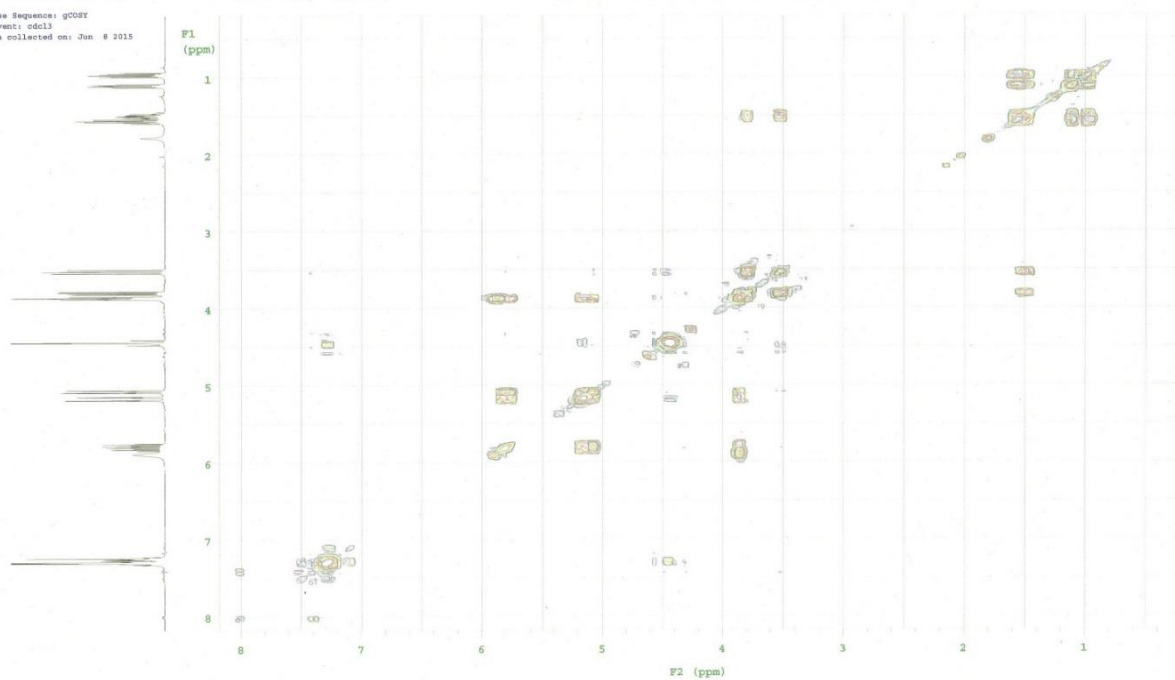
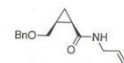


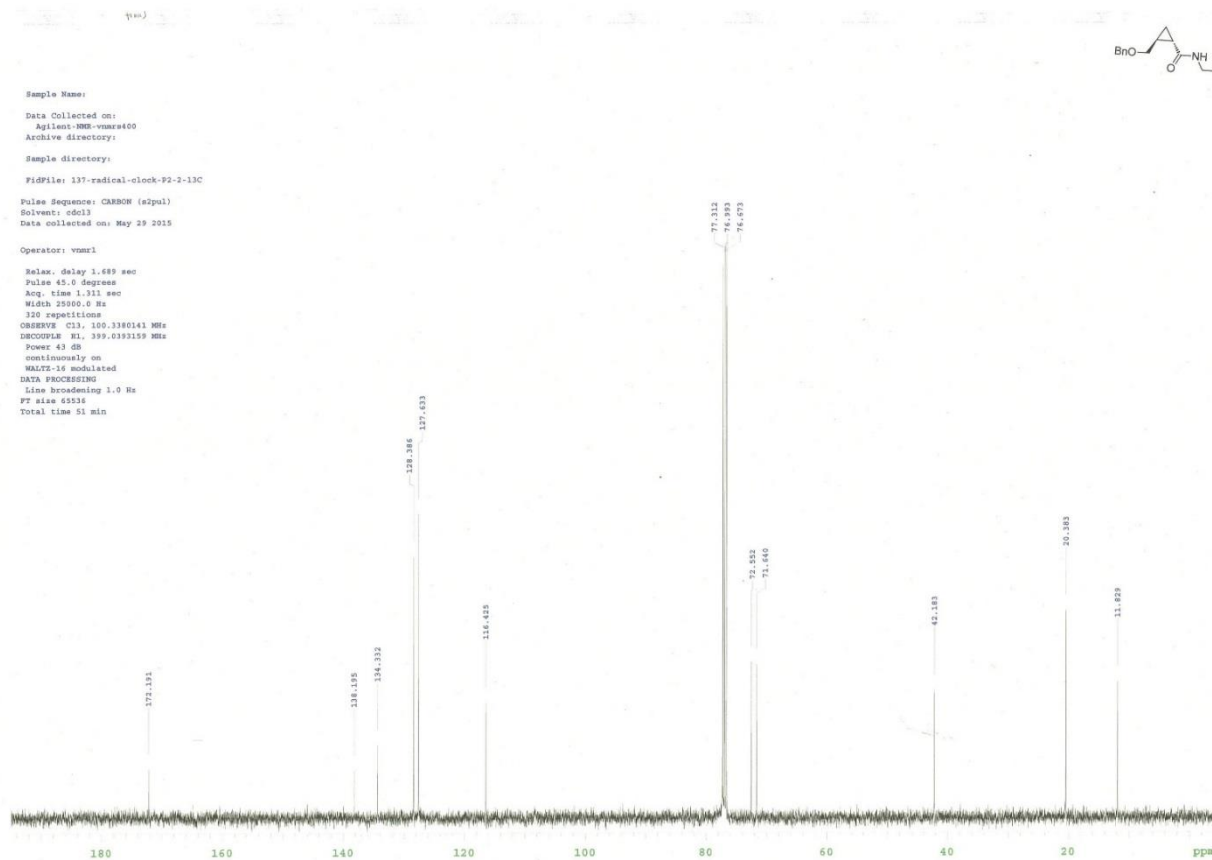
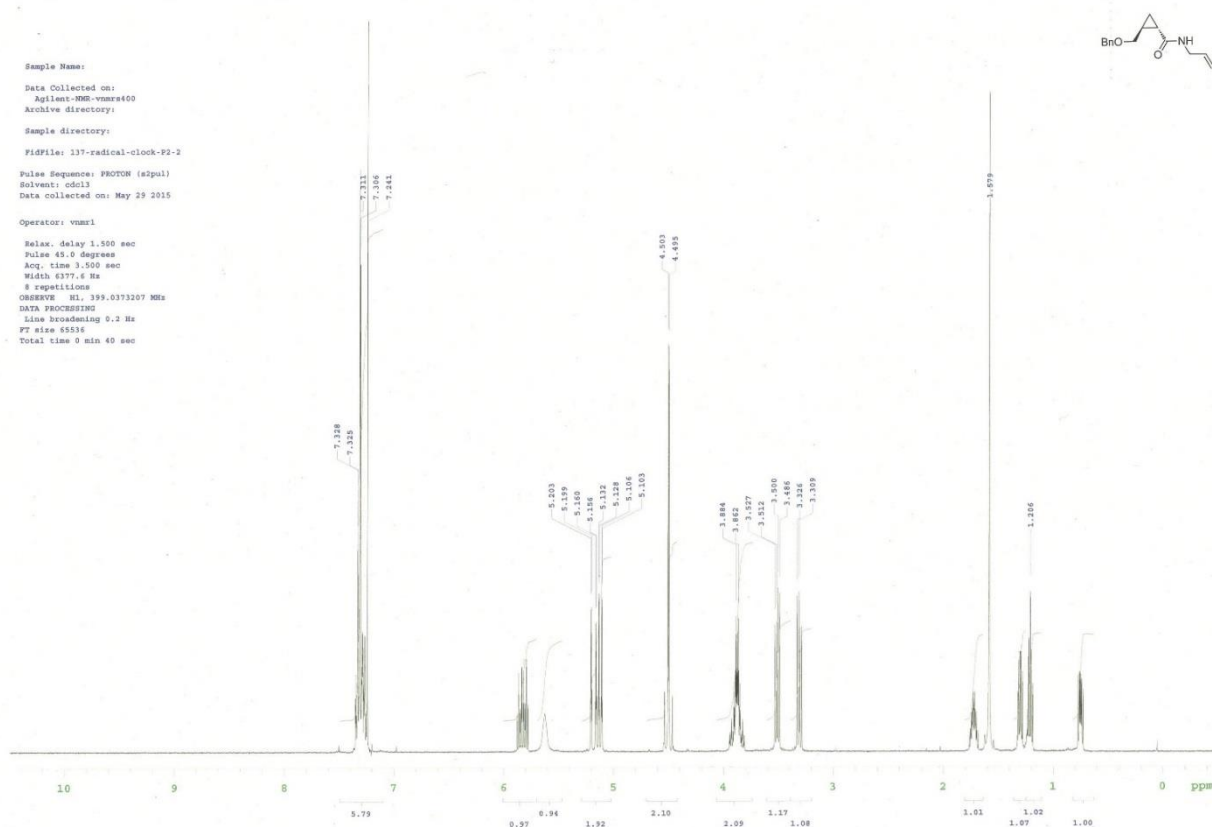


Sample Name:
 Data Collected on:
 Apilient-900-vmrst600
 Archive directory:
 Sample directory:
 Fidfile: 137-Clis-pure-30E
 Pulse Sequence: MGESE
 Solvent: cdcl3
 Data collected on: Jun 8 2015

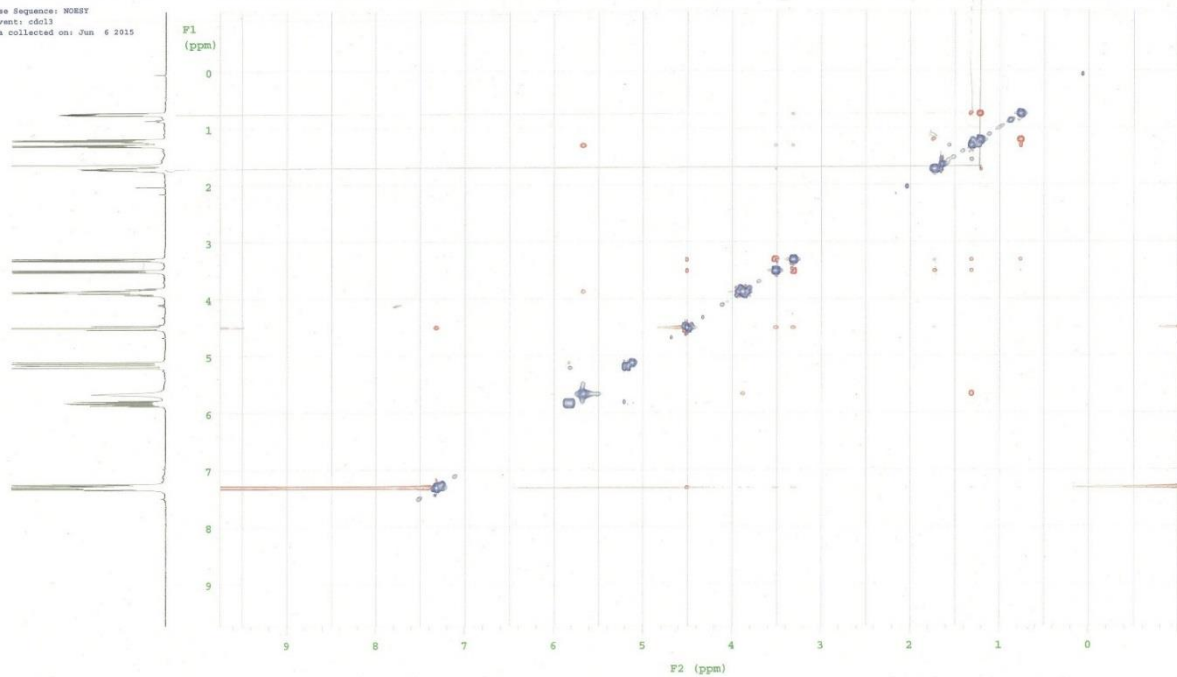


Sample Name:
 Data Collected on:
 Apilient-900-vmrst600
 Archive directory:
 Sample directory:
 Fidfile: 137-Clis-pure-Goosy
 Pulse Sequence: gCOSEY
 Solvent: cdcl3
 Data collected on: Jun 8 2015

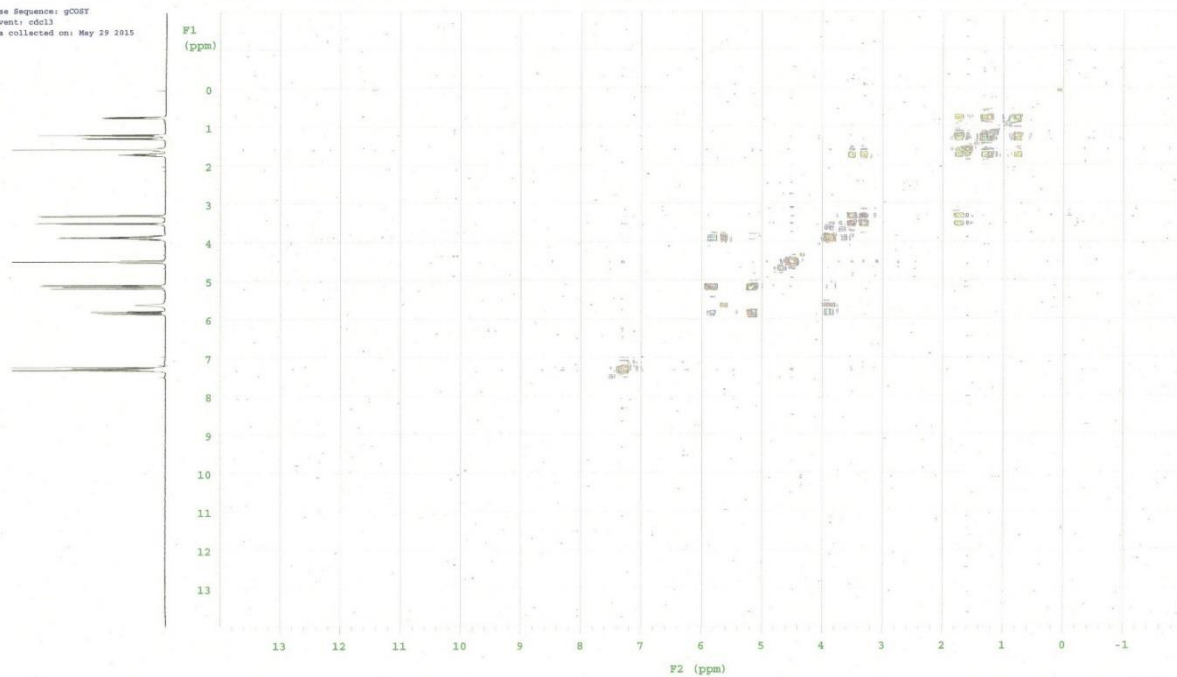




Sample Name:
 Data Collected on:
 Agilent-MMR-vnmr400
 Archive directory:
 Sample directory:
 FIDFile: 137-radical-clock-P3-6N02
 Pulse Sequence: NOESY
 Solvent: cdcl3
 Data collected on: Jun 6 2015



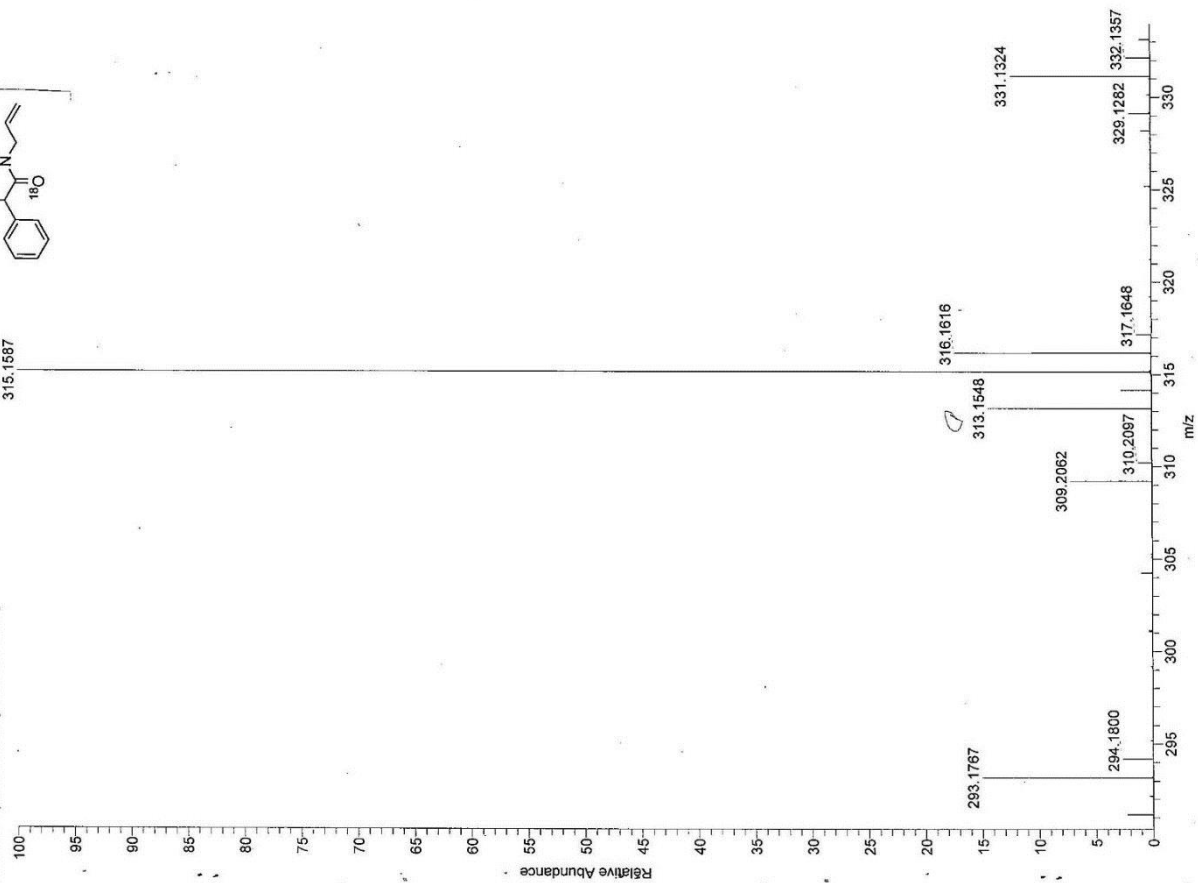
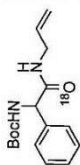
Sample Name:
 Data Collected on:
 Agilent-MMR-vnmr400
 Archive directory:
 Sample directory:
 FIDFile: 137-radical-clock-P2-2-0C08Y
 Pulse Sequence: gCOSTY
 Solvent: cdcl3
 Data collected on: May 29 2015



C:\Xcalibur\data\Unq\LNitro-18O-pure

3/20/2015 2:20:48 PM

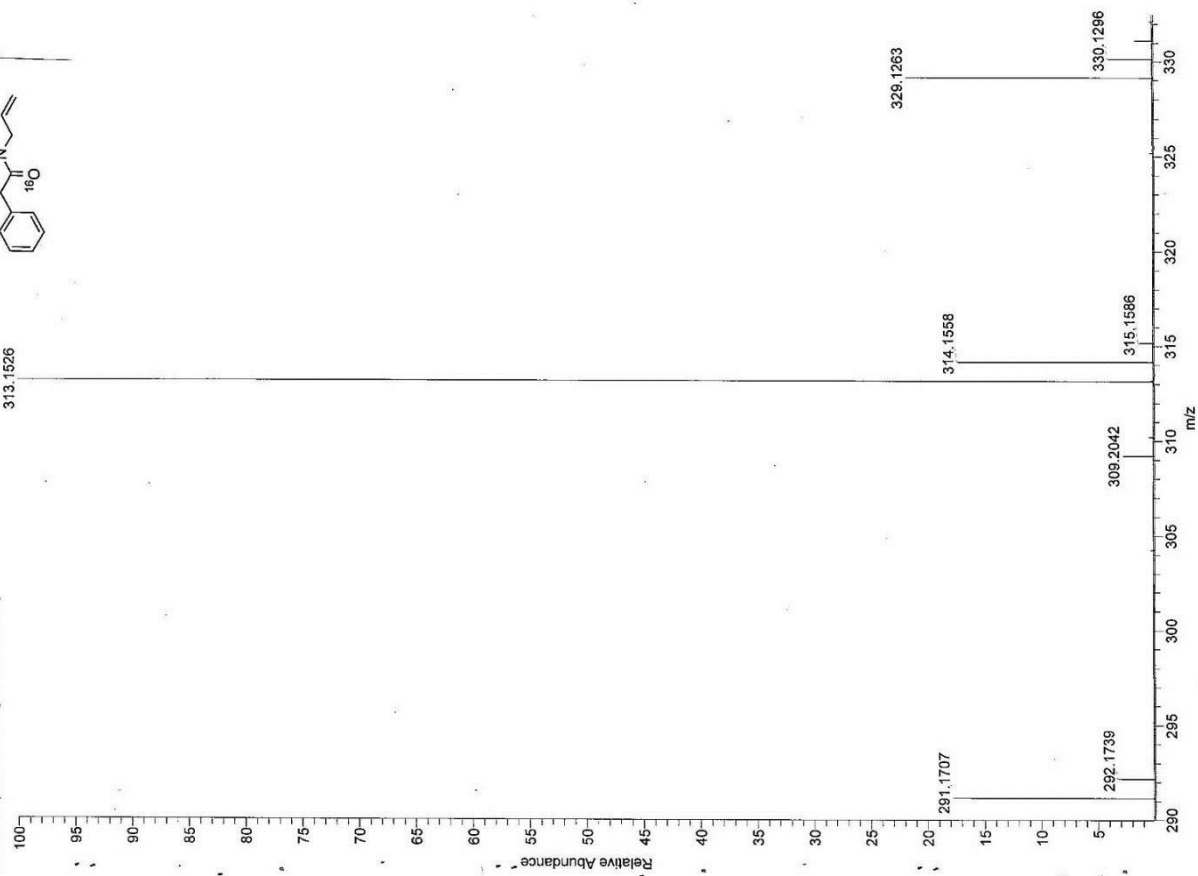
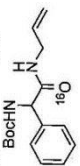
Nitro-18O-pure #1 RT: 0.01 AV: 1 NL: 3.68E7
T: FTMS + p ESI Full ms [150.00-2000.00]

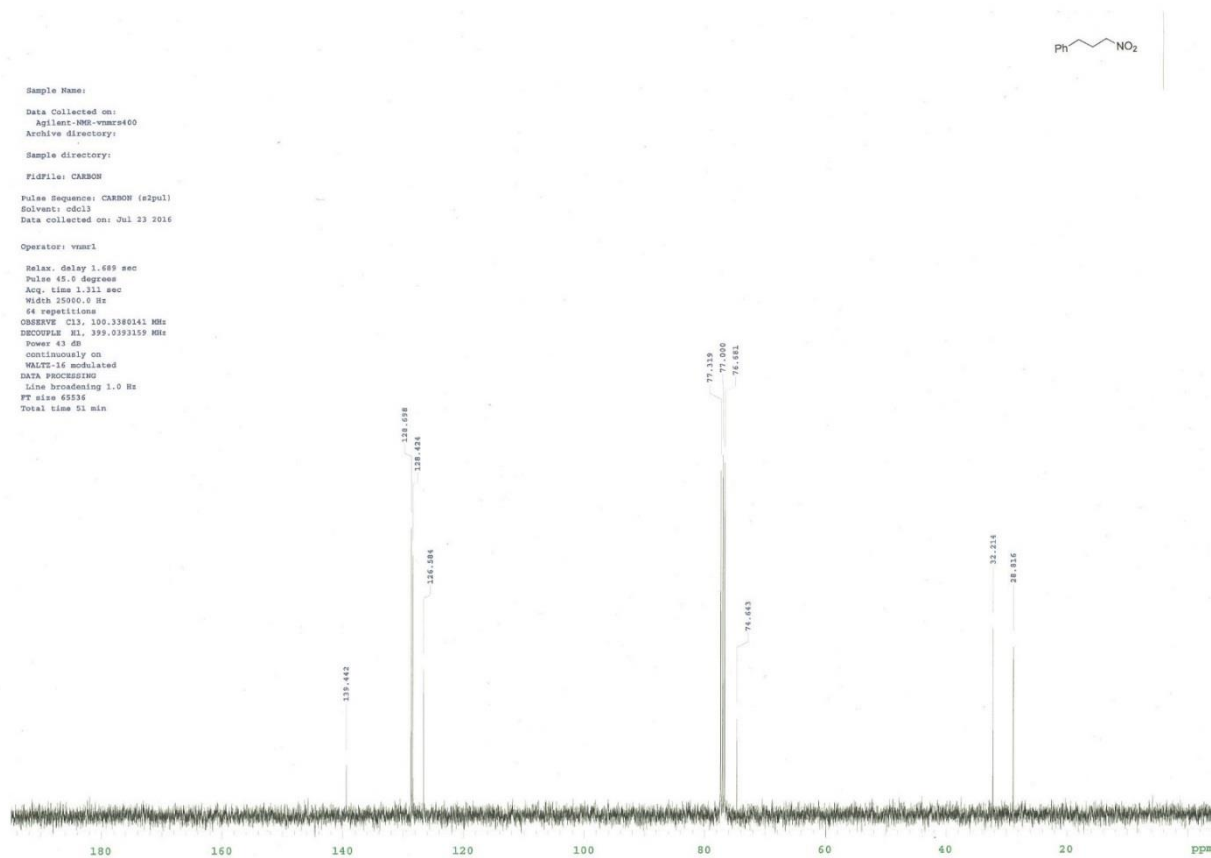
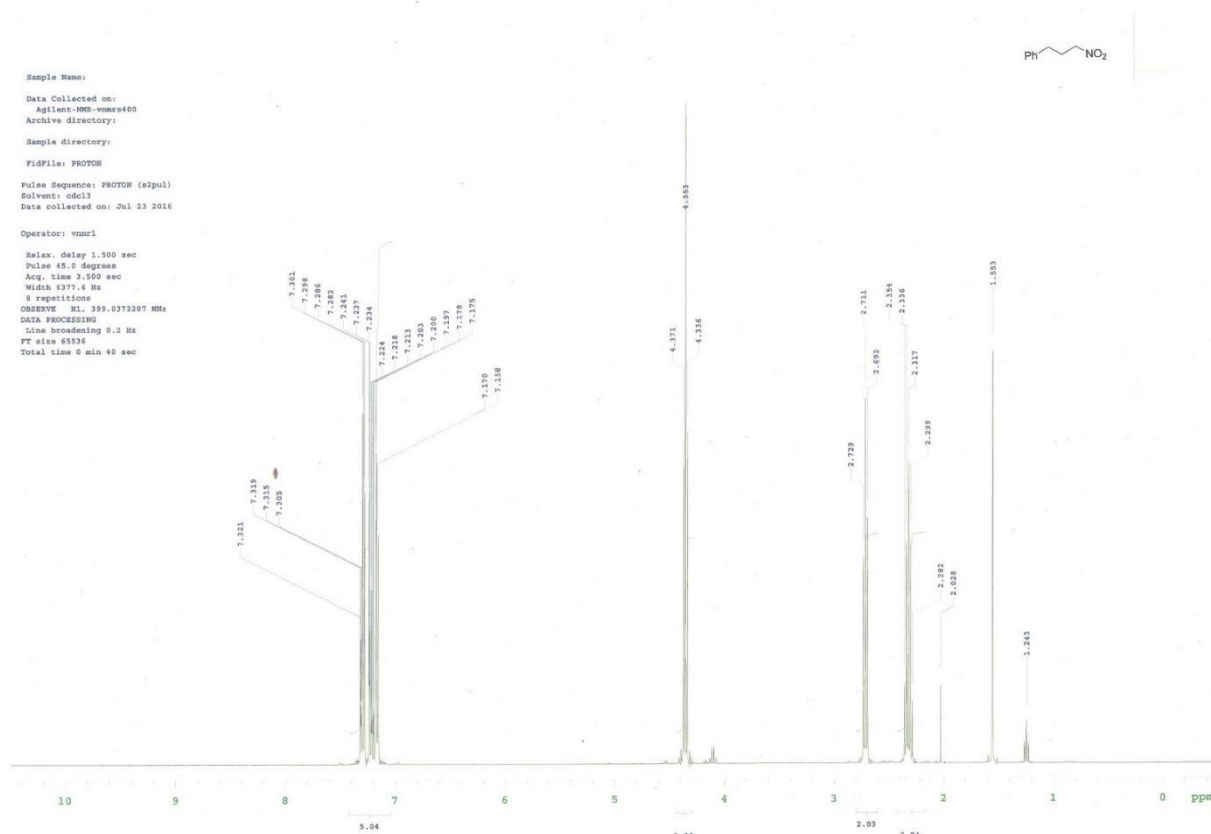


C:\Xcalibur\data\Unq\LNitro-16O-pure

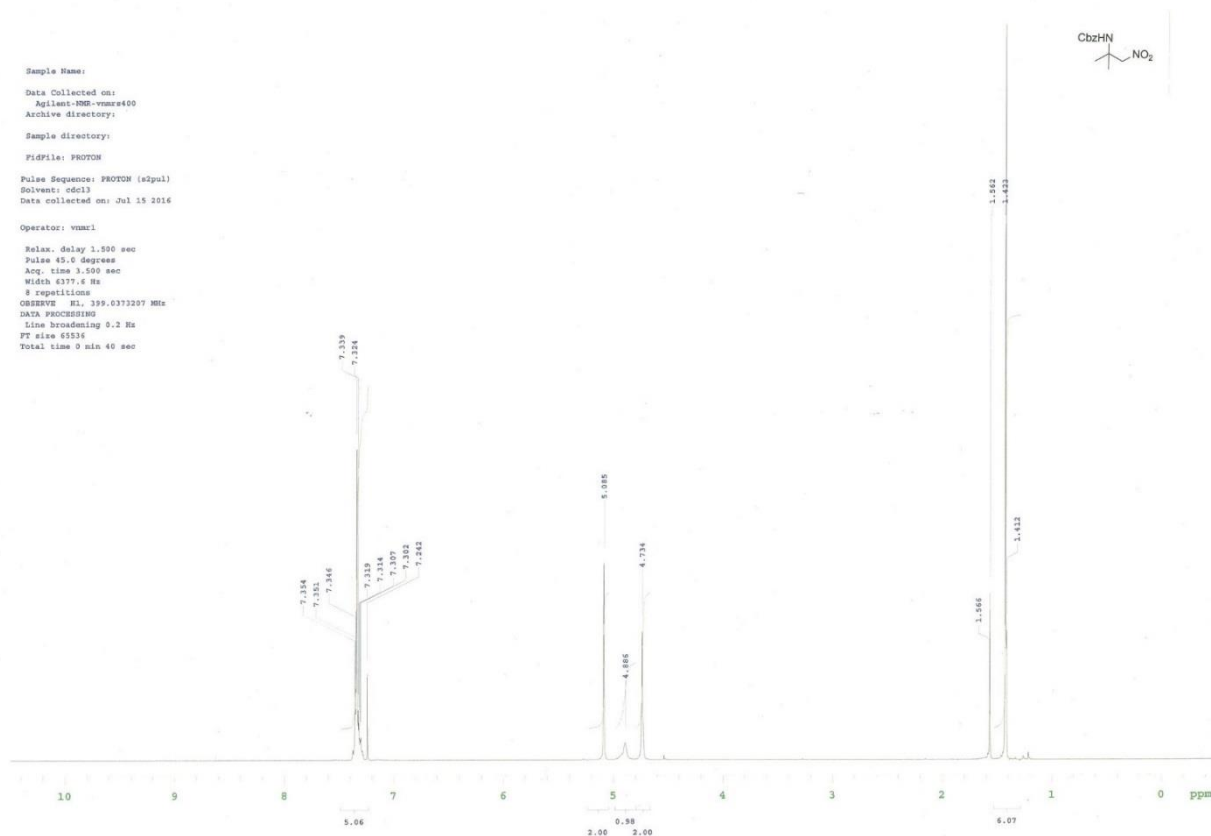
3/20/2015 2:27:18 PM

Nitro-16O-pure #1 RT: 0.01 AV: 1 NL: 1.58E7
T: FTMS + p ESI Full ms [150.00-2000.00]

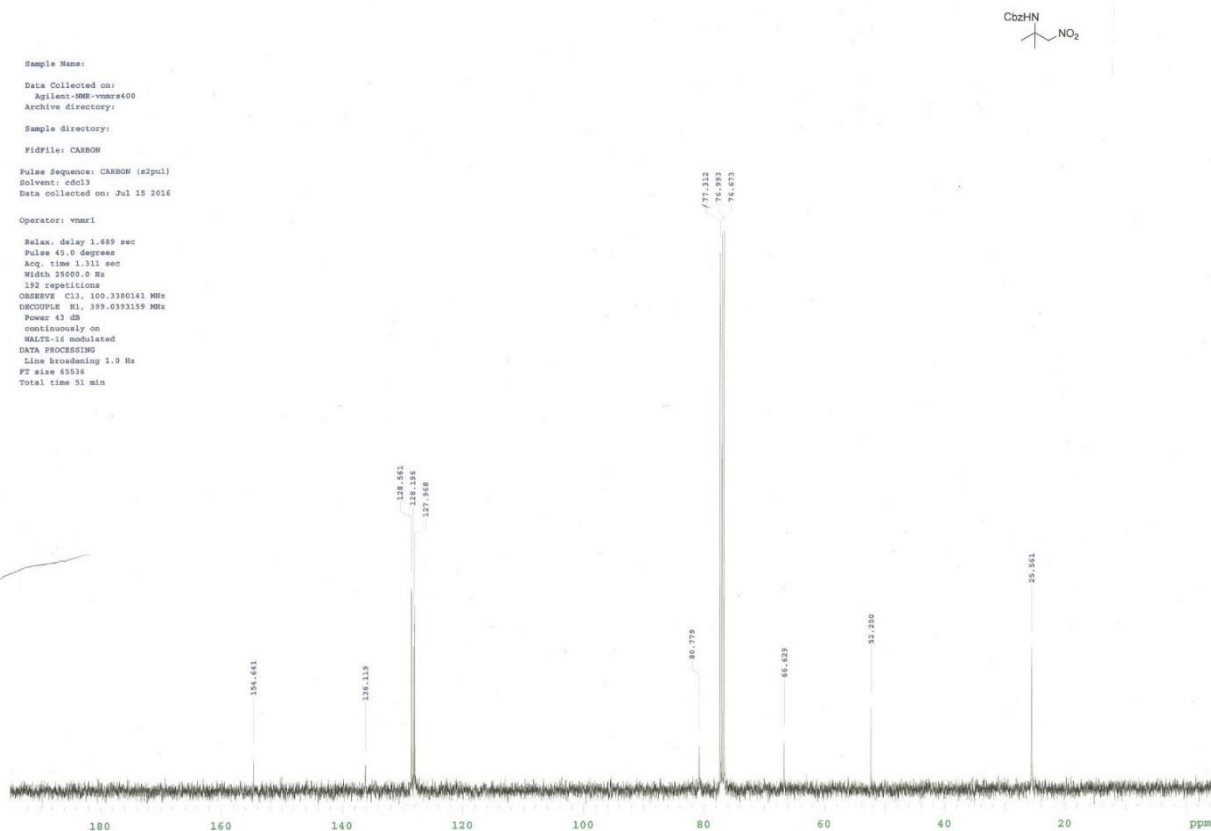


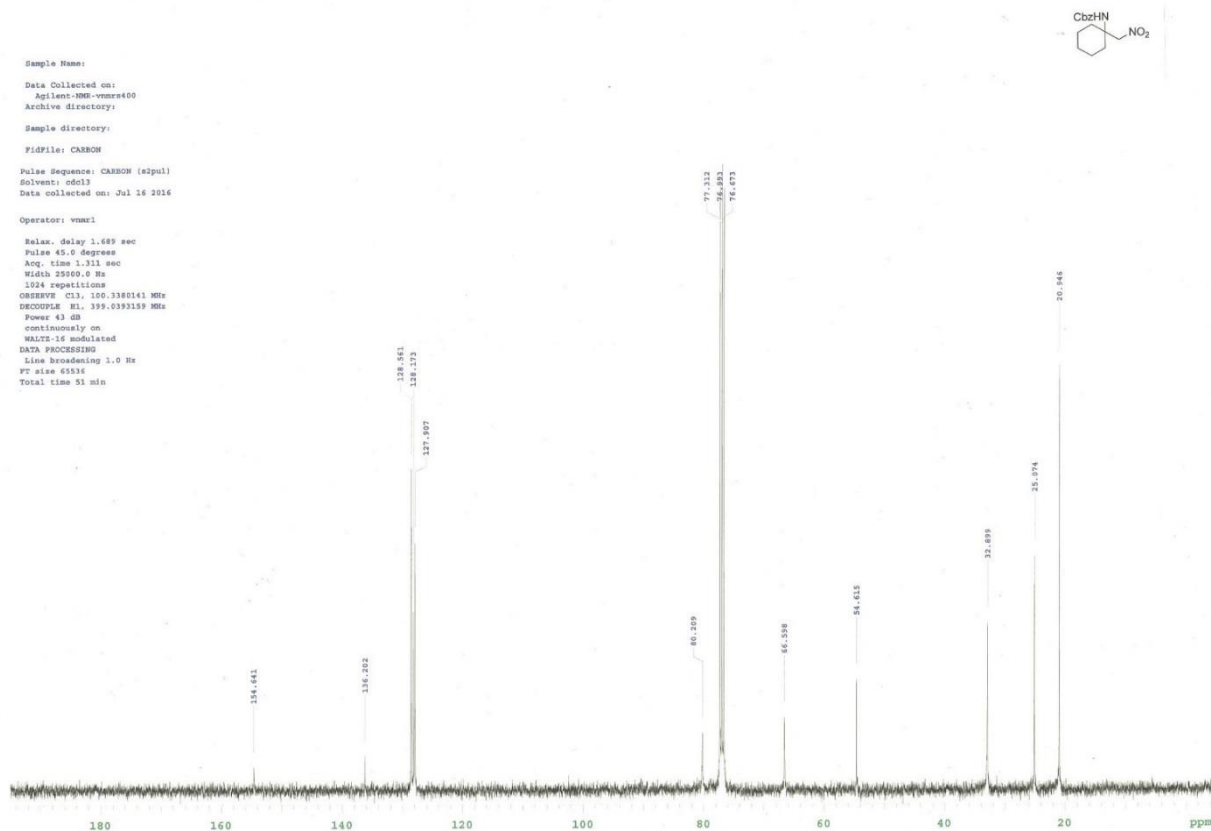
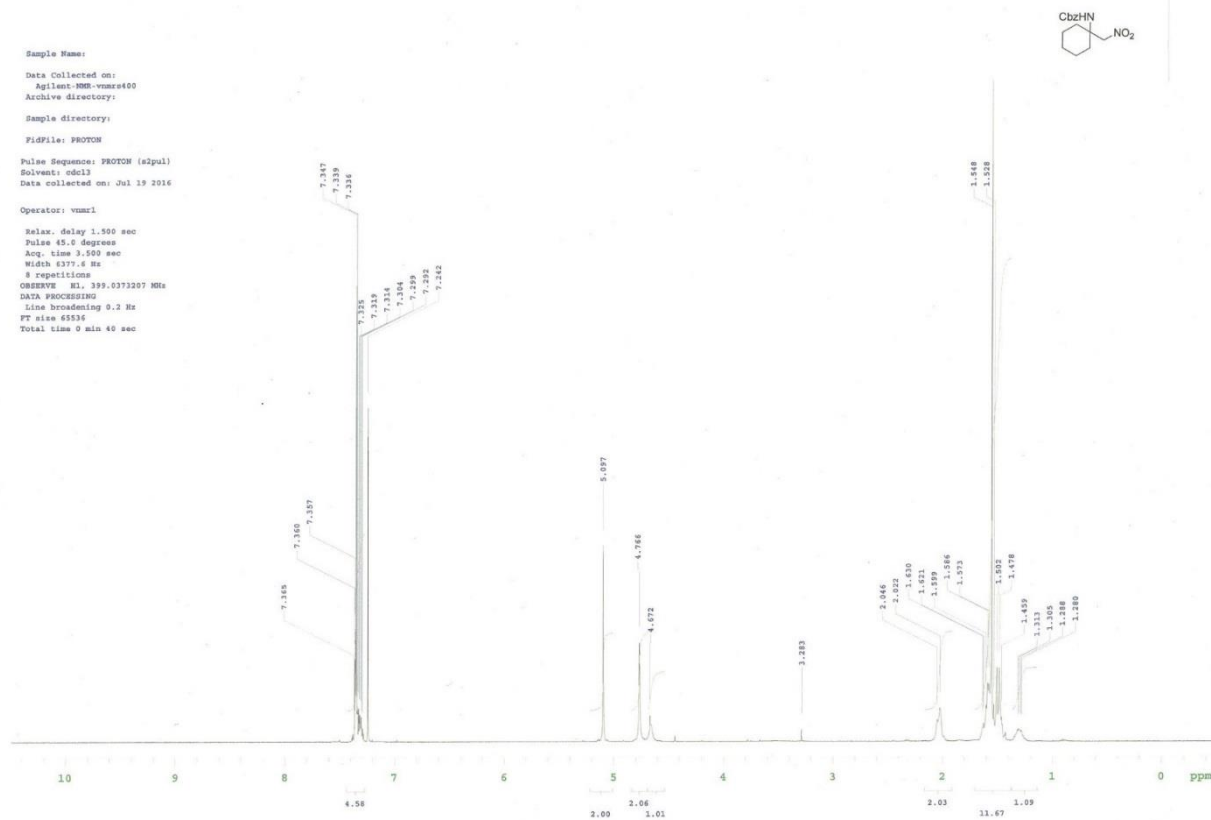


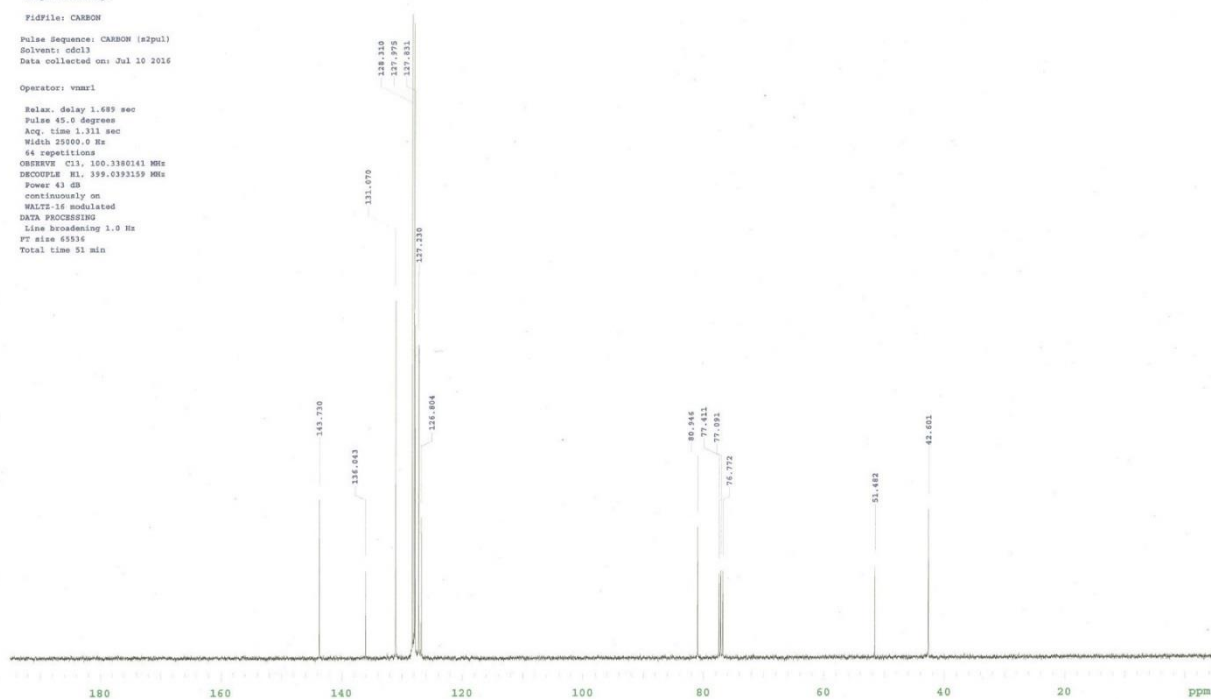
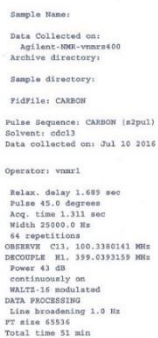
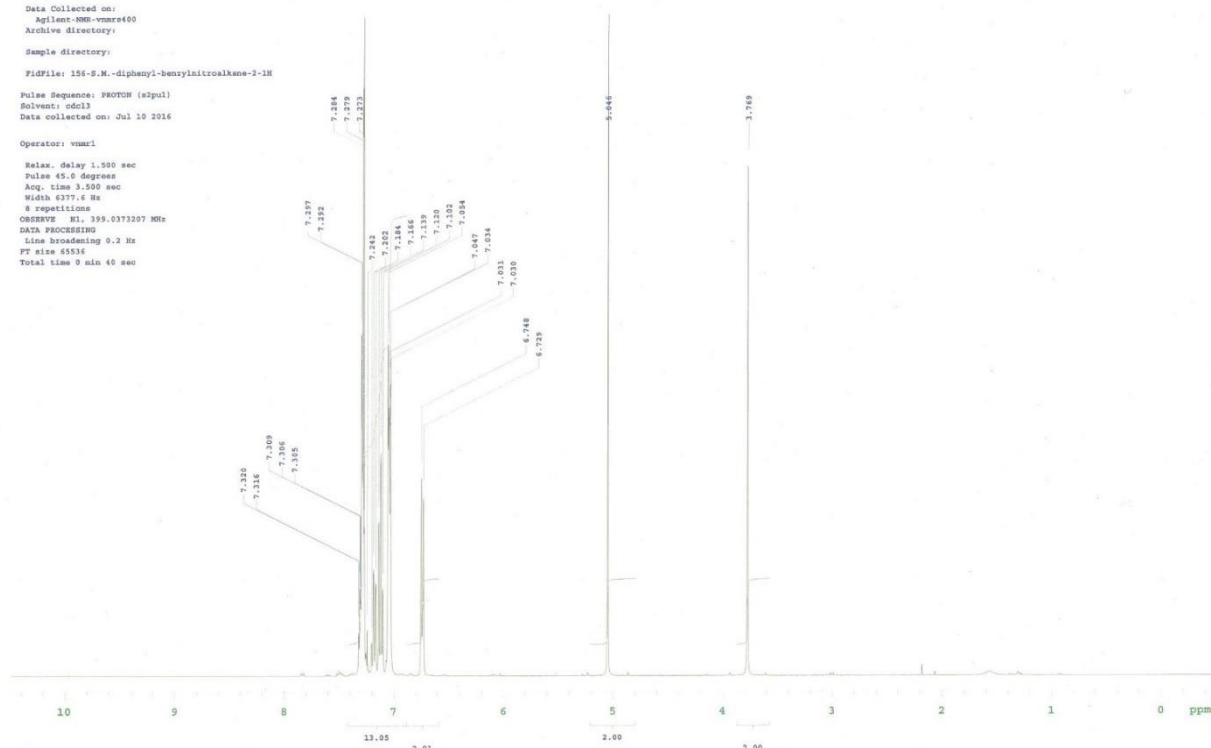
Sample Name:
 Data Collected on:
 Agilent-1H-VMR400
 Archive directory:
 Sample directory:
 FIDFile: PROTON
 Pulse Sequence: PROTON (s2pul)
 Solvent: cdcl3
 Data collected on: Jul 15 2016
 Operator: vmur1
 Relax. delay 1.550 sec
 Pulse 45.0 degrees
 Acq. time 3.550 sec
 Width 6377.6 Hz
 8 repetitions
 OBSERVE H1, 399.6372207 MHz
 DATA PROCESSING
 Line broadening 0.2 Hz
 FT size 65536
 Total time 0 min 40 sec



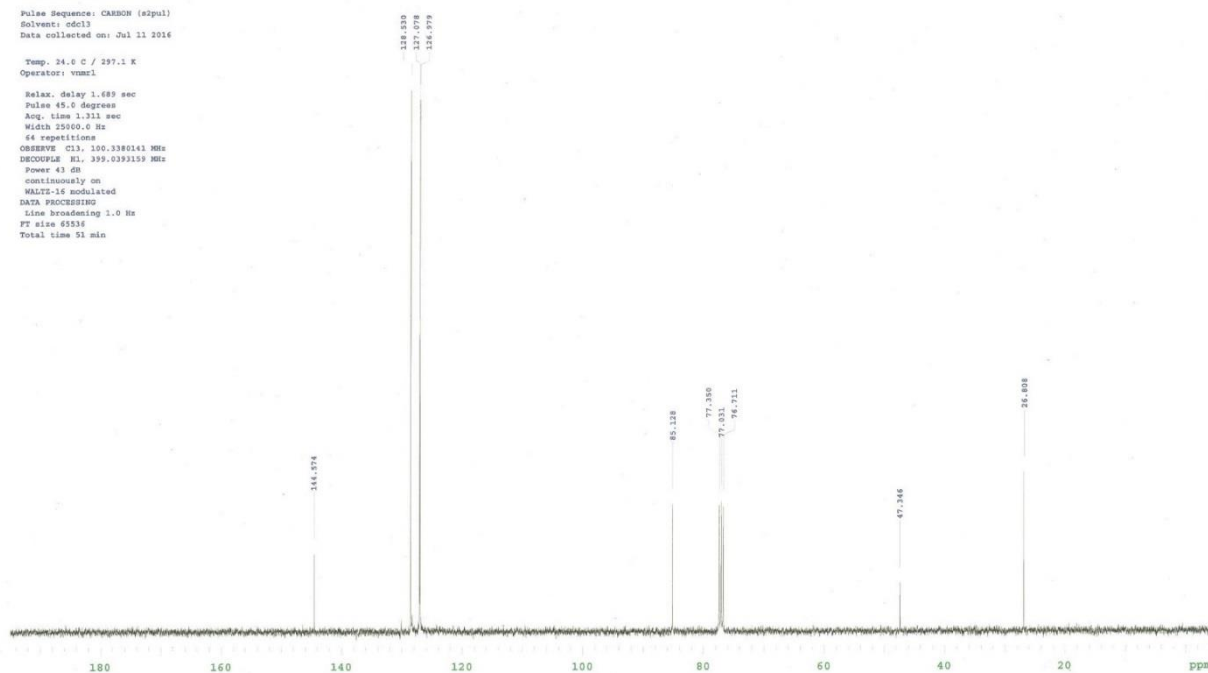
Sample Name:
 Data Collected on:
 Agilent-1H-VMR400
 Archive directory:
 Sample directory:
 FIDFile: CARBON
 Pulse Sequence: CARBON (s2pul)
 Solvent: cdcl3
 Data collected on: Jul 15 2016
 Operator: vmur1
 Relax. delay 1.689 sec
 Pulse 45.0 degrees
 Acq. time 1.311 sec
 Width 25000.0 Hz
 132 repetitions
 OBSERVE C13, 100.3386143 MHz
 DECOUPLE H1, 399.6393159 MHz
 Power 43 dB
 continuously on
 WALTZ-16 modulated
 DATA PROCESSING
 Line broadening 1.0 Hz
 FT size 65536
 Total time 51 min



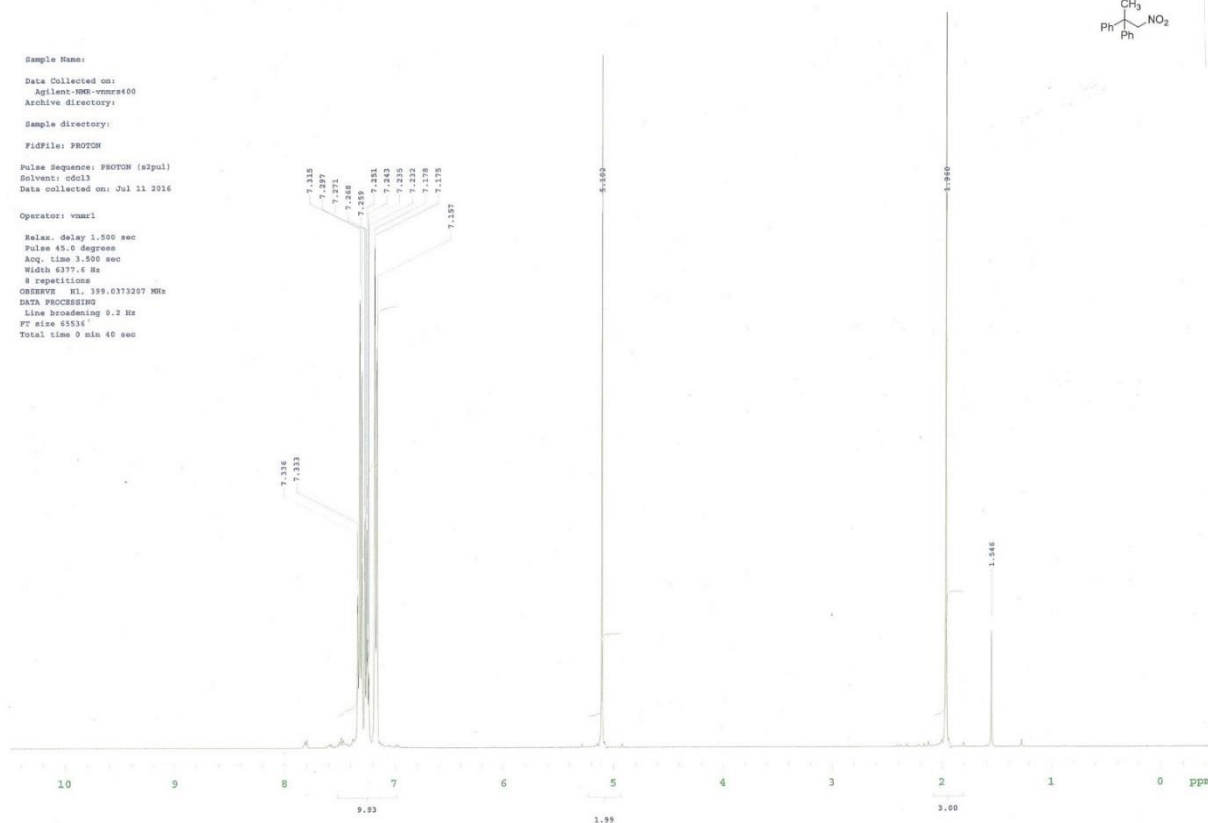




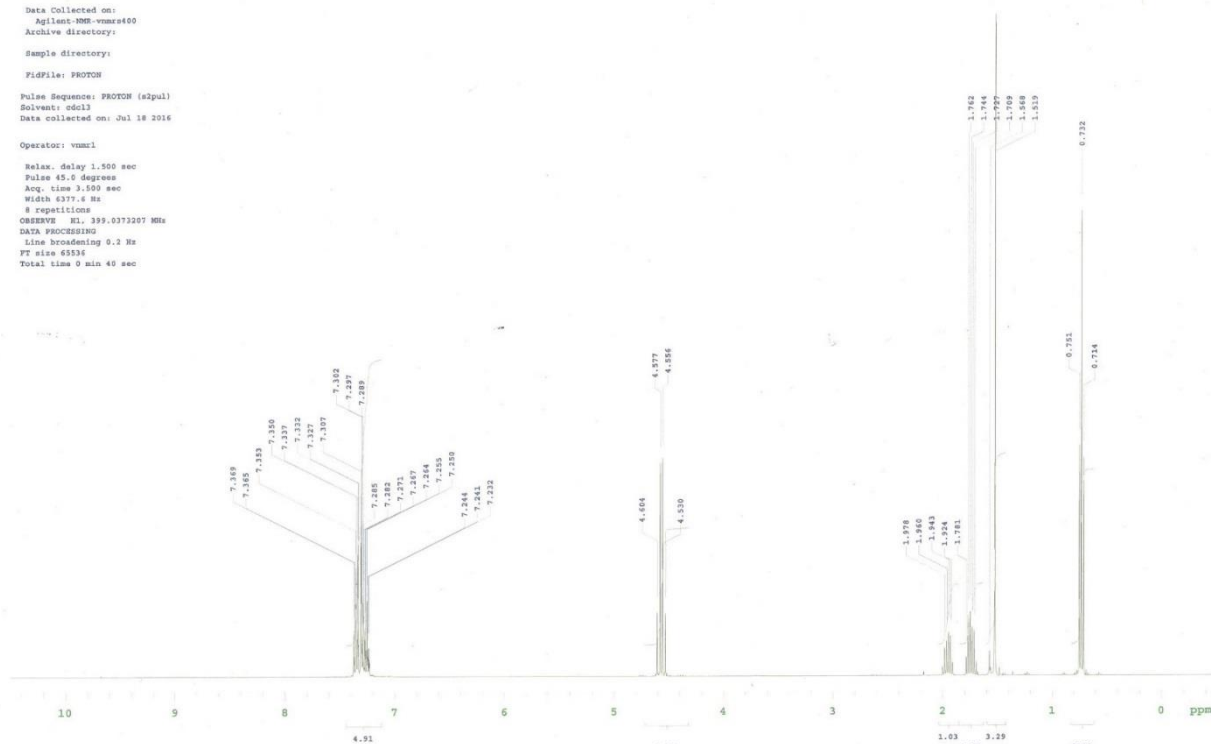
Sample Name:
 Data Collected on:
 Agilent-NMR-vnmr400
 Archive directory:
 Sample directory:
 FIDFile: CARBON
 Pulse Sequence: CARBON (s2pul)
 Solvent: cdcl3
 Data collected on: Jul 11 2016
 Temp. 24.6 C / 297.1 K
 Operator: vnmr1
 Relax. delay 1.689 sec
 Pulse 45.0 degrees
 Acq. time 1.311 sec
 Width 25040.0 Hz
 64 repetitions
 OBSERVE C13, 100.3380143 MHz
 DECOUPLE H1, 399.6393159 MHz
 Power 43 dB
 continuously on
 WALTZ-16 modulated
 DATA PROCESSING
 Line broadening 1.0 Hz
 FT size 65536
 Total time 51 min



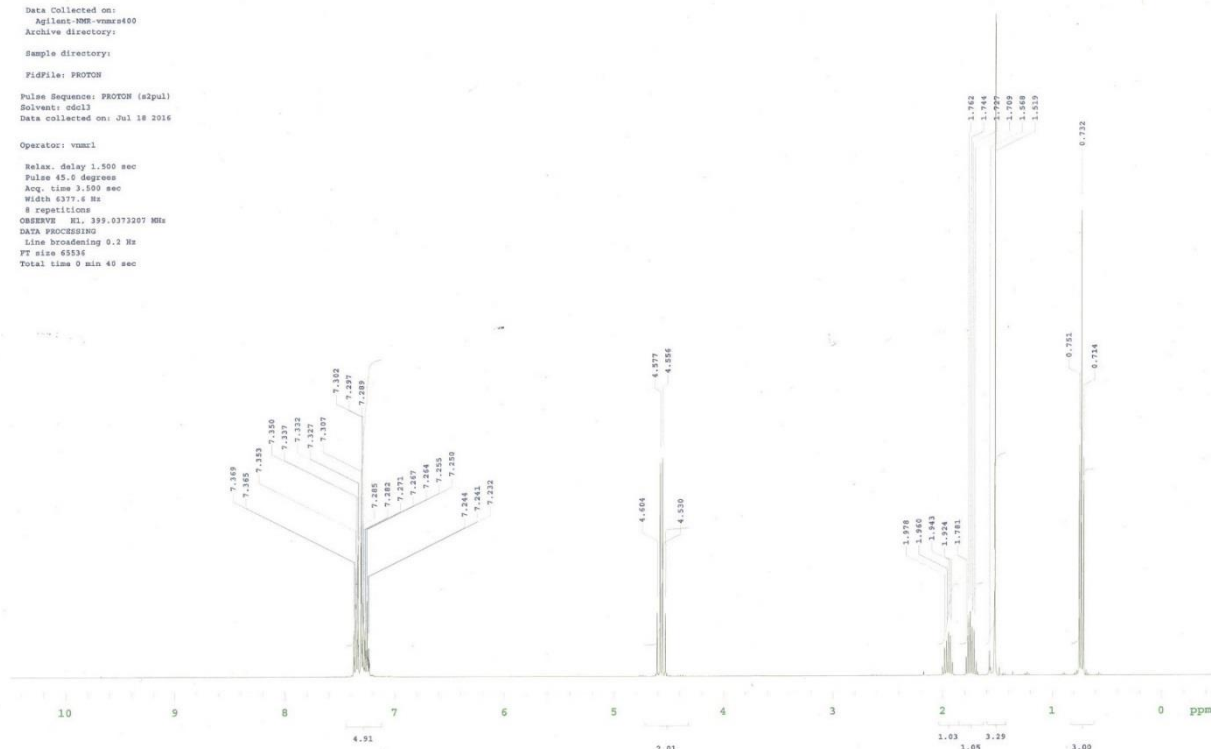
Sample Name:
 Data Collected on:
 Agilent-NMR-vnmr400
 Archive directory:
 Sample directory:
 FIDFile: PROTON
 Pulse Sequence: PROTON (s2pul)
 Solvent: cdcl3
 Data collected on: Jul 11 2016
 Operator: vnmr1
 Relax. delay 1.550 sec
 Pulse 45.0 degrees
 Acq. time 3.500 sec
 Width 6377.6 Hz
 8 repetitions
 OBSERVE H1, 399.6373297 MHz
 DATA PROCESSING
 Line broadening 0.2 Hz
 FT size 65536
 Total time 0 min 40 sec

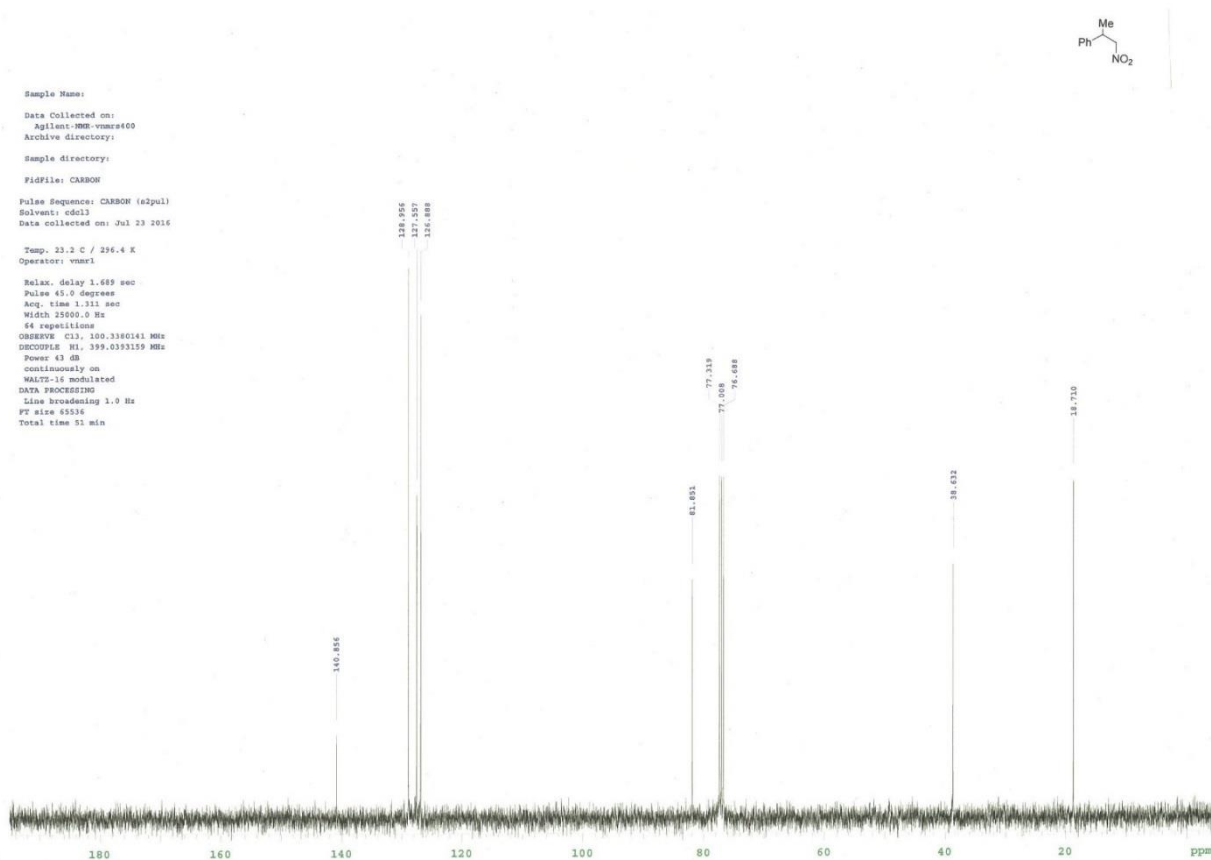
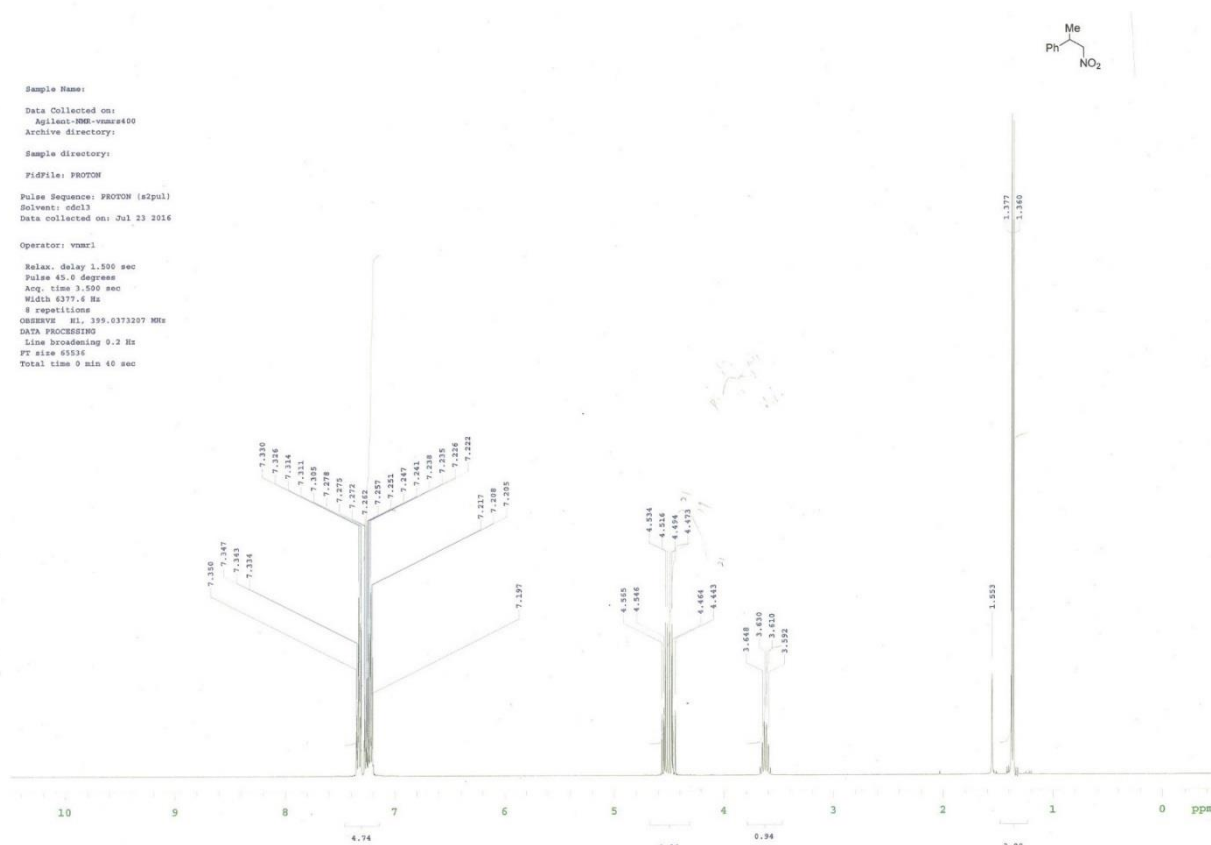


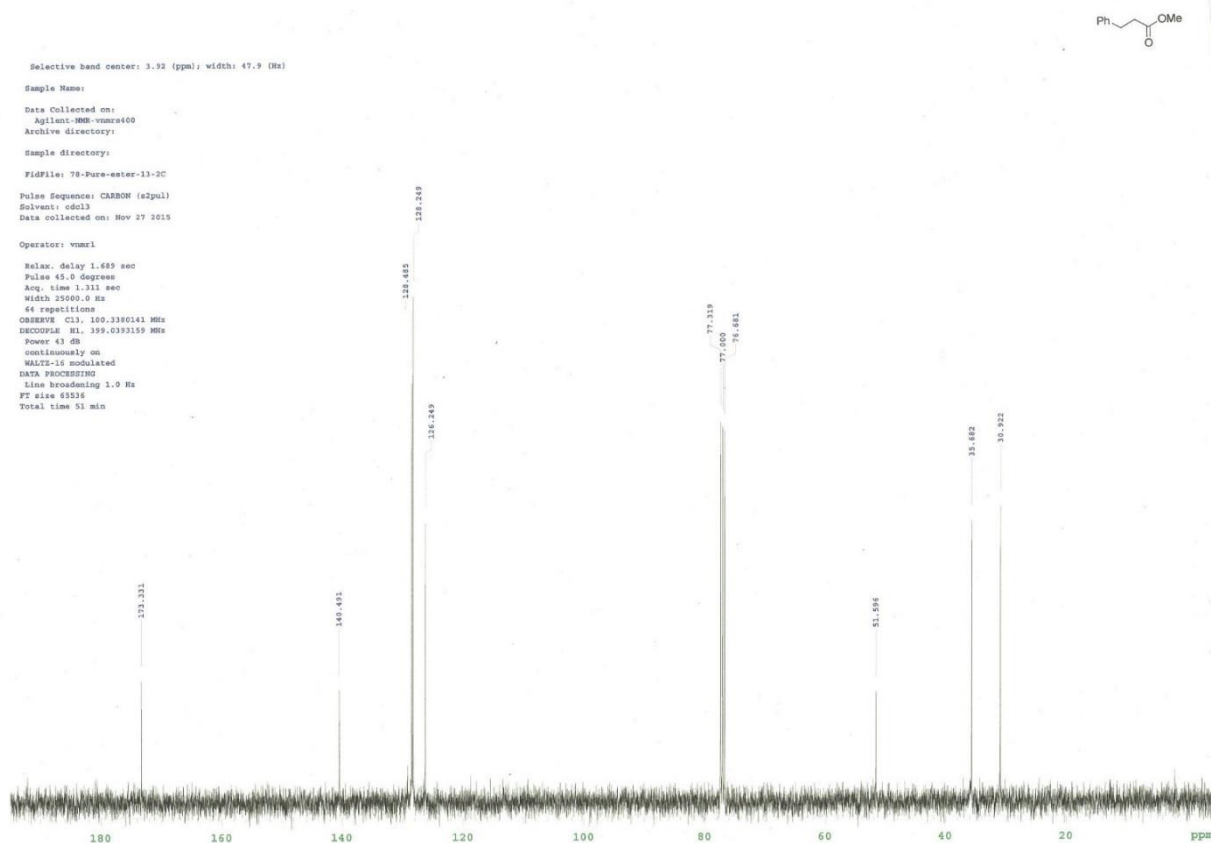
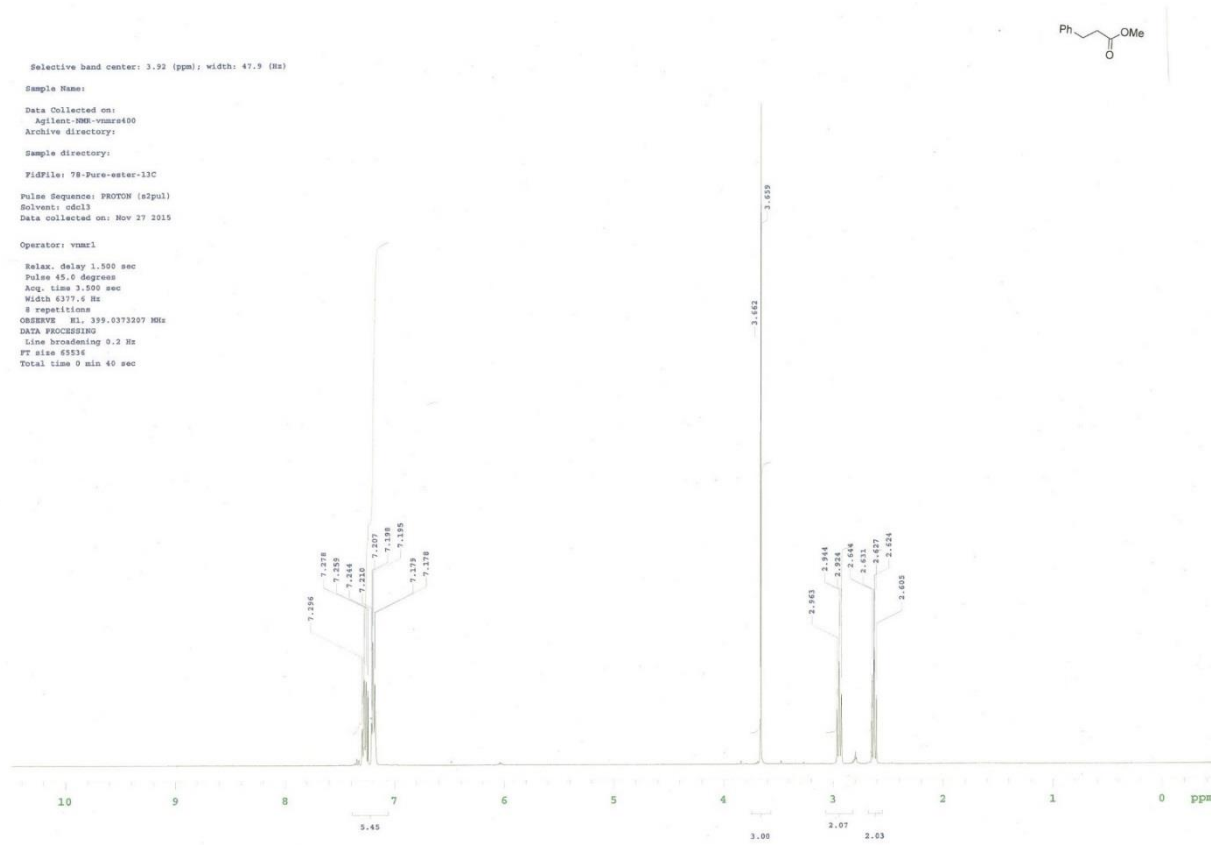
Sample Name:
 Data Collected on:
 Agilent-MMR-vnmr400
 Archive directory:
 Sample directory:
 FIDFile: PROTON
 Pulse Sequence: PROTON (s2pul)
 Solvent: cdcl3
 Data collected on: Jul 18 2016
 Operator: vnmr1
 Relax. delay 1.500 sec
 Pulse 45.0 degrees
 Acq. time 3.500 sec
 Width 6377.4 Hz
 8 repetitions
 OBSERVE K1, 399.0373207 MHz
 DATA PROCESSING
 Line broadening 0.2 Hz
 FT size 65536
 Total time 0 min 40 sec

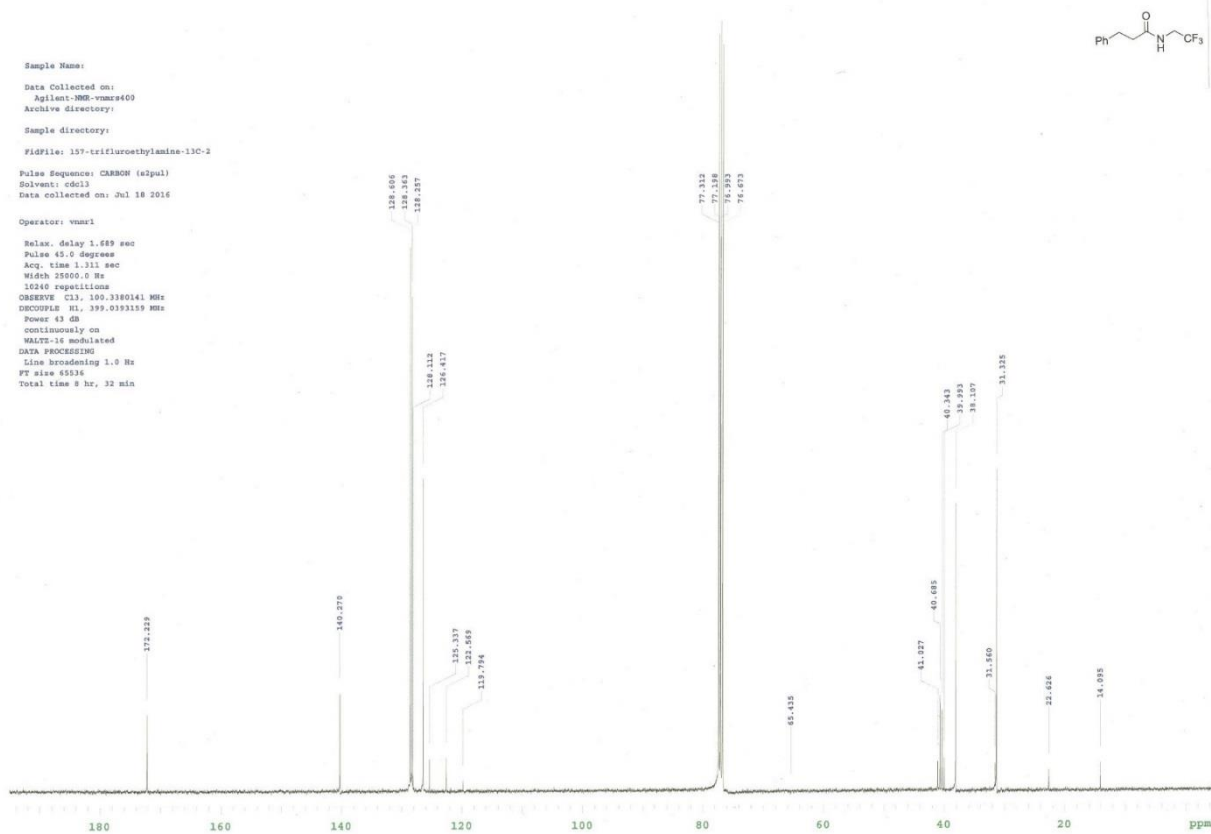
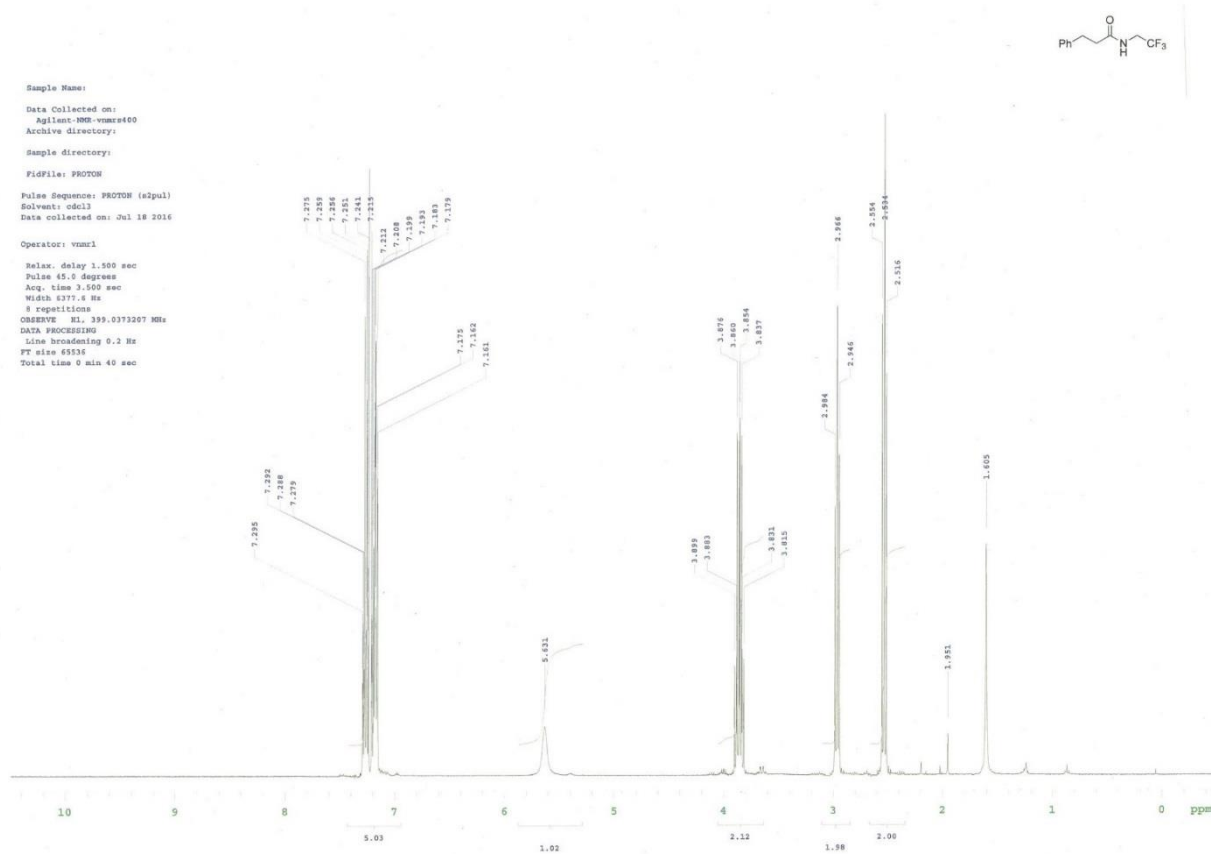


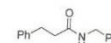
Sample Name:
 Data Collected on:
 Agilent-MMR-vnmr400
 Archive directory:
 Sample directory:
 FIDFile: PROTON
 Pulse Sequence: PROTON (s2pul)
 Solvent: cdcl3
 Data collected on: Jul 18 2016
 Operator: vnmr1
 Relax. delay 1.500 sec
 Pulse 45.0 degrees
 Acq. time 3.500 sec
 Width 6377.4 Hz
 8 repetitions
 OBSERVE K1, 399.0373207 MHz
 DATA PROCESSING
 Line broadening 0.2 Hz
 FT size 65536
 Total time 0 min 40 sec



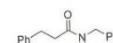
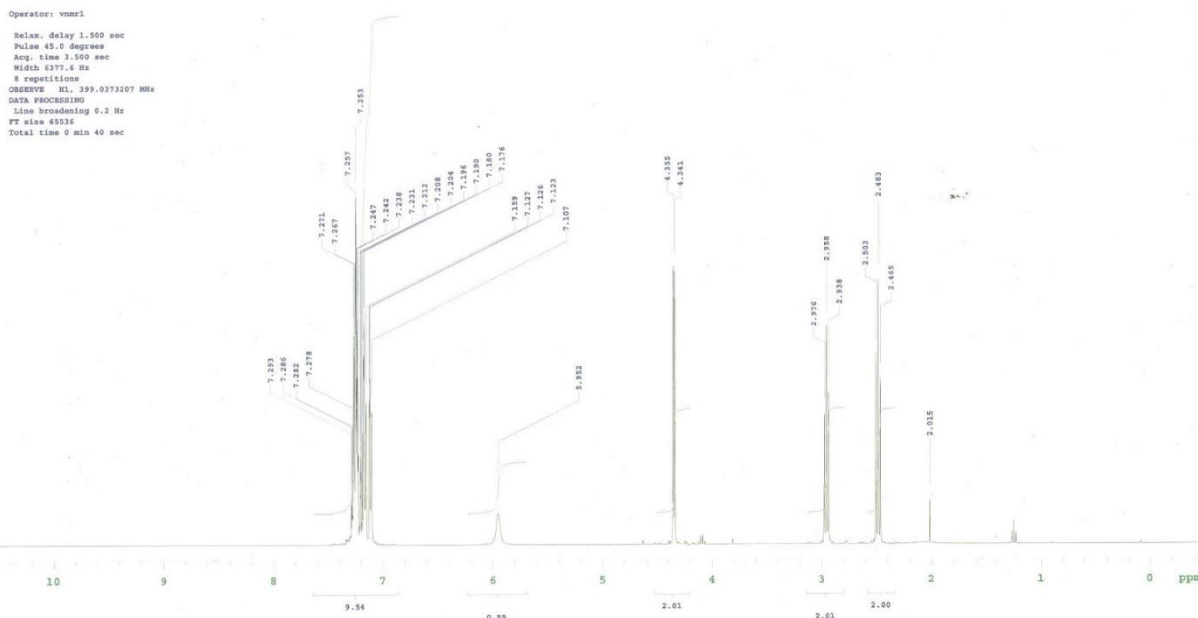




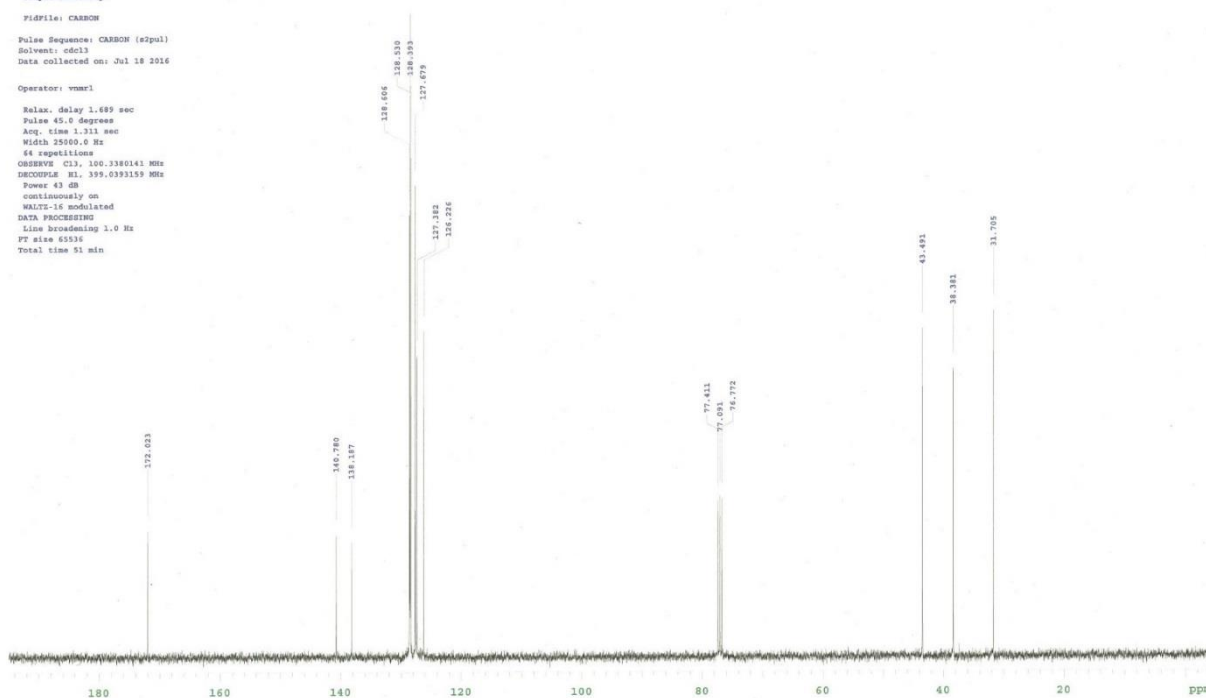




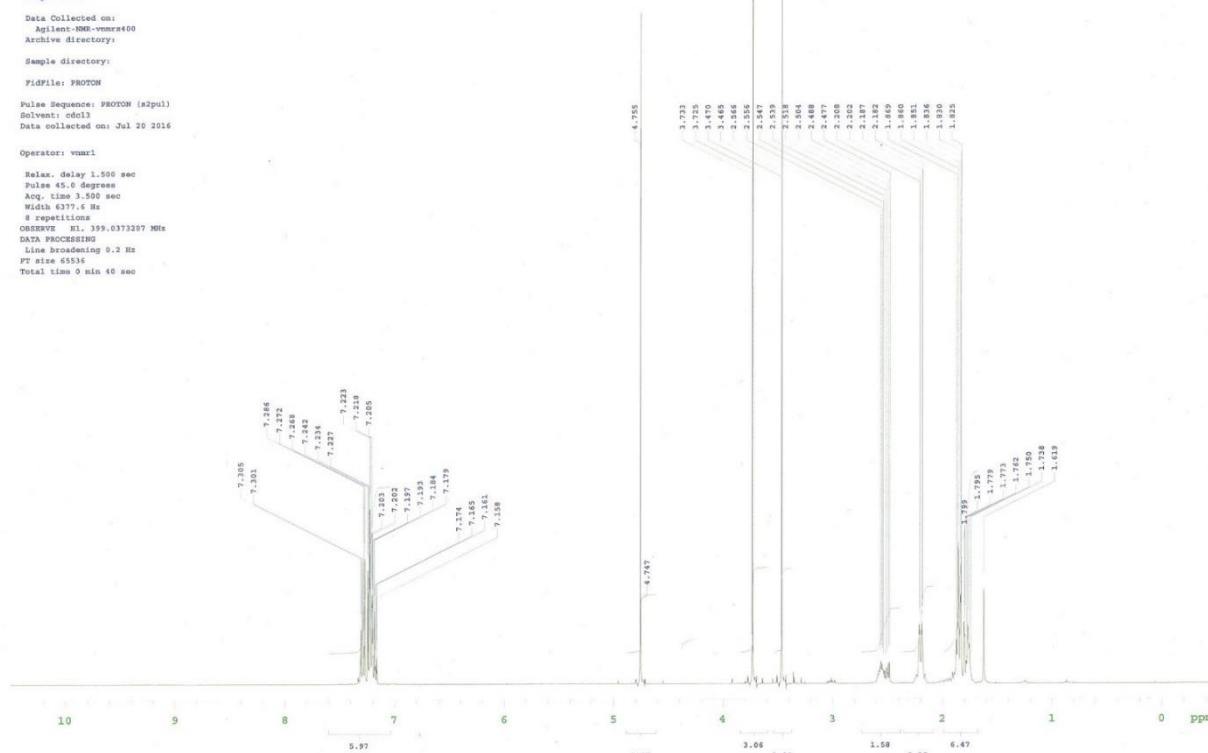
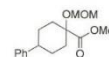
Sample Name:
Data Collected on:
Agilent-800-vnmr400
Archive directory:
Sample directory:
Fidfile: PROTON
Pulse Sequence: PROTON (s2pul)
Solvent: cdcl3
Data collected on: Jul 18 2016



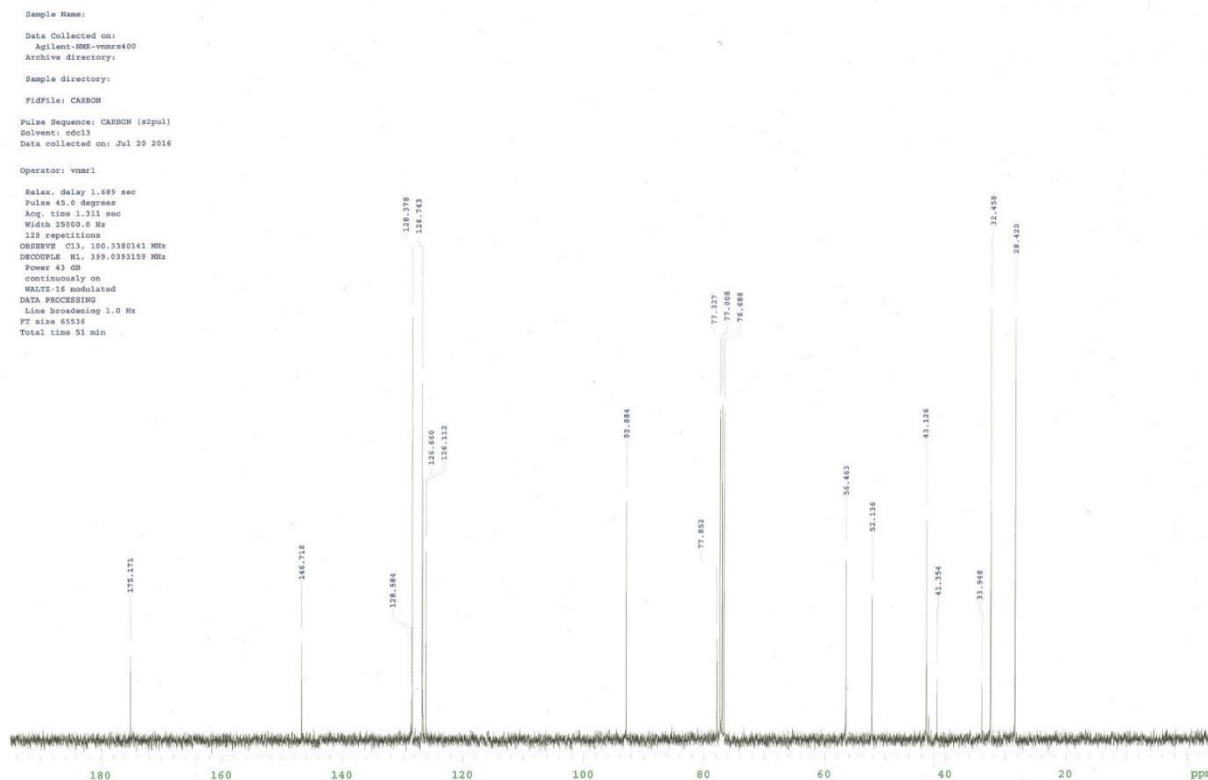
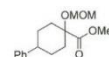
Sample Name:
Data Collected on:
Agilent-800-vnmr400
Archive directory:
Sample directory:
Fidfile: CARBON
Pulse Sequence: CARBON (s2pul)
Solvent: cdcl3
Data collected on: Jul 18 2016
Operator: vnmr1
Relax. delay 1.089 sec
Pulse 45.0 degrees
Acq. time 1.311 sec
Width 25060.0 Hz
repetitions
OBSERVE C13, 100.3380141 MHz
DECOUPLE H1, 399.0393159 MHz
Power 43 dB
continuously on
WALTZ-16 modulated
DATA PROCESSING
Line broadening 1.0 Hz
FT size 65536
Total time 51 min

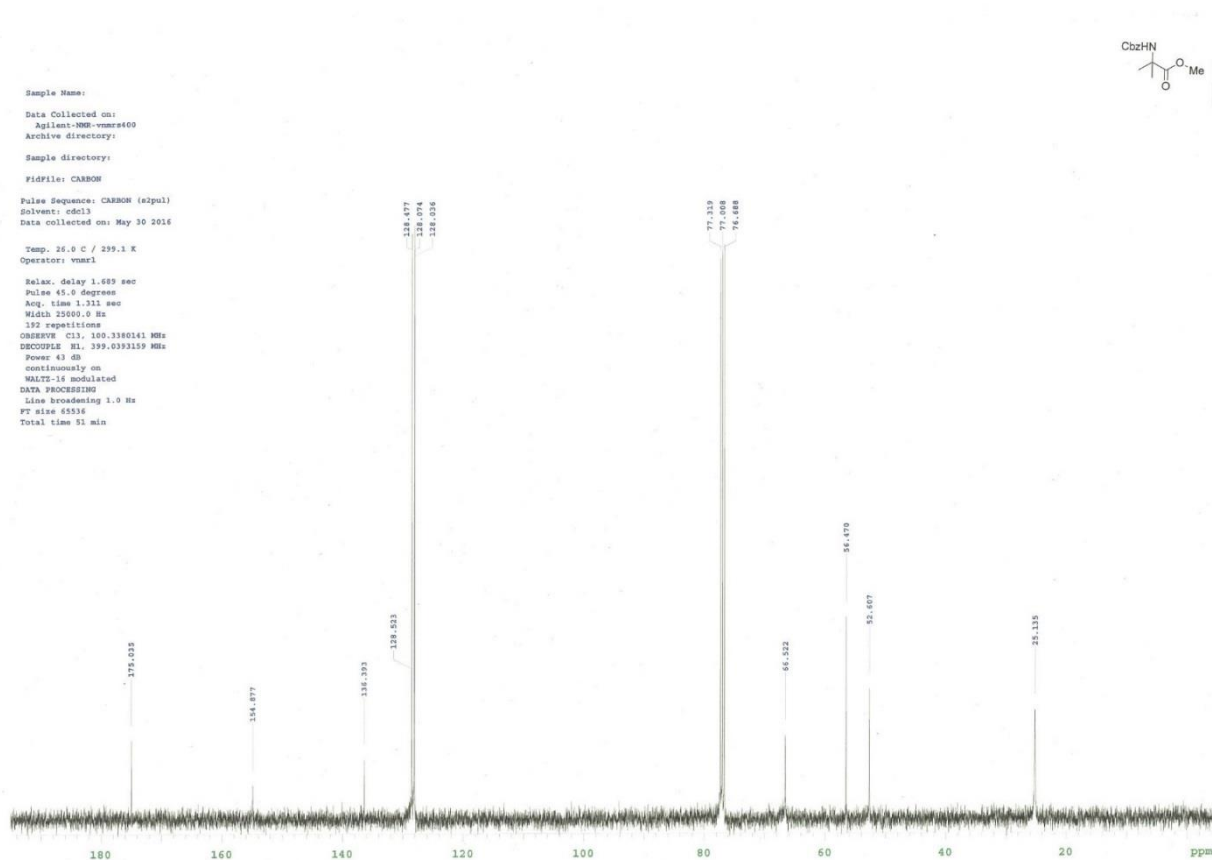
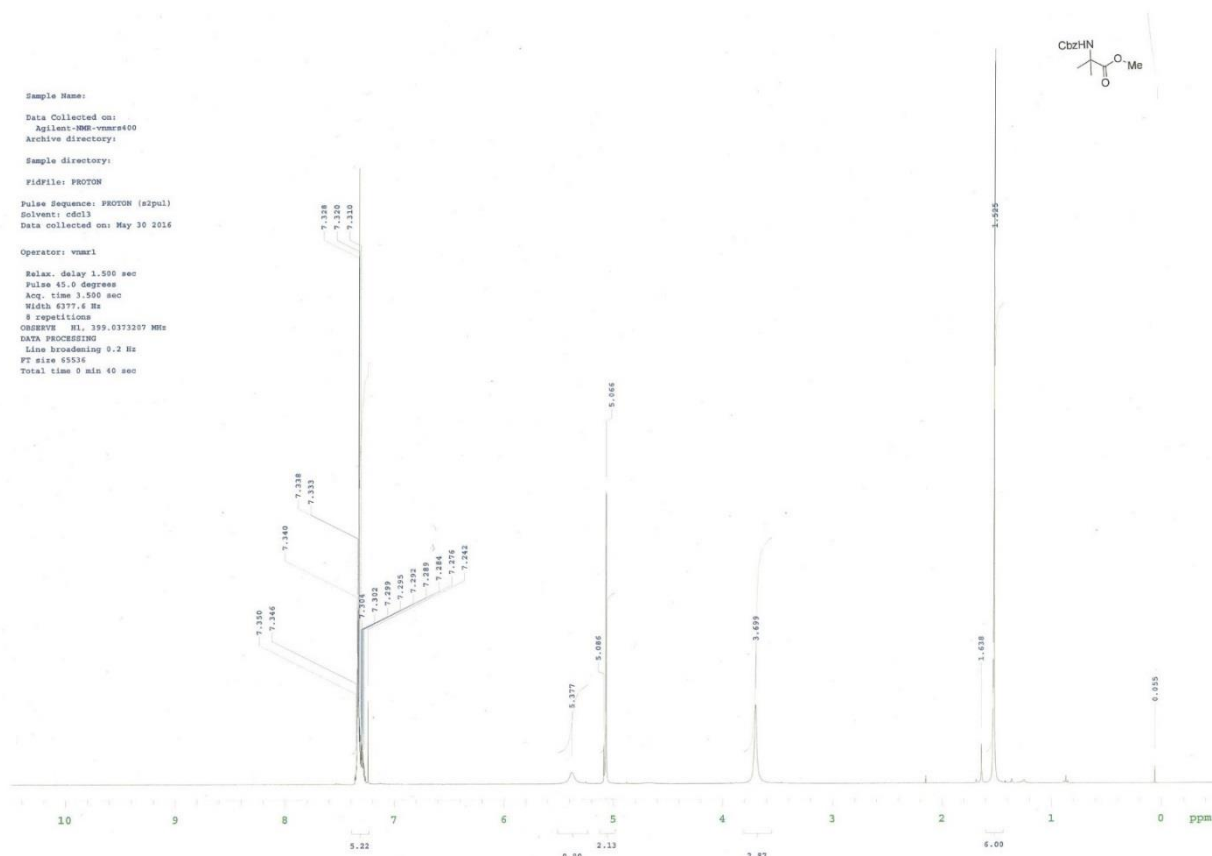


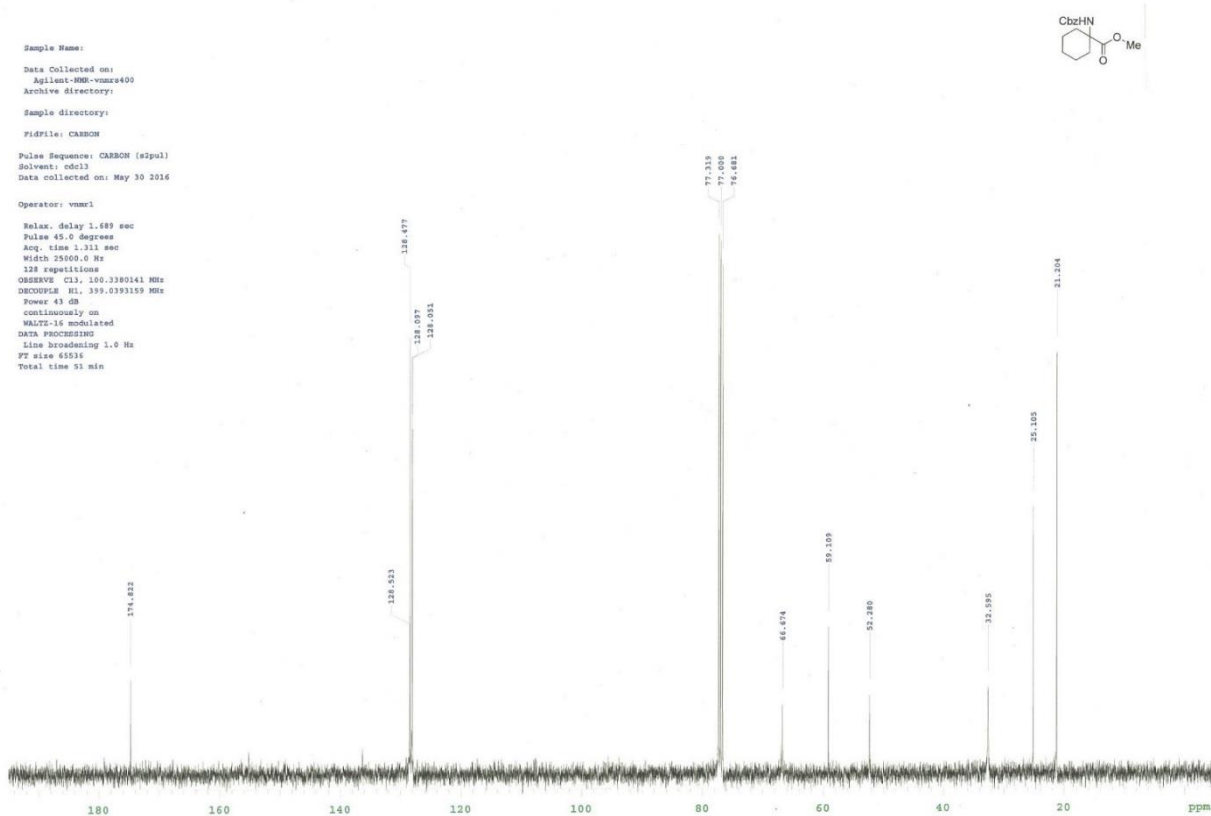
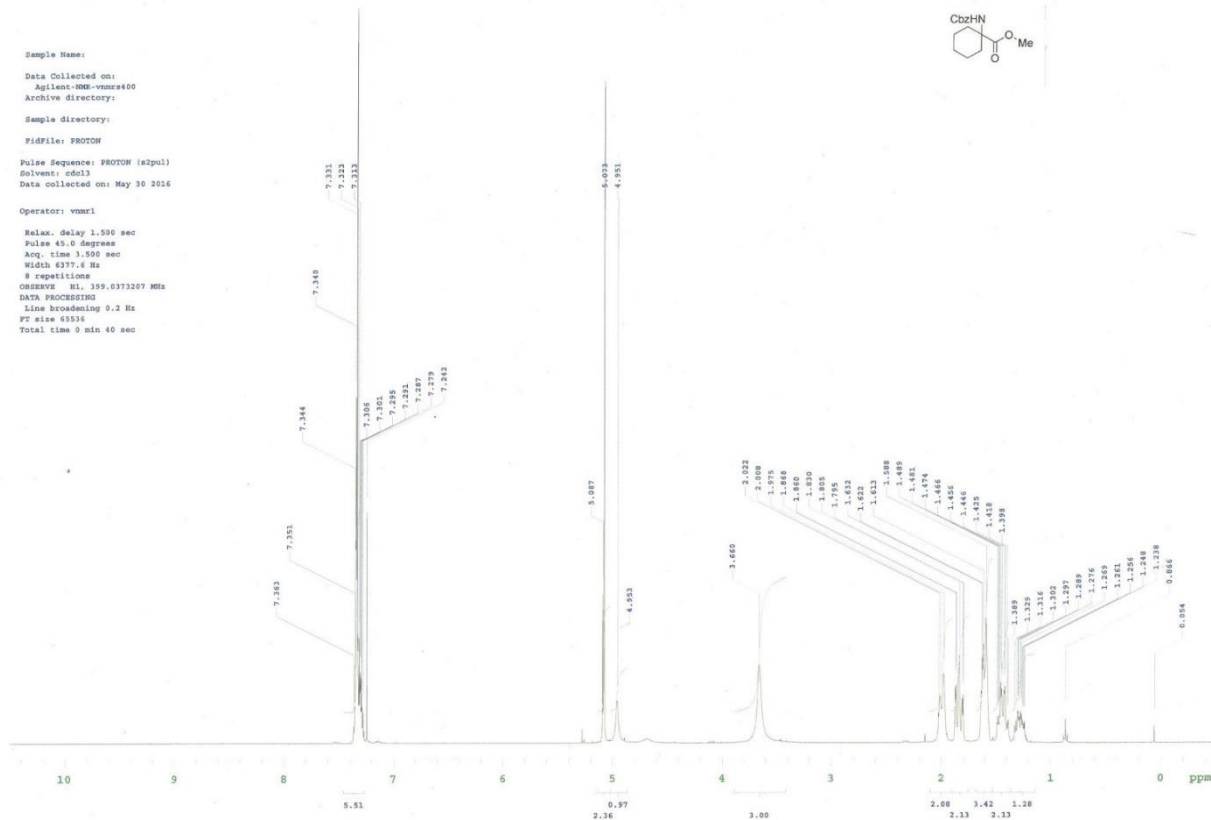
Sample Name:
 Data Collected on:
 Agilent-HM-vmr400
 Archive directory:
 Sample directory:
 FIDFile: PROTON
 Pulse Sequence: PROTON (zgpg30)
 Solvent: cdcl3
 Data collected on: Jul 20 2016
 Operator: vmr41
 Relax. delay 1.500 sec
 Pulse 45.0 degree
 Acq. time 3.500 sec
 Width 6377.6 Hz
 8 repetitions
 OBSERVE F1: 399.6373207 MHz
 DATA PROCESSING
 Line broadening 0.2 Hz
 FT size 65536
 Total time 0 min 40 sec



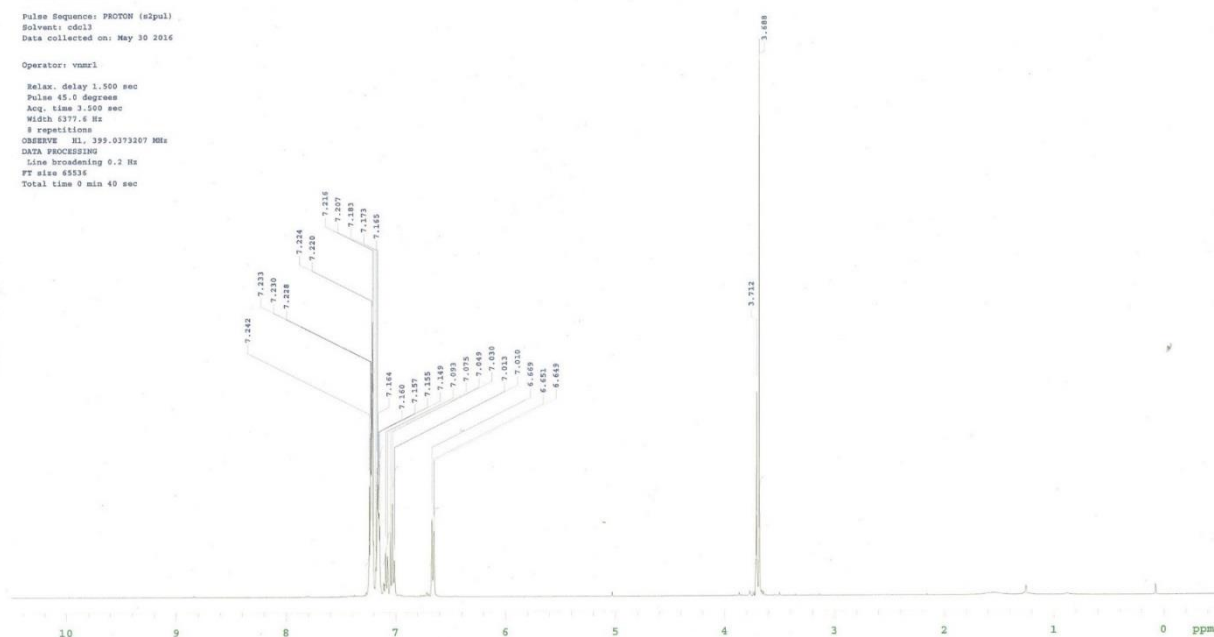
Sample Name:
 Data Collected on:
 Agilent-HM-vmr400
 Archive directory:
 Sample directory:
 FIDFile: CARBON
 Pulse Sequence: CARBON (zgpg30)
 Solvent: cdcl3
 Data collected on: Jul 20 2016
 Operator: vmr41
 Relax. delay 1.689 sec
 Pulse 45.0 degree
 Acq. time 1.313 sec
 Width 25000.0 Hz
 128 repetitions
 OBSERVE C13: 100.3380141 MHz
 DECOUPLE F1: 399.6393159 MHz
 Power 43 dB
 continuously on
 WALTZ-16 modulated
 DATA PROCESSING
 Line broadening 1.0 Hz
 FT size 65536
 Total time 51 min



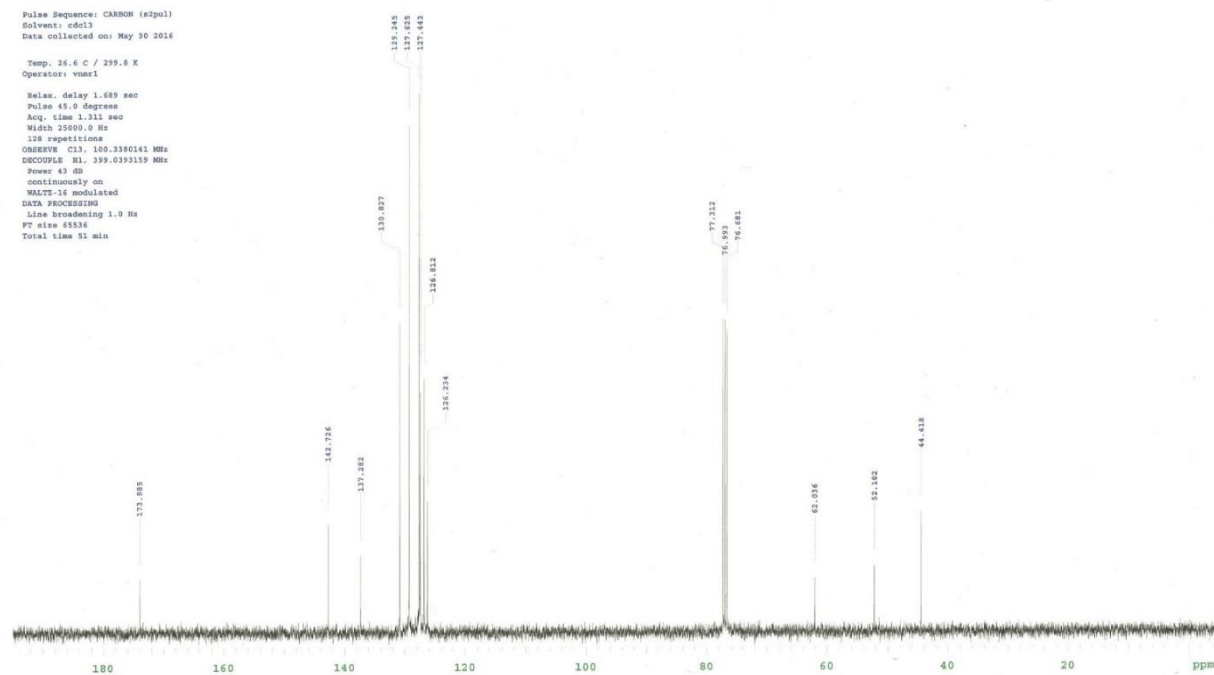


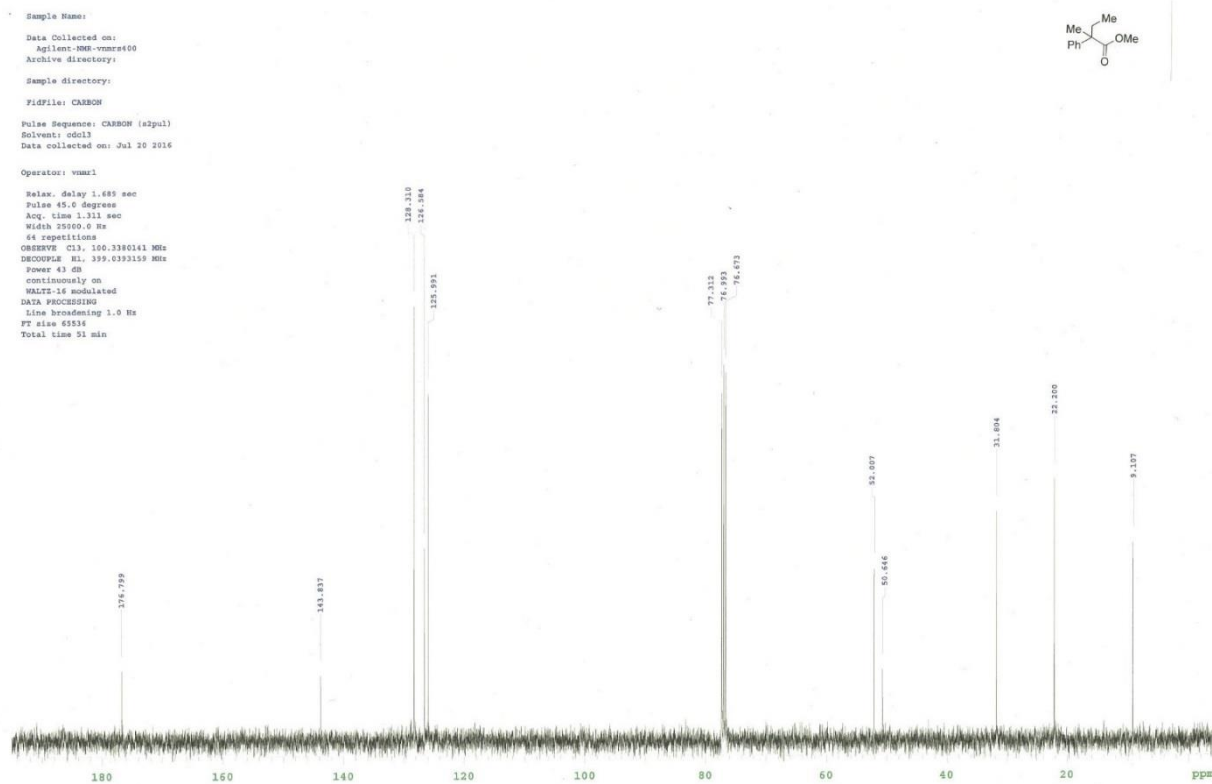
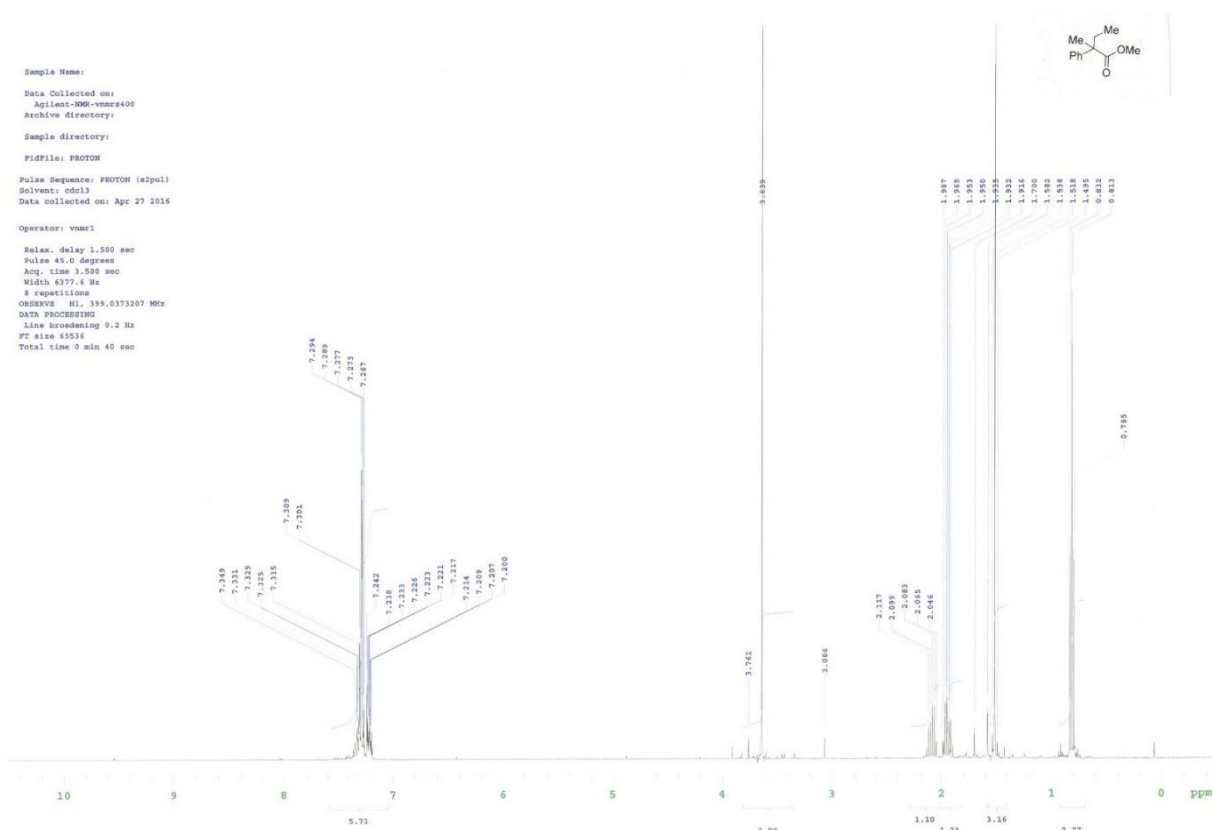


Sample Name:
 Data Collected on:
 Agilent-NMR-vnmr400
 Archive directory:
 Sample directory:
 FIDfile: PROTON
 Pulse Sequence: PROTON (s2pul)
 Solvent: cdcl3
 Data collected on: May 30 2016
 Operator: vnmr1
 Relax. delay 1.500 sec
 Pulse 45.0 degrees
 Acq. time 3.500 sec
 Width 6377.6 Hz
 8 repetitions
 OBSERVE HL 399.0373267 MHz
 DATA PROCESSING
 Line broadening 0.2 Hz
 FT size 65536
 Total time 0 min 49 sec

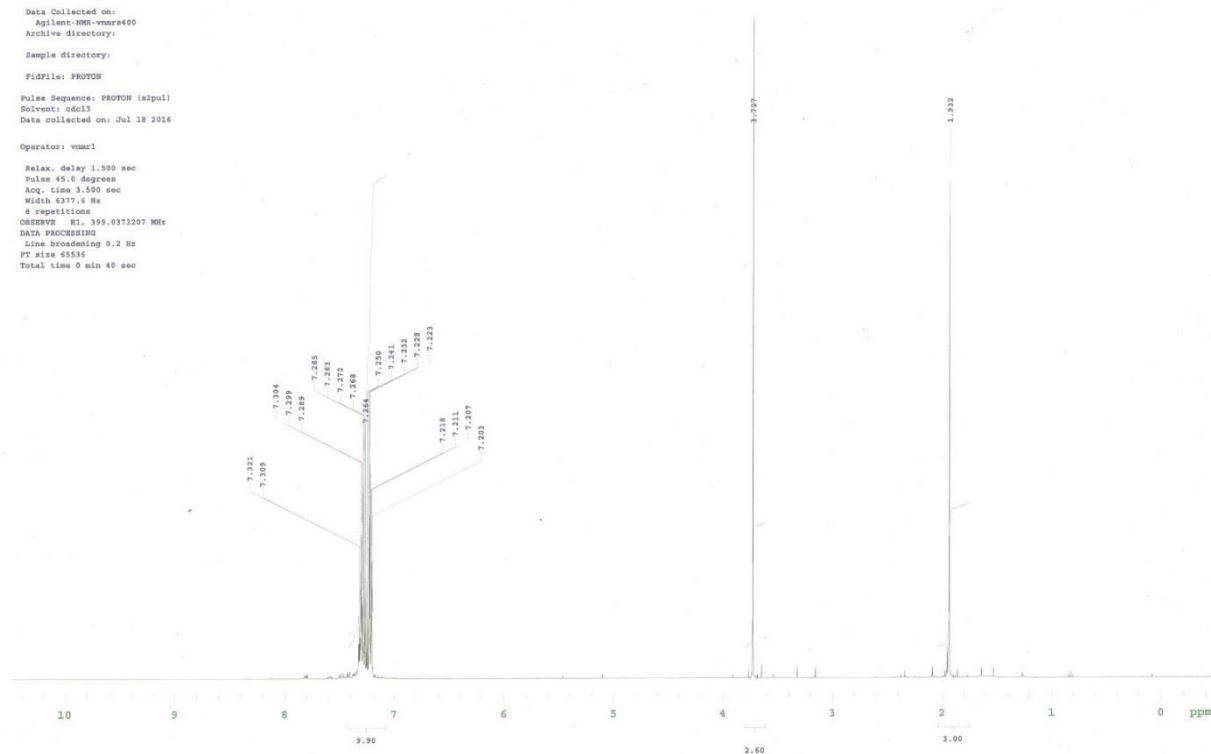


Sample Name:
 Data Collected on:
 Agilent-NMR-vnmr400
 Archive directory:
 Sample directory:
 FIDfile: CARBON
 Pulse Sequence: CARBON (s2pul)
 Solvent: cdcl3
 Data collected on: May 30 2016
 Temp. 24.6 C / 299.8 K
 Operator: vnmr1
 Relax. delay 1.689 sec
 Pulse 45.0 degrees
 Acq. time 1.311 sec
 Width 25000.0 Hz
 128 repetitions
 OBSERVE C13 100.3360141 MHz
 DECOUPLE HL 399.0393159 MHz
 Power 43 dB
 continuously on
 WALTZ-16 modulated
 DATA PROCESSING
 Line broadening 1.0 Hz
 FT size 65536
 Total time 51 min

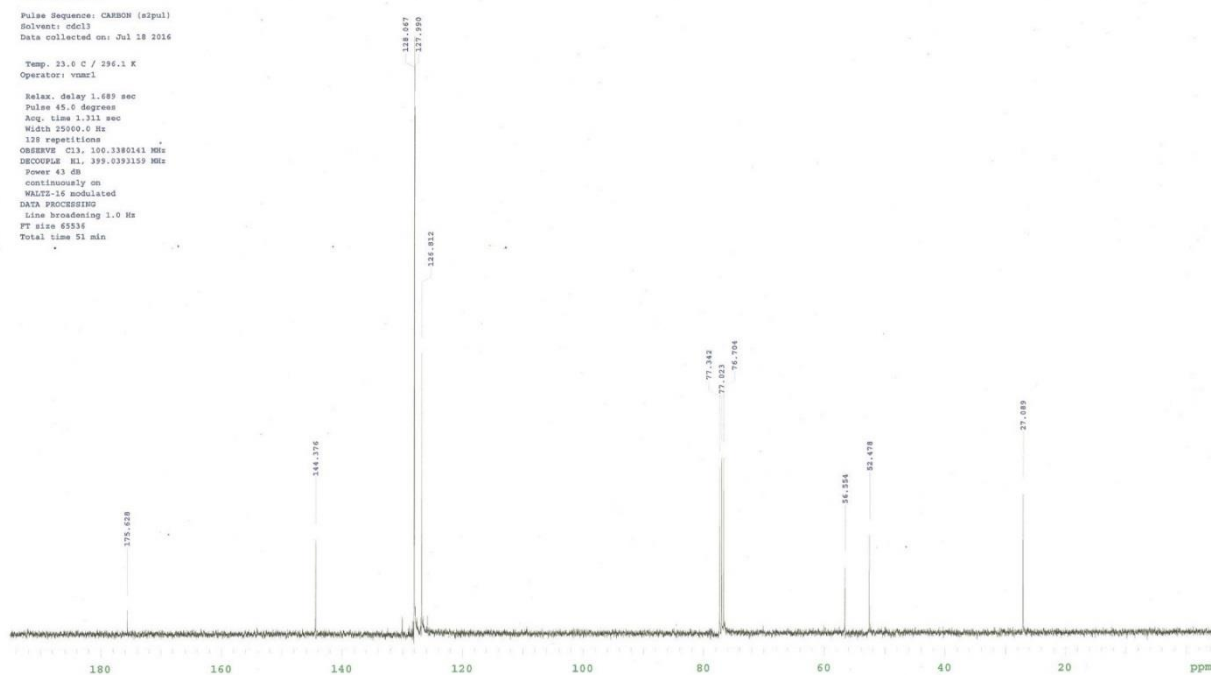




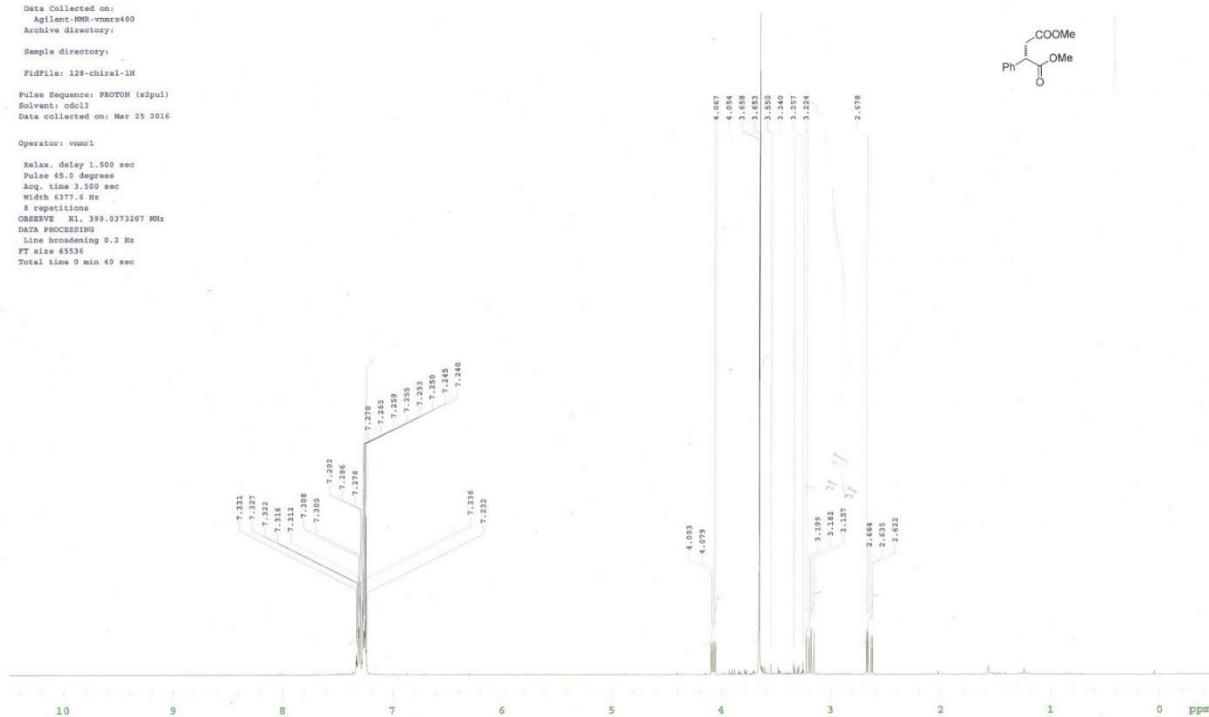
Sample Name:
 Data Collected on:
 Agilent-VNM-vmars400
 Archive directory:
 Sample directory:
 FIDFile: PROTON
 Pulse Sequence: PROTON (s2pul)
 Solvent: cdcl3
 Data collected on: Jul 18 2016
 Operator: vmars1
 Relax. delay 1.500 sec
 Pulse 45.0 degrees
 Acq. time 3.500 sec
 Width 6377.5 Hz
 8 repetitions
 OBSERVE H1, 399.6373207 MHz
 DATA PROCESSING
 Line broadening 0.2 Hz
 FT size 65536
 Total time 0 min 40 sec



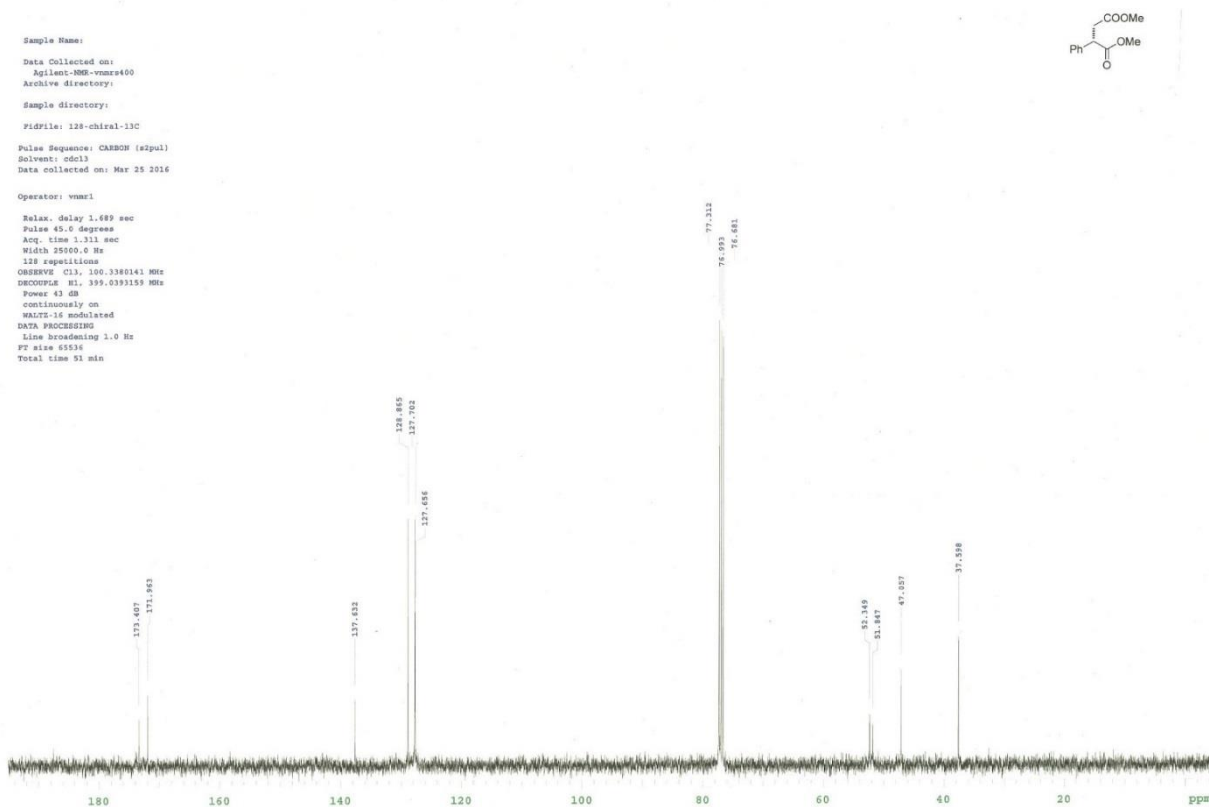
Sample Name:
 Data Collected on:
 Agilent-VNM-vmars400
 Archive directory:
 Sample directory:
 FIDFile: CARBON
 Pulse Sequence: CARBON (s2pul)
 Solvent: cdcl3
 Data collected on: Jul 18 2016
 Temp. 23.6 C / 296.1 K
 Operator: vmars1
 Relax. delay 1.689 sec
 Pulse 45.0 degrees
 Acq. time 1.313 sec
 Width 25060.0 Hz
 128 repetitions
 OBSERVE C13, 100.3380141 MHz
 DECOUPLE H1, 399.6393159 MHz
 Power 43.08
 continuously on
 WALTZ-16 modulated
 DATA PROCESSING
 Line broadening 1.0 Hz
 FT size 65536
 Total time 51 min



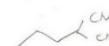
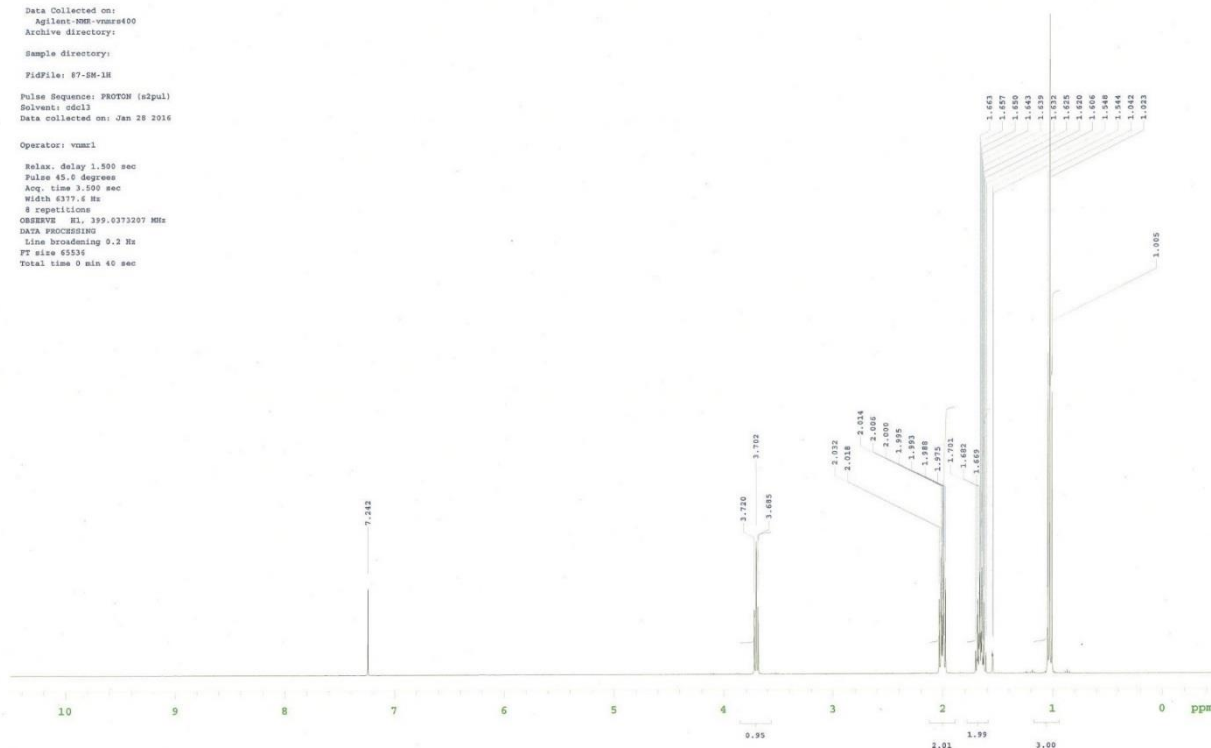
Sample Name:
 Data Collected on:
 Agilent-NMR-vnmr400
 Archive directory:
 Sample directory:
 FidFile: 128-chiral-1M
 Pulse Sequence: PROTON (s2pul)
 Solvent: cdcl3
 Data collected on: Mar 25 2016
 Operator: vnmr1
 Relax. delay 1.500 sec
 Pulse 45.0 degrees
 Acq. time 3.500 sec
 Width 6377.4 Hz
 8 repetitions
 OBSERVE H1, 399.0373207 MHz
 DATA PROCESSING
 Line broadening 0.2 Hz
 FT size 65536
 Total time 0 min 40 sec



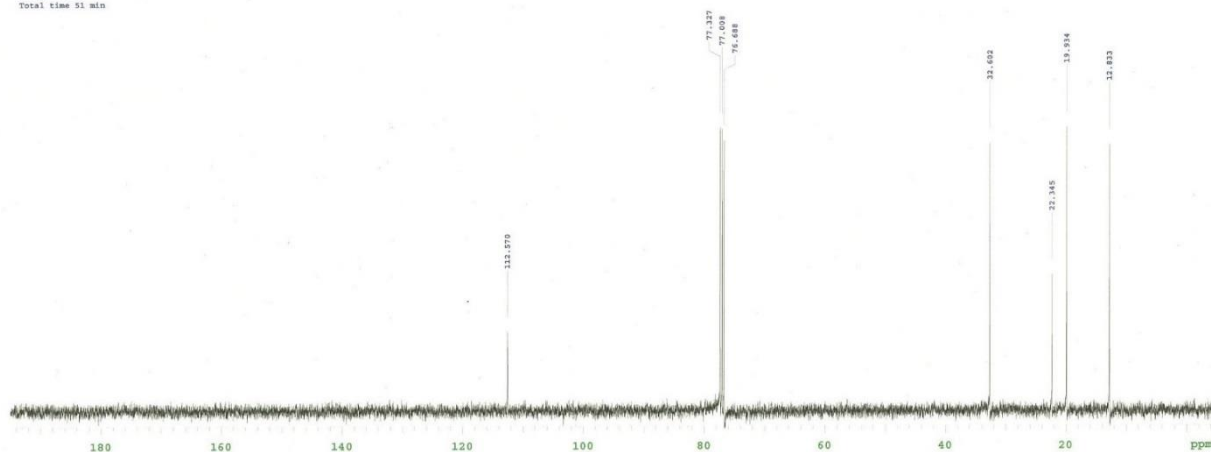
Sample Name:
 Data Collected on:
 Agilent-NMR-vnmr400
 Archive directory:
 Sample directory:
 FidFile: 128-chiral-13C
 Pulse Sequence: CARBON (s2pul)
 Solvent: cdcl3
 Data collected on: Mar 25 2016
 Operator: vnmr1
 Relax. delay 1.689 sec
 Pulse 45.0 degrees
 Acq. time 1.311 sec
 Width 35900.0 Hz
 128 repetitions
 OBSERVE C13, 100.3360141 MHz
 DECOUPLE H1, 399.039155 MHz
 Power 43 dB
 continuously on
 WALTZ-16 modulated
 DATA PROCESSING
 Line broadening 1.0 Hz
 FT size 65536
 Total time 51 min

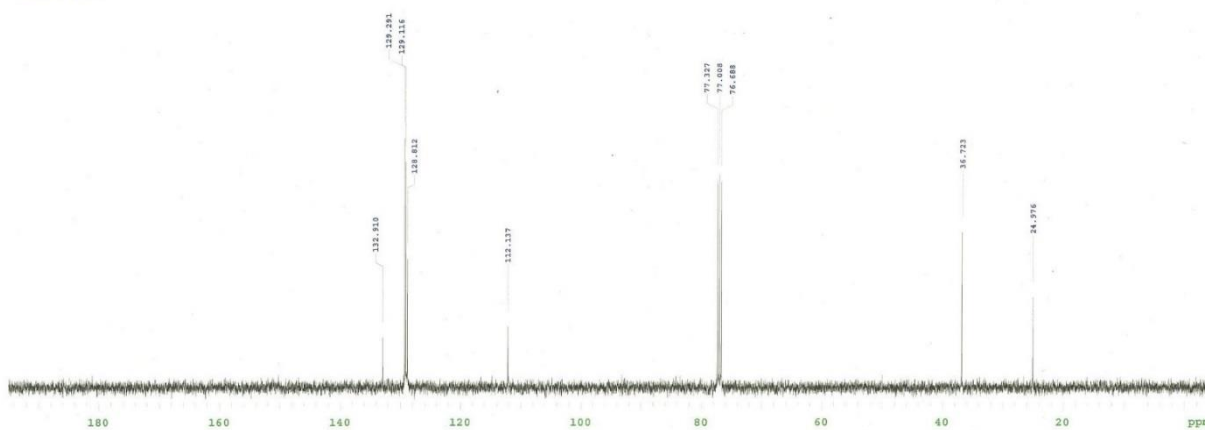
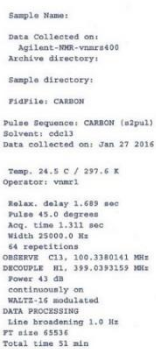
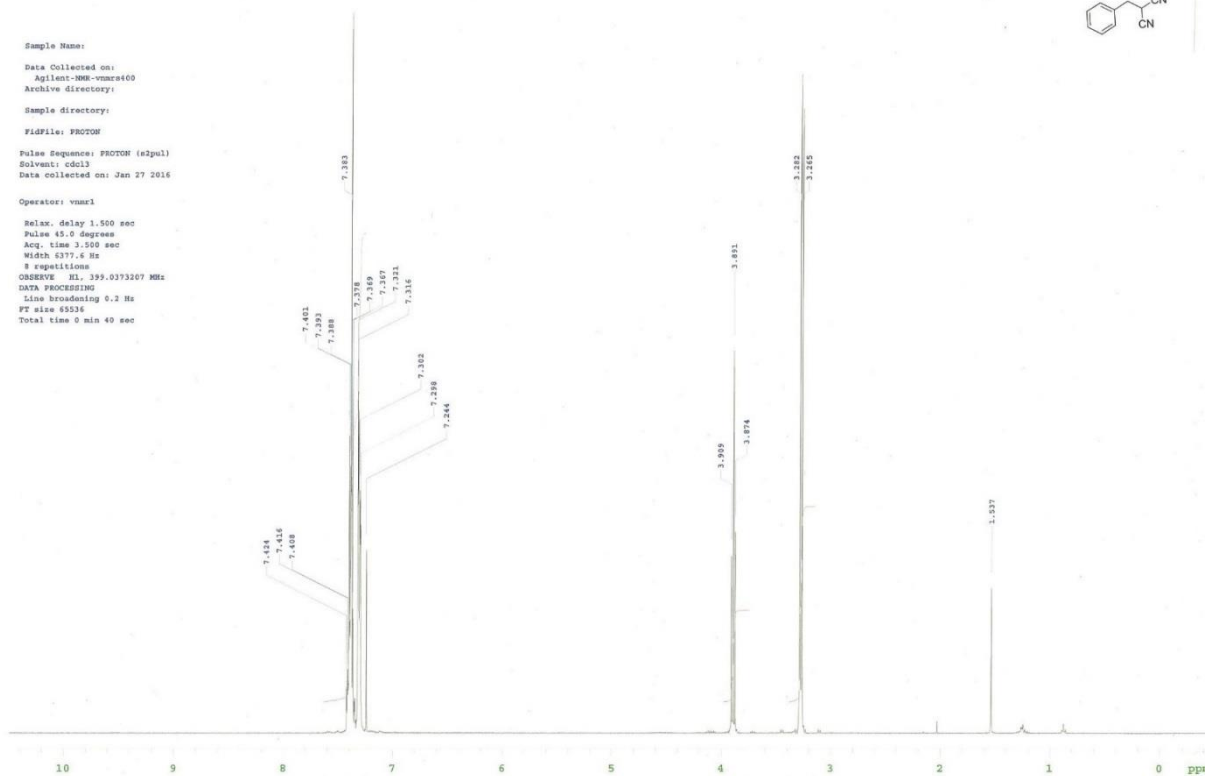


Sample Name:
 Data Collected on:
 Agilent-MMR-vnmr400
 Archive directory:
 Sample directory:
 FidFile: 87-SM-18
 Pulse Sequence: PROTON (s2pul)
 Solvent: cdcl3
 Data collected on: Jan 28 2016
 Operator: vnmr1
 Relax. delay 1.500 sec
 Pulse 45.0 degrees
 Acq. time 3.500 sec
 Width 6377.6 Hz
 6 repetitions
 OBSERVE H1, 399.0373207 MHz
 DATA PROCESSING
 Line broadening 0.2 Hz
 FT size 65536
 Total time 0 min 40 sec

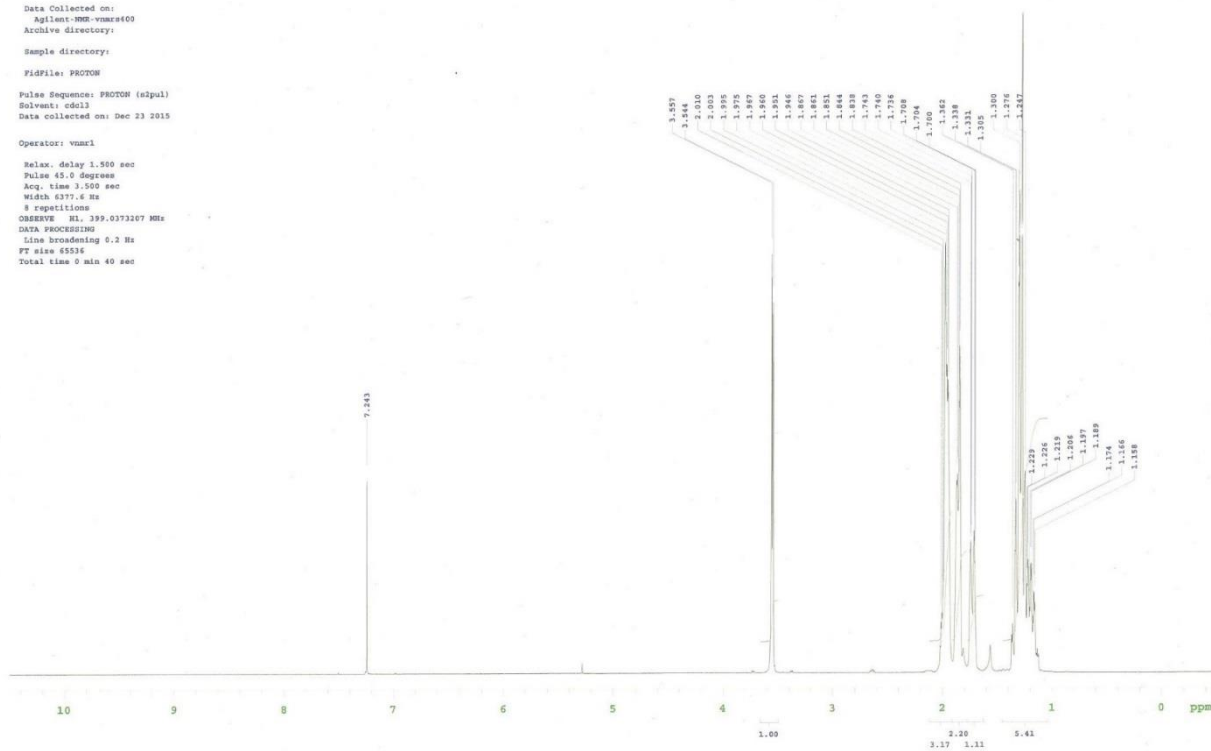


2Cl-75-TMS
 Sample Name:
 Data Collected on:
 Agilent-MMR-vnmr400
 Archive directory:
 Sample directory:
 FidFile: 87-SM-13C
 Pulse Sequence: CARBON (s2pul)
 Solvent: cdcl3
 Data collected on: Jan 28 2016
 Operator: vnmr1
 Relax. delay 1.689 sec
 Pulse 45.0 degrees
 Acq. time 1.311 sec
 Width 25000.0 Hz
 128 repetitions
 OBSERVE C13, 100.3380141 MHz
 DECOUPLE H1, 399.0373159 MHz
 Power 43 dB
 continuously on
 WALTZ-16 modulated
 DATA PROCESSING
 Line broadening 1.0 Hz
 FT size 65536
 Total time 51 min

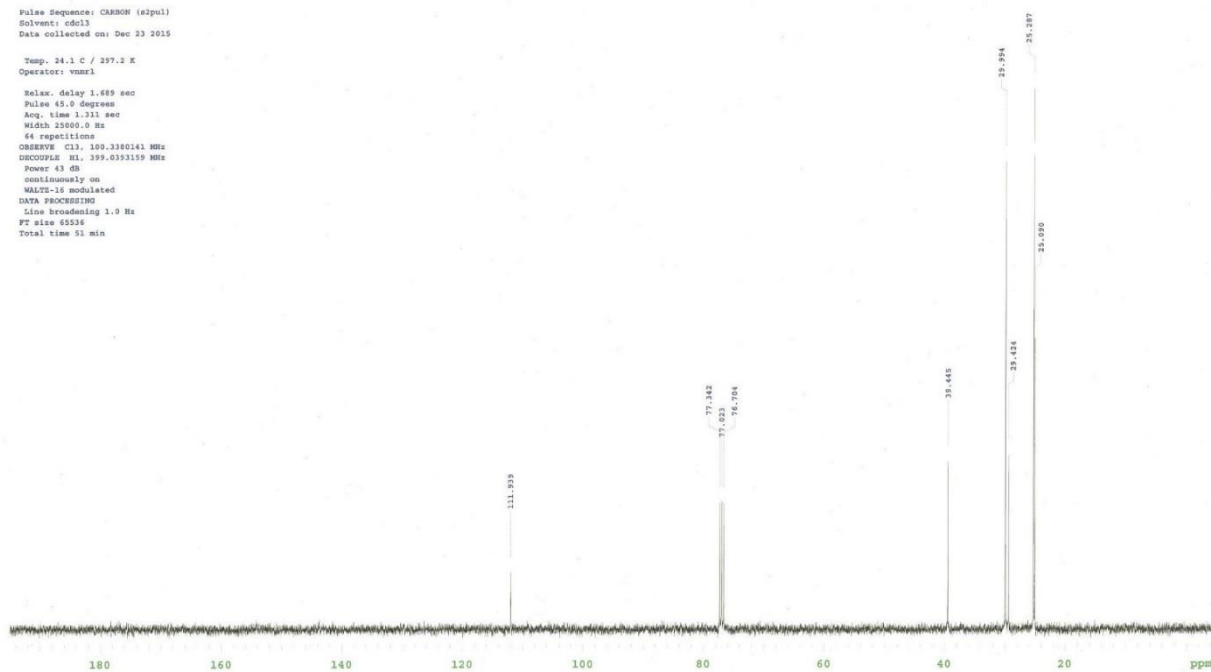




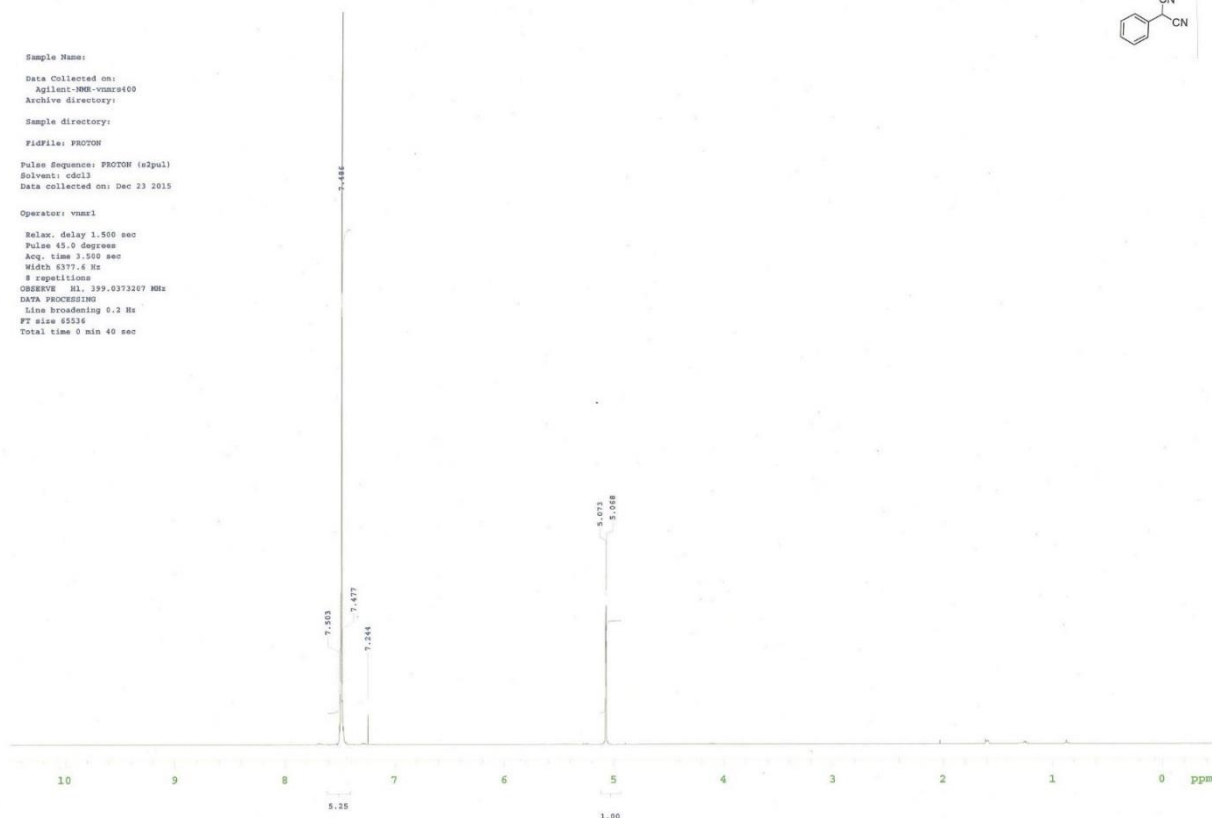
Sample Name:
 Data Collected on:
 Agilent-NMR-vnmr600
 Archive directory:
 Sample directory:
 Fidfile: PROTON
 Pulse Sequence: PROTON (s2pul)
 Solvent: cdcl3
 Data collected on: Dec 23 2015
 Operator: vnmr1
 Relax. delay 1.500 sec
 Pulse 45.0 degrees
 Acq. time 3.500 sec
 Width 6377.6 Hz
 8 repetitions
 OBSERVE HL 399.0373267 MHz
 DATA PROCESSING
 Line broadening 0.2 Hz
 FT size 65536
 Total time 0 min 40 sec



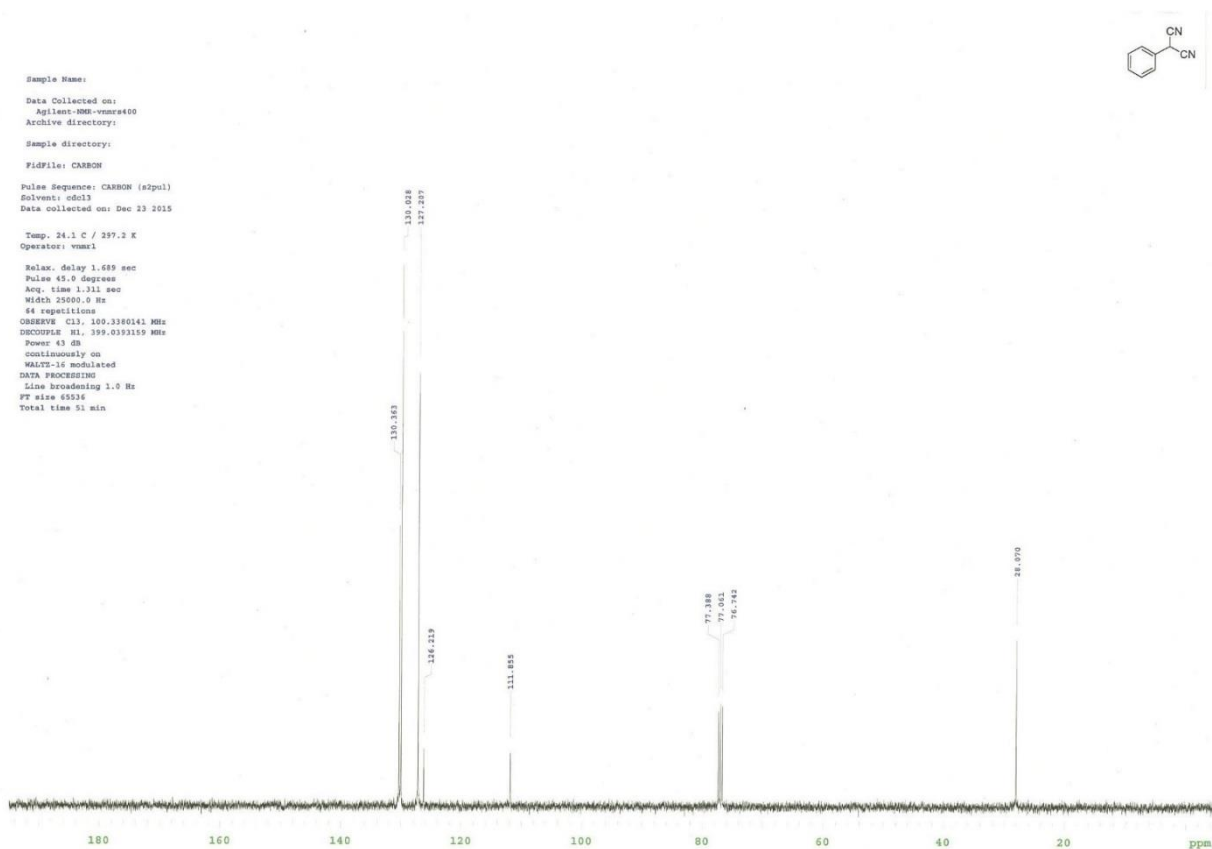
Sample Name:
 Data Collected on:
 Agilent-NMR-vnmr600
 Archive directory:
 Sample directory:
 Fidfile: CARBON
 Pulse Sequence: CARBON (s2pul)
 Solvent: cdcl3
 Data collected on: Dec 23 2015
 Temp. 24.1 C / 297.2 K
 Operator: vnmr1
 Relax. delay 1.669 sec
 Pulse 45.0 degrees
 Acq. time 1.333 sec
 Width 25000.0 Hz
 64 repetitions
 OBSERVE CH 100.3360143 MHz
 DECOUPLE HL 399.0333159 MHz
 Power 43 dB
 Continuously on
 WALTZ-16 modulated
 DATA PROCESSING
 Line broadening 3.0 Hz
 FT size 65536
 Total time 51 min

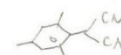


Sample Name:
 Data Collected on:
 Agilent-VNM-vmx400
 Archive directory:
 Sample directory:
 Fidfile: PROTON
 Pulse Sequence: PROTON (s2pul)
 Solvent: cdcl3
 Data collected on: Dec 23 2015
 Operator: vmx41
 Relax. delay 1.550 sec
 Pulse 45.0 degrees
 Acq. time 3.550 sec
 Width 6377.4 Hz
 8 repetitions
 OBSERVE H1, 399.0373207 MHz
 DATA PROCESSING
 Line broadening 0.3 Hz
 FT size 65536
 Total time 0 min 40 sec

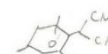
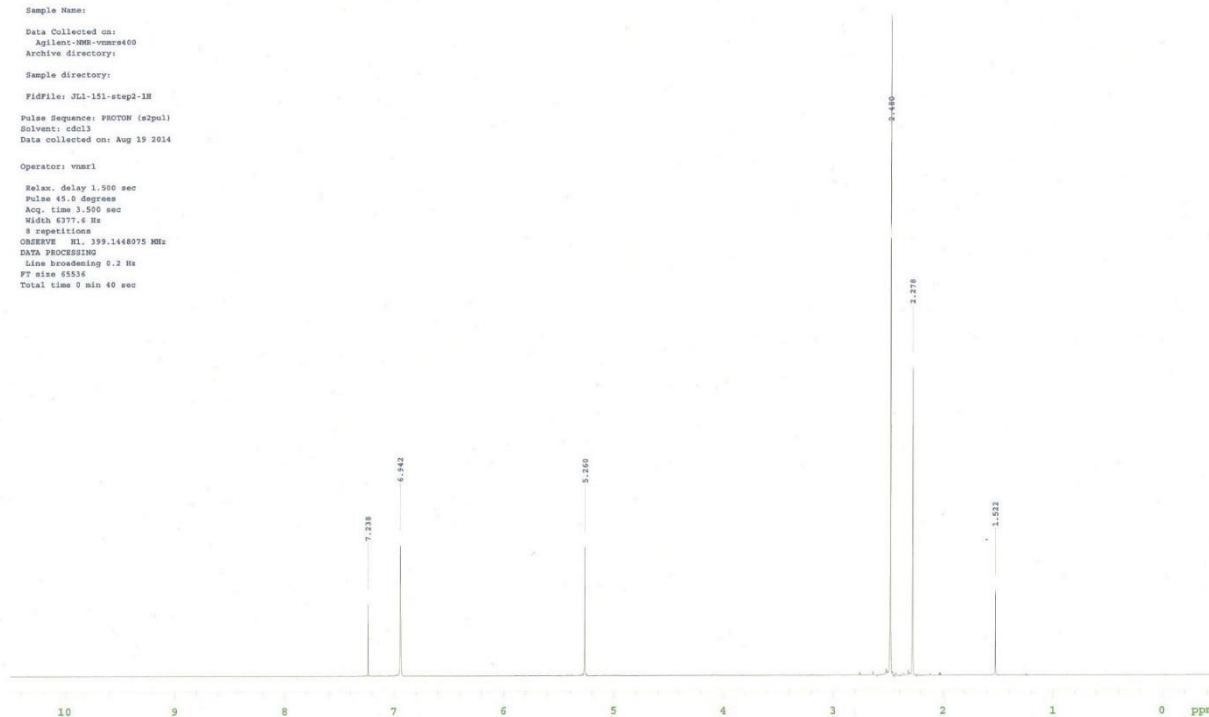


Sample Name:
 Data Collected on:
 Agilent-VNM-vmx400
 Archive directory:
 Sample directory:
 Fidfile: CARBON
 Pulse Sequence: CARBON (s2pul)
 Solvent: cdcl3
 Data collected on: Dec 23 2015
 Temp. 24.1 C / 297.2 K
 Operator: vmx41
 Relax. delay 1.689 sec
 Pulse 45.0 degrees
 Acq. time 1.311 sec
 Width 25000.0 Hz
 64 repetitions
 OBSERVE C13, 100.3360141 MHz
 DECOUPLE H1, 399.0373159 MHz
 Power 43 dB
 Continuously on
 WALTZ-16 modulated
 DATA PROCESSING
 Line broadening 1.0 Hz
 FT size 65536
 Total time 51 min

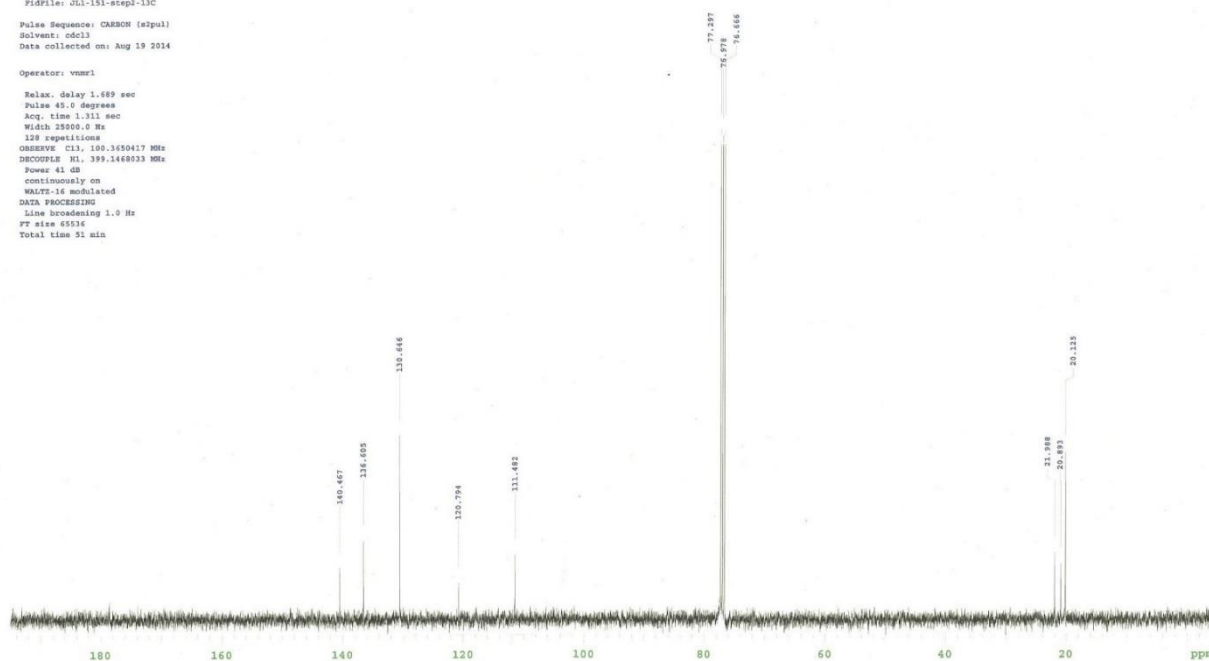




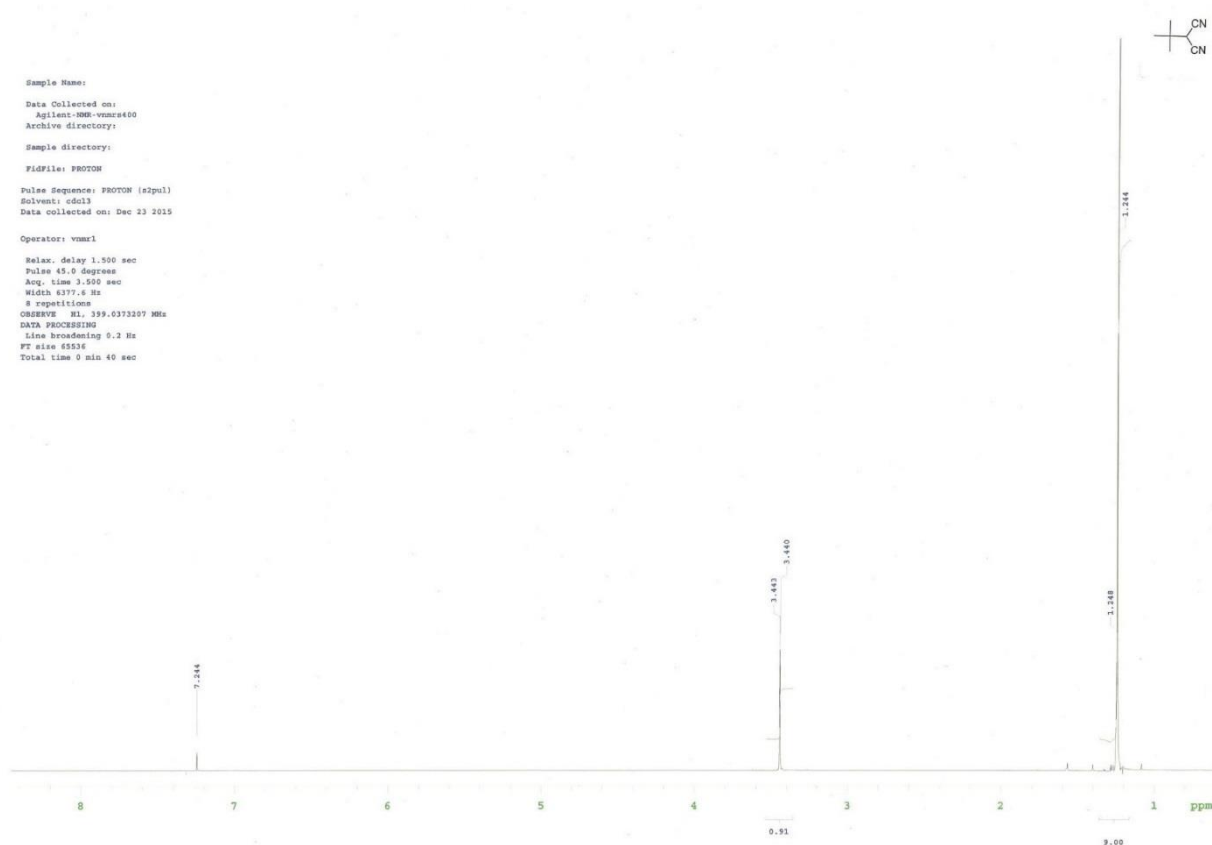
Sample Name:
 Data Collected on:
 Agilent-1H-500-mmh400
 Archive directory:
 Sample directory:
 Fidfile: JLI-151-step2-1H
 Pulse Sequence: PROTON (s2pul)
 Solvent: cdcl3
 Data collected on: Aug 19 2014
 Operator: vnmr1
 Relax. delay 1.500 sec
 Pulse 45.0 degrees
 Acq. time 3.500 sec
 Width 6377.6 Hz
 8 repetitions
 OBSERVE H1, 399.1448975 MHz
 DATA PROCESSING
 Line broadening 0.2 Hz
 FT size 65536
 Total time 9 min 40 sec



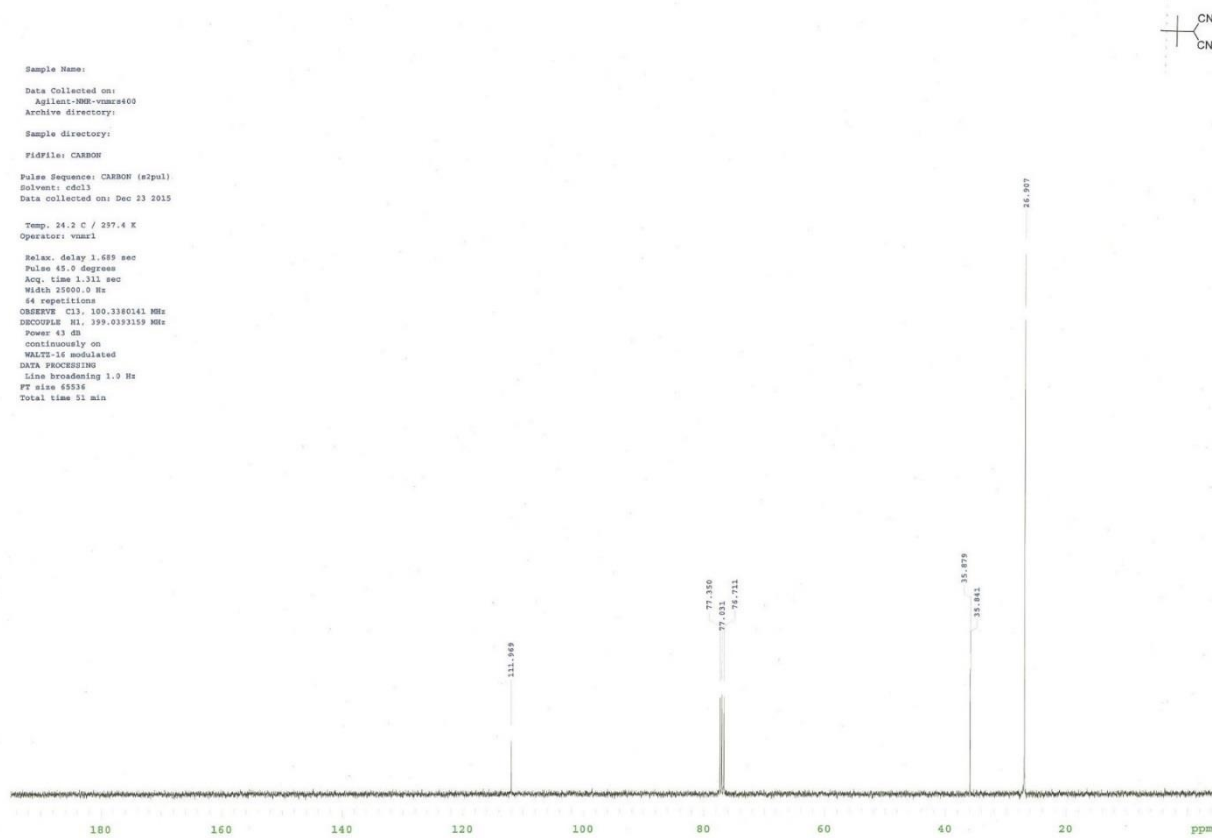
Sample Name:
 Data Collected on:
 Agilent-1H-500-mmh400
 Archive directory:
 Sample directory:
 Fidfile: JLI-151-step2-13C
 Pulse Sequence: CARBON (s2pul)
 Solvent: cdcl3
 Data collected on: Aug 19 2014
 Operator: vnmr1
 Relax. delay 1.689 sec
 Pulse 45.0 degrees
 Acq. time 1.311 sec
 Width 25000.0 Hz
 128 repetitions
 OBSERVE C13, 100.3650417 MHz
 DECOUPLE H1, 399.1448975 MHz
 Power 41 dB
 continuously on
 WALTZ-16 modulated
 DATA PROCESSING
 Line broadening 1.0 Hz
 FT size 65536
 Total time 31 min



Sample Name:
 Data Collected on:
 Agilent-NMR-vnmr400
 Archive directory:
 Sample directory:
 Fidfile: PROTON
 Pulse Sequence: PROTON (s2pul)
 Solvent: cdcl3
 Data collected on: Dec 23 2015
 Operator: vnmr1
 Relax. delay 1.500 sec
 Pulse 45.0 degrees
 Acq. time 3.500 sec
 Width 6377.6 Hz
 8 repetitions
 OBSERVE H1, 399.0373207 MHz
 DATA PROCESSING
 Line broadening 0.2 Hz
 FT size 65536
 Total time 0 min 40 sec

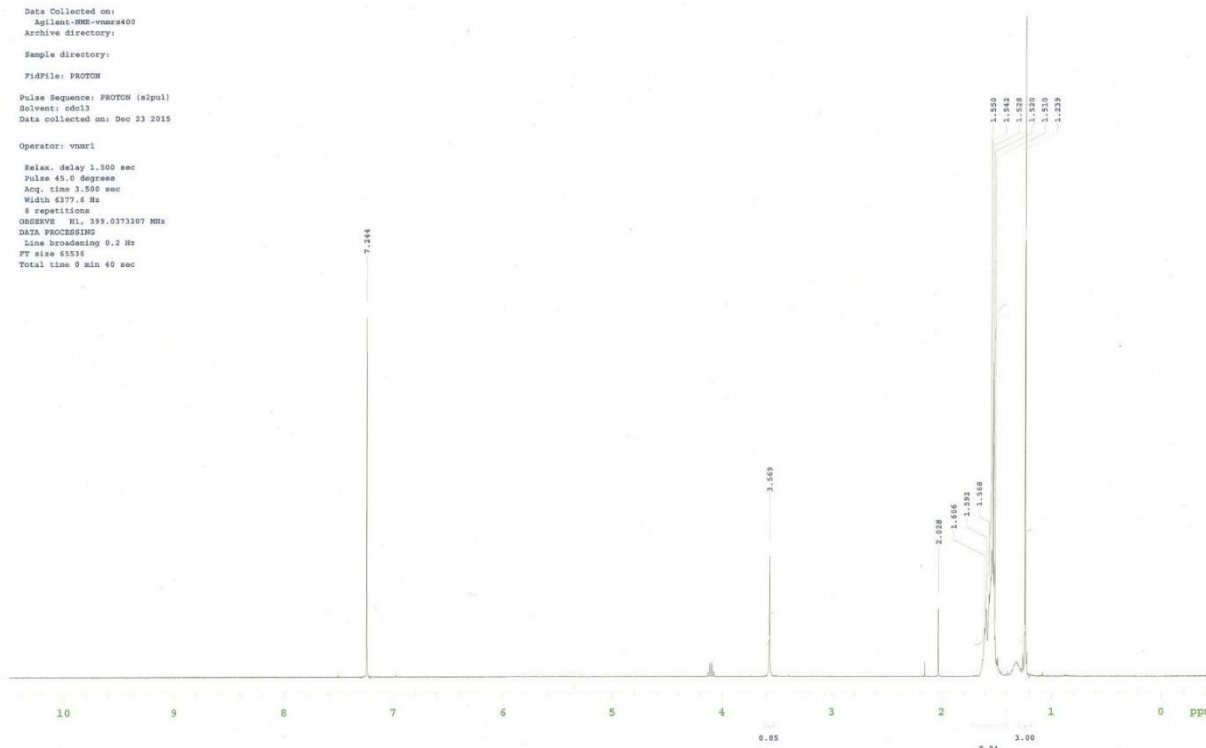


Sample Name:
 Data Collected on:
 Agilent-NMR-vnmr400
 Archive directory:
 Sample directory:
 Fidfile: CARBON
 Pulse Sequence: CARBON (s2pul)
 Solvent: cdcl3
 Data collected on: Dec 23 2015
 Temp. 24.2 C / 297.4 K
 Operator: vnmr1
 Relax. delay 1.669 sec
 Pulse 45.0 degrees
 Acq. time 1.311 sec
 Width 25000.0 Hz
 64 repetitions
 OBSERVE C13, 100.3360141 MHz
 DECOUPLE H1, 399.0373159 MHz
 Power 43 dB
 continuously on
 WALTZ-16 modulated
 DATA PROCESSING
 Line broadening 1.0 Hz
 FT size 65536
 Total time 31 min

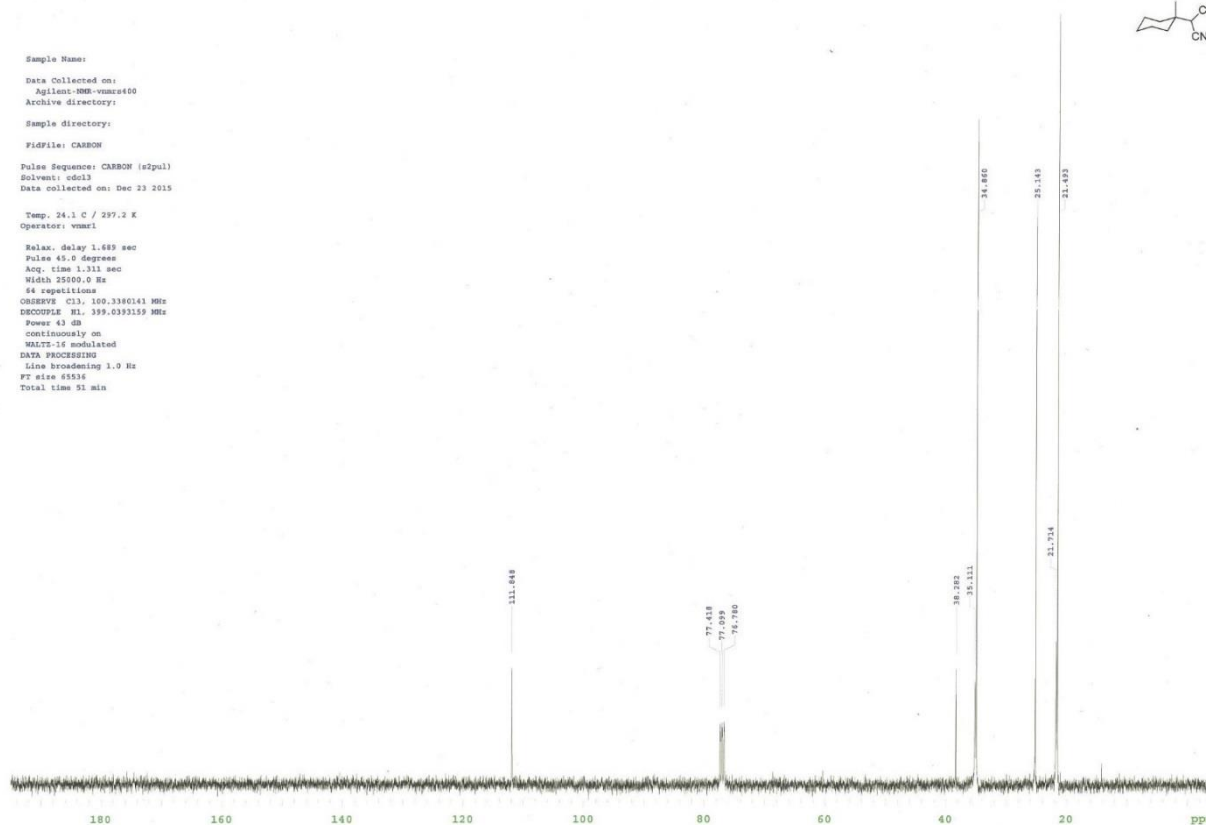


STANDARD IN OBSERVE - profile

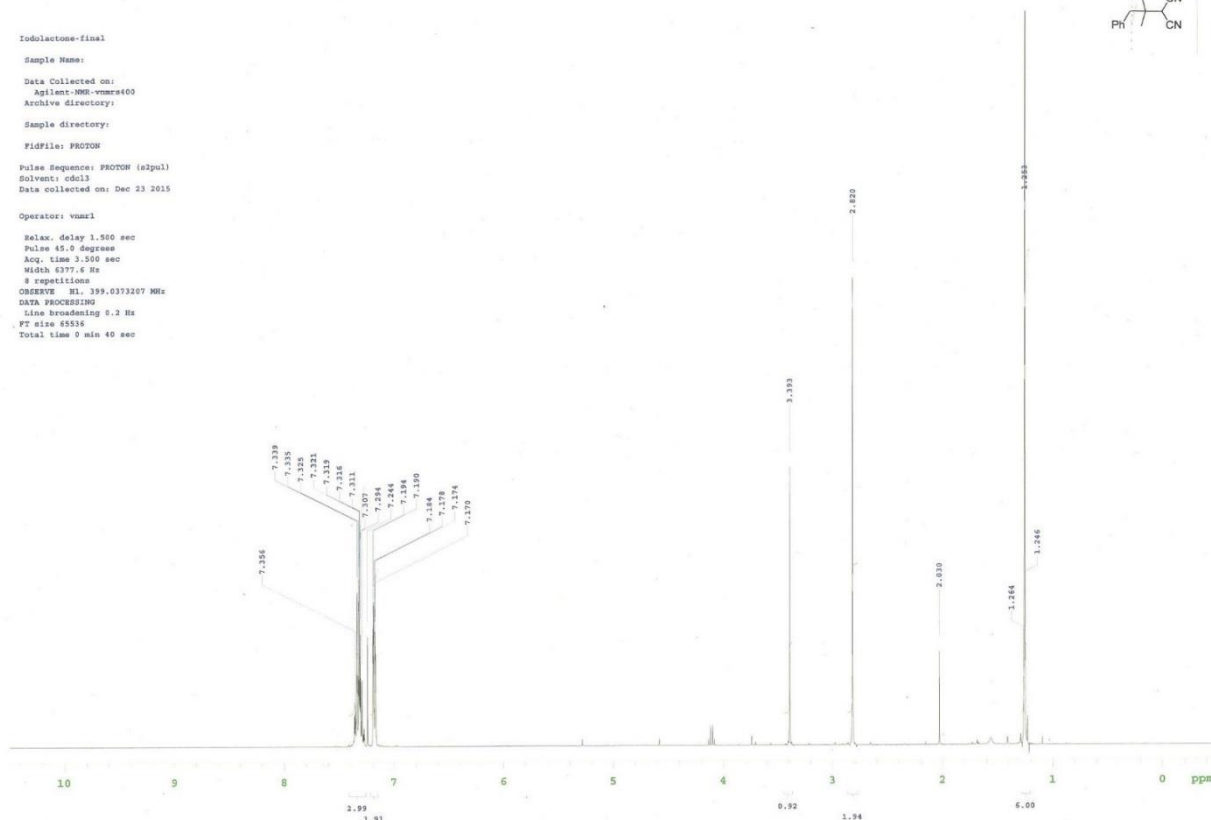
Sample Name:
Data Collected on:
Agilent-HW-vnmr400
Archive directory:
Sample directory:
FidFile: PROTON
Pulse Sequence: PROTON (s2pul)
Solvent: cdcl3
Data collected on: Dec 23 2015
Operator: vnmr1
Relax. delay 1.500 sec
Pulse 45.0 degree
Acq. time 3.550 sec
Width 6377.6 Hz
6 repetitions
OBSERVE H1, 399.0373207 MHz
DATA PROCESSING
Line broadening 9.2 Hz
FT size 65536
Total time 9 min 40 sec



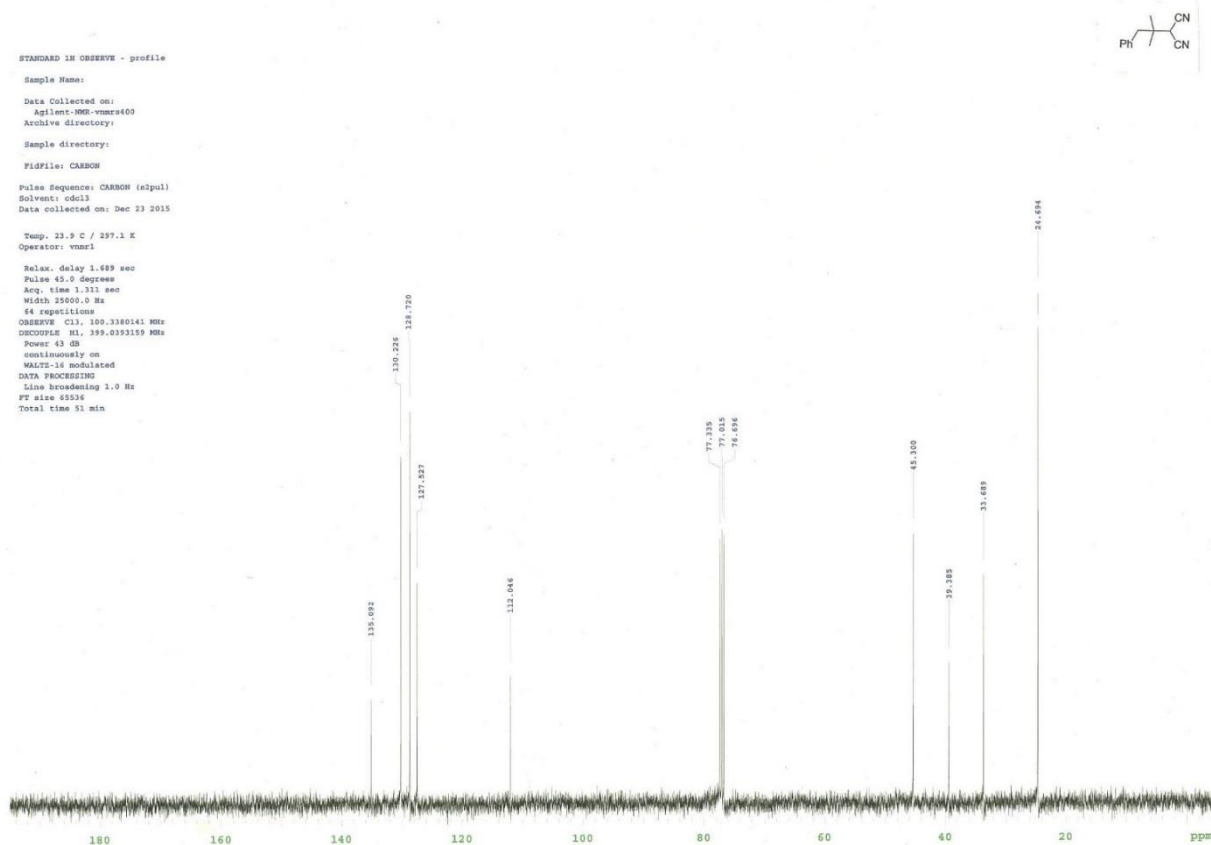
Sample Name:
Data Collected on:
Agilent-HW-vnmr400
Archive directory:
Sample directory:
FidFile: CARBON
Pulse Sequence: CARBON (s2pul)
Solvent: cdcl3
Data collected on: Dec 23 2015
Temp. 24.1 C / 297.2 K
Operator: vnmr1
Relax. delay 1.689 sec
Pulse 45.0 degree
Acq. time 1.311 sec
Width 25500.0 Hz
64 repetitions
OBSERVE C13, 100.3360143 MHz
DECOUPLE H1, 399.0393159 MHz
Power 43 dB
continuously on
WALTZ-16 modulated
DATA PROCESSING
Line broadening 1.0 Hz
FT size 65536
Total time 51 min



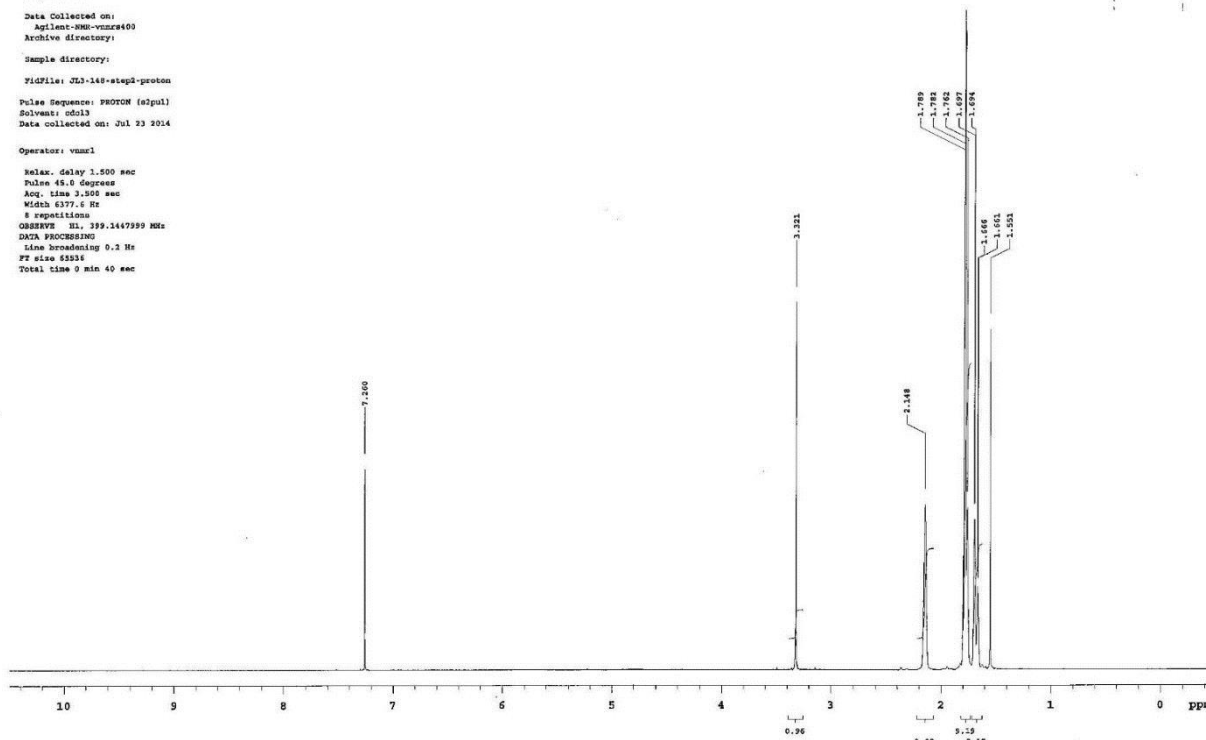
Iodolactone-final
 Sample Name:
 Data Collected on:
 Agilent-NMR-vnmr400
 Archive directory:
 Sample directory:
 Fidfile: PROTON
 Pulse Sequence: PROTON (s2pul)
 Solvent: cdcl3
 Data collected on: Dec 23 2015
 Operator: vnmr1
 Relax. delay 1.500 sec
 Pulse 45.0 degrees
 Acq. time 1.500 sec
 Width 6377.6 Hz
 8 repetitions
 OBSERVE HL 399.0373207 MHz
 DATA PROCESSING
 Line broadening 5.2 Hz
 FT size 65536
 Total time 9 min 40 sec



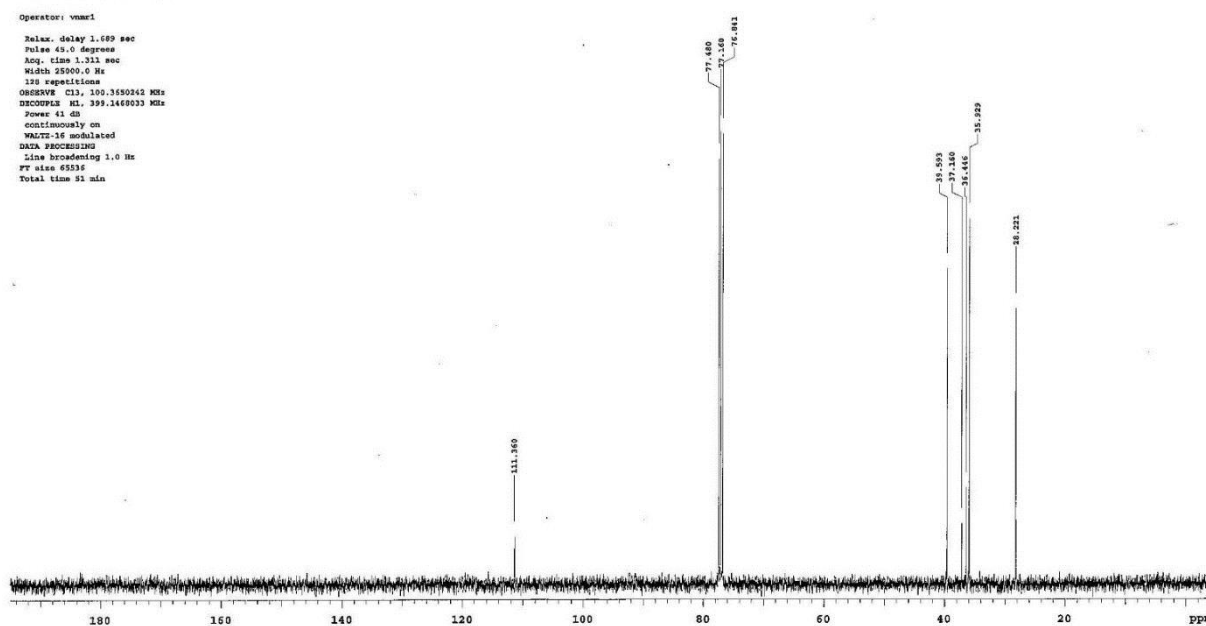
STANDARD 1H OBSERVE - profile
 Sample Name:
 Data Collected on:
 Agilent-NMR-vnmr400
 Archive directory:
 Sample directory:
 Fidfile: CARBON
 Pulse Sequence: CARBON (s2pul)
 Solvent: cdcl3
 Data collected on: Dec 23 2015
 Temp. 23.9 C / 297.1 K
 Operator: vnmr1
 Relax. delay 1.689 sec
 Pulse 45.0 degrees
 Acq. time 1.311 sec
 Width 25000.0 Hz
 64 repetitions
 OBSERVE CL3, 100.3180141 MHz
 DECOUPLE HL 399.0393159 MHz
 Power 43 dB
 continuously on
 WALTZ-16 modulated
 DATA PROCESSING
 Line broadening 1.0 Hz
 FT size 65536
 Total time 51 min

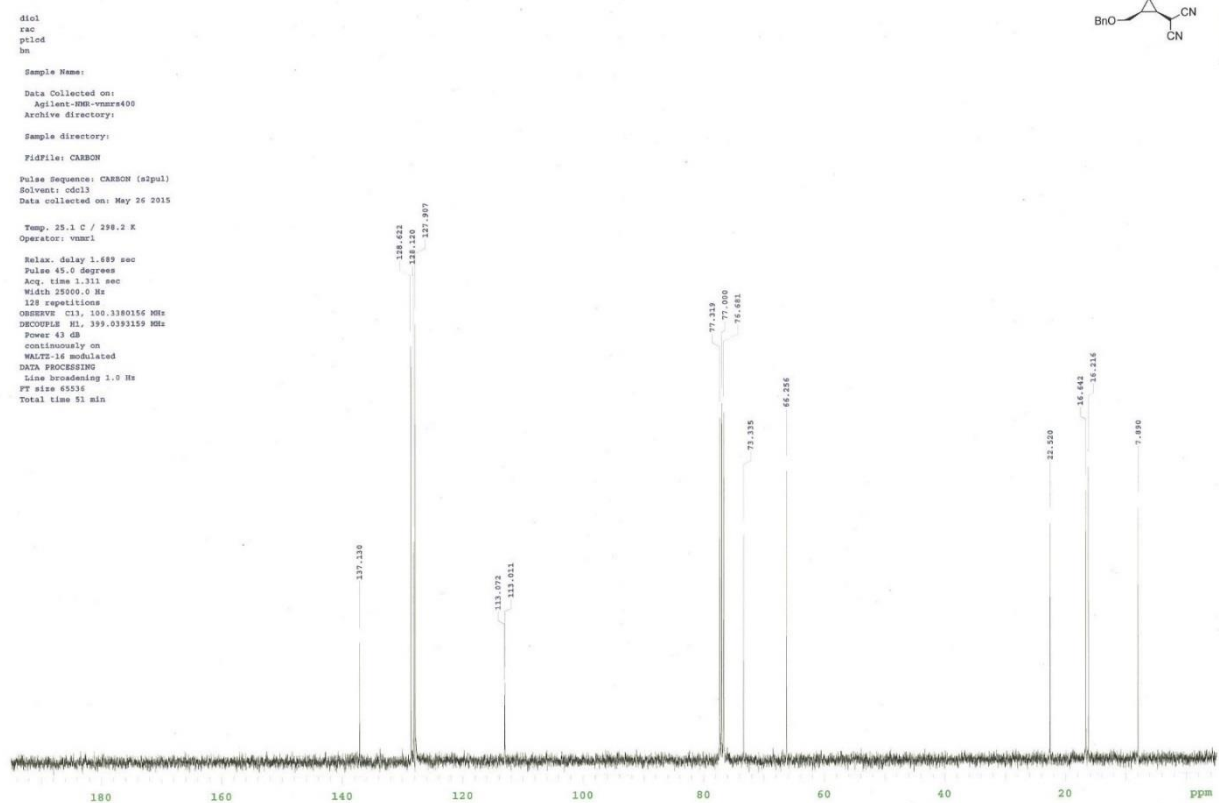
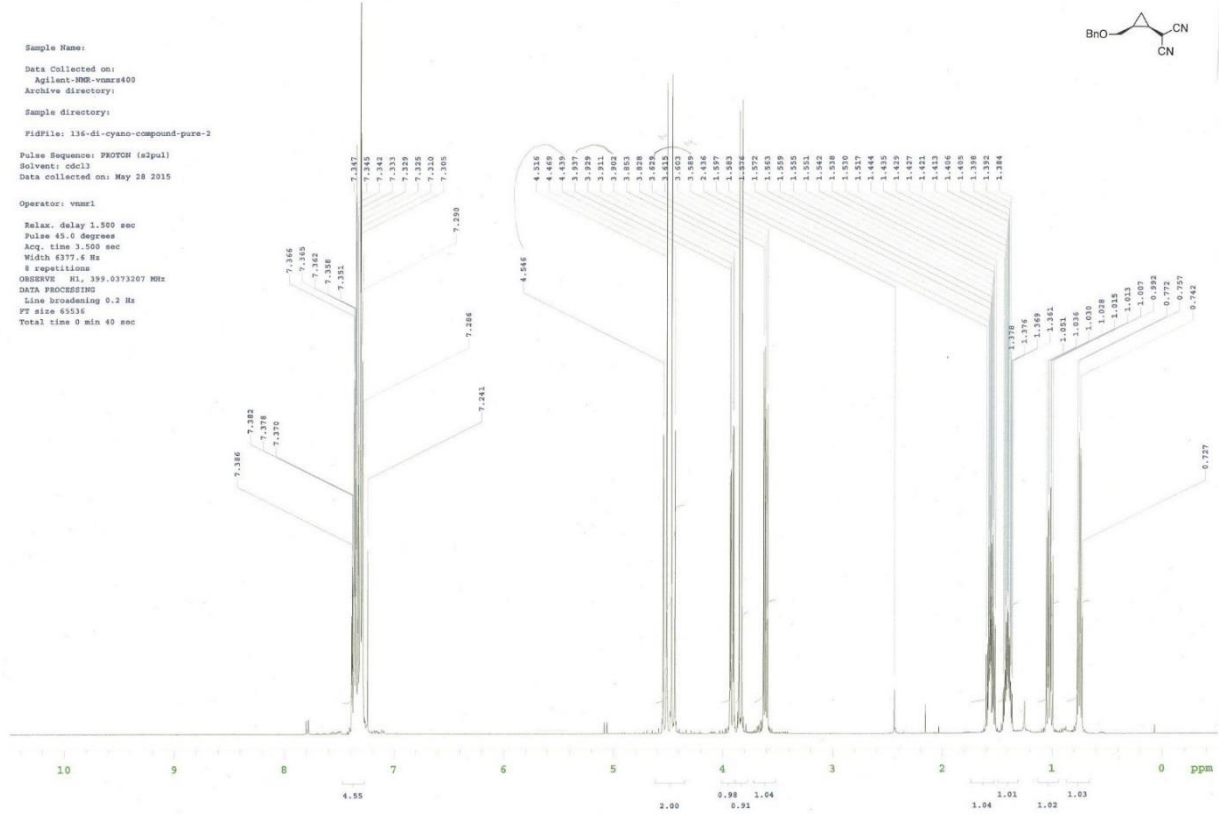


Sample Name:
 Data Collected on:
 Agilent-NMR-vnmr400
 Archive directory:
 Sample directory:
 FidFile: JLS-148-step2-proton
 Pulse Sequence: PROTON (a2pul)
 Solvent: cdcl3
 Data collected on: Jul 23 2014
 Operator: vnmr1
 Relax. delay 1.500 sec
 Pulse 45.0 degrees
 Acq. time 2.500 sec
 Width 6377.6 Hz
 8 repetitions
 OBSERVE H1. 399.1447399 MHz
 DATA PROCESSING
 Line broadening 0.2 Hz
 FT size 65536
 Total time 9 min 40 sec



Sample Name:
 Data Collected on:
 Agilent-NMR-vnmr400
 Archive directory:
 Sample directory:
 FidFile: JLS-148-step2-13C
 Pulse Sequence: CARBON (a2pul)
 Solvent: cdcl3
 Data collected on: Jul 23 2014
 Operator: vnmr1
 Relax. delay 1.689 sec
 Pulse 45.0 degrees
 Acq. time 1.311 sec
 Width 25000.0 Hz
 128 repetitions
 OBSERVE C13. 100.3550242 MHz
 DECOUPLE H1. 399.1448033 MHz
 Power 41 dB
 continuously on
 WALTZ-16 modulated
 DATA PROCESSING
 Line broadening 1.0 Hz
 FT size 65536
 Total time 51 min





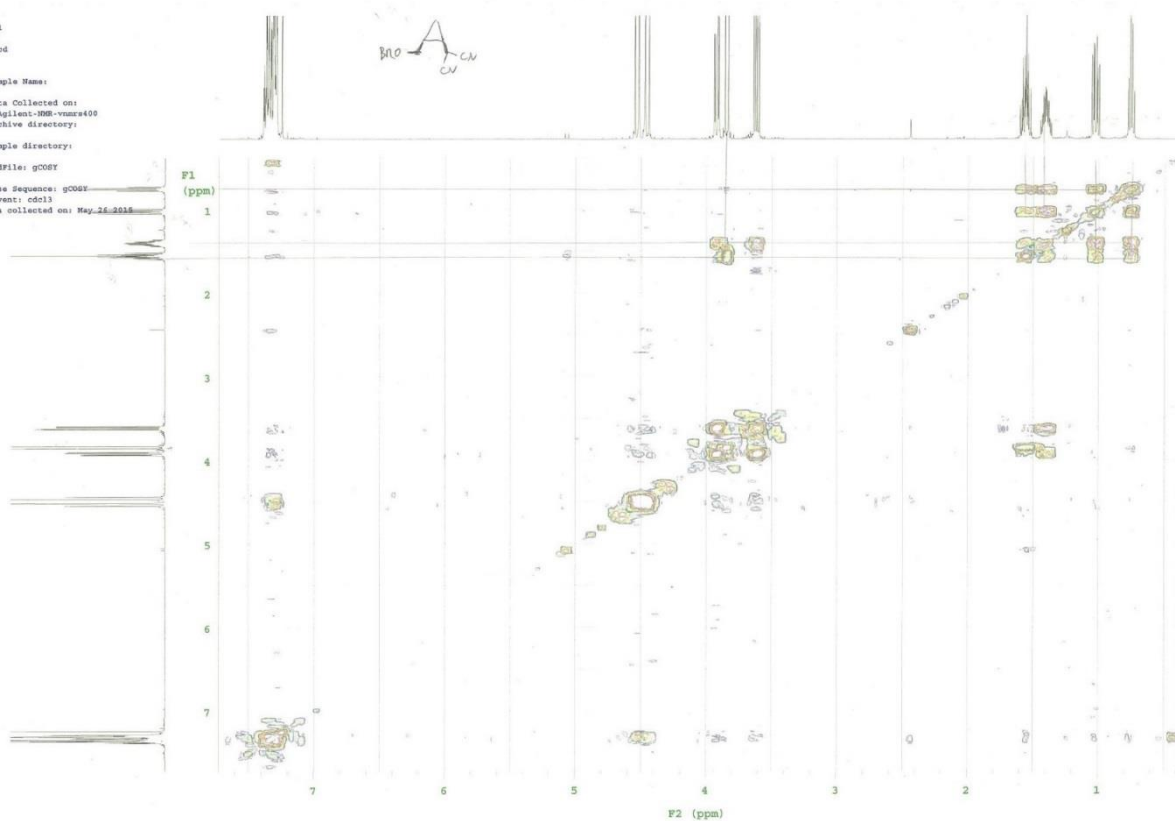
diol
rac
ptled
ba

Sample Name:

Data Collected on:
Agilent-900-vnmr400
Archive directory:

Sample directory:

FidFile: g0067
Pulse Sequence: g0067
Solvent: cdcl3
Data collected on: May 26 2015



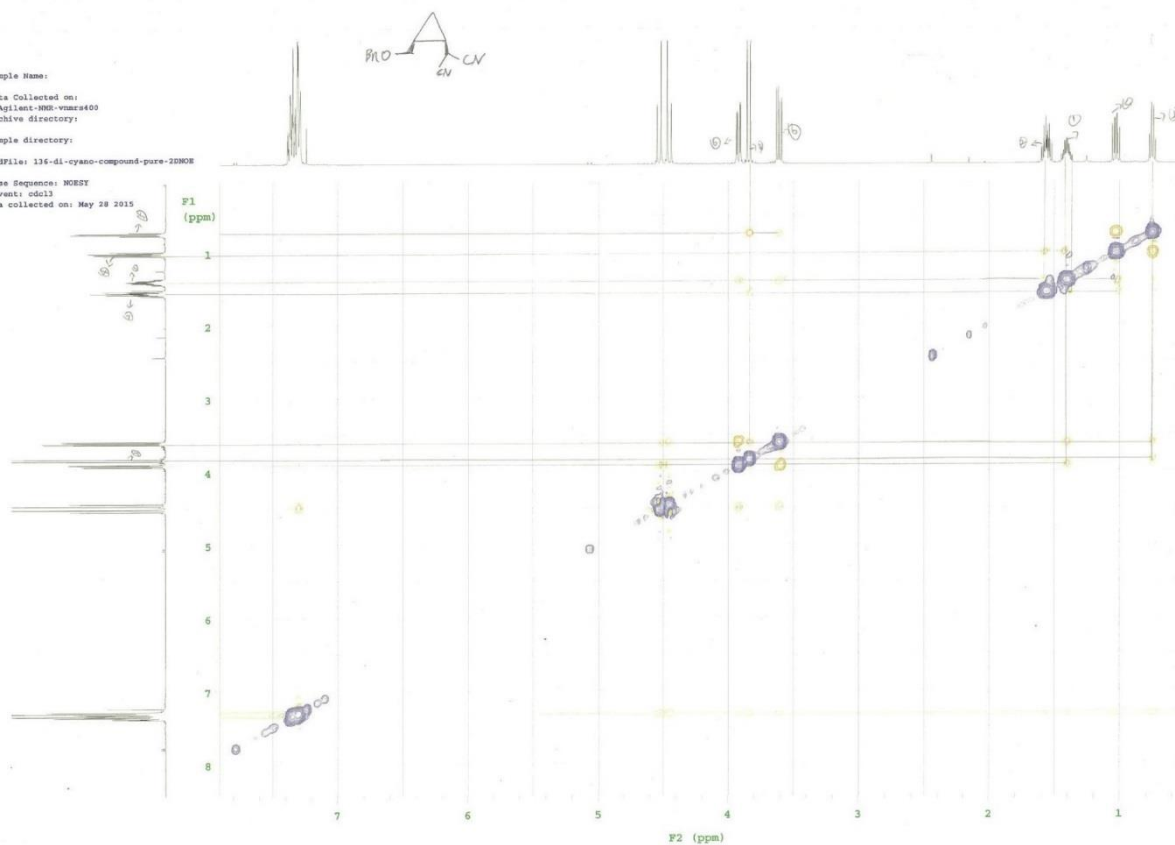
Sample Name:

Data Collected on:
Agilent-900-vnmr400
Archive directory:

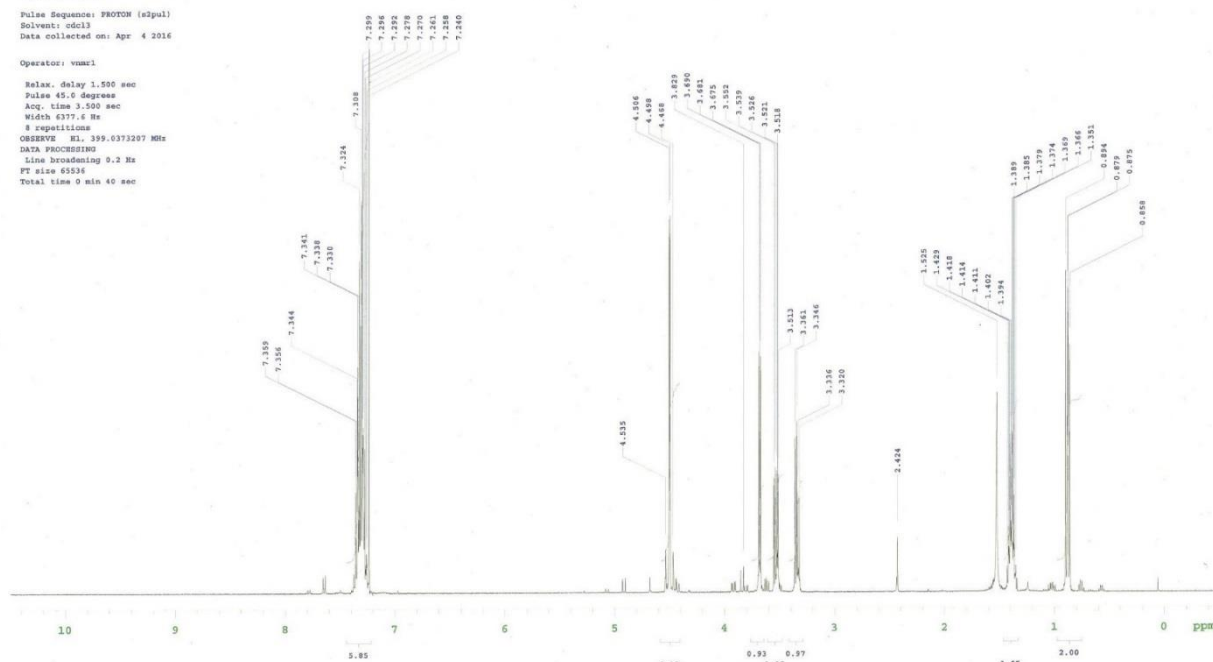
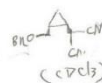
Sample directory:

FidFile: 135-di-cyano-compound-pure-2DNOE

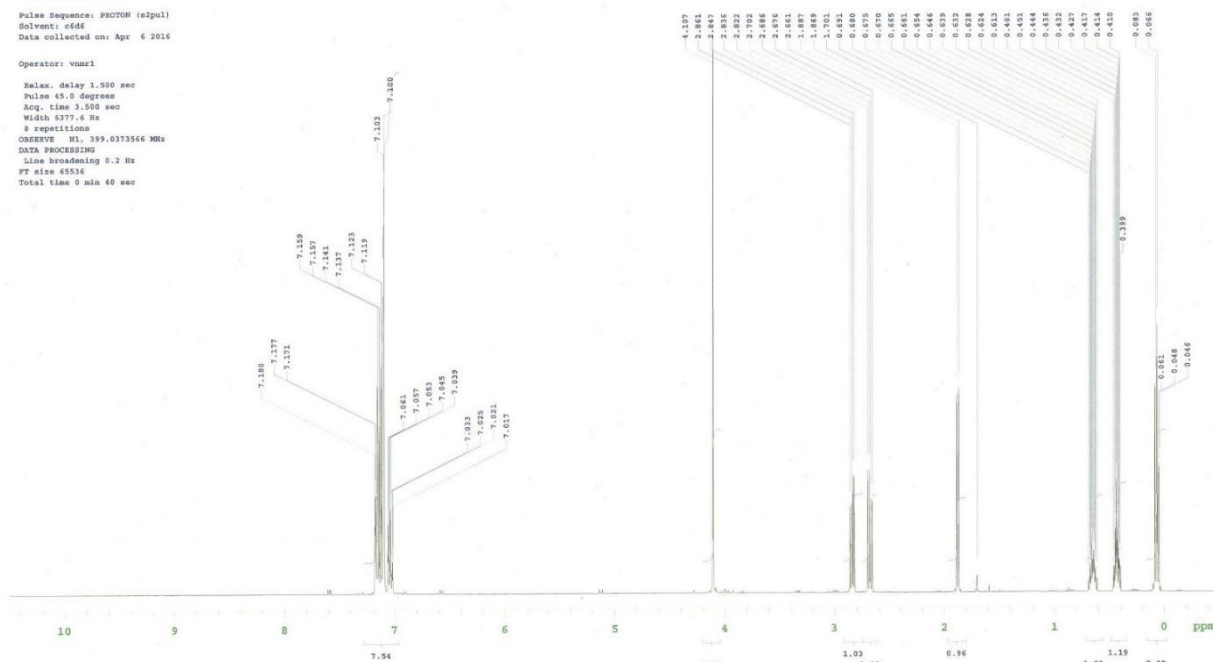
Pulse Sequence: NOESY
Solvent: cdcl3
Data collected on: May 28 2015



Sample Name:
 Data Collected on:
 Agilent-NMR-vnmr400
 Archive directory:
 Sample directory:
 FIDfile: PROTON
 Pulse Sequence: PROTON (s2pul)
 Solvent: cdcl3
 Data collected on: Apr 4 2016
 Operator: vnmr1
 Relax. delay 1.500 sec
 Pulse 45.0 degrees
 Acq. time 3.500 sec
 Width 6377.6 Hz
 8 repetitions
 OBSERVE H1, 399.0373207 MHz
 DATA PROCESSING
 Line broadening 0.2 Hz
 FT size 65536
 Total time 0 min 40 sec



Sample Name:
 Data Collected on:
 Agilent-NMR-vnmr400
 Archive directory:
 Sample directory:
 FIDfile: PROTON
 Pulse Sequence: PROTON (s2pul)
 Solvent: c6d6
 Data collected on: Apr 6 2016
 Operator: vnmr1
 Relax. delay 1.500 sec
 Pulse 45.0 degrees
 Acq. time 3.500 sec
 Width 6377.6 Hz
 8 repetitions
 OBSERVE H1, 399.0373566 MHz
 DATA PROCESSING
 Line broadening 0.2 Hz
 FT size 65536
 Total time 0 min 40 sec



STANDARD IN OBSERVE - profile

Sample Name:

Data Collected on:
Agilent-900-vnmr600

Archive directory:

Sample directory:

FidFile: CARBON

Pulse Sequence: CARBON (zgpg3)

Solvent: d2o

Data collected on: Apr 6 2016

Temp: 24.3 C / 297.4 K

Operator: vnmr1

Relax. delay 1.689 sec

Pulse 45.0 degrees

Acq. time 1.313 sec

Width 25000.0 Hz

128 repetitions

OBSERVE C13, 100.3387720 MHz

DECOUPLE H1, 399.5453410 MHz

Power 43 dB

continuously on

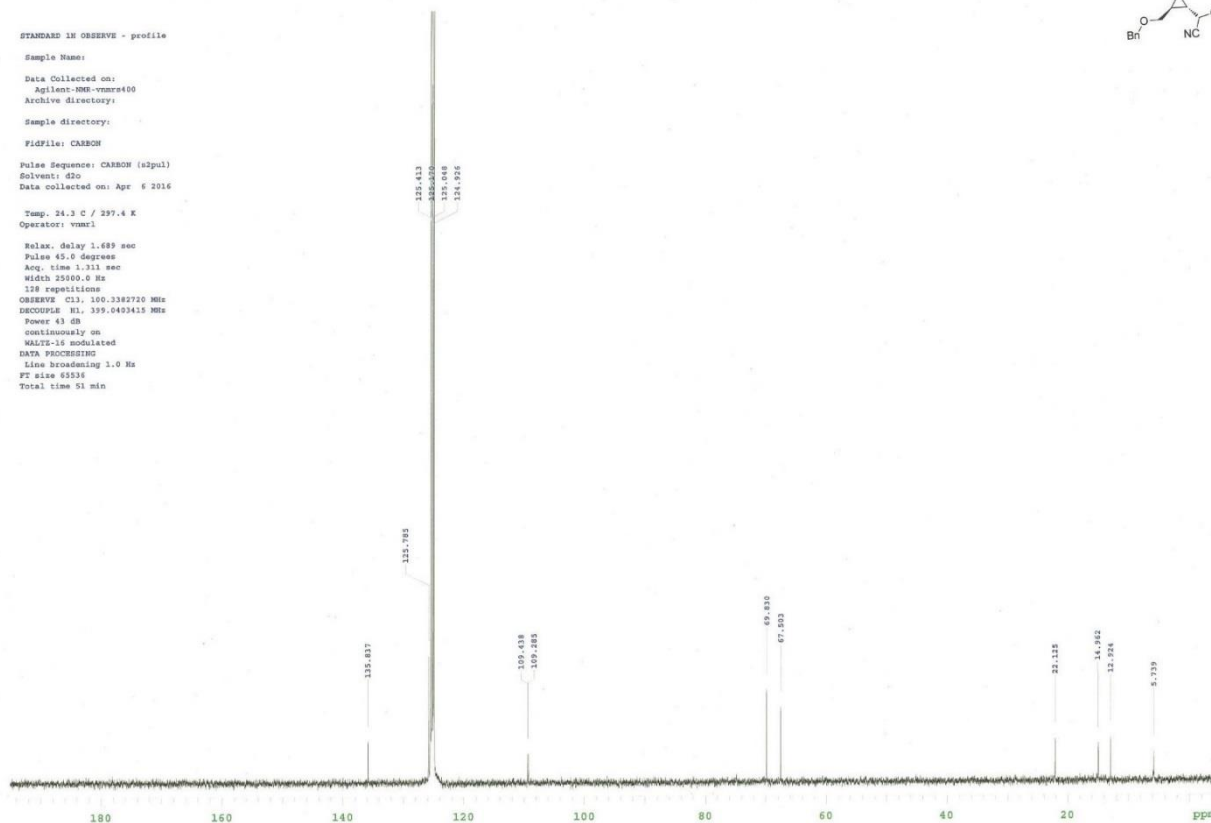
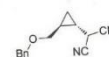
WALTZ-16 modulated

DATA PROCESSING

Line broadening 1.0 Hz

FT size 65536

Total time 51 min



Sample Name:

Data Collected on:
Agilent-900-vnmr600

Archive directory:

Sample directory:

FidFile: gCOSY

Pulse Sequence: gCOSY

Solvent: c6d6

Data collected on: Apr 1 2016

Temp: 24.3 C / 297.4 K

Operator: vnmr1

Relax. delay 1.689 sec

Pulse 45.0 degrees

Acq. time 1.313 sec

Width 25000.0 Hz

128 repetitions

OBSERVE C13, 100.3387720 MHz

DECOUPLE H1, 399.5453410 MHz

Power 43 dB

continuously on

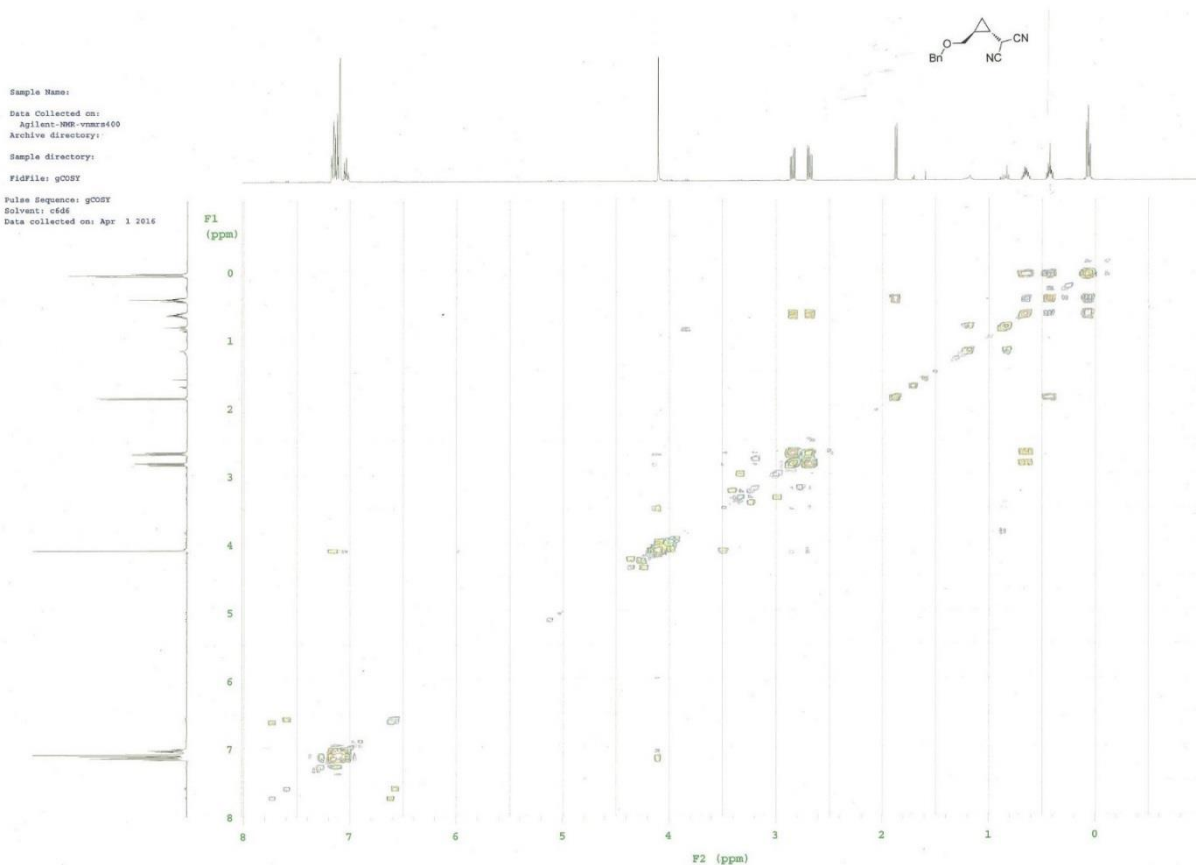
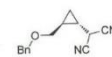
WALTZ-16 modulated

DATA PROCESSING

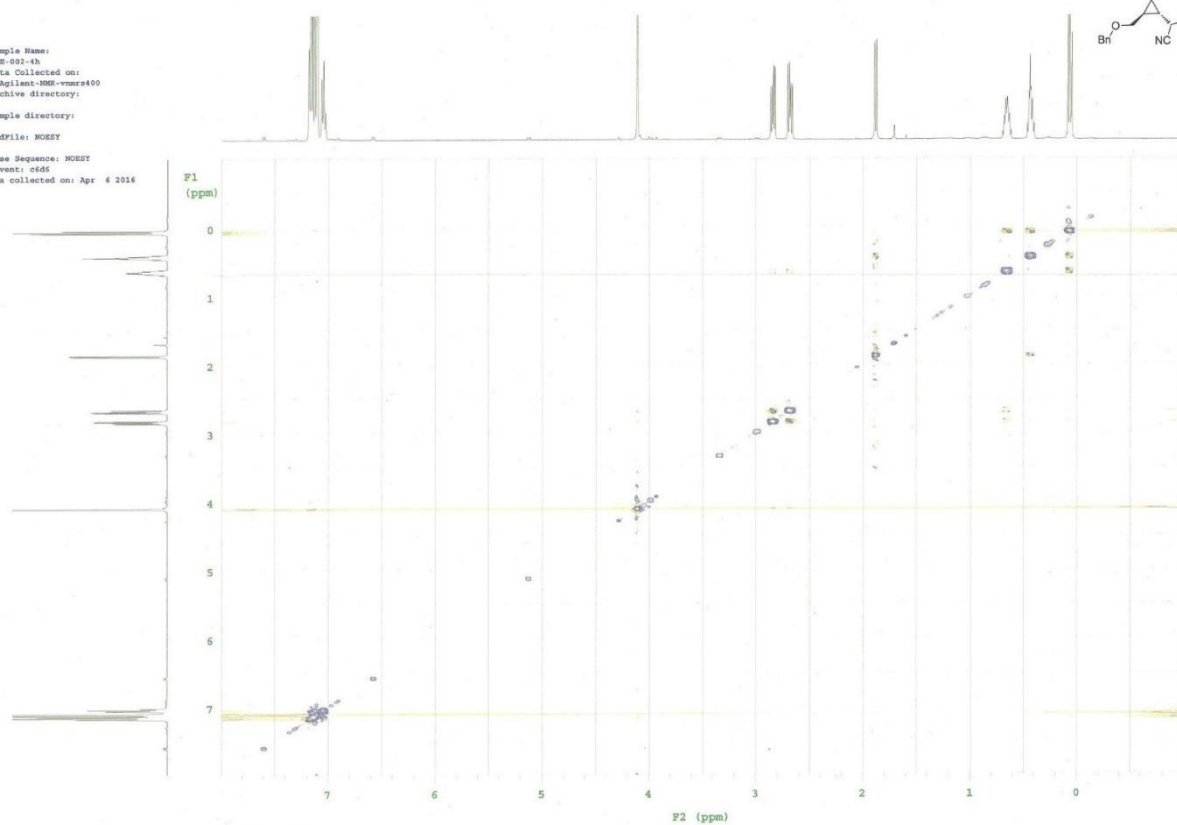
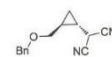
Line broadening 1.0 Hz

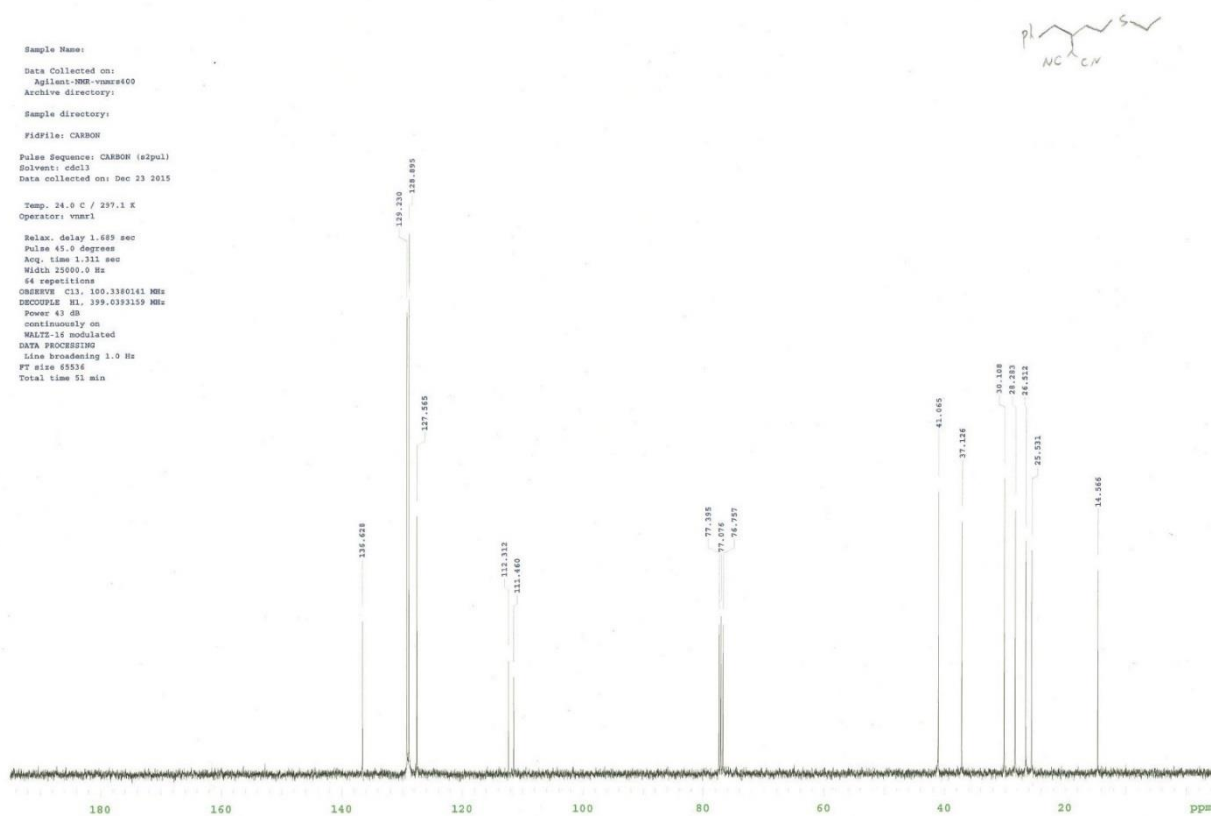
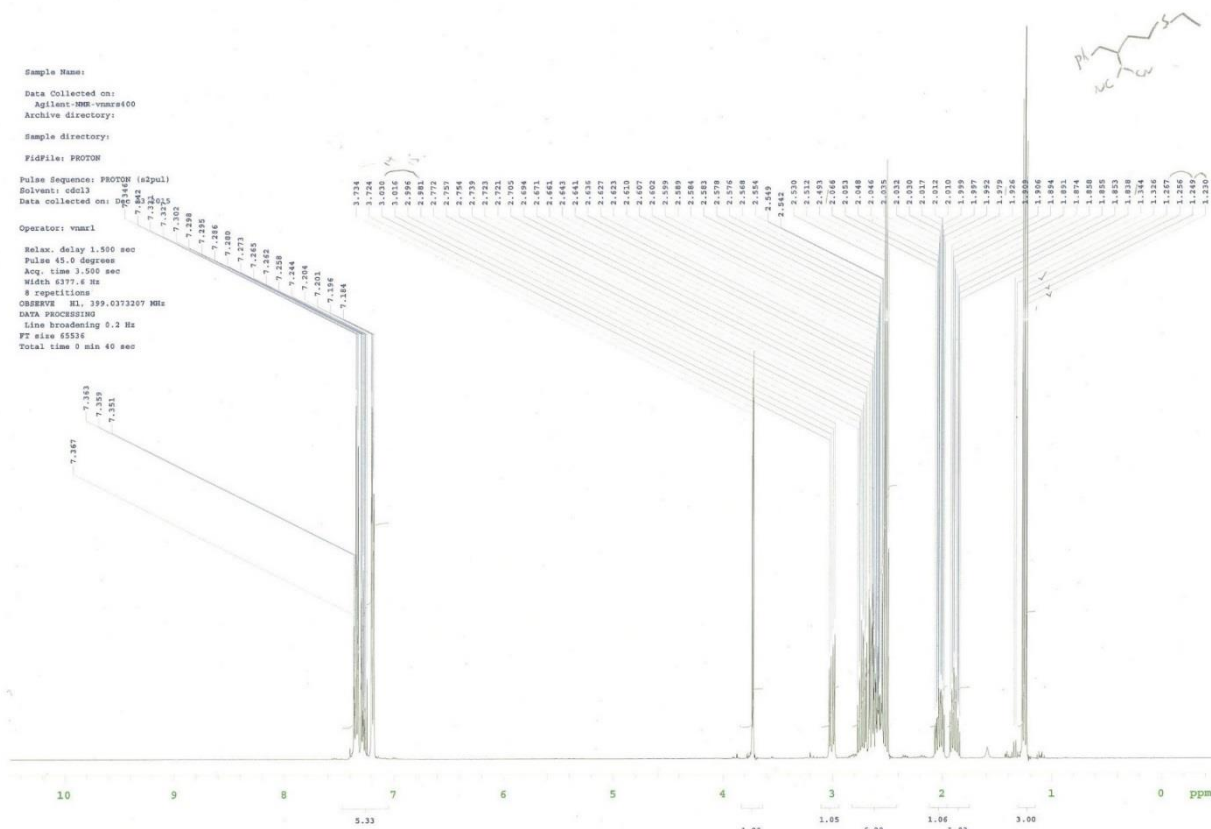
FT size 65536

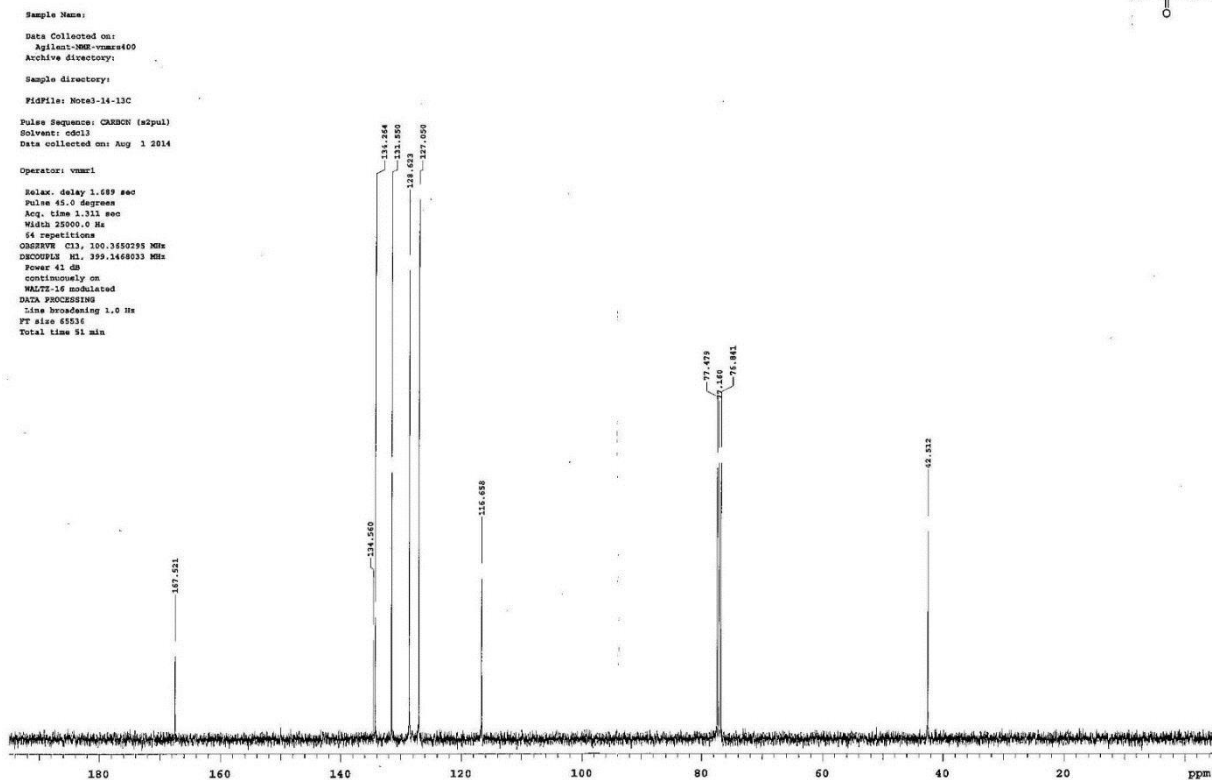
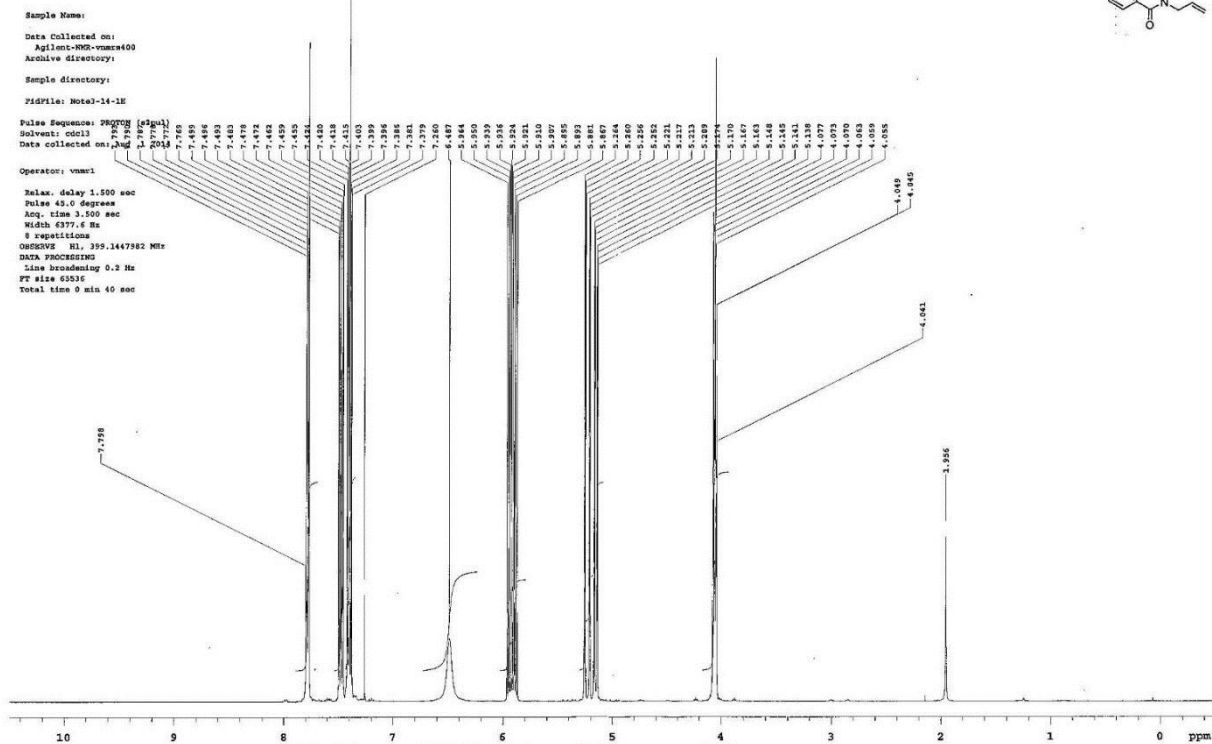
Total time 51 min

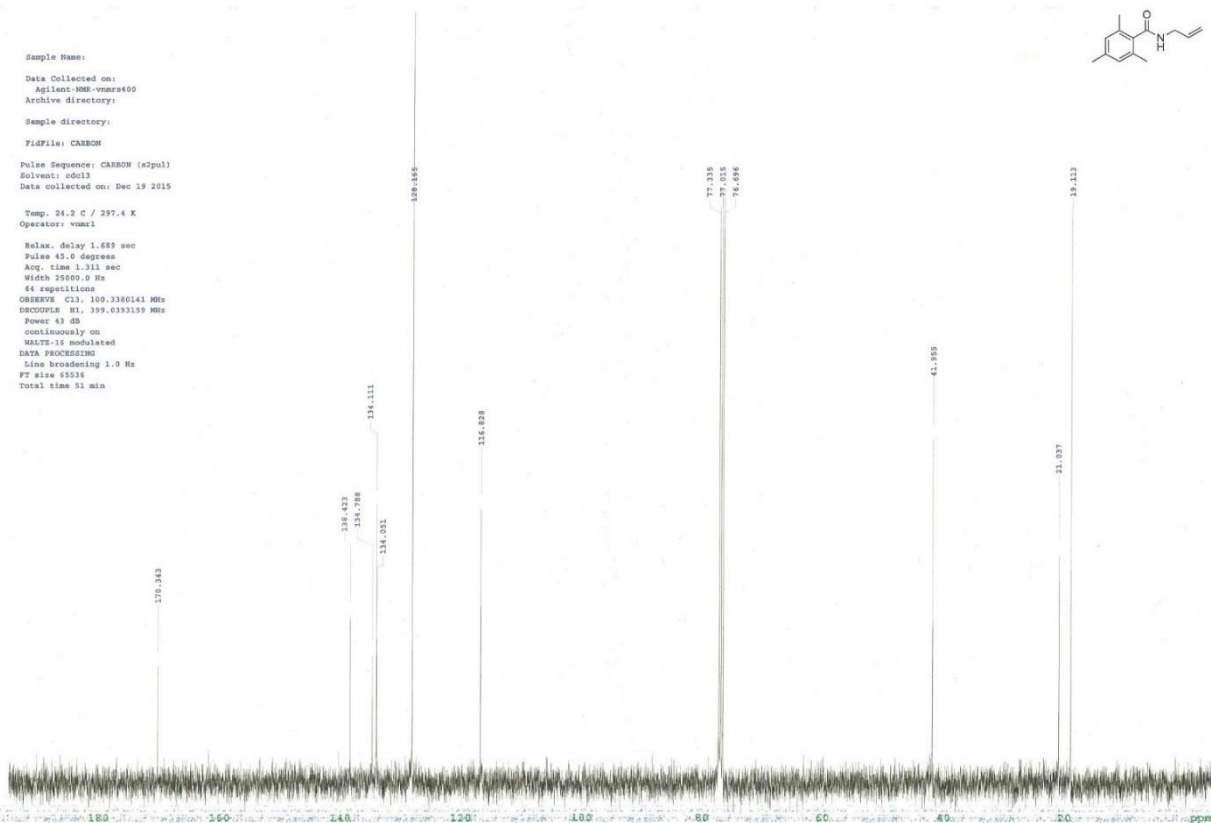
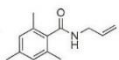
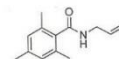


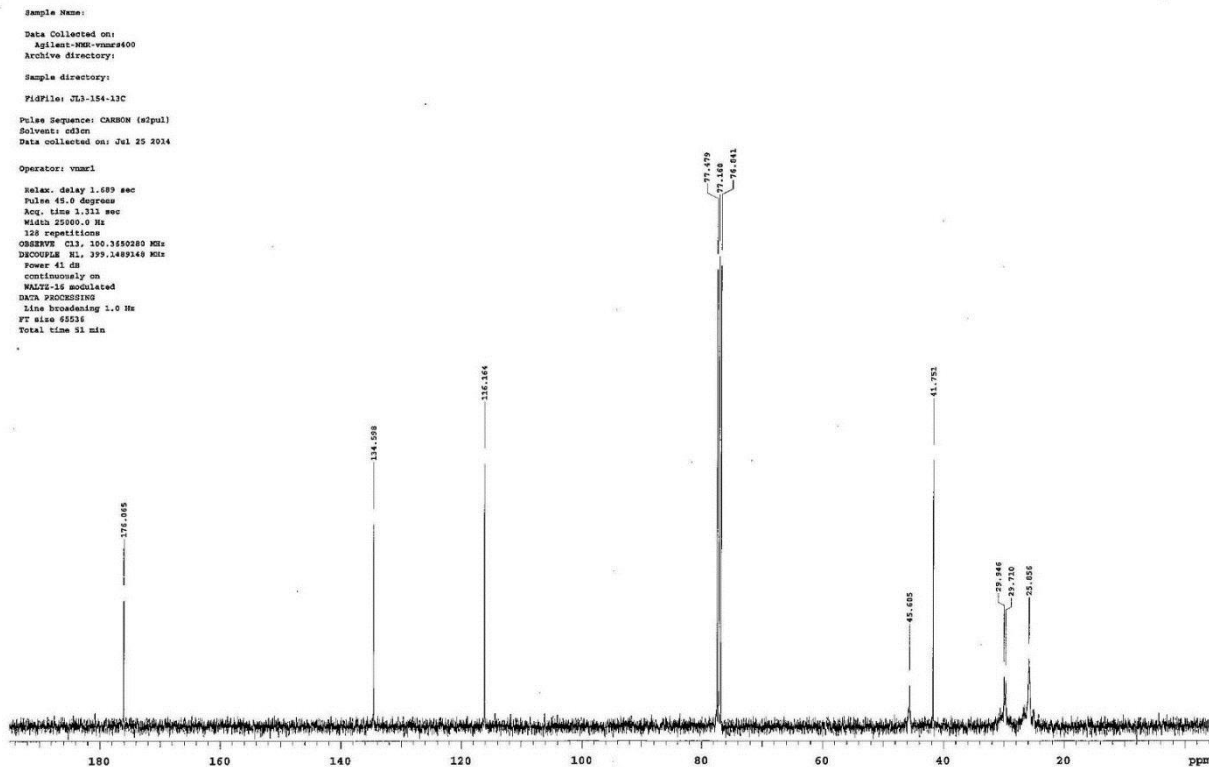
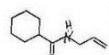
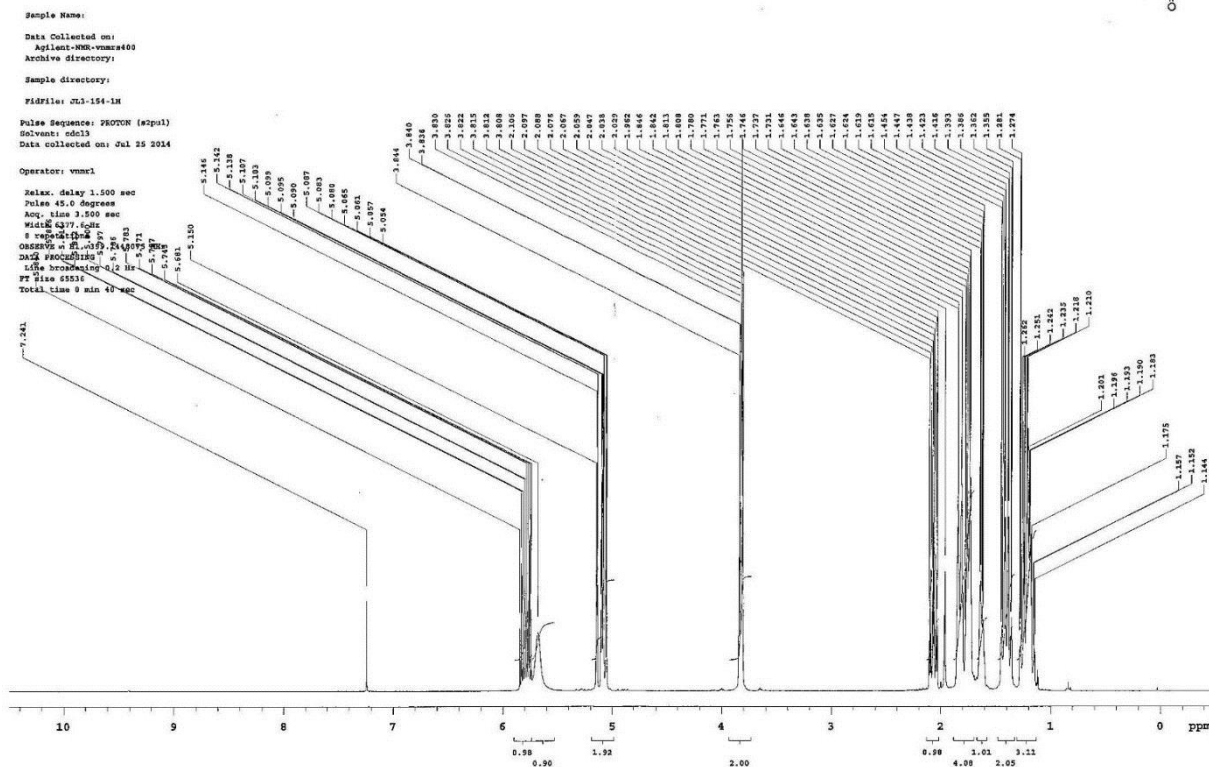
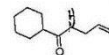
Sample Name:
E-001-4h
Data Collected on:
Agilent-1H-900-Vnmr400
Archive directory:
Sample directory:
fidFile: NOEST
Pulse Sequence: NOEST
Solvent: c6d6
Data collected on: Apr 6 2016



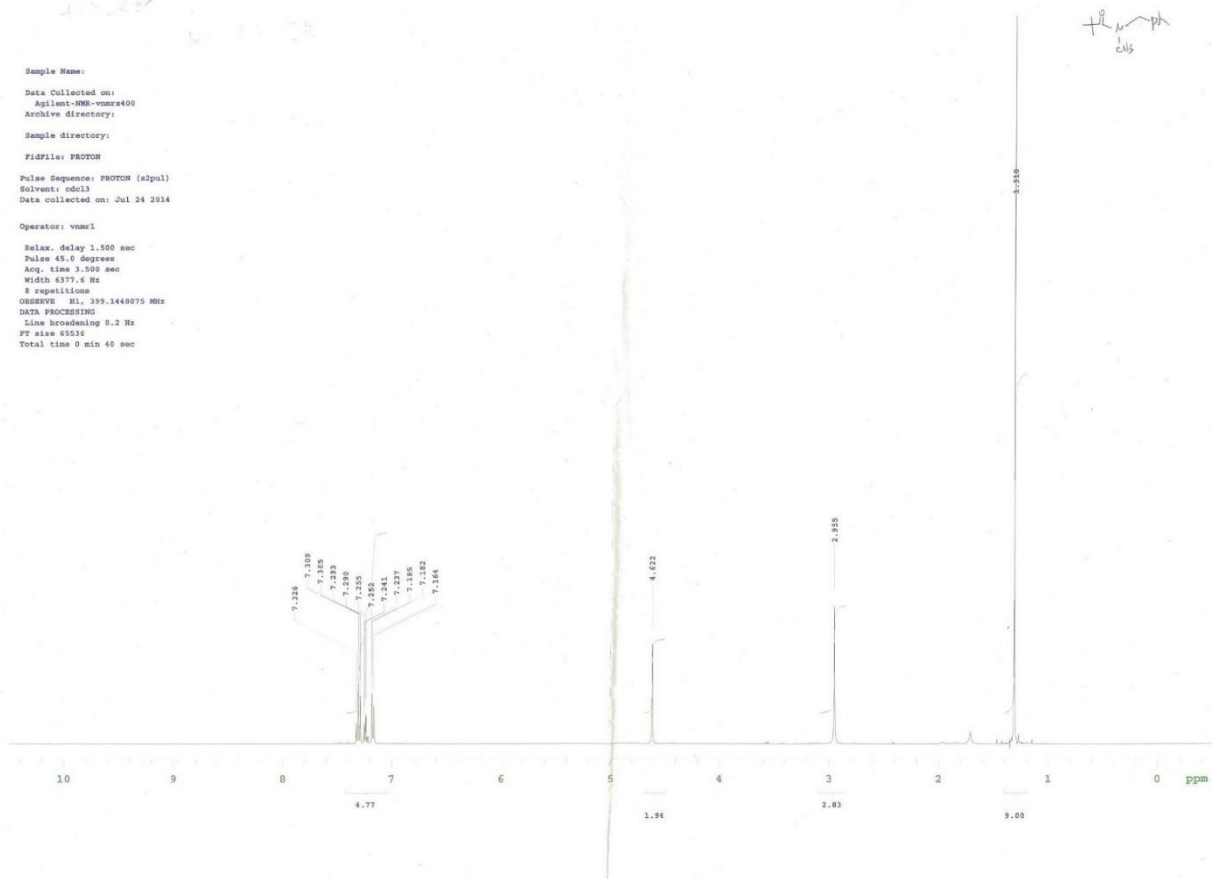




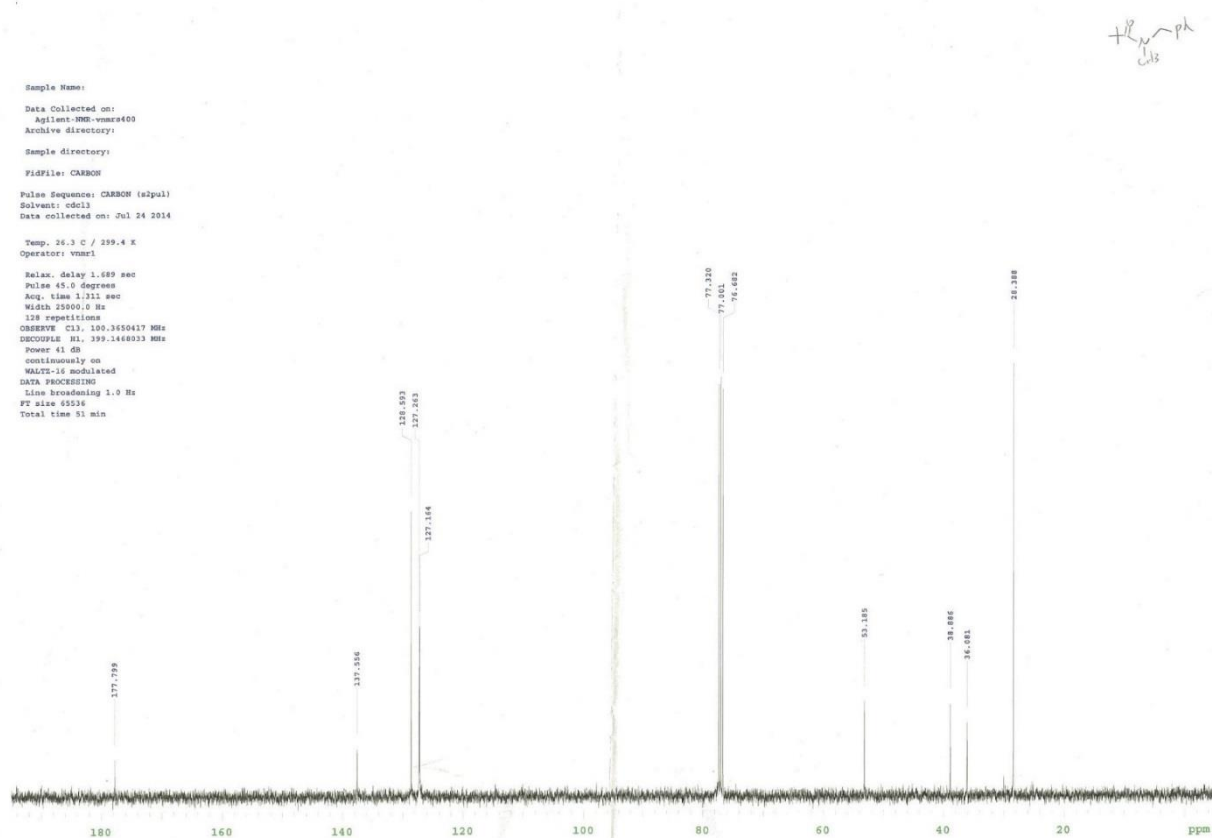


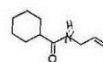


Sample Name:
 Data Collected on:
 Agilent-VNM-vmr400
 Archive directory:
 Sample directory:
 FIDFile: PROTON
 Pulse Sequence: PROTON (zgpg30)
 Solvent: cdcl3
 Data collected on: Jul 24 2014
 Operator: vmr1
 Relax. delay 1.500 sec
 Pulse 45.0 degrees
 Acq. time 3.500 sec
 Width 6377.6 Hz
 8 repetitions
 OBSERVE H1, 399.1448075 MHz
 DATA PROCESSING
 Line broadening 0.2 Hz
 FT size 65536
 Total time 9 min 40 sec

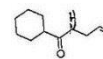
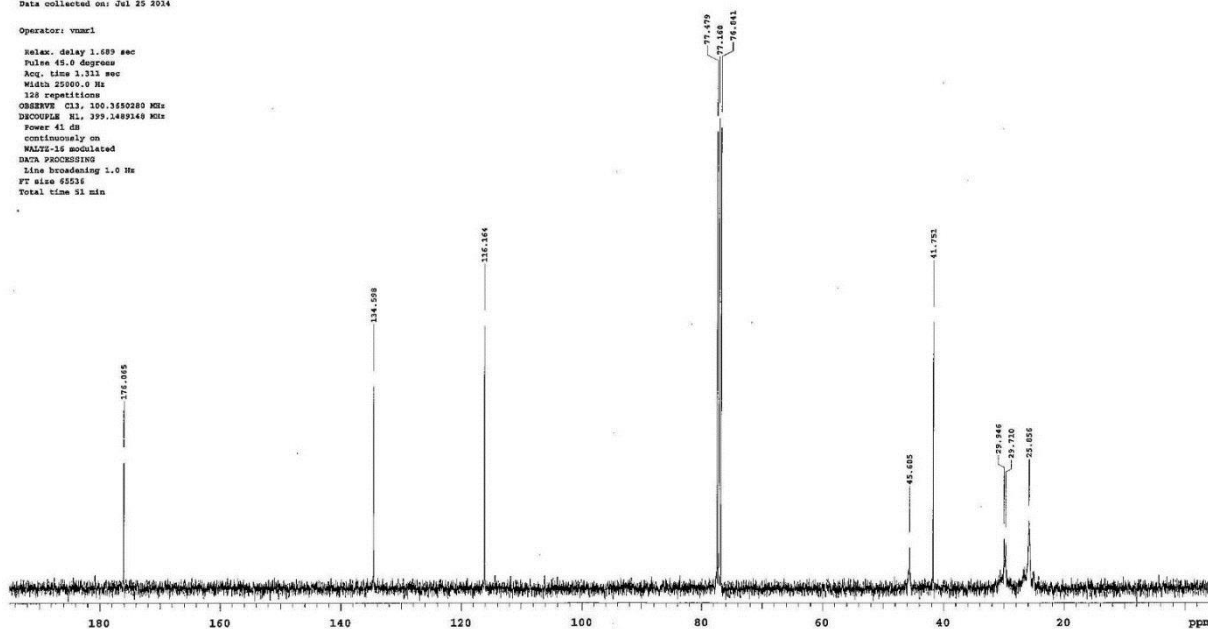


Sample Name:
 Data Collected on:
 Agilent-VNM-vmr400
 Archive directory:
 Sample directory:
 FIDFile: CARBON
 Pulse Sequence: CARBON (zgpg30)
 Solvent: cdcl3
 Data collected on: Jul 24 2014
 Temp. 26.3 C / 299.4 K
 Operator: vmr1
 Relax. delay 1.689 sec
 Pulse 45.0 degrees
 Acq. time 1.311 sec
 Width 25000.0 Hz
 128 repetitions
 OBSERVE C13, 100.6250417 MHz
 DECOUPLE H1, 399.1448075 MHz
 Power 41 dB
 continuously on
 WALTZ-16 modulated
 DATA PROCESSING
 Line broadening 1.0 Hz
 FT size 65536
 Total time 51 min

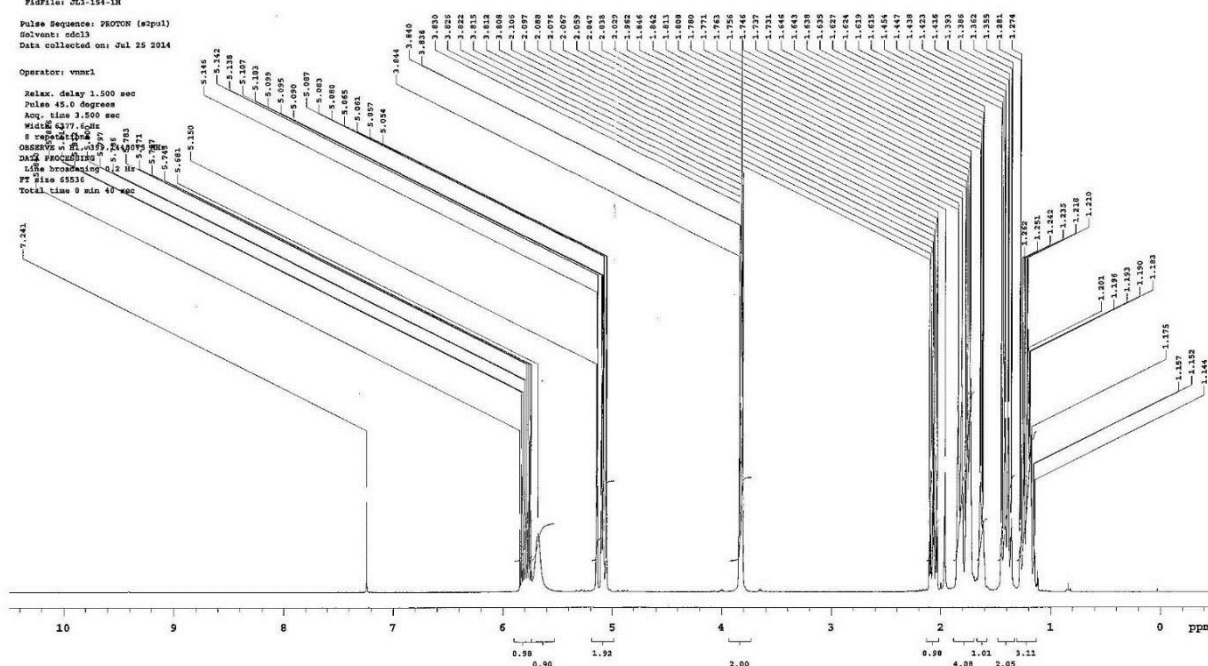




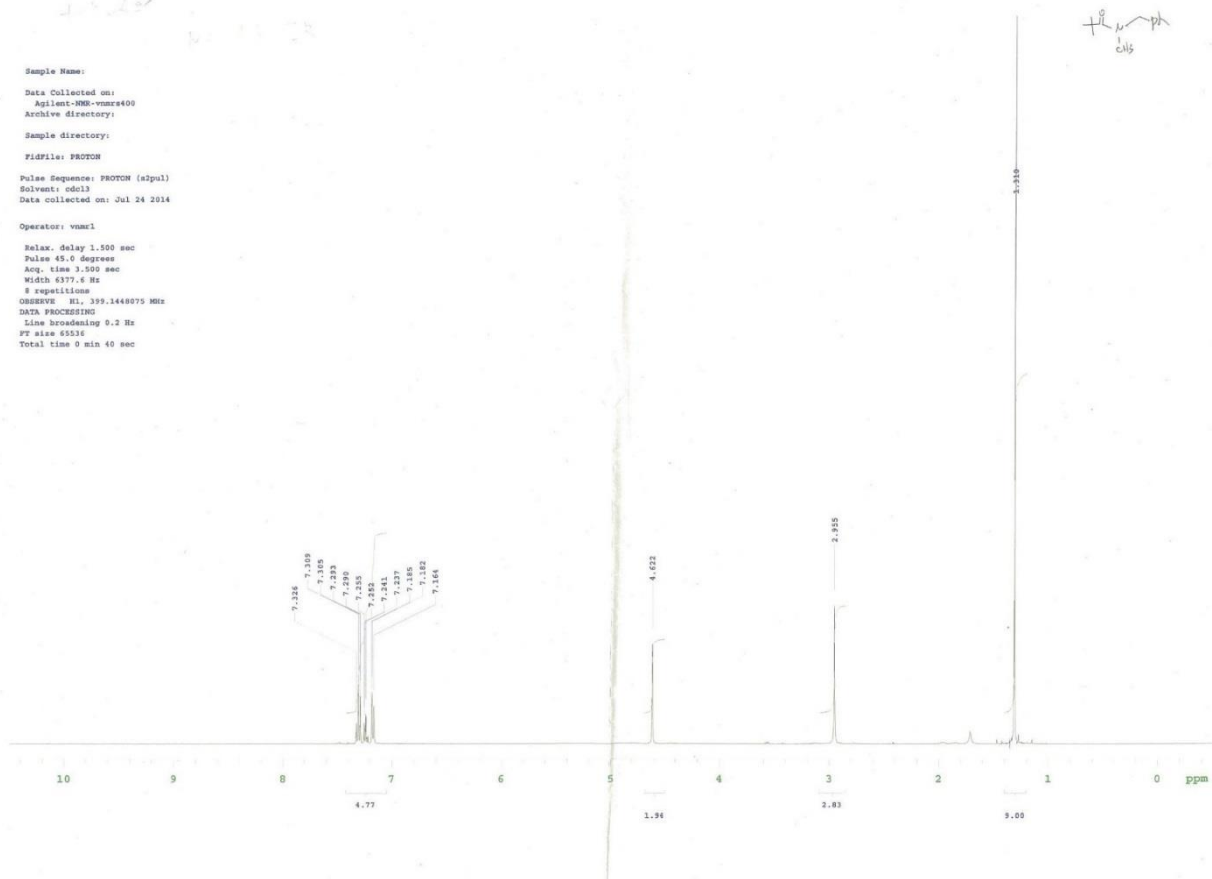
Sample Name:
Data Collected on:
Agilent-VNM-vmr400
Archive directory:
Sample directory:
Fidfile: J13-154-13C
Pulse Sequence: CARBON (zgpg30)
Solvent: cdcl3
Data collected on: Jul 25 2014
Operator: vmr1
Relax. delay 1.689 sec
Pulse 45.0 degrees
Acq. time 3.311 sec
Width 25000.0 Hz
128 repetitions
OBSERVE CH: 100.350280 MHz
DECOUPLE N1: 399.1489140 MHz
Power 41 dB
continuously on
WALTZ-16 modulated
DATA PROCESSING
Line broadening 1.0 Hz
FT size 65536
Total time 31 min



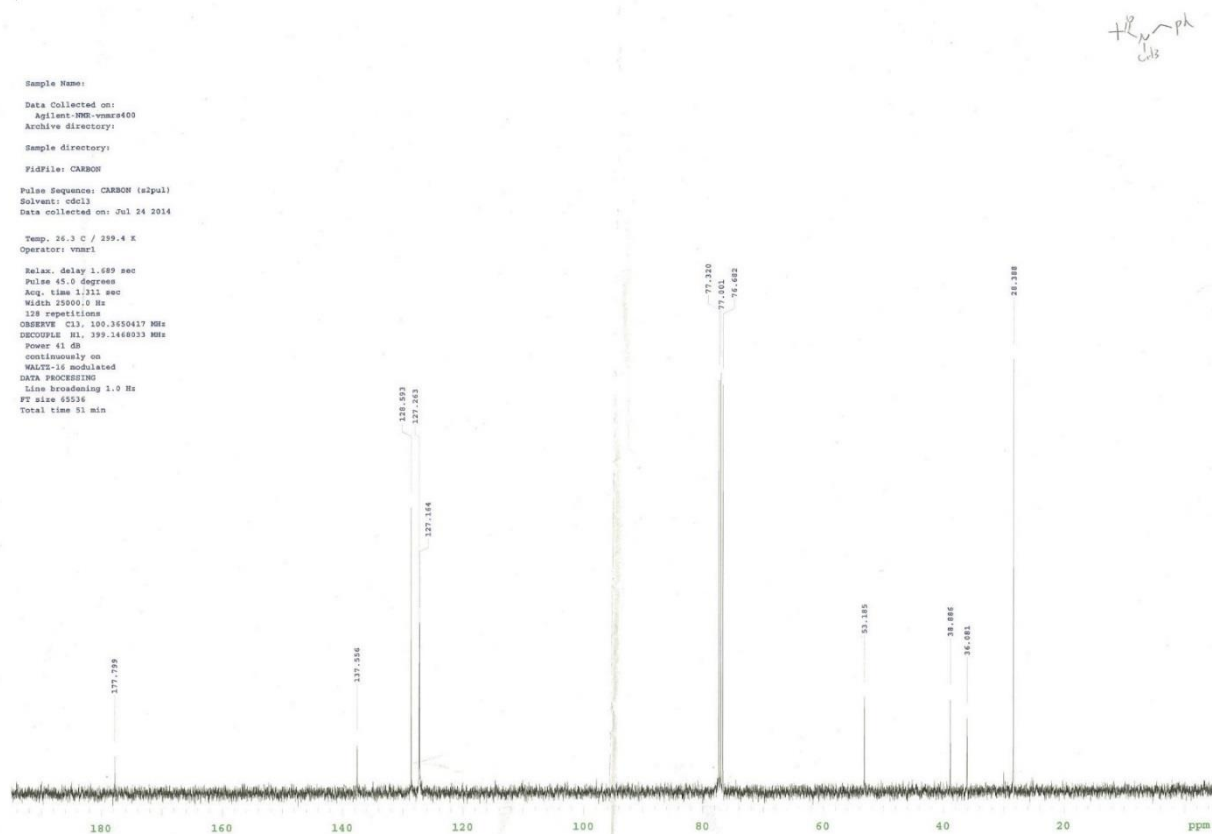
Sample Name:
Data Collected on:
Agilent-VNM-vmr400
Archive directory:
Sample directory:
Fidfile: J13-154-1H
Pulse Sequence: PROTON (zgpg30)
Solvent: cdcl3
Data collected on: Jul 25 2014
Operator: vmr1
Relax. delay 1.500 sec
Pulse 45.0 degrees
Acq. time 3.311 sec
Width 6377.60 Hz
8 repetitions
OBSERVE CH: 500.136095 MHz
DECOUPLE N1: 100.350280 MHz
DATA PROCESSING
Line broadening 0.5 Hz
FT size 65536
Total time 3 min 43 sec



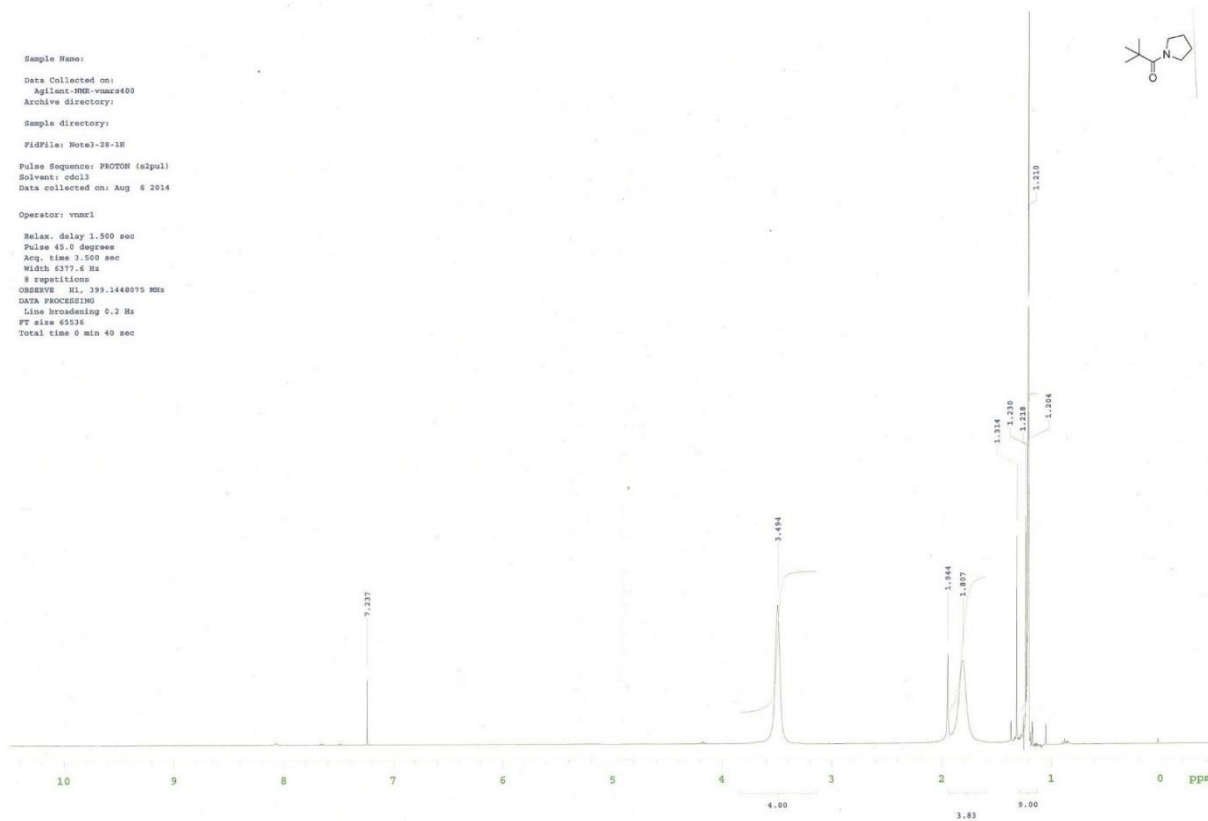
Sample Name:
 Data Collected on:
 Agilent-MS-vnmr400
 Archive directory:
 Sample directory:
 FIDFile: PROTON
 Pulse Sequence: PROTON (zgpg30)
 Solvent: cdcl3
 Data collected on: Jul 24 2014
 Operator: vnmr1
 Relax. delay 1.500 sec
 Pulse 45.0 degrees
 Acq. time 1.500 sec
 Width 6377.6 Hz
 8 repetitions
 OBSERVE H1, 399.1448075 MHz
 DATA PROCESSING
 Line broadening 0.2 Hz
 FT size 65536
 Total time 9 min 40 sec



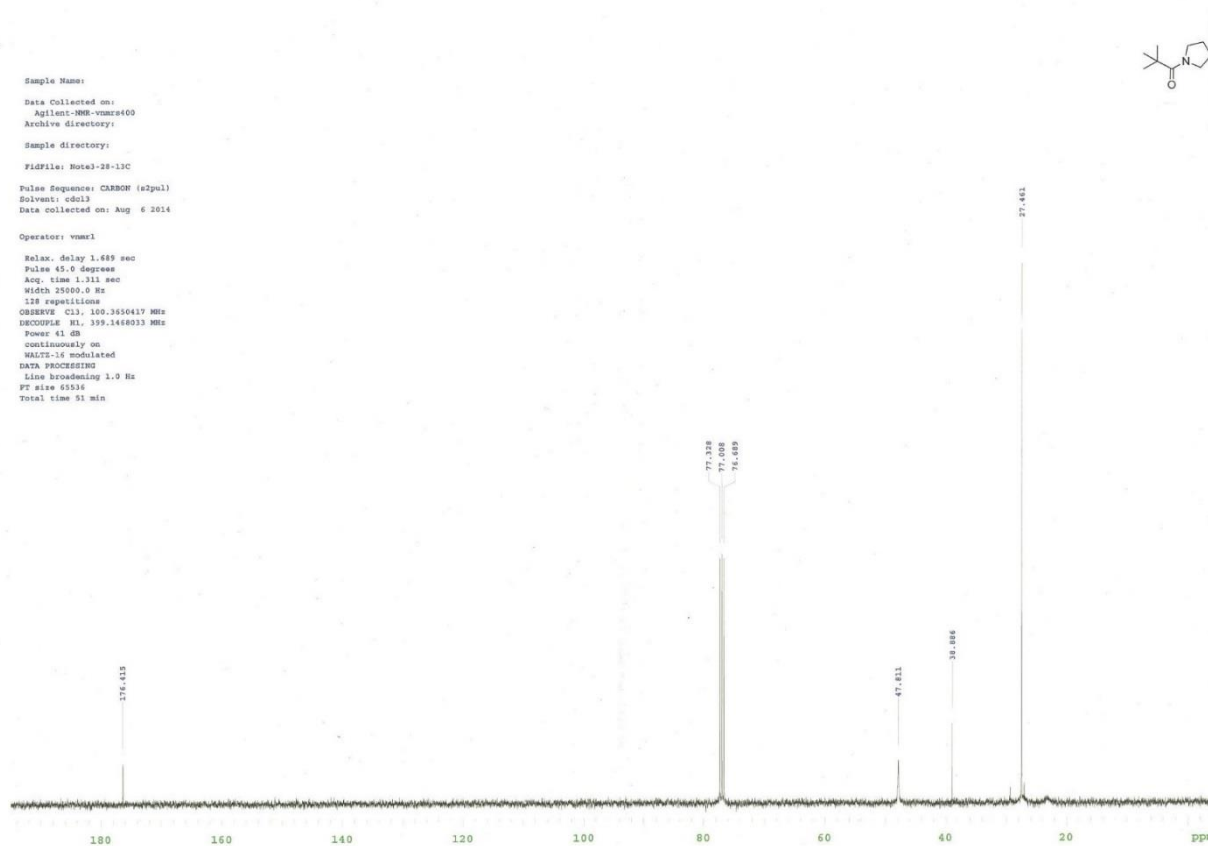
Sample Name:
 Data Collected on:
 Agilent-MS-vnmr400
 Archive directory:
 Sample directory:
 FIDFile: CARBON
 Pulse Sequence: CARBON (zgpg30)
 Solvent: cdcl3
 Data collected on: Jul 24 2014
 Temp. 26.3 C / 299.4 K
 Operator: vnmr1
 Relax. delay 1.689 sec
 Pulse 45.0 degrees
 Acq. time 1.311 sec
 Width 25000.0 Hz
 128 repetitions
 OBSERVE C13, 100.6250417 MHz
 DECOUPLE H1, 399.1448075 MHz
 Power 41 dB
 continuously on
 WALTZ-16 modulated
 DATA PROCESSING
 Line broadening 1.0 Hz
 FT size 65536
 Total time 51 min



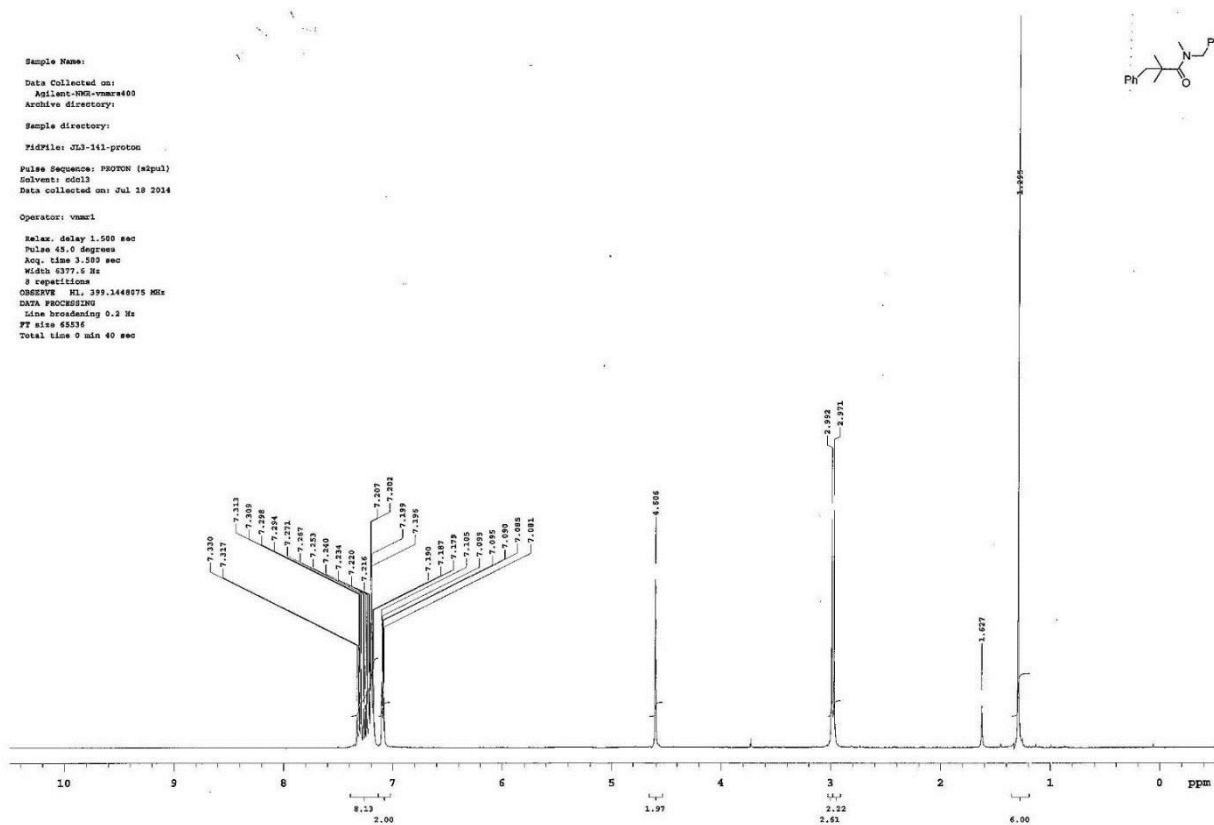
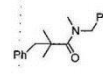
Sample Name:
 Data Collected on:
 Agilent-MMR-vnmr400
 Archive directory:
 Sample directory:
 FidFile: Note3-28-1E
 Pulse Sequence: PROTON (s2pul)
 Solvent: cdcl3
 Data collected on: Aug 6 2014
 Operator: vnmr1
 Relax. delay 1.500 sec
 Pulse 45.0 degrees
 Acq. time 1.959 sec
 Width 6377.6 Hz
 8 repetitions
 OBSERVE H1, 399.1448075 MHz
 DATA PROCESSING
 Line broadening 0.2 Hz
 FT size 65536
 Total time 0 min 40 sec



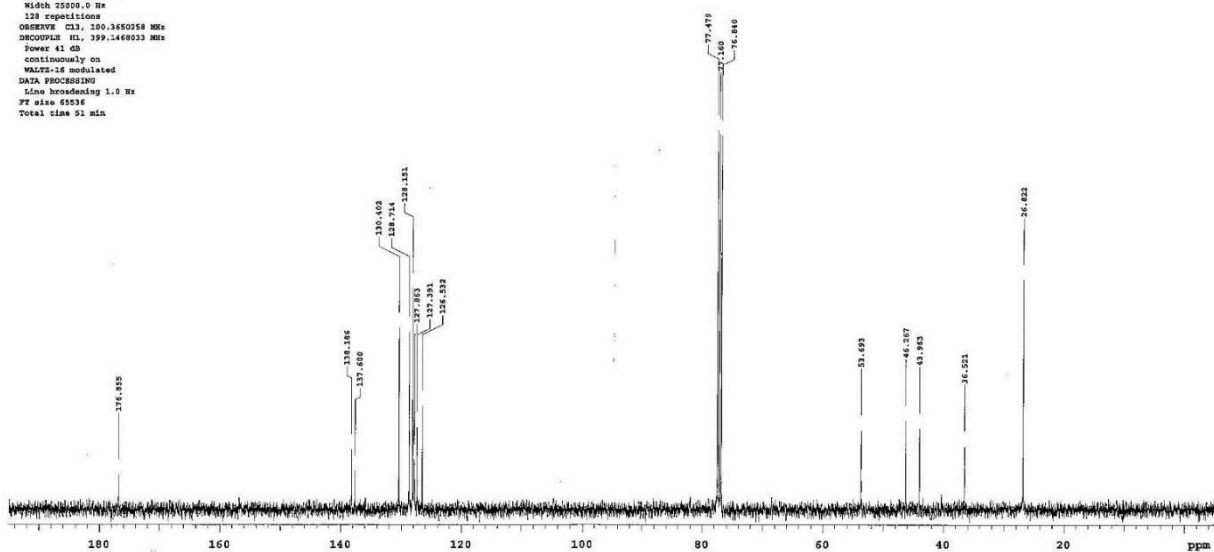
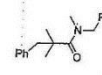
Sample Name:
 Data Collected on:
 Agilent-MMR-vnmr400
 Archive directory:
 Sample directory:
 FidFile: Note3-28-13C
 Pulse Sequence: CARBON (s2pul)
 Solvent: cdcl3
 Data collected on: Aug 6 2014
 Operator: vnmr1
 Relax. delay 1.089 sec
 Pulse 45.0 degrees
 Acq. time 1.311 sec
 Width 25000.0 Hz
 128 repetitions
 OBSERVE C13, 100.3650417 MHz
 DECOUPLE H1, 399.1448033 MHz
 Power 41 dB
 continuously on
 WALTZ-16 modulated
 DATA PROCESSING
 Line broadening 1.0 Hz
 FT size 65536
 Total time 51 min



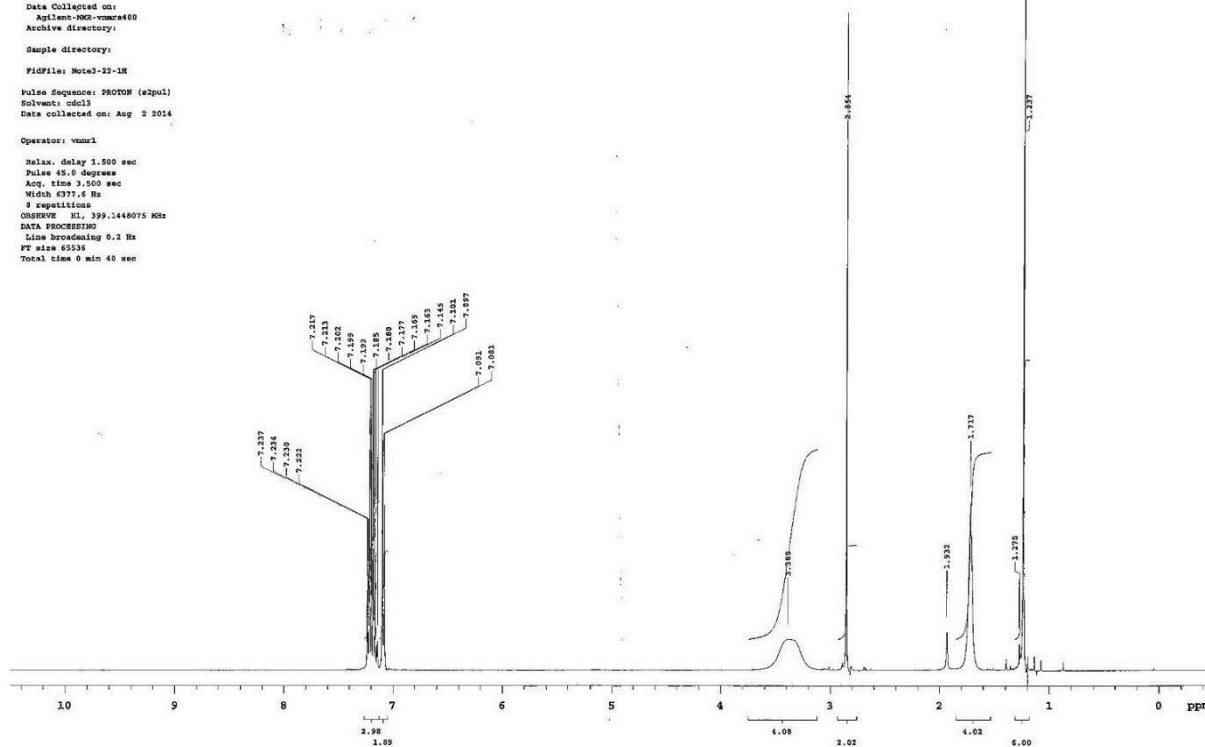
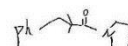
Sample Name:
 Data Collected on:
 Agilent-NMR-vnmr400
 Archive directory:
 Sample directory:
 FIDFile: JLS-141-proton
 Pulse Sequence: PROTON (zgpg3)
 Solvent: cdcl3
 Data collected on: Jul 18 2014
 Operator: vnmr1
 Relax. delay 1.500 sec
 Pulse 45.0 degrees
 Acq. time 1.500 sec
 Width 6377.6 Hz
 8 repetitions
 OBSERVE HL 299.146875 MHz
 DATA PROCESSING
 Line broadening 0.2 Hz
 FT size 65536
 Total time 9 min 40 sec



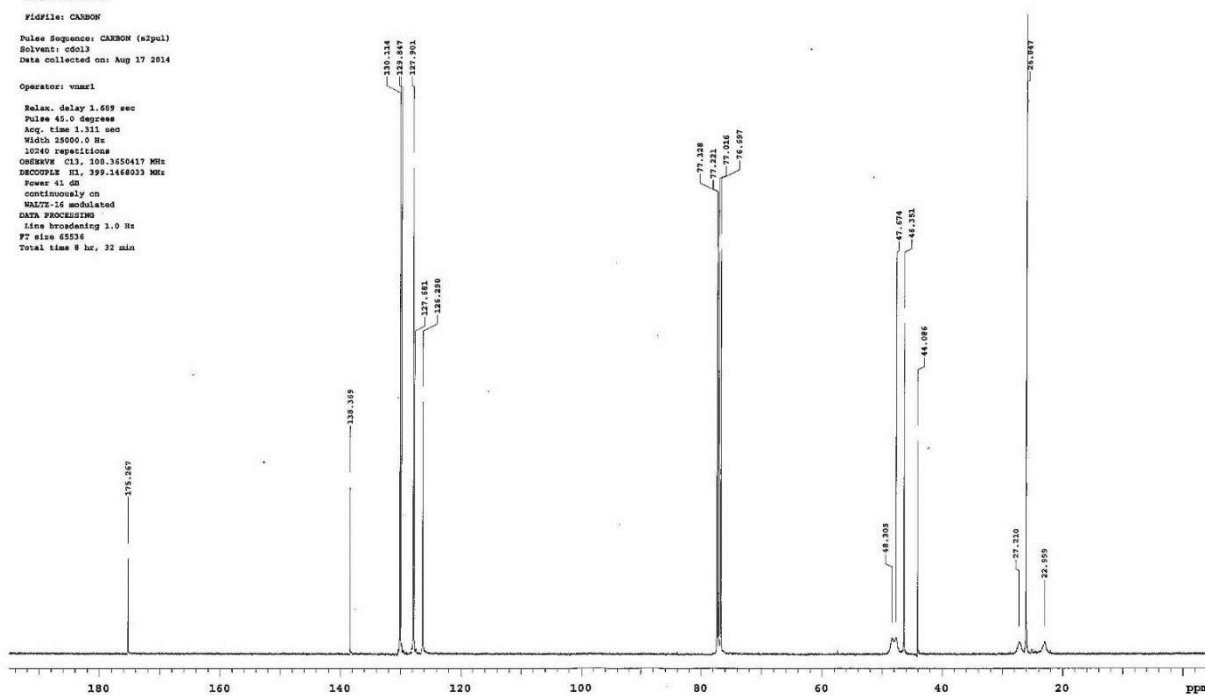
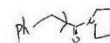
Sample Name:
 Data Collected on:
 Agilent-NMR-vnmr400
 Archive directory:
 Sample directory:
 FIDFile: CARBON
 Pulse Sequence: CARBON (zgpg3)
 Solvent: cdcl3
 Data collected on: Sep 10 2014
 Operator: vnmr1
 Temp. 24.0 C / 299.1 K
 Relax. delay 1.600 sec
 Pulse 45.0 degrees
 Acq. time 1.311 sec
 Width 23200.0 Hz
 128 repetitions
 OBSERVE CL3 100.6250558 MHz
 DECOUPLE HL 299.146875 MHz
 Power 41 dB
 continuously on
 WALTZ-16 modulated
 DATA PROCESSING
 Line broadening 1.0 Hz
 FT size 65536
 Total time 51 min



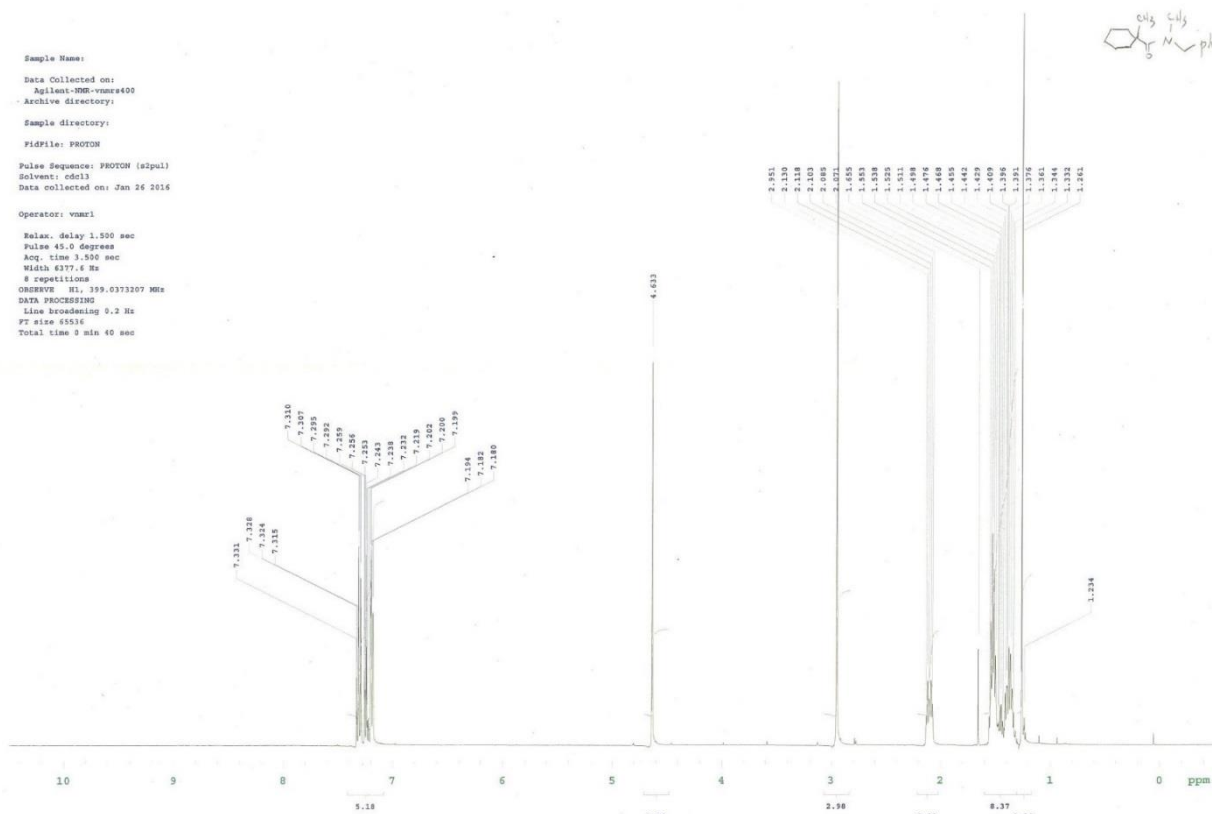
Sample Name:
 Data Collected on:
 Agilent-800-mmx400
 Archive directory:
 Sample directory:
 Fidfile: NMR3-22-1K
 Pulse Sequence: PROTON (s2pul)
 Solvent: cdcl3
 Data collected on: Aug 2 2014
 Operator: vmm1
 Relax. delay 1.500 sec
 Pulse 45.0 degrees
 Acq. time 3.500 sec
 Width 6377.6 Hz
 8 repetitions
 OBSERVE EL 399.1448075 MHz
 DATA PROCESSING
 Line broadening 0.2 Hz
 FT size 65536
 Total time 5 min 40 sec



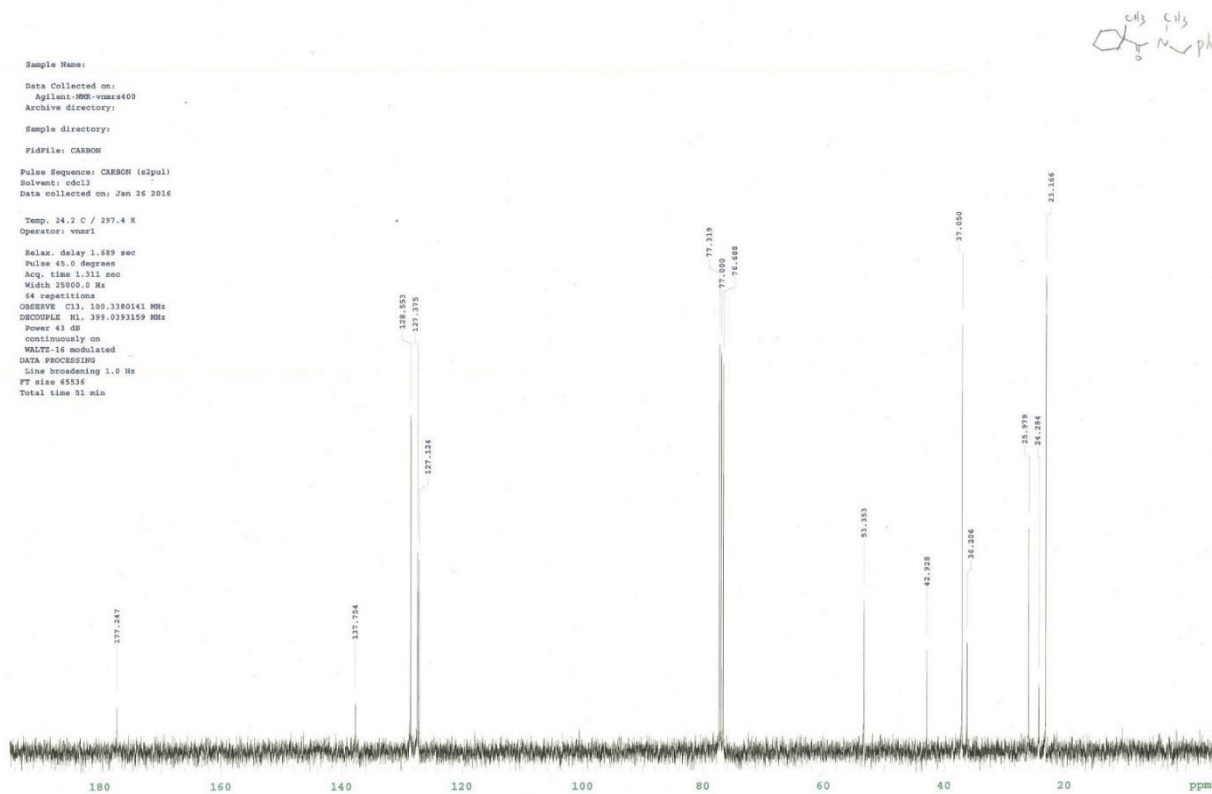
Sample Name:
 Data Collected on:
 Agilent-800-mmx400
 Archive directory:
 Sample directory:
 Fidfile: CARBON
 Pulse Sequence: CARBON (s2pul)
 Solvent: cdcl3
 Data collected on: Aug 17 2014
 Operator: vmm1
 Relax. delay 1.659 sec
 Pulse 45.0 degrees
 Acq. time 1.311 sec
 Width 24000.0 Hz
 10240 repetitions
 OBSERVE CH 100.6250417 MHz
 RECOVER EL 399.1448073 MHz
 Power 41 dB
 continuously on
 WALTZ-16 modulated
 DATA PROCESSING
 Line broadening 1.0 Hz
 FT size 65536
 Total time 9 hr, 22 min

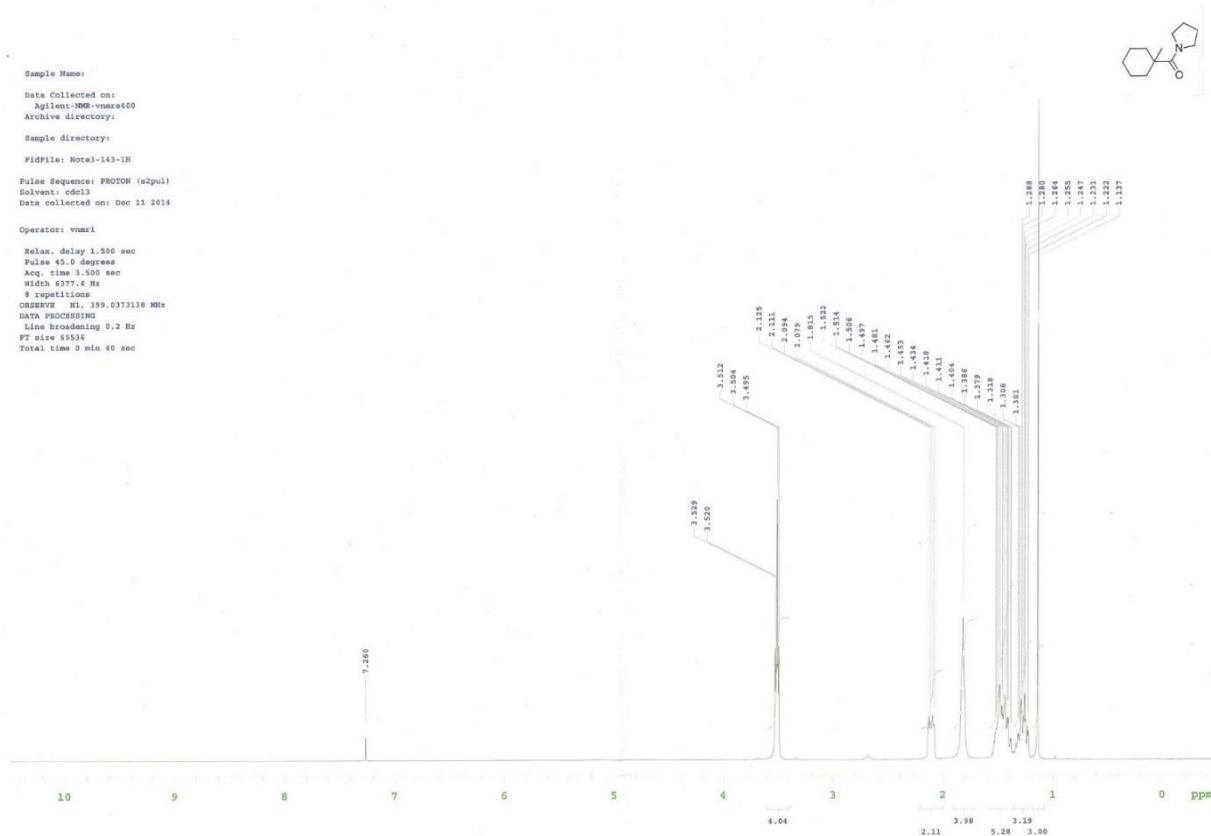
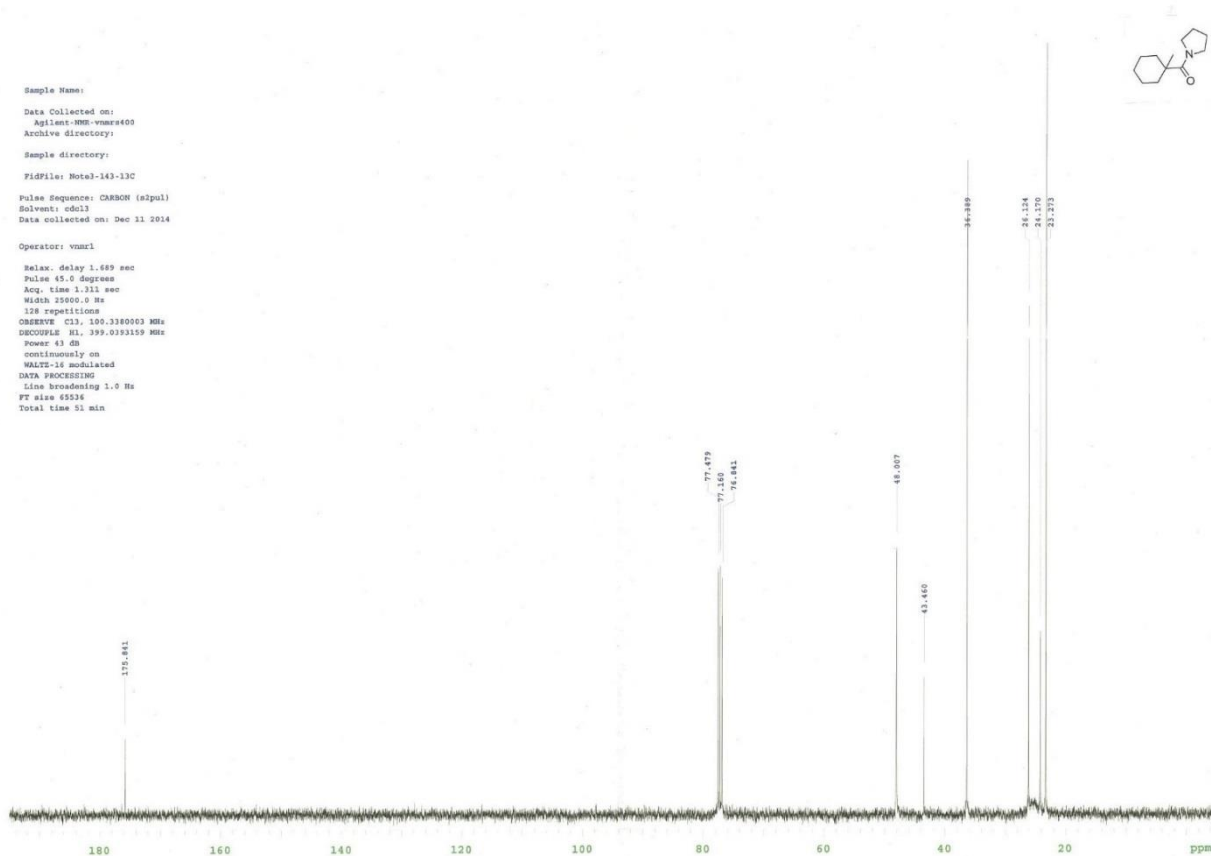


Sample Name:
 Data Collected on:
 Agilent-DMG-vnmr400
 Archive directory:
 Sample directory:
 FIDFile: PROTON
 Pulse Sequence: PROTON (s2pul)
 Solvent: cdcl3
 Data collected on: Jan 26 2016
 Operator: vnmr1
 Relax. delay 1.500 sec
 Pulse 45.0 degrees
 Acq. time 3.550 sec
 Width 6377.6 Hz
 8 repetitions
 OBSERVE H1, 399.0373207 MHz
 DATA PROCESSING
 Line broadening 9.2 Hz
 FT size 65536
 Total time 9 min 40 sec

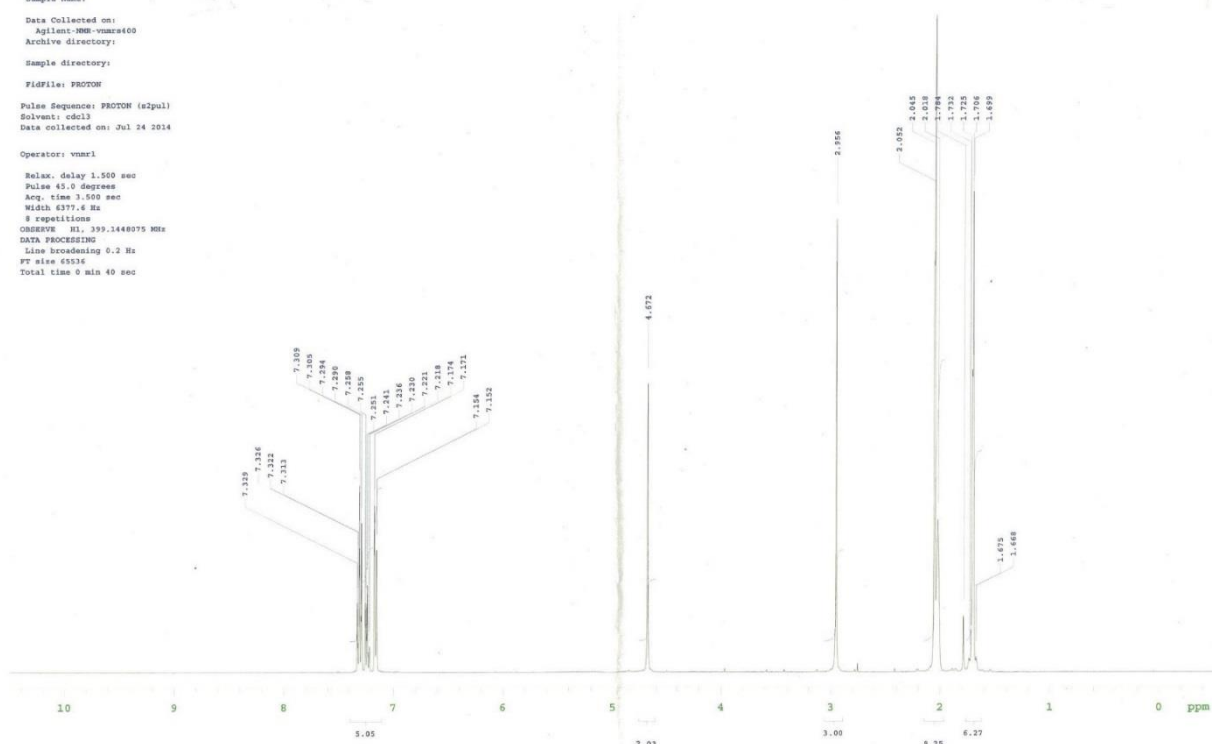


Sample Name:
 Data Collected on:
 Agilent-DMG-vnmr400
 Archive directory:
 Sample directory:
 FIDFile: CARBON
 Pulse Sequence: CARBON (s2pul)
 Solvent: cdcl3
 Data collected on: Jan 26 2016
 Temp. 24.2 C / 297.4 K
 Operator: vnmr1
 Relax. delay 1.689 sec
 Pulse 45.0 degrees
 Acq. time 1.311 sec
 Width 25000.0 Hz
 64 repetitions
 OBSERVE C13, 100.3360141 MHz
 DECOUPLE H1, 399.0393159 MHz
 Power 43 dB
 Continuously on
 WALTZ-16 modulated
 DATA PROCESSING
 Line broadening 1.0 Hz
 FT size 65536
 Total time 51 min

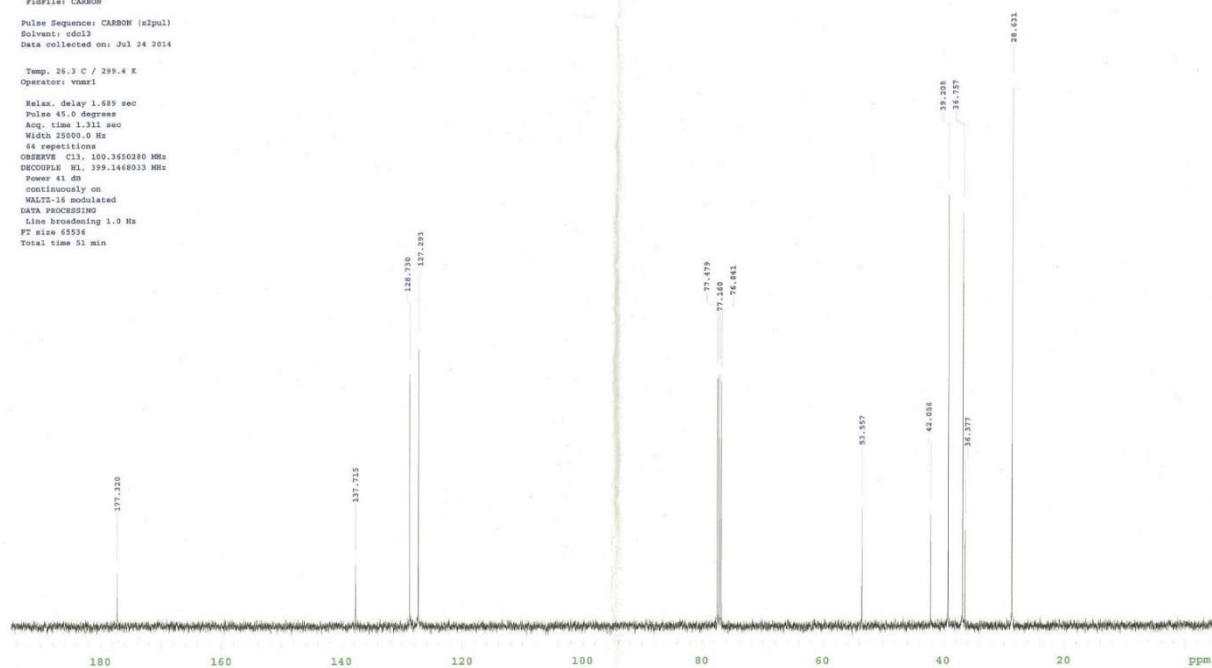




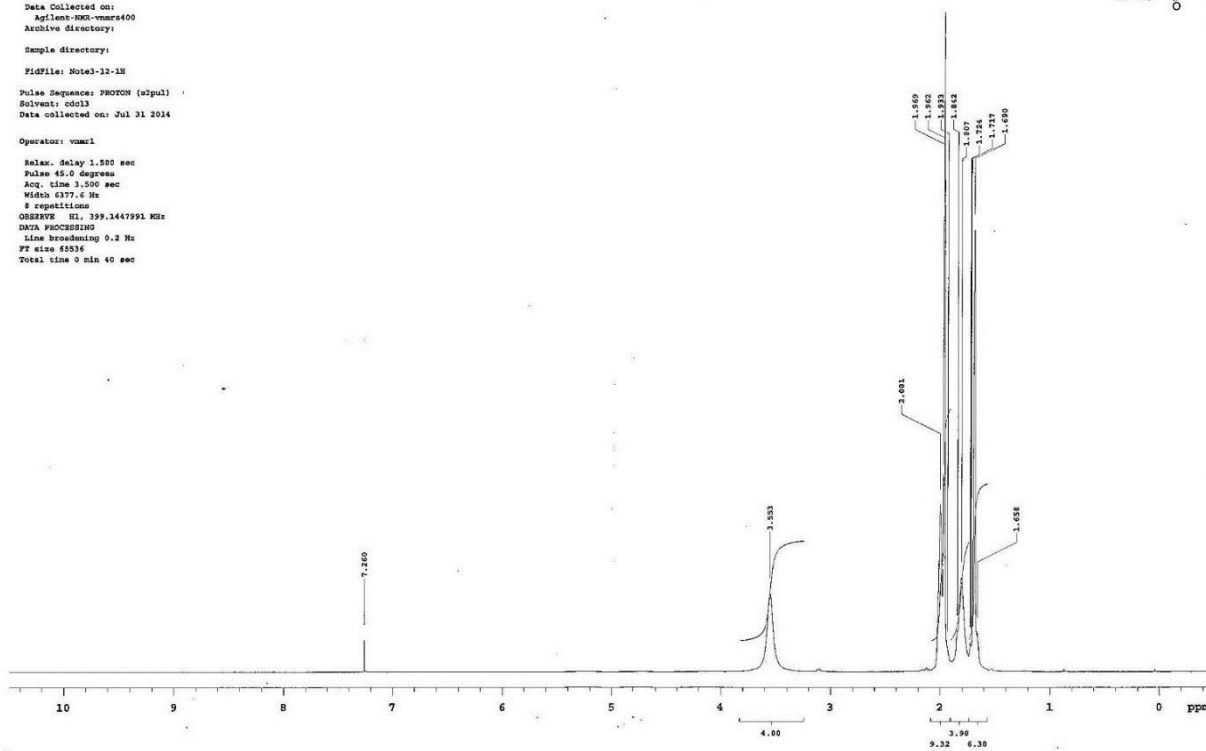
Sample Name:
 Data Collected on:
 Agilent-NMR-vnmr400
 Archive directory:
 Sample directory:
 Fidfile: PROTON
 Pulse Sequence: PROTON (e2pul)
 Solvent: cdcl3
 Date collected on: Jul 24 2014
 Operator: vnmr1
 Relax. delay 1.500 sec
 Pulse 45.0 degrees
 Acq. time 3.500 sec
 Width 6377.6 Hz
 8 repetitions
 OBSERVE H1, 399.1448075 MHz
 DATA PROCESSING
 Line broadening 0.2 Hz
 FT size 65536
 Total time 6 min 40 sec



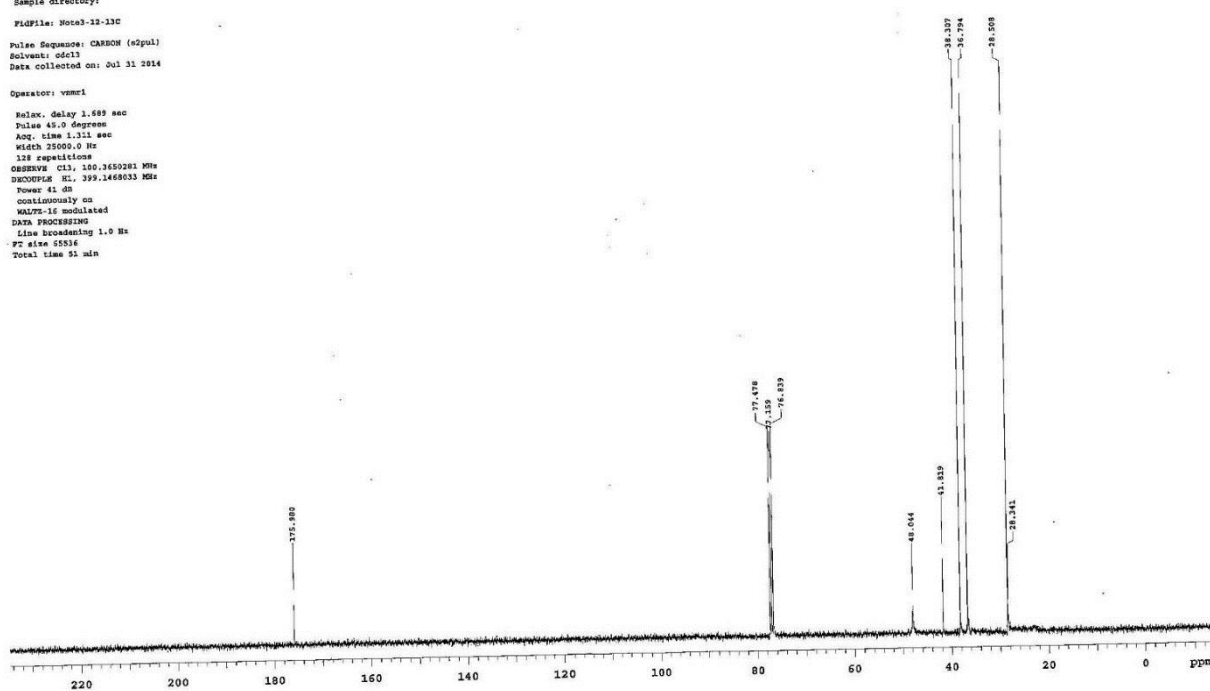
Sample Name:
 Data Collected on:
 Agilent-NMR-vnmr400
 Archive directory:
 Sample directory:
 Fidfile: CARBON
 Pulse Sequence: CARBON (e2pul)
 Solvent: cdcl3
 Date collected on: Jul 24 2014
 Temp. 24.3 C / 299.4 K
 Operator: vnmr1
 Relax. delay 1.089 sec
 Pulse 45.0 degrees
 Acq. time 1.311 sec
 Width 25000.0 Hz
 64 repetitions
 OBSERVE C13, 100.3650280 MHz
 DECOUPLE H1, 399.1448033 MHz
 Power 41 dB
 continuously on
 WALTZ-16 modulated
 DATA PROCESSING
 Line broadening 1.0 Hz
 FT size 65536
 Total time 11 min



Sample Name:
 Data Collected on:
 Agilent-VNM-600
 Archive directory:
 Sample directory:
 FIDFile: M023-12-1H
 Pulse Sequence: PROTON (zgpg30)
 Solvent: cdcl3
 Data collected on: Jul 31 2014
 Operator: vsmr1
 Relax. delay 1.200 sec
 Pulse 45.0 degree
 Acq. time 3.500 sec
 Width 6177.6 Hz
 8 repetitions
 OBSERVE F1: 399.1447991 MHz
 DATA PROCESSING
 Line broadening 0.2 Hz
 FT size 65536
 Total time 0 min 40 sec

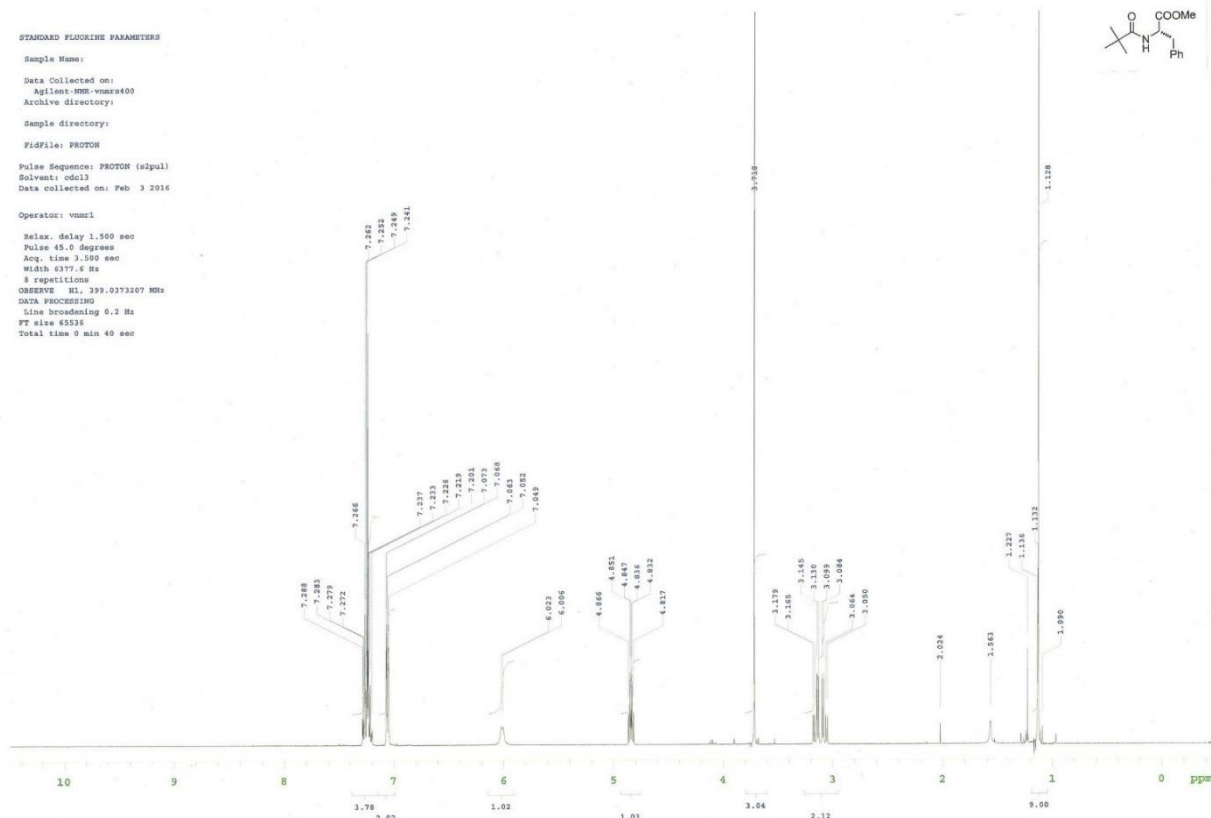


Sample Name:
 Data Collected on:
 Agilent-VNM-600
 Archive directory:
 Sample directory:
 FIDFile: M023-12-13C
 Pulse Sequence: CARBON (zgpg30)
 Solvent: cdcl3
 Data collected on: Jul 31 2014
 Operator: vsmr1
 Relax. delay 1.689 sec
 Pulse 45.0 degree
 Acq. time 1.311 sec
 Width 25000.0 Hz
 128 repetitions
 OBSERVE C13: 100.1450281 MHz
 DECOUPLE F1: 399.1447991 MHz
 Power 41 dB
 continuously on
 WALTZ-16 modulated
 DATA PROCESSING
 Line broadening 1.0 Hz
 FT size 65536
 Total time 31 min

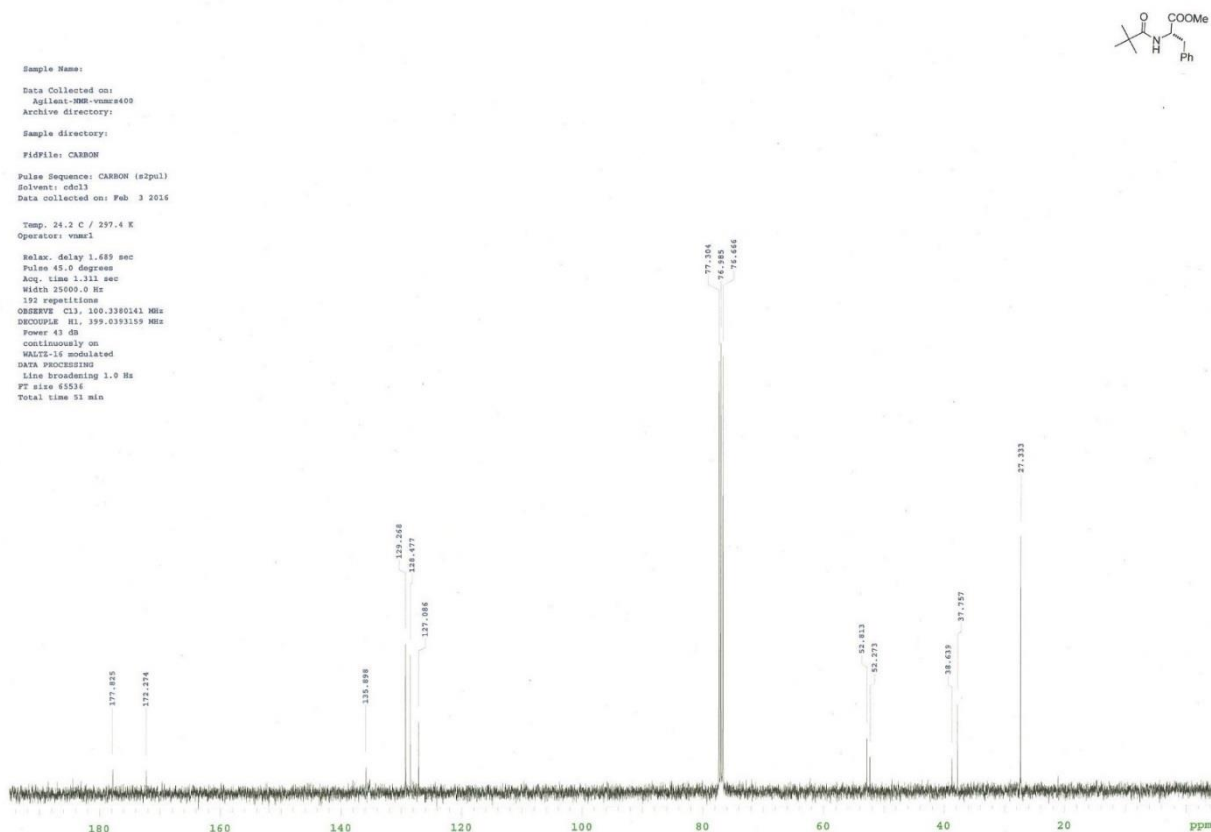


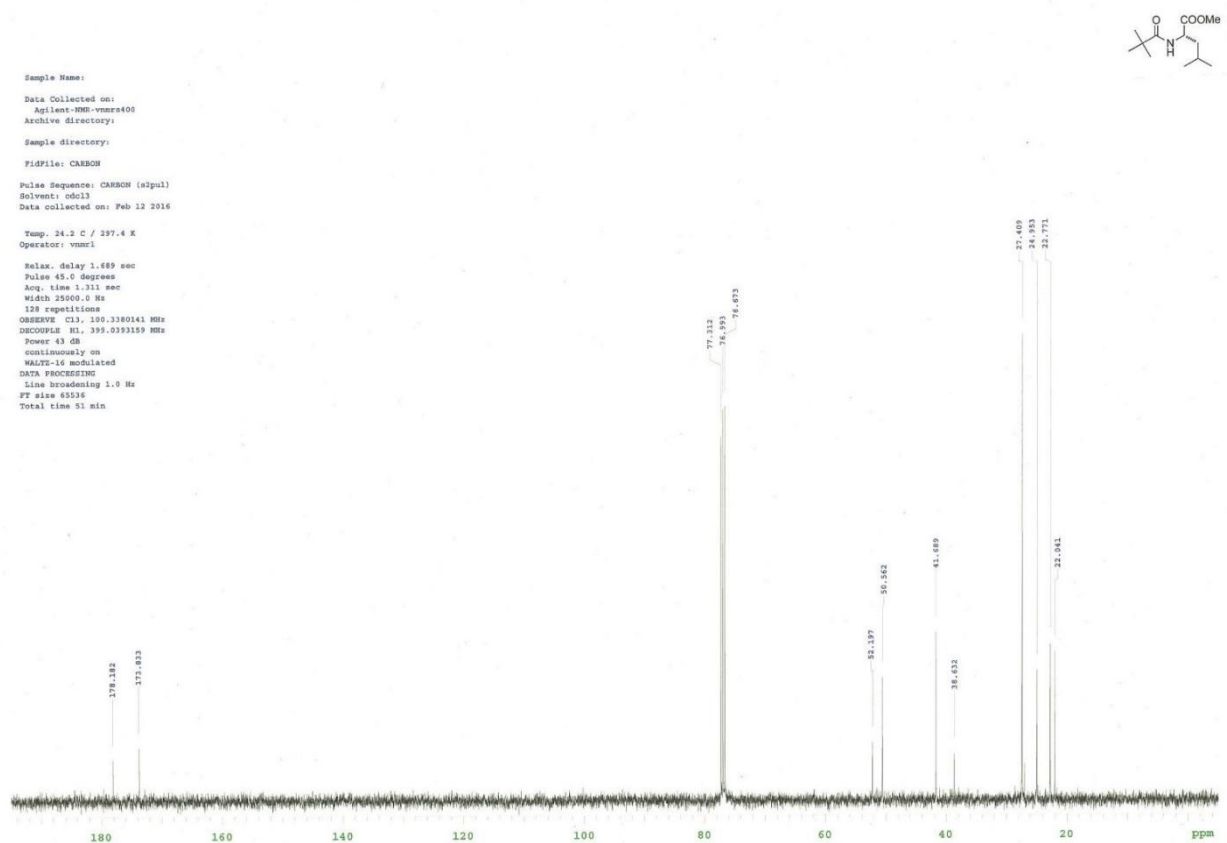
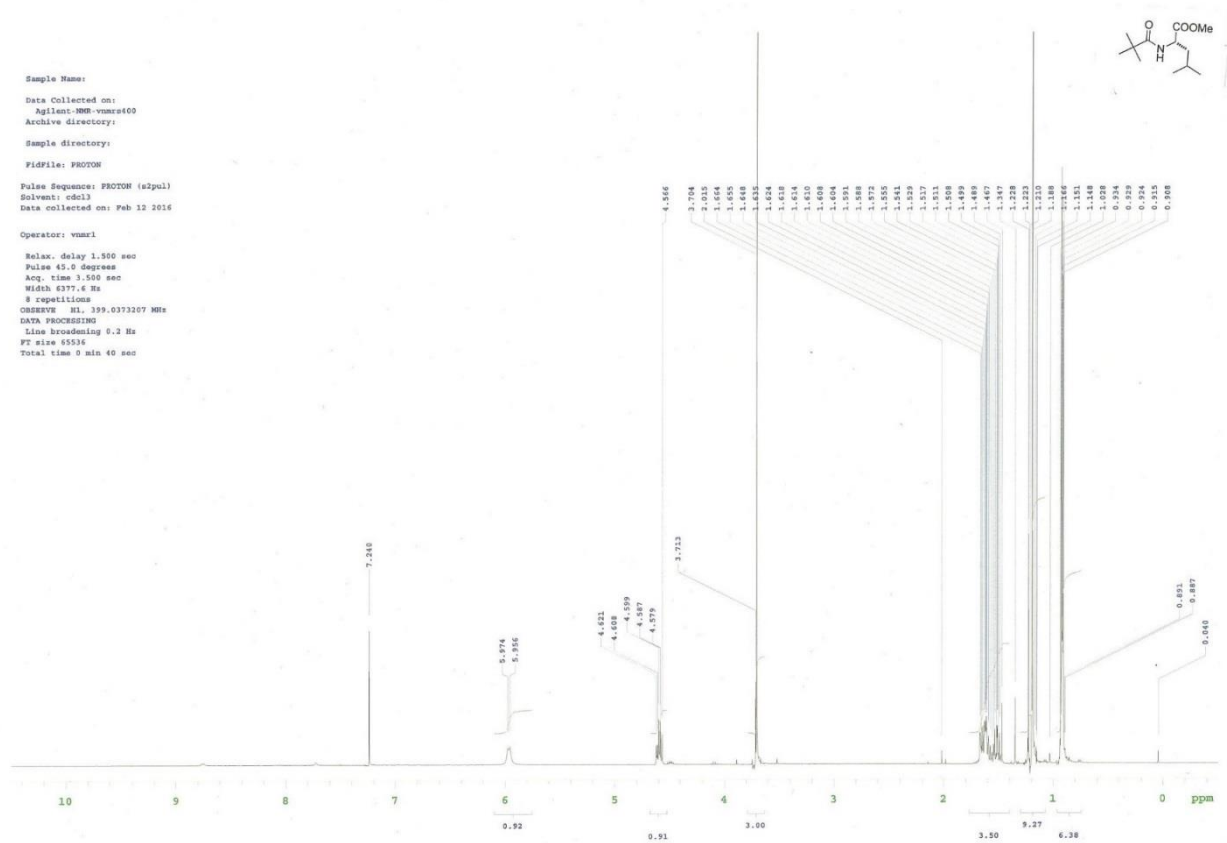
STANDARD FLUORINE PARAMETERS

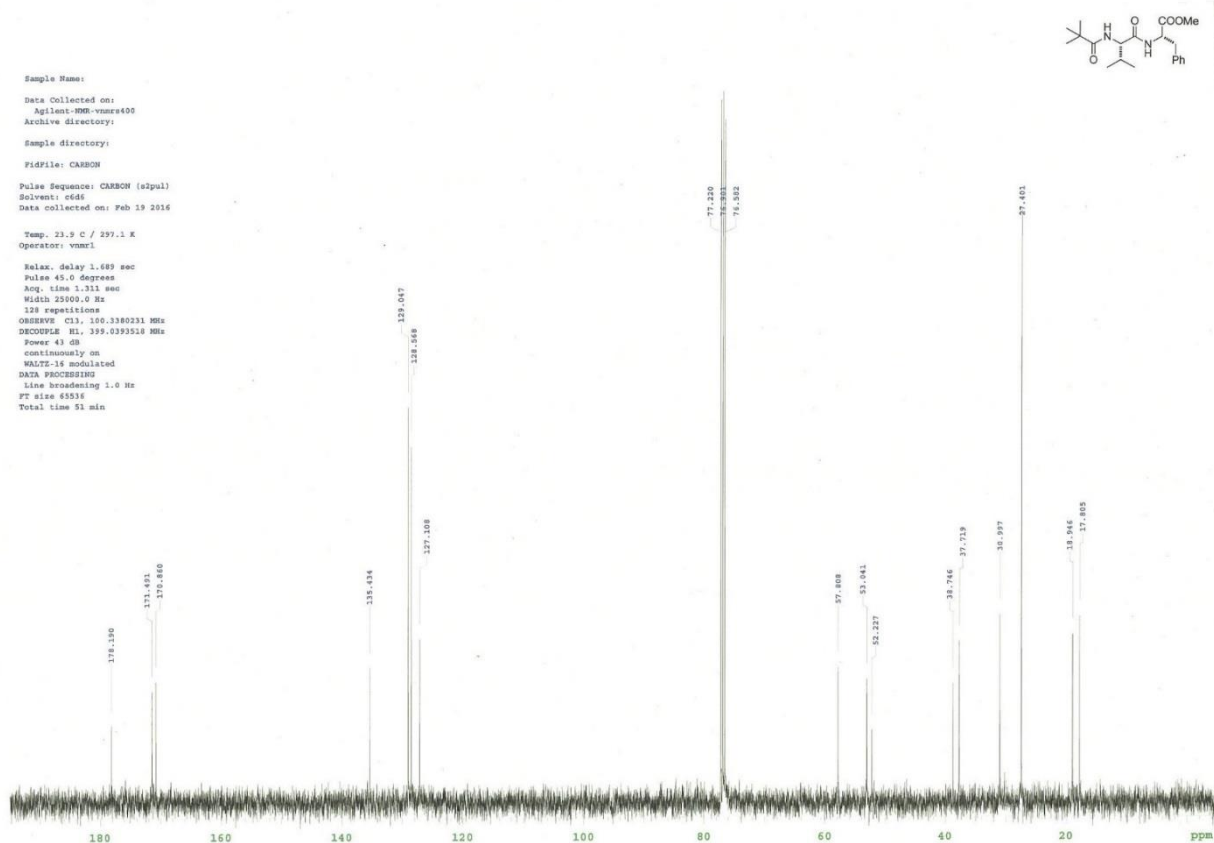
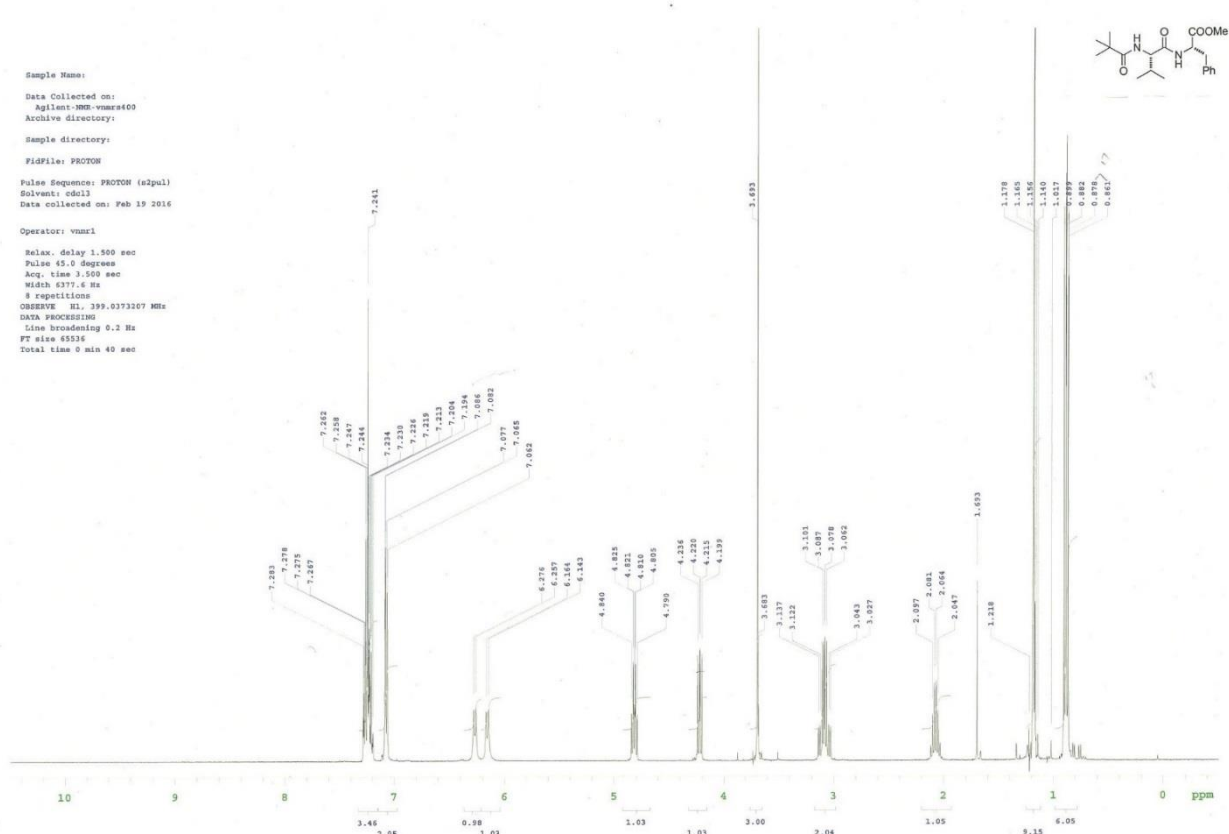
Sample Name:
 Data Collected on:
 Agilent-VNM-vmr400
 Archive directory:
 Sample directory:
 FidFile: PROTON
 Pulse Sequence: PROTON (s2pul)
 Solvent: cdcl3
 Data collected on: Feb 3 2016
 Operator: vmr41
 Relax. delay 1.500 sec
 Pulse 45.0 degrees
 Acq. time 3.500 sec
 Width 6177.6 Hz
 8 repetitions
 OBSERVE H1, 399.0373267 MHz
 DATA PROCESSING
 Line broadening 0.2 Hz
 FT size 65536
 Total time 0 min 40 sec



Sample Name:
 Data Collected on:
 Agilent-VNM-vmr400
 Archive directory:
 Sample directory:
 FidFile: CARBON
 Pulse Sequence: CARBON (s2pul)
 Solvent: cdcl3
 Data collected on: Feb 3 2016
 Temp. 24.2 C / 297.4 K
 Operator: vmr41
 Relax. delay 1.689 sec
 Pulse 45.0 degrees
 Acq. time 1.312 sec
 Width 25000.0 Hz
 192 repetitions
 OBSERVE C13, 100.3360141 MHz
 DECOUPLE H1, 399.0393159 MHz
 Power 43 dB
 Continuously on
 WALTZ-16 modulated
 DATA PROCESSING
 Line broadening 1.0 Hz
 FT size 65536
 Total time 31 min







YQ-77-after3days

Sample Name:

Data Collected on:
Agilent-NMR-vnmr400

Archive directory:

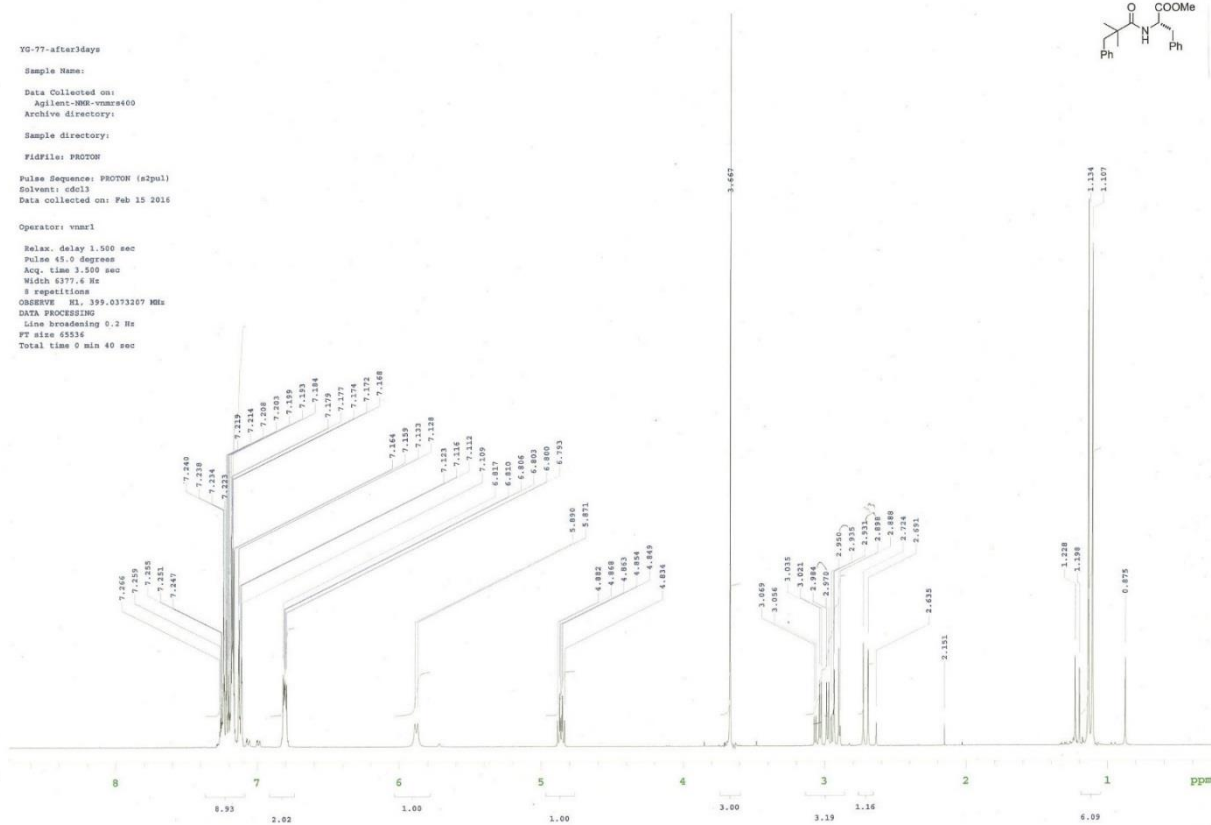
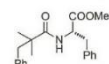
Sample directory:

Fidfile: PROTON

Pulse Sequence: PROTON (a2pul)
Solvent: cdcl3
Data collected on: Feb 15 2016

Operator: vnmr1

Relax. delay 1.560 sec
Pulse 45.0 degrees
Acq. time 3.590 sec
Width 6377.4 Hz
8 repetitions
OBSERVE HL 399.0373207 MHz
DATA PROCESSING
Line broadening 6.2 Hz
FT size 65536
Total time 9 min 40 sec



Sample Name:

Data Collected on:
Agilent-NMR-vnmr400

Archive directory:

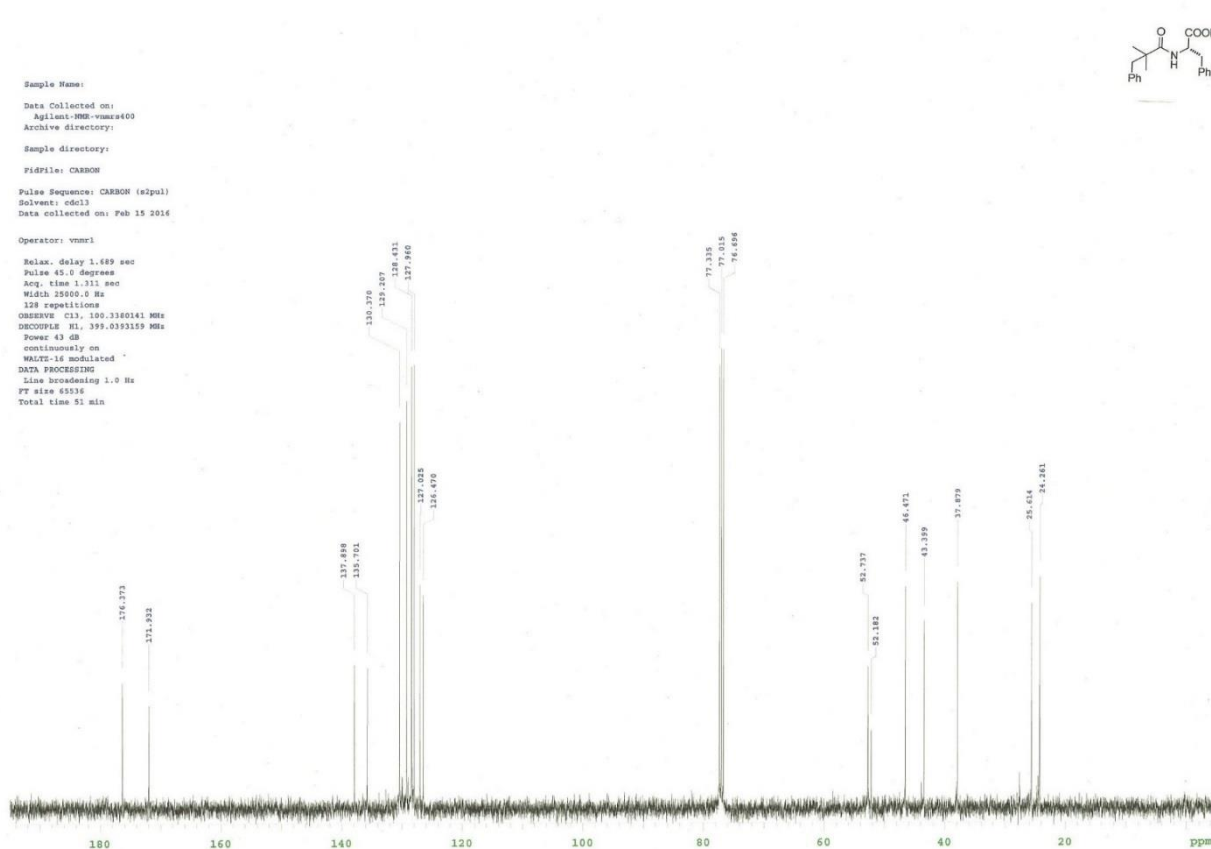
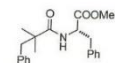
Sample directory:

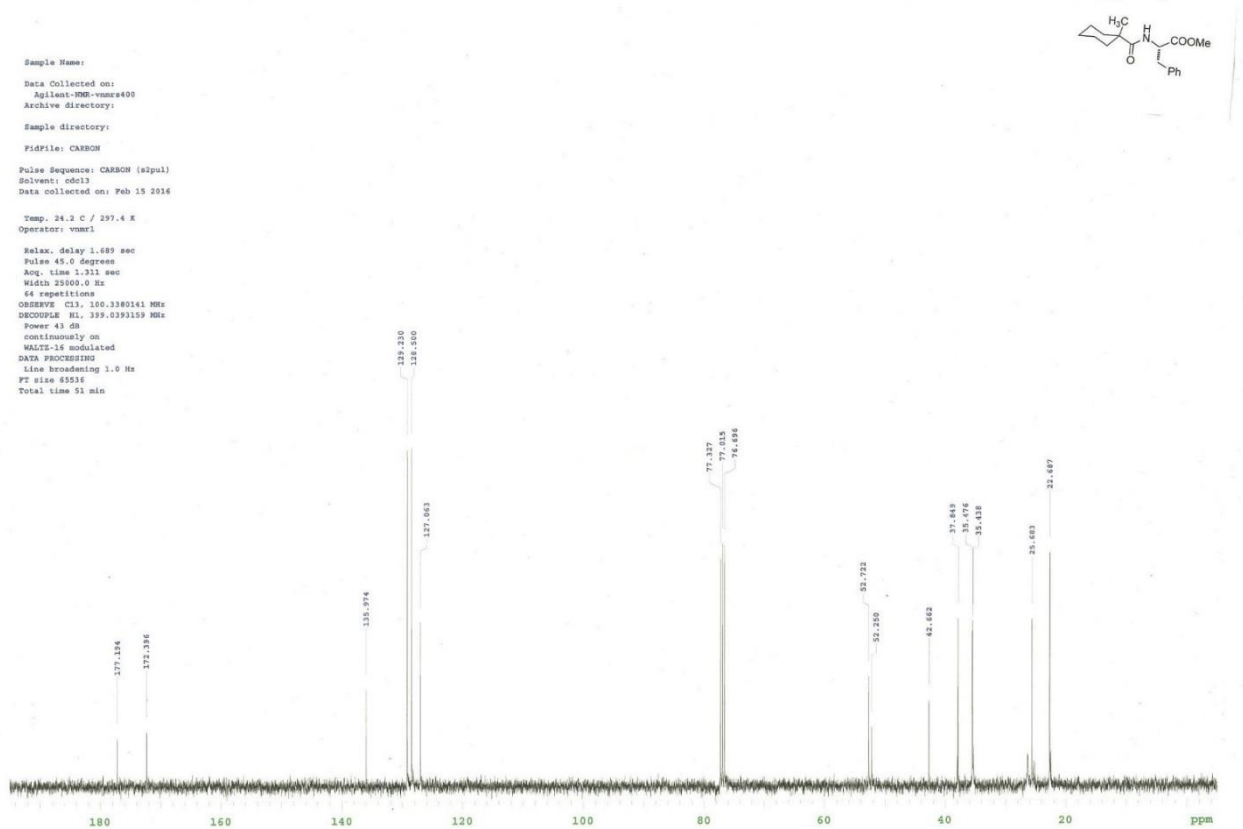
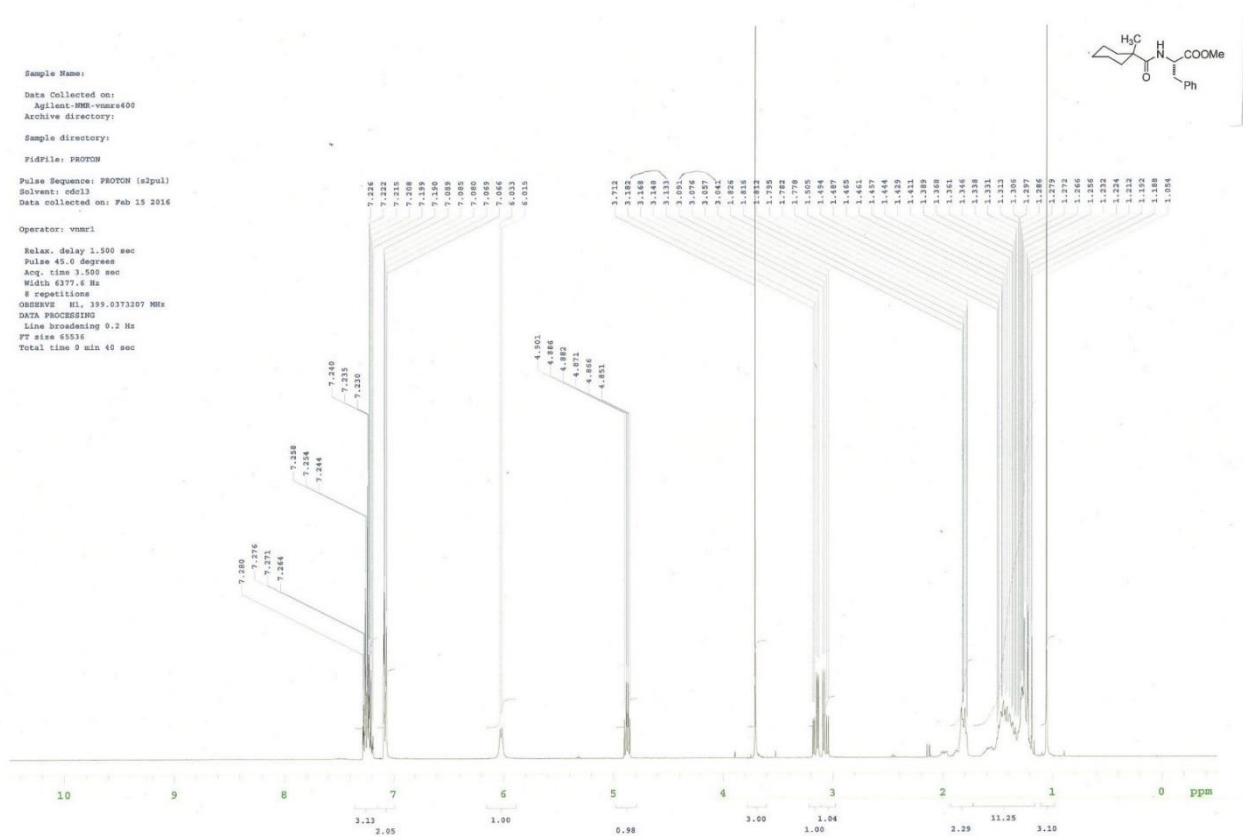
Fidfile: CARBON

Pulse Sequence: CARBON (a2pul)
Solvent: cdcl3
Data collected on: Feb 15 2016

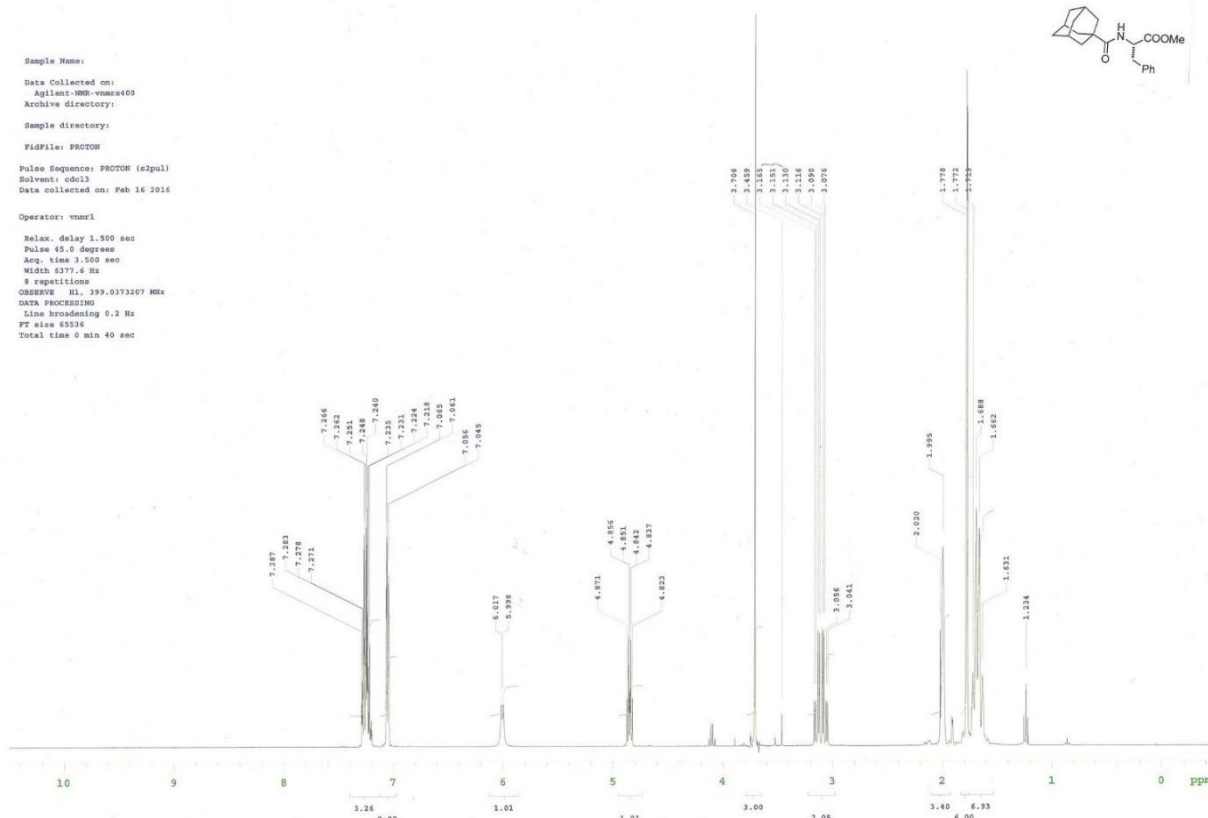
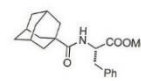
Operator: vnmr1

Relax. delay 1.669 sec
Pulse 45.0 degrees
Acq. time 1.311 sec
Width 25000.0 Hz
128 repetitions
OBSERVE CH 100.3360141 MHz
DECOUPLE HL 399.0373159 MHz
Power 43 dB
continuously on
WALTZ-16 modulated
DATA PROCESSING
Line broadening 1.0 Hz
FT size 65536
Total time 51 min

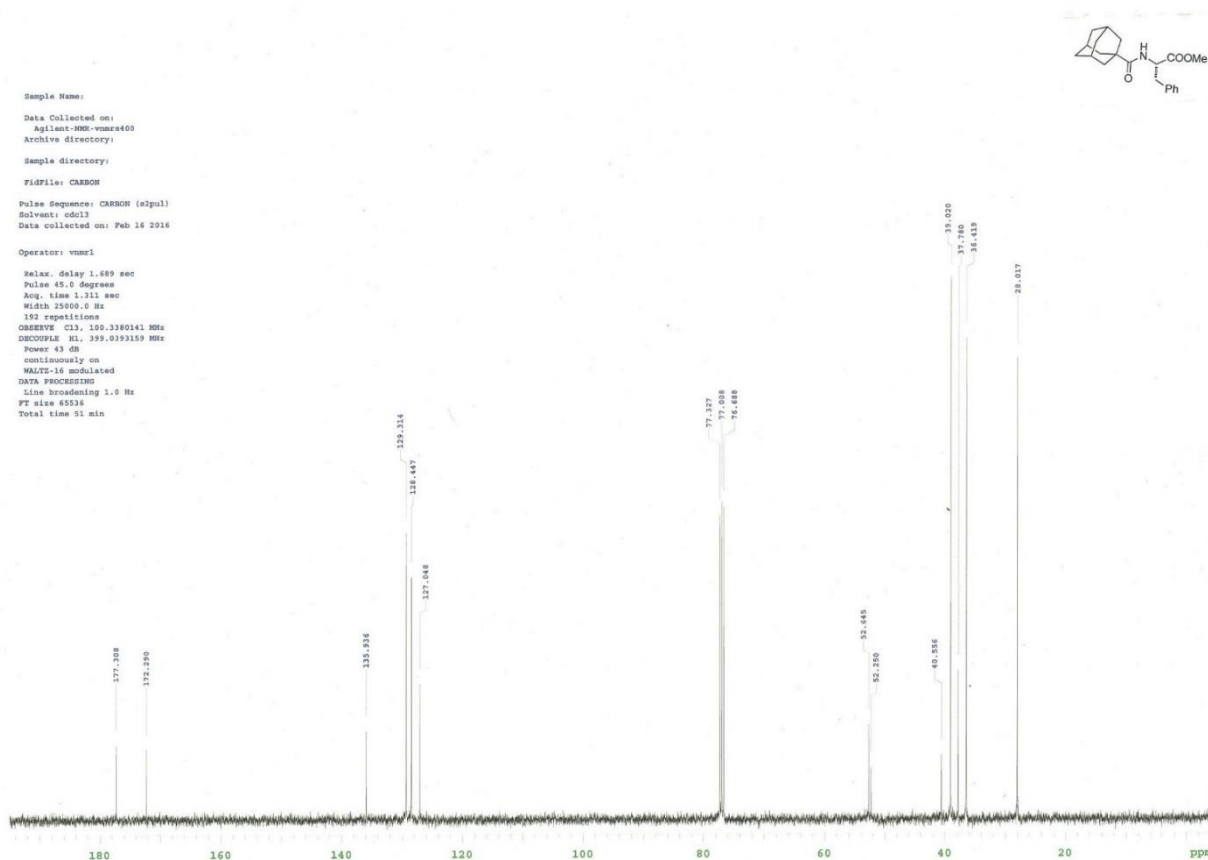
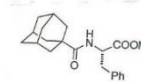


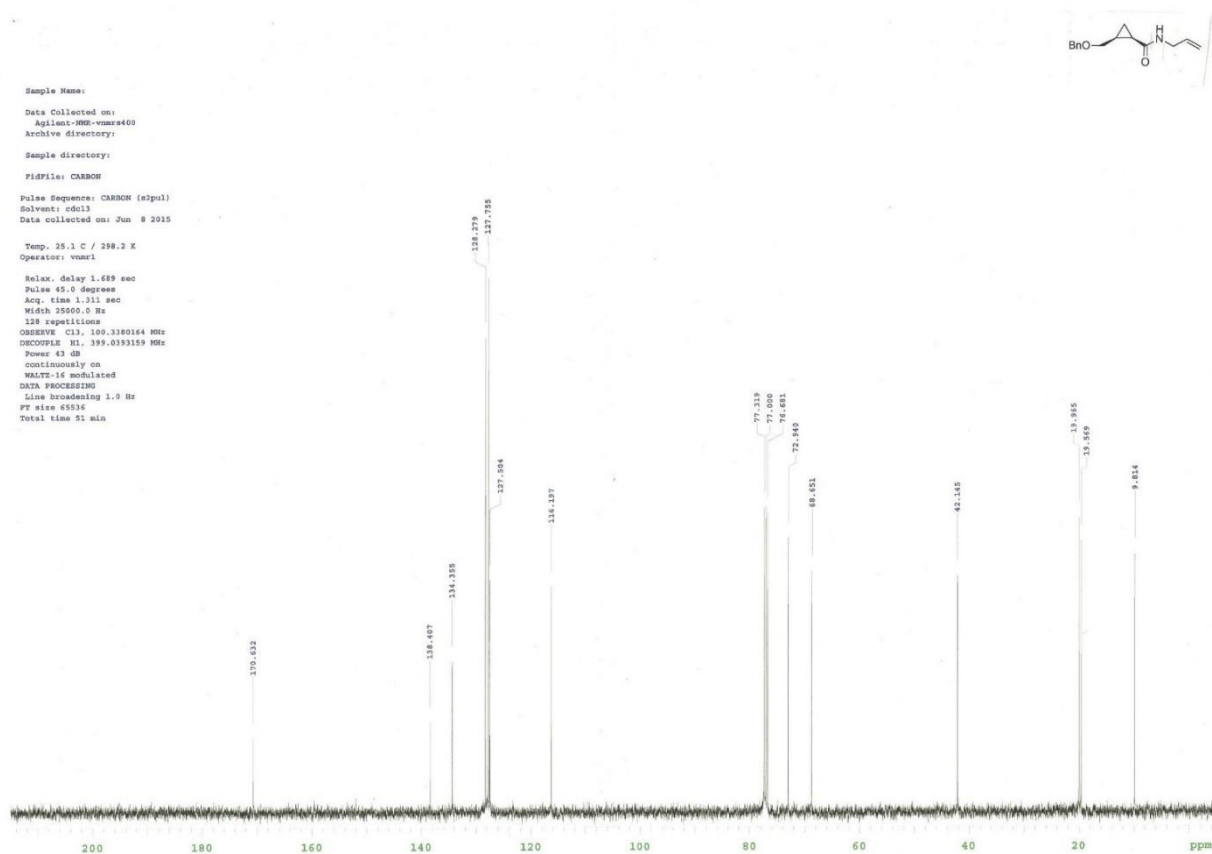
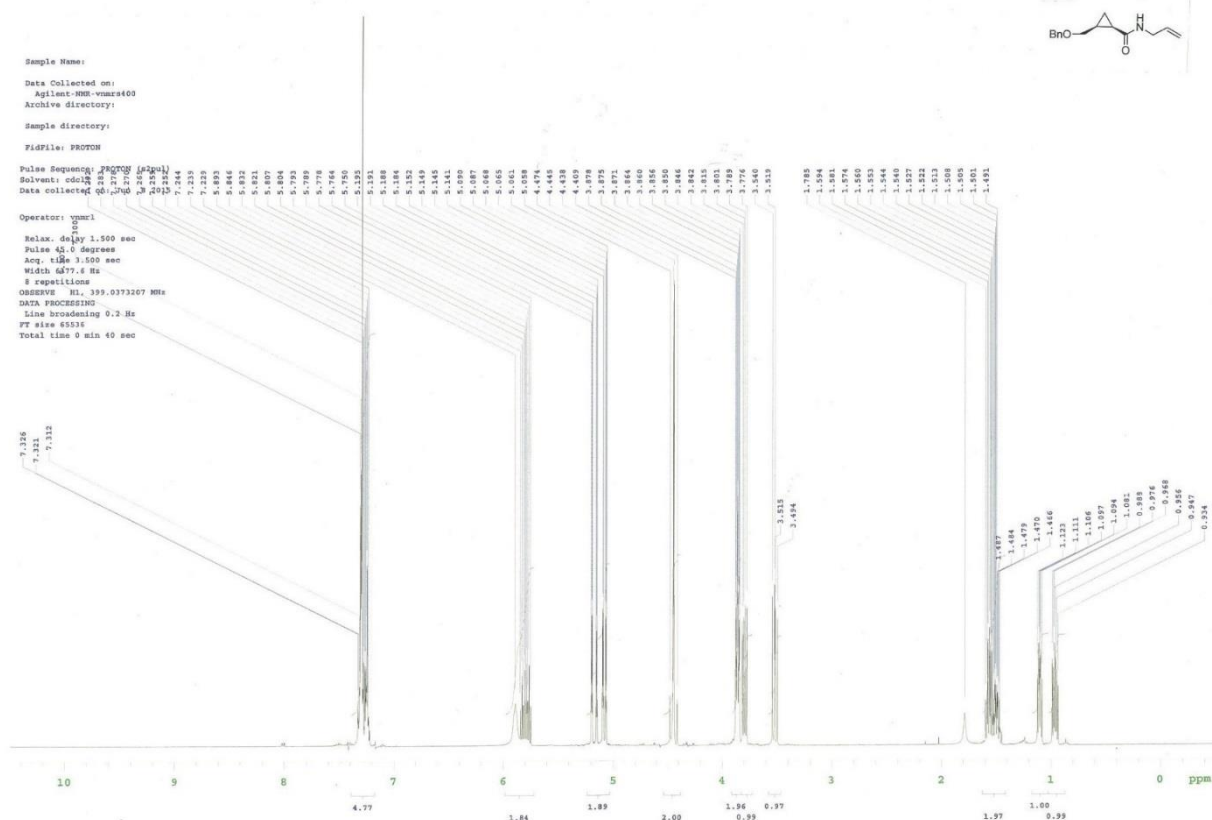


Sample Name:
 Data Collected on:
 Agilent-VNM-vmr400
 Archive directory:
 Sample directory:
 FidFile: PROTON
 Pulse Sequence: PROTON (a2pul)
 Solvent: cdcl3
 Data collected on: Feb 16 2016
 Operator: vmr1
 Relax. delay 1.500 sec
 Pulse 45.0 degrees
 Acq. time 1.550 sec
 Width 6177.6 Hz
 8 repetitions
 OBSERVE H1, 399.0173267 MHz
 DATA PROCESSING
 Line broadening 0.2 Hz
 FT size 65536
 Total time 0 min 40 sec

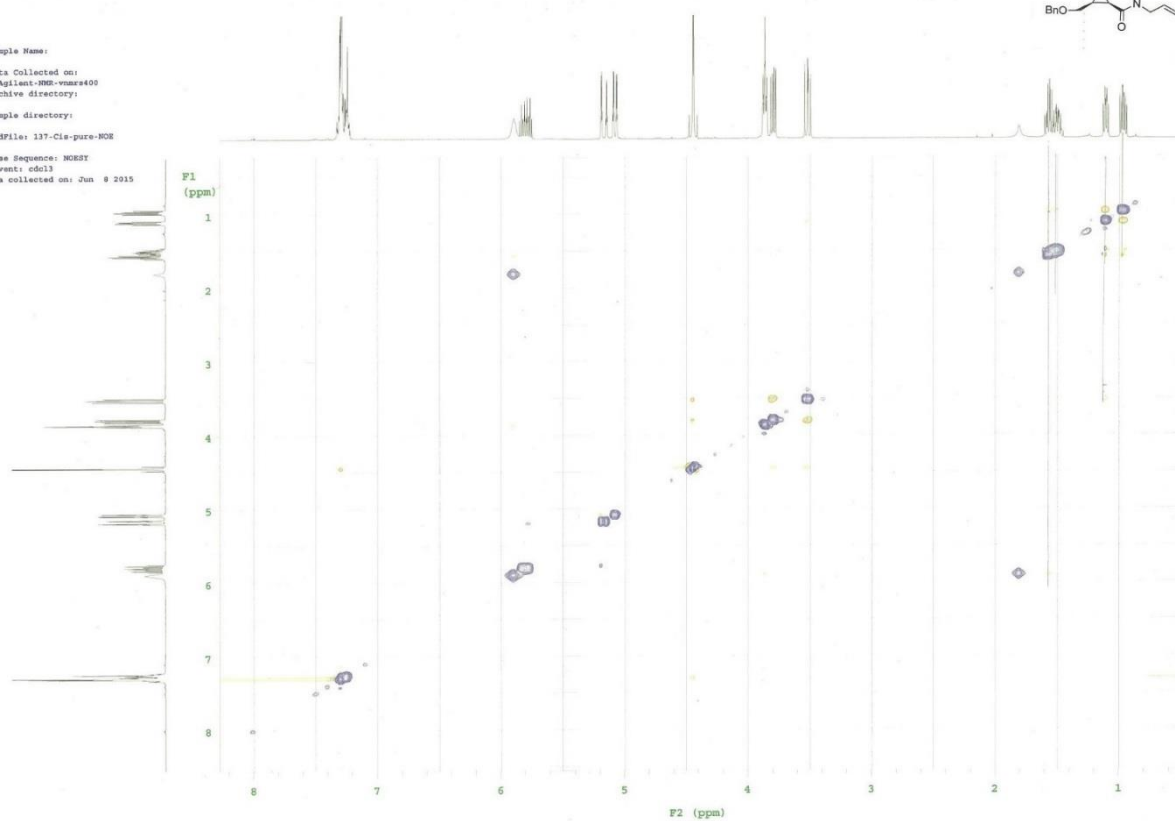
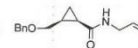


Sample Name:
 Data Collected on:
 Agilent-VNM-vmr400
 Archive directory:
 Sample directory:
 FidFile: CARBON
 Pulse Sequence: CARBON (a2pul)
 Solvent: cdcl3
 Data collected on: Feb 16 2016
 Operator: vmr1
 Relax. delay 1.669 sec
 Pulse 45.0 degrees
 Acq. time 1.311 sec
 Width 25000.0 Hz
 192 repetitions
 OBSERVE C13, 100.3380141 MHz
 DECOUPLE H1, 399.0193157 MHz
 Power 43 dB
 continuously on
 WALTZ-16 modulated
 DATA PROCESSING
 Line broadening 1.0 Hz
 FT size 65536
 Total time 51 min

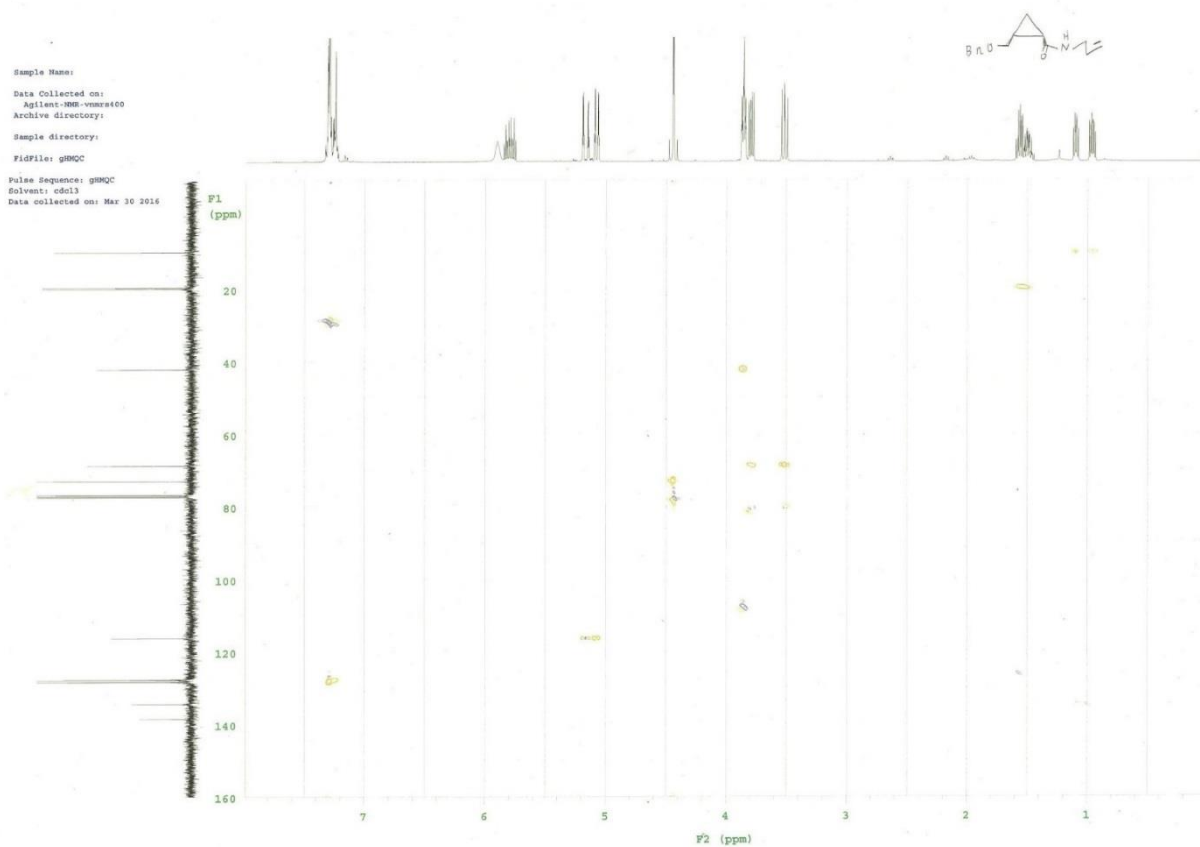




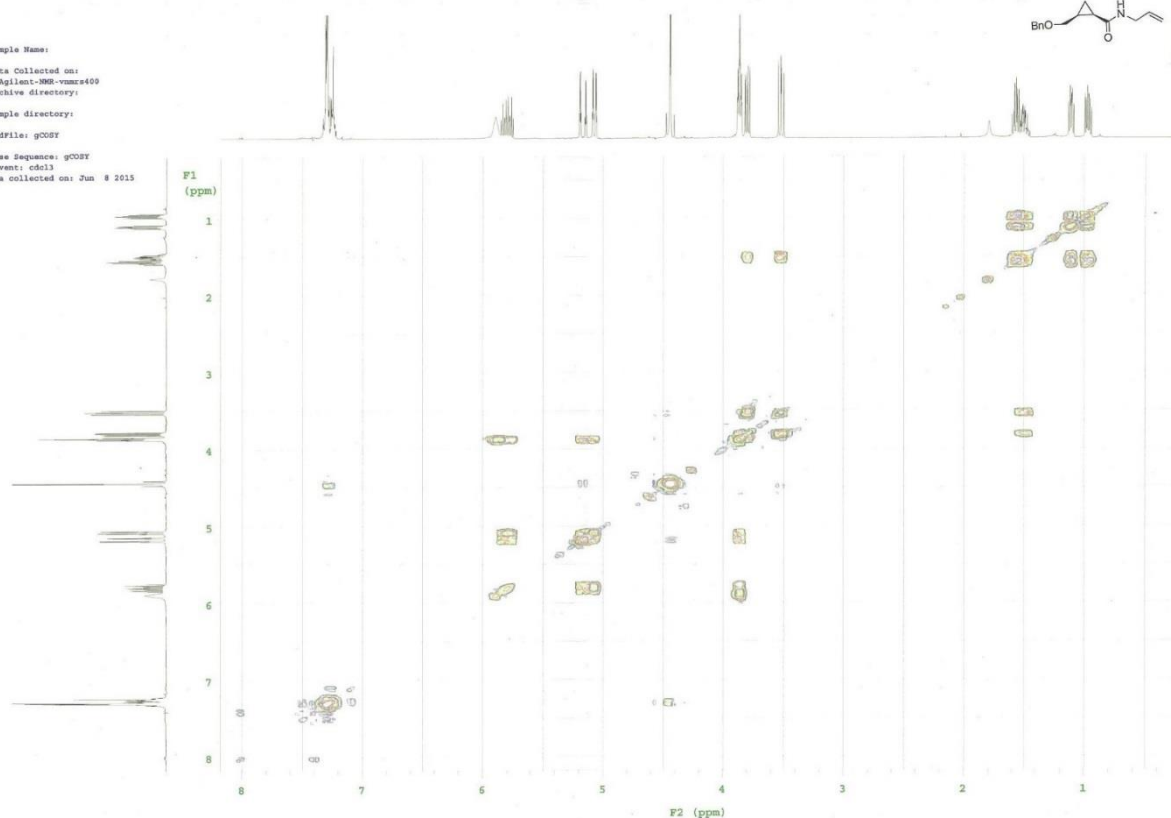
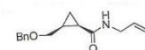
Sample Name:
 Data Collected on:
 Agilent-VNM-600
 Archive directory:
 Sample directory:
 FidFile: 137-Cis-pure-MOE
 Pulse Sequence: NOESY
 Solvent: cdcl3
 Data collected on: Jun 9 2015



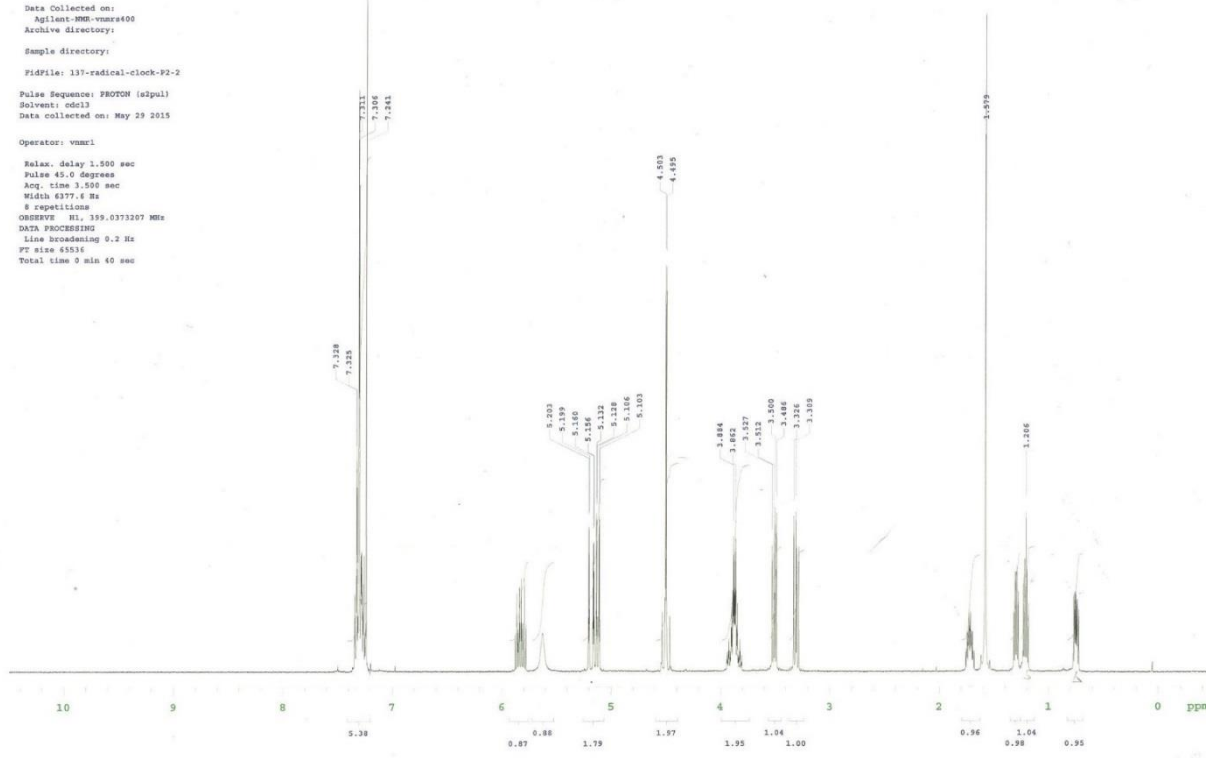
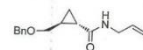
Sample Name:
 Data Collected on:
 Agilent-VNM-600
 Archive directory:
 Sample directory:
 FidFile: gbmqc
 Pulse Sequence: gbmqc
 Solvent: cdcl3
 Data collected on: Mar 30 2016



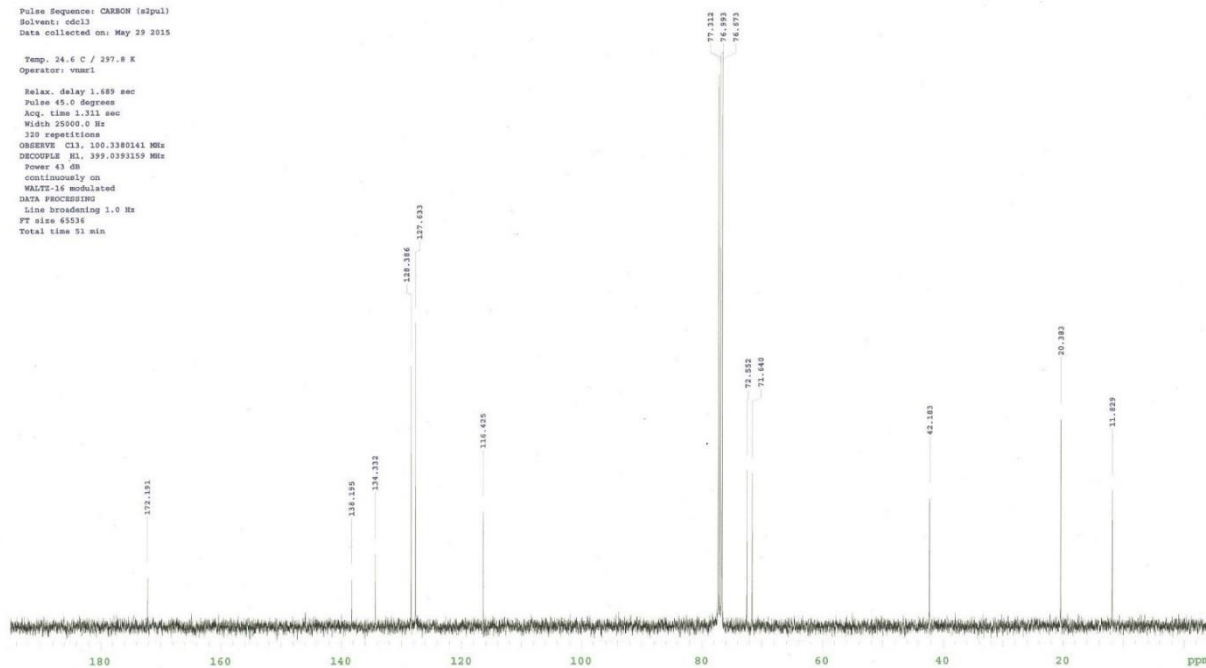
Sample Name:
 Data Collected on:
 Agilent-VNM-600MHz
 Archive directory:
 Sample directory:
 FIDfile: gCOSY
 Pulse Sequence: gCOSY
 Solvent: cdcl3
 Data collected on: Jun 9 2015



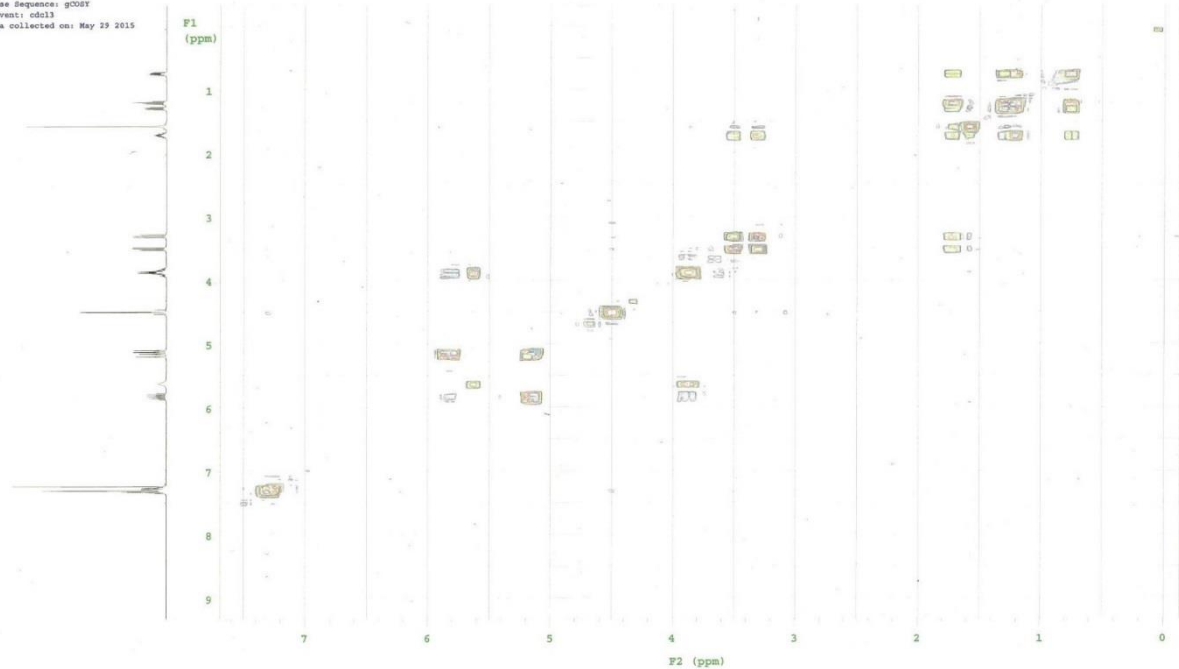
Sample Name:
 Data Collected on:
 Agilent-MMR-vnmr400
 Archive directory:
 Sample directory:
 FIDFile: 137-radical-clock-P2-2
 Pulse Sequence: PROTON (s2pul)
 Solvent: cdcl3
 Data collected on: May 29 2015
 Operator: vnmr1
 Relax, delay 1.500 sec
 Pulse 45.0 degrees
 Acq. time 3.550 sec
 Width 6377.6 Hz
 8 repetitions
 OBSERVE H1, 399.8373207 MHz
 DATA PROCESSING
 Line broadening 9.2 Hz
 FT size 65536
 Total time 3 min 40 sec



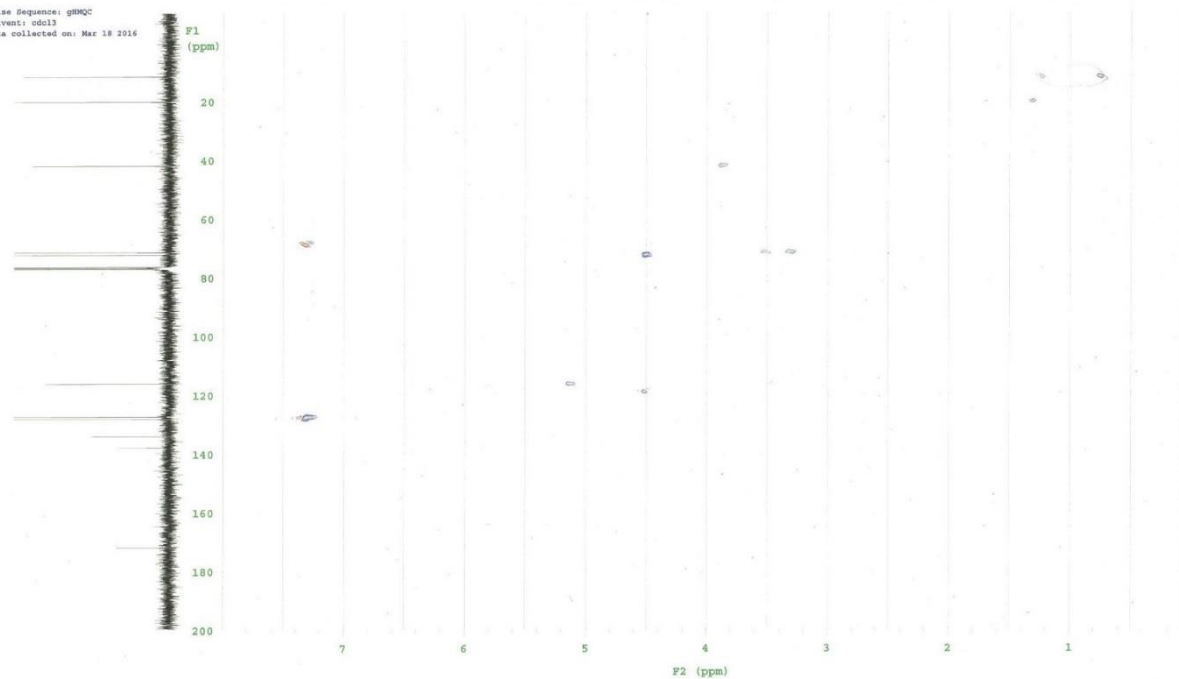
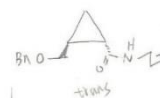
Sample Name:
 Data Collected on:
 Agilent-MMR-vnmr400
 Archive directory:
 Sample directory:
 FIDFile: CARBON
 Pulse Sequence: CARBON (s2pul)
 Solvent: cdcl3
 Data collected on: May 29 2015
 Temp. 24.6 C / 297.8 K
 Operator: vnmr1
 Relax, delay 1.689 sec
 Pulse 45.0 degrees
 Acq. time 1.311 sec
 Width 25000.0 Hz
 320 repetitions
 OBSERVE C13, 100.3380141 MHz
 DECOUPLE H1, 399.8393159 MHz
 Power 43 dB
 continuously on
 WALTZ-16 modulated
 DATA PROCESSING
 Line broadening 1.0 Hz
 FT size 65536
 Total time 51 min



Sample Name:
 Data Collected on:
 Agilent-900-vnmr400
 Archive directory:
 Sample directory:
 FIDFile: gCOST
 Pulse Sequence: gCOST
 Solvent: cdcl3
 Data collected on: May 29 2015

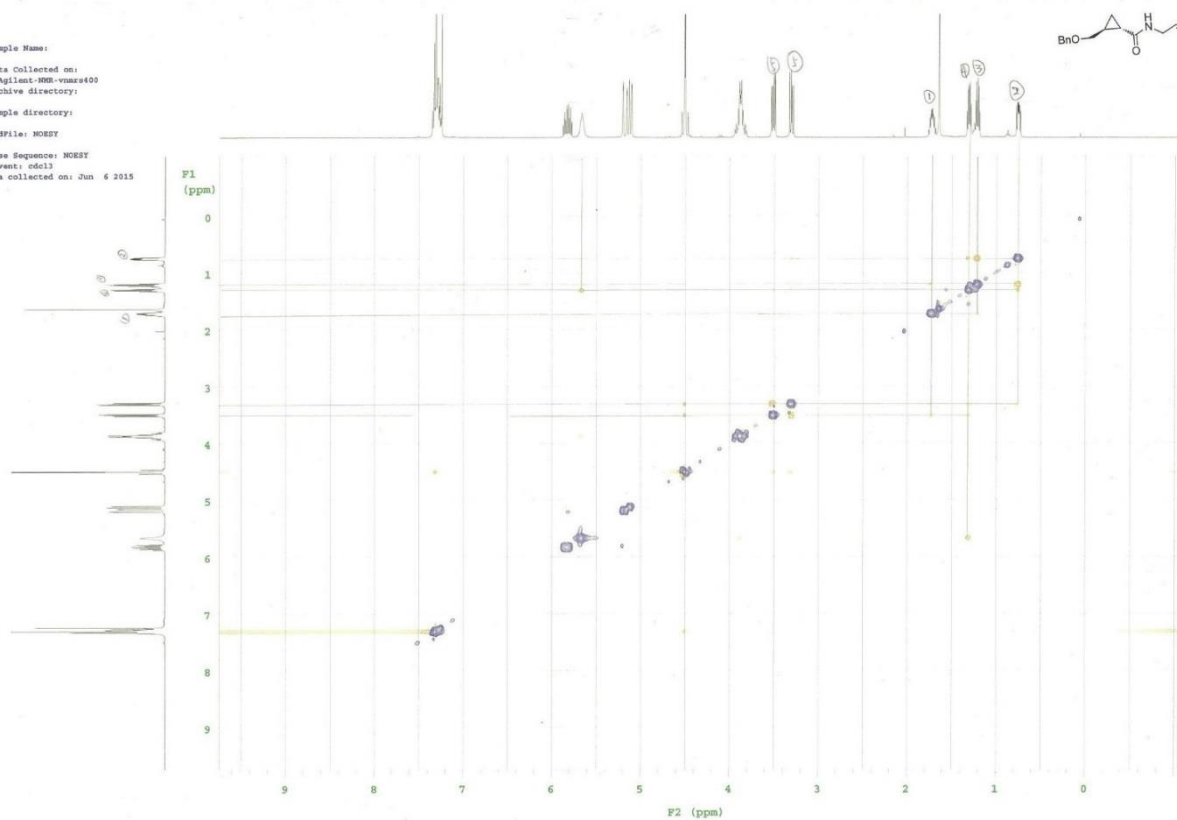
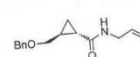


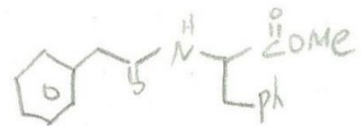
Sample Name:
 Data Collected on:
 Agilent-900-vnmr400
 Archive directory:
 Sample directory:
 FIDFile: gHMOC
 Pulse Sequence: gHMOC
 Solvent: cdcl3
 Data collected on: Mar 18 2016



Sample Name:
 Data Collected on:
 Agilent-900-mmx400
 Archive directory:
 Sample directory:
 FIDfile: M0857

Pulse Sequence: M0857
 Solvent: cdcl3
 Data collected on: Jun 6 2015

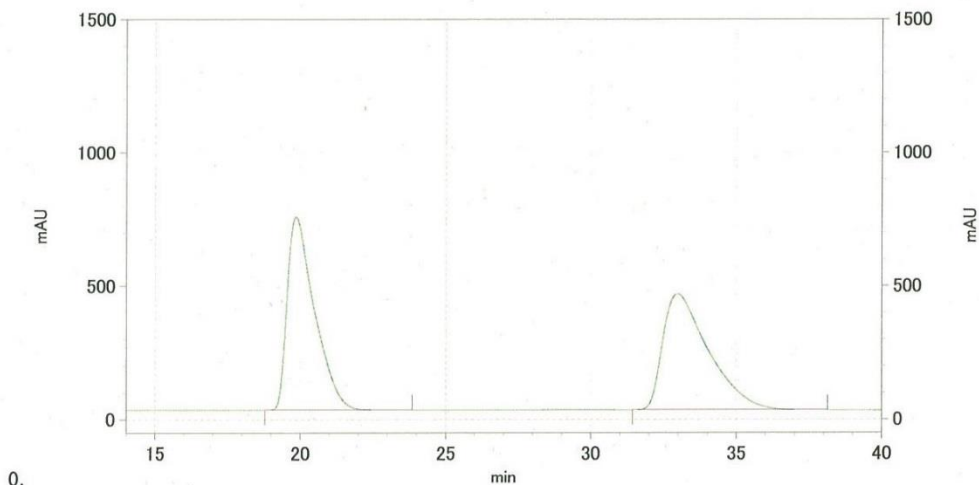




ページ 1/1

面積%レポート

データファイル名: C:\EZChrom Elite\Enterprise\Projects\Default\Data\2014-07-26 14-07-39
 LiJing 03-155 raceme chiral IC 10vs1 2ml.dat
 メソッドファイル名: C:\EZChrom Elite\Enterprise\Projects\Default\Method\50vs1 1ml.met
 ユーザー名: System
 分析日時: 2014/07/26 14:08:26
 印刷日時: 2014/07/31 14:18:13

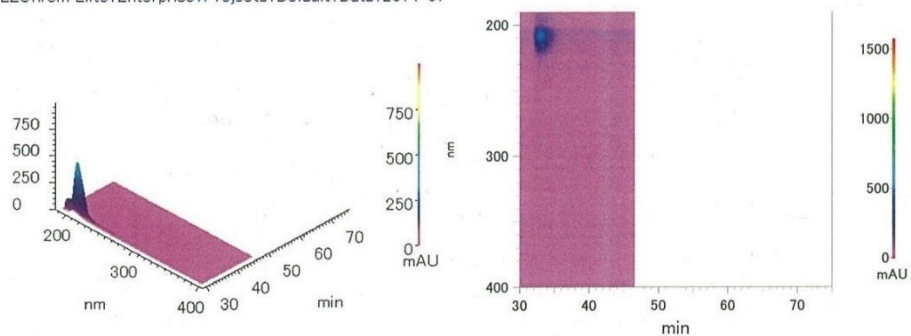


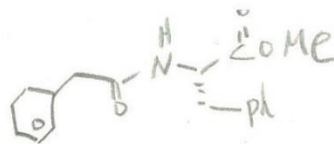
1: 207 nm, 4
nm結果

名前	保持時間	面積	面積%	ベースラインコード
	19.86	188804397	49.955	MM
	32.99	189142435	50.045	MM

トータル		377946832	100.000	
------	--	-----------	---------	--

C:\EZChrom Elite\Enterprise\Projects\Default\Data\2014-07-

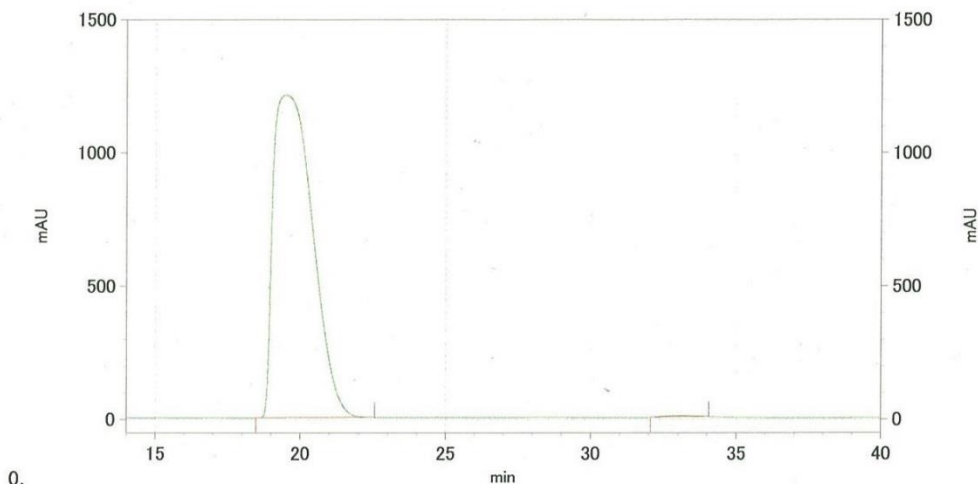




ページ 1/1

面積%レポート

データファイル名: C:\EZChrom Elite\Enterprise\Projects\Default\Data\2014-07-26 15-54-19
 LiJing 03-155 L chiral IC 10vs1 2ml.dat
 メソッドファイル名: C:\EZChrom Elite\Enterprise\Projects\Default\Method\50vs1 1ml.met
 ユーザー名: System
 分析日時: 2014/07/26 15:54:56
 印刷日時: 2014/07/31 14:26:52

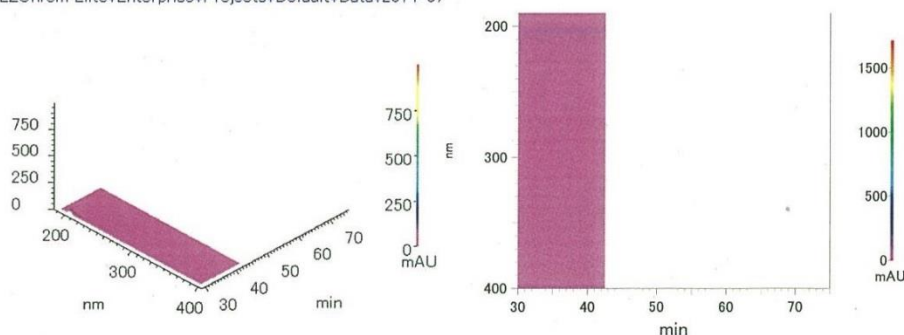


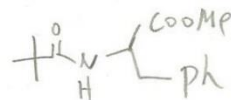
1: 207 nm, 4
nm結果

名前	保持時間	面積	面積%	ピークコメント
	19.50	456350131	99.666	MM
	33.11	1529588	0.334	MM

トータル		457879719	100.000	
------	--	-----------	---------	--

C:\EZChrom Elite\Enterprise\Projects\Default\Data\2014-07-



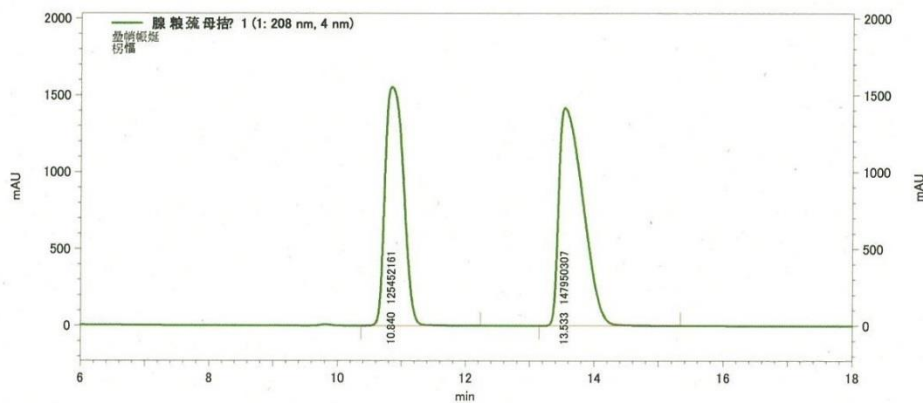


光学純度解析

データファイル C:\Users\tohoku univ\Desktop\Li-dicyano\LiJing-dicyano-IA-9\Li-ID-15-1-1mL-raceme-3.dat

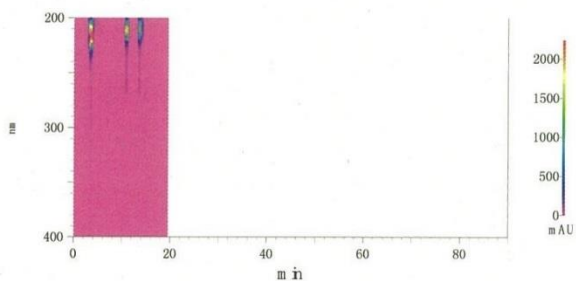
メソッド C:\VEZChrom Elite\Enterprise\Projects\Default\Method\shimasaki\Anal0126.met

取込日時 2016/02/05 13:55:00

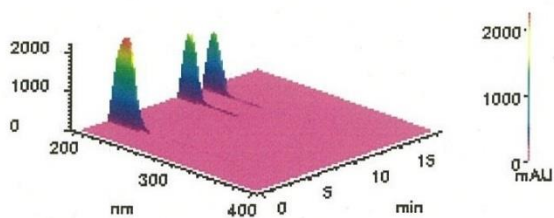


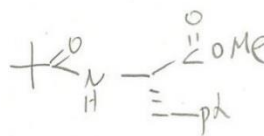
1: 208 nm, 4 nm結果

保持時間	面積	面積%	高さ	高さ%
10.840	125452161	45.886	6211830	52.269
13.533	147950307	54.114	5672546	47.731



C:\Users\tohoku univ\Desktop\Li-dicyano\LiJing-dicyano-IA-



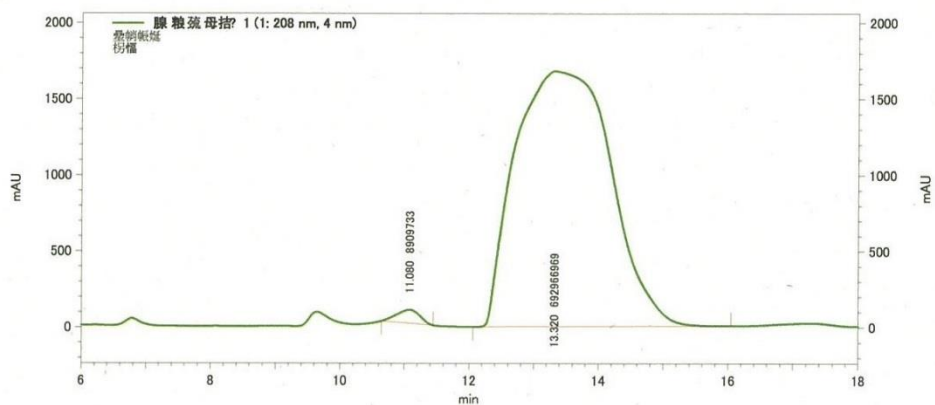


光学純度解析

データファイル C:\Users\tohoku univ\Desktop\Li-dicyano\LiJing-dicyano-IA-9\Li-ID-15-1-1mL-chiral-6. dat

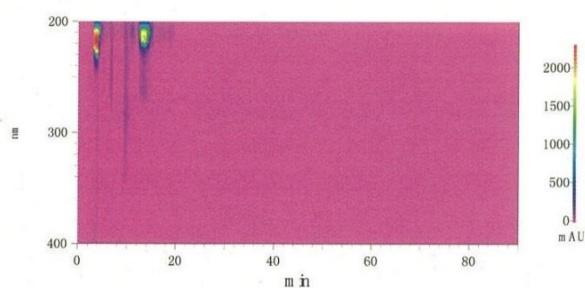
メソッド C:\EZChrom Elite\Enterprise\Projects\Default\Method\shimasaki\Anal0126.met

取込日時 2016/02/09 19:25:52

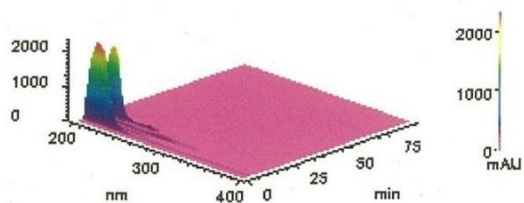


1: 208 nm, 4 nm結果

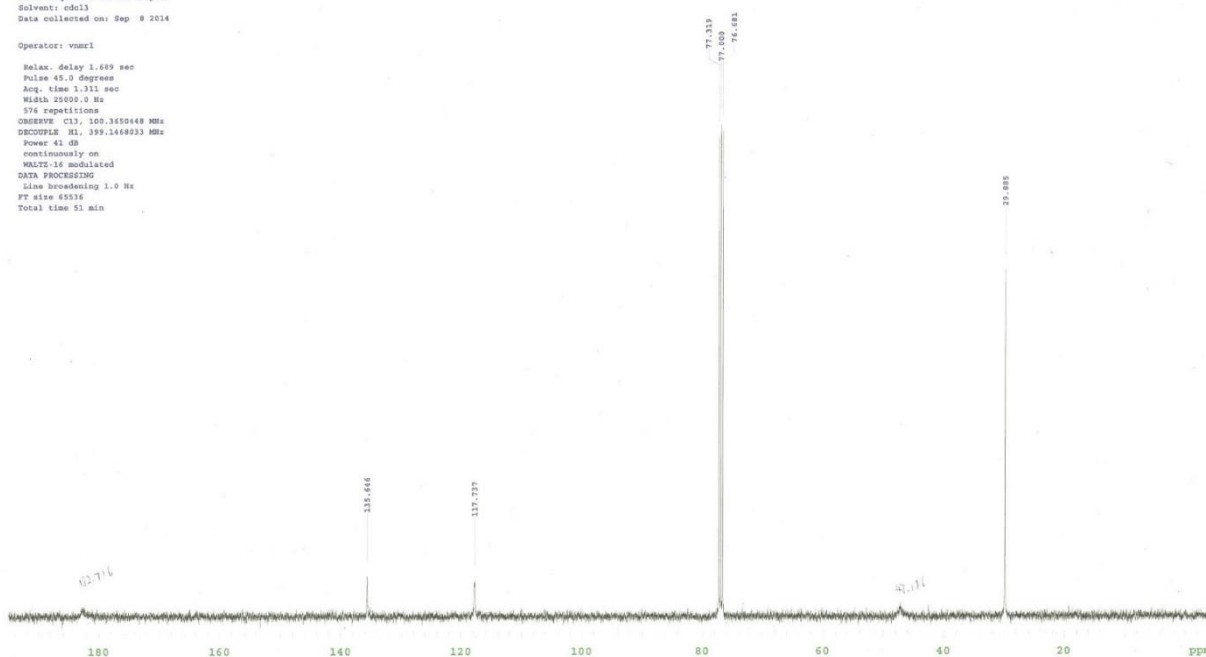
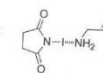
保持時間	面積	面積%	高さ	高さ%
11.080	8909733	1.269	353895	5.008
13.320	692966969	98.731	6712937	94.992



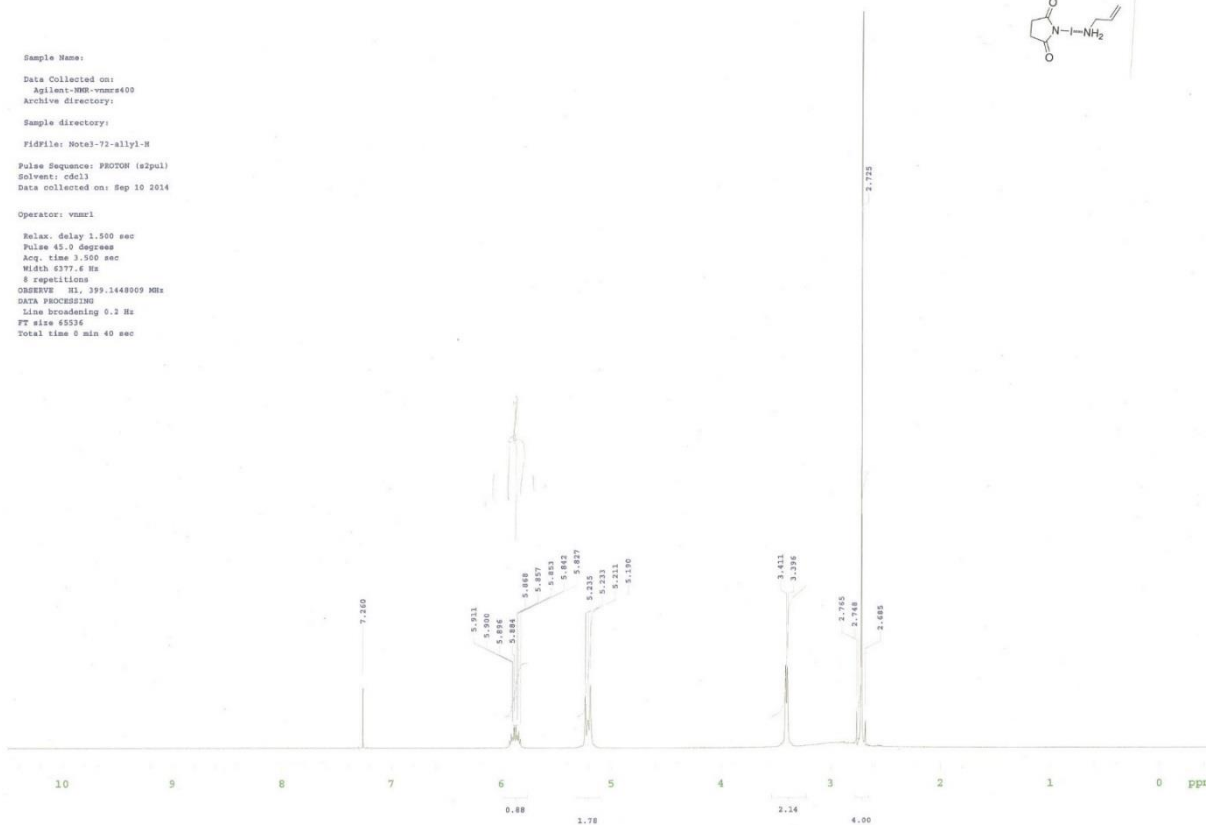
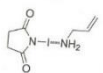
C:\Users\tohoku univ\Desktop\Li-dicyano\LiJing-dicyano-IA-



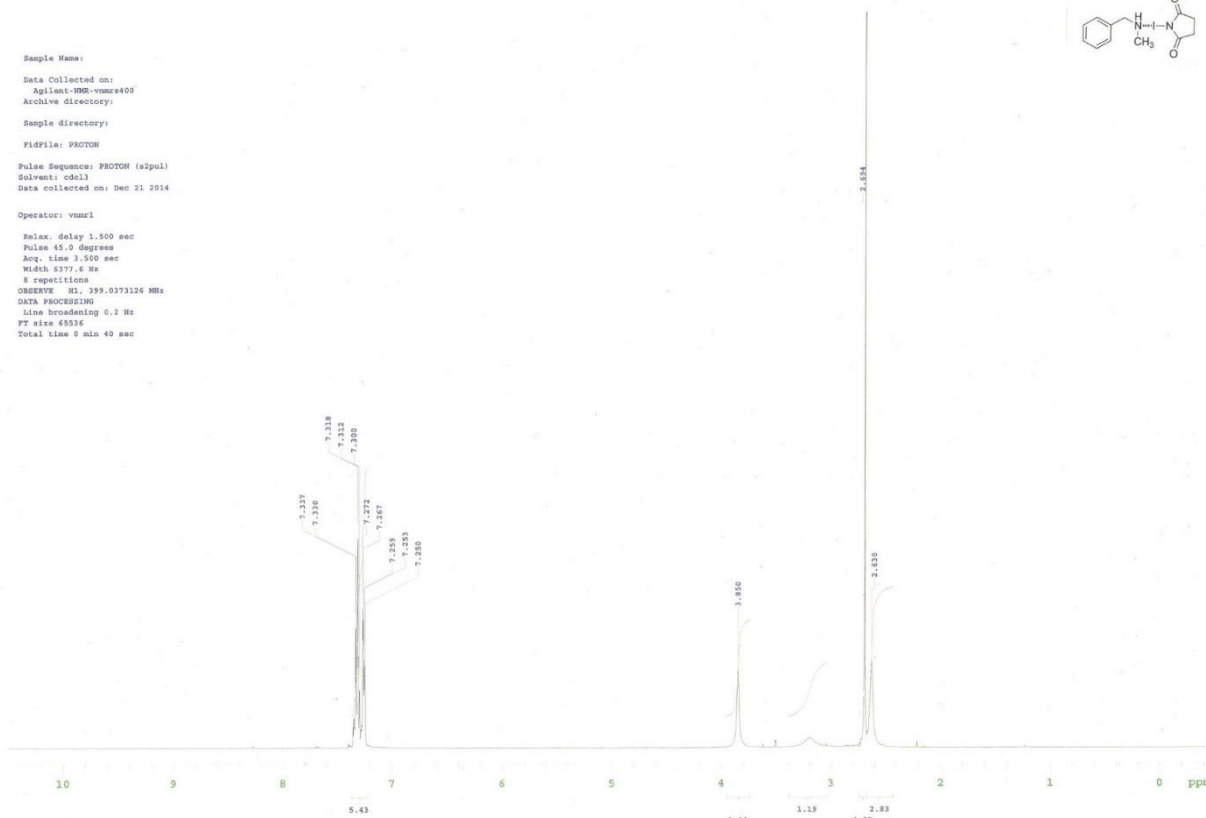
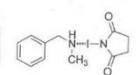
Sample Name:
 Data Collected on:
 Agilent-WMR-vnmr400
 Archive directory:
 Sample directory:
 FIDFile: Notal-72-13C
 Pulse Sequence: CARBON (s2pul)
 Solvent: cdcl3
 Data collected on: Sep 8 2014
 Operator: vnmr1
 Relax: delay 1.669 sec
 Pulse 45.0 degrees
 Acq. time 1.311 sec
 Width 25000.0 Hz
 574 repetitions
 OBSERVE C13, 100.3650468 MHz
 DECOUPLE H1, 399.1468033 MHz
 Power 41 dB
 continuously on
 WALTZ-16 modulated
 DATA PROCESSING
 Line broadening 1.0 Hz
 FT size 65536
 Total time 51 min



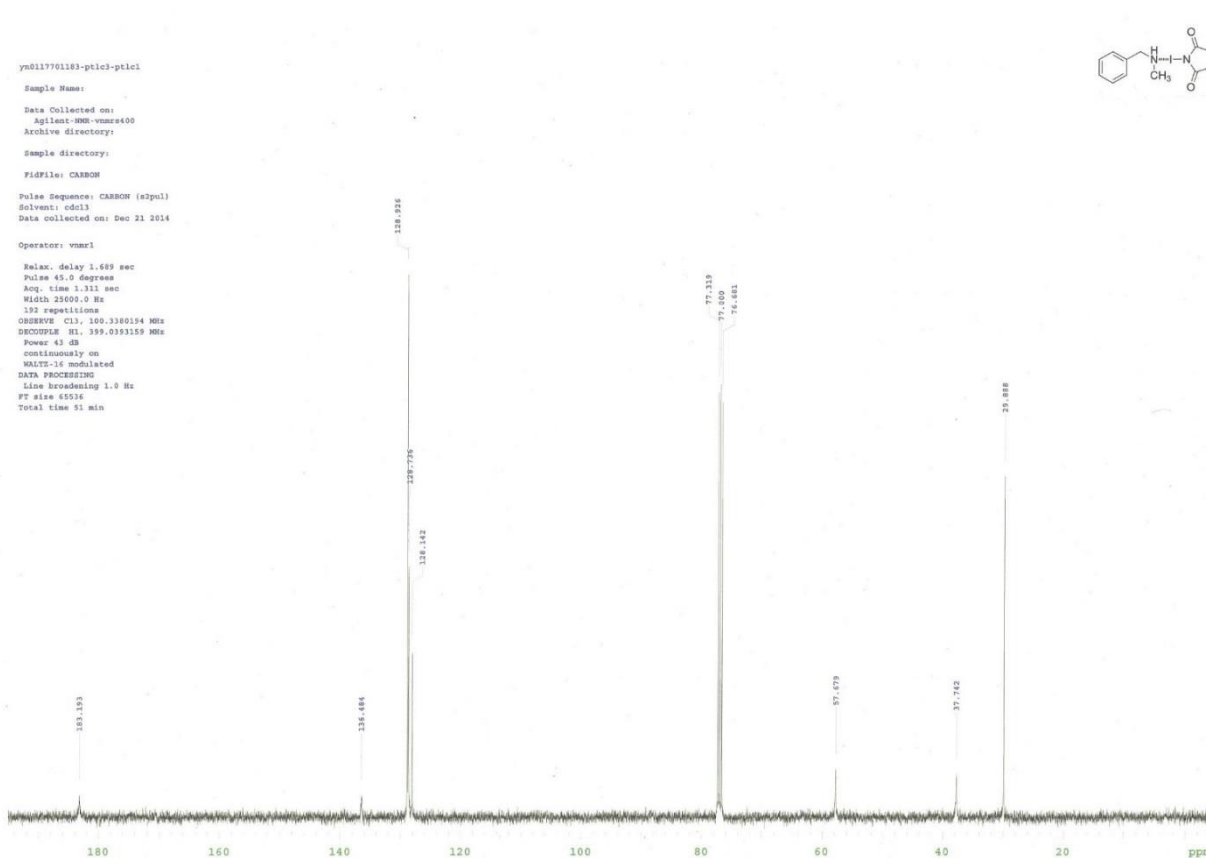
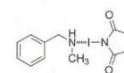
Sample Name:
 Data Collected on:
 Agilent-WMR-vnmr400
 Archive directory:
 Sample directory:
 FIDFile: Notal-72-allyl-H
 Pulse Sequence: PROTON (s2pul)
 Solvent: cdcl3
 Data collected on: Sep 10 2014
 Operator: vnmr1
 Relax: delay 1.500 sec
 Pulse 45.0 degrees
 Acq. time 3.500 sec
 Width 6177.6 Hz
 8 repetitions
 OBSERVE H1, 399.1448009 MHz
 DATA PROCESSING
 Line broadening 0.2 Hz
 FT size 65536
 Total time 8 min 40 sec



Sample Name:
 Data Collected on:
 Agilent-900-vnmr400
 Archive directory:
 Sample directory:
 FIDFile: PROTON
 Pulse Sequence: PROTON (a2pul)
 Solvent: cdcl3
 Data collected on: Dec 21 2014
 Operator: vnmr1
 Relax. delay 1.500 sec
 Pulse 45.0 degrees
 Acq. time 3.500 sec
 Width 6377.6 Hz
 8 repetitions
 OBSERVE H1, 399.0773126 MHz
 DATA PROCESSING
 Line broadening 0.2 Hz
 FT size 65536
 Total time 8 min 40 sec



yz0117701183-ptlc3-ptlc1
 Sample Name:
 Data Collected on:
 Agilent-900-vnmr400
 Archive directory:
 Sample directory:
 FIDFile: CARBON
 Pulse Sequence: CARBON (a2pul)
 Solvent: cdcl3
 Data collected on: Dec 21 2014
 Operator: vnmr1
 Relax. delay 1.689 sec
 Pulse 45.0 degrees
 Acq. time 1.311 sec
 Width 25600.0 Hz
 192 repetitions
 OBSERVE C13, 100.3380194 MHz
 DECOUPLE H1, 399.0593159 MHz
 Power 43 dB
 continuously on
 WALTZ-16 modulated
 DATA PROCESSING
 Line broadening 1.0 Hz
 FT size 65536
 Total time 51 min



2-068
2cl-dh-1/6.6-pured

Sample Name:

Data Collected on:
Agilent-WNM-vnmr400
Archive directory:

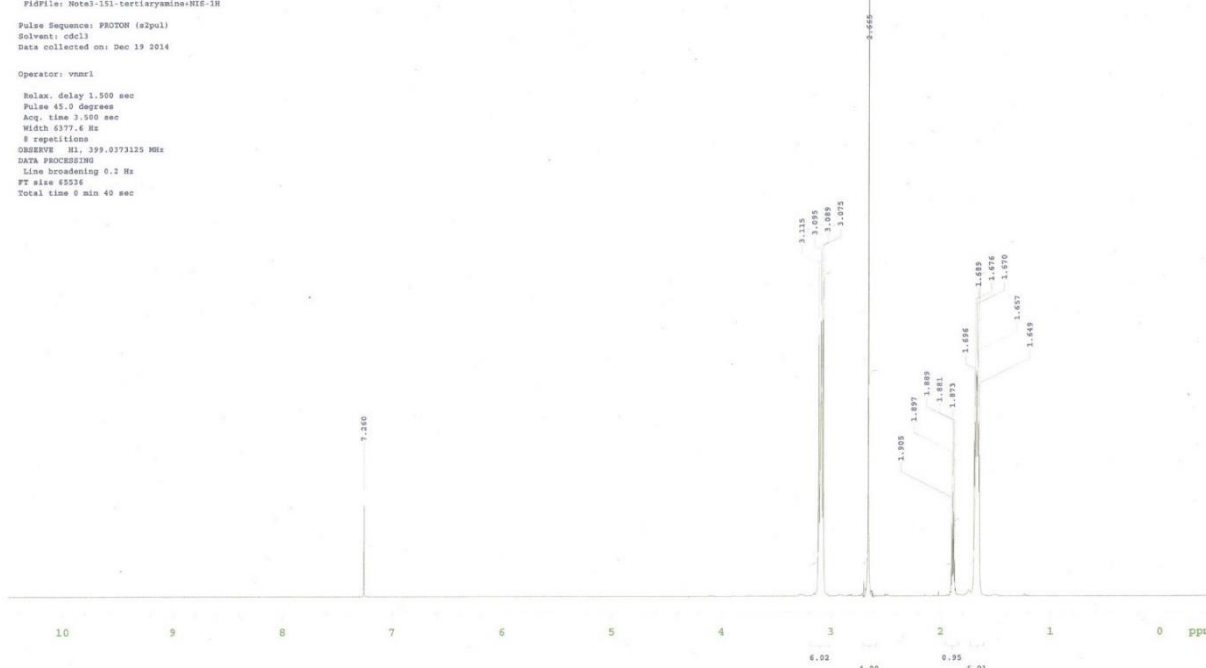
Sample directory:

FidFile: Note3-151-tertiaryamine-NIS-1H

Pulse Sequence: PROTON (s2pul)
Solvent: cdcl3
Data collected on: Dec 19 2014

Operator: vnmr1

Relax. delay 1.500 sec
Pulse 45.0 degrees
Acq. time 3.000 sec
Width 6177.6 Hz
8 repetitions
OBSERVE H1, 399.0173125 MHz
DATA PROCESSING
Line broadening 0.2 Hz
FT size 65536
Total time 9 min 40 sec



2-068
2cl-dh-1/6.6-pured

Sample Name:

Data Collected on:
Agilent-WNM-vnmr400
Archive directory:

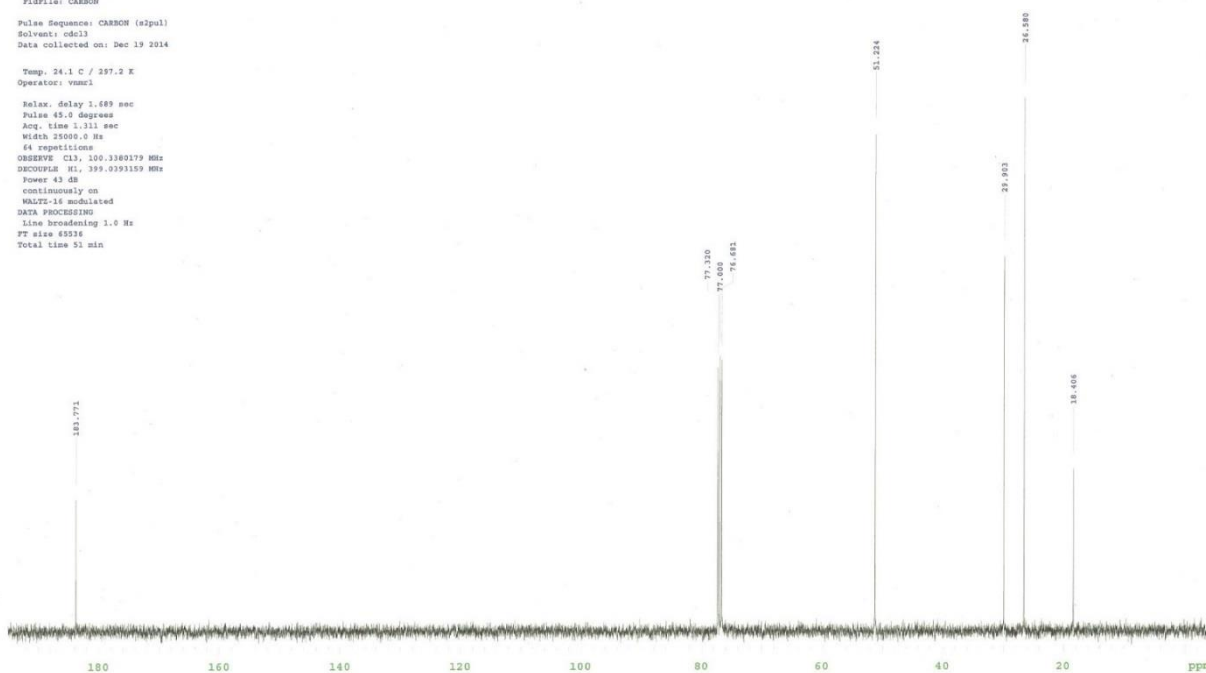
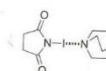
Sample directory:

FidFile: CARBON

Pulse Sequence: CARBON (s2pul)
Solvent: cdcl3
Data collected on: Dec 19 2014

Temp. 24.1 C / 297.2 K
Operator: vnmr1

Relax. delay 1.689 sec
Pulse 45.0 degrees
Acq. time 1.311 sec
Width 25000.0 Hz
64 repetitions
OBSERVE C13, 100.3180179 MHz
DECOUPLE H1, 399.0193159 MHz
Power 43 dB
continuously on
WALTZ-16 modulated
DATA PROCESSING
Line broadening 1.0 Hz
FT size 65536
Total time 51 min



2-068
2cl-0b-1/6.6-pured

Sample Name:

Data Collected on:
Agilent-NMR-vnmr400
Archive directory:

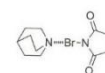
Sample directory:

FidFile: Note3-151-tertiaryamine+MB5-1M

Pulse Sequence: PROTON (a2pul)
Solvent: cdcl3
Data collected on: Dec 19 2014

Operator: vnmr1

Relax. delay 1.500 sec
Pulse 45.0 degrees
Acq. time 1.550 sec
Width 6377.6 Hz
8 repetitions
OBSERVE H1, 399.0373124 MHz
DATA PROCESSING
Line broadening 0.2 Hz
FT size 65516
Total time 8 min 40 sec



2-068
2cl-0b-1/6.6-pured

Sample Name:

Data Collected on:
Agilent-NMR-vnmr400
Archive directory:

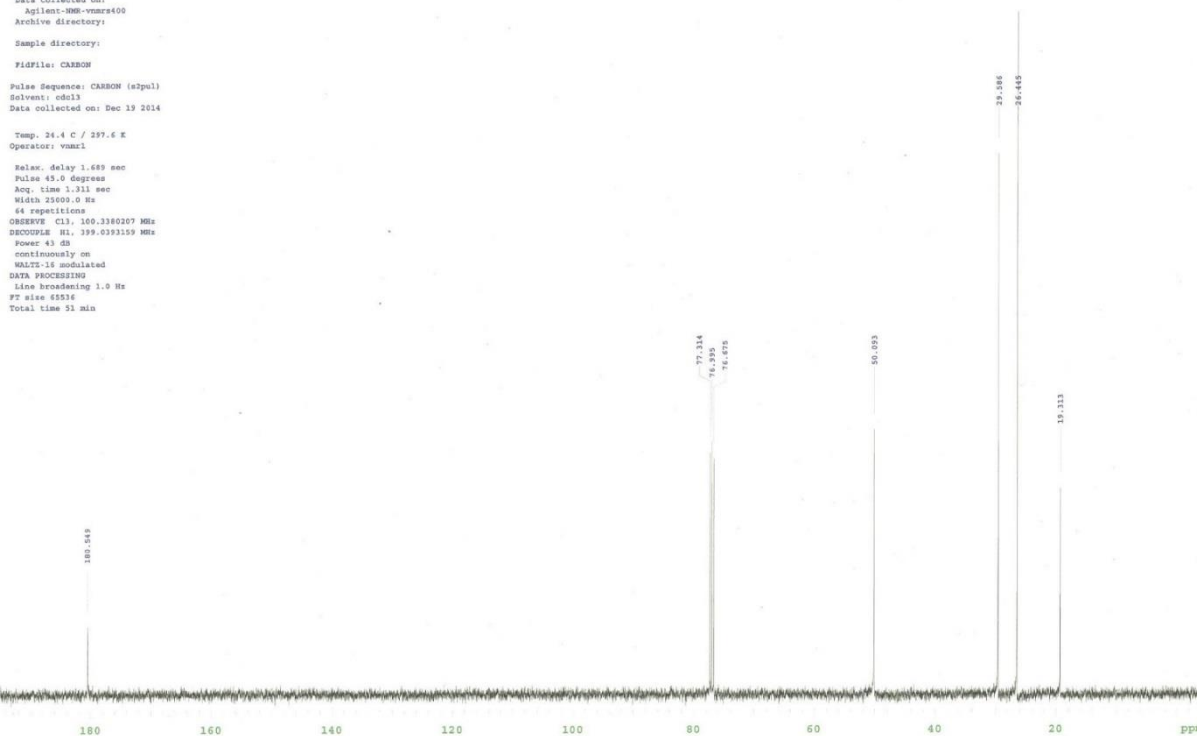
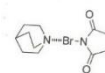
Sample directory:

FidFile: CARBON

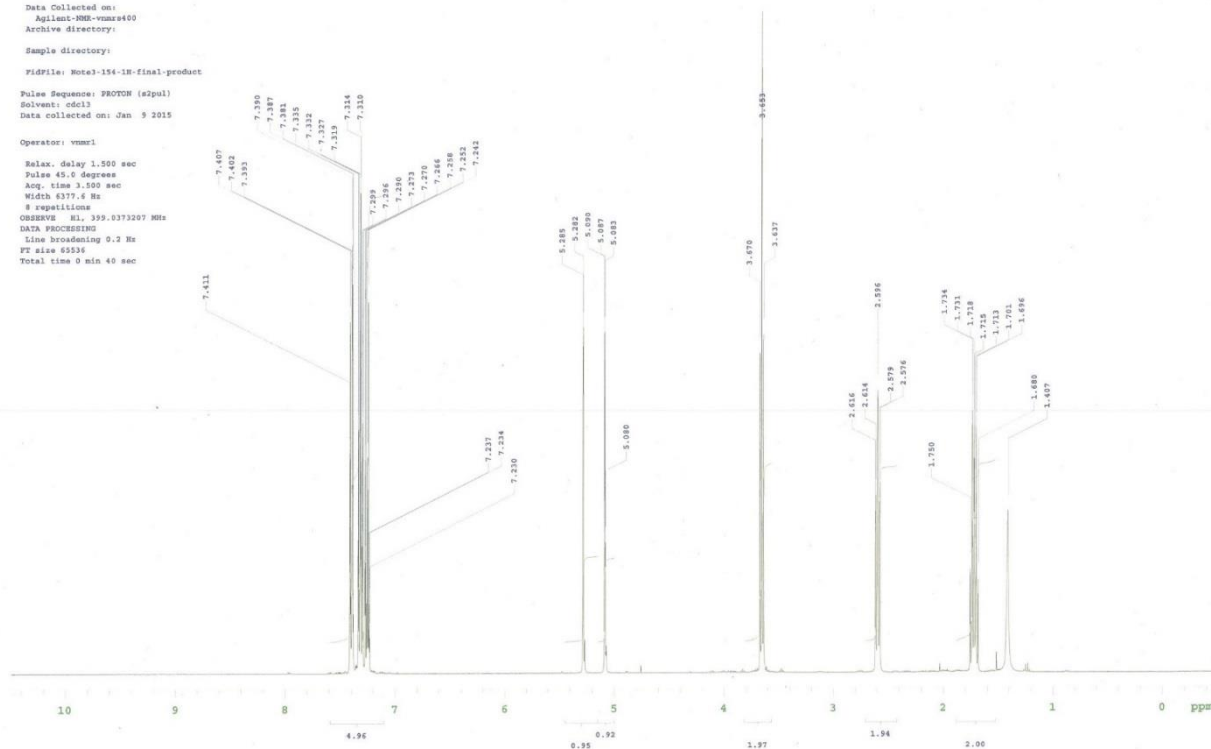
Pulse Sequence: CARBON (a2pul)
Solvent: cdcl3
Data collected on: Dec 19 2014

Temp. 24.4 C / 297.6 K
Operator: vnmr1

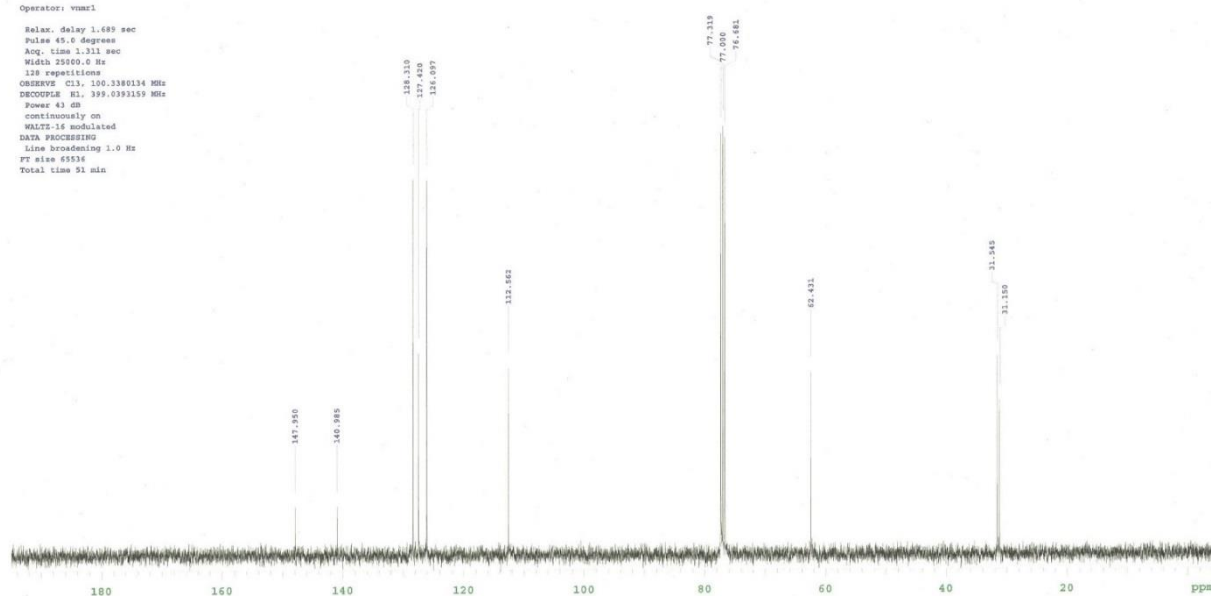
Relax. delay 1.689 sec
Pulse 45.0 degrees
Acq. time 1.311 sec
Width 21009.0 Hz
64 repetitions
OBSERVE C13, 100.3380207 MHz
DECOUPLE H1, 399.0393159 MHz
Power 45 dB
continuously on
WALTZ-16 modulated
DATA PROCESSING
Line broadening 1.0 Hz
FT size 65516
Total time 51 min



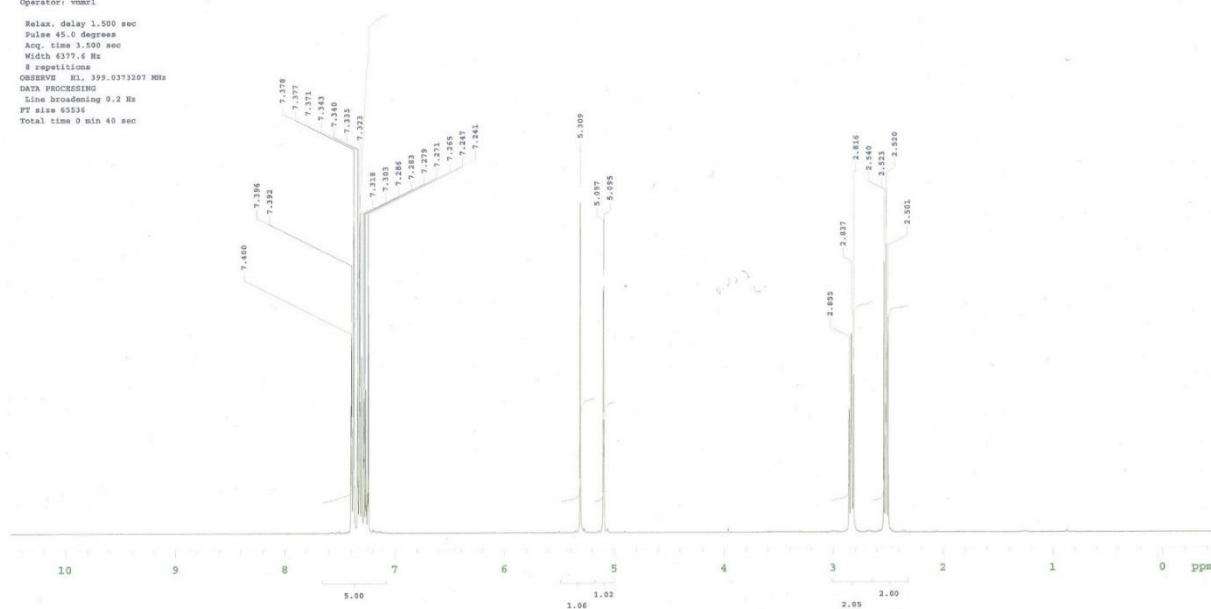
Sample Name:
Data Collected on:
Agilent-MMR-vnmr400
Archive directory:
Sample directory:
FidFile: M063-154-1H-final-product
Pulse Sequence: PROTON (s2pul)
Solvent: cdcl3
Data collected on: Jan 9 2015
Operator: vnmr1
Relax. delay 1.500 sec
Pulse 45.0 degrees
Acq. time 1.500 sec
Width 6377.6 Hz
8 repetitions
OBSERVE H1, 399.0373207 MHz
DATA PROCESSING
Line broadening 0.2 Hz
FT size 65536
Total time 0 min 40 sec



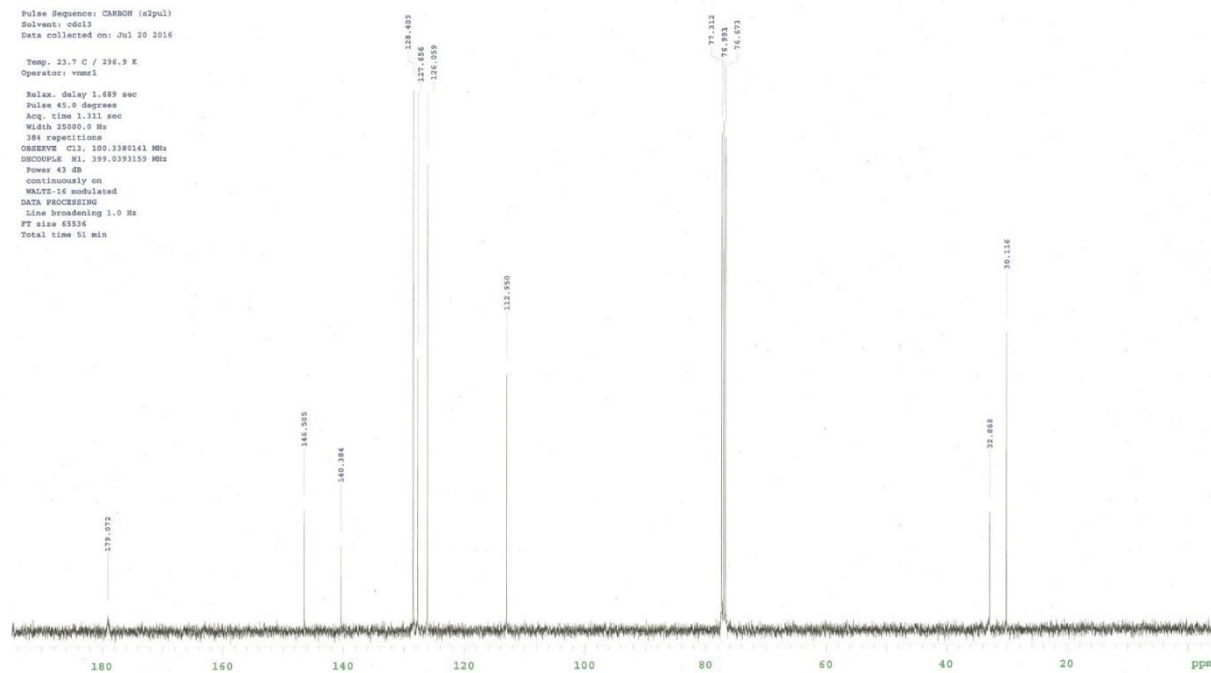
amber-unko
bluecap
Me7
Sample Name:
Data Collected on:
Agilent-MMR-vnmr400
Archive directory:
Sample directory:
FidFile: M063-154-1H-final-product-13C
Pulse Sequence: CARBON (s2pul)
Solvent: cdcl3
Data collected on: Jan 9 2015
Operator: vnmr1
Relax. delay 1.689 sec
Pulse 45.0 degrees
Acq. time 1.311 sec
Width 25000.0 Hz
128 repetitions
OBSERVE C13, 100.6300134 MHz
DECOUPLE H1, 399.0393159 MHz
Power 43 dB
continuously on
WALTZ-16 modulated
DATA PROCESSING
Line broadening 1.0 Hz
FT size 65536
Total time 51 min



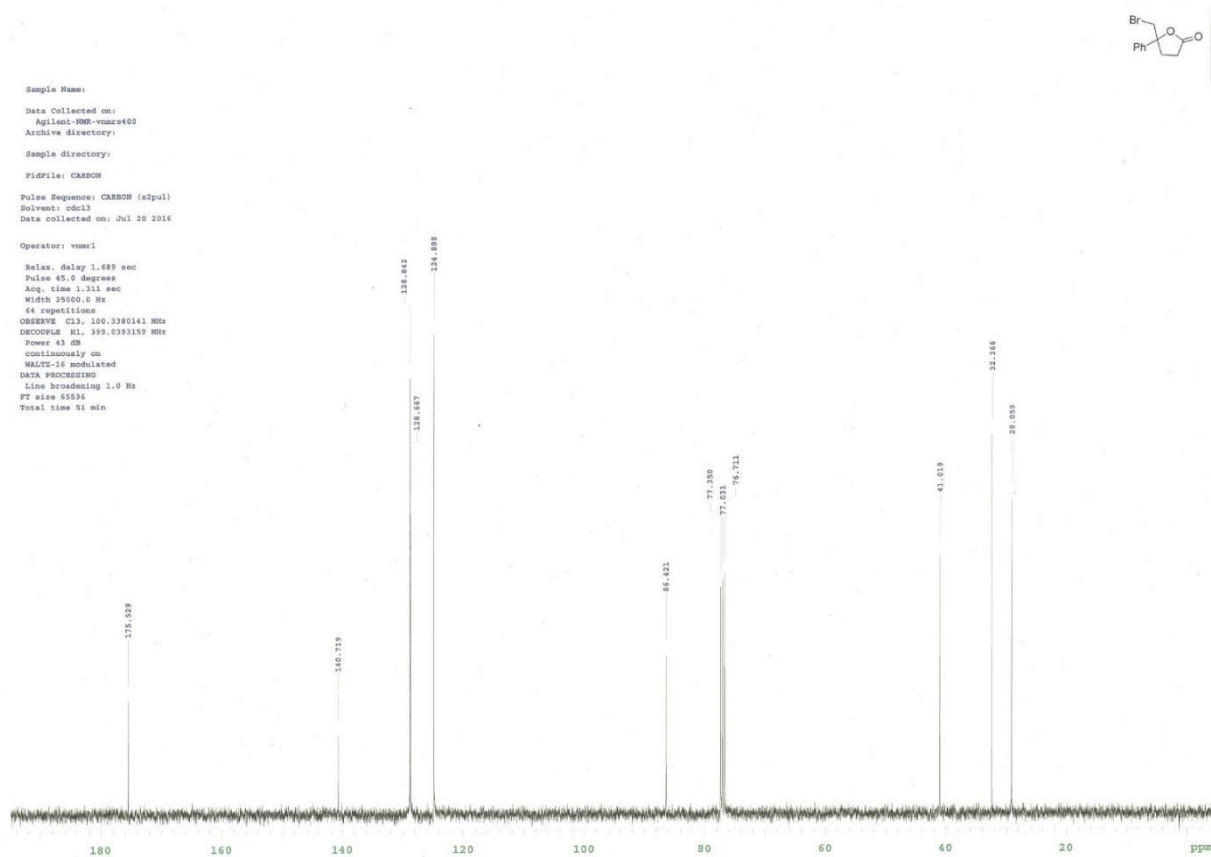
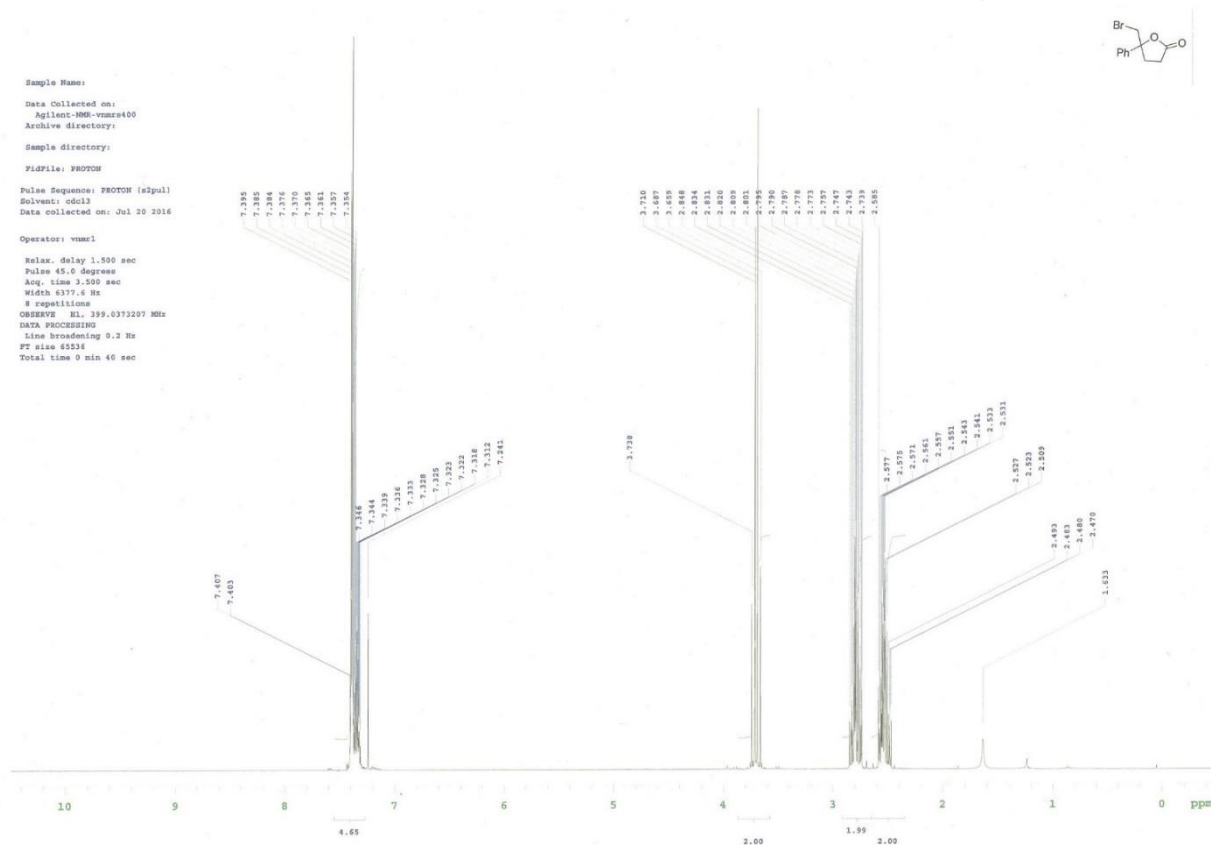
Sample Name:
 Data Collected on:
 Agilent-900-vnmr400
 Archive directory:
 Sample directory:
 FIDFile: PROTON
 Pulse Sequence: PROTON (s2pul)
 Solvent: cdcl3
 Data collected on: Jul 19 2016
 Operator: vnmr1
 Relax. delay 1.500 sec
 Pulse 45.0 degrees
 Acq. time 1.500 sec
 Width 6377.6 Hz
 8 repetitions
 OBSERVE H1, 399.0373207 MHz
 DATA PROCESSING
 Line broadening 0.2 Hz
 FT size 65536
 Total time 0 min 40 sec

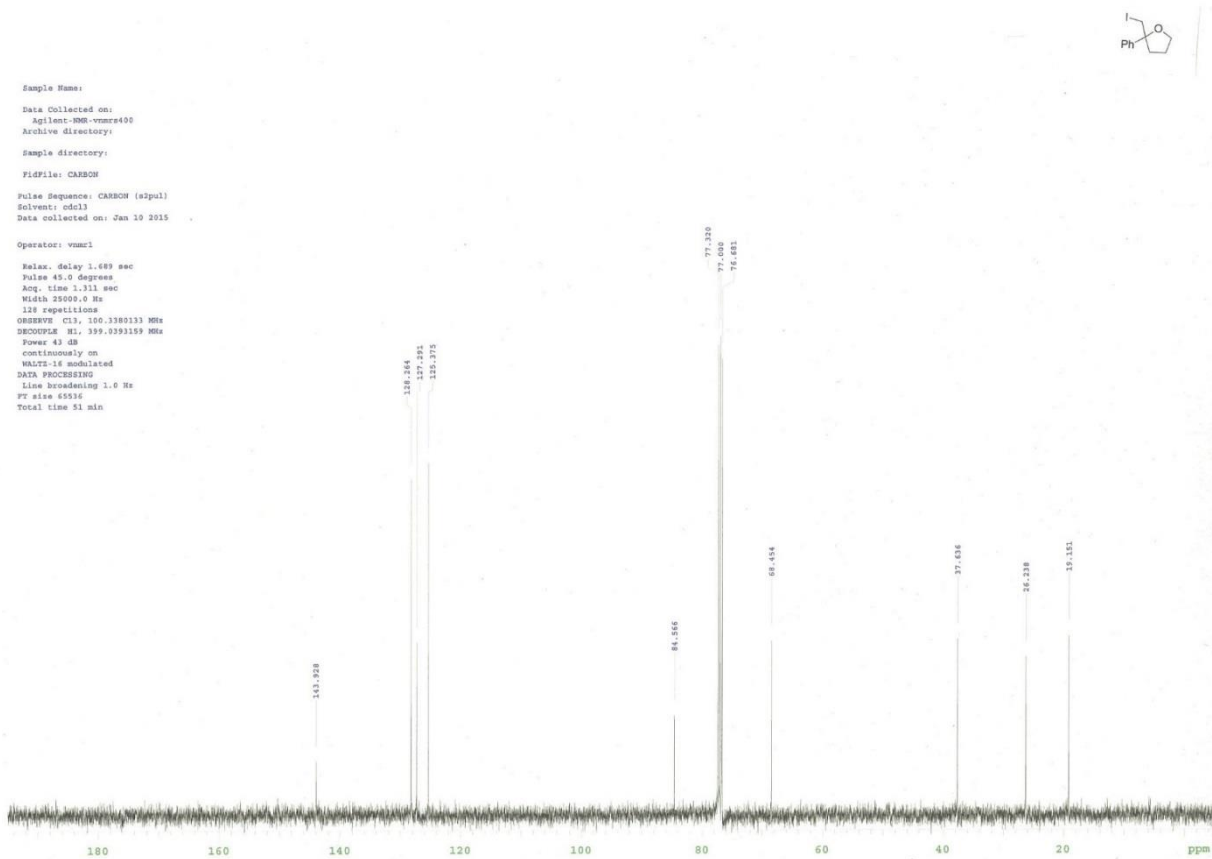
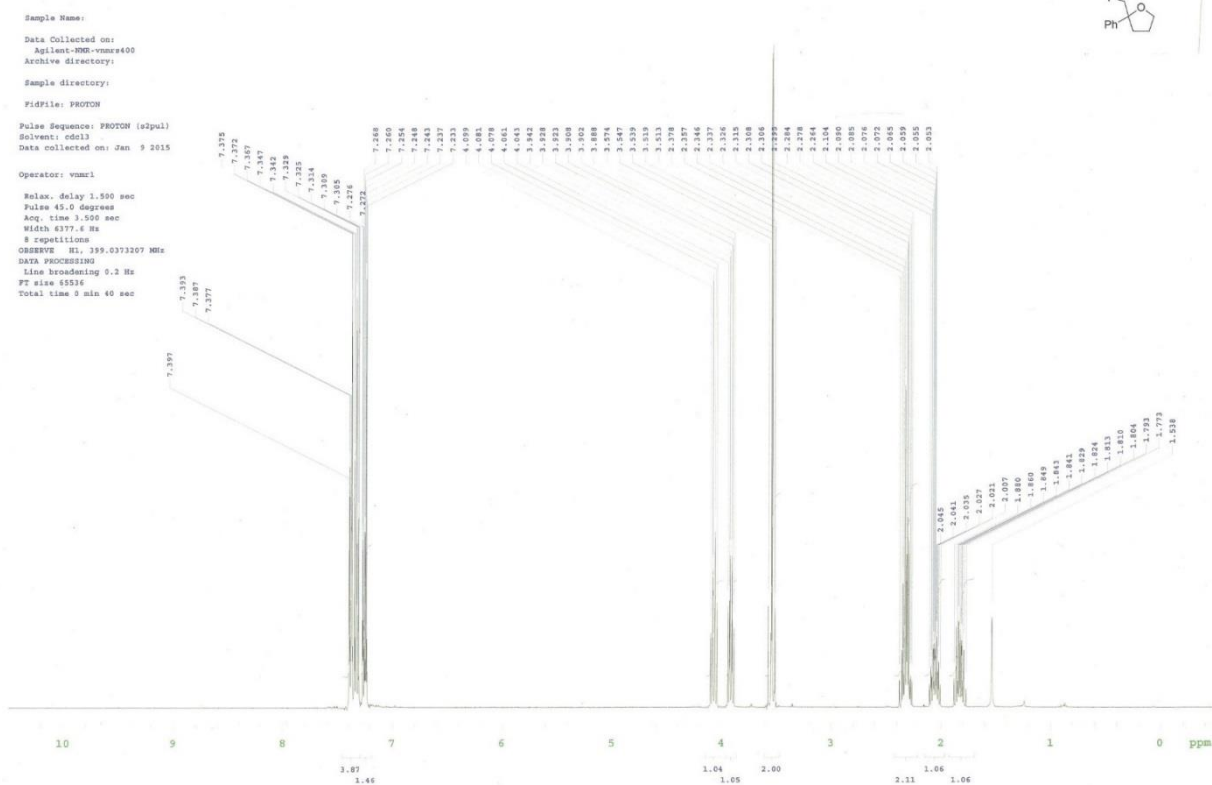


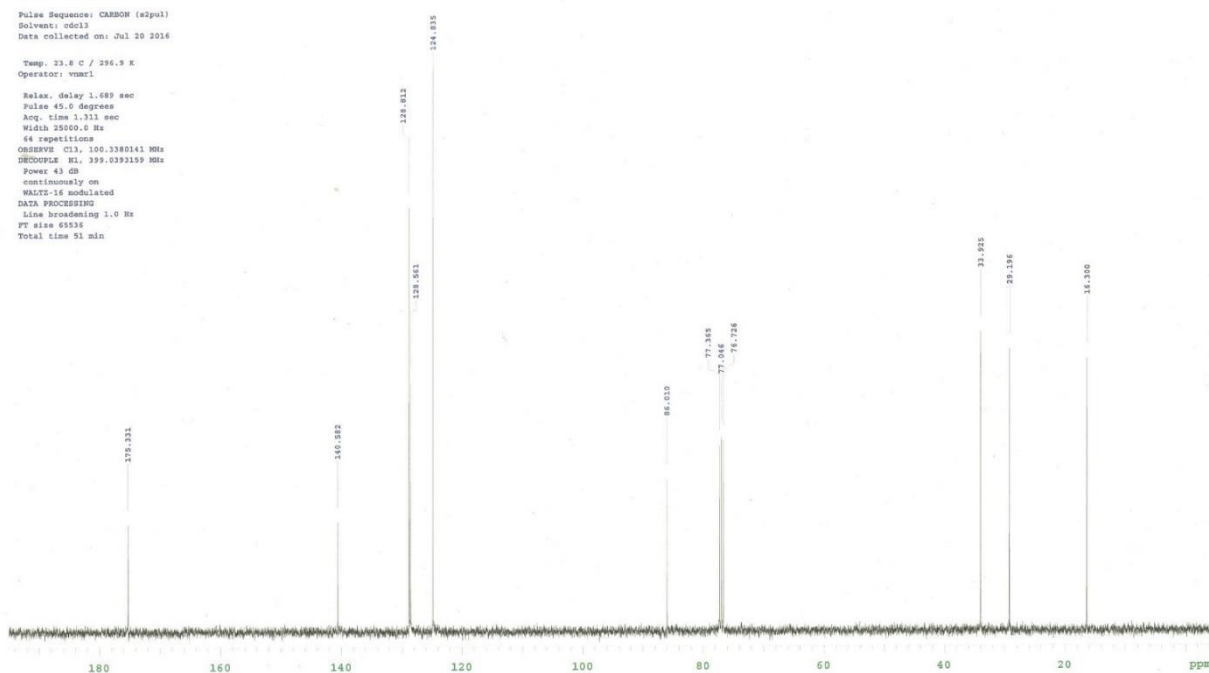
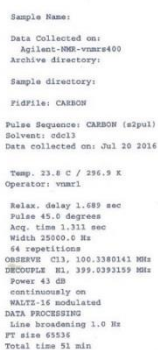
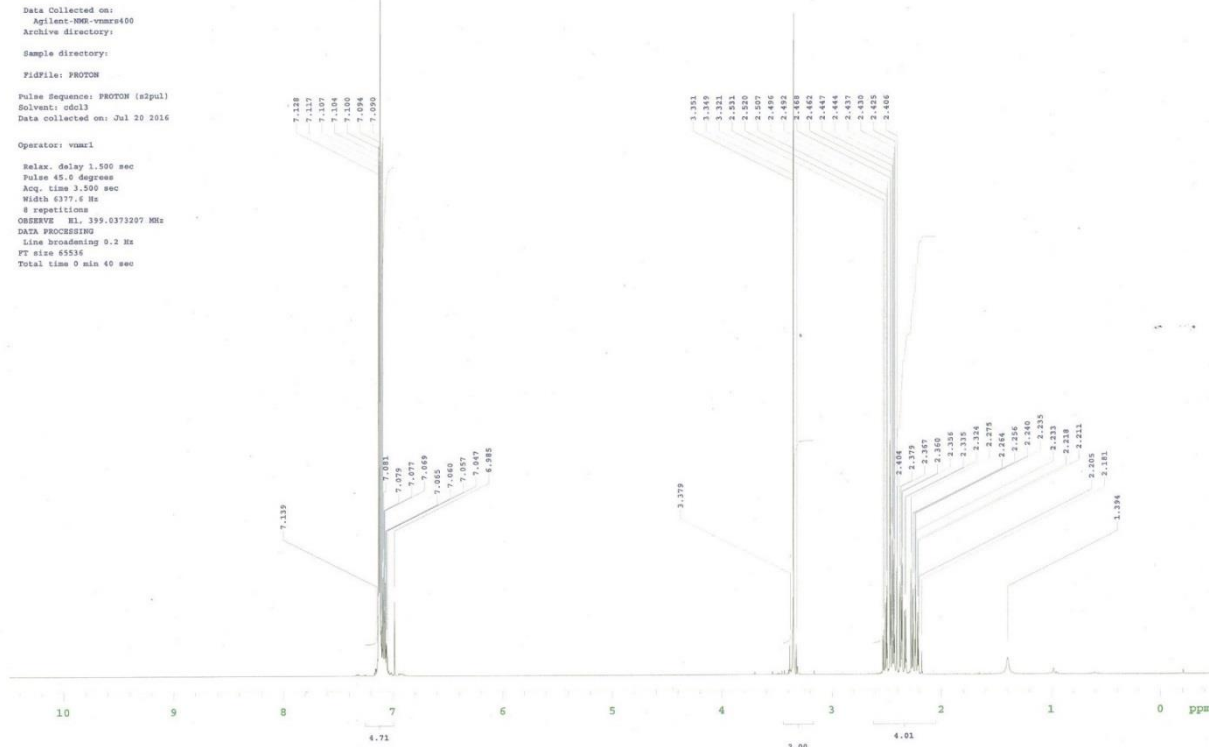
Sample Name:
 Data Collected on:
 Agilent-900-vnmr400
 Archive directory:
 Sample directory:
 FIDFile: CARBON
 Pulse Sequence: CARBON (s2pul)
 Solvent: cdcl3
 Data collected on: Jul 20 2016
 Temp. 23.7 C / 236.9 K
 Operator: vnmr1
 Relax. delay 1.689 sec
 Pulse 45.0 degrees
 Acq. time 1.311 sec
 Width 25900.0 Hz
 384 repetitions
 OBSERVE C13, 100.3382141 MHz
 DECOUPLE H1, 399.0393159 MHz
 Power 43 dB
 continuously on
 WALTZ-16 modulated
 DATA PROCESSING
 Line broadening 1.0 Hz
 FT size 65536
 Total time 51 min











Oxidative Amidation of Nitroalkanes with Amine Nucleophiles using Molecular Oxygen and Iodine

Jing Li, Martin J. Lear, Yuya Kawamoto, Shigenobu Umemiya, Alice R. Wong, Eunsang Kwon, Itaru Sato, and Yujiro Hayashi*

Abstract: The formation of amides and peptides often necessitates powerful yet mild reagent systems. The reagents used, however, are often expensive and highly elaborate. New atom-economical and practical methods that achieve such goals are highly desirable. Ideally, the methods should start with substrates that are readily available in both chiral and non-chiral forms and utilize cheap reagents that are compatible with a wide variety of functional groups, steric encumbrance, and epimerizable stereocenters. A direct oxidative method was developed to form amide and peptide bonds between amines and primary nitroalkanes simply by using I_2 and K_2CO_3 under O_2 . Contrary to expectations, a 1:1 halogen-bonded complex forms between the iodonium source and the amine, which reacts with nitronates to form α -iodo nitroalkanes as precursors to the amides.

Traditional peptide and amide synthesis involves the electrophilic derivatization and activation of a carboxylic acid into an amine-selective acylating species (Eq. (1), Figure 1; Lg = leaving group).^[1,2] There are, however, a few atypical cases of forming reactive *N*-acylating species in an oxidative manner from alcohols, aldehydes, and alkyne precursors.^[3,4] Notably, pre-synthesized α -bromo substituted nitroalkanes have been oxidized with *N*-iodosuccinimide (NIS) and molecular oxygen in the presence of amines.^[5–7] To account for the apparent umpolung in reactivity of the amine components, the intermediacy of electrophilic *N*-iodo amines and tetrahedral α -amino, α -bromo nitroalkanes were suggested.^[5,6] From a synthetic point of view, however, methods to achieve direct asymmetric access to α -bromo

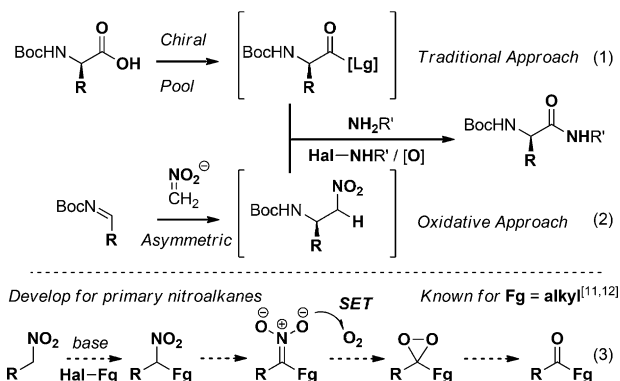


Figure 1. Traditional versus oxidative approaches to amide formation.

nitroalkanes are relatively limited in substrate scope.^[7,8] In comparison, there are a wide variety of catalytic asymmetric methods that adopt nitromethane as a simple, cheap pro-nucleophile to add to both alkyl and aryl aldehydes, imines, enals, enones, and so forth.^[9,10] Herein, our interest was to exploit these readily available primary nitroalkane substrates (Eqs. (2) and (3)) and develop a direct oxidative method to form amide and peptide bonds in a most economical and practical manner.

Our inspiration for this study started after our 2013 total synthesis of prostaglandin A_1 and E_1 methyl esters.^[11] Specifically, we discovered the base-promoted Nef conversion of a key nitroalkene into an enone product under aerobic conditions. In 2014, we extended this oxidative transformation to a wide range of nitroalkenes and nitroalkanes to produce enones and ketones, respectively (Eq. (3); Fg = alkyl).^[12] Mechanistic insights were gained from ^{18}O -labeling, nitrite/nitrate ion analysis, intramolecular thioether trapping, and radical clock experiments. In short, the formation of ketones from secondary α -alkylated nitroalkanes was shown to be consistent with a single-electron transfer (SET) mechanism from a charged *aci*-nitronate electron donor to a triplet dioxygen molecule to afford an eventual dioxirane adduct after expelling a nitrite anion. The dioxirane subsequently acts as an electrophilic source of mono-oxygen^[13] that can be captured by another nitronate anion in the surrounding basic medium.

On the basis of these recent mechanistic findings,^[12] we reasoned that secondary α -amino nitroalkanes could be formed in situ by reacting primary nitronates with electrophilic *N*-halo amines (Eq. (3); Hal = halogen, Fg = amine). These would be similarly oxidized with oxygen to afford peroxy adducts bearing amine groups and eventually trans-

[*] J. Li, Prof. Dr. M. J. Lear,^[†] Y. Kawamoto, Dr. S. Umemiya, A. R. Wong, Prof. Dr. I. Sato,^[††] Prof. Dr. Y. Hayashi
Department of Chemistry,
Graduate School of Science,
Tohoku University
6-3 Aramaki-Aza, Aoba-ku, Sendai 980-8578 (Japan)
E-mail: yhayashi@m.tohoku.ac.jp
Homepage: <http://www.ykbsc.chem.tohoku.ac.jp>
Prof. Dr. E. Kwon
Research and Analytical Center for Giant Molecules,
Graduate School of Science,
Tohoku University
Sendai 980-8578 (Japan)

[†] Present address: School of Chemistry, University of Lincoln
Brayford Pool, Lincoln LN6 7TS (UK)

[††] Present address: Faculty of Science, Ibaraki University
Ibaraki 310-8512 (Japan)

Supporting information for this article is available on the WWW
under <http://dx.doi.org/10.1002/anie.201505192>.

form into amides. At this juncture, among other mechanistic concerns, it was not certain whether the formation and reaction of *N*-iodo amines could be achieved in situ and thereby generate the requisite α -amino nitroalkane intermediates. This premise was, however, given credence by the suggestion of *N*-iodo amine and α -amino nitroalkane intermediates being reported in a series of oxidative umpolung amide synthesis (UmAS) studies.^[5–7] Herein, during the course of developing an atom-economical, direct amidation procedure of readily prepared chiral nitroalkanes,^[9,10] we describe our independent findings and ultimately propose new mechanistic aspects that have general implications both in amine/halogen-based chemistry and in UmAS chemistry.

Despite some mechanistic concerns regarding the amine component and the oxidative steps (Eq. (3)), we first elected to pursue the base-promoted oxidative coupling of the racemic nitroalkane **1**^[9] with the hydrochloride salt of (*S*)-phenylalanine methyl ester **2** and NIS in acetonitrile (Table 1). Thus, the resultant 1:1 diastereomeric mixture of the dipeptide **3** could be checked for its stereochemical integrity by NMR and HPLC analysis. In the first instance, the base was varied (entries 1–7). This quickly demonstrated K₂CO₃ (entry 4) to be superior to weaker bases such as NaOAc, which gave the α -iodo nitroalkane **4** (entry 1). Stronger bases, such as Cs₂CO₃ and K₃PO₄, gave slightly

lower yields of the dipeptide product **3** (entries 5 and 6). Soluble bases such as DBU were also found inferior to K₂CO₃ (cf. entries 4 and 7), but both conditions resulted in significant amounts of the carboxylic acid **5** (30–50% yields). The use of less electrophilic *N*-halosuccinamides did not improve the result (entries 8 and 9), and the α,α -dichloro nitroalkane **6** (X = Cl) was isolated in one case (entry 9). A change in the solvent system with NIS and adopting two equivalents of the free amine of **2** proved more successful (entries 10 to 15). In particular, the use of molecular I₂ or NIS at room temperature afforded optimal yields of dipeptide **3** (67%; entry 15). Generation of the carboxylic side-product **5** could not be avoided even under strictly anhydrous conditions.

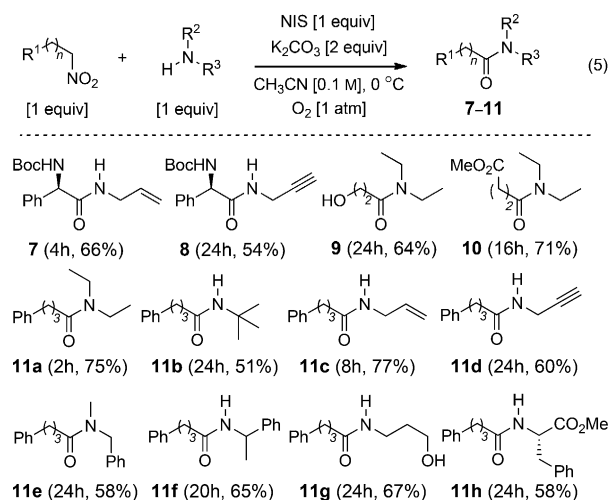
Next, we investigated the scope of the oxidative amidation method with the use of NIS (Scheme 1) and I₂ (Scheme 2). The optimal solvent for primary and secondary alkyl amines was determined to be acetonitrile (Eq. (5)). Unsaturated functional groups, such as benzyl, allyl, and alkynyl groups, remained unreacted, and the amidation method also tolerated unprotected hydroxy groups (**9**, **11g**). Extension of the method to amino acid esters with (*R*)-1^[14] was optimally performed with I₂ in 1:1 THF/toluene (Eq. (6)). Importantly, the dipeptide products (**3**, **12**) were produced with complete stereochemical integrity. No epimerization of potentially labile α -stereocenters was observed (Supporting Information). The same tolerances were found for readily prepared, chiral nitroalkyl Michael adducts^[15] (**13**→**14**, Eq. (7)) and standard protecting groups (for example, *O*-*t*Bu, *N*-Tr, *N*-Cbz, *N*-Boc; Tr = trityl = triphenylmethyl, Cbz = benzyloxycarbonyl, Boc = *tert*-butoxycarbonyl) were also found to be compatible.

To evaluate whether our initial mechanistic idea was in keeping with prior studies,^[12] we began to explore the first α -amination step of our proposal (Eq. (3)). In short, all attempts to prepare, infer, or observe the anticipated *N*-iodo amines,^[5–7] were not confirmed in our hands. Instead, we interpret our NMR data to show that amines like allylamine and α -methyl benzyl amine form a complex readily with NIS and precipitate, and these precipitates behave chemically as sources of electrophilic iodine and nucleophilic amine. For

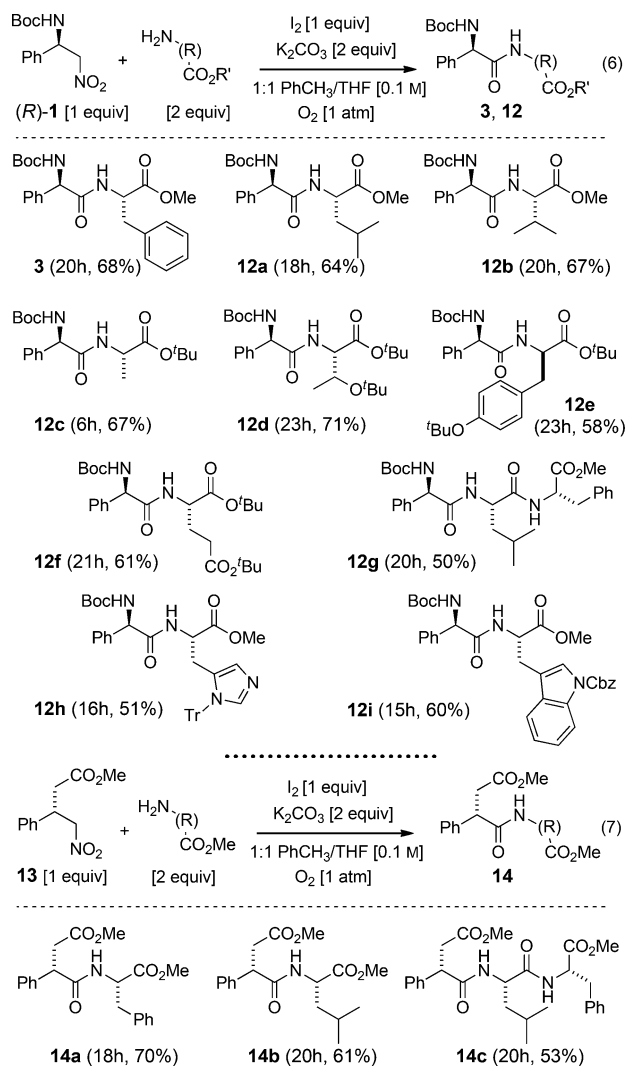
Table 1: Optimization of oxidative peptide formation.^[a]

Entry	Base	X ⁺	Solvent (t [h])	3	4	5
1	NaOAc	NIS	CH ₃ CN (5)	–	5	–
2	KOAc	NIS	CH ₃ CN (5)	20	–	–
3	Na ₂ CO ₃	NIS	CH ₃ CN (15)	5	–	–
4	K ₂ CO ₃	NIS	CH ₃ CN (3)	49	–	30
5	Cs ₂ CO ₃	NIS	CH ₃ CN (2)	30	–	–
6	K ₃ PO ₄	NIS	CH ₃ CN (3)	42	–	–
7	DBU	NIS	CH ₃ CN (12)	30	–	50
8	K ₂ CO ₃	NBS	CH ₃ CN (12)	20	–	–
9	K ₂ CO ₃	NCS	CH ₃ CN (12)	–	– ^[b]	–
10 ^[c]	K ₂ CO ₃	NIS	CH ₃ CN (2.5)	51	–	–
11 ^[c]	K ₂ CO ₃	NIS	THF (7.5)	51	–	–
12 ^[c]	K ₂ CO ₃	NIS	PhCH ₃ (48)	15	–	60
13 ^[c]	K ₂ CO ₃	NIS	DMSO (48)	15	–	30
14 ^[c,d]	K ₂ CO ₃	NIS	1:1 media (12)	59	–	30
15 ^[c,e]	K ₂ CO ₃	I ₂	1:1 media (4)	67	–	25

[a] Unless noted otherwise, all reactions were conducted with nitroalkane **1** [0.2 mmol], amine-HCl salt **2** [0.2 mmol], base [0.6 mmol], halonium (X⁺) source [0.2 mmol] at 0 °C in solvent [2 mL] under O₂ [1 atmosphere] and yields of isolated products (%) are given. [b] Dichlorinated nitroalkane **6** (X = Cl) was isolated in 10% yield. [c] For entries 10 to 15, two equivalents of the free amine **2** [0.4 mmol] and base [0.4 mmol] were used. [d] 1:1 toluene/THF mixture was used. [e] Reaction performed at room temperature with free amine **2** [0.4 mmol] and base [0.4 mmol]; a similar result was obtained with NIS [0.2 mmol] over 12 h.



Scheme 1. Oxidative amidation using NIS/O₂.



Scheme 2. Oxidative peptide formation using I_2/O_2 .

example, these 1:1 NIS/amine precipitates can be employed directly in our base-promoted nitroalkane amidation procedure with similar success (cf. Eq. (4)), and they also react with electrophilic Boc₂O to form standard NH-Boc amides slowly (Supporting Information). Eventually, we were able to obtain a single-crystal X-ray crystallographic structure for the allylamine/NIS complex **15** (Figure 2).

This evidence of a halogen bonded amine complex **15** and isolating an α -iodo nitroalkane **4** (Table 1, entry 1) clearly puts our proposed α -amination (Eq. (3), Fg = NHR) into question. Suspecting α -iodination was occurring first, and thus the mono-iodide **4** as an early intermediate, we first checked for its formation by reacting the *aci*-nitronate anion of **1** with **15** or NIS alone (Scheme 3). This being the case in

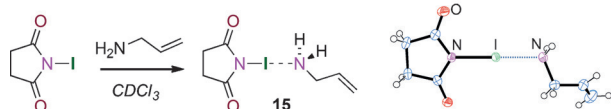
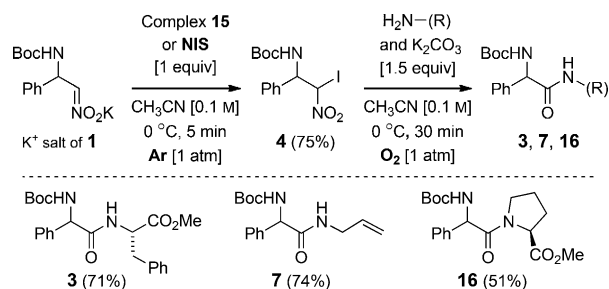


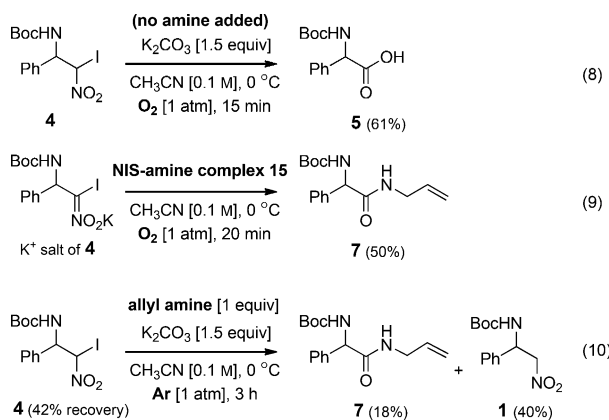
Figure 2. ORTEP X-ray crystal structure of 1:1 NIS-allylamine (**15**) with ellipsoids set at 30% probability level.



Scheme 3. Formation and oxidative amidation of α -iodo nitroalkane **4**.

75% yield, pre-prepared **4** was tested for its ability to form amides directly. Electrophilic halogen sources were omitted and **4** was reacted in the presence of K₂CO₃, O₂, and a slight excess of allylamine or phenylalanine methyl ester **2**. The anticipated amides were isolated in good yields at 0 °C within 30 min. The iodo nitroalkane **4** was even reactive enough to couple with the methyl ester of L-proline, a secondary amino ester often displaying unique reactivity, giving its respective dipeptide **16** in 51% yield.

Notably, we did not observe the intermediacy or isolate any α -amino nitroalkane product, as either we proposed in Equation (3)^[12] or as reported in umpolung amide synthesis (UmAS) studies.^[5–7] This was the case even by directly reacting pre-formed *N*-bromo amines (or **15**, see above) with the *aci*-nitronate of **1**; in fact, this generated the α -bromo analogue of **4** in good yields.^[16] Having confirmed the α -iodide **4** as the primary intermediate, two possible pathways to form the amide product **7** were considered; one pathway being where an oxygen molecule first reacts with **4** before the amine component, and in the other pathway the amine reacts with **4** first. Thus, the relative reactivities of the amine and oxygen components were investigated through a set of control experiments (Scheme 4). Here, we found the α -iodide **4** reacted readily with O₂ within 15–20 min, giving good yields of the oxidized products **5** or **7** (cf. Eq. (8) and (9)). In the absence of O₂, the amine reacts with **4** relatively slowly and inefficiently over 3 h (cf. Eq. (10)). These results support the



Scheme 4. Control experiments to discern relative reactivity of **4** to O₂ and amine components.

initial reaction of O₂ with **4**, as opposed to the α-iodide **4** first reacting with the amine component.^[17]

Collectively, our findings are consistent with the reaction sequence as illustrated in Figure 3. We thus propose an *aci*-nitronate anion, once formed under the basic conditions from

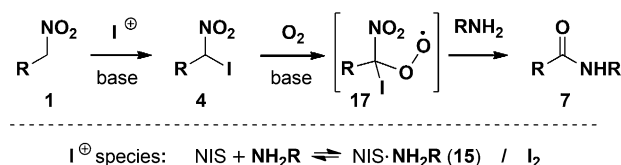


Figure 3. Proposed oxidative conversion of nitroalkanes **1** into amide products **7** by α-iodinated intermediates **4**.

the primary nitroalkane **1**, will first become α-iodinated with NIS from the halogen bonded amine complex **15** or I₂, to afford the mono-iodide **4**. From this intermediate onwards, several addition-elimination pathways, under either radical or ionic reaction modes, can be proposed to afford the amide product **7**.^[5–7] Among such possibilities, we currently favor the formation of a peroxy radical^[18] **17**, which can cyclize and expel a mono-iodine or nitrite radical to form a reactive dioxirane intermediate (cf. Eq. (3)).^[12] Further mechanistic evidence is being actively pursued in our group to provide a more complete and consistent picture of this non-trivial oxidative process.^[17,19]

In closing, several synthetic virtues of this oxidative amidation method are noteworthy (Schemes 1, 2, and 3). The method is straightforward in operation, chemoselective in functional group tolerance, and stereochemically robust to potentially epimerizable substrates and products. Importantly, a whole range of primary nitroalkane starting materials for our reaction method can be readily prepared in chiral form through a plethora of asymmetric methods.^[9,10,14,15] Further improvements and extension of the mechanistic rationales presented herein to construct more challenging amide bonds are ongoing in our laboratories.^[17,19] The implications of amine-complexed, halogen bonded, electrophilic iodine species to our understanding of amine-based, asymmetric catalytic events will be published in due course.^[20,21]

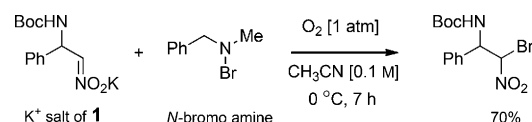
Acknowledgements

This work was supported by a Grant-in-Aid for Scientific Research on Innovative Areas “Advanced Molecular Transformations by Organocatalysts” from The Ministry of Education, Culture, Sports, Science and Technology, Japan, and the Multidimensional Materials Science Leaders Program (to M.J.L.).

Keywords: amidation · halogen bonding · iodination · peptide formation · umpolung

How to cite: *Angew. Chem. Int. Ed.* **2015**, *54*, 12986–12990
Angew. Chem. **2015**, *127*, 13178–13182

- [1] A. El-Faham, F. Albericio, *Chem. Rev.* **2011**, *111*, 6557–6602.
- [2] E. Valeur, M. Bradley, *Chem. Soc. Rev.* **2009**, *38*, 606–631.
- [3] V. R. Pattabiraman, J. W. Bode, *Nature* **2011**, *480*, 471–479.
- [4] Recent decarboxylative/oxidative amidations of α-ketoacids: a) J. Liu, Q. Liu, H. Yi, C. Qin, R. Bai, X. Qi, Y. Lan, A. Lei, *Angew. Chem. Int. Ed.* **2014**, *53*, 502–506; *Angew. Chem.* **2014**, *126*, 512–516; b) I. Pusterla, J. W. Bode, *Angew. Chem. Int. Ed.* **2012**, *51*, 513–516; *Angew. Chem.* **2012**, *124*, 528–531.
- [5] B. Shen, D. M. Makley, J. N. Johnston, *Nature* **2010**, *465*, 1027–1032.
- [6] J. P. Shackleford, B. Shen, J. N. Johnston, *Proc. Natl. Acad. Sci. USA* **2012**, *109*, 44–46.
- [7] Recent studies of oxidative umpolung amide synthesis (UmAS): a) K. E. Schwietzer, B. Shen, J. P. Shackleford, M. W. Leighty, J. N. Johnston, *Org. Lett.* **2014**, *16*, 4714–4717; b) M. W. Leighty, B. Shen, J. N. Johnston, *J. Am. Chem. Soc.* **2012**, *134*, 15233–15236; c) K. E. Schwietzer, J. N. Johnston, *Chem. Sci.* **2015**, *6*, 2590–2595.
- [8] R. W. Woolfolk, M. Cowperthwaite, R. Shaw, *Thermochim. Acta* **1973**, *5*, 409–414.
- [9] A. Noble, J. C. Anderson, *Chem. Rev.* **2013**, *113*, 2887–2939.
- [10] Selected organocatalytic enantioselective aza-Henry reactions: a) T. Okino, S. Nakamura, T. Furukawa, Y. Takemoto, *Org. Lett.* **2004**, *6*, 625–627; b) B. M. Nugent, R. A. Yoder, J. N. Johnston, *J. Am. Chem. Soc.* **2004**, *126*, 3418–3419; c) T. P. Yoon, E. N. Jacobsen, *Angew. Chem. Int. Ed.* **2005**, *44*, 466–468; *Angew. Chem.* **2005**, *117*, 470–472.
- [11] Y. Hayashi, S. Umekiya, *Angew. Chem. Int. Ed.* **2013**, *52*, 3450–3452; *Angew. Chem.* **2013**, *125*, 3534–3536.
- [12] S. Umekiya, K. Nishino, I. Sato, Y. Hayashi, *Chem. Eur. J.* **2014**, *20*, 15753–15759.
- [13] W. Adam, M. Makosza, C. R. Saha-Moller, C. G. Zhao, *Synlett* **1998**, 1335–1336.
- [14] Organocatalytic enantioselective formation of **1**: C. Palomo, M. Oiarbide, A. Laso, R. Lopez, *J. Am. Chem. Soc.* **2005**, *127*, 17622–17623.
- [15] Organocatalytic enantioselective formation of **13**: H. Gotoh, H. Ishikawa, Y. Hayashi, *Org. Lett.* **2007**, *9*, 5307–5309.
- [16] For the synthesis of *N*-bromo amines, see: a) J. E. M. N. Klein, H. Müller-Bunz, P. Evans, *Org. Biomol. Chem.* **2009**, *7*, 986–995; b) E. J. Corey, C.-P. Chen, G. A. Reichard, *Tetrahedron Lett.* **1989**, *30*, 5547–5550.



- [17] As insightfully suggested by the reviewers, additional halogenation could be occurring on **4** (cf. Eqs. (9) and (10), Scheme 4) and extra iodonium sources could be regenerated under the aerobic conditions. These possibilities, and the potential for catalysis in the iodine component, are being further explored. For mechanistically related iodine catalyzed and promoted coupling reactions, see: a) D. Liu, A. Lei, *Chem. Asian J.* **2015**, *10*, 806–823; b) S. Tang, K. Liu, Y. Long, X. Qi, Y. Lan, A. Lei, *Chem. Commun.* **2015**, *51*, 8769–8772; c) S. Tang, K. Liu, Y. Long, X. Gao, M. Gao, A. Lei, *Org. Lett.* **2015**, *17*, 2404–2407; d) S. Tang, Y. Wu, W. Liao, R. Bai, C. Liu, A. Lei, *Chem. Commun.* **2014**, *50*, 4496–4499.
- [18] For a related mechanistic rationale and peroxy adduct generation from haloalkanes, see: a) X. Ge, K. L. M. Hoang, M. L. Leow, X.-W. Liu, *RSC Adv.* **2014**, *4*, 45191–45197; b) J. M. Beames, F. Liu, L. Lu, M. I. Lester, *J. Am. Chem. Soc.* **2012**, *134*, 20045–20048.

- [19] Besides UmAS and other possibilities, see Refs. [5,6,7a,12,17,18], the exact mechanistic details and sequence of events for the addition of dioxygen and the exact stage of introduction of the amine component to an α -iodo nitroalkane **4**, for example, through a peroxy species like **17**, remains to be elucidated.
- [20] Examples of assumed *N*-halogenated ammonium-based catalytic intermediates may be found in the following critical review: S. E. Denmark, W. E. Kuester, M. T. Burk, *Angew. Chem. Int. Ed.* **2012**, *51*, 10938–10953; *Angew. Chem.* **2012**, *124*, 11098–11113.
- [21] For general work and concepts in halogen bonding, see: “Halogen Bonding: Fundamentals and Applications”: *Structure and Bonding*, Vol. 126 (Eds.: D. M. P. Mingos, P. Metrangolo, G. Resnati), Springer, Berlin, **2008**.

Received: June 7, 2015

Revised: July 18, 2015

Published online: September 9, 2015

Synthetic Methods

Mechanism of Oxidative Amidation of Nitroalkanes with Oxygen and Amine Nucleophiles by Using Electrophilic Iodine

Jing Li,^[a] Martin J. Lear,^[b] Eunsang Kwon,^[c] and Yujiro Hayashi*^[a]

Abstract: Recently, we developed a direct method to oxidatively convert primary nitroalkanes into amides that entailed mixing an iodonium source with an amine, base, and oxygen. Herein, we systematically investigated the mechanism and likely intermediates of such methods. We conclude that an amine–iodonium complex first forms through N–halogen bonding. This complex reacts with *aci*-nitronates to give both α -iodo- and α,α -diiodonitroalkanes, which can act as alternative sources of electrophilic iodine and also generate an extra equimolar amount of I^+ under O_2 . In particular, evidence supports α,α -diiodonitroalkane intermediates reacting with molecular oxygen to form a peroxy adduct; alternatively, these tetrahedral intermediates rearrange anaerobically to form a cleavable nitrite ester. In either case, activated esters are proposed to form that eventually reacts with nucleophilic amines in a traditional fashion.

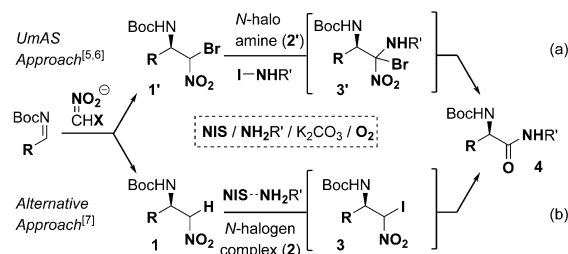


Figure 1. Oxidative approaches to umpolung amide synthesis (UmAS).^[5–7]

Later mechanistic studies supported such tetrahedral intermediates **3'** coupling with molecular oxygen in a homogenic manner to eventually form the amide products **4** (Figure 1a).^[6] Through a systematic study of our recently developed oxidative amidation procedure on unsubstituted nitroalkanes **1**,^[7] we now provide evidence that the tetrahedral intermediates are more likely α,α -dihalogenated nitroalkanes derived from α -halonitroalkanes like **1'** or **3** (Figure 1b). Under our reaction conditions, we propose that there is no umpolung of reactivity in the amine component and an extra equivalent of iodonium source is generated in the process.

Thus, having discovered^[8] and developed^[9] a Nef conversion of nitroalkenes and nitroalkanes into their carbonyl counterparts under base and oxygen, we recently extended our mechanistic understanding of such oxidative conversions into an atom-economical and direct amidation of primary nitroalkanes **1** by mixing in I_2 or NIS with amines (Figure 1b).^[7] During these amidation studies, we could not confirm the intermediacy of *N*-iodoamines **2'** or early-stage α -aminonitroalkanes **3'** derived from **1** as anticipated from UmAS rationales (Figure 1a).^[5a,b,6] Instead, we isolated a halogen bonded amine–NIS complex **2**, which was shown to form the α -iodonitroalkane **3** (Figure 1b) through its anion, and realized data that put the mechanistic basis of UmAS into question (*vide infra*). We thus began to discern each step and intermediate of these clearly interrelated schemes in a systematic and precise fashion (Scheme 1).

In particular, we noted the anaerobic reaction of monoiodide **3** with allylamine and K_2CO_3 not only produced the amide **4** (18%), but also a significant amount (40%) of the deiodinated nitroalkane **1** (Scheme 1a).^[7] Without the amine under O_2 , carboxylic acid **5** was generated from **3** (Scheme 1b). These results led to the idea that the monoiodide **3** could act as a source of electrophilic iodine for α -carbanions, as opposed to reacting with amines to generate *N*-haloamines (**2'**).^[6] This would logically produce a hitherto unobserved diiodide inter-

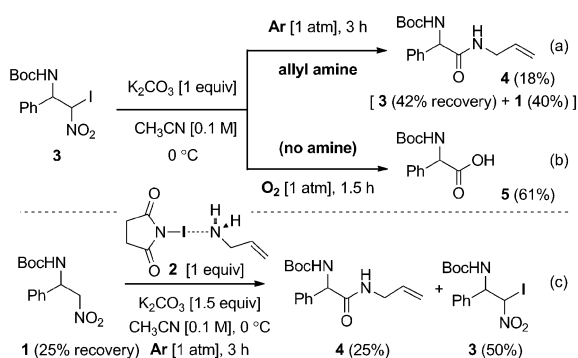
The structural and functional importance of the amide bond to natural products and bioactive small molecules is clear.^[1] Yet, the efficient synthesis of amides and peptides with simple reagents is still a challenge.^[2] Several alternative oxidative and decarboxylative methods to form amides and peptides have been developed over the last decade.^[3] Related interest has also been in the use of iodine-based reagents to promote or catalyze C–N amine bond formations.^[4] In 2010, a major advancement in oxidative amidation was disclosed by the Johnston group with the use of *N*-iodosuccinimide (NIS) and is termed umpolung amide synthesis (UmAS).^[5] The method centers on α -bromo-substituted nitroalkanes **1'** reacting with electrophilic *N*-iodoamines **2'** (in situ generated with NIS) to form reactive tetrahedral α -amino- α -bromonitroalkanes **3'** (Figure 1).

[a] J. Li, Prof. Dr. Y. Hayashi
Department of Chemistry, Graduate School of Science, Tohoku University
Aza Aramaki, Aoba-ku, Sendai 980-8578 (Japan)
E-mail: yhayashi@m.tohoku.ac.jp
Homepage: <http://www.ykbsc-chem.com/>

[b] Dr. M. J. Lear
School of Chemistry, University of Lincoln
Brayford Pool, Lincoln LN6 7TS (UK)

[c] Prof. Dr. E. Kwon
Research and Analytical Center for Giant Molecules
Graduate School of Science, Tohoku University
Sendai 980-8578 (Japan)

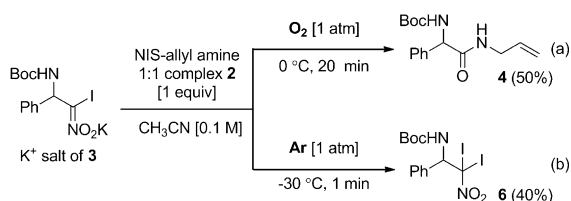
Supporting information for this article and ORCID for one of the authors can be found under <http://dx.doi.org/10.1002/chem.201600549>.



Scheme 1. Control amidation study of protonated nitroalkanes **1** and **3**.

mediate (vide infra) and the isolated deiodinated compound **1**. We thus decided to react the starting nitroalkane **1** directly with the NIS–amine complex **2** under Ar (Scheme 1c). Notably, about 25% of the starting nitroalkane **1**, 50% of the α -iodonitroalkane **3**, and 25% of the amide product **4** were produced under Ar with one equivalent of the 1:1 NIS–amine complex **2**. This means that a 25% yield of amide **4** required 50% of the iodinating reagent **2** under anaerobic conditions (cf. Schemes 1a and 1c).

Suspecting the need for iodine transfer by **3**, we studied the reactivity of the pure anion of **3** with one equivalent of the NIS–amine complex **2** under O₂ and under Ar (Scheme 2). The



Scheme 2. Control amidation study of the pure anion of **3**.

aerobic conditions produced the amide **4** in moderate yields in 20 min when conducted at 0 °C (Scheme 2a). Markedly, the potassium salt of **3** rapidly produced the diiodide **6** at –30 °C with the NIS–amine complex **2** when the reaction was stopped within 1 min (Scheme 2b). Longer reaction times or higher temperatures produced the expected amide **4**, and diiodide **6** was not observed. Although the anion of **3** transformed into amide **4** with NIS–amine complex **2** under O₂ (Scheme 2a), **3** readily oxidized with O₂ to carboxylic acid **5** in the absence of amine and iodonium sources (cf. Scheme 1b). In such cases, we observed I₂ being generated and, among other possibilities, these control experiments (cf. Schemes 1 and 2) reinforced the idea that the amide **4** and carboxylic acid **5** can be derived from the corresponding α,α -diiodonitroalkane **6**, which is generated by sequential bis-iodination of **1** via intermediate **3**.

Considering such types of dihalogenated species **6** as reactive tetrahedral intermediates to the amide **4**, as alternatives to α -amino- α -bromonitroalkanes **3'**,^[6] we prepared and compared the reactivity of dihalonitroalkanes **6** (X¹, X²=Cl, Br, and/or I)

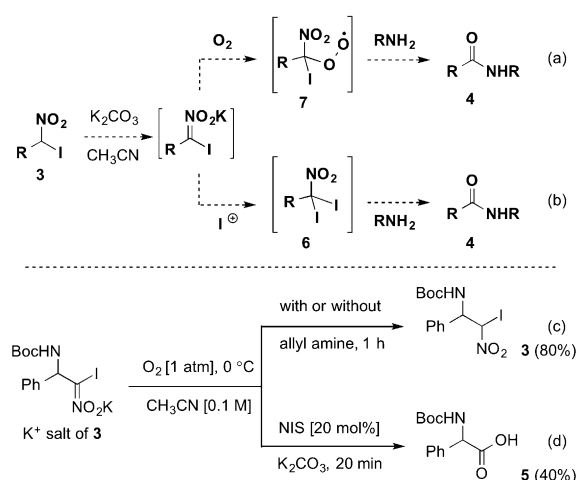
Table 1. Direct amidation of dihalogenated nitroalkanes **6**.^[a]

Entry	X ¹	X ²	Yield under Ar [%] ^[b]	Yield under O ₂ [%] ^[c]
1	Cl	Cl	trace	< 5
2	Cl	Br	35	20
3	Cl	I	48	72
4 ^[d]	Br	Br	10	31
5	Br	I	55	70
6 ^[e]	I	I	50	60

[a] Unless noted otherwise, all reactions were conducted with dihalogenated nitroalkanes **6** (0.1 mmol), allyl amine (0.15 mmol), and K₂CO₃ (0.15 mmol) at 0 °C in CH₃CN (1 mL) under O₂ or Ar (1 atm); isolated yields are given. [b] Reactions under Ar were conducted over 48 h, except entry 6, which was over 1 h. [c] Reactions under O₂ were conducted over 24 h, except entry 6, which was over 20 min. [d] Reaction conducted at room temperature. [e] Diiodide of **6** was unstable and used immediately after preparation.

under both Ar and O₂ (Table 1; see the Supporting Information for X-ray of bromo/iodo **6**). The experiments clearly showed that the amide **4** formed directly from the dihalide intermediate **6**, whereby higher reactivity and yield resulted with the introduction of at least one iodine substituent. Exceptional reactivity, within 20–60 min, was observed with the unstable diiodide **6** (X¹, X²=I), which likely accounted for our difficulty in observing **6** during our initial amidation studies, unlike the dihalide.^[7]

In combination with Scheme 2, the results in Table 1 are consistent with the consecutive bis-iodination of the starting nitroalkane **1** and then monoiodide **3** through their respective *aci*-nitronates. However, at this juncture, it was still not clear whether the anion of **3** first reacted with oxygen, for example, either directly or through SET and radical coupling (Scheme 3a) or with an iodonium source, for example, with I₂, NIS or the halogen bonded NIS–complex **2** (Scheme 3b). We thus consid-

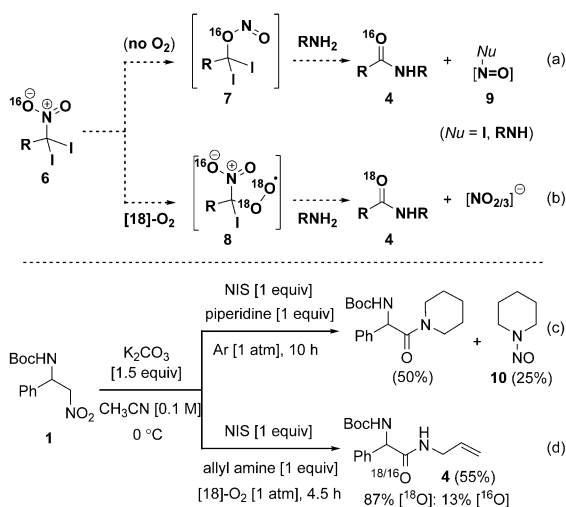


Scheme 3. Pathway selection and reactivity of anion of **3** with O₂ and NIS.

ered two pathways for the formation of amide **4** from monoiodide **3** and performed another set of control experiments with the potassium salt of **3** (Schemes 3 c and 3 d).

First, with or without amine being present, the experiments clearly demonstrated that, in the absence of an iodonium source, molecular oxygen does not react with the *aci*-nitronate intermediate of **3** at all (Scheme 3 c). Thus, SET transfer mechanisms or immediate anionic attack onto O₂ to afford radical^[10] or anionic^[9] oxygen adducts directly from **3** do not operate. It is more likely the case of molecular oxygen reacting with the diiodinated nitroalkane **6**, as first evidenced during the experiments shown in Scheme 2. Second, in the presence of 20 mol % of NIS and absence of amine, carboxylic acid **5** was isolated in a yield of 40% after aqueous work-up (Scheme 3 d). Here, we suggest the diiodide intermediate **6** can regenerate an extra equivalent of the iodonium source (*vide infra*).

Such suggestions have clear experimental precedence in a recent UmAS study.^[6] The difference herein is that we propose tetrahedral α -iodo- α -halonitroalkane **6** instead of α -amino- α -halonitroalkane **3'** as the key intermediate that reacts with oxygen. Further evidence presented in the UmAS-labeling study^[6] also showed that the residual H₂¹⁸O and N¹⁸O₂-labeled α -halonitroalkanes **3** do not result in significantly ¹⁸O-enriched amides **4** under ¹⁶O₂. Thus, having the dioxygen directly reacting with the anion of **3**, two UmAS-like pathways to form the amide **4** were reasoned to occur by the tetrahedral α,α -diiodo-nitroalkane **6**, and not by its α -amino- α -bromo counterpart **3'**^[6] (Scheme 4). Both radical and ionic modes were considered



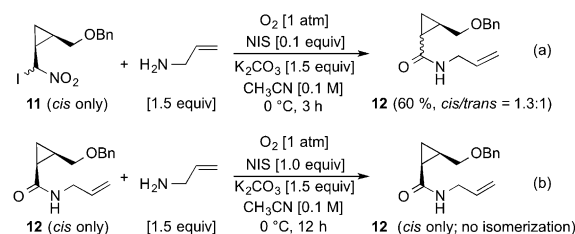
Scheme 4. Nitroso-trapping and $^{18}\text{O}_2$ -labelling studies of **1**.

feasible, and the generation of *N*-nitrosoamines **9** (Nu = amine)^[11] was also deemed possible as products from previously related^[5b] diiodo nitrites **7**, the rearranged adducts of **6** (Scheme 4a). The fate of the nitro group was thus uncertain under anaerobic and aerobic conditions, for example, to form either nitrate or nitrite salts from the congested peroxyxynitroalkane **8** (Scheme 4b), and a further set of control experiments were performed to discern such fates (Schemes 4c and 4d).

Specifically, we measured the resultant concentration of nitrate/nitrite salts and the level of ^{18}O incorporation by converting **1** into **4** under $^{18}\text{O}_2$.^[9]

In the event, *p*-iperidine was chosen as a less volatile amine reactant than allylamine, which allowed for the anticipated and known *N*-nitrosoamine **10**^[11] to be isolated reliably (Scheme 4c). Under Ar, **10** was isolated in 25% yield. Under O₂, **10** was isolated in 11% yield. The formed nitrosyl iodide **9** (Nu=I) would be expected to also convert to I₂ and NO gas.^[12] The fact that *N*-nitrosoamines were isolated supports the existence of nitrite intermediates **7** under the UmAS reaction conditions. Next, isotope labelling experiments with allylamine as the nucleophile revealed an 87% of ¹⁸O incorporation in the amide product **4**, which was isolated in a chemical yield of 55% under ¹⁸O₂ (Scheme 4d). The resultant nitro-derived salt ratios were calculated to be 36% nitrite (NO₂⁻) and 4–6% nitrate (NO₃⁻) under O₂, whereas 3% NO₂⁻ and 1–2% NO₃⁻ were detected under anaerobic conditions (see the Supporting Information). Although the data supports the nitro–nitrite rearrangement (**6** to **7**; Scheme 4a) as the predominant fate of the nitro functionality of **1** under anaerobic conditions, it also suggests that both pathways can occur concomitantly under aerobic conditions. Presumably, the proximity and local concentration of solvated O₂ gas to diiodide **6** will be a factor in pathway selection, and NO_{2/3} salt counts were found to be low due to *N*-nitrosoamine formation and loss of NO gas (and I₂) through species like I–N=O.^[12]

Next, we performed radical clock experiments (Scheme 5).^[9, 13] Thus, the pure *cis*-cyclopropanes **11** and **12** were prepared and reacted with the allylamine under our oxidative conditions. Starting from *cis*-**11**, a 1.3:1 *cis/trans* ratio of



Scheme 5. Radical clock control experiments of pure *cis*-11 and *cis*-12.

12 was generated in 60% yield (Scheme 5a). In order to exclude epimerization occurring after amide formation, the purified *cis*-cyclopropyl amide **12** was similarly treated with NIS, K₂CO₃ and O₂. This gave complete recovery of the *cis*-cyclopropyl amide, even after 12 h (Scheme 5b). These results support the existence of a cyclopropylcarbiny radical being generated and undergoing ring opening/closure.

Lastly, the regeneration and intermediacy of putative iodonium sources need to be considered under our reaction conditions (Figure 2). In other words, presuming that diiodide **6** is the key intermediate, the oxidative amidation of the mono-iodonitroalkane **3** (in the absence of additional NIS or I_2) is expected to occur by an initial iodine transfer to its anion to afford the diiodide **6** and eventually regenerate an equivalent

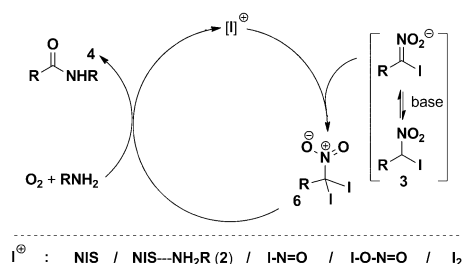


Figure 2. Generic process to regenerate an iodonium source.

amount of the iodinating agent. Furthermore, despite observing the iodo precursor **3** being oxidized to carboxylic acid **5** with oxygen under basic conditions (cf. Scheme 1 b), oxygen does not react with the anion of **3** first (cf. Scheme 3 c), but more likely O_2 reacts with the diiodide **6** after it forms through iodine transfer of **3** to its nitronate anion (cf. Scheme 2 b and Table 1). Moreover, the oxidative amidation of the nitroalkane starting material **1** only requires one equivalent of NIS in the presence of O_2 .^[7] In accordance with the latest UmAS report,^[6] we similarly suggest an extra equivalent of I_2 , $I-N=O$ ^[12] and/or $I-ONO$ species is generated under the reaction conditions (Figure 2). These iodonium species can thus react under either radical or ionic reaction modes and allow the amide oxidation state of **4** to be achieved from monoiodide **3**.

Collectively, our findings are consistent with the mechanism illustrated in Figure 3. We thus propose the primary nitroalkane **1** first becomes α -iodinated with NIS from the halogen-bonded amine complex **2** to afford the monoiodide **3** (Figure 3 a). After further deprotonation, the α -iodo *aci*-nitronate

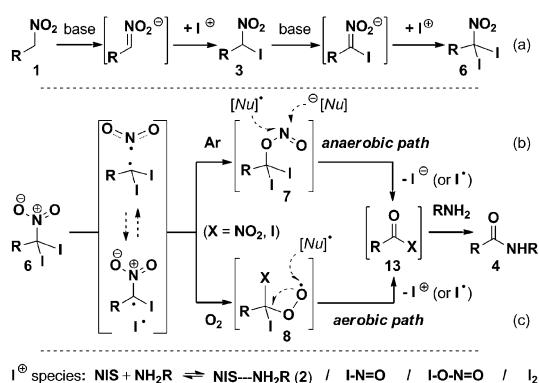


Figure 3. Proposed oxidative amidation of **1** by α -iodide **3** and diiodide **6**.

becomes α -iodinated with another iodonium species (I^+) to afford the diiodide **6**. We propose it is this congested, tetrahedral diiodinated nitroalkane **6** that can either rearrange in a homogenic, anaerobic manner to form the nitrite ester **7** (Figure 3 b) or react with the molecular oxygen to afford peroxy radical adduct **8** (Figure 3 c). From these intermediates onwards, several additive–eliminative pathways, under either radical or ionic reaction modes, can be proposed to afford the amide product **4**.^[9–11] On the basis of prior studies, one sugges-

tion for such latter stage is that the peroxy radical **8** cyclizes and expels either a mono-iodine or nitrite radical to form a reactive dioxirane intermediate, which can react with the anion of **3** (Figure 3).^[9] The peroxy radical **8** could also couple with a nearby radical derived from **6** to form homo- or heterodimers.^[14] In either case, the dioxygenated intermediates would fragment to the acylating species **13**. Besides other possibilities,^[10] the exact mechanistic details of such latter amine addition stages (through **7/8** and **13**) remains to be supported by further studies. However, we do provide indirect evidence for the anaerobic formation of the nitrite ester **7** by isolation of the *N*-nitrosoamine **10**.

In conclusion, our mechanistic rationales, as depicted in Figure 2 and Figure 3, are consistent with all of the reported data and observations that have been obtained during previously published umpolung amide synthesis (UmAS) studies^[5,6] and our recent work.^[7] Critically, the key differences in our conclusions include: 1) the intermediacy of a reactive tetrahedral dihalogenated species like **6**, and not α -amino halonitroalkane **3'**; 2) the halogen bonding of NIS with amines to form iodonium complexes like **2**, and not electrophilic *N*-iodoamine **2'**; and 3) the late-stage nucleophilic addition of amines to oxygenated intermediates like **7** or **8**, or a subsequently derived traditional acyl precursor **13**, to give the amide products **4**.

Keywords: amides · iodine · peroxides · radicals · umpolung

- [1] a) N. Sewald, H. D. Jakubke, in *Peptides: Chemistry and Biology*, Wiley-VCH, Weinheim (Germany), **2002**; b) *The Amide Linkage: Structural Significance in Chemistry, Biochemistry and Materials Science* (Eds.: A. Greenberg, C. M. Breneman, J. F. Liebman), Wiley, **2003**; c) *Peptide Drug Discovery and Development* (Eds.: M. Castanho, N. Santos), Wiley-VCH, Weinheim (Germany), **2011**.
- [2] a) E. Valeur, M. Bradley, *Chem. Soc. Rev.* **2009**, *38*, 606–631; b) A. El-Faham, F. Albericio, *Chem. Rev.* **2011**, *111*, 6557–6602.
- [3] For leading, recent literature on oxidative amidations using oxygen and/or halonium sources as oxidants, see: a) J. Liu, Q. Liu, H. Yi, C. Qin, R. Bai, X. Qi, Y. Lan, A. Lei, *Angew. Chem. Int. Ed.* **2014**, *53*, 502–506; *Angew. Chem.* **2014**, *126*, 512–516; b) D. Leow, *Org. Lett.* **2014**, *16*, 5812–5815; c) O. P. S. Patel, D. Anand, R. K. Maurya, P. P. Yadav, *Green Chem.* **2015**, *17*, 3728–3732; d) A. Alanthadka, C. U. Maheswari, *Adv. Synth. Catal.* **2015**, *357*, 1199–1203; e) S. Khamarui, R. Maiti, D. K. Maiti, *Chem. Commun.* **2015**, *51*, 384–387.
- [4] For the virtues of iodine-mediated reactions and iodine-based additives in synthesis, including oxidative aminations, see: a) S. Minakata, *Acc. Chem. Res.* **2009**, *42*, 1172–1182; b) M. Uyanik, K. Ishihara, *ChemCatChem* **2012**, *4*, 177–185; c) P. Finkbeiner, B. Nachtsheim, *Synthesis* **2013**, 979–999; d) S. Tang, Y. Wu, W. Liao, R. Bai, C. Liu, A. Lei, *Chem. Commun.* **2014**, *50*, 4496–4499; e) C. Martínez, K. Muniz, *Angew. Chem. Int. Ed.* **2015**, *54*, 8287–8291; *Angew. Chem.* **2015**, *127*, 8405–8409.
- [5] Initial discovery and mechanistic rationale of oxidative umpolung amide synthesis (UmAS): a) B. Shen, D. M. Makley, J. N. Johnston, *Nature* **2010**, *465*, 1027–1032; b) J. P. Shackleford, B. Shen, J. N. Johnston, *Proc. Natl. Acad. Sci. USA* **2012**, *109*, 44–46. Application of UmAS in synthesis: c) M. W. Leighty, B. Shen, J. N. Johnston, *J. Am. Chem. Soc.* **2012**, *134*, 15233–15236; d) K. E. Schwietz, J. N. Johnston, *Chem. Sci.* **2015**, *6*, 2590–2595; e) K. E. Schwietz, J. N. Johnston, *Chem. Commun.* **2016**, *52*, 152–155.
- [6] Presently accepted mechanism of oxidative umpolung amide synthesis (UmAS): K. E. Schwietz, B. Shen, J. P. Shackleford, M. W. Leighty, J. N. Johnston, *Org. Lett.* **2014**, *16*, 4714–4717.
- [7] J. Li, M. J. Lear, Y. Kawamoto, S. Umemiyama, A. Wong, E. Kwon, I. Sato, Y. Hayashi, *Angew. Chem. Int. Ed.* **2015**, *54*, 12986–12990; *Angew. Chem.* **2015**, *127*, 13178–13182.

- [8] Y. Hayashi, S. Umekiya, *Angew. Chem. Int. Ed.* **2013**, *52*, 3450–3452; *Angew. Chem.* **2013**, *125*, 3534–3536.
- [9] S. Umekiya, K. Nishino, I. Sato, Y. Hayashi, *Chem. Eur. J.* **2014**, *20*, 15753–15759.
- [10] For peroxy-adduct generation from dihaloalkanes, see: a) X. Ge, K. L. M. Hoang, M. L. Leow, X.-W. Liu, *RSC Adv.* **2014**, *4*, 45191–45197; b) J. M. Beames, F. Liu, L. Lu, M. I. Lester, *J. Am. Chem. Soc.* **2012**, *134*, 20045–20048.
- [11] N. Tokitoh, R. J. Okazaki, *Bull. Chem. Soc. Jpn.* **1987**, *60*, 3291–3297.
- [12] P. W. Atkins, T. L. Overton, J. P. Rourke, M. T. Weller, F. A. Armstrong, In *Inorganic Chemistry: The Group 15 Elements*, 6th ed., Oxford University Press, Oxford (UK), **2014**, p. 424.
- [13] Radical clock studies: a) E. L. Spence, G. J. Langley, T. D. H. Bugg, *J. Am. Chem. Soc.* **1996**, *118*, 8336–8343; b) T. Benkovics, J. Du, I. A. Guzei, T. P. Yoon, *J. Org. Chem.* **2009**, *74*, 5545–5552; c) J. F. Van Humbeck, S. P. Simonovich, R. R. Knowles, D. W. C. MacMillan, *J. Am. Chem. Soc.* **2010**, *132*, 10012–10014; d) E. Arceo, I. D. Jurberg, A. Alvarez-Fernandez, P. Melchiorre, *Nature Chem.* **2013**, *5*, 750–756.
- [14] H. Shimakoshi, Y. Hisaeda, *Angew. Chem. Int. Ed.* **2015**, *54*, 15439–15443; *Angew. Chem.* **2015**, *127*, 15659–15663.

Received: February 2, 2016
Published online on March 3, 2016

Amides

International Edition: DOI: 10.1002/anie.201603399
German Edition: DOI: 10.1002/ange.201603399Sterically Demanding Oxidative Amidation of α -Substituted Malononitriles with Amines Using O_2

Jing Li, Martin J. Lear,* and Yujiro Hayashi*

Abstract: An efficient amidation method between readily available 1,1-dicyanoalkanes and either chiral or nonchiral amines was realized simply with molecular oxygen and a carbonate base. This oxidative protocol can be applied to both sterically and electronically challenging substrates in a highly chemoselective, practical, and rapid manner. The use of cyclopropyl and thioether substrates support the radical formation of α -peroxy malononitrile species, which can cyclize to dioxiranes that can monooxygenate malononitrile α -carbanions to afford activated acyl cyanides capable of reacting with amine nucleophiles.

Reaching high levels of cost economy and atom efficiency for an organic reaction is particularly challenging when faced with highly functionalized substrates and energetically demanding bond formations. This goal translates into finding simple reagent systems as well as practical reaction conditions and work-up procedures, so as to produce very little reagent-based byproducts and reaction-based side-products. There is thus a continual need to develop highly chemoselective methods with low-molecular-weight reagents to minimize side-reactions and thus the molecular wastes derived from both the reagents and the reactants. The efficient and rapid formation of amides and peptides falls into such a challenge. Indeed, although the amide bond plays a pivotal role in organic, biological, and materials chemistry,^[1] it still presents a great synthetic challenge when confronted with sterically or electronically demanding substrates.^[2] Seminal synthetic methods to making such challenging or complex amides have been reported by the groups of Bode, Rawal, Danishefsky, and Schafmeister.^[3]

Adding to such challenges is a drive to develop new ways to make amide bonds by activating nontraditional substrates oxidatively, as represented by the methods from the groups of Milstein, Rovis, Johnston, Bode, Lei, and Garg, as well as ours.^[4,5] Stemming from recent mechanistic insights^[5c,d] into the umpolung amide synthesis (UmAS) method of Johnston

and co-workers,^[4c] we now present our oxidative advancement of the masked acyl cyanide (MAC) method to make amides, which was introduced by Yamamoto and co-workers^[6] in 1990 and elegantly exploited in 2013 by the group of Rawal.^[3c] Specifically, we disclose the direct, oxygen-based conversion of 1,1-dicyanoalkanes to make hindered amides and peptides in high yield and stereochemical integrity. This mild, yet powerful method simply entails stirring α -substituted malononitriles with chiral or nonchiral amines in acetonitrile under O_2 with a carbonate base.

The stimulus for this work began during our discovery and development of the base-promoted Nef oxidation of nitroalkenes or nitroalkanes to form their ketones with oxygen (Figure 1 a).^[5a,b] During the further development of a direct halogenative method to form amides under aerobic condi-

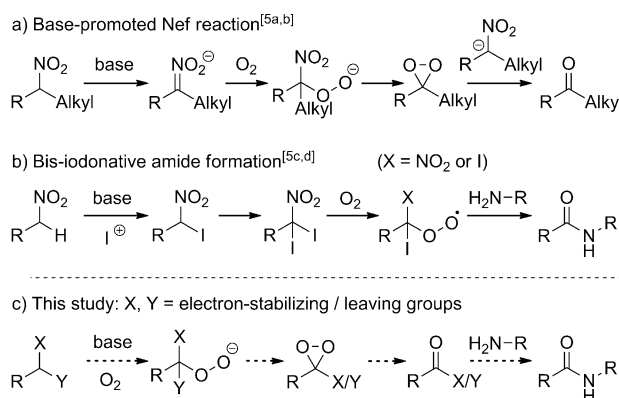


Figure 1. Mechanistic rationales for oxidative amidation.

tions,^[5c] we isolated α,α -diiodinated nitroalkanes (Figure 1 b) and recognized the mechanistic need to make intermediates that bear two electron-stabilizing groups, X and Y (Figure 1 c).^[5d] These substituents can thus not only stabilize transient radicals and anions, but also act as one- or two-electron leaving groups. We thus proposed to explore an oxidative amidation sequence via putative dioxirane intermediates, which can act as sources of electrophilic monooxygen and transform into reactive acyl derivatives to form amide bonds in a new powerful way.

First, we explored NO₂,^[7] CN,^[8] SO₂R,^[9] and PO(OR)₂^[10] as suitable X/Y groups for the proposed oxidative amidation sequence (Figure 1 c). These studies are summarized in Table 1. Under our recently established oxidative conditions,^[5c] reactions of either α -sulfonyl- or α -chloro-substituted nitroalkanes **1** with allylamine (**2**) did not produce the amide product **3** at all (entries 1 and 2). Suspecting the need for

[*] J. Li, Prof. Dr. Y. Hayashi
Department of Chemistry, Graduate School of Science
Tohoku University
Aza Aramaki, Aoba-ku, Sendai 980-8578 (Japan)
E-mail: yhayashi@m.tohoku.ac.jp
Homepage: <http://www.ykbsc.chem.tohoku.ac.jp>
Dr. M. J. Lear
School of Chemistry, University of Lincoln
Brayford Pool, Lincoln LN6 7TS (UK)
E-mail: mlear@lincoln.ac.uk
Homepage: <http://staff.lincoln.ac.uk/mlear>

Supporting information for this article can be found under:
<http://dx.doi.org/10.1002/anie.201603399>.

Table 1: Screening of functionality for oxidative amide formation.^[a]

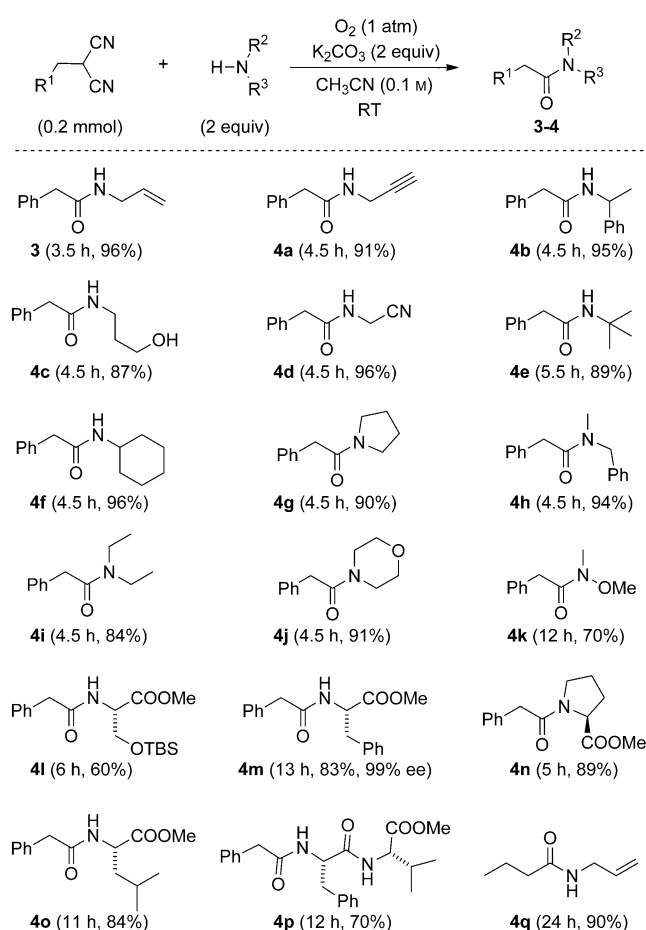
Entry	X	Y	t [h]	Yield [%] ^[b]
1	NO ₂	SO ₂ Ph	12	< 5
2	NO ₂	Cl	12	< 5
3	CN	CN	3.5	96
4	CN	SO ₂ Ph	90	70
5	CN	PO(OEt) ₂	60	< 5
6	CN	COOMe	60	< 5
7	CN	OTs	24	< 5

[a] Reactions were conducted with **1** (0.2 mmol), the allyl amine **2** (0.4 mmol), and K₂CO₃ (0.4 mmol) at room temperature under O₂ (1 atm). [b] Yield of the isolated product. Ts = 4-toluenesulfonyl.

alternative electron-withdrawing groups to facilitate single-electron transfer (SET) mechanisms with O₂,^[5b] we prepared and explored various α -substituted nitrile derivatives (**1**, X = CN). To our delight, when the 1,1-dicyanide **1** (X, Y = CN) was exposed to the amine **2** in the presence of K₂CO₃ under O₂, the desired amide was generated in 96% chemical yield within 3.5 hours at room temperature (entry 3). Further studies revealed the cooperative nature of CN and SO₂Ph groups in **1**, which gave a 70% yield of **3**, albeit over three days (entry 4). Otherwise, only trace amounts of the amide **3** were observed (entries 5–7).

With appropriate functionality and initial reaction conditions in place for the 1,1-dicyanide **1** (X, Y = CN), the scope of the oxidative amidation method was first investigated by changing the amine component (Scheme 1). Common functional groups, such as allyl, propargyl and benzyl amines, displayed high reactivity to amide formation (**3**, **4a/b**). The unprotected hydroxy amine generated the corresponding amide **4c** chemoselectively in 87% yield and the electron-deficient 2-aminoacetonitrile gave the desired amide in 96% yield (**4d**). Amines with increasing steric hindrance, including *tert*-butylamine, cyclohexylamine, pyrrolidine, *N*-methylbenzylamine, diethylamine, and morpholine, all gave the desired amides in greater than 80% yield (**4e–j**). The reaction conditions were also found suitable for Weinreb amide formation (**4k**). Notably, coupling of **1** with amino-acid methyl esters or an amine-free dipeptide generated the corresponding amides and peptides in 70–84% yields upon isolation (**4l–p**) without epimerization. Also, 2-propylmalononitrile reacts with allylamine to give the desired amide **4q** in 90% yield.

Next, our aim was to apply this oxidative method to more challenging amides (see Table S2 in Supporting Information for optimization studies). In short, we studied the α -*tert*-butyl malononitrile **5** (R¹ = *t*Bu) and *N*-methylbenzylamine for optimization to the sterically hindered amide **6a**, whereby Cs₂CO₃ was demonstrated to be superior, at elevated temperatures, to bases like K₂CO₃, KOAc, and K₃PO₄, as well as to stronger bases like KO^{*t*}Bu and CsOH (Scheme 2; Conditions A or B). To prevent carboxylic acid formation, presum-

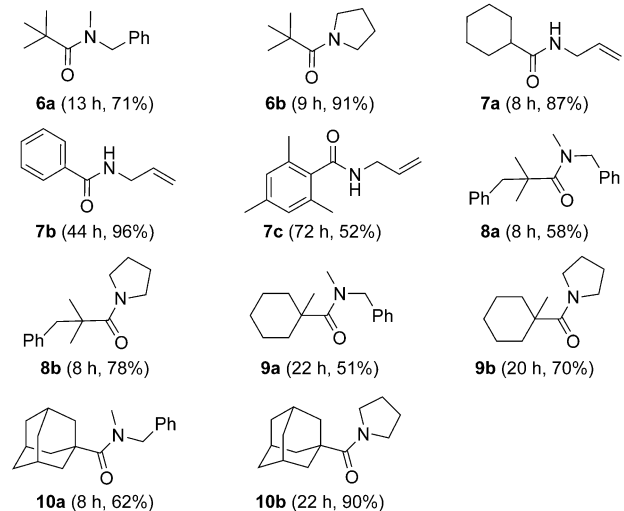
**Scheme 1.** Oxidative amidation of unhindered α -alkylated malononitriles. TBS = *tert*-butyldimethylsilyl.

ably derived by **5** reacting with residual water, strictly anhydrous conditions were adopted and predried 4 Å molecular sieves and Cs₂CO₃ with two equivalents of amine gave the amide **6a** reliably in 71% yield. We thus explored the scope of these simple oxidative conditions for making other challenging amide and peptide systems (Scheme 2). Besides the notable formation of the congested aromatic amide **7c** with allylamine, the formation of the amides **6–10** proceeded in good yield at 50 °C, despite both sides of the amide bond being fully substituted (Conditions A). Furthermore, chiral amino-acid methyl esters and amides could be coupled with sterically hindered malononitriles in acceptable yields and reaction times at 70 °C (Conditions B) with complete stereochemical integrity in the amine component (see the Supporting Information).

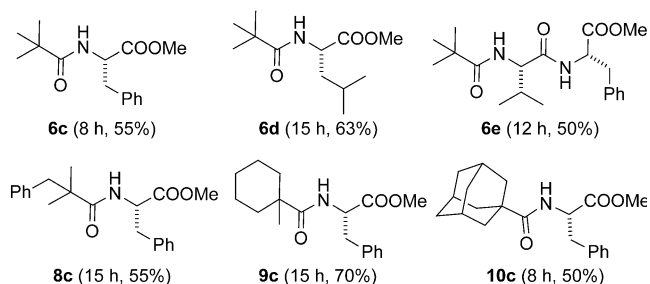
On the basis of our previous mechanistic studies into making ketones^[5b] and amides^[5c,d] from nitroalkanes, one plausible pathway for the oxidative amidation of malononitriles with amines is proposed in Figure 2. Thus, the α -substituted malononitrile first deprotonates to generate the anion **11**, which is then capable of SET and addition with molecular oxygen, either directly or indirectly. If a radical pair is produced, they would couple to form the peroxide adduct **13**.^[5,11] In either case, **13** can cyclize and expel cyanide anion to form the reactive dioxirane intermediate **14** (see the



Conditions A – malononitrile (0.2 mmol) + amine (0.4 mmol) at 50 °C



Conditions B – malononitrile (0.4 mmol) + amine (0.2 mmol) at 70 °C



Scheme 2. Oxidative amidation of sterically hindered α -alkylated malononitriles and steric N-capping of amino-acid esters/peptides. M.S. = molecular sieves.

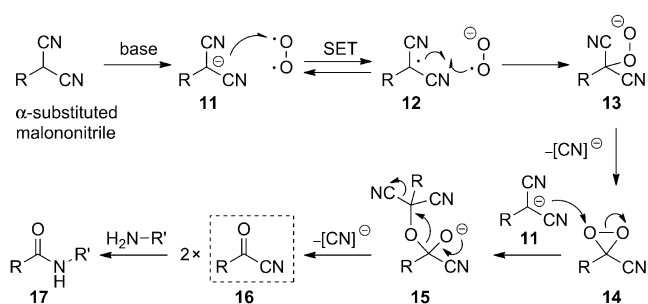
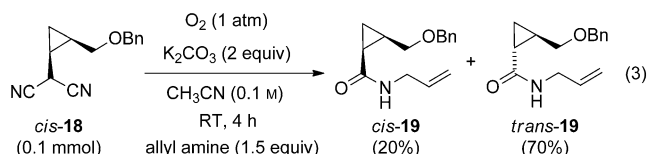
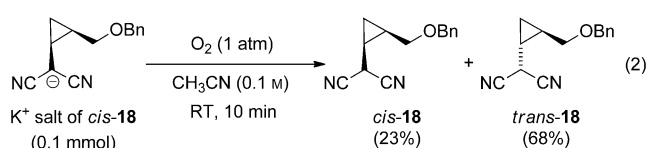
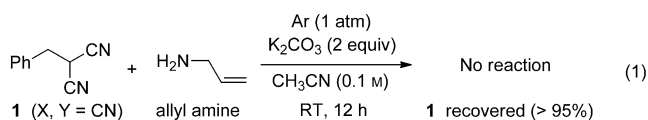


Figure 2. Proposed mechanism of amide formation via the acyl cyanide **16**.

Supporting Information for an alternative O_2 addition pathway to eliminate cyanate anions via a four-membered adduct through **12** or **13**). In turn, electrophilic mono-oxygen transfer from **14** to another 1,1-dicyano carbanion (**11**) produces a bis(tetrahedral) adduct **15** which can fragment into two

acylating species (**16**) capable of being intercepted by the amine nucleophile. It is conceivable that the initial steps between the intermediates **11/12** can be considered to be reversible. A selection of control reactions were carried out to evaluate this mechanistic proposal (also see the Supporting Information).

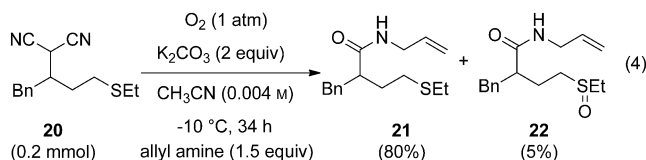
The role of O_2 was considered first [Eq. (1)]. When **1** ($\text{X}, \text{Y} = \text{CN}$) was mixed with allyl amine in the presence of K_2CO_3 under argon, the amide **3** was not formed and **1** was recovered completely. This outcome is in stark contrast to when the reaction was conducted under O_2 (Scheme 1; 96 % yield of **3**). Next, the reaction of molecular oxygen with **11** was considered. Based on our Nef study to make ketones from secondary nitroalkanes,^[5b] and related reports for ketone formation from monocyanide compounds using O_2 ,^[11] processes involving SET were deemed feasible (Figure 2). Thus to determine the existence of a radical species like **12**, we prepared the α -cyclopropyl malononitrile *cis*-**18** as its pure *cis* isomer for suitable radical clock experiments.^[12] Exposure of the preformed potassium salt of *cis*-**18** to O_2 for 10 minutes gave a 1:3 *cis*-**18**/*trans*-**18** mixture in 90 % yield [Eq. (2)]. Control experiments with added TEMPO (1.0 equiv) and under strictly O_2 -free atmosphere gave near complete recovery of *cis*-**18** (around 90%). Moreover, when *cis*-**18** was exposed to the allylamine in the presence of K_2CO_3 under O_2 , the cyclopropyl amide was isolated as a 1:3.5 *cis*-**19**/*trans*-**19** mixture in 90 % yield after 4 hours [Eq. (3)]. Further experiments demonstrated a mixture of *cis*-**18** and *cis*-**19** to be isomerically stable to the reaction conditions under argon (see the Supporting Information). Collectively, these results support the anion **11** reacting reversibly with O_2 via SET to form the radical **12**, which can conceivably couple with superoxide to form the peroxide adduct **13** as shown in Figure 2.



The fate of the cyano groups was also considered. Thus, the quantities of cyanide and cyanate anions were determined by ion chromatography as produced from the reaction given in the generation of **3** in Scheme 1. With respect to a total

theoretical yield of 2 equivalents, cyanate ions were detected in low yield (7.6%), whereas cyanide ions were formed in high yield (84.8%; see the Supporting Information). On the basis of these results, we further suggest that **13** cyclizes to form the dioxirane intermediate **14**, thus releasing the first equivalent of cyanide, after which the second equivalent of cyanide would be generated after amine addition to the proposed acyl cyanide **16** to give the amide product **17** (Figure 2).

Next, to support the electrophilic dioxirane intermediate **14**, intramolecular thioether-trapping experiments were performed in O₂-saturated CH₃CN, such that the reaction of the anion **11** with molecular O₂ would be independent of the concentration of **11** [Eq. (4)].^[5b] In the event, the δ -ethyl-sulfonyl β -benzyl malononitrile **20** was prepared and reacted under dilute conditions at –20 °C. This reaction gave the oxidized sulfinyl amide **22** reliably in 5% yield. The direct oxidation of **20** or the sulfide product **21** by O₂ was excluded by additional control experiments at room temperature for over 48 hours (see the Supporting Information).



In summary, we have presented a new powerful way to construct challenging amide bonds between α -substituted malononitriles and amines under O₂. The oxidative amidation proceeds under mild reaction conditions, is highly practical, and simply employs cheap inorganic carbonate bases. Mechanistic studies support an initial SET pathway between the anion **11** of the α -substituted malononitrile and O₂ (via radical **12**) to form the α -peroxide adduct **13** as a precursor to the dioxirane **14**, which generates acyl cyanide (**16**) via the formation and fragmentation of bis(tetrahedral) adducts **15** (Figure 2). Notably, our method does not require the formation of either congested pre-oxidized hydroxy malononitriles as masked acyl cyanides (MAC)^[3c,d,6] or congested halogenated nitroalkanes as precursors to activated esters,^[4c,5c,d] and therefore offers good substrate scope for sterically hindered systems. It is thus reasoned that the SET induced addition of O₂ to **11** proceeds in a relatively unencumbered way to generate the acyl cyanide **16**, which is known to react readily with amines (or alcohols) in a mild manner.^[13] This process compares favorably to either making and reacting acid chlorides with metal cyanides or by activating carboxylic acids with traditional reagents (e.g. with phosphorocyanidates).^[2,14] Lastly, we anticipate this method to find wide synthetic use in difficult N-terminal capping amidations and throughout the chemical sciences.^[1,2,15]

Acknowledgments

We thank the School of Chemistry, University of Lincoln, UK for funding to make this article open access.

Keywords: amides · amines · peroxides · radicals · reaction mechanisms

How to cite: *Angew. Chem. Int. Ed.* **2016**, *55*, 9060–9064
Angew. Chem. **2016**, *128*, 9206–9210

- [1] a) N. Sewald, H. D. Jakubke in *Peptides: Chemistry and Biology*, Wiley-VCH, Weinheim, **2002**; b) “The Amide Linkage: Structural Significance”: *Chemistry, Biochemistry and Materials Science* (Eds.: A. Greenberg, C. M. Breneman, J. F. Liebman), Wiley, New York, **2003**; c) *Peptide Drug Discovery and Development* (Eds.: M. Castanho, N. Santos), Wiley-VCH, Weinheim, **2011**.
- [2] a) E. Valeur, M. Bradley, *Chem. Soc. Rev.* **2009**, *38*, 606–631; b) A. El-Faham, F. Albericio, *Chem. Rev.* **2011**, *111*, 6557–6602.
- [3] Seminal methods to making challenging amide bonds: a) V. R. Pattabiraman, J. W. Bode, *Nature* **2011**, *480*, 471–479; b) G. Schäfer, C. Matthey, J. W. Bode, *Angew. Chem. Int. Ed.* **2012**, *51*, 9173–9175; *Angew. Chem.* **2012**, *124*, 9307–9310; c) K. S. Yang, A. E. Nibbs, Y. E. Turkmen, V. H. Rawal, *J. Am. Chem. Soc.* **2013**, *135*, 16050–16053; d) K. S. Yang, V. H. Rawal, *J. Am. Chem. Soc.* **2014**, *136*, 16148–16151; e) Y. Rao, X. Li, S. J. Danishefsky, *J. Am. Chem. Soc.* **2009**, *131*, 12924–12926; f) Z. Z. Brown, C. E. Schafmeister, *J. Am. Chem. Soc.* **2008**, *130*, 14382–14383.
- [4] Leading oxidative methods to making amide bonds using alternative starting materials: a) C. Gunanathan, Y. Ben-David, D. Milstein, *Science* **2007**, *317*, 790–792; b) H. U. Vora, T. Rovis, *J. Am. Chem. Soc.* **2007**, *129*, 13796–13797; c) B. Shen, D. M. Makley, J. N. Johnston, *Nature* **2010**, *465*, 1027–1032; d) I. Pusterla, J. W. Bode, *Angew. Chem. Int. Ed.* **2012**, *51*, 513–516; *Angew. Chem.* **2012**, *124*, 528–531; J. Liu, Q. Liu, H. Yi, C. Qin, R. Bai, X. Qi, Y. Lan, A. Lei, *Angew. Chem. Int. Ed.* **2014**, *53*, 502–506; *Angew. Chem.* **2014**, *126*, 512–516; e) L. Hie, N. F. F. Nathel, X. Hong, Y.-F. Yang, K. N. Houk, N. K. Garg, *Angew. Chem. Int. Ed.* **2016**, *55*, 2810–2814; *Angew. Chem.* **2016**, *128*, 2860–2864.
- [5] Discovery, development, and mechanistic studies of the base-promoted Nef reaction and oxidative amidation of nitroalkanes by O₂: a) Y. Hayashi, S. Umemiya, *Angew. Chem. Int. Ed.* **2013**, *52*, 3450–3452; *Angew. Chem.* **2013**, *125*, 3534–3536; b) S. Umemiya, K. Nishino, I. Sato, Y. Hayashi, *Chem. Eur. J.* **2014**, *20*, 15753–15759; c) J. Li, M. J. Lear, Y. Kawamoto, S. Umemiya, A. Wong, E. Kwon, I. Sato, Y. Hayashi, *Angew. Chem. Int. Ed.* **2015**, *54*, 12986–12990; *Angew. Chem.* **2015**, *127*, 13178–13182; d) J. Li, M. J. Lear, E. Kwon, Y. Hayashi, *Chem. Eur. J.* **2016**, *22*, 5538–5542.
- [6] Seminal development of masked acyl cyanides (MAC): H. Nemoto, Y. Kubota, Y. Yamamoto, *J. Org. Chem.* **1990**, *55*, 4515–4516.
- [7] R. Ballini, M. Petrini, *Tetrahedron* **2004**, *60*, 1017–1047.
- [8] A. McNally, C. K. Prier, D. W. C. MacMillan, *Science* **2011**, *334*, 1114–1117.
- [9] M. Y. Chang, C. Y. Tsai, *Tetrahedron Lett.* **2014**, *55*, 5548–5550.
- [10] J. Motoyoshiya, T. Ikeda, S. Tsuboi, T. Kusaura, Y. Takeuchi, S. Hayashi, S. Yoshioka, Y. Takaguchi, H. Aoyama, *J. Org. Chem.* **2003**, *68*, 5950–5955.
- [11] Related reports on ketone formation from alkyl nitriles using O₂: a) S. S. Kulp, M. J. McGee, *J. Org. Chem.* **1983**, *48*, 4097–4098; b) N. Rabjohn, C. A. Harbert, *J. Org. Chem.* **1970**, *35*, 3240–3243; c) S. H. Kim, K. H. Kim, J. N. Kim, *Adv. Synth. Catal.* **2011**, *353*, 3335–3339.
- [12] a) E. L. Spence, G. J. Langley, T. D. H. Bugg, *J. Am. Chem. Soc.* **1996**, *118*, 8336–8343; b) T. Benkovics, J. Du, I. A. Guzei, T. P. Yoon, *J. Org. Chem.* **2009**, *74*, 5545–5552; c) J. F. Van Humbeck, S. P. Simonovich, R. R. Knowles, D. W. C. MacMillan, *J. Am. Chem. Soc.* **2010**, *132*, 10012–10014; d) E. Arceo, I. D. Jurberg,

- A. Alvarez-Fernandez, P. Melchiorre, *Nat. Chem.* **2013**, *5*, 750–756.
- [13] Current oxidative methods to acyl cyanide intermediates are limited to unhindered mono- or bisnitriles and use peroxy reagents: a) Y. Sugiura, Y. Tachikawa, Y. Nagasawa, N. Tada, A. Itoh, *RSC Adv.* **2015**, *5*, 70883–70886; b) M. Brünjes, M. J. Ford, H. Dietrich, K. Wilson, *Synlett* **2015**, *26*, 1365–1370; c) X. Chen, T. Chen, Q. Li, Y. Zhou, L.-B. Han, S.-F. Yin, *Chem. Eur. J.* **2014**, *20*, 12234–12238; for amide and ester formations, see: d) S.-I. Murahashi, T. Naota, N. Nakajima, *Tetrahedron Lett.* **1985**, *26*, 925–928; e) S. Förster, O. Tverskoy, G. Helmchen, *Synlett* **2008**, 2803–2806; f) T. Arai, T. Moribatake, H. Masum, *Chem. Eur. J.* **2015**, *21*, 10671–10675.
- [14] For classical and emerging methods to acyl cyanides, see: a) S. Hünig, R. Schaller, *Angew. Chem. Int. Ed. Engl.* **1982**, *21*, 36–49; *Angew. Chem.* **1982**, *94*, 1–15; b) S. Takuma, Y. Hamada, T. Shioiri, *Chem. Pharm. Bull.* **1982**, *30*, 3147–3135; c) S. Lundgren, E. Wingstrand, C. Moberg, *Adv. Synth. Catal.* **2007**, *349*, 364–372; d) H. H. Choi, Y. H. Son, M. S. Jung, E. J. Kung, *Tetrahedron Lett.* **2011**, *52*, 2312–2315.
- [15] For peptide N-terminal capping, see: A. J. Doig, R. L. Baldwin, *Protein Sci.* **1995**, *4*, 1325–1336; Ongoing work pertains to preventing β -amino epimerization of chiral malononitriles (see Ref. [13e,f]) prior to acyl cyanide formation. Also oxidative esterification studies with O₂ show promise. For example, the reaction of **1** (as in Table 1, entry 3) with methanol (5 equiv) instead of allyl amine **2** proceeds in 85 % yield.

Received: April 6, 2016

Revised: May 9, 2016

Published online: June 14, 2016